Three-loop QCD corrections from massive quarks to deep-inelastic structure functions and operator matrix elements

Dissertation
zur Erlangung des wissenschaftlichen Grades
Dr. rer. nat.

eingereicht an der Fakultät Physik
der Technischen Universität Dortmund

vorgelegt von

Arnd Behring[a,b]

geboren am 19.04.1986 in Bielefeld

Dortmund
April 2016

Betreuer: Prof. Dr. Johannes Blümlein[a,b]

[a] Technische Universität Dortmund, Fakultät Physik
Otto-Hahn-Str. 4, D-44227 Dortmund
[b] Deutsches-Elektronen-Synchrotron, DESY
Platanenallee 6, D-15738 Zeuthen

Contents

List of Publications

Parts of the results presented in this thesis have already been published in the following articles.

Journal articles

- A. Behring, I. Bierenbaum, J. Blümlein, A. De Freitas, S. Klein and F. Wißbrock, "The logarithmic contributions to the $O(\alpha_s^3)$ asymptotic massive Wilson coefficients and operator matrix elements in deeply inelastic scattering", Eur. Phys. J. C **74** (2014) 3033, [arXiv:1403.6356 [hep-ph]].

- J. Ablinger, A. Behring, J. Blümlein, A. De Freitas, A. Hasselhuhn, A. von Manteuffel, M. Round, C. Schneider and F. Wißbrock, "The 3-Loop Non-Singlet Heavy Flavor Contributions and Anomalous Dimensions for the Structure Function $F_2(x, Q^2)$ and Transversity", Nucl. Phys. B **886** (2014) 733, [arXiv:1406.4654 [hep-ph]].

- J. Ablinger, A. Behring, J. Blümlein, A. De Freitas, A. von Manteuffel and C. Schneider, "The 3-loop pure singlet heavy flavor contributions to the structure function $F_2(x, Q^2)$ and the anomalous dimension", Nucl. Phys. B **890** (2014) 48, [arXiv:1409.1135 [hep-ph]].

- A. Behring, J. Blümlein, A. De Freitas, A. von Manteuffel and C. Schneider, "The 3-Loop Non-Singlet Heavy Flavor Contributions to the Structure Function $g_1(x, Q^2)$ at Large Momentum Transfer", Nucl. Phys. B **897** (2015) 612, [arXiv:1504.08217 [hep-ph]].

- A. Behring, J. Blümlein, A. De Freitas, A. Hasselhuhn, A. von Manteuffel and C. Schneider, "$O(\alpha_s^3)$ heavy flavor contributions to the charged current structure function $xF_3(x, Q^2)$ at large momentum transfer", Phys. Rev. D **92** (2015) 114005, [arXiv:1508.01449 [hep-ph]].

- J. Ablinger, A. Behring, J. Blümlein, A. De Freitas, A. von Manteuffel and C. Schneider, "Calculating Three Loop Ladder and V-Topologies for Massive Operator Matrix Elements by Computer Algebra", Comput. Phys. Commun. **202** (2016) 33, [arXiv:1509.08324 [hep-ph]].

Conference Proceedings

- A. Behring, J. Blümlein, A. De Freitas, T. Pfoh, C. Raab, M. Round, J. Ablinger, A. Hasselhuhn, C. Schneider, F. Wißbrock and A. von Manteuffel, "New Results on the 3-Loop Heavy Flavor Corrections in Deep-Inelastic Scattering", PoS **RADCOR 2013** (2013) 058, [arXiv:1312.0124 [hep-ph]].

- J. Ablinger, A. Behring, J. Blümlein, A. De Freitas, A. Hasselhuhn, A. von Manteuffel, C. Raab, M. Round, C. Schneider and F. Wißbrock, "Recent progress on the calculation of three-loop heavy flavor Wilson coefficients in deep-inelastic scattering", PoS **LL2014** (2014) 041, [arXiv:1407.3638 [hep-ph]].

Contents

- J. Ablinger, A. Behring, J. Blümlein, A. De Freitas, A. Hasselhuhn, A. von Manteuffel, C. Raab, M. Round, C. Schneider and F. Wißbrock, "3-loop heavy flavor Wilson coefficients in deep-inelastic scattering", Nucl. Part. Phys. Proc. **258-259** (2015) 41, [`arXiv:1409.1804 [hep-ph]`].

- J. Ablinger, A. Behring, J. Blümlein, A. De Freitas , A. Hasselhuhn, A. von Manteuffel, C. Raab, M. Round, C. Schneider and F. Wißbrock, "3-Loop Corrections to the Heavy Flavor Wilson Coefficients in Deep-Inelastic Scattering", PoS **EPS-HEP2015** (2016) 504, [`arXiv:1602.00583 [hep-ph]`].

1. Introduction

Scattering experiments play a crucial role in the exploration of the internal structure of matter already since the early days of nuclear and particle physics. Several pivotal results have been obtained from observations of particle scattering with atomic targets. Rutherford, Geiger and Marsden conducted experiments in which they observed the scattering of α particles off gold atoms in a thin foil [1–4]. Rutherford compared the experimentally observed distribution of scattered particles to theoretical calculations in different models [5]. The comparison revealed that the data favoured a model in which atoms are composite objects comprising negatively charged electrons and the positive charge concentrated in a nucleus and disfavoured the picture in which the electrons are embedded in a continuous cloud of positive charge as previously assumed by Thomson [6]. This combination of scattering experiments and their theoretical interpretation has henceforth been a prevailing pattern in nuclear and particle physics. The nucleus is made up of protons, discovered by Rutherford in 1919 [7], and neutrons, discovered by Chadwick in 1932 [8]. Both discoveries were made in scattering experiments where radioactive sources were used to provide high-energetic probes and the observation of the scattered particles allowed conclusions about the structure of the scattering target. The measurement of the anomalous magnetic moment of the nucleons [9–11] showed that it deviated from the value expected for point particles and proved that nucleons are extended objects. The approach of using scattering experiments to investigate the nucleon substructure proved successful again when Hofstadter and collaborators performed quasi-elastic scattering experiments with protons [12]. They could resolve the charge distribution of the proton, measure its charge radius and show that the boundary of nucleons is not sharp.

Experiments at Stanford Linear Accelerator Center (SLAC) in the late 1960s [13–16], cf. also [17–19], probed the internal structure of protons by scattering high energy electrons off a liquid hydrogen target. The cross section showed several peaks in the invariant mass distribution of the hadronic final state, which correspond to the elastic scattering peak and several nucleon resonances. At even larger virtualities $Q^2 = -q^2 > 2\,\mathrm{GeV}^2$ they also measured the continuum contribution of what is called *deep-inelastic* scattering (DIS). Here q^2 is the square of the 4-momentum carried by the exchanged photon. In this kinematic region the differential cross section can be parametrised by several structure functions F_i, which carry the information about the substructure of the nucleon. The data suggested that the structure functions would become (approximately) independent of Q^2 the further Q^2 was increased. This independence of Q^2, known as *scaling*, was predicted for DIS by Bjorken [20] based on an analysis of current algebra. One can define the Bjorken scaling variable $x = Q^2/2M\nu$, where ν is the energy transfer from the lepton to the proton in the laboratory frame and M is the nucleon mass. In the *Bjorken limit* one keeps x fixed but goes to the limit of $Q^2 \to \infty$ and $\nu \to \infty$. In this limit, instead of the absolute momentum scales Q^2 and ν, the structure functions depend solely on the dimensionless ratio x. Increasing the scale Q^2 corresponds to an increase of the spatial resolution. Since independence of an absolute energy or length scale is realised for point-like objects, the scaling behaviour hints towards point-like constituents inside the proton.

Feynman was then able to demonstrate that the assumption of point-like scattering centres inside the proton could reproduce the observed scaling behaviour [21–23]. He called those quasi-free particles *partons*. In his model a highly virtual electro-weak gauge boson, emitted by the lepton, probes the proton at such short time scales that it finds effectively free particles. There-

fore, the photon or weak bosons scatter elastically off the quasi-free partons. The cross section is then given by the incoherent sum over scattering off the individual partons. Each of these cross sections is weighted by the parton distribution functions (PDFs) $f_i(x_i)$. They describe the probability of finding a massless parton of type i inside the proton carrying a fraction x_i of the proton's longitudinal momentum. Conclusions about the spin of such partons can be drawn from the ratio of the scattering cross sections for longitudinally (L) and transversally (T) polarised photons with nucleons, $R = \sigma_\text{T}/\sigma_\text{L}$. For spin $1/2$ constituents R should be small. In the naive parton model with spin $1/2$ partons the Callan-Gross relation [24] even predicts $R = 0$. On the other hand, spin 0 constituents, for example, would entail large values for R. The ratio can be related to the structure functions of deep-inelastic scattering. While the first measurements did not yet allow to disentangle the individual structure functions, later measurements [14] showed that R is small. This supported the hypothesis of spin $1/2$ constituents and ruled out other approaches to deep-inelastic scattering, like vector meson dominance models [25, 26].

During the 1940s and 1950s experiments using cosmic rays and later also experiments at particle accelerators showed the existence of a large number of particles and resonances that were classified by their quantum numbers such as spin, parity, isospin or strangeness. In order to organize the strongly interacting states (hadrons), Gell-Mann [27] and Ne'eman [28], cf. also [29], extended the SU(2) symmetry of nuclear isospin to an SU(3) description, which incorporated strangeness into the symmetry structure. The mesons (hadrons with integer spin) could be organized into a singlet and an octet representation and the baryons (hadrons with half-integer spin) were represented as approximate octets and a decuplet. Besides grouping the states, the symmetry allowed the derivation of mass formulae for those hadrons [27, 30, 31]. At that time, the existence and mass of the spin $3/2$ baryon Ω^- with strangeness $S = -3$ was a prediction of this scheme. The observation of this baryon [32] in bubble chamber experiments at Brookhaven National Laboratory with the predicted mass was a strong indication for the correctness of this approach.

Shortly thereafter Gell-Mann [33] and independently Zweig [34] introduced the concept of hypothetical constituents of hadrons as fundamental triplets of the SU(3) symmetry. Zweig called these entities *aces* while Gell-Mann called them *quarks*: The proposal was to have an up quark with charge $+2/3$ and down and strange quarks with charge $-1/3$. Later the term *flavour* was coined to refer to the fact that there are several types of quarks, distinguished only by their mass and charge. Taking quarks to carry spin $1/2$ and fractional charges as stated above, one can form mesons as quark-antiquark states and baryons as states formed by three quarks.

With quarks as spin $1/2$ constituents for the observed hadrons and experimental data suggesting point-like spin $1/2$ partons being responsible for scaling in DIS, identifying quarks as partons was a next logical step that yielded the quark-parton model [35]. This means that quarks are not only mathematical entities but real constituents of protons and prompts the question whether one can observe free quarks in nature, which are not bound inside hadrons. To this date free quarks have not been observed despite intense searches [36].

Another problem arose from the fact that, since quarks are fermions, they must obey the spin-statistics theorem [38–42] and therefore have an antisymmetric wave function. However, the assumption of three equally flavoured spin $1/2$ quarks in a spin $3/2$ baryon like the Ω^- (sss), Δ^{++} (uuu) or Δ^- (ddd) would yield a symmetric wave function. This problem was noted by Greenberg and he proposed para-Fermi-statistics [43] for the quarks to resolve this difficulty. This was later shown to be equivalent to a new quantum number, now called *colour*, which is based on a separate SU(3)$_\text{c}$ symmetry [44–47]. The colour degree of freedom allows to anti-symmetrise the baryon wave function and thus to reconcile it with the spin-statistics theorem. Further support for the existence of colour and the number of colours $N_c = 3$ comes from the ratio of the hadronic e^+e^- annihilation cross section to the cross section of $e^+e^- \to \mu^+\mu^-$, the decay width of $\pi^0 \to 2\gamma$ if fractional charges are assumed, and the ratio of the hadronic and leptonic τ

lepton decay widths. All of these quantities involve some hadronic initial or final state and the introduction of constituents of hadrons with three colours introduces extra factors of N_c which are needed to produce agreement between theoretical predictions and experimental observations. Since no coloured objects were observed as free states in the detectors, it was postulated that the physical spectrum can only contain colourless objects, i.e. singlets under $\mathrm{SU}(3)_c$. A consequence of this postulate would be that free quarks or gluons cannot be observed since they are triplets or octets under colour.

On the theoretical side, quantum field theory had been very successfully applied to electromagnetism in the form of quantum electrodynamics (QED). One of the main tools in the application of QED is the perturbative expansion in the coupling constant. Its smallness ensures good agreement of already the first terms of the perturbative series with experimental observations. Motivated by the success of QED, attempts were made to apply quantum field theory also to the strong interactions. This turned out to be unsuccessful at first since the coupling constant of the strong interactions is large at low scales and thereby prevents the successful use of perturbation theory. As an alternative, other approaches to strong interactions were developed. This includes methods like Regge theory where one deduces scattering cross sections from the analyticity of the S-Matrix and crossing relations. Gell-Mann proposed current-algebra where only the commutation relations of currents are assumed without the necessity of an underlying field theory. Other approaches included the bootstrap model, the vector dominance model, the dual resonance model or models on a purely phenomenological basis like the parton model, mentioned above. While they explained some parts of the experimental data of that time reasonably well, they were found unsatisfactory with the advent of precise data at higher energies, notably the DIS data from the SLAC-MIT experiment [13–16].

The investigation of gauge theories with non-abelian gauge groups, pursued by Yang and Mills in 1954 [48], was a cornerstone of what would later become the quantum field theory of strong interactions. Non-abelian gauge theories, later called Yang-Mills theories, were not regarded much for some time since the theory predicted massless vector particles, gauge bosons analogous to the photon of QED, which were, however, not observed in nature. A peculiar feature of this type of gauge theories is that the non-commutativity of their symmetry generators induces self-interaction between the gauge bosons. Foundations for the later applications of these theories were laid by Faddeev and Popov, who found a way to consistently quantize Yang-Mills fields [49], and Veltman and 't Hooft, who proved the renormalisability of Yang-Mills fields [50–55]. Yang-Mills theories would soon prove instrumental for DIS and the electroweak Standard Model [56–58].

The observation of approximate scaling in DIS could be explained if the underlying theory has the property of asymptotic freedom: If the coupling strength decreases for increasing scales, scattering at high momentum transfer would effectively probe an ensemble of non-interacting particles. In contrast, all known field theories in four dimensions at that time showed increasing coupling strength with increasing scale (see, e.g. [59, 60]). Progress arose after Gross and Wilczek [61] as well as Politzer [62], cf. also [63], showed that Yang-Mills theories enjoy asymptotic freedom. Their renormalisation group analysis revealed that these theories can have a negative β-function and therefore a diminishing coupling constant in the ultraviolet (UV) regime.

In the application of Yang-Mills theories to the strong interactions Nambu [45] as well as Fritzsch, Gell-Mann and Leutwyler suggested [64, 65] to identify the non-abelian symmetry with the $\mathrm{SU}(3)_c$ colour degree of freedom of quarks and to use an octet of vector bosons (gluons) as force carriers. Quarks transform as triplets in the fundamental representation, whereas gluons transform in the adjoint representation. This theory was named quantum chromodynamics (QCD) and turned out to be rather successful in describing the strong interactions: Being a Yang-Mills theory based on $\mathrm{SU}(3)_c$, it has asymptotic freedom, which is compatible with the observed behaviour of the DIS structure functions. The gauging of colour as a local gauge symmetry implies

the strong force. Finally, it was conjectured [66, 67] that the infrared divergences of the theory, which are enhanced by the self-interactions of the massless gluons, can explain confinement of coloured states as a dynamical effect.

Asymptotic freedom also opened up the possibility to apply perturbation theory at short distances where the coupling is weak. For this, another development of that time was crucial: The operator product expansion developed by Wilson [68], cf. also [69–74], which allowed a systematic separation of long and short distance contributions. It had direct application in DIS since here, the scattering cross section can be described by a product of two electromagnetic current operators [75, 76]. It can be shown that the most relevant contributions come from light-like separations of the currents. Therefore, we can apply the operator product expansion on the light-cone [71, 77, 78], called light-cone expansion. It allows to express products of operators in terms of local operators, which describe physics at long distances, and coefficient functions, which describe the short distance phenomena. The local operators are regular in the limit of light-like separation while the coefficient functions carry the singularities of the original product in this limit. As mentioned above, theories which enjoy asymptotic freedom have weak coupling at short distances and therefore allow to calculate the coefficient functions perturbatively. Hence, the structure functions of DIS depend on the coefficient functions, also called *Wilson coefficients*, and matrix elements of the local operators. It is possible to order the relevance of the individual operators in the light-cone limit by the degree of singularity of the corresponding Wilson coefficient. An analysis reveals that the singularity depends on the difference between the canonical dimension of the operator and its spin – a quantity called twist [79] – and that the operators of lowest twist are most relevant. In the case of DIS the operators of twist 2 are the first that contribute.

How the structure functions depend on the scale Q^2 is of course of particular interest since it addresses the question of scaling (independence from Q^2). After all, QCD is not a free theory and contrary to the assumption of the naive parton model, there are interactions between the partons. It turns out, however, that the leading-order behaviour in perturbation theory in the twist-2 approximation reproduces the free field result up to calculable logarithmic corrections in Q^2 and therefore exhibits approximate Bjorken scaling [67, 80, 81]. The scale behaviour is governed by the renormalisation group equations [82–87] and in particular the anomalous dimensions of the local operators, which were calculated at leading order in [67, 80, 81]. Thus, even quantitative predictions of the scaling violations were possible in QCD, at least in limited kinematic regions probed given typical experimental resolutions available in the 1970s. Subsequent experimental investigations [88, 89] indeed found scaling violations which were in agreement with those predicted from QCD – a finding which led to a greater acceptance of QCD as the correct theory of the strong interactions. Applying an inverse Mellin transformation to the renormalisation group equations and anomalous dimensions of the light-cone operators allows to translate the expressions to x space [71, 80, 81, 90–93]. At leading twist, these quantities can be given an interpretation in the parton picture [94–98]. The matrix elements of the local operators correspond to parton distribution functions, and their scale dependence is described by a set of integro-differential equations. The anomalous dimensions of the local operators at leading twist are equivalent to splitting functions P_{ij} which give the probability to find a parton of type i when probing a parton of type j.

Many experiments thereafter measured deep-inelastic lepton-hadron scattering processes. While the first experiments were fixed target experiments, later also collider experiments were realised. They allowed for an exploration of larger virtualities Q^2 and smaller values of x. So far the largest range of kinematical parameters was accessible with the HERA collider [99, 100] at DESY. Its detectors H1 [101], ZEUS [102] and HERMES [103] probed protons at virtualities ranging from $Q^2 = 0.045\,\mathrm{GeV}^2$ to $50\,000\,\mathrm{GeV}^2$ and $6 \cdot 10^{-7} \leq x \leq 0.65$ [100].

To keep up with the increasing experimental precision, also the theoretical calculations had

to be extended to higher accuracy. Therefore, higher orders in perturbation theory beyond the leading order (LO) were needed. As a first step, the 1-loop QCD corrections to the coefficient functions to unpolarised DIS were calculated [104, 105], cf. also [106], mainly at the end of the 1970s. Also the next-to-leading order (NLO) corrections to the anomalous dimensions in the unpolarised case [104, 107–118] were obtained. The 2-loop QCD corrections to the massless Wilson coefficients followed during the next 15 years [118–128]. The step to next-to-next-to-leading order (NNLO) was first taken for sum rules [129] and a series of fixed moments of the anomalous dimensions and Wilson coefficients [130–134]. Finally, also the expressions for general values of the Mellin variable N and parton momentum fraction x were obtained for the NNLO anomalous dimensions [135, 136] and the massless 3-loop Wilson coefficients [137, 138]. There are even a few fixed moments for the unpolarised non-singlet anomalous dimension available at 4-loop order [139–142]. The anomalous dimensions and massless Wilson coefficients are single-scale quantities and are expressible in terms of nested harmonic sums [143, 144] in N space and in terms of a certain class of iterated integrals called harmonic polylogarithms [145] in x space. These mathematical objects obey algebraic and structural relations [146–148] which allow to reduce the expressions to a small number of basis sums or integrals. For the 3-loop Wilson coefficients and anomalous dimensions this was achieved in [149].

Besides the scattering of unpolarised leptons with nucleons, experiments have also investigated scattering of polarised leptons and nucleons. The polarisation of both probe and target gives insight into the spin structure of the nucleons. Here more independent structure functions arise and additional operators contribute. Therefore, the description of polarised DIS requires the separate calculation of polarised Wilson coefficients and anomalous dimensions. The Wilson coefficients for the structure function g_1 are known up to $\mathcal{O}(\alpha_s^3)$ [150–153] and the structure function g_2 is related to g_1 by the Wandzura-Wilczeck relation [154]. The polarised anomalous dimensions were calculated to LO in [96, 155, 156], to NLO in [157–159] and to NNLO in [160, 161].

In charged current DIS, a charged electro-weak gauge boson $W^\pm$ is exchanged instead of a photon. The parity-violating nature of the weak current allows new structure functions to contribute. They can be used to disentangle the flavour structure of the nucleons. Corrections to the corresponding Wilson coefficients were calculated at 1-loop order in [105, 106] and later to 2-loop [118, 122] and 3-loop order [153, 162, 163].

Besides the nearly massless up, down and strange quarks which were part of Gell-Mann's original proposal for the quark model, heavier quarks were observed as well. In 1974 the existence of a fourth quark was inferred from narrow resonances in e^+e^- collisions, called ψ and ψ' and observed at SLAC [164, 165], and a pp resonance, called J and observed at BNL [166]. The J and ψ states turned out to be the same particle and were found to be consistent with the interpretation as a quark-antiquark bound state of the new quark. The quark was called *charm quark* and had been postulated on several occasions before [167–172], cf. also [173], and was particularly welcome in the context of anomaly cancellation [174, 175] and the suppression of flavour-changing neutral currents through the Glashow-Iliopulos-Maiani mechanism [176]. Another quark, now called *bottom quark*, was found three years later as the Υ resonance, a $b\bar{b}$ bound state observed at Fermilab [177]. The most recent quark discovery was the *top quark*, also observed at Fermilab [178–180] in 1995. In contrast to the other quarks, the top quark, however, decays on such short time scales that it cannot form hadrons.

In the parton picture, all partons are massless particles. Quarks, on the other hand, do have masses. For the up, down and strange quarks the massless approximation is generally justified already at energies of a few GeV. Other flavours, starting with the charm quark, have masses larger than $1\,\text{GeV}$ and cannot be treated as massless over the whole range allowed kinematically. The top quark has a mass of $m_t \approx 173\,\text{GeV}$ [37] and is too heavy to be produced in the DIS experiments carried out so far, but charm and bottom quarks have to be taken into account.

1. Introduction

The influence of such heavy quarks on DIS was considered in theoretical calculations soon after the discovery of the charm quark. At the end of the 1970s, the leading-order contributions to the structure functions were calculated [181–185]. For photon exchange heavy quarks start to appear at $\mathcal{O}(\alpha_s)$ and are produced by photon gluon fusion ($\gamma g \rightarrow Q\bar{Q}$). Also the scaling behaviour of heavy quarks turns out to be different from that of massless quarks. Therefore, the study of heavy quarks can give a handle on the otherwise rather loosely constrained gluon distribution. This motivated the calculation of the NLO corrections [186–188]. At NLO also quark-initiated reactions start to contribute, but the gluon contributions stay dominant. Similar developments were carried out for polarised [151, 189–193] and charged current scattering [194–199].

While the NLO calculation of heavy quark contributions to unpolarised DIS were first given semi-analytically [186–188][1] for general kinematics, it was later found [201] that the heavy flavour Wilson coefficients factorise in the limit of large virtuality compared to the heavy quark mass ($Q^2 \gg m^2$). In this asymptotic region the Wilson coefficients can be written as the Mellin convolution of the massless Wilson coefficients and massive operator matrix elements (OME). The approximation is valid in the limit where power corrections in m^2/Q^2 can be discarded. By comparing to the exact NLO calculation it was found [202] that for the unpolarised structure function $F_2(x, Q^2)$ the approximation holds for $Q^2 \gtrsim 10m^2$ at the percent level, which covers large parts of the kinematic range relevant at HERA. On the other hand, for the structure function $F_L(x, Q^2)$ the approximation becomes reliable only for $Q^2 \gtrsim 800m^2$ due to the presence of terms proportional to $(m^2/Q^2) \ln(m^2/Q^2)$. The OMEs are matrix elements of the light-cone operators between partonic states and they contain the complete dependence on the heavy quark mass that remains in this limit. Moreover, the OMEs are process independent, while the process dependence is then carried by the massless Wilson coefficients.

The massive OMEs do not only appear in the asymptotic description of the heavy flavour Wilson coefficients, but also in the definition of PDFs in a variable flavour number scheme (VFNS) [193, 202, 203]. The VFNS describes the transition of PDFs in a scheme with N_F massless and one massive quark to a scheme with $N_F + 1$ massless quarks. In the new scheme, the massive quark is treated as massless and is assigned a PDF which is obtained by matching to the N_F flavour scheme at some matching scale μ. Here the massive OMEs enter as matching coefficients. Having such a scheme is relevant for experiments at energy scales much larger than the heavy quark mass, such as those carried out at the LHC. Treating the heavy quarks purely perturbatively would yield logarithms of large scale ratios involving the heavy quark mass. Through the VFNS the heavy quarks are treated as effectively massless above a matching scale, which removes their mass scale from the problem.

At NLO the massive OMEs were calculated in [201, 202] and checked in a recalculation in [204, 205]. In addition to the check of the NLO results, also expressions needed for the extension of the results to 3-loop order were obtained [206, 207]. In these calculations the authors obtained the 2-loop OMEs through direct integration of the Feynman parameter integrals in N space. This was possible by employing Mellin-Barnes representations [208–210] and by expressing the Feynman parameter integrals in terms of higher hypergeometric functions [211–214]. The resulting sums could then be simplified and expressed as nested harmonic sums. The development was not only interesting as a recalculation, but also since the same methods are applicable also at the next order in perturbation theory. Since the massless Wilson coefficients and the anomalous dimensions are already known at NNLO, the calculation of the massive OMEs at NNLO would allow for a NNLO description of the heavy flavour contribution to DIS in the asymptotic region. A first step in that direction was taken in 2009 with the calculation of a series of moments for the massive OMEs and the extension of the renormalisation procedure to 3-loop order [193, 203, 215]. This calculation also verified the parts of the NNLO anomalous dimensions which are proportional to

---

[1] A numerical implementation in Mellin space was presented in [200].

the colour factor T_F through independent calculations. The moments were obtained by mapping the diagrams to massive tadpoles through appropriate projectors and the use of the `FORM` [216] program `MATAD` [217]. For phenomenological applications, however, the expressions for general values of the Mellin variable N are necessary, which requires different calculational techniques. Since then, several partial results working towards the goal of a complete asymptotic NNLO description were completed. We will give a brief review of of these developments in Section 2.8.

Overall, DIS has been and still is an important tool to establish and test QCD as the correct theory of strong interactions. Moreover, DIS is used to obtain information which cannot be predicted from QCD. Using the theory predictions and comparing to the accumulated data of almost half a century of experiments, one can extract several important quantities. For example, DIS allows to determine the non-perturbative PDFs rather precisely. They are universal quantities and can therefore be reused for the prediction of other hadronic collisions like for example pp collisions which are currently investigated at centre-of-mass energies of $\sqrt{s} = 13\,\mathrm{TeV}$ at the LHC at CERN. Precise knowledge of the PDFs is a prerequisite for drawing accurate conclusions from hadronic collisions – be it for precision measurements of Standard Model parameters or searches for effects of new physics. Modern global analyses [100, 218–222] use deep-inelastic scattering, along with other processes, to fit phenomenological parametrisations of the PDFs to the data. Moreover, information from deep-inelastic scattering provides access to theory parameters like the strong coupling constant $\alpha_s(m_Z^2)$. It can be determined at the level of $\mathcal{O}(1\%)$ in modern NNLO analyses [223–225]. Finally, also the masses of charm and bottom quarks can be extracted, see for example [226]. Given the small experimental uncertainties, NNLO corrections have to be taken into account in the analyses mentioned above. This includes contributions from massive quarks like the charm and bottom quarks. It is the aim of this thesis to contribute to extending the description of heavy quark corrections to deep-inelastic scattering to 3-loop order.

In this thesis, we present results in the context of the long-term project to calculate the massive OMEs at 3-loop order which are required to extend the description of the heavy flavour contributions to DIS and the VFNS to NNLO. In Chapter 2, we review the basic formalism to describe deep-inelastic scattering and contributions from massive quarks. We discuss the relevant kinematic variables, the description via structure functions and the interpretation in the parton model, as well as the light-cone expansion in the context of QCD and the factorisation of the heavy flavour Wilson coefficients into massive OMEs and massless Wilson coefficients. Moreover, we explain the VFNS and renormalisation procedure for OMEs. The chapter closes with a brief summary of the status of the calculation of the massive OMEs.

We calculate the OMEs in a diagrammatic approach, which involves generating Feynman diagrams and solving the associated Feynman integrals. To handle the large number of integrals, integration-by-parts identities [227–233] are used to eliminate relations among the integrals and to reduce them to a much smaller number of master integrals. These master integrals have to be solved and their results must be assembled into the result for the complete OME. We present an outline of the major steps involved in this calculation in Section 3.1 and collect some properties of the nested sums and iterated integrals which appear in the results in Section 3.2. Since one of the most demanding tasks is the calculation of the master integrals, we explain the techniques we use in Section 3.3. These methods include introducing a Feynman parametrisation and identifying the integrals as generalised hypergeometric functions and related functions [211–214, 234–239] to arrive at a sum representation or to use Mellin-Barnes integrals [208–210] to the same end. These sum representations are subsequently simplified in terms of nested sums using the summation algorithms [240–251], which are implemented in the `Mathematica` packages `Sigma` [241, 252, 253], `EvaluateMultiSums` and `SumProduction` [254–257], as well as `HarmonicSums` [258–263]. Another important technique is the calculation of master integrals via differential equations [264–268]. We use a formal power series ansatz to translate the differential equations into difference equations and solve those by uncoupling them into a scalar recurrence and solving that in terms of nested

sums with the packages mentioned above.

In Chapter 4, we apply the techniques to calculate the flavour non-singlet OME for even and odd values of the Mellin variable N. The even moments corresponds to the matrix element of the vector operator and the odd moments to the axial-vector operator. Moreover, we also calculate the OME of the tensor operator, which is relevant for the transversity structure functions. Besides the OMEs, we also obtain the N_F-dependent parts of the non-singlet anomalous dimensions. The OMEs enter the asymptotic factorisation of the heavy flavour Wilson coefficients for $Q^2 \gg m^2$ and we discuss their influence on the unpolarised structure function $F_2(x, Q^2)$, the polarised structure function $g_1(x, Q^2)$ and the charged current structure function $xF_3(x, Q^2)$. In the latter two cases, we also comment on the associated sum rules. Finally, we examine the non-singlet matching relation in the VFNS. Chapter 5 deals with the pure-singlet OME and its application. We first present the calculation of the OME and of the pure-singlet anomalous dimension, which we obtain as a by-product of the calculation. This is the first independent recalculation of the pure-singlet anomalous dimension, which was first found in the massless case in [136]. We then give the pure-singlet asymptotic heavy flavour Wilson coefficient and illustrate its impact on the structure function $F_2(x, Q^2)$. Diagrams with ladder- and V-topology are an important class of diagrams which contribute to several OMEs. We select a sample of twelve diagrams from $A_{Qg}^{(3)}$ and discuss their calculation in Chapter 6. Here the method of differential equations plays a crucial role to calculate all required master integrals. Using similar methods, we also calculate the $\mathcal{O}(\varepsilon^0)$ term of the gluonic OME $A_{gg,Q}^{(3)}$ in Chapter 7. This OME enters the matching relation for the gluon PDFs in the VFNS. In Chapter 8, we use the known fixed moments for the OMEs [193, 203] to compare the relative importance of the individual OMEs in the context of the heavy flavour Wilson coefficients and the VFNS. Chapter 9 contains the conclusions. The Feynman diagrams in this thesis have been drawn using `Axodraw` [269].

2. Deep-inelastic scattering

In this chapter, we review the basic formalism which is used to describe deep-inelastic scattering (DIS) processes in the context of quantum chromodynamics. In particular, we collect the definitions which lead up to the description of the contributions from heavy quarks in terms of operator matrix elements, since these are the quantities which we calculate here.

2.1. Kinematics of deep-inelastic scattering

The power of deep-inelastic lepton-hadron scattering lies in using stable, non-strongly interacting elementary particles to probe composite particles. The electro-weak interaction of leptons is well understood, which makes leptons excellent probes for the substructure of composite particles like hadrons. In a classical DIS experiment, a beam of leptons (electrons, muons or neutrinos) is shot at a fixed target or a second beam consisting of hadrons (usually protons or nuclear targets containing both protons and neutrons). The lepton then scatters off the hadron inelastically. While the lepton is just deflected in this process, the hadron disintegrates into a complicated final state involving a number of particles. DIS is usually carried out as an inclusive experiment in which all possible hadronic final states that are allowed by quantum number conservation are taken into account. At lowest order of electro-weak theory, the lepton exchanges one electro-weak gauge boson with the hadron. This is the Born approximation and we will confine our discussion to this approximation, assuming that radiative corrections to the lepton system have already been carried out [270]. The gauge boson can be a photon, a Z^0 or a $W^\pm$ boson.

The kinematic situation is sketched in Fig. 2.1. An incoming lepton with four-momentum $k = (E, \vec{k})$ scatters off a hadron with initial momentum $P = (E_P, \vec{P})$ which results in a scattered lepton of momentum $k' = (E', \vec{k'})$ and a hadronic final state carrying collective momentum P'. The scattering is mediated by exchange of one electro-weak gauge boson which carries momentum $q = k - k'$. Obviously, the momenta of the initial state hadron and of the initial and final state lepton are on their respective mass shells, $k^2 = m_\ell^2$ and $k'^2 = m_{\ell'}^2$ and $P^2 = M^2$, where $m_{\ell(\ell')}$ is the mass of the incoming (outgoing) lepton and M is that of the initial state hadron. Since the momentum P' describes a collection of particles, there is no on-shell condition for this momentum and we denote its invariant hadronic mass by $W^2 = P'^2$.

Several useful kinematic variables can be defined in a Lorentz-invariant way, which however take physically intuitive forms in certain reference frames. For two-particle scattering, the Mandelstam variable s, defined as

$$s = (P + k)^2,\tag{2.1}$$

characterises the initial state and reduces to the square of the total energy in the centre-of-momentum frame. Since the gauge boson is exchanged in the t-channel, it has space-like momentum and its squared four-momentum q^2 is negative. Therefore, it is common practice to define

$$Q^2 = -q^2 = -(k - k')^2\tag{2.2}$$

and to call this quantity the virtuality of the gauge boson. The name reflects the fact that in the case of photon exchange it measures how far off the mass shell ($q^2 = 0$) the boson is. In Born
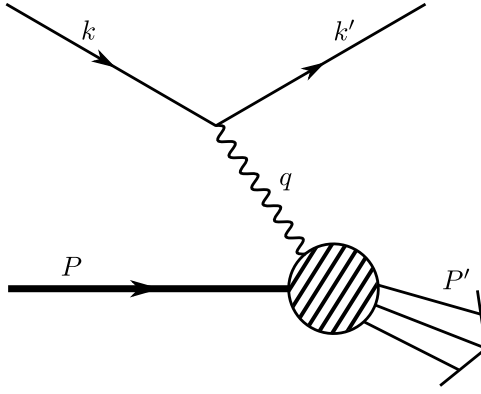
Figure 2.1.: Sketch of the kinematic setup for deep-inelastic lepton-hadron scattering in Born approximation: The upper line denotes the lepton, the wavy line represents the electro-weak gauge boson and the lower line stands for the hadronic part of the reaction.

approximation it coincides with the Mandelstam variable t up to a sign, $Q^2 = -t$. We define ν as

$$\nu = \frac{P.q}{M} = \frac{W^2 + Q^2 - M^2}{2M} \qquad (2.3)$$

such that in the rest frame of the hadron (target system) it becomes the energy transfer from the leptons to the hadronic system, $\nu = E_{\mathrm{TS}} - E'_{\mathrm{TS}}$. Furthermore, it proves to be useful to define the Bjorken scaling variable [35, 271]

$$x = \frac{-q^2}{2P.q} = \frac{Q^2}{2M\nu} = \frac{Q^2}{W^2 + Q^2 - M^2} \qquad (2.4)$$

and the inelasticity

$$y = \frac{P.q}{P.k} = \frac{2M\nu}{s - M^2 - m_\ell^2} = \frac{W^2 + Q^2 - M^2}{s - M^2 - m_\ell^2} \ . \qquad (2.5)$$

In the target system, the inelasticity can be interpreted as the energy transfer from the lepton to the hadron system relative to the energy of the incoming lepton, $y = (E_{\mathrm{TS}} - E'_{\mathrm{TS}})/E_{\mathrm{TS}}$.

The scattering process is called *deep-inelastic* if the virtuality Q^2 and the invariant mass of the final state W^2 are sufficiently large. For nucleon (i.e. proton or neutron) targets a reasonable requirement is $Q^2 \geq 4\,\mathrm{GeV}^2$ and $W^2 \geq 4\,\mathrm{GeV}^2$ [272]. Below these limits there are significant contributions from nucleon resonances, while above them the continuum contribution dominates. This continuum contribution is the matter of interest in DIS experiments, since it contains information about the internal structure of the hadron. For the discussions in this thesis, we neglect the masses of the leptons $m_\ell = 0$ and drop terms of order M^2/Q^2. The latter are called *target mass corrections* and can become important at low values of Q^2 and large values of x [273–277]. Moreover, we will specialise the discussion to the case of nucleons in the initial state.

Both the leptons and the nucleons are spin $^1/_2$ particles. The nucleon spin is described by the spin four-vector S, which we normalise as $S^2 = -M^2$. It fulfils $P.S = 0$ and can be decomposed into a longitudinal and transverse component with respect to the beam axis. In the nucleon rest frame the components take a particularly simple form if we align the z-axis with the beam axis,

$$S_{\mathrm{L}} = M(0,0,0,1)\,, \qquad\qquad S_{\mathrm{T}} = M(0,\cos(\beta),\sin(\beta),0)\,, \qquad (2.6)$$

where β is the angle of the nucleon spin direction in the plane transverse to the beam axis.

For unpolarised scattering, there are three independent variables necessary to describe the kinematics of the scattering process. One variable describes the initial state for which we can choose for example the Mandelstam variable s. The two other variables, such as x and Q^2, characterise the final state configuration. If we describe scattering of polarised particles additional angular variables are necessary to describe the orientation of the spins.

The physical region of phase space is determined by a number of constraints. The total energy must account for at least the mass of the initial state nucleon, $s \geq M^2$. Baryon number conservation requires at least one baryon in the final state which leads to $W^2 \geq m_p^2$, where m_p is the proton mass, since the proton is the lightest baryon. Moreover, for vanishing lepton masses, the virtuality must be non-negative, $Q^2 \geq 0$, as must be the energy transfer to the hadronic system, $\nu \geq 0$. Then we deduce from Eq. (2.5) that $0 \leq y \leq 1$. The limit $y \to 0$ requires the energy transfer to the hadronic system ν to vanish, which corresponds to exact forward scattering. Considering proton scattering, we use

$$W^2 = (P + q)^2 = m_p^2 + Q^2 \frac{1 - x}{x} \geq m_p^2 \tag{2.7}$$

to show that $0 \leq x \leq 1$. The elastic situation, where $W^2 = m_p^2$, corresponds to the limit $x \to 1$. Since at most three kinematic variables can be independent, there are of course relations between the above invariants. A particularly useful one is

$$Q^2 = xy(s - M^2) \approx xys. \tag{2.8}$$

This allows to estimate the lowest attainable value of x for a given virtuality. In particular, we get for HERA kinematics

$$x \gtrsim \frac{Q^2}{10^5 \, \text{GeV}^2}. \tag{2.9}$$

2.2. Cross section and structure functions

The calculations presented in this thesis concern the QCD corrections from massive quarks to inclusive deep-inelastic lepton-nucleon scattering. In particular, the results will be applied to three situations: Unpolarised scattering mediated by photons, photon-mediated polarised scattering and unpolarised scattering mediated by charged currents ($W^\pm$ bosons). Therefore, we discuss the cross-sections which are relevant for these three cases and suppress contributions from weak neutral currents for brevity.

The matrix element for inclusive lepton-hadron scattering in the Born approximation of electroweak theory reads [75, 76]

$$\mathcal{M}_i = \bar{u}(k', \lambda')\gamma_\mu(g_{V,i} + g_{A,i}\gamma_5)u(k, \lambda)\frac{e^2}{D_i(q^2)} \left\langle P' \middle| J_i^\mu(0) \middle| P, S \right\rangle, \tag{2.10}$$

where u and $\bar{u}$ are the Dirac spinors describing the initial and final state leptons with helicities λ and λ', respectively. We denote the electromagnetic unit of charge by e and the Dirac matrices by γ_μ and γ_5, cf. also Appendix A. The nucleon initial state with momentum P and spin S has the state vector $|P, S\rangle$ and the hadronic final state is described by $|P'\rangle$. Depending on the gauge boson that mediates the scattering, indicated by the index i, the vector coupling $g_{V,i}$, the axial-vector coupling $g_{A,i}$ and the propagator factor $D_i(q^2)$ take different values. For photons we get

$$g_{V,\gamma} = 1, \qquad g_{A,\gamma} = 0, \qquad D_\gamma(q^2) = q^2, \tag{2.11}$$

while for W bosons they are

$$g_{V,W^\pm} = 1\,, \qquad g_{A,W^\pm} = -1\,, \qquad D_{W^\pm}(q^2) = 2\sqrt{2}\sin\theta_{\rm W}(q^2 - M_W^2)\,, \qquad (2.12)$$

where M_W is the mass of the W boson and $\theta_{\rm W}$ is the weak mixing angle. The current operator $J_i^\mu(0)$ is the electromagnetic ($i = \gamma$) or the weak charged current ($i = W^\pm$). The former is hermitian $J_\gamma^{\mu\dagger} = J_\gamma^\mu$, while for the latter hermitian conjugation connects W^+ and W^- couplings by $J_{W^+}^\mu = J_{W^-}^{\mu\dagger}$.

In order to obtain the differential cross section for inclusive scattering, we have to insert the squared matrix element into the cross section, sum over all allowed hadronic final states and integrate over their respective phase space. The form of the matrix element Eq. (2.10) allows us to decompose the cross section into a leptonic tensor $L_{\mu\nu}$ and a hadronic tensor $W_{\mu\nu}$. First, we write this retaining all dependence on initial and final state spins [276, 278, 279]

$$\frac{{\rm d}^3\sigma(\lambda, \lambda', S)}{{\rm d}x\,{\rm d}y\,{\rm d}\phi} = \frac{y\alpha^2}{Q^4} \sum_{i\in\{\gamma, W^+, W^-\}} \eta_i(Q^2)L_{\mu\nu}^i W_i^{\mu\nu}\,. \qquad (2.13)$$

Here $\alpha = e^2/(4\pi)$ denotes the electromagnetic fine structure constant. If the polarisation of the final state lepton is not observed, we have to sum over its helicity states λ'. For unpolarised scattering, we also average over the spins of the initial state lepton and the nucleon, after which the integration over the azimuthal angle ϕ of the scattered lepton becomes trivial. The normalisation constants $\eta_i(Q^2)$ absorb the propagator factors and allow for a uniform notation across the different channels. They read

$$\eta_\gamma(Q^2) = 1\,, \qquad (2.14)$$

$$\eta_{W^\pm}(Q^2) = \frac{1}{2}\frac{G_F^2 Q^4}{(4\pi)^2\alpha^2}\left(\frac{M_W^2}{Q^2 + M_W^2}\right)^2\,, \qquad (2.15)$$

where G_F is the Fermi constant which describes the weak strength of the interaction,

$$G_F = \frac{e^2}{4\sqrt{2}\sin\theta_{\rm W}M_W^2}\,. \qquad (2.16)$$

The leptonic tensor with all polarisation information is then given by

$$L_{\mu\nu}^i = \left[\bar{u}(k', \lambda')\gamma_\mu(g_{V,i} + g_{A,i}\gamma_5)u(k, \lambda)\right]^\dagger \left[\bar{u}(k', \lambda')\gamma_\nu(g_{V,i} + g_{A,i}\gamma_5)u(k, \lambda)\right]\,, \qquad (2.17)$$

which for unpolarised, photon-mediated scattering becomes

$$\frac{1}{2}\sum_{\lambda, \lambda'} L_{\mu\nu}^{\rm em} = 2\left(k_\mu k_\nu' + k_\nu k_\mu' - \frac{Q^2}{2}g_{\mu\nu}\right)\,. \qquad (2.18)$$

The same expression arises both for leptons and anti-leptons in the initial state. Keeping the polarisation information of the initial state lepton, but summing over the final state lepton polarisation λ' yields the expression for polarised scattering

$$\sum_{\lambda'} L_{\mu\nu}^{\rm em} = 2\left(k_\mu k_\nu' + k_\nu k_\mu' - \frac{Q^2}{2}g_{\mu\nu} + i\varepsilon_{\mu\nu\rho\sigma}2\lambda k^\rho q^\sigma\right)\,. \qquad (2.19)$$

Finally, we give the expression for unpolarised charged current scattering, in which we average over λ and sum λ', but where there is an axial-vector coupling present,

$$\frac{1}{2}\sum_{\lambda, \lambda'} L_{\mu\nu}^{W^-} = 4\left(k_\mu k_\nu' + k_\nu k_\mu' - \frac{Q^2}{2}g_{\mu\nu} + i\varepsilon_{\mu\nu\rho\sigma}k^\rho k'^\sigma\right)\,. \qquad (2.20)$$

The hadronic tensor, on the other hand, contains the matrix element of the current operator between hadronic initial and final states. Since we have to sum or integrate over all unobserved degrees of freedom of the hadronic final state and since we sum over all allowed final states, we can use the completeness of states together with the positivity of the energy to write the hadronic tensor as a commutator of the currents between nucleon states,

$$W^i_{\mu\nu}(P, S, q) = \frac{1}{4\pi} \int d^4z \, e^{iq\cdot z} \, \langle P, S|[J^{i\dagger}_\mu(z), J^i_\nu(0)]|P, S\rangle \,. \tag{2.21}$$

A similar expression, where the current commutator is replaced by a time-ordered product, arises as the amplitude for Compton scattering of virtual photon with a nucleon for forward kinematics,

$$T^i_{\mu\nu}(P, S, q) = i \int d^4z \, e^{iq\cdot z} \, \langle P, S|\mathrm{T}[J^{i\dagger}_\mu(z)J^i_\nu(0)]|P, S\rangle \,, \tag{2.22}$$

where $\mathrm{T}[\dots]$ is the time ordered product of its arguments. In fact, the two tensors are related by the optical theorem, see e.g. [75],

$$W^i_{\mu\nu}(P, S, q) = \frac{1}{2\pi} \operatorname{Im} T^i_{\mu\nu}(P, S, q)\,. \tag{2.23}$$

At times, it is more convenient to deal with a time ordered product rather than the commutator of currents. By using translation invariance, one can also show that the crossing operation $q \to -q$, $\mu \leftrightarrow \nu$, which interchanges the initial and final state leptons, yields $T^\gamma_{\mu\nu}(P, S, -q) = T^\gamma_{\mu\nu}(P, S, q)$ for the electromagnetic case, i.e. the amplitude is even under this operation. However, in the charged current case, the crossing operation acts on the Compton amplitude as $T^{W^\pm}_{\nu\mu}(P, S, -q) = T^{W^\mp}_{\mu\nu}(P, S, q)$. In order to discuss objects with even or odd behaviour under crossing, it is useful to define the combinations, [280, 281],

$$T^{W^+ \pm W^-}_{\mu\nu} = T^{W^+}_{\mu\nu} \pm T^{W^-}_{\nu\mu} \,, \tag{2.24}$$

which behave like $T^{W^+ \pm W^-}_{\mu\nu}(P, S, -q) = \pm T^{W^+ \pm W^-}_{\mu\nu}(P, S, -q)$.

A direct evaluation of the hadronic tensor is not possible because of the strongly interacting, composite nucleon states. Nevertheless, we can parametrise it, using what is commonly known as *structure functions*, by making an ansatz using all possible Lorentz structures and imposing symmetry principles and conservation laws, see e.g. [272, 282]. In general, 14 independent structure functions are required to describe the hadronic tensor [276, 280] but under the assumptions made here, only five structure functions appear,

$$W_{\mu\nu}(P, S, q) = \frac{1}{2x}\left(g_{\mu\nu} + \frac{q_\mu q_\nu}{Q^2}\right) F_L(x, Q^2) + \frac{2x}{Q^2}\left(P_\mu P_\nu + \frac{q_\mu P_\nu + q_\nu P_\mu}{2x} - \frac{Q^2}{4x^2}g_{\mu\nu}\right) F_2(x, Q^2)$$
$$+ i\varepsilon_{\mu\nu\rho\sigma}\left(\frac{P^\rho q^\sigma}{2P\cdot q}F_3(x, Q^2) + \frac{q^\rho S^\sigma}{P\cdot q}g_1(x, Q^2) + \frac{q^\rho[(P\cdot q)S^\sigma + (S\cdot q)p^\sigma]}{(P\cdot q)^2}g_2(x, Q^2)\right)\,. \tag{2.25}$$

We choose to use the structure function $F_L(x, Q^2)$. An alternative choice would be to use $F_1(x, Q^2)$ which is related to $F_L(x, Q^2)$ and $F_2(x, Q^2)$ by

$$F_1(x, Q^2) = \frac{F_2(x, Q^2) - F_L(x, Q^2)}{2x} \tag{2.26}$$

By contracting the hadronic and leptonic tensors and averaging over the initial state spins, we arrive at the differential cross section for unpolarised, photon-mediated scattering

$$\frac{d^2\sigma^{\gamma,\mathrm{unp}}}{dx\,dy} = \int_0^{2\pi} d\phi \, \frac{1}{4} \sum_{\lambda, \lambda', S} \frac{d^3\sigma^\gamma(\lambda, \lambda', S)}{dx\,dy\,d\phi}$$
$$= \frac{2\pi\alpha^2}{xyQ^2}\left[\left(1 + (1 - y)^2\right) F_2(x, Q^2) - y^2 F_L(x, Q^2)\right]\,. \tag{2.27}$$

2. Deep-inelastic scattering

The cross section for polarised leptons and hadrons, on the other hand, is given by

$$\frac{\mathrm{d}^2\sigma^{\gamma,\mathrm{pol}}}{\mathrm{d}x\,\mathrm{d}y} = \frac{2\pi\alpha^2}{Q^4}\lambda_N^p f^p s\left[S_1^p(x,y)g_1(x,Q^2) + S_2^p(x,y)g_2(x,Q^2)\right], \tag{2.28}$$

where λ_N^p denotes the degree of nucleon polarisation and we use the following short-hands for the cases of longitudinal $(p = L)$ and transversal $(p = T)$ polarisation of the nucleon

$$f^L = 1 \qquad\qquad f^T = \cos(\beta - \phi)\frac{\mathrm{d}\phi}{2\pi}\sqrt{\frac{4M^2x}{sy}\left[1 - y - \frac{M^2xy}{s}\right]}$$

$$S_1^L = 2xy\left[(2-y) - 2\frac{M^2}{s}xy\right] \qquad S_1^T = 2xy^2$$

$$S_2^L = -8x^2y\frac{M^2}{s} \qquad\qquad S_2^T = 4xy. \tag{2.29}$$

The angle ϕ is the azimuthal angle of the outgoing lepton on which there is a non-trivial dependence in the case of transverse nucleon polarisation. In this case, β is the direction of the nucleon spin in the transverse plane, see Eq. (2.6). For unpolarised charged current scattering, the differential cross section reads

$$\frac{\mathrm{d}^2\sigma^{\nu(\bar\nu)}}{\mathrm{d}x\,\mathrm{d}y} = \frac{G_F^2 s}{4\pi}\frac{M_W^4}{(Q^2 + M_W^2)^2}$$
$$\times\left[\left(1+(1-y)^2\right)F_2^{W^\pm}(x,Q^2) - y^2 F_L^{W^\pm}(x,Q^2) \pm \left(1-(1-y)^2\right)xF_3^{W^\pm}(x,Q^2)\right] \tag{2.30}$$

$$\frac{\mathrm{d}^2\sigma^{\ell(\bar\ell)}}{\mathrm{d}x\,\mathrm{d}y} = \frac{G_F^2 s}{4\pi}\frac{M_W^4}{(Q^2 + M_W^2)^2}$$
$$\times\left[\left(1+(1-y)^2\right)F_2^{W^\mp}(x,Q^2) - y^2 F_L^{W^\mp}(x,Q^2) \pm \left(1-(1-y)^2\right)xF_3^{W^\mp}(x,Q^2)\right]. \tag{2.31}$$

The $\pm$ signs refer to incoming neutrinos (anti-neutrinos) or charged leptons (anti-leptons). For calculational purposes it is advantageous to consider combinations of structure functions which have an even or odd behaviour under crossing. To achieve this, we can consider the sum or difference of the lepton and anti-lepton cross sections, in analogy to Eq. (2.24). We introduce the shorthands

$$F_2^{W^++W^-} = F_2^{W^+} + F_2^{W^-}, \qquad\qquad F_2^{W^+-W^-} = F_2^{W^+} - F_2^{W^-}, \tag{2.32}$$
$$F_L^{W^++W^-} = F_L^{W^+} + F_L^{W^-}, \qquad\qquad F_L^{W^+-W^-} = F_L^{W^+} - F_L^{W^-}, \tag{2.33}$$
$$F_3^{W^++W^-} = F_3^{W^+} - F_3^{W^-}, \qquad\qquad F_3^{W^+-W^-} = F_3^{W^+} + F_3^{W^-}, \tag{2.34}$$

where the combinations of the left column appear in the sum of cross sections and the combinations of the right column appear in the differences. Note the opposite signs for the F_3 combinations.[1]

---

[1] We use the convention that the superscript $W^+ \pm W^-$ refers to the sum and difference of the cross sections. This agrees with [198], while the convention of [153] refers to the sum and difference of the structure functions, which exactly swaps $F_3^{W^++W}$ and $F_3^{W^+-W}$.

2.3. DIS in the parton model

The fact that we cannot evaluate the hadronic tensor directly has led us to parametrise it in terms of structure functions. These depend on two kinematic variables, like ν and Q^2 and describe the behaviour of the cross section beyond what is expected for point-like scattering centres. For smooth, extended objects, the structure functions are expected to fall rapidly, which was confirmed for protons in quasi-elastic scattering experiments at SLAC [12].

Bjorken investigated the hadronic tensor using current algebra, which assumes commutation rules for the currents based on the commutation rules of free fields. From this analysis he predicted [20] that the structure functions become independent of Q^2 in the *Bjorken limit* where we take $Q^2 \to \infty$ and $\nu \to \infty$ while keeping the ratio Q^2/ν fixed. This property became known as *scaling* and suggested using the dimensionless ratio $x = Q^2/2M\nu$ to describe the structure functions in the Bjorken limit. The absence of an absolute length scale in the structure functions hints towards scattering off point-like particles: Increasing the spatial resolution of the probe by increasing the virtuality Q^2 does not lead to a different scattering behaviour for point-like objects, except for trivial kinematic dependence. The scaling behaviour was confirmed approximately in the deep-inelastic region by experiments at SLAC [13–16] for the range of Q^2 accessible at that time.

The parton model, put forward by Feynman [21–23], allowed to explain the observed behaviour. In this model, the proton consists of several point-like particles, called *partons*. The leptons scatter off the proton by exchanging photons with the partons. Since the photon is highly virtual, the time scale of interaction for the photon is assumed to be very short compared to the time scale on which the partons interact with each other. Thus, the photon effectively probes a proton with "frozen" internal interactions, which leads to elastic scattering off one individual parton. The cross section for lepton-proton scattering is then given by an incoherent sum over the individual electron-parton cross sections, weighted by the probability to find a parton with a fraction ξ of the proton's momentum P. The hadronic tensor becomes, [272],

$$W_{\mu\nu} = \frac{1}{4\pi} \sum_q \int_0^1 \mathrm{d}\xi \, f_q(\xi) \frac{2P^0}{2p^0} |\mathcal{M}_q|^2 2\pi \delta(p'^2 - m^2) \,, \tag{2.35}$$

with the squared partonic matrix element

$$|\mathcal{M}_q|^2 = 2e_q^2 \left(p_\mu p'_\nu + p_\nu p'_\mu - g_{\mu\nu} p{\cdot}p' \right) \,, \tag{2.36}$$

where p and p' are the initial and final state momenta of the partons. The initial state momentum of the parton is related to the momentum of the proton by $p = \xi P$. This is based on the assumption that the partons are collinear to the proton, i.e. that transverse momenta can be neglected, and leads to the *collinear parton model*. The sum over q extends over all parton species found in the proton, e_q is the electromagnetic charge of the parton and $f_q(\xi)$ describes the number density of partons of type q with momentum fraction ξ inside the proton. The δ-distribution enforces the on-shell condition of the final state parton where m is its mass. For massless partons the δ-distribution enforces $\xi = x$. Contracting the hadronic tensor in Eq. (2.35) with the leptonic tensor in Eq. (2.18) leads to the cross section

$$\frac{\mathrm{d}^2\sigma}{\mathrm{d}x \, \mathrm{d}y} = \frac{2\pi\alpha^2}{xyQ^2} \sum_q e_q^2 x f_q^2(x) \left[1 + (1-y)^2 \right] \,. \tag{2.37}$$

The index q runs over all active quark and anti-quark species. A comparison with Eq. (2.27)

yields for the structure functions F_2 and F_L

$$F_2(x, Q^2) = \sum_q e_q^2 x f_q^2(x) \tag{2.38}$$

$$F_L(x, Q^2) = 0 \,. \tag{2.39}$$

We see two key predictions of the parton model in this result: The structure functions are independent of Q^2 and the longitudinal structure function vanishes. The latter is known as the Callan-Gross relation [24] and implies $F_2(x, Q^2) = 2x F_1(x, Q^2)$ for spin-$\frac{1}{2}$ quarks and anti-quarks.

2.4. Quantum chromodynamics and the light-cone expansion

By construction Feynman's parton model does not make any statements about the interactions between the partons, except for requiring that the partons are non-interacting at very high energy scales. In Quantum Chromodynamics (QCD) the binding force is mediated by gluons [45, 64, 65] and the partons are identified with quarks and gluons. Over the course of the years since its inception, QCD has been repeatedly and successfully tested and is by now the established theory of strong interactions. Its application to DIS yields a good description of the scattering processes also beyond leading order. The results can be interpreted in the parton picture by extending the parton model to the QCD-improved parton model. Therefore, we review some basic facts about QCD and its application to DIS to the extent necessary for the remaining chapters. A more in-depth treatment can be found in many reviews and textbooks, see e.g. [75, 76, 272, 283, 284].

QCD is a gauge theory, i.e. a theory which is invariant under local symmetry transformations. In the case of QCD the underlying symmetry group is $\mathrm{SU(3)_{colour}}$, which is to say that the colour degrees of freedom of the quarks can be transformed locally without changing the theory if a corresponding change is made to the gluon fields. The gluons then mediate a force between all coloured objects. Since $\mathrm{SU(3)}$ is a non-abelian group, additional terms arise which correspond to interactions of gluons among themselves. This is a characteristic feature of non-abelian gauge theories, also called Yang-Mills theories [48]. The Lagrangian of QCD is given by, see e.g. [76],

$$\mathcal{L} = \sum_q \bar{\psi}_q (i\slashed{\partial} - m_q) \psi_q + g_s \sum_q \bar{\psi}_q \gamma_\mu t^a \psi_q B_a^\mu - \frac{1}{4} G_a^{\mu\nu} G_{a\mu\nu}$$
$$- \frac{1}{2(1-\xi)} (\partial_\mu B_a^\mu)(\partial_\nu B_a^\nu) + (\partial_\mu \bar{\omega}_a) \left[\delta_{ab} \partial^\mu - g_s f_{abc} B_c^\mu \right] \omega_b \,, \tag{2.40}$$

where the gluon field strength tensor $G_a^{\mu\nu}$ is given by

$$G_a^{\mu\nu} = \partial^\mu B_a^\nu - \partial^\nu B_a^\mu + g_s f_{abc} B_b^\mu B_c^\nu \tag{2.41}$$

in terms of the gluon field B_a^μ. The indices a, b, c are in the adjoint representation of the colour algebra and the Dirac spinors ψ_q, representing the quark fields of flavour q with mass m_q, transform as colour triplets in the fundamental representation. The t^a are the generators of the colour algebra which fulfil commutation relations determined by the structure constants f^{abc}

$$[t^a, t^b] = i f^{abc} t^c \,. \tag{2.42}$$

The strong coupling constant is denoted by g_s, but also the following notations will be used

$$\alpha_s = \frac{g_s^2}{4\pi} \,, \qquad\qquad a_s = \frac{\alpha_s}{4\pi} = \frac{g_s^2}{(4\pi)^2} \,. \tag{2.43}$$

The first line of Eq. (2.40) corresponds to the classical Lagrangian, while the quantisation procedure introduced by Faddeev and Popov [49] requires the introduction of ghost fields $\bar{\omega}$ and ω as well as a gauge fixing term. We choose to work in the covariant Lorentz gauges, which depend on a gauge parameter ξ. The gluon propagator is then given by, cf. [76],

$$i\delta_{ab}\left[\frac{-g^{\mu\nu}}{k^2 + i\varepsilon} + \xi\frac{k^\mu k^\nu}{(k^2 + i\varepsilon)^2}\right], \qquad (2.44)$$

which takes a particularly simple form for $\xi = 0$ (Fermi-Feynman gauge). This gauge is economic, especially for higher order calculations, due to the reduced number of terms that each propagator introduces. Therefore, we will work in this gauge for the remainder of this thesis.

After quantisation, QCD requires renormalisation to remove divergences which arise in the ultraviolet (UV) limit. It was shown by 't Hooft and Veltman [50–53] that it is indeed possible to absorb the infinities into suitable redefinitions of fields, masses and coupling constants. Through this procedure the coupling constant acquires a scale dependence, which is described by the renormalisation group equation. A renormalisation group analysis by Politzer, Gross and Wilczek [61, 62], cf. also [63], revealed that the QCD coupling constant vanishes towards infinite momentum scales at lowest order in the coupling constant. This property is called *asymptotic freedom* and gives a justification for the assumption of the parton model that the partons behave essentially like free particles for very high momentum transfer. Nevertheless, the theory becomes strongly interacting at low scales, which precludes a naive application of perturbation theory. One first has to separate the contribution at high scales, which can be treated perturbatively, from those at low scales, which are intrinsically non-perturbative.

For the purposes of deep-inelastic scattering, this task is accomplished by the operator product expansion, proposed by Wilson and others [68–70, 72–74]. It was originally formulated to express products of local operators in the limit of short distances. Products of local operators are usually highly singular in this limit. The operator product expansion allows to express them as a series of regular, local operators and coefficient functions, called *Wilson coefficients*, which carry the singularities. The product of current operators in the hadronic tensor of Eq. (2.21), however, requires a slightly different expansion. It can be shown that the hadronic tensor is dominated by contributions from light-like separations of the currents, $z^2 \approx 0$.

The concept of the operator product expansion at short distances was generalised to light-like distances and is then called *light-cone expansion* [71, 77, 78]. The light-cone expansion can be applied most conveniently to the virtual forward amplitude for Compton scattering, which is related to the hadronic tensor via the optical theorem, see Eq. (2.23). It has the general form [68, 70, 71, 77, 78]

$$\lim_{z^2 \to 0} \mathrm{T}[J(z)J(0)] \sim \sum_{i,N,\tau} \bar{C}_{i,\tau}^N(z^2, \mu_\mathrm{F}^2) z_{\mu_1} \dots z_{\mu_N} O_{i,\tau}^{\mu_1 \dots \mu_N}(0, \mu_\mathrm{F}^2), \qquad (2.45)$$

written here for scalar currents. Here the local operators $O_{i,\tau}^{\mu_1 \dots \mu_N}(z^2, \mu_\mathrm{F}^2)$ are regular in the limit $z^2 \to 0$, while the Wilson coefficients $\bar{C}_{i,\tau}^N(z^2, \mu_\mathrm{F}^2)$ are c-number functions which carry the singularities of the time ordered product in the limit $z^2 \to 0$. The scale μ_F^2 is the factorisation scale at which the operator product expansion is defined: If we include composite operators in a theory, these develop additional UV singularities which are not removed by the renormalisation of the masses, couplings and fields of the theory. Thus, we need to introduce an additional renormalisation of the composite operators in order to render them finite, cf. e.g. [285]. Therefore, the renormalised operators are scale dependent and in order to write down the light-cone expansion, we have to fix a scale μ_F^2 for the renormalised operators at which we define the expansion. In addition, the renormalisation of QCD introduces another scale μ_R^2 at which the renormalisation procedure is defined. If we choose to regularise the UV divergences by continuing the number of

dimensions to $D = 4 + \varepsilon$, as we will do, another scale μ_D^2 arises from the requirement that the coupling constant should remain dimensionless. In general, these are three separate scales which have to be treated independently. However, we will identify these three scales in the following, and write only $\mu^2 = \mu_D^2 = \mu_F^2 = \mu_R^2$.

The sum in Eq. (2.45) extends over all operators which are compatible with the quantum numbers of the operator product on the left-hand side. The index i addresses the different sets of allowed operators, which are distinguished for example by their flavour symmetries and fields involved. Moreover, the operators differ by their spin N, i.e. their transformation properties under the Lorentz group, which ranges up to infinity in the sum. Finally, it is possible to define the twist τ of an operator O as the difference of its canonical mass dimension d_O and its spin, [79],

$$\tau = d_O - N \,. \tag{2.46}$$

It determines the degree of divergence of the coefficients functions, as can be seen from dimensional analysis: Suppose that the two current operators have mass dimension d_J. Since the mass dimension of the operators is d_O and that of the vectors z^{μ_i} is $-N$, the coefficient functions must have mass dimension $d_C = 2d_J + N - d_O$. Thus, the coefficient functions behave like

$$\bar{C}_{i,\tau}^N(z^2, \mu^2) \propto \left(\frac{1}{z^2}\right)^{d_J - \tau/2} \tag{2.47}$$

in the limit $z^2 \to 0$. Strictly speaking, this is only true for free field theory, but due to asymptotic freedom of QCD, the scaling dimensions of the operators receive only logarithmic corrections. This implies that the dominant, i.e. most singular, contributions arise from the operators of lowest twist. Taking only the most singular terms into account is called the leading twist approximation. It can be shown that the results of the leading twist approximation agree with the QCD-improved parton model [272, 283, 284]. If we insert the light-cone expansion into the Compton amplitude, only the local operators act on the nucleon states. These hadronic operator matrix elements contain the non-perturbative information about the low scale behaviour of the product. The coefficient functions on the other hand express the behaviour at high scales. Due to asymptotic freedom of QCD, they can be calculated in perturbation theory.

To discuss the application of the light-cone expansion to DIS, we first need to specify the currents J_μ^i which enter the hadronic tensor. For the electromagnetic and charged weak currents they read, [76],

$$J_\mu^\gamma(z) = \sum_i e_i \bar{\psi}_i(z) \gamma_\gamma \psi_i(z) \,, \tag{2.48}$$

$$J_\mu^{W^+}(z) = \sum_{i=u,c} \sum_{j=d,s} \bar{\psi}_i V_{ij} \gamma_\mu (1 - \gamma_5) \psi_j \,, \tag{2.49}$$

where the e_i denote the charges of the quarks and the V_{ij} are the Cabibbo-Kobayashi-Maskawa (CKM) matrix elements [286, 287]. For the charged current, we give its form for four active flavours u, d, s, c. The light-cone expansion for the time-ordered product of two electromagnetic currents is then [77, 78, 105, 284]

$$
\begin{aligned}
T_{\mu\nu} = \sum_{N,i} &\left\{ \left[Q^2 g_{\mu\mu_1} g_{\nu\mu_2} + g_{\mu\mu_1} q_\nu q_{\mu_2} + q_\mu q_{\mu_1} g_{\nu\mu_2} - g_{\mu\nu} q_{\mu_1} q_{\mu_2} \right] C_{i,2}\left(N, \frac{Q^2}{\mu^2}\right) \right. \\
&+ \left[g_{\mu\nu} + \frac{q_\mu q_\nu}{Q^2} \right] q_{\mu_1} q_{\mu_2} C_{i,L}\left(N, \frac{Q^2}{\mu^2}\right) - i\varepsilon_{\alpha\beta\mu\nu} g_{\alpha\mu_1} q_\beta q_{\mu_2} C_{i,3}\left(N, \frac{Q^2}{\mu^2}\right) \right\} \\
&\times q_{\mu_3} \dots q_{\mu_N} \left(\frac{2}{Q^2}\right)^N O_i^{\mu_1\dots\mu_N} \,.
\end{aligned}
\tag{2.50}
$$

In the unpolarised case, the twist-2 operators are, [282],

$$O^{\text{NS}}_{q,r;\mu_1\ldots\mu_N} = i^{N-1}\,\mathbf{S}\left[\bar{\psi}\gamma_{\mu_1}D_{\mu_2}\ldots D_{\mu_N}\frac{\lambda_r}{2}\psi\right] - \text{trace terms}\,, \tag{2.51}$$

$$O^{\text{S}}_{q;\mu_1\ldots\mu_N} = i^{N-1}\,\mathbf{S}\left[\bar{\psi}\gamma_{\mu_1}D_{\mu_2}\ldots D_{\mu_N}\psi\right] - \text{trace terms}\,, \tag{2.52}$$

$$O^{\text{S}}_{g;\mu_1\ldots\mu_N} = 2i^{N-2}\,\mathbf{S}\,\text{Tr}\left[G^a_{\mu_1\alpha}g^{\alpha\beta}D_{\mu_2}\ldots D_{\mu_{N-1}}G^a_{\beta\mu_N}\right] - \text{trace terms}\,, \tag{2.53}$$

where $\mathbf{S}$ indicates a symmetrisation of the Lorentz indices $\mu_1,\ldots,\mu_N$ and Tr is the trace in the fundamental representation of the colour algebra. The spinors ψ are the quark fields, $G^a_{\mu\nu}$ is the gluon field strength tensor and D_μ denotes the gauge-covariant derivative. The non-singlet operator, marked by the superscript NS, transforms in the adjoint representation of the flavour group SU(N_F) through the group's generator λ_r, while the other two operators are singlets under the flavour group, indicated by the superscript S. The subscripts q and g refer to the quark and gluon operators, respectively. The trace terms ensure that the operators have a definite spin N under Lorentz transformations, which requires the operators to be traceless, symmetric tensors. In the polarised case, additional operators contribute

$$O^{\text{NS},5}_{q,r;\mu_1\ldots\mu_N} = i^{N-1}\,\mathbf{S}\left[\bar{\psi}\gamma_5\gamma_{\mu_1}D_{\mu_2}\ldots D_{\mu_N}\frac{\lambda_r}{2}\psi\right] - \text{trace terms}\,, \tag{2.54}$$

$$O^{\text{S},5}_{q;\mu_1\ldots\mu_N} = i^{N-1}\,\mathbf{S}\left[\bar{\psi}\gamma_5\gamma_{\mu_1}D_{\mu_2}\ldots D_{\mu_N}\psi\right] - \text{trace terms}\,, \tag{2.55}$$

$$O^{\text{S},5}_{g;\mu_1\ldots\mu_N} = 2i^{N-2}\,\mathbf{S}\,\text{Tr}\left[\frac{1}{2}\varepsilon^{\mu_1\alpha\beta\gamma}G^a_{\beta\gamma}D_{\mu_2}\ldots D_{\mu_{N-1}}G^a_{\alpha\mu_N}\right] - \text{trace terms}\,. \tag{2.56}$$

Calculating the hadronic matrix elements of these operators yields

$$\langle P|O^{\mu_1\ldots\mu_N}_i(0,\mu^2)|P\rangle = A_i(N,\mu^2)P^{\mu_1}\ldots P^{\mu_N} + \text{trace terms}\,. \tag{2.57}$$

Upon inserting the above into the light-cone expansion of $T_{\mu\nu}$, we obtain

$$T_{\mu\nu} = 2\sum_{N,i}\frac{1}{x^{N-1}}\left\{\frac{2x}{Q^2}\left[P_\mu P_\nu + \frac{P_\mu q_\nu + P_\nu q_\mu}{2x} - \frac{Q^2}{4x^2}g_{\mu\nu}\right]C_{i,2}\left(N,\frac{Q^2}{\mu^2}\right)\right.$$
$$\left. + \frac{1}{2x}\left[g_{\mu\nu} + \frac{q_\mu q_\nu}{Q^2}\right]C_{i,L}\left(N,\frac{Q^2}{\mu^2}\right) - i\varepsilon_{\mu\nu\alpha\beta}\frac{P^\alpha q^\beta}{2Q^2}C_{i,3}\left(N,\frac{Q^2}{\mu^2}\right)\right\}A_i\left(N,\mu^2\right)\,. \tag{2.58}$$

The sum is only convergent for $x > 1$, which is outside the physical region for DIS, given by $0 \le x \le 1$. We can however, analytically continue the above result to the physical region using dispersion relations. Employing furthermore the optical theorem, we arrive at expressions for the Mellin moments of the structure functions

$$\int_0^1 dx\, x^{N-2}F_L(x,Q^2) = \sum_i A_i(N,\mu^2)C_{i,L}\left(N,\frac{Q^2}{\mu^2}\right)\,, \tag{2.59}$$

$$\int_0^1 dx\, x^{N-2}F_2(x,Q^2) = \sum_i A_i(N,\mu^2)C_{i,2}\left(N,\frac{Q^2}{\mu^2}\right)\,, \tag{2.60}$$

$$\int_0^1 dx\, x^{N-1}F_3(x,Q^2) = \sum_i A_i(N,\mu^2)C_{i,3}\left(N,\frac{Q^2}{\mu^2}\right)\,, \tag{2.61}$$

where we sum over the singlet and non-singlet quark operators as well as the gluon operator. These integrals have the form of a particular integral transformation:

2. Deep-inelastic scattering

In general, we define the Mellin moments of a function $f(x)$ as the integral transformation [288]

$$\mathrm{M}[f](N) = \int_0^1 \mathrm{d}x\, x^{N-1} f(x)\,, \tag{2.62}$$

which is also called the Mellin transformation of f. When we speak of Mellin moments, we usually take N as integer, but of course the definition can be extended to complex N as long as the integral converges. Moreover, we can define the Mellin convolution of two functions $f(x)$ and $g(x)$ as

$$[f \otimes g](x) = \int_0^1 \mathrm{d}z_1 \int_0^1 \mathrm{d}z_2\, \delta(x - z_1 z_2) f(z_1) g(z_2)\,. \tag{2.63}$$

It is diagonalised by the Mellin transformation, i.e. the Mellin transformation of $f \otimes g$ is the product of the Mellin moments of f and g,

$$\mathrm{M}[f \otimes g](N) = \mathrm{M}[f](N)\, \mathrm{M}[g](N)\,. \tag{2.64}$$

There also exists an inverse Mellin transformation which is given by

$$f(x) = \frac{1}{2\pi i} \int_{c-i\infty}^{c+i\infty} \mathrm{d}s\, x^{-s}\, \mathrm{M}[f](s)\,. \tag{2.65}$$

The integration contour is parallel to the imaginary axis and $c \in \mathbb{R}$ is chosen in such a way, that the contour lies to the right of all singularities of $\mathrm{M}[f](s)$. The application of this inversion requires $\mathrm{M}[f](N)$ to be defined for complex N. If the Mellin moments of a function $f(x)$ are known for all integers N, Carlson's theorem [289, 290] guarantees the uniqueness of an analytic continuation within a certain class of functions.[2] It is enough to know either the even or odd moments of the function to construct an analytic continuation from those moments.

The form of Eqs. (2.59) to (2.61) indicates that the structure functions are Mellin convolutions of two functions. This interpretation is compatible with the form of the structure functions in the parton model, cf. Section 2.3. We are led to the QCD-improved parton model, if we identify the hadronic operator matrix elements $A_i(N)$ with the Mellin moments of parton distribution functions and the Wilson coefficients $C_i(N)$ with the Mellin transformations of coefficient functions $C_i(x)$. Since the operator matrix elements depend on a factorisation scale μ^2, also the PDFs in the QCD-improved parton model become scheme- and scale-dependent quantities. As such they loose their direct probabilistic interpretation beyond leading order. They have to be interpreted as scheme dependent quantities, in a similar way as, for example, coupling constants.

The light-cone expansion itself is an operator identity and is valid independently of the states on which the operators act. Therefore, the Wilson coefficients are independent of the states as well and can be obtained by choosing particularly convenient states, such as single quark or gluon states, and calculating both the left- and right-hand sides of the expansion. This calculation can be carried out perturbatively, if we choose very high scales μ^2 at which the coupling constant is small due to asymptotic freedom. Since physical observables cannot depend on the arbitrary factorisation scale μ^2, we can derive renormalisation group equations which allow to translate these results to other scales. After applying the light-cone expansion, the process dependence is carried by the Wilson coefficients, while the dependence on the external states is contained in the operator matrix elements or equivalently in the PDFs. The PDFs are universal in the sense that they are process-independent and once they are known, they can be used for describing the nucleon structure in different scattering processes involving nucleons.

---

[2]See [261] for a precise statement of the theorem and a discussion of the application to the present case.

Starting from PDFs for each quark flavour k, denoted by $f_k(x, \mu^2)$, and corresponding anti-quark distributions $\bar{f}_k(x, \mu^2)$, as well as a gluon PDF $G(x, \mu^2)$, we can define PDF combinations whose moments can be identified with operator matrix elements, based on their flavour symmetries. The gluon PDF can be readily identified with the gluon operator. The singlet quark operator finds its correspondence in the singlet PDF combination

$$\Sigma(x, \mu^2) = \sum_{k=1}^{N_F} \left[f_k(x, \mu^2) + \bar{f}_k(x, \mu^2) \right] , \qquad (2.66)$$

and the non-singlet PDF combination

$$\Delta_k(x, \mu^2) = f_k(x, \mu^2) + f_k(x, \mu^2) - \frac{\Sigma(x, \mu^2)}{N_F} \qquad (2.67)$$

corresponds to the non-singlet operator. Here N_F denotes the number of light flavours.

With these conventions the structure functions $F_2(x, Q^2)$ and $F_L(x, Q^2)$ can be written as

$$F_i(x, Q^2) = x \frac{1}{N_F} \sum_{k=1}^{N_F} e_k^2 \left[C_{q,i}^{\mathrm{S}} \left(x, \frac{Q^2}{\mu^2} \right) \otimes \Sigma(x, \mu^2) + C_{g,i}^{\mathrm{S}} \left(x, \frac{Q^2}{\mu^2} \right) \otimes G(x, \mu^2) \right.$$
$$\left. + N_F C_{q,i}^{\mathrm{NS}} \left(x, \frac{Q^2}{\mu^2} \right) \otimes \Delta_k(x, \mu^2) \right] , \qquad (2.68)$$

where $i \in \{2, L\}$ and the first index of the Wilson coefficients indicates whether the contributing processes are initiated by a quark (q) or a gluon (g). A corresponding expression in N space is obtained by applying the Mellin transformation to both sides, which expresses all quantities by their moments and turns the convolutions into simple products. To simplify the notation we will use the same symbols for the Wilson coefficients, PDFs, etc. in x- and N space and distinguish both representations just by their argument. Since all diagrams which contribute to the non-singlet Wilson coefficient also contribute to the quark singlet coefficient, it is convenient to split up the latter into a non-singlet (NS) and a pure-singlet (PS) contribution via

$$C_{q,i}^{\mathrm{S}} = C_{q,i}^{\mathrm{NS}} + C_{q,i}^{\mathrm{PS}} . \qquad (2.69)$$

Inserting this into Eq. (2.68) yields a very similar expression, in which the non-singlet Wilson coefficient multiplies the PDF combination $f_k(x, \mu^2) + \bar{f}_k(x, \mu^2)$ instead of $\Delta_k(x, \mu^2)$. In the remainder of this thesis, we will frequently make use of this decomposition since it simplifies the organisation of the calculations from a diagrammatic point of view: Diagrams belong either to the non-singlet or pure-singlet part and do not have to be considered more than once. Because of this convention and in accordance with earlier literature [201, 202], we will sometimes refer to the combination $f_k(x, \mu^2) + \bar{f}_k(x, \mu^2)$ as a non-singlet PDF combination, even if it is not a non-singlet quantity in the sense of the evolution equations, to be discussed below.

Since the calculation of the Wilson coefficients involves massless particles, infrared divergences appear in limits where massless particles become collinear or soft. The soft singularities cancel between real and virtual corrections due to the inclusiveness of the structure functions. Furthermore, the Kinoshita-Lee-Nauenberg theorem [291, 292] asserts that collinear singularities of the final state cancel, but since the twist-2 approximation implies that we only take a single parton as initial states into account, the collinear singularities of the initial state remain. They factorise and can be absorbed into a redefinition of the PDFs. To this end, we introduce transition functions Γ_{ij} which contain precisely the collinear singularities of the Wilson coefficients. The singularities of the *bare* Wilson coefficients $C_{a,i}^b$ are cancelled by the transition functions so that

the renormalised Wilson coefficient $C_{a,i} = \sum_j C_{a,j}^b \Gamma_{ji}$ are finite. Analogously, the bare PDFs f_k^b are renormalised by the inverse transition functions. For only massless partons, the factorisation can be written in N space schematically as

$$F_a(N, Q^2) = \sum_{i,j,k} C_{a,i}^b \left(N, \frac{Q^2}{\mu^2} \right) \Gamma_{ij} \Gamma_{jk}^{-1} f_k^b(N, \mu^2) \tag{2.70}$$

$$= \sum_k C_{a,k} \left(N, \frac{Q^2}{\mu^2} \right) f_k(N, \mu^2) . \tag{2.71}$$

For QCD with massless quarks, the transition functions are given by the inverse of the operator renormalisation constants $\Gamma_{ij} = Z_{ij}^{-1}$ and the collinear singularities of the coefficient functions correspond to the UV divergences of the operators. A similar factorisation will play an important role for the case of N_F massless and a single massive quark in the asymptotic region where $Q^2 \gg m^2$, which we will discuss in the next section.

The dependence of the Wilson coefficients and PDFs on the factorisation scale μ^2 is a remnant of the fact that we have to choose a scale for the renormalised operators in terms of which we define the light-cone expansion. Taking all orders of perturbation theory into account, the dependence on this scale has to cancel in physical observables like the structure functions. Together with the renormalisation group equations for the operators this allows to derive renormalisation group equations for the structure functions and Wilson coefficients.

The twist-2 operators are renormalised by introducing renormalisation constants Z

$$O_{q,r;\mu_1...\mu_N}^{NS} = Z^{NS}(\mu^2) O_{q,r;\mu_1...\mu_N}^{NS,R}(\mu^2) , \tag{2.72}$$

$$O_{i;\mu_1...\mu_N}^{S} = Z_{ij}^{S}(\mu^2) O_{j;\mu_1...\mu_N}^{S,R}(\mu^2) , \quad i \in \{q, g\} , \tag{2.73}$$

where a sum over $j \in \{q, g\}$ is implied in the second line and the superscript R marks the renormalised operators. The non-singlet operators do not mix under renormalisation so that their renormalisation constants are scalar. In fact, they are also independent of the adjoint flavour index r, see e.g. [76, 131]. However, the singlet quark and gluon operators do mix under renormalisation since they carry the same quantum numbers. Thus, their renormalisation constants take the form of a 2×2 matrix. The corresponding anomalous dimensions are defined as

$$\gamma_{qq}^{NS} = Z^{-1,NS}(\mu^2) \mu \frac{\partial}{\partial \mu} Z^{NS}(\mu^2) , \tag{2.74}$$

$$\gamma_{ij}^{S} = Z_{ik}^{-1,S}(\mu^2) \mu \frac{\partial}{\partial \mu} Z_{ij}^{S}(\mu^2) . \tag{2.75}$$

Starting from the scale independence of the bare operators, we can derive evolution equations for the renormalised operators and in turn also for the moments of the PDFs. For the non-singlet combination they read

$$\frac{d}{d \ln(\mu^2)} \Delta_k(N, \mu^2) = -\frac{1}{2} \gamma_{qq}^{NS} \Delta_k(N, \mu^2) , \tag{2.76}$$

while for the singlet and gluon PDF they are

$$\frac{d}{d \ln(\mu^2)} \begin{pmatrix} \Sigma(N, \mu^2) \\ G(N, \mu^2) \end{pmatrix} = -\frac{1}{2} \begin{pmatrix} \gamma_{qq} & \gamma_{qg} \\ \gamma_{gq} & \gamma_{gg} \end{pmatrix} \begin{pmatrix} \Sigma(N, \mu^2) \\ G(N, \mu^2) \end{pmatrix} . \tag{2.77}$$

At the level of twist-2 operators, the anomalous dimensions are related to the Mellin transformations of the splitting functions $P_{ij}(z)$, which describe the collinear emission of a parton of type i with momentum fraction z from a parton of type j. The relation is given by [71, 80, 81, 90–93]

$$\gamma_{ij}(N) = -M[P_{ij}](N) . \tag{2.78}$$

The renormalisation group equations of the moments of the PDFs correspond to the DGLAP evolution equations in x space [96–98].

To shorten the notation, we define the total derivative with respect to the scale μ^2 as [86, 87]

$$\mathcal{D}(\mu^2) = \mu^2 \frac{\partial}{\partial \mu^2} + \beta(a_s(\mu^2)) \frac{\partial}{\partial a_s(\mu^2)} - \gamma_m(a_s(\mu^2)) m(\mu^2) \frac{\partial}{\partial m(\mu^2)} \,, \tag{2.79}$$

where we made use of the β-function of the strong coupling constant and the mass anomalous dimension, which are given by

$$\beta(a_s(\mu^2)) = \mu^2 \frac{\partial a_s(\mu^2)}{\partial \mu^2} \,, \tag{2.80}$$

$$\gamma_m(a_s(\mu^2)) = -\frac{\mu^2}{m(\mu^2)} \frac{\partial m(\mu^2)}{\partial \mu^2} \,. \tag{2.81}$$

The independence of the structure functions from the factorisation scale then yields a renormalisation group equation for it,

$$\mathcal{D}(\mu^2) F_i(x, Q^2) = 0 \,. \tag{2.82}$$

Upon combining this with the factorised form of $F_i(x, Q^2)$ in Eq. (2.68) and the evolution equations of the PDFs, Eqs. (2.76) and (2.77), we obtain evolution equations for the Wilson coefficients

$$\frac{\mathrm{d}}{\mathrm{d}\ln(\mu^2)} C_{q,i}^{\mathrm{NS}}(N, Q^2/\mu^2) = \frac{1}{2} \gamma_{qq}^{\mathrm{NS}} C_{q,i}^{\mathrm{NS}}(N, Q^2/\mu^2) \,, \tag{2.83}$$

$$\frac{\mathrm{d}}{\mathrm{d}\ln(\mu^2)} \begin{pmatrix} C_{q,i}^{\mathrm{S}}(N, Q^2/\mu^2) \\ C_{g,i}^{\mathrm{S}}(N, Q^2/\mu^2) \end{pmatrix} = \frac{1}{2} \begin{pmatrix} \gamma_{qq} & \gamma_{gq} \\ \gamma_{qg} & \gamma_{gg} \end{pmatrix} \begin{pmatrix} C_{q,i}^{\mathrm{S}}(N, Q^2/\mu^2) \\ C_{g,i}^{\mathrm{S}}(N, Q^2/\mu^2) \end{pmatrix} \,. \tag{2.84}$$

Note that the anomalous dimension matrix in Eq. (2.84) is transposed compared to Eq. (2.77) and that the sign on the right hand side of the evolution equations for the Wilson coefficients is opposite to the sign in the corresponding equations for the PDFs.

The perturbative expansions of the anomalous dimensions γ_{ij} are known at leading order since the early days of QCD [67, 80, 81, 96]. Also their NLO [104, 107–118] and NNLO [130–136] terms are known. The corresponding Wilson coefficients for unpolarised scattering by photon-exchange with only massless quarks were obtained at 1-loop [104, 105], 2-loop [118–128] and 3-loop order [137, 138]. Similar discussions as above can of course be given for polarised scattering, where the anomalous dimensions of the operators in Eqs. (2.54) to (2.56) were calculated in [96, 155, 156] to LO and to NLO in [157–159]. Finally, also the NNLO results are available in the literature [160, 161].

If we calculate the Wilson coefficients for a fixed factorisation scale μ^2, the expressions will depend on the scale ratio Q^2/μ^2 through powers of logarithms of the form $\ln^l(Q^2/\mu^2)$, where $l \in \mathbb{N}$. Adopting the notation of [293], we can write the expansion of the Wilson coefficients in a_s as

$$C_{i,a} = \sum_{k=0}^{\infty} a_s^k C_{i,a}^{(k)} = c_{i,a}^{(0)} + \sum_{k=1}^{\infty} a_s^k \left(c_{i,a}^{(k)} + \sum_{l=1}^{k} c_{i,a}^{(k,l)} \ln^l \left(\frac{Q^2}{\mu^2} \right) \right) \,, \tag{2.85}$$

where the subscripts i and a indicates the initial parton and the structure function respectively. At each order of the perturbative expansion, the logarithmic coefficients $c_{i,a}^{(k,l)}$ are completely determined by the renormalisation group equations. The anomalous dimensions, β-function and lower order constant terms $c_{i,a}^{(k)}$ suffice to express them. By also expanding the anomalous dimensions and β-function

$$\beta = \sum_{k=0}^{\infty} a_s^{k+2} \beta_k \,, \qquad\qquad \gamma_{ij} = \sum_{k=0}^{\infty} a_s^{k+1} \gamma_{ij}^{(k)} \,, \tag{2.86}$$

inserting all this into the renormalisation group equations of the Wilson coefficients, Eqs. (2.83) and (2.84), and comparing coefficients in a_s and $\ln(Q^2/\mu^2)$, we can derive expressions for $c_{i,a}^{(k,l)}$. Explicit expressions up to $\mathcal{O}\!\left(a_s^3\right)$ can be found in [293]. We will make use of this in the upcoming chapters, as presentations of results in the literature often omit these terms altogether through the scale choice $\mu^2 = Q^2$, precisely because they can be reconstructed using the renormalisation group equations.

2.5. Heavy flavour contributions

So far, we have mainly discussed contributions to deep-inelastic scattering in a theory with only massless quarks. This is certainly justified for the u, d and s quarks. Their current masses [37]

$$m_u \approx 2\,\mathrm{MeV}\,, \qquad m_d \approx 5\,\mathrm{MeV}\,, \qquad m_s \approx 100\,\mathrm{MeV}\,, \qquad (2.87)$$

are below the QCD scale $\Lambda_{\mathrm{QCD}} \propto 200 - 300\,\mathrm{MeV}$ and are therefore produced non-perturbatively. We can assign generic PDFs to these quarks which describe their non-perturbative features and treat them as massless in perturbative calculations. The other three quarks of the Standard Model, the c, b and t quarks, on the other hand, have pole masses of [37]

$$m_c = (1.67 \pm 0.07)\,\mathrm{GeV}\,, \qquad m_b = (4.78 \pm 0.06)\,\mathrm{GeV}\,, \qquad m_t = (174.6 \pm 1.9)\,\mathrm{GeV}\,, \qquad (2.88)$$

respectively, which are much larger than the QCD scale. Therefore, these quarks are produced radiatively and assigning a generic PDF to them is not justified.

In all DIS experiments carried out so far, the energy was never large enough for top quark pair production. Though kinematically possible at HERA, single top quark production [294–297] was not observed there [298, 299], cf. also [300].

Charm and bottom quarks, however, contribute both as final state particles and in virtual corrections. Due to confinement, the real production of charm and bottom quarks must yield hadrons with charm or bottom content. For the charm quark, these are in particular D mesons, where a charm (or anti-charm) quark is combined with a light quark, and the $c\bar{c}$ resonances, of which the J/Ψ meson is the lightest. Especially at low values of x the contributions from heavy quarks to the structure functions can be substantial. A precise knowledge of the heavy flavour corrections is therefore important for precision analyses of the DIS world data. This concerns the determination of the QCD scale Λ_{QCD}, the heavy quark masses and the PDFs.

The calculations discussed in this thesis are applicable to the inclusive structure functions. Their heavy quark contributions are defined as the structure functions for both massless and massive quarks minus the contributions from just the massless quarks. We will first discuss the case of a *fixed flavour number scheme* (FFNS) with N_F massless quarks, which are assumed to be constituents of the nucleon and described by a generic PDF, and a single massive quark, which is produced only through perturbative processes. In the next section we will also consider a *variable flavour number scheme* (VFNS), where the number of light flavours is adapted depending on the scale of the process considered. A plausible choice at HERA is to treat the up, down and strange quarks as light ($N_F = 3$) and the charm quark as the heavy quark. The bottom quark is heavier than the charm quark by about a factor three. Up to $\mathcal{O}\!\left(a_s^2\right)$, the bottom quark can be included into the FFNS with $N_F = 3$ by just adding the heavy flavour contributions with the charm quark mass replaced by that of the bottom quark. Starting at $\mathcal{O}\!\left(a_s^3\right)$, however, diagrams with two separate heavy quark lines arise. Such diagrams depend on the ratio of the masses m_c^2/m_b^2. We confine our discussion to the case of a single heavy quark flavour and refer to [301, 302] for the case of two distinct masses.

In a FFNS with N_F light quark flavours, we can split the inclusive structure functions into contributions from light quarks and gluons and contributions involving heavy quarks. In case of $F_2(x, Q^2)$ we have

$$F_2(x, Q^2) = F_2^{\mathrm{l}}(x, Q^2) + F_2^{\mathrm{h}}(x, Q^2), \tag{2.89}$$

where the light part $F_i^{\mathrm{l}}(x, Q^2)$ is essentially given by Eq. (2.68) and the heavy part reads

$$
\begin{aligned}
F_2^{\mathrm{h}}&(x, N_F + 1, Q^2, m^2) = \\
&x\Bigg\{ \sum_{k=1}^{N_F} e_k^2 \Bigg[L_{q,2}^{\mathrm{NS}}\left(x, N_F+1, \frac{Q^2}{\mu^2}, \frac{m^2}{\mu^2}\right) \otimes \Big[f_k(x, \mu^2, N_F) + \bar{f}_k(x, \mu^2, N_F) \Big] \\
&+ \frac{1}{N_F} L_{q,2}^{\mathrm{PS}}\left(x, N_F+1, \frac{Q^2}{\mu^2}, \frac{m^2}{\mu^2}\right) \otimes \Sigma(x, \mu^2, N_F) \\
&+ \frac{1}{N_F} L_{g,2}^{\mathrm{S}}\left(x, N_F+1, \frac{Q^2}{\mu^2}, \frac{m^2}{\mu^2}\right) \otimes G(x, \mu^2, N_F) \Bigg] \\
&+ e_Q^2 \Bigg[H_{q,2}^{\mathrm{PS}}\left(x, N_F+1, \frac{Q^2}{\mu^2}, \frac{m^2}{\mu^2}\right) \otimes \Sigma(x, \mu^2, N_F) \\
&+ H_{g,2}^{\mathrm{S}}\left(x, N_F+1, \frac{Q^2}{\mu^2}, \frac{m^2}{\mu^2}\right) \otimes G(x, \mu^2, N_F) \Bigg] \Bigg\}.
\end{aligned}
\tag{2.90}
$$

The argument $N_F + 1$ of the heavy flavour Wilson coefficients has to be read symbolically in that it refers to N_F massless and a single massive flavour. We distinguish the Wilson coefficients in which the photon couples to the light quark, denoted by L, from those where it couples to the heavy quark, denoted by H. The former are multiplied by the charges e_k of the light quarks while the latter are multiplied by the heavy quark charge e_Q. Analogous to the massless case, cf. Eq. (2.69), we have split up the quarkonic singlet coefficient into a non-singlet (NS) and a pure-singlet (PS) part. This split gives rise to the PDF combination $f_k(x, \mu^2) + \bar{f}_k(x, \mu^2)$ as discussed before. For unpolarised photon-mediated scattering, there is no $H_{q,2}^{\mathrm{NS}}$ since it would require a heavy quark in the initial state, which contradicts our assumptions in the FFNS.

The lowest order contributions from heavy flavours arise from the virtual-photon-gluon fusion process $\gamma^* g \to Q\bar{Q}$, which is of order $\mathcal{O}(a_s)$ and contributes to the Wilson coefficient $H_{g,2}^{\mathrm{S}}$. The leading-order process was calculated using various methods in [181–185]. At $\mathcal{O}(a_s^2)$, besides corrections to $H_{g,2}^{\mathrm{S}}$, there are also non-vanishing contributions to the non-singlet and pure-singlet Wilson coefficients $L_{q,2}^{\mathrm{NS}}$ and $H_{q,2}^{\mathrm{PS}}$. In the relevant diagrams for the non-singlet coefficient $L_{q,2}^{\mathrm{NS}}$ the photon couples to a massless quark line which is connected to a massless quark in the initial state. The heavy quark appears either through pair production or virtual corrections. Diagrams for $H_{q,2}^{\mathrm{PS}}$ are initiated by massless quarks as well, but the photon couples directly to a heavy quark line. The NLO expressions were given in [186–188] as semi-numerical computer programs due to the complexity of the phase space integrals for certain subprocesses.[3] In the inclusive description $L_{g,2}^{\mathrm{S}}$ already starts at $\mathcal{O}(a_s^2)$ due to self-energy corrections from heavy quarks, but the first non-trivial contributions enter one order higher. The Wilson coefficient $L_{q,2}^{\mathrm{PS}}$ contributes from $\mathcal{O}(a_s^3)$ onwards since three separate fermion lines have to be present in diagrams contributing here: The external quark is massless, the photon couples to a separate massless quark line and at the same time a massive quark has to be present.

Even though the NLO results could only be obtained in semi-numerical form for general kinematic configurations, it has been shown in [202] that analytic expressions can be obtained

---

[3] An implementation in Mellin space was given in [200].

in the asymptotic limit $Q^2 \gg m^2$. In this limit the inclusive Wilson coefficients factorise into the massless Wilson coefficients $C_{i,a}$ and massive operator matrix elements (OMEs) A_{ij}. The factorisation holds up to power corrections which are suppressed by powers of m^2/Q^2. As long as such power corrections can be neglected, the asymptotic form of the Wilson coefficients describes the heavy flavour contributions to the structure functions. However, it is important to stress that the factorisation holds only for the inclusive structure functions where heavy quarks enter both as real particles in the final state and as virtual corrections to the production of massless partons. By comparing the asymptotic expressions to the exact results at NLO, it was shown in [201] that the asymptotic representation of the structure function $F_2(x, Q^2)$ holds for $Q^2/m^2 \gtrsim 10$. The factorisation of the longitudinal structure function $F_L(x, Q^2)$ starts to be valid only at much higher scales $Q^2/m^2 \gtrsim 800$.

The heart of the factorisation is the observation that for large momentum transfer Q^2 the massive quark behaves essentially like a massless particle. The terms which are not power suppressed in the limit $Q^2 \gg m^2$ are those terms which form the mass singularities in the limit $m^2 \to 0$. Similar to the case of light quarks discussed before, the soft singularities as well as final state collinear singularities cancel due to the inclusiveness of the structure functions. However, the collinear singularities of the initial state remain but factorise. By absorbing the additional singularities from the heavy quark into the PDFs as well, we would arrive at a scheme for $N_F + 1$ massless quarks where we assign a PDF to the heavy quark in the massless limit. This is called a zero-mass variable flavour number scheme and will be discussed in greater detail in the next section. Instead of absorbing the collinear singularities into the PDFs, we can also use the transition functions to reconstruct the asymptotic behaviour of the heavy flavour Wilson coefficients [201, 202]. The transition functions of this factorisation are given by the massive operator matrix elements A_{Qj} and $A_{ij,Q}$ which will be discussed below. The factorisation relation for the non-singlet Wilson coefficients reads in N space, [202, 203],

$$C_{q,a}^{\mathrm{NS}}\left(N, N_F, \frac{Q^2}{\mu^2}\right) + L_{q,a}^{\mathrm{NS}}\left(N, N_F + 1, \frac{Q^2}{\mu^2}, \frac{m^2}{\mu^2}\right) =$$
$$A_{qq,Q}^{\mathrm{NS}}\left(N, N_F + 1, \frac{m^2}{\mu^2}\right) C_{q,a}^{\mathrm{NS}}\left(N, N_F + 1, \frac{Q^2}{\mu^2}\right), \tag{2.91}$$

where we neglect power suppressed terms. For the singlet part the factorisation relations become more complex due to operator mixing. Suppressing the dependence on N and the scale ratios Q^2/μ^2 and m^2/μ^2 for brevity, one finds

$$
\begin{aligned}
C_{q,a}^{\mathrm{PS}}(N_F) + L_{q,a}^{\mathrm{PS}}(N_F + 1) &= \left[A_{qq,Q}^{\mathrm{NS}}(N_F + 1) + A_{qq,Q}^{\mathrm{PS}}(N_F + 1) + A_{Qq}^{\mathrm{PS}}(N_F + 1)\right] \\
&\quad \times N_F \tilde{C}_{q,a}^{\mathrm{PS}}(N_F + 1) + A_{qq,Q}^{\mathrm{PS}}(N_F + 1) C_{q,a}^{\mathrm{NS}}(N_F + 1) \\
&\quad + A_{gq,Q}(N_F + 1) N_F \tilde{C}_{g,a}^{\mathrm{S}}(N_F + 1), \tag{2.92} \\
C_{g,a}^{\mathrm{S}}(N_F) + L_{g,a}^{\mathrm{S}}(N_F + 1) &= A_{gg,Q}(N_F + 1) N_F \tilde{C}_{g,a}^{\mathrm{S}}(N_F + 1) \\
&\quad + A_{qg,Q}(N_F + 1) C_{q,a}^{\mathrm{NS},S}(N_F + 1) \\
&\quad + \left[A_{qg,Q}(N_F + 1) + A_{Qg}(N_F + 1)\right] N_F \tilde{C}_{q,a}^{\mathrm{PS}}(N_F + 1). \tag{2.93}
\end{aligned}
$$

Similarly, the factorisation relations for the $H_{i,a}$ read

$$
\begin{aligned}
H_{q,a}^{\mathrm{PS}}(N_F + 1) &= A_{Qq}^{\mathrm{PS}}(N_F + 1) \left[C_{q,a}^{\mathrm{NS}}(N_F + 1) + \tilde{C}_{q,a}^{\mathrm{PS}}(N_F + 1)\right] \\
&\quad + \left[A_{qq,Q}^{\mathrm{NS}}(N_F + 1) + A_{qq,Q}^{\mathrm{PS}}(N_F + 1)\right] \tilde{C}_{q,a}^{\mathrm{PS}}(N_F + 1) \\
&\quad + A_{gq,Q}(N_F + 1) \tilde{C}_{g,a}^{\mathrm{S}}(N_F + 1), \tag{2.94}
\end{aligned}
$$

$$H_{g,a}^{\mathrm{S}}(N_F + 1) = A_{gg,Q}(N_F + 1)\tilde{C}_{g,a}^{\mathrm{S}}(N_F + 1) + A_{qg,Q}(N_F + 1)\tilde{C}_{q,a}^{\mathrm{PS}}(N_F + 1)$$
$$+ A_{Qg}(N_F + 1)\left[C_{q,a}^{\mathrm{NS}}(N_F + 1) + \tilde{C}_{q,a}^{\mathrm{PS}}(N_F + 1)\right]. \tag{2.95}$$

The argument $N_F + 1$ of the massive OMEs and heavy flavour Wilson coefficients refers to N_F massless and one massive flavour, while the arguments of the massless Wilson coefficients always refer to the number of massless flavours only. In order to shorten the expressions, we make use of the following shorthands

$$\tilde{f}(N_F) = \frac{f(N_F)}{N_F}, \qquad\qquad \tilde{f}(N_F + 1) = \frac{f(N_F + 1)}{N_F + 1}, \tag{2.96}$$

and for later use, we also define

$$\hat{f}(N_F) = f(N_F + 1) - f(N_F), \qquad\qquad \hat{\tilde{f}}(N_F) = \frac{f(N_F + 1)}{N_F + 1} - \frac{f(N_F)}{N_F}. \tag{2.97}$$

The massive operator matrix elements appearing above are given by the local twist-2 light-cone operators between massless, on-shell gluon or quark states, calculated in the theory with N_F massless and a single massive quark and have the structure,

$$A_{ij}\left(N, N_F + 1, \frac{m^2}{\mu^2}\right)(p^{\mu_1} \ldots p^{\mu_N} + \text{trace terms}) = \langle j|O_i^{\mu_1 \cdots \mu_N}|j\rangle, \tag{2.98}$$

where the external state j can be either a gluon (g) or a quark (q) and the index i distinguishes the operators. The loop corrections from purely massless diagrams vanish in dimensional regularisation for $p^2 = 0$ since these are scaleless integrals. Only the tree-level contributions from the massless partons as well as higher order corrections involving massive quarks remain. After the factorisation, all mass dependence is carried by the massive OMEs, except for power suppressed terms.

In order to calculate the massive operator matrix elements A_{ij}, we make use of the fact that they are closely related to connected two-point Green's functions with operator insertions. The external gluon or massless quark states are on-shell $(p^2 = 0)$ and no momentum leaves or enters through the operator. Since the Lorentz structure factorises from the A_{ij}, cf. Eq. (2.98) and [283], we contract the operators with the source term

$$J_{\mu_1 \ldots \mu_N} = \Delta_{\mu_1} \ldots \Delta_{\mu_N}, \tag{2.99}$$

where Δ is an arbitrary light-like vector $(\Delta^2 = 0)$, so that all trace terms vanish. In addition, we extract the spinors $u(p, s)$ and polarisation vectors $\epsilon^\mu(p)$ of the external quarks or gluons, thereby exposing the colour, Dirac and Lorentz tensor structure. We write

$$\bar{u}_k(p, s)\hat{G}_q^{\mathrm{NS},kl}\lambda_r u_l(p, s) = J_{\mu_1 \ldots \mu_N} \langle q, k|O_{q,r}^{\mathrm{NS},\mu_1 \cdots \mu_N}|q, l\rangle_Q, \tag{2.100}$$

$$\bar{u}_k(p, s)\hat{G}_i^{kl} u_l(p, s) = J_{\mu_1 \ldots \mu_N} \langle q, k|O_i^{\mu_1 \cdots \mu_N}|q, l\rangle_Q, \qquad i \in \{q, g, Q\}, \tag{2.101}$$

$$\epsilon^\mu(p)\hat{G}_{i,\mu\nu}^{ab}\epsilon^\nu(p) = J_{\mu_1 \ldots \mu_N} \langle g, \mu, a|O_i^{\mu_1 \cdots \mu_N}|g, \nu, b\rangle_Q, \qquad i \in \{q, g, Q\}, \tag{2.102}$$

where k, l and a, b are indices in the fundamental and adjoint representation of the colour group, respectively. The subscript Q denotes the presence of a heavy quark. Note, that even though the external fields are extracted from $\hat{G}_i$, self-energy contributions on external legs are still included. The hat indicates that the relations are written at the unrenormalised level. Beyond leading order, contributions to the singlet matrix elements with external gluon or quark states arise from all three types of singlet operators – purely gluonic operators $(i = g)$, operators involving light quarks $(i = q)$ and the heavy quark operators $(i = Q)$.

To extract the massive OMEs from the Green's functions, we can define projectors which project out the relevant colour, Dirac and Lorentz structures. For external quarks, we use the projector, [201, 203],

$$
P_{q,kl}\hat{G}_q^{kl} = \frac{\delta_{kl}}{N_c}(\Delta.p)^{-N}\frac{1}{4}\operatorname{Tr}\left[\slashed{p}\hat{G}_q^{kl}\right] , \tag{2.103}
$$

where N_c is the number of colours, which is of course $N_c = 3$ for QCD. Two different projectors can be used for external gluons,

$$
P_{g,ab}^{(1),\mu\nu}\hat{G}_{i,\mu\nu}^{ab} = \frac{\delta_{ab}}{N_c^2 - 1}\frac{-g^{\mu\nu}}{D-2}(\Delta.p)^{-N}\hat{G}_{i,\mu\nu}^{ab} , \tag{2.104}
$$

$$
P_{g,ab}^{(2),\mu\nu}\hat{G}_{i,\mu\nu}^{ab} = \frac{\delta_{ab}}{N_c^2 - 1}\frac{1}{D-2}(\Delta.p)^{-N}\left(-g^{\mu\nu} + \frac{p^\mu\Delta^\nu + p^\nu\Delta^\mu}{\Delta.p}\right)\hat{G}_{i,\mu\nu}^{ab} . \tag{2.105}
$$

The second variant of the gluonic projector eliminates unphysical polarisations of the external gluons at the cost of more complicated integrals. The first projector, on the other hand, includes these unphysical gluon polarisations in the sums over μ and ν, which have to be removed by including additional diagrams with external ghost fields. Since the computational complexity is lower for the latter approach, we use $P_{g,ab}^{(1),\mu\nu}$. In [203] the physical projector has been used for a few low moments as a cross-check on the calculation.

The massive OMEs are then calculated using the projectors in Eqs. (2.103) and (2.104) and the Feynman rules for QCD and the operator insertions, which are collected for convenience in Appendix B. Denoting the completely unrenormalised OMEs with a double hat, we have

$$
\hat{\hat{A}}_{gq,Q}\left(N, \frac{\hat{m}^2}{\mu^2}, \varepsilon\right) = P_{q,kl}\hat{G}_g^{kl} , \qquad \hat{\hat{A}}_{qg,Q}\left(N, \frac{\hat{m}^2}{\mu^2}, \varepsilon\right) = P_{g,ab}^{(1),\mu\nu}\hat{G}_{q,\mu\nu}^{ab} , \tag{2.106}
$$

$$
\hat{\hat{A}}_{qq,Q}^{\mathrm{S}}\left(N, \frac{\hat{m}^2}{\mu^2}, \varepsilon\right) = P_{q,kl}\hat{G}_q^{kl} , \qquad \hat{\hat{A}}_{Qg}\left(N, \frac{\hat{m}^2}{\mu^2}, \varepsilon\right) = P_{g,ab}^{(1),\mu\nu}\hat{G}_{Q,\mu\nu}^{ab} , \tag{2.107}
$$

$$
\hat{\hat{A}}_{qq,Q}^{\mathrm{NS}}\left(N, \frac{\hat{m}^2}{\mu^2}, \varepsilon\right) = P_{q,kl}\hat{G}_q^{\mathrm{NS},kl} , \qquad \hat{\hat{A}}_{gg,Q}\left(N, \frac{\hat{m}^2}{\mu^2}, \varepsilon\right) = P_{g,ab}^{(1),\mu\nu}\hat{G}_{g,\mu\nu}^{ab} , \tag{2.108}
$$

$$
\hat{\hat{A}}_{Qq}^{\mathrm{PS}}\left(N, \frac{\hat{m}^2}{\mu^2}, \varepsilon\right) = P_{q,kl}\hat{G}_Q^{kl} , \tag{2.109}
$$

and in analogy to Eq. (2.69) we define a pure-singlet OME by

$$
A_{qq,Q}^{\mathrm{PS}} = A_{qq,Q}^{\mathrm{S}} - A_{qq,Q}^{\mathrm{NS}} . \tag{2.110}
$$

2.6. Variable flavour number scheme

The factorisation of the heavy flavour Wilson coefficients described in the previous section is based on the mass factorisation of the heavy quark for $Q^2 \to \infty$. In this limit, the heavy quark becomes effectively light and in the FFNS the logarithm of the scale ratio $\ln(Q^2/m^2)$ becomes large. For large but not too large values of Q^2, we can use the asymptotic form of the heavy flavour Wilson coefficients to describe the structure functions. Here the heavy quark is treated purely perturbatively and appears only through radiative corrections. At even larger virtualities Q^2, the logarithms will eventually become so large that they have to be resummed. For this purpose, we can switch to a scheme in which the heavy quark is treated as an additional massless quark and assign a PDF to it. In this $(N_F + 1)$-flavour scheme, the *heavy* quark is treated as completely massless and the scale evolution of its PDF is governed by the renormalisation group equations of the theory with $N_F + 1$ massless quarks. The connection between the two schemes

is established by matching them at a certain scale μ^2, where both descriptions are valid. We call a $(N_F + 1)$-flavour scheme obtained in this way a *zero mass variable flavour number scheme* (ZMVFNS).

Several definitions of variable flavour number schemes exist in the literature [202, 303–305]. We will follow [202] for this discussion. The definition of [202] was extended to NNLO in [203]. In the ZMVFNS the massless $(N_F + 1)$-flavour structure functions are matched to the asymptotic form of the FFNS structure functions, retaining only terms which are not power-suppressed by powers of m^2/Q^2. Based on the factorisation relations Eqs. (2.91) to (2.95) the matching relations for the PDFs become, [202, 203],

$$
\begin{aligned}
f_k(N_F + 1, N, \mu^2, m^2) + \bar{f}_k(N_F + 1, N, \mu^2, m^2) = \\
A_{qq,Q}^{\mathrm{NS}}\left(N, N_F + 1, \frac{\mu^2}{m^2}\right)\left[f_k(N_F, N, \mu^2) + \bar{f}_k(N_F, N, \mu^2)\right] \\
+ \frac{1}{N_F} A_{qq,Q}^{\mathrm{PS}}\left(N, N_F + 1, \frac{\mu^2}{m^2}\right)\Sigma(N_F, N, \mu^2) \\
+ \frac{1}{N_F} A_{qg,Q}\left(N, N_F + 1, \frac{\mu^2}{m^2}\right)G(N_F, N, \mu^2),
\end{aligned}
\tag{2.111}
$$

$$
\begin{aligned}
f_Q(N_F + 1, N, \mu^2, m^2) + \bar{f}_Q(N_F + 1, N, \mu^2, m^2) = \\
A_{Qq}^{\mathrm{PS}}\left(N, N_F + 1, \frac{\mu^2}{m^2}\right)\Sigma(N_F, N, \mu^2) \\
+ A_{Qg}\left(N, N_F + 1, \frac{\mu^2}{m^2}\right)G(N_F, N, \mu^2),
\end{aligned}
\tag{2.112}
$$

$$
\begin{aligned}
G(N_F + 1, N, \mu^2, m^2) = \\
A_{gq,Q}\left(N, N_F + 1, \frac{\mu^2}{m^2}\right)\Sigma(N_F, N, \mu^2) \\
+ A_{gg,Q}\left(N, N_F + 1, \frac{\mu^2}{m^2}\right)G(N_F, N, \mu^2).
\end{aligned}
\tag{2.113}
$$

The PDFs on the left-hand side refer to the $(N_F + 1)$-flavour scheme, while the PDFs on the right-hand side are the PDFs in the FFNS, depending on N_F massless flavours. The PDF combination $f_Q + \bar{f}_Q$ is the new PDF assigned to the heavy quark Q. Due to the appearance of the massive OMEs A_{ij}, the new PDFs depend on the heavy quark mass. By combining Eqs. (2.111) and (2.112) we can write down the singlet and non-singlet PDF combinations,

$$
\begin{aligned}
\Sigma(n_f + 1, N, \mu^2, m^2) = \left[A_{qq,Q}^{\mathrm{NS}}\left(N, N_F + 1, \frac{\mu^2}{m^2}\right) + A_{qq,Q}^{\mathrm{PS}}\left(N, N_F + 1, \frac{\mu^2}{m^2}\right)\right. \\
\left. + A_{Qq}^{\mathrm{PS}}\left(N, N_F + 1, \frac{\mu^2}{m^2}\right)\right]\Sigma(N_F, N, \mu^2) \\
+ \left[A_{qg,Q}\left(N, N_F + 1, \frac{\mu^2}{m^2}\right) + A_{Qg}\left(N, N_F + 1, \frac{\mu^2}{m^2}\right)\right]G(N_F, N, \mu^2),
\end{aligned}
\tag{2.114}
$$

$$
\begin{aligned}
\Delta_k(N_F + 1, N, \mu^2, m^2) = f_k(N_F + 1, N, \mu^2, m^2) + \bar{f}_k(N_F + 1, N, \mu^2, m^2) \\
- \frac{1}{N_F + 1}\Sigma(N_F + 1, N, \mu^2, m^2).
\end{aligned}
\tag{2.115}
$$

When choosing the matching scale, we have to keep in mind that both descriptions have to be valid at this scale. Therefore, the appropriate scale depends on the process under consideration,

as was discussed for example in [306]. In particular, the description is bound to break down near the heavy quark threshold: There it is no longer justified to treat the heavy quark as massless. Thus, the ZMVFNS is only valid for $Q^2/m^2 \gg 1$. The FFNS with exact dependence on the heavy quark mass, on the other hand, is well suited to describe the heavy flavour contributions near the threshold. Its validity is bounded by the requirement that the size of the logarithms $\ln(Q^2/m^2)$ should not spoil the perturbative convergence, i.e. $a_s \ln(Q^2/m^2) \lesssim 1$. This suggests to combine the ZMVFNS and the exact description in the FFNS into a *general mass variable flavour number scheme* (GMVFNS) [202, 303–305, 307], which smoothly interpolates between both schemes. One example is the BMSN scheme [202, 308] where the structure function is defined by

$$F_2^{\mathrm{BMSN}}(N_F) = F_2^{\mathrm{exact}}(N_F) + F_2^{\mathrm{ZMVFNS}}(N_F + 1) - F_2^{\mathrm{asympt}}(N_F) \,. \tag{2.116}$$

The exact mass dependence near threshold is captured by $F_2^{\mathrm{exact}}(N_F)$, which depends on N_F massless quarks, while the massless description of the heavy quark is provided by F_2^{ZMVFNS}, which uses the massless Wilson coefficients for $N_F + 1$ massless quarks along with the PDFs defined above. In order to avoid double counting, the asymptotic form $F_2^{\mathrm{asympt}}(N_F)$, which discards power corrections, is subtracted. It has been shown in [308] that $F_2^{\mathrm{BMSN}}(N_F)$ smoothly interpolates between the threshold region and the asymptotic region.

The discussion so far implicitly assumed that only a single heavy quark needs to be decoupled. If there is a strong hierarchy between the masses of heavy quarks, the matching procedure can be iterated for each quark individually. However, for charm and bottom quarks the ratio of masses $\rho = m_c^2/m_b^2 \sim 0.1$ requires careful assessment as to whether the hierarchy is sufficient for a sequential decoupling. Starting from 3-loop order, the decoupling is complicated further by the appearance of diagrams with two massive quarks with different masses, cf. [301, 302].

The massive OMEs which we calculate in this thesis enter the matching relations of the ZM-VFNS, thereby contributing to its extension to NNLO.

2.7. Renormalisation of massive operator matrix elements

The calculation of the massive operator matrix elements involves both ultraviolet (UV) and infrared (IR) divergent Feynman integrals, which have to be regularised. We use dimensional regularisation [309–312], where we analytically continue the dimensionality of space-time to D dimensions. The divergences show up as poles of the regularised integrals in a Laurent expansion around $\varepsilon = D - 4$ and can be removed by renormalisation and mass factorisation.

Calculations within dimensional regularisation require to find generalisations for all objects which depend on the dimension of space-time. Most obviously, the momentum integration must be suitably generalised. For the calculations at hand, the first step is to perform a Wick rotation, which leaves us with integrals over Euclidean momenta k that we continue to D dimensions. In practice, the Wick-rotated Feynman integrals can all be brought into the form

$$\int \frac{\mathrm{d}^D k}{(2\pi)^D} \frac{(k^2)^r}{(k^2 + R^2)^m} = \frac{1}{(4\pi)^{D/2}} \frac{\Gamma(r + D/2)\Gamma(m - r - D/2)}{\Gamma(D/2)\Gamma(m)} (R^2)^{r-m+D/2} \,. \tag{2.117}$$

This integral vanishes if $R = 0$, i.e. if there is no external scale, like masses or other momenta, involved in the integral [285]. The Γ-functions $\Gamma(z)$ [313, 314] arising on the right hand side are defined for complex arguments z. For $\mathrm{Re}\, z > 0$ the integral representation

$$\Gamma(z) = \int_0^\infty \mathrm{d}t \, e^{-t} t^{z-1} \tag{2.118}$$

converges and an analytic continuation in z is obtained from the functional equation

$$\Gamma(z + 1) = z\Gamma(z) \,. \tag{2.119}$$

As can be seen from the functional equation, the Γ-function has poles for $z = 0, -1, -2, \dots$. In Eq. (2.117), these poles correspond exactly to the divergences of the momentum integrals for $\varepsilon = D - 4 \to 0$. Choosing a complex ε, the divergences show up as poles in the principal part of the Laurent series of the Γ-functions. The Laurent series around negative integers can be inferred from combining the functional equation with the expansion of the Γ-function around $z = 1$,

$$\Gamma(1 - \varepsilon) = \exp(\varepsilon \gamma_{\mathrm{E}}) \exp\left(\sum_{i=2}^{\infty} \frac{\zeta_i}{i} \varepsilon^i\right), \quad |\varepsilon| < 1, \tag{2.120}$$

where γ_{E} is the Euler-Mascheroni constant and ζ_i denotes Riemann's zeta function evaluated at the integers,

$$\zeta_i = \sum_{k=1}^{\infty} \frac{1}{k^i}, \quad 2 \le i \in \mathbb{N}. \tag{2.121}$$

Thus, by defining the momentum integration by Eq. (2.117), we regularise divergences from UV and IR regions of the loop momenta as well as collinear divergences from collinear emission of massless particles. Using dimensional regularisation has the advantage that it keeps Lorentz and gauge invariance of the integrals intact.

Besides the momentum integration, we have to treat also the Lorentz contractions and the Clifford algebra of Dirac matrices in D dimensions. The corresponding relations are collected in Appendix A. A problem arises in the generalisation of γ_5 since it is an inherently four dimensional object [309]. A possible prescription is the replacement [309, 315–319]

$$\gamma_\mu \gamma_5 = \frac{i}{6} \varepsilon_{\mu\nu\rho\sigma} \gamma^\nu \gamma^\rho \gamma^\sigma, \tag{2.122}$$

where the Levi-Civita symbol is contracted in D dimensions according to

$$\varepsilon_{\alpha\beta\gamma\delta} \varepsilon_{\mu\nu\rho\sigma} = \begin{vmatrix} g_{\alpha\mu} & g_{\alpha\nu} & g_{\alpha\rho} & g_{\alpha\sigma} \\ g_{\beta\mu} & g_{\beta\nu} & g_{\beta\rho} & g_{\beta\sigma} \\ g_{\gamma\mu} & g_{\gamma\nu} & g_{\gamma\rho} & g_{\gamma\sigma} \\ g_{\delta\mu} & g_{\delta\nu} & g_{\delta\rho} & g_{\delta\sigma} \end{vmatrix}. \tag{2.123}$$

In general, the prescription described above violates the Ward identity of the axial current and requires a finite renormalisation of the axial current to restore this Ward identity [129, 319]. However, in this thesis we will only discuss the non-singlet contributions to the polarised and charged-current Wilson coefficients. The non-singlet OME can be calculated using an anti-commuting γ_5 due to a Ward-Takahashi identity [320, 321] which we will discuss in Section 4.1.

In dimensional regularisation the unrenormalised D-dimensional coupling constant $\hat{g}_{s,D}$ aquires a mass dimension, to ensure that the action remains dimension-less. We can make this explicit by defining a dimensionless coupling $\hat{g}_s$ and introducing an arbitrary mass scale μ_{D},

$$\hat{g}_{s,D} = \mu_{\mathrm{D}}^{-\varepsilon/2} \hat{g}_s. \tag{2.124}$$

As mentioned above, we identify this scale with the factorisation and renormalisation scales and write only μ, dropping the subscript D.

Once the divergences are made explicit via regularisation, they can be removed consistently via renormalisation and mass factorisation, such that afterwards the limit $\varepsilon \to 0$ can be taken. Dimensional regularisation allows for a convenient renormalisation scheme, called *minimal subtraction* (MS) scheme [322], in which only the pole terms of the Laurent expansion are absorbed

2. Deep-inelastic scattering

into the renormalisation constants. A slight modification simplifies expressions even more: Each loop integration will introduce an overall factor

$$S_\varepsilon = \exp\left[\frac{\varepsilon}{2}(\gamma_E - \ln(4\pi))\right], \tag{2.125}$$

where γ_E is the Euler-Mascheroni constant. It arises from the Γ-functions in Eq. (2.117) and the normalisation of the measure of integration, together with the relation Eq. (2.120). In the MS scheme, S_ε is simply expanded, which introduces the constants γ_E and $\ln(4\pi)$ into the results. Since this factor arises purely from the regularisation prescription, we can define the renormalisation scheme such that S_ε is absorbed into the renormalisation constants at each order, thereby eliminating γ_E and $\ln(4\pi)$ from the results altogether. This scheme is called the *modified minimal subtraction* ($\overline{\text{MS}}$) scheme [105] and we will frequently employ it.

A renormalisation procedure for massive operator matrix elements was worked out up to $\mathcal{O}(a_s^3)$ in [193, 203]. We briefly summarise the steps involved following the presentations in [193, 199, 203]. As the starting point we use the unrenormalised OMEs obtained from the connected Green's functions as defined in Eqs. (2.100) to (2.102). Note that only the external fields are removed but the self-energy corrections on external legs are still present. Since we work in dimensional regularisation and we have massless, on-shell external particles, all self-energy corrections involving only massless fields vanish. Furthermore, the fact that we are interested in on-shell OMEs ensures that the operators do not mix with non-gauge invariant operators and do not pick up unphysical contributions from the breakdown of the equations of motion, which would have to be dealt with if the external particles were off-shell [116, 323–325]. The renormalisation now proceeds in four steps: Mass renormalisation, coupling constant renormalisation, operator renormalisation and mass factorisation.

The renormalisation of the heavy quark mass is carried out multiplicatively in the on-mass-shell (OMS) scheme and we replace the bare mass $\hat{m}$ by

$$\hat{m} = Z_m m = m\left[1 + \hat{a}_s\left(\frac{m^2}{\mu^2}\right)^{\varepsilon/2}\delta m_1 + \hat{a}_s^2\left(\frac{m^2}{\mu^2}\right)^\varepsilon \delta m_2 + \mathcal{O}(\hat{a}_s^3)\right], \tag{2.126}$$

where the expansion coefficients of the renormalisation constant are [326–329]

$$\delta m_1 = C_F\left[\frac{6}{\varepsilon} - 4 + \left(4 + \frac{3}{4}\zeta_2\right)\varepsilon\right] \tag{2.127}$$

$$= \frac{\delta m_1^{(-1)}}{\varepsilon} + \delta m_1^{(0)} + \delta m_1^{(1)}\varepsilon, \tag{2.128}$$

$$\begin{aligned}\delta m_2 = C_F\Bigg\{&\frac{1}{\varepsilon^2}\Big(18C_F - 22C_A + 8T_F(N_F + N_H)\Big) + \frac{1}{\varepsilon}\Big(-\frac{45}{2}C_F + \frac{91}{2}C_A \\ &- 14T_F(N_F + N_H)\Big) + C_F\Big(\frac{199}{8} - \frac{51}{2}\zeta_2 + 48\ln(2)\zeta_2 - 12\zeta_3\Big) \\ &+ C_A\Big(-\frac{605}{8} + \frac{5}{2}\zeta_2 - 24\ln(2)\zeta_2 + 6\zeta_3\Big) \\ &+ T_F\Big[N_F\Big(\frac{45}{2} + 10\zeta_2\Big) + N_H\Big(\frac{69}{2} - 14\zeta_2\Big)\Big]\Bigg\}\end{aligned} \tag{2.129}$$

$$= \frac{\delta m_2^{(-2)}}{\varepsilon^2} + \frac{\delta m_2^{(-1)}}{\varepsilon} + \delta m_2^{(0)}. \tag{2.130}$$

The expressions are given for N_F massless and N_H massive quarks, which we will specialise to $N_H = 1$ in the following.

Most commonly, the coupling constant of QCD is renormalised in the $\overline{\text{MS}}$ scheme by reexpressing the bare coupling $\hat{a}_s$ in terms of the multiplicatively renormalised coupling $a_s^{\overline{\text{MS}}}$, which are related by

$$\hat{a}_s = \left(Z_g^{\overline{\text{MS}}}(\varepsilon, N_F) \right)^2 a_s^{\overline{\text{MS}}}(\mu^2)$$
$$= a_s^{\overline{\text{MS}}}(\mu^2) \left[1 + \delta a_{s,1}^{\overline{\text{MS}}}(N_F) a_s^{\overline{\text{MS}}}(\mu^2) + \delta a_{s,2}^{\overline{\text{MS}}}(N_F) \left(a_s^{\overline{\text{MS}}}(\mu^2) \right)^2 + \mathcal{O}\left(\left(a_s^{\overline{\text{MS}}} \right)^3 \right) \right]. \quad (2.131)$$

The expansion coefficients for the renormalisation constant $Z_g^{\overline{\text{MS}}}$ can be related to the β-function, cf. Eq. (2.86),

$$\delta a_{s,1}^{\overline{\text{MS}}}(N_F) = \frac{2}{\varepsilon} \beta_0(N_F), \quad (2.132)$$

$$\delta a_{s,2}^{\overline{\text{MS}}}(N_F) = \frac{4}{\varepsilon} \beta_0^2(N_F) + \frac{1}{\varepsilon} \beta_1(N_F), \quad (2.133)$$

where the coefficients of the β-function in the $\overline{\text{MS}}$ scheme are given by [61–63, 330–332]

$$\beta_0(N_F) = \frac{11}{3} C_A - \frac{4}{3} T_F N_F, \quad (2.134)$$

$$\beta_1(N_F) = \frac{34}{3} C_A^2 - 4 \left(\frac{5}{3} C_A + C_F \right) T_F N_F. \quad (2.135)$$

The factorisation relations in Eqs. (2.91) to (2.95) require strictly on-shell external states for the massive OMEs. In order to preserve this condition also after renormalisation, we have to ensure that the heavy quark contributions to the gluon self-energy $\Pi_H(p^2, m^2)$ vanish at zero momentum, i.e. $\Pi_H(0, m^2) = 0$. A consistent implementation of this condition is possible by absorbing the corresponding contributions into the renormalisation of the coupling constant. This defines a MOM scheme for the coupling constant, which is conveniently stated in the background field formalism [333–335], see also [76]. The renormalisation constant of the background field can be split into a light and a heavy flavour part according to $Z_A = Z_{A,l} + Z_{A,H}$. It is related to the renormalisation constant Z_g of the coupling constant by

$$Z_A = Z_g^{-2}. \quad (2.136)$$

Only the heavy quark contributions are affected by the renormalisation condition stated above and we choose the common $\overline{\text{MS}}$ scheme for the light quarks, i.e.

$$Z_{A,l} = \left(Z_g^{\overline{\text{MS}}}(\varepsilon, N_F) \right)^{-2}. \quad (2.137)$$

A strictly massless on-shell gluon is then enforced by the condition, [203],

$$\Pi_{H,\text{BF}} + Z_{A,H} = 0, \quad (2.138)$$

which leads to the coupling renormalisation constant in the MOM scheme

$$Z_g^{\text{MOM}}(\varepsilon, N_F + 1, \mu^2, m^2) = \frac{1}{(Z_{A,l} + Z_{A,H})^{1/2}}. \quad (2.139)$$

Instead of Eq. (2.131) we have to use, [203],

$$\hat{a}_s = \left(Z_g^{\text{MOM}}(\varepsilon, N_F + 1, \mu^2, m^2) \right)^2 a_s^{\text{MOM}}(\mu^2, m^2)$$
$$= a_s^{\text{MOM}}(\mu^2, m^2) \left[1 + \delta a_{s,1}^{\text{MOM}} a_s^{\text{MOM}}(\mu^2, m^2) \right.$$
$$\left. + \delta a_{s,2}^{\text{MOM}} \left(a_s^{\text{MOM}}(\mu^2, m^2) \right)^2 + \mathcal{O}\left(\left(a_s^{\text{MOM}} \right)^3 \right) \right] \quad (2.140)$$

with

$$\delta a_{s,1}^{\mathrm{MOM}} = \frac{2}{\varepsilon} \left[\beta_0(N_F) + \beta_{0,Q} f(\varepsilon) \right], \tag{2.141}$$

$$\delta a_{s,2}^{\mathrm{MOM}} = \left[\frac{\beta_1(N_F)}{\varepsilon} + \frac{4}{\varepsilon^2} \left(\beta_0(N_F) + \beta_{0,Q} f(\varepsilon) \right)^2 \right.$$
$$\left. + \frac{1}{\varepsilon} \left(\frac{m^2}{\mu^2} \right)^\varepsilon \left(\beta_{1,Q} + \varepsilon \beta_{1,Q}^{(1)} + \varepsilon^2 \beta_{1,Q}^{(2)} \right) \right] + \mathcal{O}(\varepsilon^2), \tag{2.142}$$

where

$$f(\varepsilon) = \left(\frac{m^2}{\mu^2} \right)^{\varepsilon/2} \exp \left(\sum_{i=2}^\infty \frac{\zeta_i}{2} \left(\frac{\varepsilon}{2} \right)^i \right) \tag{2.143}$$

and the coefficients of the heavy quark contributions to the β-function in the MOM scheme read, [203],

$$\beta_{0,Q} = \hat{\beta}_0(N_F) = -\frac{4}{3} T_F, \tag{2.144}$$

$$\beta_{1,Q} = \hat{\beta}_1(N_F) = -4 \left(\frac{5}{3} C_A + C_F \right) T_F, \tag{2.145}$$

$$\beta_{1,Q}^{(1)} = -\frac{32}{9} T_F C_A + 15 T_F C_F, \tag{2.146}$$

$$\beta_{1,Q}^{(2)} = -\frac{86}{27} T_F C_A - \frac{31}{4} T_F C_F - \zeta_2 \left(\frac{5}{3} T_F C_A + T_F C_F \right). \tag{2.147}$$

We mark the OMEs after mass and coupling constant renormalisation with only a single hat, $\hat{A}_{ij}$. At the end of the renormalisation procedure, after operator renormalisation and mass factorisation have been carried out, the coupling constant can be translated back into the $\overline{\mathrm{MS}}$ scheme by using the relations to the bare coupling, Eqs. (2.131) and (2.140), to find a finite renormalisation which connects both schemes.

Composite operators introduce additional UV divergences which have to be removed via operator renormalisation. This is of course already true for the purely massless theory, where they are removed by the Z factors defined in Eqs. (2.72) and (2.73). Already there one has to take care to disentangle the UV and IR divergences since both give rise to $1/\varepsilon^k$ poles in dimensional regularisation. Even more care is necessary if one of the quarks is massive. Therefore, the renormalisation procedure of [203] first deals with slightly off-shell OMEs where only UV divergences occur. For N_F massless and one massive flavour, the operator matrix elements can be subdivided into two contributions

$$\hat{A}_{ij}(p^2, m^2, \mu^2, a_s^{\mathrm{MOM}}, N_F + 1) = \hat{A}_{ij} \left(\frac{-p^2}{\mu^2}, a_s^{\overline{\mathrm{MS}}}, N_F \right) + \hat{A}_{ij}^Q(p^2, m^2, \mu^2, a_s^{\mathrm{MOM}}, N_F + 1), \tag{2.148}$$

where the first part contains only contributions from the massless fields, while the second part covers also the rest. The MOM scheme of the coupling constant is defined such that its contribution from the massless quarks reduces to the $\overline{\mathrm{MS}}$ scheme. We first discuss the renormalisation of the massless part.

The Z factors for the massless theory can be reconstructed from the anomalous dimensions according to Eqs. (2.74) and (2.75), order by order in perturbation theory. With them, the

massless OMEs for N_F flavours are renormalised by

$$A_{qq}^{\text{NS}}\left(\frac{-p^2}{\mu^2}, a_s^{\overline{\text{MS}}}, N_F\right) = Z_{qq}^{-1,\text{NS}}(a_s^{\overline{\text{MS}}}, N_F, \varepsilon)\hat{A}_{qq}^{\text{NS}}\left(\frac{-p^2}{\mu^2}, a_s^{\overline{\text{MS}}}, N_F, \varepsilon\right), \quad (2.149)$$

$$A_{ij}\left(\frac{-p^2}{\mu^2}, a_s^{\overline{\text{MS}}}, N_F\right) = Z_{ik}^{-1}(a_s^{\overline{\text{MS}}}, N_F, \varepsilon)\hat{A}_{kj}\left(\frac{-p^2}{\mu^2}, a_s^{\overline{\text{MS}}}, N_F, \varepsilon\right), \quad (2.150)$$

where $i, j \in \{q, g\}$, and the coupling constant is renormalised in the $\overline{\text{MS}}$ scheme. The renormalisation of the OMEs with one massive quark then requires the same Z factors, but with N_F replaced by $N_F + 1$ and $a_s^{\overline{\text{MS}}}$ reexpressed in terms of a_s^{MOM}. This allows us to write down the renormalisation of the massive OME,

$$\hat{A}_{ij}(p^2, m^2, \mu^2, a_s^{\text{MOM}}, N_F + 1) = Z_{ik}(a_s^{\text{MOM}}, N_F + 1, \varepsilon)\bar{A}_{kj}(p^2, m^2, \mu^2, a_s^{\text{MOM}}, N_F + 1), \quad (2.151)$$

where the renormalised OME is denoted by $\bar{A}_{kj}$. If we now want to extract just the renormalised heavy flavour part, we can split up the renomalised OME in analogy to Eq. (2.148) and subtract the massless flavour part to arrive at

$$\begin{aligned}
\bar{A}_{ij}^Q(p^2, m^2, \mu^2, a_s^{\text{MOM}}, N_F + 1) &= Z_{ik}^{-1}(a_s^{\text{MOM}}, N_F + 1, \mu^2)\hat{A}_{kj}^Q(p^2, m^2, \mu^2, a_s^{\text{MOM}}, N_F + 1) \\
&+ Z_{ik}^{-1}(a_s^{\text{MOM}}, N_F + 1, \mu^2)\hat{A}_{kj}\left(\frac{-p^2}{\mu^2}, a_s^{\overline{\text{MS}}}, N_F\right) \\
&- Z_{ik}^{-1}(a_s^{\overline{\text{MS}}}, N_F, \mu^2)\hat{A}_{kj}\left(\frac{-p^2}{\mu^2}, a_s^{\overline{\text{MS}}}, N_F\right).
\end{aligned} \quad (2.152)$$

Finally, we have to take the limit $p^2 \to 0$ which removes the only external scale from all purely massless loop integrals and therefore eliminates all loop contributions to the unrenormalised massless OMEs so that only their tree-level contribution remains,

$$\hat{A}_{ij}\left(0, a_s^{\overline{\text{MS}}}, N_F\right) = \delta_{ij}. \quad (2.153)$$

After the UV divergences have been removed through operator renormalisation, $\bar{A}_{ij}^Q$ has only collinear divergences left. These are removed via mass factorisation,

$$\bar{A}_{ij}^Q\left(\frac{m^2}{\mu^2}, a_s^{\text{MOM}}, N_F + 1\right) = A_{ik}^Q\left(\frac{m^2}{\mu^2}, a_s^{\text{MOM}}, N_F + 1\right)\Gamma_{kj}(N_F). \quad (2.154)$$

Here the transition functions $\Gamma_{ij}(N_F)$ are related to the massless renormalisation constants for N_F flavours. If all quarks were massless, the transition functions would be exactly the inverse of the operator Z factors,

$$\Gamma_{ij} = Z_{ij}^{-1}. \quad (2.155)$$

However, since only the massless subdiagrams give rise to collinear divergences, the transition functions refer to the N_F flavour case. Note, that the heavy quark contributions to the OME $\bar{A}_{ik}^Q$ do not have a tree-level contribution. Therefore, the transition functions in Eq. (2.154) contribute at most up to $\mathcal{O}(a_s^2)$ for the 3-loop OMEs. The tree-level part δ_{ij}, which is required for the heavy quark factorisation in Eqs. (2.91) to (2.95), is added back to A_{ij}^Q after renormalisation and mass factorisation.

Based on the renormalisation procedure summarised here, the renormalised massive OMEs can be expressed in terms of the constant terms of the ε expansion of the unrenormalised OMEs together with the expansions coefficients of the β-function, the mass renormalisation constant and the anomalous dimensions. Explicit expressions were derived in [193, 203]. For those OMEs which we explicitly discuss, we will give these expressions in the respective chapters of this thesis.

2.8. Status of the calculation of the massive OMEs at 3-loop order

There are seven massive operator matrix elements for the unpolarised operators Eqs. (2.51) to (2.53) and one more if we include the non-singlet operator for transversity. Considering the perturbative expansions of the asymptotic heavy flavour Wilson coefficients, Eqs. (2.91) to (2.95), and of the matching relations in the variable flavour number scheme, Eqs. (2.111) to (2.115), it becomes apparent that all OMEs are required to 3-loop order for a full $\mathcal{O}\left(a_s^3\right)$ description. For the structure functions the OMEs A_{Qg}, A_{Qq}^{PS}, $A_{qq,Q}^{\mathrm{PS}}$, $A_{qq,Q}^{\mathrm{NS}}$ and $A_{qg,Q}$ are required up to 3-loop order, while the gluonic OMEs $A_{gg,Q}$ and $A_{gq,Q}$ only contribute with their 2-loop terms. However, the VFNS also requires the latter two up to 3-loop order for the 3-loop matching relation of the gluon density.

The OMEs have been the subject of several investigations so far: They were calculated up to $\mathcal{O}\left(a_s^2\right)$ in [201, 202] for unpolarised operators and in [191] for polarised operators. The 2-loop OMEs were recalculated and corrected in [204, 205]. The 2-loop calculations were extended to include the $\mathcal{O}(\varepsilon)$ terms in [206, 207]. This is an important prerequisite for extending the calculation to 3-loop order since the $\mathcal{O}(\varepsilon)$ terms of the 2-loop results enter through renormalisation. At 3-loop order a series of fixed moments up to $N = 10\ldots14$, depending on the OME, was calculated in [193, 203] for the unpolarised OMEs and moments for the non-singlet OME for transversity were calcualted at 2- and 3-loop order in [215].

The long-term project to calculate the massive 3-loop OMEs for general values of N builds upon the calculations of [193, 203], but requires very different techniques. This thesis contributes to this project. Progress towards this goal which was made outside the context of this thesis includes the calculation of all diagrams which have a closed loop of fermions and where the operator insertion is located on a light quark line [336]. They are all proportional to N_F and, therefore, form a separately renormalisable colour factor. The OMEs $A_{qq,Q}^{\mathrm{PS}}$ and $A_{qg,Q}$ only receive contributions from diagrams of this class. Thus, their calculation in the cited reference marked the completion of the first massive OMEs for general N at 3-loop order. The corresponding diagrams for gluonic operator insertions, i.e. the OMEs $A_{gg,Q}^{(3)}$ and $A_{gq,Q}^{(3)}$, were presented in [337]. Another class of diagrams which have two 1-loop bubble insertions, one of which is massless, were calculated separately and published in [338]. These diagrams do not form a separate colour factor but were selected on topological grounds due to their suitability for a certain technological approach to their calculation. Moreover, the general N solution for the OME $A_{gq,Q}$ at $\mathcal{O}\left(a_s^3\right)$ was obtained in [339]. The diagrams with two heavy quark loops constitute a separate colour factor, proportional to T_F^2. For the OME $A_{gg,Q}$ general N expressions for this colour factor were obtained in [340]. As mentioned before, there are also 3-loop diagrams with two different massive quarks which contribute to the OMEs. Such diagrams were dealt with in [301, 302, 341, 342]. More technical aspects of the calculations were discussed in [343], where scalar prototypes of ladder diagrams were calculated, and in [344], where an application of the method of hyperlogarithms [345, 346] to massive diagrams with local operator insertions was developed and applied to several scalar diagrams with Benz-, ladder- and V-topologies.

In this thesis, we describe the caluclation of two complete OMEs and partial results for two more. In Chapter 4, we discuss the calculation the non-singlet OME $A_{qq,Q}^{\mathrm{NS},(3)}$ for even and for odd values of N. For the non-singet OME, this corresponds to the unpolarised and polarised case, respectively. We also describe the application of this OME in the asymptotic heavy flavour Wilson coefficients for the structure functions $F_2(x, Q^2)$, $g_1(x, Q^2)$ and $xF_3(x, Q^2)$ as well as its role in the matching relations of the VFNS. Moreover, we calculate the unpolarised pure-singlet OME $A_{Qq}^{\mathrm{PS},(3)}$ and the corresponding heavy flavour Wilson coefficient $H_{q,2}^{\mathrm{PS}}$ in Chapter 5. We also calculate a set of diagrams with ladder- and V-topologies which contribute to $A_{Qg}^{(3)}$, see

Chapter 6. Finally, for the gluonic OME $A_{gg,Q}^{(3)}$, we obtain the constant term of the ε-expansions of the unrenomalised OME. We describe its calculation in Chapter 7.

3. Calculation of massive operator matrix elements

The calculation of the massive OMEs requires the calculation of Feynman diagrams with local operator insertions. In several previous calculations, see Section 2.8, the occurring Feynman integrals were computed directly and the methods developed there are still useful for the calculations at hand. However, the large number of diagrams and scalar integrals necessitate the use of relations between scalar integrals to reduce their number to a manageable size. Integration-by-parts (IBP) identities for Feynman integrals [231–233], which are based on the divergence theorem [227–230], provide such a reduction to a small set of master integrals. We therefore explain below, how integration-by-parts identities can be used in the context of Feynman integrals with local operator insertions and how the arising master integrals can be calculated.

In Section 3.1, we give an overview of the steps involved in the calculation of the OMEs, starting from the generation of the relevant Feynman diagrams, up to the point where the unrenormalised results for the OMEs are obtained. The results of the Feynman integrals are expressed in terms of certain classes of nested sums and iterated integrals. We collect the definitions of the classes which appear here in Section 3.2. Several techniques for calculating the master integrals are discussed in Section 3.3.

3.1. Outline of the calculation

The starting point for all calculations of the massive OMEs is their definition in terms of connected Green's functions as given in Eqs. (2.100) to (2.102). In the following we will summarise the steps required in order to obtain an expression for the unrenormalised OMEs for general N. Figure 3.1 contains a schematic representation of the major steps involved in the calculation. Once this result is available, it can be subjected to the renormalisation procedure outlined in Section 2.7.

Generate Feynman diagrams We use the program `QGRAF` [347] to generate all Feynman diagrams associated to the respective Green's functions. Its output is a description of the diagrams in terms of edges and vertices. `QGRAF` generates the diagrams according to a model file, which specifies the quantum field theory with its vertices and propagators, and according to constraints on the external particles, the loop order and topological requirements like the presence of certain fields. For the massive OMEs at least one heavy quark propagator must always be present. The treatment of local operators insertions within `QGRAF` was worked out in [193, 203]. The crucial point is to implement the requirement of having exactly one vertex from the set of vertices that represent operator insertions. For this purpose, an auxiliary scalar field ϕ is added as an external particle and all vertices corresponding to operator insertions are extended by one such field. Operators with two fermion legs and $n \in \{0, 1, 2, 3\}$ gluons legs are represented by couplings of the form

$$\bar{\psi} \underbrace{g \ldots g}_{n \text{ times}} \psi \phi \,, \tag{3.1}$$

3. Calculation of massive operator matrix elements

```
┌─────────────────────────┐
│  Topological constraints │
│  for Feynman diagrams    │
└─────────────────────────┘
            │
            │  Generate all diagrams
            ▼
                                      Construct integral families
                                      Find required sectors
┌─────────────────────┐                              ┌─────────────────────┐
│ Diagram descriptions │ ──────────────────────────→ │  Integral families,  │
└─────────────────────┘                              │   Required sectors   │
            │                                         └─────────────────────┘
            │  Insert Feynman rules                             │
            │  Apply projectors for OMEs                        │  Calculate
            │  Simplify Dirac and colour algebra                │  reductions
            ▼                                                   ▼
┌─────────────────────┐                              ┌─────────────────────┐
│  Diagrams in terms of │                            │    Reductions to     │
│    scalar integrals   │                            │   master integrals   │
└─────────────────────┘                              │ for all required sectors │
            │                                         └─────────────────────┘
            │  Resum operators into generating functions
            │  Apply momentum shifts
            │  Identify integrals as members of integral family
            ▼
┌─────────────────────┐        ┌─────────────────┐
│  Diagrams in terms of │ ────→ │ List of occuring │
│    scalar integrals   │       │ scalar integrals │
│ (from integral families) │    └─────────────────┘
└─────────────────────┘                  │
            │                            │  Select required reductions
            │                            ▼
            │                   ┌─────────────────┐
            │  Insert reductions ◄─ │ Replacements for │
            │                   │ scalar integrals │
            ▼                   └─────────────────┘
┌─────────────────────┐        ┌─────────────────┐
│  Diagrams in terms of │ ────→ │ List of required │
│   master integrals    │       │ master integrals │
└─────────────────────┘        └─────────────────┘
            │                            │ Calculate master integrals
            │                            ▼
            │  Insert master integrals ◄─ │ Results for │
            │                            │ master integrals │
            ▼
┌─────────────────────┐
│ Diagrams in generating │
│ function representation │
└─────────────────────┘
            │
            │  Extract Nth moment
            ▼
┌─────────────────────┐
│  Results for diagrams │
│      in N space       │
└─────────────────────┘
```
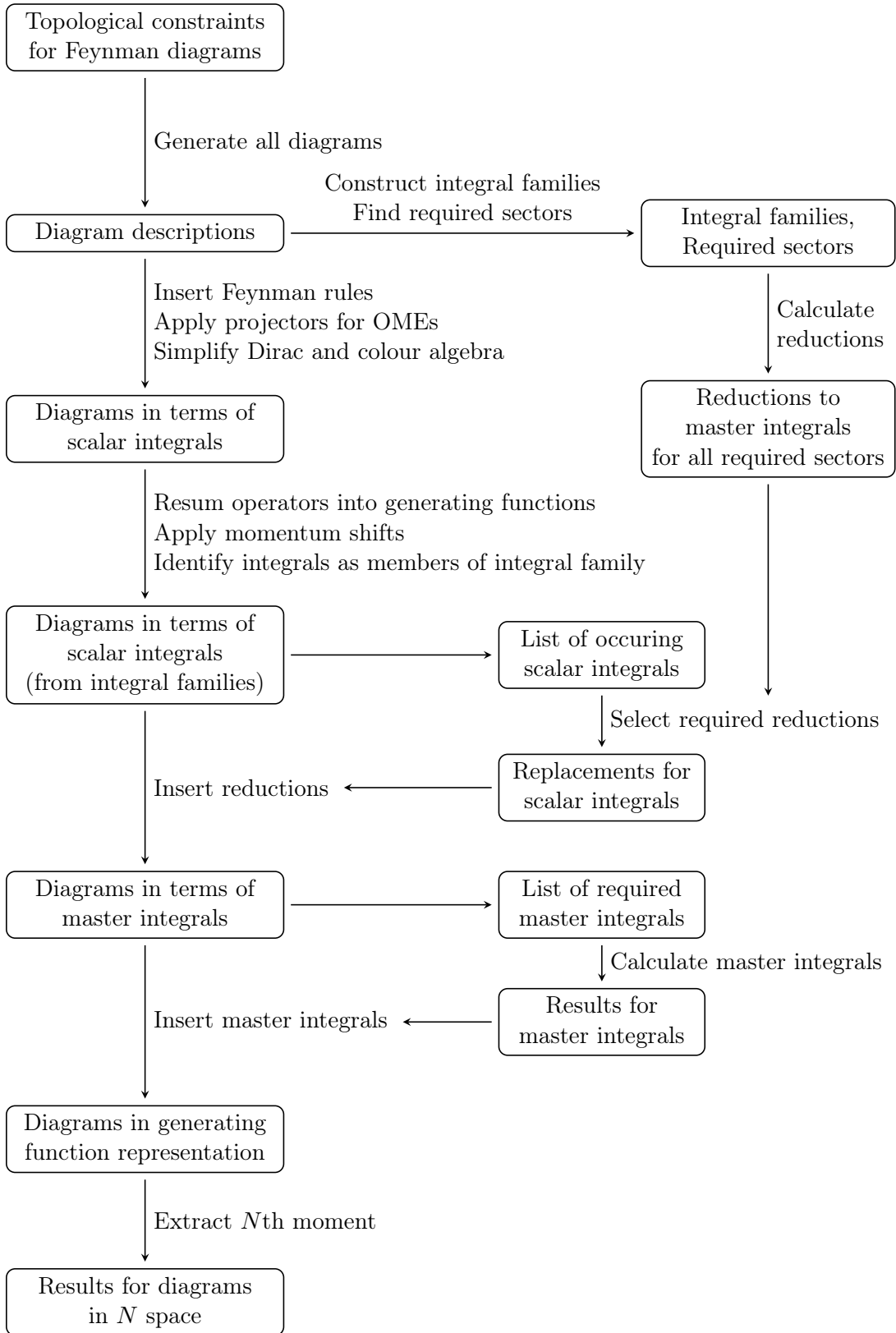
Figure 3.1.: Schematic outline of the major steps involved in the calculation of the unrenormalised massive operator matrix elements.

where ψ and $\bar{\psi}$ denote the fermion legs and g the gluon legs. The operators with $n \in \{2, 3, 4\}$ gluon legs are represented by

$$\underbrace{g \dots g}_{n \text{ times}} \phi \,. \tag{3.2}$$

The field ϕ is made non-propagating and we require one external field ϕ in addition to the two gluons or fermions required by the OME. If we generate only connected diagrams, this enforces exactly one coupling of ϕ to the rest of the diagram. By dropping the field ϕ and setting the momentum flowing through the ϕ leg to zero, we obtain the diagrams for OMEs with exactly one operator insertion.

The relevant diagrams for the massive OMEs were generated according to the procedure described above for the calculation of fixed moments in [193, 203]. We reuse this setup for the following calculations. The renormalisation procedure for the OMEs requires to calculate also reducible diagrams with massive self-energy corrections inserted on the external legs. Since the calculation of such diagrams factorises into the one-particle irreducible parts of the diagrams, we generate only the one-particle irreducible diagrams for the OMEs and add the self-energy parts at the end of the calculation. The required expressions for the heavy quark contributions to the quark and and gluon self-energies were calculated in [193, 203].

Simplify diagrams to scalar integrals The next step is to insert the Feynman rules for QCD and local operator insertions, see Appendix B, and to apply the projectors given in Eqs. (2.103) and (2.104). A `FORM` [216] program which accomplishes this task was also developed for [193, 203]. The application of the projectors contracts all Lorentz-, spinor- and colour indices so that the resulting expressions are scalar objects. The program also performs the traces of Dirac matrices for the fermion lines and reduces the colour generators to the colour factors by using the `FORM` package `color.h` [348].

At the end of this step, all diagrams are expressed as linear combinations of scalar integrals of the form

$$\int \frac{\mathrm{d}^D k_1}{(2\pi)^D} \frac{\mathrm{d}^D k_2}{(2\pi)^D} \frac{\mathrm{d}^D k_3}{(2\pi)^D} \frac{\left(\prod_{i,j}(k_i.k_j)^{\lambda_{i,j}}\right)\left(\prod_i (p.k_i)^{\lambda_i}\right)\left(\prod_i (\Delta.k_i)^{\alpha_i}\right)}{\prod_i (p_i^2 - m_i^2)^{\nu_i}} \, \mathrm{OP}_\alpha^{(n)}(\tilde{p}_1, \dots, \tilde{p}_\alpha)\,. \tag{3.3}$$

Here p denotes the external momentum flowing through the diagram, with $p^2 = 0$, and the p_i are linear combinations of internal and external momenta which flow through the propagators of the diagram. Since each propagator can be either massive or massless, m_i can either be zero or the heavy quark mass m. The exponents $\lambda_{i,j}$, λ_i, α_i and ν_i are integers. The operators introduce the polynomial $\mathrm{OP}_\alpha^{(n)}(\tilde{p}_1, \dots, \tilde{p}_\alpha)$ of order n in the scalar products $\Delta.\tilde{p}_i$, where the $\tilde{p}_i$ are linear combinations of the momenta flowing through the propagators adjacent to the vertex. Its concrete form depends on the type of operator insertion at hand and its location in the diagram. As can be seen from the Feynman rules in Appendix B, up to four different scalar products can occur in the polynomial. It can always be brought into one of the forms

$$\mathrm{OP}_1^{(n)}(\tilde{p}_1) = (\Delta.\tilde{p}_1)^n \,, \tag{3.4}$$

$$\mathrm{OP}_2^{(n)}(\tilde{p}_1, \tilde{p}_2) = \sum_{j=0}^{n} (\Delta.\tilde{p}_1)^j (\Delta.\tilde{p}_2)^{n-j} \,, \tag{3.5}$$

$$\mathrm{OP}_3^{(n)}(\tilde{p}_1, \tilde{p}_2, \tilde{p}_3) = \sum_{j=0}^{n} \sum_{l=0}^{j} (\Delta.\tilde{p}_1)^{n-j} (\Delta.\tilde{p}_2)^{j-l} (\Delta.\tilde{p}_3)^l \,, \tag{3.6}$$

3. Calculation of massive operator matrix elements

$$\mathrm{OP}_4^{(n)}(\tilde{p}_1, \tilde{p}_2, \tilde{p}_3, \tilde{p}_4) = \sum_{j=0}^{n} \sum_{l=0}^{j} \sum_{m=0}^{l} (\Delta.\tilde{p}_1)^{n-j} (\Delta.\tilde{p}_2)^{j-l} (\Delta.\tilde{p}_3)^{l-m} (\Delta.\tilde{p}_4)^{m}, \qquad (3.7)$$

where n is related to the Mellin variable N by an integer shift which depends on the type of operator. The coefficients of the integrals in Eq. (3.3) are polynomials in the colour factors, the space-time dimension D, the heavy quark mass m^2 and the scalar product $\Delta.p$.

Construction of integral families   Due to the large number of scalar integrals, it is necessary to use available relations between the integrals to eliminate redundancies and reduce the number of integrals which have to be calculated explicitly. Integration-by-parts identities for Feynman integrals [231–233] offer such a possibility. They can be used to derive a homogeneous system of linear equations fulfilled by the scalar integrals. The system is solved to express all occurring scalar integrals in terms of a small number of *master integrals*. Several public and private software packages exists to derive such IBP relations [349–354]. We choose to use `Reduze 2` [353, 354] which is a `C++` program based on Laporta's algorithm [355].[1]

A complication arises from the operator insertions, whose Feynman rules introduce scalar products raised to a symbolic power, cf. Eqs. (3.4) to (3.7). Laporta's algorithm on the other hand requires all propagators and scalar products to be raised to definite integer powers. To circumvent this problem, we can resum the operators into generating functions by multiplying with a tracing variable t^N and summing over N. The polynomials OP, which contain the dependence on N, are transformed into propagator-like terms [340, 343]. For example, the polynomial involving only one momentum can be summed using the geometric series, yielding

$$\sum_{N=0}^{\infty} t^N \mathrm{OP}_1^{(N)}(\tilde{p}_1) = \sum_{N=0}^{\infty} t^N (\Delta.\tilde{p}_1)^N = \frac{1}{1 - t\Delta.\tilde{p}_1}. \qquad (3.8)$$

Polynomials with more momenta can be factorised into independent geometric series by using the Cauchy product,

$$\sum_{i=0}^{\infty} a_i \sum_{j=0}^{\infty} b_j = \sum_{i=0}^{\infty} \sum_{j=0}^{i} a_j b_{i-j}, \qquad (3.9)$$

read backwards. For the polynomial with two momenta we get

$$\sum_{N=0}^{\infty} t^N \mathrm{OP}_2^{(N)}(\tilde{p}_1, \tilde{p}_2) = \sum_{N=0}^{\infty} t^N \sum_{j=0}^{N} (\Delta.\tilde{p}_1)^j (\Delta.\tilde{p}_2)^{N-j} = \sum_{i=0}^{\infty} t^i (\Delta.\tilde{p}_1)^i \sum_{j=0}^{\infty} t^j (\Delta.\tilde{p}_2)^j$$

$$= \frac{1}{(1 - t\Delta.\tilde{p}_1)(1 - t\Delta.\tilde{p}_2)}. \qquad (3.10)$$

Repeating this recursively allows to sum also the higher order polynomials analogously

$$\sum_{N=0}^{\infty} t^N \mathrm{OP}_3^{(N)}(\tilde{p}_1, \tilde{p}_2, \tilde{p}_3) = \frac{1}{(1 - t\Delta.\tilde{p}_1)(1 - t\Delta.\tilde{p}_2)(1 - t\Delta.\tilde{p}_3)}, \qquad (3.11)$$

$$\sum_{N=0}^{\infty} t^N \mathrm{OP}_4^{(N)}(\tilde{p}_1, \tilde{p}_2, \tilde{p}_3, \tilde{p}_4) = \frac{1}{(1 - t\Delta.\tilde{p}_1)(1 - t\Delta.\tilde{p}_2)(1 - t\Delta.\tilde{p}_3)(1 - t\Delta.\tilde{p}_4)}. \qquad (3.12)$$

These generating functions can now be treated as artificial propagators, which depend only linearly on the momentum. They are raised to definite integer powers and can be handled within

---

[1] `Reduze 2` uses the libraries `GiNaC` [356] and `Fermat` [357].

Laporta's algorithm. In order to recover the Nth moment, one can expand around $t = 0$ and extract the coefficient of t^N. Both representations are equivalent and we will use the more convenient one, depending on the task to be solved.

To apply `Reduze 2`, we have to label the scalar integrals in a systematic way. For this purpose, `Reduze 2` uses the concept of integral families. An integral family is an ordered set of propagators which is complete and minimal in the following sense: Completeness refers to the property that any scalar product of internal momenta with internal and external momenta can be expressed in terms of linear combinations of inverse propagators and kinematic invariants. Minimality means that removal of any propagator from the set will violate completeness. Within this framework, each integral is uniquely described by specifying the integral family it belongs to and by giving the powers to which each propagator of the integral family is raised.

Since the integral families are constructed for the resummed operators, it is convenient to introduce a graphical representation for the linear propagators. The resummation of the operator insertion with just two fermion legs (FF) yields a single linear propagator which can be depicted as

$$p \rightarrow \bigotimes \rightarrow p \longrightarrow p \xrightarrow{\quad\triangleright\quad} p\,, \tag{3.13}$$

where p is the momentum flowing through the operator and the triangle marks the direction of the momentum through the linear propagator. Analogously, the operator insertion with two fermions and one gluon (FFV) can be represented by

$$p_1 \rightarrow \bigotimes \rightarrow p_2 \longrightarrow p_1 \xrightarrow{\quad} \xrightarrow{\quad} p_2\,. \tag{3.14}$$

Note that the relative direction of the momenta p_1 and p_2 is important since the propagators depend linearly on the momenta. The Feynman rule of the operator insertion with two fermions and two gluons (FFVV) has two terms which differ by the momenta involved in the sum. This finds its correspondence in two terms with different linear propagators whose diagrammatic representation is

$$\tag{3.15}$$

Finally, the operator insertion with two fermions and three gluons (FFVVV) has six terms,


$$\tag{3.16}$$

Similar patterns can be found for the gluonic operators (VV, VVV and VVVV), where, however, more combinatorial possibilities arise.

In our case, there are three internal (k_1, k_2 and k_3) and two external momenta (p and Δ). Thus, each integral family must consist of nine standard and three linear propagators. However, a single integral can contain at most eight standard propagators. Therefore, no single integral completely determines an integral family, and we have a freedom in choosing the ninth propagator. By economically constructing the integral families, we can try to cover all scalar integrals by a minimal number of families. Moreover, it is advantageous to construct integral families which have a large number of permutation symmetries. The number of required integral families is driven mainly by the number and placement of massive lines and by the location of the operator

insertions. Also note that a diagram can have several terms which are covered by different integral families.

The construction of the integral families for the massive OMEs was completed before work on this thesis was started and was described in [358]. We summarise it here since it allows to discuss the characteristics of the integrals that occur in the following. To construct the integral families for this project, first families were constructed for the 3-loop self-energy diagrams without operator insertions. Their topologies are either Benz-, ladder- or crossed box topologies or subtopologies thereof. Since the only massive particle is a fermion and since the external particles are massless, there has to be at least one closed massive loop in each diagram. The massive lines can of course be placed along different loops. It was found that the diagrams without operators can be covered by six integral families: Three families cover the planar topologies, i.e. Benz and ladder diagrams, and three families are required for the non-planar crossed-box diagrams. In the following we will refer to the planar families by B1, B3 and B5 and to the non-planar families by C1, C2 and C3. The number distinguishes different routings of the massive lines. As examples we can consider the diagrams
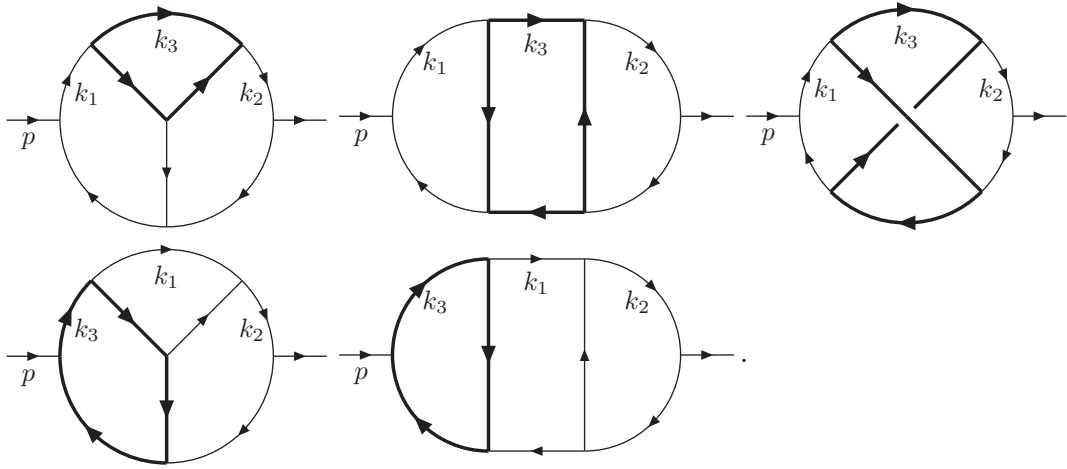
Here thick lines represent massive propagators, while thin lines denote massless propagators. All four planar diagrams depicted here are covered by the integral family B1 and the non-planar diagram requires the family C1. The propagators for the respective families are given by

$$
\begin{aligned}
P_{\text{B1},1} &= k_1^2 & P_{\text{C1},1} &= k_1^2 \\
P_{\text{B1},2} &= (k_1 - p)^2 & P_{\text{C1},2} &= (k_1 - p)^2 \\
P_{\text{B1},3} &= k_2^2 & P_{\text{C1},3} &= k_2^2 \\
P_{\text{B1},4} &= (k_2 - p)^2 & P_{\text{C1},4} &= (k_2 - p)^2 \\
P_{\text{B1},5} &= k_3^2 & P_{\text{C1},5} &= k_3^2 - m^2 \\
P_{\text{B1},6} &= (k_1 - k_3)^2 - m^2 & P_{\text{C1},6} &= (k_1 - k_3)^2 - m^2 \\
P_{\text{B1},7} &= (k_2 - k_3)^2 - m^2 & P_{\text{C1},7} &= (k_2 - k_3)^2 - m^2 \\
P_{\text{B1},8} &= (k_1 - k_2)^2 & P_{\text{C1},8} &= (k_1 + k_2 - k_3 - p)^2 \\
P_{\text{B1},9} &= (k_3 - p)^2 - m^2 & P_{\text{C1},9} &= (k_3 - p)^2 - m^2 \,.
\end{aligned}
$$

The families constructed in this way can be extended to cover also the linear propagators. To this end, the operator insertions in all diagrams are replaced by the linear propagators using the graphical notation described above. To cover scalar products of the light-like vector Δ with the loop momenta, the families had to be extended by three linear propagators in accordance with the properties of completeness and minimality. Depending on the placement of the linear

propagators, each of the six operator-less families can be extended into different families, differing by the choice of linear propagators. In addition to the conditions for the operator-less families, we require that the momentum flowing through each linear propagator is also present in one of the standard propagators. The families were then constructed by decomposing the 5- and 4-leg vertices first, which usually fixed the choice of all linear propagators up to an overall sign. Starting from the diagrams with the most involved vertices and working towards simpler diagrams allowed to fix all families.

In total, 24 integral families suffice to cover all diagrams for all massive OMEs. Five families are based on the operator-less family B1 and will be referred to as B1a to B1e, where the last letter distinguishes the sets of linear propagators added to the standard propagators of B1. Three families are based on B3 (denoted B3a to B3c) and six on B5 (B5a to B5f). The non-planar diagrams are covered by two families based on C1, four based on C2 and four based on C3, each following a similar naming scheme. The inverse propagators of the family B1a, for example, are given by

$$
\begin{aligned}
P_{\text{B1a},i} &= P_{\text{B1},i}\,, \text{ for } 1 \leq i \leq 9\,, \\
P_{\text{B1a},10} &= 1 - t\Delta.(k_3 - k_1)\,, \\
P_{\text{B1a},11} &= 1 - t\Delta.k_3\,, \\
P_{\text{B1a},12} &= 1 - t\Delta.(k_3 - k_2)\,.
\end{aligned}
$$

In Appendix C we collect the definitions propagators for all families that occur in this project.

In addition to the families explained above, the reductions also require the *crossed* version of each family where all momenta are reversed ($k_i \to -k_i$ and $p \to -p$). Reversing all momenta in one of the scalar integrals is equivalent to multiplying the integral by $(-1)^N$ for the moments or to performing the transformation $t \to -t$ for the generating functions.

There are only three linear propagators in each family which have to be chosen such that we can express $\Delta.k_1$, $\Delta.k_2$ and $\Delta.k_3$ as linear combinations of these propagators. Therefore, diagrams with operator insertions adjacent to an external leg require special treatment. Let us consider the case of a FFV operator with one external leg. Its two linear propagators belong to the same loop and carry the same loop momentum. They only differ by the external momentum p. An example would be

$$
\frac{1}{(1 - t\Delta.k_3)(1 - t(\Delta.k_3 - \Delta.p))}\,. \tag{3.17}
$$

These two linear propagators cannot be part of an integral family at the same time since then three linear propagators would not suffice to express all three scalar products of Δ with the loop momenta. Instead, we perform a partial fraction decomposition

$$
\frac{1}{(1 - t\Delta.k_3)(1 - t(\Delta.k_3 - \Delta.p))} = \frac{1}{t\Delta.p}\left(\frac{1}{1 - t\Delta.k_3} - \frac{1}{1 - t(\Delta.k_3 - \Delta.p)}\right)\,, \tag{3.18}
$$

which splits the diagrams into two parts with one linear propagator less. The two parts can be handled separately and, if necessary, even mapped to different integral families. Similarly, if more than three linear propagators occur at the same time, like for the FFVVV operator, at least two of the linear propagators in each term have to belong to the same loop (for 3-loop diagrams) and can be treated in the same way as above.

Once the integral families are fixed, the scalar integrals can be expressed by specifying an integral family f and the powers ν_i to which the inverse propagators $P_{f,i}$ of this family are raised, where $1 \leq i \leq 12$. Then we can write

$$
I^f_{\nu_1 \nu_2 \nu_3 \nu_4 \nu_5 \nu_6 \nu_7 \nu_8 \nu_9; \nu_{10} \nu_{11} \nu_{12}} = \int \frac{\mathrm{d}^D k_1}{(2\pi)^D} \frac{\mathrm{d}^D k_2}{(2\pi)^D} \frac{\mathrm{d}^D k_3}{(2\pi)^D} \prod_{i=1}^{12} \frac{1}{P_{f,i}^{\nu_i}}\,. \tag{3.19}
$$

3. Calculation of massive operator matrix elements

By allowing for negative powers ν_i also scalar products can be expressed as linear combinations of such integrals due to the completeness of families. We use the convention that the first nine propagators are standard propagators involving the loop momenta and p, while the last three propagators are artificial, linear propagators which arise from the operators.

The integrals within each family are organised into sectors. A sector is a subset of propagators of a family. Each integral belongs to exactly one sector, defined by the set of its propagators which appear in the denominator ($\nu_i > 0$). We call a sector S_1 a subsector of another sector S_2, if the propagators in S_1 are a subset of the propagators in S_2. This induces a partial order on the integrals. `Reduze 2` finds all IBP relations for the integrals of a sector and all its subsectors as well as relations between different sectors that arise from shifts of the loop momenta. Therefore, we have to identify which sectors of each integral family are required to cover all scalar integrals.

Calculate reductions Given the descriptions of the integral families and the relevant sectors, we instruct `Reduze 2` to find all reduction relations for these sectors and their respective subsectors. When calculating the reductions, there is a freedom of choice which scalar integrals should be considered as master integrals. At the level of integral families, we choose planar topologies over non-planar ones and families with fewer massive lines over those with more. Moreover, we prefer families with a larger number of permutation symmetries. Within the families, integrals with fewer different propagators are considered easier and are therefore preferred as master integrals. Finally, we choose integrals with higher powers in the denominator over integrals with scalar products in the numerator, i.e. negative powers ν_i.

The output of `Reduze 2` are the reduction relations for the scalar integrals, organised into a set of text files which take up about 2.1 TB of disk space. This covers all scalar integrals for all relevant sectors within the ranges of powers specified for the reductions. Later, it is possible to extract the reduction relations for a list of scalar integrals which actually occur in the diagrams.

Express diagrams in terms of scalar integrals from integral families At this point, the diagrams are still expressed in terms of general scalar integrals of the form given in Eq. (3.3) and in general the momenta assigned to the propagators do not yet match any of the integral families. To make use of the reductions to master integrals, we have to first resum the operators using the generating functions. Next, all scalar integrals of the diagram must be mapped to the integral families and their propagators by identifying the relevant integral family for a diagram and finding suitable shifts of the loop momenta

$$k_i = \sum_{j=1}^3 a_{ij} k'_j + b_i p \,, \tag{3.20}$$

with $a_{ij}, b_i \in \{-1, 0, 1\}$, such that all propagators match the form dictated by the integral family. In the simplest case, all scalar integrals belong to the same integral family and require the same shift of momenta. For diagrams with operator insertions whose Feynman rules have several terms or where the operator is adjacent to an external leg (see above), the diagram has to be split into several parts which are mapped separately. Given the number of diagrams, it is still feasible to search for the family and shift by an exhaustive search. Since the coefficients a_{ij} and b_i are from a finite set and since there is only a finite number of families, there is a finite number of possible family assignments and momentum shifts. The number of possible shifts can be further reduced by requiring that the shift has to be bijective. Moreover, there are several possible combinations of family assignments and momentum shifts due to permutation symmetries within the families and equivalences of sectors across families. We can terminate the search after finding the first instance that works. Finally, we perform the search in an order which tries more plausible mappings first, in the sense that we first try families which cover many diagrams and shifts

in which many coefficients a_{ij} and b_i are zero. The exhaustive search can be implemented in `Mathematica`.

Once the integral family and momentum shifts are known, we can apply the shifts and express each scalar product of internal momenta with internal or external momenta uniquely by a linear combination of inverse propagators. The scalar integrals are then expressed completely as rational functions of the inverse propagators $P_{f,i}$. From this, we can directly read off the powers $\nu_{f,i}$ and hence write the diagrams $D(t)$ as linear combinations of scalar integrals from the integral families,

$$D(t) = \sum_i c_i(t) I_i(t) , \qquad (3.21)$$

where the coefficients $c_i(t)$ are polynomials in $t\Delta.p$, the mass m and the dimensional regulator ε. The index i labels all scalar integrals $I_i(t)$. The scalar integrals are in the form of Eq. (3.19).

Express diagrams in terms of master integrals As mentioned above, the reductions calculated by `Reduze 2` cover many more scalar integrals than actually appear in the diagrams. Therefore, we compile a list of scalar integrals for which a reduction to master integrals is indeed required and extract the necessary reductions. The reductions express the scalar integrals $I_i(t)$ as linear combinations of master integrals $M_j(t)$, where j labels all master integrals,

$$I_i(t) = \sum_j d_{ij}(t) M_j(t) , \qquad (3.22)$$

with coefficients $d_{ij}(t)$ that are now rational functions of $t\Delta.p$, the mass m and ε. Combining Eq. (3.21) with Eq. (3.22) provides a representation of the diagram as a linear combination of master integrals

$$D(t) = \sum_j b_j(t) M_j(t) , \qquad (3.23)$$

with the coefficients

$$b_j(t) = \sum_i c_i(t) d_{ij}(t) . \qquad (3.24)$$

Calculation of master integrals In the end, we would like to calculate the diagrams as Laurent expansions in the dimensional regulator ε, expanded up to the constant term (ε^0). Thus, it suffices to also calculate the master integrals as truncated Laurent expansions, but since the coefficients of the master integrals are now rational functions in ε, we have to expand them to higher orders whenever the coefficients $b_j(t)$ contain poles in ε. If the highest pole occurring in $b_j(t)$ is ε^{-n}, we must calculate the corresponding master integral $M_j(t)$ up to order ε^n. Taking all diagrams into account, the highest appearing pole in the coefficients determines the overall order to which a particular master integral is required.

Calculating the master integrals $M_j(t)$ is one of the most demanding tasks in the calculation of the massive OMEs. A number of techniques have been developed for calculating these master integrals. We will describe those which are used in this thesis in more detail in Section 3.3. All these methods have in common that we do not directly calculate the master integrals in their generating function representation, but rather we calculate the moments $M_j(N)$ of the generating function

$$M_j(t) = \sum_{N=0}^{\infty} t^N M_j(N) . \qquad (3.25)$$

The $M_j(N)$ are simplified to nested sums using the summation algorithms [240–251] implemented in the packages `Sigma` [241, 252, 253], `HarmonicSums` [258–263], `EvaluateMultiSums` and `SumProduction` [254–257]. For some integrals a small number of coefficients $M_j(N)$ must be given explicitly for $N = 0, \ldots, n_0$ since the representation for general N has poles or removable poles for these low values of N. Instead of Eq. (3.25), the master integrals take the form

$$M_j(t) = \sum_{N=0}^{n_0} t^N \tilde{M}_{j,N} + \sum_{N=n_0+1}^{\infty} t^N M_j(N) \,, \qquad (3.26)$$

where $\tilde{M}_{j,N}$ denotes the fixed moment N of the master integral M_j. After obtaining the moments of the master integrals $M_j(N)$, we write the generating functions $M_j(t)$ as formal power series (Eq. (3.25)) without actually performing the summation over N. Inserting this form of the master integrals into the diagrams, Eq. (3.23) in principle gives us a result for the generating function of the moments of the diagram.

Extracting the result in N space   Our goal is to obtain the final result for the diagrams in N space up to the constant term in ε. The master integrals $M_j(t)$, obtained in the previous step, are already given as expansions in ε. Thus, we have to expand the coefficients $b_j(t)$ in ε and insert the expanded coefficients back into the diagrams Eq. (3.23).

At each order of the expansion in ε, we now have to extract the Nth moment of the generating function. This is accomplished by expanding in t around $t = 0$ and extracting the coefficient of t^N. Since the master integrals are already given as a formal power series in t, only their coefficients have to be expanded. The latter are rational functions in t so that their expansion is rather straightforward. The resulting infinite series has to be combined with the power series of the master integrals via the Cauchy product. The final expressions are again simplified to nested sums. The expansion in ε, the extraction of the Nth moment and the simplification steps are provided by the routine `GetMomentAndSimplify` from the package `SumProduction`, which uses the function `GetMoment` from the package `HarmonicSums`.

3.2. Nested sums and iterated integrals

The results of calculations in quantum field theory frequently involve special functions and numbers. In this section, we collect the definitions of those special functions and numbers which are relevant for the massive OMEs. For more in-depth introductions to these and related topics we refer, for example, to [359, 360] and the references therein. The special functions fall into two broad categories: On the one hand, results for general values of the Mellin variable N, which arise directly from the light-cone expansion, are most naturally expressed in terms of nested sums. On the other hand, the results can also be translated to x space via an inverse Mellin transform, which relates nested sums to iterated integrals. In both cases, special numbers like zeta values and multiple zeta values [361] arise.

Nested sums are sums of the general form

$$\sum_{i_1=1}^{N} a_1(i_1) \sum_{i_2=1}^{i_1} a_2(i_2) \cdots \sum_{i_k-1}^{i_{k-1}} a_k(i_k) \,, \qquad (3.27)$$

where $N \in \mathbb{N}$ and at the jth level of the nesting the summation index i_j only appears in the summand $a_j(i_j)$ and as the upper limit of the next sum. We call k the depth of the nesting. A prominent example for this class of sums are the harmonic sums [143, 144]. They are

generalisations of the harmonic numbers and are defined recursively as

$$S_{m_1,\ldots,m_k}(N) = \sum_{i=1}^{N} \frac{(\text{sign}(m_1))^i}{i^{|m_1|}} S_{m_2,\ldots,m_k}(i) \,, \qquad S_{\emptyset} = 1 \,, \qquad (3.28)$$

with $m_1,\ldots,m_k \in \mathbb{Z} \setminus \{0\}$. The m_j are called indices and the sum of their absolute values $w = |m_1| + \cdots + |m_k|$ is called the weight of the sum. The analytic continuation of harmonic sums to $N \in \mathbb{C}$ has been discussed in [147, 148, 362]. It can be obtained from the asymptotic expansion at $N \to \infty$ together with the shift relations fulfilled by the harmonic sums. In the limit $N \to \infty$, the harmonic sums $S_k(N)$ with positive $k \geq 2$ converge to zeta values, i.e. the Riemann zeta function evaluated at integer argument k,

$$S_k(\infty) = \lim_{N \to \infty} S_k(N) = \sum_{i=1}^{\infty} \frac{1}{i^k} = \zeta(k) = \zeta_k \,, \quad k \geq 2 \,. \qquad (3.29)$$

For $k = 1$ the sum is the usual harmonic series and diverges logarithmically. The same limit for general harmonic sums leads to multiple zeta values [361],

$$\sigma_{k_1,\ldots,k_m} = \lim_{N \to \infty} S_{k_1,\ldots,k_m}(N) \,. \qquad (3.30)$$

In calculations of massive Feynman diagrams, in particular the constant [217, 363–367]

$$
\begin{aligned}
B_4 = {}& -8\sigma_{-3,-1} - \frac{13}{2}\zeta_2 + 12\zeta_4 \\
= {}& -4\zeta_2 \ln^2(2) + \frac{2}{3}\ln^4(2) - \frac{13}{2}\zeta_4 + 16\,\text{Li}_4\Big(\frac{1}{2}\Big) \approx -1.762800093\ldots \qquad (3.31)
\end{aligned}
$$

appears. The definition of harmonic sums can be extended to generalised harmonic sums or S-sums [261, 368], defined as

$$S_{m_1,\ldots,m_k}(x_1,\ldots,x_k; N) = \sum_{i=1}^{N} \frac{x_1^i}{i^{m_1}} S_{m_2,\ldots,m_k}(x_2,\ldots,x_k; i) \,, \quad S_{\emptyset} = 1 \,, \qquad (3.32)$$

where the indices are positive natural numbers $m_1,\ldots,m_k \in \mathbb{N}$ and we have in addition non-zero, real parameters $x_1,\ldots,x_k \in \mathbb{R} \setminus \{0\}$. The harmonic sums are a special case for $x_1,\ldots,x_k \in \{-1,1\}$. Another generalisation are cyclotomic harmonic sums [260]

$$S_{\{a_1,b_1,c_1\},\ldots,\{a_k,b_k,c_k\}}(x_1,\ldots,x_k; N) =$$

$$\sum_{i=1}^{N} \frac{x_1^i}{(a_1 k + b_1)^{c_1}} S_{\{a_2,b_2,c_2\},\ldots,\{a_k,b_k,c_k\}}(x_2,\ldots,x_k; i) \,, \quad S_{\emptyset} = 1 \,, \qquad (3.33)$$

with $a_j, c_j \in \mathbb{N}$, $b_j \in \mathbb{N}_0$ and $x_j \in \mathbb{R} \setminus \{0\}$. Finally, we can also allow for binomial weights in the summands and obtain iterated binomial sums [262, 369–371]. The summands have the form

$$a_j(n) = \binom{2n}{n}^{b_j} \frac{x_j^n}{n^{m_j}} \,, \qquad (3.34)$$

where $m_j \in \mathbb{N}$, $b_j \in \{-1, 0, 1\}$ and $x_j \in \mathbb{R} \setminus \{0\}$. We do not introduce any notation for binomially weighted sums here, since it is usually more transparent to explicitly write down the sums.

Nested sums fulfil quasi-shuffle (or stuffle relations) [143, 144, 147, 368, 372]. They arise from the product of two sums, if we split up the summation ranges according to

$$\left(\sum_{i=1}^{N} a_i\right)\left(\sum_{j=1}^{N} b_j\right) = \sum_{i=1}^{N} a_i \sum_{j=1}^{i} b_j + \sum_{j=1}^{N} b_j \sum_{i=1}^{j} a_i - \sum_{i=1}^{N} a_i b_i \,. \qquad (3.35)$$

3. Calculation of massive operator matrix elements

For generalised harmonic sums, for example, Eq. (3.35) amounts to

$$S_{a_1,\ldots,a_k}(x_1,\ldots,x_k;N)S_{b_1,\ldots,b_k}(y_1,\ldots,y_k;N) =$$

$$\sum_{i=1}^{N} \frac{x_1^i}{i^{a_1}} S_{a_2,\ldots,a_k}(x_2,\ldots,x_k;i)S_{b_1,\ldots,b_l}(y_1,\ldots,y_l;i)$$

$$+ \sum_{i=1}^{N} \frac{y_1^i}{i^{b_1}} S_{b_2,\ldots,b_l}(y_2,\ldots,y_l;i)S_{a_1,\ldots,a_k}(x_1,\ldots,x_k;i)$$

$$- \sum_{i=1}^{N} \frac{(x_1 y_1)^i}{i^{a_1+b_1}} S_{a_2,\ldots,a_k}(x_2,\ldots,x_k;i)S_{b_2,\ldots,b_l}(y_2,\ldots,y_l;i) , \tag{3.36}$$

which can be applied recursively This leads to algebraic relations among the sums which allow to eliminate some of the sums from expressions. Systematically applying these relations, one can reduce them to a smaller set of basis sums [143, 144, 146, 147]. The package `HarmonicSums` [258–263] provides routines and precomputed tables for such reductions.

Nested sums are closely related to iterated integrals [373–375], which are integrals of the form

$$\int_0^x \mathrm{d}x_1\, a_1(x_1) \int_0^{x_1} \mathrm{d}x_2\, a_2(x_2) \ldots \int_0^{x_{k-1}} \mathrm{d}x_k\, a_k(x_k) . \tag{3.37}$$

The integrands $a_j(x_j)$ are functions from an a set of functions $\mathfrak{A}$ called *alphabet*. The elements of the alphabet are called letters. If we choose the rational functions

$$\mathfrak{A} = \left\{ f_1(x) = \frac{1}{1-x}, f_0(x) = \frac{1}{x}, f_{-1}(x) = \frac{1}{1+x} \right\} , \tag{3.38}$$

we obtain the class of functions known as harmonic polylogarithms (HPLs) [145]

$$H_{\underbrace{0,\ldots,0}_{k \text{ times}}}(x) = \frac{1}{k!} \ln^k(x) , \tag{3.39}$$

$$H_m(x) = \int_0^x \mathrm{d}y\, f_m(y) , \quad m \neq 0 , \tag{3.40}$$

$$H_{m_1,\ldots,m_k}(x) = \int_0^x \mathrm{d}y\, f_{m_1}(y) H_{m_2,\ldots,m_k}(y) . \tag{3.41}$$

The number of integrations k is called the weight of the HPL. Special cases of harmonic polylogarithms include the classical polylogarithms [376, 377]

$$\mathrm{Li}_n(x) = H_{\underbrace{0,\ldots,0,1}_{n-1 \text{ times}}}(x) \tag{3.42}$$

and the Nielsen integrals [377–380]

$$\mathsf{S}_{n,p}(x) = \frac{(-1)^{n+p-1}}{(n-1)!p!} \int_0^1 \frac{\mathrm{d}z}{z} \ln^{n-1}(z) \ln^p(1-xz) = H_{\underbrace{0,\ldots,0}_{n \text{ times}},\underbrace{1,\ldots,1}_{p \text{ times}}}(x) . \tag{3.43}$$

The Mellin transformation, cf. Eq. (2.62), relates HPLs to harmonic sums and conversely the inverse Mellin transforms of harmonic sums can be expressed in terms of HPLs. Moreover, harmonic sums appear as expansion coefficients in power series expansions of HPLs at argument

$x = 0$. The representation of certain harmonic sums as Mellin transformations of HPLs requires the introduction of +-distributions $[f(x)]_+$, which are defined according to

$$\int_0^1 dx \, [f(x)]_+ g(x) = \int_0^1 dx \, f(x)[g(x) - g(1)] \,. \tag{3.44}$$

With their help, we can express, for example, the harmonic sum $S_1(N)$ as

$$S_1(N) = \int_0^1 dx \, x^{N-1} \left(1 - \left[\frac{1}{1-x}\right]_+\right) = \int_0^1 dx \, x^{N-1} - \int_0^1 dx \, \frac{x^{N-1} - 1}{1 - x} \,. \tag{3.45}$$

Similarly, δ-distributions are necessary, to express constants in N space as Mellin integrals. We will repeatedly refer to these notions, when discussing results in x space.

Cyclotomic harmonic polylogarithms [260] are a generalisation of HPLs which are based on the cyclotomic polynomials $\Phi_n(x)$ [381], defined as

$$\Phi_n(x) = \prod_{\substack{1 \leq k \leq n \\ \gcd(k,n)=1}} \left(x - e^{2\pi i \frac{k}{n}}\right) \,. \tag{3.46}$$

Based on these polynomials, on can consider iterated integrals over the alphabet

$$\mathfrak{A} = \left\{f_0(x) = \frac{1}{x}\right\} \cup \left\{f_{(n;b)}(x) = \frac{x^b}{\Phi_n(x)} \,\middle|\, n \in \mathbb{N}, b \in \mathbb{N}_0, b < \varphi(n)\right\} \,, \tag{3.47}$$

where $\varphi(n)$ is Euler's totient function. The condition $b < \varphi(n)$ ensures that the degree of the polynomial in the denominator is larger than that of the numerator. The letters $f_0(x) = x^{-1}$, $f_{(1;0)}(x) = (x-1)^{-1}$ and $f_{(2,0)} = (x+1)^{-1}$ are, up to a sign of $f_{(1;0)}$, exactly the letters which generate the HPLs. The cyclotomic HPLs are then defined by, [260],

$$H_{\underbrace{0,\ldots,0}_{k \text{ times}}}(x) = \frac{1}{k!} \ln^k(x) \,, \tag{3.48}$$

$$H_{(n;b)}(x) = \int_0^x dy \, f_{(n;b)}(y) \,, \quad m \neq 0 \,, \tag{3.49}$$

$$H_{(n_1;b_1),\ldots,(n_k;b_k)}(x) = \int_0^x dy \, f_{(n_1;n_1)}(y) H_{(n_2;b_2),\ldots,(n_k;b_k)}(y) \,. \tag{3.50}$$

The Mellin transformation of cyclotomic HPLs are linear combinations of cyclotomic harmonic sums.

Other relevant alphabets include letters of the form

$$f_a(x) = \frac{1}{x - a} \tag{3.51}$$

for $a \in \mathbb{C}$, which lead to hyperlogarithms [373, 374], and letters which include square roots [262], like for example

$$\frac{1}{(x + a)\sqrt{x + b}} \,, \quad \frac{1}{\sqrt{x + a}\sqrt{x + b}} \,, \quad a, b \in \mathbb{Q} \,, \tag{3.52}$$

which are related to the iterated binomial sums of Eq. (3.34) via Mellin transformations. For further details we refer to [262].

Similar to the quasi-shuffle relations of nested sums, one can derive shuffle relations for iterated integrals. The idea is to split up the region of integration into simplices. The basic case is

$$\int_0^x \mathrm{d}y\, f(y) \int_0^x \mathrm{d}z\, g(z) = \int_0^x \mathrm{d}y\, f(y) \int_0^y \mathrm{d}z\, g(z) + \int_0^x \mathrm{d}z\, g(z) \int_0^z \mathrm{d}y\, f(y) \,. \qquad (3.53)$$

For HPLs this translates to

$$
\begin{aligned}
H_{a_1,\dots,a_k}(x) H_{b_1,\dots,b_k}(x) = {} & \int_0^x \mathrm{d}y\, f_{a_1}(y) H_{a_2,\dots,a_k}(y) H_{b_1,\dots,b_l}(y) \\
& + \int_0^x \mathrm{d}y\, f_{b_1}(y) H_{a_1,\dots,a_k}(y) H_{b_2,\dots,b_l}(y) \,.
\end{aligned}
\qquad (3.54)
$$

Recursive application then yields algebraic relations among the HPLs which can be used to reduce all HPLs of a given weight to a basis composed of a smaller number of functions. Algorithms for such reductions [145–148] are, for example, implemented in the package `HarmonicSums`.

Since the calculation of the master integrals heavily relies on the package `Sigma` [241, 252, 253] and related packages, we introduce the notion of indefinite nested product-sum expressions: Given a field $\mathbb{K}$ and a variable N which is algebraically independent over $\mathbb{K}$, an indefinite nested product-sum expression with respect to N is any expression which can be constructed from N, a finite number of constants from $\mathbb{K}$, the operations $(+, -, \cdot, /)$ and sums and products of the form $\sum_{i=l}^N f(i)$ and $\prod_{i=l}^N f(i)$, where $l \in \mathbb{N}$ and $f(i)$ is an indefinite nested product-sum expression with respect to i which is free of N. In particular, the nested sums discussed in this section fall into this class. The relevance of this definition for the calculations in this thesis derives from the fact that the algorithms implemented in `Sigma` deal with objects from this class. For example, `Sigma` provides routines to solve linear recurrences of the form

$$a_0(N) f(N) + \cdots + a_m(N) f(N + m) = b(N) \,,$$

where $a_0(N), \dots, a_m(N)$ are polynomials in N over $\mathbb{K}$ and $b(N)$ is an indefinite nested sum-product expression. It finds all solutions to the recurrence which can be expressed as indefinite nested sum-product expressions. Moreover, the package `EvaluateMultiSums` [254–257], which builds on `Sigma`, allows to simplify definite multiple sums in terms of indefinite nested product-sum expressions, if such a simplification exists.

3.3. Calculational tools for master integrals

While the approach outlined above is tailored to the use of IBP identities and reductions to master integrals, the methods developed before for the calculation of integrals with operator insertions can be applied for the calculation of master integrals as well. By working on the moments of the master integrals $M_j(N)$ instead of the generating functions $M_j(t)$, we can directly apply those methods for scalar integrals. This involves introducing a Feynman parametrisation and solving the resulting integrals in terms of special functions, like Euler Beta functions or higher hypergeometric functions [211–214, 234–239]. In more involved cases, the Feynman parameter integrals can be treated using Mellin-Barnes integrals [208–210]. In both cases, the solutions are formulated in terms of nested finite and infinite sums. These sum representations can be simplified to indefinite nested product-sum expressions using the summation algorithms implemented in the `Mathematica` packages `Sigma`, `HarmonicSums`, `EvaluateMultiSums` and `SumProduction`. The methods based on special functions are explained in more detail in Section 3.3.2 and the Mellin-Barnes techniques are discussed in Section 3.3.3.

In addition, the reductions to master integrals offer the opportunity to employ another technique for calculating the master integrals: The master integrals fulfil differential equations which

can be derived using IBP relations. Provided we can calculate appropriate initial values, differential equations turn out to be a powerful method for these calculations. The differential equations are derived for the generating functions of the master integrals by differentiating with respect to the tracing variable t. This results in coupled systems of first order ordinary differential equations. We can translate them into coupled systems of difference equations by inserting a formal power series ansatz for the master integrals. These can be uncoupled to linear recurrences with the help of uncoupling algorithms [382] implemented in the package `OreSys` [383] and solved using the tools mentioned above. In Section 3.3.4 we explain this method.

Some of the master integrals required for this project are also calculated using the multivariate Almkvist-Zeilberger algorithm [384, 385], which allows to compute recurrences for the integrals. These can be solved subsequently by `Sigma`. The algorithm is implemented in the package `MultiIntegrate` [259]. For details on this approach we refer to [259, 268].

3.3.1. Feynman parametrisations and related tools

Several techniques which we use for calculating the master integrals are based on a Feynman parameter representation. Therefore, we briefly review how it is derived. Our starting point is a scalar integral with an operator insertion in N space. Since we will apply the method to master integrals, we will confine the discussion the case where only scalar products of the light-like vector Δ and loop momenta k_i, i.e. one of the polynomials $\mathrm{OP}_\alpha^{(N)}(\tilde{p}_1, \ldots, \tilde{p}_\alpha)$, are present in the numerator. Thus, the integrals are of the form

$$\int \frac{\mathrm{d}^D k_1}{(2\pi)^D} \frac{\mathrm{d}^D k_2}{(2\pi)^D} \frac{\mathrm{d}^D k_3}{(2\pi)^D} \frac{\mathrm{OP}_\alpha^{(N)}(\tilde{p}_1, \ldots, \tilde{p}_\alpha)}{P_1^{\nu_1} \ldots P_9^{\nu_9}} . \tag{3.55}$$

We can now select a loop momentum k_j, take the set of propagators through which k_j flows and combine them using a Feynman parametrisation, see e.g. [76],

$$\prod_{i=1}^n \frac{1}{P_i^{\nu_i}} = \frac{\Gamma(\nu)}{\prod_{i=1}^n \Gamma(\nu_i)} \left(\prod_{i=1}^n \int \mathrm{d}x_i \, x_i^{\nu_i - 1} \right) \left[\sum_{i=1}^n x_i P_i \right]^{-\nu} \delta \left(1 - \sum_{i=1}^n x_i \right) , \tag{3.56}$$

where $\nu = \sum_{i=1}^n \nu_i$. After a suitable shift of the loop momentum k_j, we can use Eq. (2.117) to perform the integration over $\mathrm{d}^D k_j$. After the loop integral is carried out, only scalar products of Δ with the external momentum p or the remaining loop momenta will be left [107], see also [204, 386]. After introducing a Feynman parametrisation, we are frequently faced with integrals of the form

$$I_n = \int \frac{\mathrm{d}^D k}{(2\pi)^D} (\Delta.k + \Delta.q)^n f(k^2) , \tag{3.57}$$

where $n \in \mathbb{N}$, q is any linear combination of momenta which does not involve k and $f(k^2)$ is of the form of the integrand in Eq. (2.117). By splitting up $(\Delta.k + \Delta.q)^n$ using the binomial theorem and explicitly writing out the scalar product $\Delta.k$, we arrive at a sum of tensor integrals

$$I_n = \sum_{j=0}^n \binom{n}{j} (\Delta.q)^{n-j} \left(\prod_{i=1}^j \Delta_{\mu_i} \right) \int \frac{\mathrm{d}^D k}{(2\pi)^D} \left(\prod_{i=1}^j k^{\mu_i} \right) f(k^2) . \tag{3.58}$$

Since Δ is light-like, i.e. $\Delta^2 = 0$, here only the term for $j = 0$ survives and we get

$$I_n = (\Delta.q)^n \int \frac{\mathrm{d}^D k}{(2\pi)^D} f(k^2) . \tag{3.59}$$

3. Calculation of massive operator matrix elements

Repeating the procedure above loop momentum by loop momentum, we solve the D-dimensional integrations over the loop momenta at the cost of introducing integrals over Feynman parameters. The resulting integral representations differ depending on the order in which the loop momenta are integrated. Usually, it is advantageous to start with the simplest subtopologies with the fewest propagators and to perform the loop integrations of more peripheral loops first. If two otherwise equivalent choices exist, we prefer the one where loop momenta not occurring in the operator are integrated out first. In this way, we obtain polynomials in the Feynman parameters which are raised to powers $\gamma = a + \varepsilon b$, where a, b are rational numbers and ε is the dimensional regulator. Moreover, the operator gives rise to polynomials in the Feynman parameters which are raised to integer powers, i.e. the Mellin variable N or the summation indices of the sums from Eqs. (3.4) to (3.7).

Working loop by loop, we introduce a family of Feynman parameters for each loop momentum. If there are p distinct propagators in a ℓ-loop integral, $p + \ell - 1$ Feynman parameters are required this way. The resulting integrals contain ℓ δ-distributions according to Eq. (3.56). Each of them can be used to eliminate one integration over a Feynman parameter by

$$
\int_0^1 dy_1 \ldots \int_0^1 dy_n \int_0^1 dx \, \delta(1 - x - Y) f(x, y_1, \ldots, y_n) =
$$
$$
\int_0^1 dy_1 \ldots \int_0^1 dy_n \, \theta(Y)\theta(1 - Y) f(1 - Y, y_1, \ldots, y_n), \tag{3.60}
$$

where we use the shorthand $Y = \sum_{i=1}^n y_i$. The first step function $\theta(Y)$ does not restrict the region of integration any further and can be dropped. The restriction from the second step function $\theta(1 - Y)$, on the other hand, can be removed by rescaling the integration variables appropriately. Rescaling for example y_1 yields

$$
\int_0^1 dy_1 \ldots \int_0^1 dy_n \, \theta(1 - y_1 - Y_1) f(1 - y_1 - Y_1, y_1, \ldots, y_n) =
$$
$$
\int_0^1 dy_1 \ldots \int_0^1 dy_n \, \theta(1 - Y_1)(1 - Y_1) f((1 - y_1)(1 - Y_1), y_1(1 - Y_1), \ldots, y_n), \tag{3.61}
$$

where

$$
Y_k = \sum_{\substack{i=1 \\ i \neq k}}^n y_i, \quad k \in \mathbb{N}. \tag{3.62}
$$

Recursive application of such rescalings allow us to map the region of integration back to the unit hypercube $[0, 1]^n$ thereby eliminating all step functions. In general, the order in which we rescale the Feynman parameters changes the resulting expression. If we decide to eliminate all δ-distributions and step functions, we are thus faced with three types of choices to make: Choosing the order of integrating the loop momenta, choosing the Feynman parameter for eliminating the δ-distribution and choosing the order of rescalings to reduce the step functions. In addition, it can be useful to leave certain step functions untouched since they can be later on absorbed into the integral representation of Appell hypergeometric functions, which we discuss in the next subsection. All choices obviously lead to equivalent integrals, whose concrete form, however, differs drastically. A set of useful heuristics for obtaining suitable Feynman integrals were formulated in [199, 340]. The aim of these guidelines is to keep the number of Feynman parameters which are raised to powers containing the Mellin parameter N or summation indices to a minimum.

After mapping all integrations over Feynman parameters back to the unit hypercube, it is sometimes advantageous to perform certain transformations which map the region of integration

back onto itself. The simplest example is the mapping $x_i \to 1-x_i'$, whose Jacobian exactly reverts the interchange of integration limits. Two useful transformations involving two parameters were mentioned in [387]. The first one can be used to merge a product xy into a new variable x' by defining

$$x' = xy\,, \qquad x = x' + y' - x'y'\,, \qquad \left|\frac{\partial(x,y)}{\partial(x',y')}\right| = \frac{1-x'}{x'+y'-x'y'}\,. \qquad (3.63)$$
$$y' = \frac{x(1-y)}{x'+y'-x'y'}\,, \qquad y = \frac{x'}{x'+y'-x'y'}\,,$$

This transformation is equivalent to reconstructing and eliminating certain δ-distributions and step functions, see e.g. [199]. It is useful in order to reduce the number of Feynman parameters which are involved in the operator, as in

$$\int_0^1 dx \int_0^1 dy\, (xy)^N f(x,y) = \int_0^1 dx \int_0^1 dy\, \frac{(1-x')x'^N}{x'+y'-x'y'} f\left(x'+y'-x'y', \frac{x'}{x'+y'-x'y'}\right)\,. \qquad (3.64)$$

Moreover, it is sometimes applicable to factor expressions containing $1 - xy$ into expressions involving only x, y, $(1-x)$ and $(1-y)$. Take as an example the expression

$$I = \int_0^1 dx \int_0^1 dy\, x^a (1-x)^b y^c (1-y)^d (1-xy)^e\,, \qquad (3.65)$$

where $a, b, c, d, e \in \mathbb{C}$ such that the integral converges. Applying Eq. (3.63), we obtain

$$I = \int_0^1 dx' \int_0^1 dy'\, x'^c (1-y')^b y'^d (1-x')^{1+b+d+e} (x'+y'-x'y')^{a-c-d-1}\,. \qquad (3.66)$$

Under a transformation $x' \to 1 - x''$ and $y' \to 1 - y''$ the term $x' + y' - x'y'$ becomes $1 - x''y''$. Thus, a simplification occurs if $a = c + b + 1$ and the last term vanishes.

The second transformation from [387] is useful to combine differences of Feynman parameters $x - y$ into a single Feynman parameter. Here we have to distinguish the regions $x > y$ and $x < y$. We split the region of integration accordingly and map the integration back to $[0,1]^2$ in each part. For $x > y$ we use

$$x' = x - y\,, \qquad x = x' + y' - x'y'\,, \qquad \left|\frac{\partial(x,y)}{\partial(x',y')}\right| = 1 - x'\,, \qquad (3.67)$$
$$y' = \frac{y}{1-x+y}\,, \qquad y = (1-x')y'\,,$$

while for $x < y$ the transformation reads

$$x' = y - x\,, \qquad x = (1-x')(1-y')\,, \qquad \left|\frac{\partial(x,y)}{\partial(x',y')}\right| = 1 - x'\,. \qquad (3.68)$$
$$y' = \frac{1-y}{1+x-y}\,, \qquad y = 1 - y'(1-x')\,,$$

A useful application is, for example,

$$\int_0^1 dx \int_0^1 dy\, (x-y)^N f(x,y) = \int_0^1 dx' \int_0^1 dy'\, x'^N (1-x') \Big[f\left(x' + y' - x'y', (1-x')y'\right)$$
$$+ (-1)^N f\left((1-y')(1-x'), 1 - y'(1-x')\right) \Big]\,, \qquad (3.69)$$

which is again useful in order to prevent the proliferation of the Mellin variable N in the integral being considered.

Finally, the resulting Feynman parameter integrals can be solved with the help of special functions, Mellin-Barnes representations and summation techniques. We will discuss these in the following subsections and follow [268].

3.3.2. Hypergeometric function techniques

Having derived a representation in terms of integrals over Feynman parameters, we now have to solve those integrals. We will review the definitions of some special functions which are useful for integrating the Feynman parameters and afterwards illustrate their use by means of several examples. The main idea of the approach described here is to solve the integrals in terms of special functions, which can either be directly expressed as products of Γ-functions or which allow for a convergent series representation which contain Γ-functions. After expanding in ε, the sums are simplified to nested sums and products using the `Mathematica` packages `Sigma`, `HarmonicSums`, `EvaluateMultiSums` and `SumProduction`.

In the easiest case, when one of the Feynman parameters x_i only occurs linearly in one of the polynomials, i.e. as $(y + y'x_i)^a$, where y and y' are polynomials involving other Feynman parameters except x_i, it can be integrated trivially. If a Feynman parameter only occurs in the combination $x^a(1 - x)^b$, we can use the integral representation of the Euler Beta function

$$B(a, b) = \int_0^1 dx\, x^{a-1}(1 - x)^{b-1}\,. \tag{3.70}$$

It converges for $\operatorname{Re} a > 0$ and $\operatorname{Re} b > 0$ in the Riemann-Lebesgue sense, but through analytic continuation it can be extended to the whole complex plane except for non-positive integers a and b. The Beta function is related to the Γ-function through

$$B(a, b) = \frac{\Gamma(a)\Gamma(b)}{\Gamma(a + b)}\,. \tag{3.71}$$

From this relation it becomes obvious that the Beta function has poles at $a, b \in 0, -1, -2, \ldots$ and that expansions around integer values of a and b can be obtained from the expansion of the Γ-function, Eq. (2.120).

In addition to the factors appearing in the Beta integral, we frequently encounter terms of the form $(1 - xz)^\gamma$ where z can consist of one or several further Feynman parameters. These structures can be expressed as a Gauß hypergeometric function $_2F_1$ [211–214, 388],

$$_2F_1 \begin{bmatrix} a, b\,; \\ c\,; \end{bmatrix} = \frac{1}{B(b, c - b)} \int_0^1 dx\, x^{b-1}(1 - x)^{c-b-1}(1 - xz)^{-a}\,. \tag{3.72}$$

For $z = 1$, this immediately simplifies to the Beta integral and we arrive at the Gauß summation theorem [211, 214]

$$_2F_1 \begin{bmatrix} a, b\,; \\ c\,; \end{bmatrix} = \frac{\Gamma(c)\Gamma(c - a - b)}{\Gamma(c - a)\Gamma(c - b)}\,. \tag{3.73}$$

In general, the $_2F_1$ has a series representation

$$_2F_1 \begin{bmatrix} a, b\,; \\ c\,; \end{bmatrix} = \sum_{n=0}^{\infty} \frac{(a)_n (b)_n}{(c)_n} \frac{z^n}{n!}\,, \tag{3.74}$$

which converges for $|z| \leq 1$ and for $z = 1$ if $\operatorname{Re}(c - a - b) > 0$ [211, 214]. Moreover, c may not be a negative integer. The Pochhammer symbol $(a)_n$ appearing in the series is defined as

$$(a)_n = a(a + 1)\ldots(a + n - 1)\,, \quad n \in \mathbb{N}, a \in \mathbb{C} \tag{3.75}$$
$$(a)_0 = 1\,. \tag{3.76}$$

In particular, we see from the definition that $(-a)_n = 0$ for $a \in \mathbb{N}$ and $a < n$. Thus, the series in Eq. (3.74) terminates after a finite number of terms if either a or b are negative integers. For $a \in \mathbb{C} \setminus (-\mathbb{N})$ we can also write

$$(a)_n = \frac{\Gamma(a+n)}{\Gamma(a)} \,. \tag{3.77}$$

If $|z| > 1$ the series in Eq. (3.74) diverges, but we can perform an analytic continuation in z to map for example z to $z/(z-1)$ which maps the interval $[1, \infty]$ to $[0, 1]$. An example for such a continuation is [214]

$$\,_2F_1 \begin{bmatrix} a, b\,; \\ c\,; \end{bmatrix} z = (1-z)^{-a} \,_2F_1 \begin{bmatrix} a, c-b\,; \\ c\,; \end{bmatrix} \frac{z}{z-1} \,. \tag{3.78}$$

Another example for a transformation of the argument is given by [388]

$$\,_2F_1 \begin{bmatrix} a, b\,; \\ c\,; \end{bmatrix} z = \frac{\Gamma(c)\Gamma(c-a-b)}{\Gamma(c-a)\Gamma(c-b)} \,_2F_1 \begin{bmatrix} a, b\,; \\ a+b-c+1\,; \end{bmatrix} 1-z$$
$$+ (1-z)^{c-a-b} \frac{\Gamma(c)\Gamma(a+b-c)}{\Gamma(a)\Gamma(b)} \,_2F_1 \begin{bmatrix} c-a, c-b\,; \\ c-a-b+1\,; \end{bmatrix} 1-z \,, \tag{3.79}$$

which is useful when the argument z contains several Feynman parameters of the form $z = 1 - xy$. They are mapped to $z' = xy$ and point towards generalised hypergeometric functions, which we discuss next.

We generalise the series Eq. (3.74) by introducing more Pochhammer symbols. For $p \in \mathbb{N}$ we write [214]

$$\,_{p+1}F_p \begin{bmatrix} a_1, \ldots, a_{p+1}\,; \\ b_1, \ldots, b_p\,; \end{bmatrix} z = \sum_{n=0}^{\infty} \frac{(a_1)_n \ldots (a_{p+1})_n}{(b_1)_n \ldots (b_p)_n} \frac{z^n}{n!} \,. \tag{3.80}$$

This function is called the generalised hypergeometric function $\,_{p+1}F_p$. The series makes apparent that if any pair of parameters a_i and b_j are identical, they cancel and the function simplifies to a $\,_pF_{p-1}$. For the convergence of the series it is again sufficient that $|z| < 1$ or if $z = 1$ we need

$$\mathrm{Re} \left(\sum_{i=1}^{p} b_i - \sum_{i=1}^{p+1} a_i \right) > 0 \,. \tag{3.81}$$

The generalised hypergeometric function $\,_{p+1}F_p$ permits an integral representation which is constructed recursively from the integral representation of $\,_pF_{p-1}$. This allows us to connect its integral representation to that of the $\,_2F_1$. Each step of the recursion, called Euler transformation, reduces p by one and reads, [214],

$$\,_{p+1}F_p \begin{bmatrix} a_1, \ldots, a_p, c\,; \\ b_1, \ldots, b_{p-1}, d\,; \end{bmatrix} z = \frac{1}{B(c, d-c)} \int_0^1 \mathrm{d}x \, x^{c-1} (1-x)^{d-c-1} \,_pF_{p-1} \begin{bmatrix} a_1, \ldots, a_p\,; \\ b_1, \ldots, b_{p-1}\,; \end{bmatrix} xz \,. \tag{3.82}$$

While solving Feynman parameter integrals, we are frequently faced with polynomials in the Feynman parameters, which can be integrated by this type of recursion.

The Appell functions [214, 235] are a different generalisation of the hypergeometric function. They have two independent variables instead of one. For our purposes, the Appell function of the first kind, F_1, is most useful. It has a double integral representation

$$F_1 \begin{bmatrix} a, b, b'\,; \\ c\,; \end{bmatrix} x, y = \frac{\Gamma(c)}{\Gamma(b)\Gamma(b')\Gamma(c-b-b')} \int_0^1 \mathrm{d}u \int_0^1 \mathrm{d}v \, \theta(1-u-v)$$
$$u^{b-1} v^{b'-1} (1-u-v)^{c-b-b'-1} (1-ux-vy)^{-a} \,, \tag{3.83}$$

3. Calculation of massive operator matrix elements

which involves a step function limiting the region of integration to $u, v \geq 0, u + v \leq 1$. This is the motivation behind the statement in the previous subsection that it is sometimes useful to leave some of the step functions untouched. Appell functions are particularly useful for diagrams where two loop momenta can be integrated completely independently, as for example in ladder diagrams [193, 199, 343]. There is also a one-dimensional integral representation for this function which reads [214]

$$
F_1 \begin{bmatrix} a, b, b' ; \\ c ; \end{bmatrix} x, y = \frac{1}{B(a, c-a)} \int_0^1 \mathrm{d}u \, u^{a-1}(1-u)^{c-a-1}(1-ux)^{-b}(1-uy)^{-b'} . \tag{3.84}
$$

The Appell F_1 function has a series representation given by

$$
F_1 \begin{bmatrix} a, b, b' ; \\ c ; \end{bmatrix} x, y = \sum_{m=0}^{\infty} \sum_{n=0}^{\infty} \frac{(a)_{m+n} \, (b)_m \, (b')_n}{(c)_{m+n}} \frac{x^m}{m!} \frac{y^n}{n!} , \tag{3.85}
$$

which converges for $|x| < 1$ and $|y| < 1$. For $|x| > 1$ and $|y| > 1$ the function can be analytically continued using

$$
F_1 \begin{bmatrix} a, b, b' ; \\ c ; \end{bmatrix} x, y = (1-x)^{-b}(1-y)^{-b'} F_1 \begin{bmatrix} c-a, b, b' ; \\ c ; \end{bmatrix} \frac{x}{x-1}, \frac{y}{y-1} . \tag{3.86}
$$

Examples We now discuss some examples for master integrals which can be solved using the methods described above. For these examples, we will set $\Delta.p = 1$ and $m = 1$ and omit a global factor of $iS_\varepsilon^3/(4\pi)^6$. The first integral we consider is $J_1 = I_{110010111;110}^{\mathrm{B1a}}$ which reads

$$
J_1 = \int \frac{\mathrm{d}^D k_1}{(2\pi)^D} \frac{\mathrm{d}^D k_2}{(2\pi)^D} \frac{\mathrm{d}^D k_3}{(2\pi)^D} \frac{\sum_{j=0}^{N}(\Delta.k_3)^j(\Delta.k_3 - \Delta.k_1)^{N-j}}{P_1 P_2 P_5 P_7 P_8 P_9} , \tag{3.87}
$$

where the propagators P_i are those of family B1a, see Appendix C.

We work loop by loop, dealing with k_1 and k_3 first, which can be integrated independently, and treating the integration over k_2 last. The integral requires five Feynman parameters, which can be brought into the form

$$
J_1 = -\int_0^1 \mathrm{d}x_1 \dots \int_0^1 \mathrm{d}x_5 \, \Gamma\left(-\tfrac{3}{2}\varepsilon\right) x_2^{-1+\varepsilon/2}(1-x_2)^{\varepsilon/2}x_4^{-1-\varepsilon}(1-x_4)^{-\varepsilon}x_5^{\varepsilon}(1-x_5)^{-\varepsilon/2}
$$

$$
\times \sum_{j=0}^{N}[x_3(1-x_4) - x_1(1-x_2) + (x_4 - x_2)(x_1(1-x_5) + x_3 x_5)]^j
$$

$$
\times [x_3(1-x_4) + x_4(x_1(1-x_5) + x_3 x_5)]^{N-j} . \tag{3.88}
$$

The two polynomials which are raised to j and $N - j$ originate from the operator insertion and will be called the operator part in the following. If we were only interested in the case $N = 0$, i.e. the integral without any operator insertion, the integral could be done completely in terms of Beta functions using Eq. (3.70). By repeatedly applying the binomial theorem,

$$
(x + y)^n = \sum_{k=0}^{n} \binom{n}{k} x^k y^{n-k} , \tag{3.89}
$$

to all sums in the operator part we can split everything into Beta-like factors x_i and $1 - x_i$. Of course, each such split introduces a finite sum which has to be performed in the end. Therefore, our goal is to use this this option sparingly and solve as many integrals as possible without

introducing additional sums. As a first step, we reorder the sum from the operator insertion using

$$\sum_{j=0}^{N} A^j B^{N-j} = \frac{A^{N+1} - B^{N+1}}{A - B} = \sum_{j=0}^{N} \binom{N+1}{j}(A-B)^{N-j} B^j \tag{3.90}$$

to eliminate common terms between the two polynomials of the operator part. With this, J_1 reads

$$J_1 = -\int_0^1 dx_1 \dots \int_0^1 dx_5 \, \Gamma\left(-\tfrac{3}{2}\varepsilon\right) x_2^{-1+\varepsilon/2}(1-x_2)^{\varepsilon/2} x_4^{-1-\varepsilon}(1-x_4)^{-\varepsilon} x_5^{\varepsilon}(1-x_5)^{-\varepsilon/2}$$
$$\times \sum_{j=0}^{N} \binom{N+1}{j} \left[x_4(1-x_5)(x_1-x_3)+x_3\right]^j \left[x_2 x_5(x_1-x_3)-x_1\right]^{N-j}. \tag{3.91}$$

Now we use the binomial theorem twice – to split off x_3 and $(-x_1)$, respectively – and we obtain

$$J_1 = -\int_0^1 dx_1 \cdots \int_0^1 dx_5 \, \Gamma\left(-\tfrac{3}{2}\varepsilon\right) \sum_{j=0}^{N}\sum_{k=0}^{j}\sum_{i=0}^{N-j}(-1)^{N-j-i}\binom{N+1}{j}\binom{j}{k}\binom{N-j}{i}$$
$$\times x_1^{N-j-i} x_2^{i-1+\varepsilon/2}(1-x_2)^{\varepsilon/2} x_3^{j-k} x_4^{k-1-\varepsilon}(1-x_4)^{-\varepsilon}$$
$$\times x_5^{i+\varepsilon}(1-x_5)^{k-\varepsilon/2}(x_1-x_3)^{i+k}. \tag{3.92}$$

The integrations over x_2, x_4 and x_5 yield Beta functions and the integration over x_1 and x_3 is done using

$$\int_0^1 dx \int_0^1 dy \; x^{a-1} y^{b-1}(x-y)^{c-1} = \frac{\Gamma(c)}{a+b+c-1}\left(\frac{\Gamma(b)}{\Gamma(b+c)} - (-1)^c \frac{\Gamma(a)}{\Gamma(a+c)}\right), \tag{3.93}$$

which leads to

$$J_1 = -\sum_{j=0}^{N}\sum_{k=0}^{j}\sum_{i=0}^{N-j} \Gamma\left(-\tfrac{3}{2}\varepsilon\right)(-1)^{N-j-i}\binom{N+1}{j}\binom{j}{k}\binom{N-j}{i}\frac{(i+k)!}{N+2}$$
$$\times \left[(-1)^{i+k}\frac{(N-j-i)!}{(N-j+k+1)!} + \frac{(j-k)!}{(i+j+1)!}\right]\Gamma(i+\varepsilon/2)$$
$$\times \Gamma(1+\varepsilon/2)\frac{\Gamma(k-\varepsilon)\Gamma(1-\varepsilon)}{\Gamma(k+1-2\varepsilon)}\frac{\Gamma(k+1-\varepsilon/2)}{\Gamma(i+k+2+\varepsilon/2)}. \tag{3.94}$$

This triple sum can be performed using the summation methods based on difference fields and rings which are implemented in `Sigma` and `EvaluateMultiSums`, together with the routines of `HarmonicSums` to speed up the elimination of relations between harmonic sums. For further details on these packages and the underlying algorithms we refer to [254–257] and the references therein. Up to $\mathcal{O}(\varepsilon^0)$ we obtain

$$J_1 = \frac{1}{N+2}\left\{\frac{1}{\varepsilon^3}\left[-\frac{4}{3}S_1 - \frac{4(2N+3)}{3(N+1)(N+2)} - \frac{4(-1)^N}{3(N+2)}\right] + \frac{1}{\varepsilon^2}\left[\frac{2(4N^2+7N+1)}{3(N+1)(N+2)^2}\right.\right.$$
$$+ (-1)^N \left(\frac{2(2N^3+6N^2+9N+7)}{3(N+1)^2(N+2)^2} - \frac{2S_1}{3(N+2)}\right) - S_1^2 + \frac{2(N-2)(2N+3)}{3(N+1)(N+2)}S_1$$
$$\left.+ S_2 - \frac{4}{3}S_{-2}\right] + \frac{1}{\varepsilon}\left[-\left(\frac{4N^2-6N-1}{3(N+1)^2} + \frac{5}{6}S_2 + \frac{\zeta_2}{2}\right)S_1 + \frac{6N^2+19N+6}{6(N+1)(N+2)}S_1^2\right.$$

$$
\begin{aligned}
&+\left(\frac{2\left(2N^2-5\right)}{3(N+1)(N+2)}-2S_1\right)S_{-2}-\frac{\left(6N^2+17N+16\right)S_2}{6(N+1)(N+2)}-S_{2,1}+\frac{4}{3}S_{-2,1}\\
&+(-1)^N\left(-\frac{4N^5+24N^4+57N^3+60N^2+16N-11}{3(N+1)^3(N+2)^3}-\frac{S_1^2+9S_2+3\zeta_2}{6(N+2)}\right.\\
&+\frac{2N^3+12N^2+21N+13}{3(N+1)^2(N+2)^2}S_1\Bigg)-\frac{8N^5+46N^4+100N^3+104N^2+63N+27}{3(N+1)^3(N+2)^3}\\
&-\frac{7}{18}S_1^3+\frac{2}{9}S_3-\frac{2}{3}S_{-3}-\frac{(2N+3)\zeta_2}{2(N+1)(N+2)}\Bigg]+\left(-\frac{12N^3+50N^2+59N+62}{12(N+1)^2(N+2)}\right.\\
&-\frac{25S_2}{24}-\frac{3\zeta_2}{8}\Bigg)S_1^2+\left(\frac{8N^4+12N^3-22N^2-53N-66}{6(N+1)^3(N+2)}+\frac{\left(10N^2-N-36\right)S_2}{12(N+1)(N+2)}\right.\\
&-2S_3-\frac{3}{2}S_{2,1}+2S_{-2,1}+\frac{(N-2)(2N+3)\zeta_2}{4(N+1)(N+2)}+\frac{7\zeta_3}{6}\Bigg)S_1+\frac{65}{48}S_2^2+\frac{7S_4}{24}-\frac{1}{3}S_{-4}\\
&+\frac{16N^7+140N^6+508N^5+979N^4+1065N^3+623N^2+130N-35}{6(N+1)^4(N+2)^4}+\frac{2}{3}S_{-2,2}\\
&+\left(\frac{2N^2-5}{3(N+1)(N+2)}-S_1\right)S_{-3}-\frac{\left(4N^2+31N+63\right)S_3}{18(N+1)(N+2)}+\frac{\left(2N^2+4N-1\right)S_{2,1}}{2(N+1)(N+2)}\\
&+\left(-\frac{3}{2}S_1^2+\frac{2N^2+2N-3}{(N+1)(N+2)}S_1-\frac{4N^4+12N^3+13N^2+21N+25}{3(N+1)^2(N+2)^2}-\frac{3}{2}S_2\right.\\
&-\frac{\zeta_2}{2}\Bigg)S_{-2}+\left(\frac{12N^4+70N^3+151N^2+178N+102}{12(N+1)^2(N+2)^2}+\frac{3\zeta_2}{8}\right)S_2-\frac{4}{3}S_{-2,1,1}\\
&+\frac{4N^2+7N+1}{4(N+1)(N+2)^2}\zeta_2+\frac{3}{2}S_{3,1}+\frac{2}{3}S_{-3,1}-\frac{2\left(2N^2-5\right)}{3(N+1)(N+2)}S_{-2,1}-\frac{1}{2}S_{2,1,1}\\
&+\frac{7(2N+3)\zeta_3}{6(N+1)(N+2)}+(-1)^N\Bigg[-\frac{S_1^3}{36(N+2)}+\frac{2N^3+12N^2+21N+13}{12(N+1)^2(N+2)^2}S_1^2\\
&-\left(\frac{4N^5+36N^4+129N^3+240N^2+226N+79}{6(N+1)^3(N+2)^3}+\frac{3S_2}{4(N+2)}+\frac{\zeta_2}{4(N+2)}\right)S_1\\
&+\frac{8N^7+72N^6+274N^5+562N^4+656N^3+434N^2+183N+67}{6(N+1)^4(N+2)^4}-\frac{S_{2,1}}{N+2}\\
&+\frac{2N^3+6N^2+9N+7}{4(N+1)^2(N+2)^2}\zeta_2+\frac{6N^3+28N^2+47N+31}{4(N+1)^2(N+2)^2}S_2+\frac{21\zeta_3-25S_3}{18(N+2)}\Bigg]\\
&+\frac{14N^2+59N+30}{36(N+1)(N+2)}S_1^3-\frac{5}{48}S_1^4\Bigg\}.
\end{aligned}
\tag{3.95}
$$

We use the shorthand $S_{\vec{a}}=S_{\vec{a}}(N)$, suppressing the argument N, to compactify the notation. The result is expressed in terms of harmonic sums up to weight $w=4$ and its calculation takes 4828 seconds. The linear term in ε is also required for some diagrams and its calculation takes 50339 seconds. Here harmonic sums up to weight $w=5$ enter.

Next, we consider the master integral $J_2=I_{011011011;100}^{\text{B1a}}$, whose solution involves hypergeometric functions in addition to the Beta functions encountered before. We start from the D-dimensional momentum integral

$$
J_2=\int\frac{\mathrm{d}^Dk_1}{(2\pi)^D}\frac{\mathrm{d}^Dk_2}{(2\pi)^D}\frac{\mathrm{d}^Dk_3}{(2\pi)^D}\frac{(\Delta.k_3-\Delta.k_1)^N}{P_2P_3P_5P_6P_8P_9}.
\tag{3.96}
$$

The propagators P_i refer to family B1a, cf. Appendix C. Working in the order k_2, k_1, k_3, we

arrive at the Feynman parametrisation

$$J_2 = -\int_0^1 dx_1 \ldots \int_0^1 dx_5\ \Gamma\left(-\tfrac{3}{2}\varepsilon\right) x_1^{\varepsilon/2}(1-x_1)^{\varepsilon/2}(1-x_2)^{-1-\varepsilon/2}x_3^{\varepsilon}(1-x_3)^{N-\varepsilon}$$
$$\times\ x_5^{N+1}(1-x_5)^{-1-\varepsilon}(x_4-x_2)^N(1-x_3x_5)^{\frac{3}{2}\varepsilon}\,. \tag{3.97}$$

The integral over x_1 results in a Beta function and the integral over x_4 is trivial. To integrate x_5, we use Eq. (3.72) and obtain a hypergeometric function $_2F_1$

$$J_2 = -\int_0^1 dx_2\int_0^1 dx_3\ \Gamma\left(-\tfrac{3}{2}\varepsilon\right)\frac{\Gamma\left(1+\varepsilon/2\right)^2}{\Gamma(2+\varepsilon)}\left((1-x_2)^{N+1}+(-1)^N x_2^{N+1}\right)$$
$$\times\ \frac{1}{N+1}(1-x_2)^{-1-\varepsilon/2}x_3^{\varepsilon}(1-x_3)^{N-\varepsilon}$$
$$\times\ \frac{\Gamma(N+2)\Gamma(-\varepsilon)}{\Gamma(N+2-\varepsilon)}\,_2F_1\left[\begin{matrix}-\tfrac{3}{2}\varepsilon, N+2\,;\\ N+2-\varepsilon\,;\end{matrix}x_3\right]\,. \tag{3.98}$$

For the integral over x_3 we use the recursive definition of the generalised hypergeometric functions and get a $_3F_2$ function evaluated at argument 1, which however simplifies to a $_2F_1$,

$$_3F_2\left[\begin{matrix}-\tfrac{3}{2}\varepsilon, 1+\varepsilon, N+2\,;\\ N+2, N+2-\varepsilon\,;\end{matrix}1\right]=\,_2F_1\left[\begin{matrix}-\tfrac{3}{2}\varepsilon, 1+\varepsilon\,;\\ N+2-\varepsilon\,;\end{matrix}1\right]\,, \tag{3.99}$$

since two parameters are identical. Now, by using Gauß' theorem, Eq. (3.73), we write the $_2F_1$ in terms of just Γ-functions and finally perform also the integral over x_2. The result reads

$$J_2 = -\Gamma\left(-\tfrac{3}{2}\varepsilon\right)\frac{\Gamma\left(1+\varepsilon/2\right)^2\Gamma(1+\varepsilon)\Gamma(N+1-\varepsilon)\Gamma(-\varepsilon)\Gamma\left(N+1-\varepsilon/2\right)}{\Gamma(2+\varepsilon)\Gamma(N+1-2\varepsilon)\Gamma\left(N+2+\varepsilon/2\right)}$$
$$\times\left(\frac{1}{(N+1)(N+1-\varepsilon/2)}+(-1)^N\frac{\Gamma(N+1)\Gamma\left(-\varepsilon/2\right)}{\Gamma\left(N+2-\varepsilon/2\right)}\right)\,. \tag{3.100}$$

It is valid to all orders in ε and its expansion up to the constant term is

$$J_2 = \frac{1}{(N+1)^2}\left\{\frac{4}{3\varepsilon^3}(-1)^N+\frac{2}{3\varepsilon^2}\left[(-1)^N\left(S_1-2\right)\frac{1}{N+1}\right]+\frac{1}{\varepsilon}\left[\frac{2}{3(N+1)}\right.\right.$$
$$+(-1)^N\left(\frac{4N^2+8N+5}{3(N+1)^2}+\frac{1}{6}S_1^2-\frac{2}{3}S_1+\frac{13}{6}S_2+\frac{\zeta_2}{2}\right)-\frac{4N^2+8N+5}{6(N+1)^3}$$
$$-\frac{4S_2+\zeta_2}{4(N+1)}+(-1)^N\left[\left(\frac{4N^2+8N+5}{6(N+1)^2}+\frac{13}{12}S_2+\frac{\zeta_2}{4}\right)S_1+\frac{1}{36}S_1^3-\frac{1}{6}S_1^2\right.$$
$$\left.-\frac{4N^2+8N+5}{3(N+1)^2}-\frac{13}{6}S_2+\frac{55}{18}S_3-\frac{\zeta_2}{2}-\frac{7}{6}\zeta_3\right]+\varepsilon\left[\frac{4N^2+8N+5}{6(N+1)^3}+\frac{S_2}{N+1}\right.$$
$$+(-1)^N\left[\frac{4N^2+8N+5}{24(N+1)^2}\left(S_1^2-4S_1+13S_2+3\zeta_2\right)+\left(\frac{13}{48}S_2+\frac{\zeta_2}{16}\right)S_1^2-\frac{13}{12}S_1S_2\right.$$
$$+\left(\frac{55}{36}S_3-\frac{\zeta_2}{4}-\frac{7}{12}\zeta_3\right)S_1+\frac{13}{16}\zeta_2S_2+\frac{\left(4N^2+6N+3\right)\left(4N^2+10N+7\right)}{12(N+1)^4}$$
$$+\frac{1}{288}S_1^4-\frac{1}{36}S_1^3+\frac{169}{96}S_2^2-\frac{55}{18}S_3+\frac{241}{48}S_4-\frac{173}{160}\zeta_2^2+\frac{7}{6}\zeta_3\right]-\frac{3S_3}{2(N+1)}$$
$$\left.\left.\left.+\frac{\zeta_2}{4(N+1)}+\frac{7\zeta_3}{12(N+1)}\right]\right\}\,. \tag{3.101}$$

3. Calculation of massive operator matrix elements

The example of master integral J_2 is peculiar in the sense that the result in Eq. (3.100) does not involve any sums. In general, hypergeometric functions arising from this approach will result in infinite sums which requires using the symbolic summation tools mentioned above. An example for such an integral is $J_3 = I^{\text{B5c}}_{110100110;110}$ which reads

$$J_3 = \int \frac{\mathrm{d}^D k_1}{(2\pi)^D} \frac{\mathrm{d}^D k_2}{(2\pi)^D} \frac{\mathrm{d}^D k_3}{(2\pi)^D} \frac{\sum_{j=0}^{N}(\Delta.k_1)^j(\Delta.k_1 - \Delta.k_3)^{N-j}}{P_1 P_2 P_4 P_7 P_8}, \tag{3.102}$$

where the definition of the propagators P_i for family B5c can be found in Appendix C. Note that k_3 only appears in one massive propagator and the operator. Its integration does not require any Feynman parameter. We subsequently integrate k_2 and k_1 and arrive at the following Feynman parametrisation:

$$J_3 = \int_0^1 \mathrm{d}x \int_0^1 \mathrm{d}y \int_0^1 \mathrm{d}z \; \Gamma(-1-\varepsilon/2)\Gamma(-\varepsilon) \sum_{j=0}^{N}(-x)^{N-j}y^{N-j+\varepsilon/2}(1-y)^{-\varepsilon/2}$$

$$\times z^{N-j+1}(1-z)^{-1-\varepsilon/2}(1-xz)^j(1-yz)^\varepsilon. \tag{3.103}$$

We use the binomial theorem to split $(1-xy)^j$ and integrate over x trivially. The integrals over y and z lead to a $_3F_2$ function evaluated at 1 by means of Eq. (3.72) and Eq. (3.82). Thus, we have

$$J_3 = \Gamma(-1-\varepsilon/2)\Gamma(-\varepsilon) \sum_{j=0}^{N}\sum_{k=0}^{j} \frac{(-1)^{N-j+k}}{N-j+k+1}\binom{j}{k}$$

$$\times \frac{\Gamma(N-j+k+2)\Gamma(-\varepsilon/2)}{\Gamma(N-j+k+2-\varepsilon/2)} \frac{\Gamma(N-j+1+\varepsilon/2)\Gamma(1-\varepsilon/2)}{\Gamma(N-j+2)}$$

$$\times \, _3F_2\left[\begin{matrix} -\varepsilon, N-j+1+\frac{\varepsilon}{2}, N-j+k+2 \,; \\ N-j+2, N-j+k+2-\frac{\varepsilon}{2} \,; \end{matrix} 1\right]. \tag{3.104}$$

In contrast to the previous example, this $_3F_2$ does not simply reduce to Γ-functions, but it can be written as a convergent series

$$J_3 = \Gamma(-1-\varepsilon/2)\Gamma(-\varepsilon/2)\Gamma(1-\varepsilon/2) \sum_{j=0}^{N}\sum_{k=0}^{j} \frac{(-1)^{N-j+k}}{N-j+k+1}\binom{j}{k}$$

$$\times \sum_{n=0}^{\infty} \frac{\Gamma(n-\varepsilon)\Gamma(n+N-j+1+\varepsilon/2)\Gamma(n+N-j+k+2)}{n!\,\Gamma(n+N-j+2)\Gamma(n+N-j+k+2-\varepsilon/2)}. \tag{3.105}$$

The expansion in ε and the subsequent simplification of the sums can be done using the routines provided by `EvaluateMultiSums`. It uses `Sigma` to find nested indefinite product-sum expressions for finite sums. First, the infinite sum is treated and simplified as a partial sum, depending on a symbolic upper limit a and finally the limit $a \to \infty$ is performed. Routines for taking limits of harmonic sums and their generalisations are implemented in `HarmonicSums`, which is used internally by `EvaluateMultiSums`. We obtain the result up to the constant term in ε after 3011 seconds in terms of harmonic sums

$$J_3 = \frac{1}{\varepsilon^3}\left[-\frac{4}{(N+1)^2} + \frac{8(-1)^N}{(N+1)^2} - 4S_2 - 8S_{-2}\right] + \frac{1}{\varepsilon^2}\left[\frac{2(N-2)}{(N+1)^3} - \frac{4(-1)^N N}{(N+1)^3} - 4S_1 S_2\right.$$

$$\left. + \frac{2(N-1)}{N+1}S_2 - 6S_3 + \left(\frac{4(N-1)}{N+1} - 8S_1\right)S_{-2} - 4S_{-3} + 4S_{2,1} + 8S_{-2,1}\right]$$

$$
\begin{aligned}
&+ \frac{1}{\varepsilon}\Bigg[\frac{-N^2+N+9}{(N+1)^4} + \frac{2(-1)^N\left(N^2+N-3\right)}{(N+1)^4} + \left(-\frac{3}{2(N+1)^2} + \frac{3(-1)^N}{(N+1)^2} - \frac{3}{2}S_2\right. \\
&- 3S_{-2}\Bigg)\zeta_2 + \left(\frac{2(N-1)}{N+1}S_2 - 6S_3 + 4S_{2,1} + 8S_{-2,1}\right)S_1 - 2S_1^2 S_2 + \frac{3(N-1)}{N+1}S_3 \\
&+ \left(-\frac{4(-1)^N}{(N+1)^2} + \frac{3-N^2}{(N+1)^2}\right)S_2 + 3S_2^2 + 2S_4 + \left(-\frac{8(-1)^N}{(N+1)^2} - \frac{2(N-1)}{N+1} - 4S_1^2\right. \\
&+ \frac{4(N-1)S_1}{N+1} + 4S_2\Bigg)S_{-2} + 4S_{-2}^2 + \left(\frac{2(N-1)}{N+1} - 4S_1\right)S_{-3} + 2S_{-4} + 6S_{3,1} \\
&- \frac{2(N-1)}{N+1}S_{2,1} - \frac{4(N-1)}{N+1}S_{-2,1} + 4S_{-2,2} + 4S_{-3,1} - 4S_{2,1,1} - 8S_{-2,1,1}\Bigg] \\
&+ \frac{(N-4)\left(N^2+4N+6\right)}{2(N+1)^5} + \Bigg[\frac{3(N-2)}{4(N+1)^3} - \frac{3(-1)^N N}{2(N+1)^3} + \frac{3(N-1)S_2}{4(N+1)} - \frac{3}{2}S_1 S_2 \\
&- \frac{9}{4}S_3 + \left(\frac{3(N-1)}{2(N+1)} - 3S_1\right)S_{-2} - \frac{3}{2}S_{-3} + \frac{3}{2}S_{2,1} + 3S_{-2,1}\Bigg]\zeta_2 + \left(\frac{2(-1)^N-1}{2(N+1)^2}\right. \\
&- \frac{1}{2}S_2 - S_{-2}\Bigg)\zeta_3 - \frac{(-1)^N}{(N+1)^5}\left(N^3+2N^2-2N-10\right) + \Bigg[\frac{4(-1)^N}{(N+1)^2}S_2 + 3S_2^2 \\
&+ \frac{N-1}{N+1}\left(3S_3 - 2S_{2,1} - 4S_{-2,1} - S_2\right) + 2S_4 + 6S_{3,1} + 4S_{-2,2} + 4S_{-3,1} - 4S_{2,1,1} \\
&- 8S_{-2,1,1}\Bigg]S_1 + \left(\frac{N-1}{N+1}S_2 - 3S_3 + 2S_{2,1} + 4S_{-2,1}\right)S_1^2 + \left(\frac{2(-1)^N(N+3)}{(N+1)^3}\right. \\
&+ \frac{N^3+N^2-3N-9}{2(N+1)^3} - \frac{4}{3}S_3 - 4S_{2,1} - 12S_{-2,1}\Bigg)S_2 - \frac{2}{3}S_1^3 S_2 - \frac{9}{2}S_5 + 4S_1 S_{-2}^2 \\
&+ \left(\frac{6(-1)^N}{(N+1)^2} + \frac{5-3N^2}{2(N+1)^2}\right)S_3 + \frac{N-1}{N+1}\Bigg[-2S_{-2}^2 - \frac{3}{2}S_2^2 - S_4 + (2S_1-1)S_{-3} \\
&+ \left(1 - 2S_1 + 2S_1^2 - 2S_2\right)S_{-2} - S_{-4} + S_{2,1} + 2S_{-2,1} - 3S_{3,1} - 2S_{-2,2} - 2S_{-3,1} \\
&+ 2S_{2,1,1} + 4S_{-2,1,1}\Bigg] + \Bigg[\frac{4(-1)^N(N+3)}{(N+1)^3} + \left(\frac{8(-1)^N}{(N+1)^2} + 4S_2\right)S_1 - \frac{4}{3}S_1^3 - \frac{8}{3}S_3 \\
&+ 8S_{2,1} - 4S_{-2,1}\Bigg]S_{-2} + \left(\frac{4(-1)^N}{(N+1)^2} - 2S_1^2 + 2S_2\right)S_{-3} + 2S_1 S_{-4} - S_{-5} + 4S_{2,3} \\
&- \frac{4(-1)^N}{(N+1)^2}\left(S_{2,1} + 2S_{-2,1}\right) + 8S_{2,-3} - 3S_{4,1} - 6S_{-2,3} + 8S_{-2,-3} - 2S_{-4,1} + 2S_{2,2,1} \\
&- 8S_{2,1,-2} - 6S_{3,1,1} - 12S_{-2,1,-2} - 4S_{-2,2,1} - 4S_{-3,1,1} + 4S_{2,1,1,1} + 8S_{-2,1,1,1}\,. \quad (3.106)
\end{aligned}
$$

Similar approaches are successful for other master integrals as well. The integration into hypergeometric functions and their generalisations works whenever we can find a way to transform the integrand into a form which can be identified as the integral representation of a generalised hypergeometric function and if the resulting function has a convergent series representation. Instances where this fails have to be treated by other methods, one of which uses Mellin-Barnes integrals. We discuss this in the next subsection.

3.3.3. Mellin-Barnes representations

Mellin-Barnes integrals are complex contour integrals which are closely related to hypergeometric functions [208, 209, 214]. The Gauß' hypergeometric function $_2F_1$ can be written as the complex

3. Calculation of massive operator matrix elements

contour integral,

$$
{}_2F_1 \begin{bmatrix} a, b\,; \\ c\,; \end{bmatrix} = \frac{1}{2\pi i} \frac{\Gamma(c)}{\Gamma(a)\Gamma(b)} \int_{-i\infty}^{i\infty} d\sigma \frac{\Gamma(a+\sigma)\Gamma(b+\sigma)\Gamma(-\sigma)}{\Gamma(c+\sigma)} (-z)^{\sigma}, \tag{3.107}
$$

where the contour stretches from $-i\infty$ to $i\infty$ such that all poles of $\Gamma(a+\sigma)$ and $\Gamma(b+\sigma)$ are to the left of the contour and the poles of $\Gamma(-\sigma)$ are to the right. It can be applied to manipulate hypergeometric functions, but it is also useful for Feynman diagram calculations in the form, see e.g. [389],

$$
\frac{1}{(A+B)^{\lambda}} = \frac{1}{2\pi i} \int_{-i\infty}^{i\infty} d\sigma \frac{\Gamma(-\sigma)\Gamma(\lambda+\sigma)}{\Gamma(\lambda)} \frac{A^{\sigma}}{B^{\lambda+\sigma}} . \tag{3.108}
$$

Again, the poles of $\Gamma(-\sigma)$ should be on the right hand side of the contour and those of $\Gamma(\lambda+\sigma)$ on the left hand side. The connection to Eq. (3.107) can be seen by choosing $a = \lambda$, $b = c$, $z = -A/B$ in Eq. (3.107) and multiplying the expression by $B^{-\lambda}$. The idea behind this formula is to transform sums raised to real powers into products at the cost of introducing a contour integral for each such split. We will apply this technique to Feynman parameter integrals, where A and B are polynomials in the Feynman parameters. After introducing the contour integral, we interchange the order of integration over the complex contour with the integrations over the remaining Feynman parameters. The latter can usually be performed in terms of Beta functions, which in turn can be written as Γ-functions using Eq. (3.71).

To interchange the order of integration, we have to ensure that the result of the Feynman parameter integrals is integrable along the contour. This means that we have to choose the contour such that it separates the poles of Γ-functions in the numerator with argument $z + \sigma$ from those of Γ-functions with $z' - \sigma$, where $z, z' \in \mathbb{C}$ are expressions which can depend on the regulator ε, N and summation parameters. The poles of the former Γ-functions are located at $\sigma = -(z+k), k \in \mathbb{N} \cup \{0\}$ and the poles of the latter are located at $\sigma = z' + k$. In the simplest case there is a straight contour parallel to the imaginary axis which fulfils this condition. In general, however, there can be pairs of Γ-functions with $\mathrm{Re}\, z > \mathrm{Re}\, z'$, which means that the contour has to wind around the poles of these Γ-functions such that it separates the two types of poles. Moreover, it is possible, that there are pairs of Γ-functions $\Gamma(z+\sigma)$ and $\Gamma(z'-\sigma)$ such that in the limit $\varepsilon \to 0$ we get $z \to z'$. One solution in these cases is to fix the integration contour for $\varepsilon \in \mathbb{C} \setminus \{0\}$ and analytically continue to $\varepsilon \to 0$ [389–391]. While bringing $\varepsilon \to 0$, the location of the poles of the Γ-functions changes. Every time a pole crosses the contour, the residue of the integrand at this pole has to be taken and added separately. The `Mathematica` packages `MB` [392] and `MBresolve` [393] offer routines to find contours and perform the analytic continuation. After the analytic continuation, the integrand can be expanded in ε around zero.

Once the contour is fixed and all integrals over Feynman parameters have been performed, the remaining contour integrals have to be carried out. In practice, we can check whether Barnes' lemmas [209, 210, 214] or their corollaries are applicable, see also [389]. For example, Barnes' first lemma states

$$
\frac{1}{2\pi i} \int_{-i\infty}^{i\infty} d\sigma\, \Gamma(\lambda_1+\sigma)\Gamma(\lambda_2+\sigma)\Gamma(\lambda_3-\sigma)\Gamma(\lambda_4-\sigma) =
$$
$$
\frac{\Gamma(\lambda_1+\lambda_3)\Gamma(\lambda_1+\lambda_4)\Gamma(\lambda_2+\lambda_3)\Gamma(\lambda_2+\lambda_4)}{\Gamma(\lambda_1+\lambda_2+\lambda_3+\lambda_4)} . \tag{3.109}
$$

If the lemmas and their corollaries are not applicable, we can close the contour to the left or to the right such that the arc added to the contour does not change the value of the integral. Finally, we apply the residue theorem and take the residues at the poles enclosed by the contour. Since

the Γ-function and its derivatives have poles at zero and all negative integers, taking residues results in infinite sums. These sums are then simplified using the packages `EvaluateMultiSums`, `Sigma` and `HarmonicSums`, as explained in the previous subsection.

Example As an example, we consider the master integral $J_4 = I_{001011011;010}^{\text{B1a}}$, which reads

$$J_4 = \int \frac{\mathrm{d}^D k_1}{(2\pi)^D} \frac{\mathrm{d}^D k_2}{(2\pi)^D} \frac{\mathrm{d}^D k_3}{(2\pi)^D} \frac{(\Delta.k_3)^N}{P_3 P_5 P_6 P_8 P_9} \,. \tag{3.110}$$

For the definition of the propagators P_i for family B1a see Appendix C. We want to calculate this integral up to the quadratic term in ε. Working loop by loop, we choose the order k_2, k_1, k_3 since that way, we integrate the momentum appearing in the operator last and we can integrate two purely massless propagators, P_3 and P_8, first. The resulting Feynman parametrisation is

$$J_4 = \int_0^1 \mathrm{d}w \int_0^1 \mathrm{d}x \int_0^1 \mathrm{d}y \int_0^1 \mathrm{d}z \, \Gamma\left(-1 - \tfrac{3}{2}\varepsilon\right) w^N x^{\varepsilon/2}(1-x)^{\varepsilon/2} y^{1+\varepsilon}(1-y)^{-1-\varepsilon}$$
$$\times z^{N+1}(1-z)^{-2-\varepsilon}(1-yz)^{1+\frac{3}{2}\varepsilon} \,. \tag{3.111}$$

If we try to integrate this using hypergeometric functions, as outlined above, we arrive at

$$J_4 = \frac{\Gamma\left(-1 - \tfrac{3}{2}\varepsilon\right)}{N+1} \Gamma(1+\varepsilon/2)^2 \Gamma(-\varepsilon) \frac{\Gamma(N+2)\Gamma(-1-\varepsilon)}{\Gamma(N+1-\varepsilon)} {}_3F_2\left[\begin{matrix} N+2, -1-\tfrac{3}{2}\varepsilon, 2+\varepsilon\,; \\ N+1-\varepsilon, 2\,; \end{matrix} 1\right]. \tag{3.112}$$

The condition Eq. (3.81) for the convergence of the series representation of the ${}_3F_2$ is not met and we instead use a Mellin-Barnes representation. Starting again from Eq. (3.111), the integrals over w and x are performed as before and we make the change of variables $z \to 1-z$. This leaves us with

$$J_4 = \int_0^1 \mathrm{d}y \int_0^1 \mathrm{d}z \, \frac{\Gamma\left(-1 - \tfrac{3}{2}\varepsilon\right)}{N+1} \frac{\Gamma(1+\varepsilon/2)^2}{\Gamma(2+\varepsilon)} \frac{y^{1+\varepsilon}(1-y)^{-1-\varepsilon} z^{-2-\varepsilon}(1-z)^{N+1}}{(1-y+zy)^{-1-\frac{3}{2}\varepsilon}} \,. \tag{3.113}$$

We split $(1-y+zy)^{-1-3\varepsilon/2}$ using Eq. (3.108) and solve the integrations over y and z in terms of Beta functions. Thus, we arrive at a single contour integration

$$J_4 = \frac{1}{2\pi i} \int_{\gamma-i\infty}^{\gamma+i\infty} \mathrm{d}\sigma \, \Gamma(-\sigma) \Gamma\left(\sigma - 1 - \tfrac{3}{2}\varepsilon\right) \frac{\Gamma\left(1+\varepsilon/2\right)^2}{\Gamma(2+\varepsilon)} \frac{\Gamma(\sigma+2+\varepsilon)\Gamma\left(-\sigma+1+\varepsilon/2\right)}{\Gamma\left(3+\tfrac{3}{2}\varepsilon\right)}$$
$$\times \frac{\Gamma(\sigma-1-\varepsilon)\Gamma(N+1)}{\Gamma(\sigma+N+1-\varepsilon)} \,, \tag{3.114}$$

where the integration contour runs parallel to the imaginary axis and crosses the real axis at $\gamma \in \mathbb{R}$. The task is now to find values for ε and γ such that the condition that all poles of $\Gamma(\sigma - 1 - 3/2\varepsilon)$, $\Gamma(\sigma + 2 + \varepsilon)$ and $\Gamma(\sigma - 1 - \varepsilon)$ are left of the contour and those of $\Gamma(-\varepsilon)$ and $\Gamma(-\sigma + 1 + \varepsilon/2)$ are right of it. This task can be automated using the `Mathematica` package MB [392] and for the problem at hand we find $\gamma = -\tfrac{1}{8}$ and $\varepsilon = -\tfrac{13}{8}$. The integrand now has to be analytically continued to $\varepsilon \to 0$, taking the residue at each pole of the Γ-functions in the integrand which crosses the contour during this process. Here we have to add the residues at $\sigma = 1 + \tfrac{3}{2}\varepsilon$, $\sigma = \tfrac{3}{2}\varepsilon$, $\sigma = 1 + \varepsilon$ and $\sigma = \varepsilon$. The MB package automates also this step. After the analytic continuation, the integrand can be expanded in ε. We obtain the following expression

$$J_4 = J_4' + \frac{\Gamma\left(1+\tfrac{\varepsilon}{2}\right)^2 \Gamma(-\varepsilon)}{\Gamma(2+\varepsilon)\Gamma\left(3+\tfrac{3\varepsilon}{2}\right)} \left[-\Gamma(2+2\varepsilon)\left(\frac{2\Gamma\left(-\tfrac{\varepsilon}{2}\right)^2}{N+1} + \Gamma\left(-1-\tfrac{\varepsilon}{2}\right)\Gamma\left(1-\tfrac{\varepsilon}{2}\right)\right)\right.$$
$$\left. + \Gamma(N+1)\Gamma\left(\tfrac{\varepsilon}{2}\right)\left(\frac{\Gamma\left(-1-\tfrac{3}{2}\varepsilon\right)\Gamma\left(3+\tfrac{5}{2}\varepsilon\right)}{\Gamma\left(N+2+\tfrac{\varepsilon}{2}\right)} - \frac{4\Gamma\left(1-\tfrac{3}{2}\varepsilon\right)\Gamma\left(2+\tfrac{5}{2}\varepsilon\right)}{3(\varepsilon-2)\Gamma\left(N+1+\tfrac{\varepsilon}{2}\right)}\right)\right]. \tag{3.115}$$

3. Calculation of massive operator matrix elements

The second term corresponds to the sum of residues which arise in the process of analytic continuation, while the first term J_4' is the contour integral, given after expansion in ε by

$$
J_4' = \frac{1}{2\pi i} \int_{\gamma-i\infty}^{\gamma+i\infty} d\sigma \; \frac{\Gamma(N+1)\Gamma(1-\sigma)\Gamma(\sigma-1)^2\Gamma(-\sigma)\Gamma(\sigma+2)}{\Gamma(\sigma+N+1)} \left[\frac{1}{2} \right.
$$

$$
+ \varepsilon \left(\frac{1}{2}\psi(\sigma+N+1) + \frac{1}{4}\psi(1-\sigma) - \frac{5}{4}\psi(\sigma-1) + \frac{1}{2}\psi(\sigma+2) - \frac{13}{8} \right)
$$

$$
+ \varepsilon^2 \left(\frac{1}{4}\psi(1-\sigma)\psi(\sigma+N+1) + \frac{1}{4}\psi(\sigma+N+1)^2 + \frac{1}{4}\psi'(\sigma+2) \right.
$$

$$
+ \frac{1}{2}\psi(\sigma+2)\psi(\sigma+N+1) - \frac{13}{8}\psi(\sigma+N+1) - \frac{1}{4}\psi'(\sigma+N+1)
$$

$$
+ \frac{1}{16}\psi(1-\sigma)^2 - \frac{5}{8}\psi(\sigma-1)\psi(1-\sigma) + \frac{1}{4}\psi(\sigma+2)\psi(1-\sigma)
$$

$$
- \frac{13}{16}\psi(1-\sigma) + \frac{25}{16}\psi(\sigma-1)^2 + \frac{1}{4}\psi(\sigma+2)^2 + \frac{65}{16}\psi(\sigma-1)
$$

$$
- \frac{5}{4}\psi(\sigma-1)\psi(\sigma+2) - \frac{13}{8}\psi(\sigma+2) + \frac{1}{16}\psi'(1-\sigma) + \frac{13}{16}\psi'(\sigma-1)
$$

$$
\left. \left. - \frac{5}{4}\psi(\sigma-1)\psi(\sigma+N+1) - \frac{11}{96}\pi^2 + \frac{115}{32} \right) + \mathcal{O}(\varepsilon^3) \right]. \tag{3.116}
$$

Here $\psi(z)$ and $\psi^{(k)}(z), k \in \mathbb{N}$ denote the polygamma function and its derivatives

$$
\psi(z) = \frac{1}{\Gamma(z)}\frac{d}{dz}\Gamma(z), \qquad\qquad \psi^{(k)}(z) = \frac{d^k}{dz^k}\psi(z). \tag{3.117}
$$

The contour integral over $d\sigma$ can be performed by closing the contour in the left or right half plane and summing the residues of the integrand at all enclosed poles. We choose to close the contour to the right: Closing it to the left requires to take the residues at $\sigma = -k$, where $k \geq 1, k \in \mathbb{N}$, and we would have to distinguish the cases $k \leq N$ and $k > N$ since $\Gamma(\sigma+N+1)$ and $\psi(\sigma+N+1)$ develop poles only in the latter case. To close the contour to the right, we have to take residues at $\sigma = k, k \in \mathbb{N} \cup \{0\}$. We obtain

$$
J_4' = a_0 + a_1 + \sum_{k=2}^{\infty} \frac{(k+1)\Gamma(k-1)\Gamma(N+1)}{2(k-1)\Gamma(k+N+1)} \left(b_0 + \varepsilon b_1 + \varepsilon^2 b_2 \right), \tag{3.118}
$$

where a_0 and a_1 are the lowest two residues at $\sigma = 0, 1$, which have to be taken separately, and b_0, b_1 and b_2 are given by

$$
b_0 = S_1(k+N) - S_1(k) + \frac{2k^2+3k-1}{(k-1)k(k+1)}, \tag{3.119}
$$

$$
b_1 = \left(\frac{13k^3-26k^2-25k+10}{4(k-1)k(k+1)} \right)(S_1(k) - S_1(k+N)) - \frac{3}{2}S_1(k+N)S_1(k) - \frac{3}{4}S_2(k)
$$

$$
+ \frac{3}{4}S_2(k+N) + \frac{3}{4}S_1(k+N)^2 + \frac{3}{4}S_1(k)^2 - \frac{26k^4-47k^3-64k^2+51k-14}{4(k-1)^2k^2(k+1)}, \tag{3.120}
$$

$$
b_2 = \frac{39k^3-70k^2-63k+26}{16(k-1)k(k+1)} \left[2S_1(k)S_1(k+N) - S_2(k+N) - S_1(k)^2 - S_1(k+N)^2 \right]
$$

$$
- \frac{7}{8}S_1(k+N)^2S_1(k) + \frac{7}{8}S_1(k+N)S_1(k)^2 + \frac{39k^3-118k^2-135k+50}{16(k-1)k(k+1)}S_2(k)
$$

$$
+ \frac{115k^5-453k^4+471k^3+341k^2-310k+84}{16(k-1)^2k^2(k+1)} \left[S_1(k+N) - S_1(k) \right]
$$

$$+ \left(\frac{7}{8} S_2(k+N) - \frac{19}{8} S_2(k) + \frac{3}{8} \zeta_2 \right) \left[S_1(k+N) - S_1(k) \right] + \frac{7}{24} S_1(k+N)^3$$

$$+ \frac{7}{12} S_3(k+N) - \frac{7}{24} S_1(k)^3 - \frac{43}{12} S_3(k) + \frac{3\left(2k^2 + 3k - 1\right)}{8(k-1)k(k+1)} \zeta_2 + 3\zeta_3$$

$$+ \frac{230k^6 - 895k^5 + 937k^4 + 725k^3 - 1071k^2 + 598k - 124}{16(k-1)^3 k^3 (k+1)} . \tag{3.121}$$

The summation over k can be performed using `EvaluateMultiSums` and within 160 seconds we obtain the result for J_4,

$$J_4 = \frac{1}{N+1} \Bigg\{ \frac{8}{3\varepsilon^3} + \frac{1}{\varepsilon^2} \left[\frac{N^2 - 9N - 8}{3(N+1)} + \frac{2}{3} S_1 \right] + \frac{1}{\varepsilon} \Bigg[\frac{N^2 - 2}{3(N+1)} S_1 - \frac{1}{6} S_1^2 - \frac{1}{6} S_2 + \zeta_2$$

$$- \frac{19N^3 + 18N^2 - 13N - 8}{12(N+1)^2} \Bigg] + S_{2,1} + \frac{2N^2 + 9N + 2}{12(N+1)} \left(S_1^2 + S_2 \right) + \frac{N^2 - 9N - 8}{8(N+1)} \zeta_2$$

$$+ \left(-\frac{19N^3 + 60N^2 + 59N + 16}{12(N+1)^2} - \frac{5}{12} S_2 + \frac{\zeta_2}{4} \right) S_1 - \frac{5}{36} S_1^3 - \frac{5}{18} S_3 - \frac{7}{3} \zeta_3$$

$$+ \frac{229N^4 + 835N^3 + 1119N^2 + 665N + 160}{48(N+1)^3} + \varepsilon \Bigg[\frac{N^2 - 2}{2(N+1)} S_{2,1} - \frac{1}{2} S_{3,1} + \frac{5}{2} S_{2,1,1}$$

$$+ \left(\frac{N^2 - 2}{8(N+1)} \zeta_2 + \frac{229N^4 + 1039N^3 + 1749N^2 + 1289N + 346}{48(N+1)^3} - \frac{13}{36} S_3 - \frac{7}{12} \zeta_3 \right.$$

$$\left. - \frac{1}{2} S_{2,1} \right) S_1 + \frac{4N^2 + 27N + 10}{72(N+1)} \left(3S_1 S_2 + S_1^3 + 2S_3 \right) - \frac{7\left(N^2 - 9N - 8\right)}{24(N+1)} \zeta_3$$

$$- \frac{19N^3 + 18N^2 - 13N - 8}{32(N+1)^2} \zeta_2 - \left(\frac{19N^3 + 81N^2 + 95N + 28}{24(N+1)^2} + \frac{13}{48} S_2 + \frac{\zeta_2}{16} \right) S_1^2$$

$$- \left(\frac{19N^3 + 81N^2 + 95N + 28}{24(N+1)^2} + \frac{\zeta_2}{16} \right) S_2 - \frac{13}{288} S_1^4 - \frac{37}{96} S_2^2 - \frac{25}{48} S_4 - \frac{173}{80} \zeta_2^2$$

$$- \frac{2239N^5 + 11312N^4 + 22366N^3 + 21592N^2 + 10171N + 1888}{192(N+1)^4} \Bigg]$$

$$+ \varepsilon^2 \Bigg[- \left(\frac{29}{288} S_2 + \frac{5}{96} \zeta_2 \right) S_1^3 - \frac{38N^3 + 183N^2 + 226N + 68}{144(N+1)^2} \left(S_1^3 + 3S_1 S_2 + 2S_3 \right)$$

$$- \frac{29}{2880} S_1^5 + \frac{2N^2 + 9N + 2}{32(N+1)} \left(\zeta_2 S_1^2 + 8S_1 S_{2,1} + 8S_{3,1} \right) - \frac{173\left(N^2 - 9N - 8\right)}{640(N+1)} \zeta_2^2$$

$$+ \left(\frac{7}{48} \zeta_3 - \frac{29}{144} S_3 - \frac{5}{8} S_{2,1} \right) S_1^2 + \frac{56N^2 + 279N + 74}{192(N+1)} S_2^2 - \frac{179}{120} S_5 + \frac{7}{4} S_{2,3}$$

$$+ \frac{8N^2 + 63N + 26}{576(N+1)} \left(S_1^4 + 6S_1^2 S_2 + 8S_1 S_3 \right) + \left(-\frac{5}{4} S_{3,1} - \frac{5}{32} \zeta_2 S_2 - \frac{7\left(N^2 - 2\right)}{24(N+1)} \zeta_3 \right.$$

$$- \frac{2239N^5 + 12560N^4 + 28096N^3 + 31330N^2 + 17401N + 3838}{192(N+1)^4} - \frac{149}{192} S_2^2$$

$$- \frac{173}{320} \zeta_2^2 - \frac{89}{96} S_4 + \frac{7}{4} S_{2,1,1} \Bigg) S_1 - \frac{19N^3 + 60N^2 + 59N + 16}{32(N+1)^2} \left(\zeta_2 S_1 + 4S_{2,1} \right)$$

$$- \frac{N^2 + 18N + 10}{4(N+1)} S_{2,1,1} + \frac{229N^4 + 1141N^3 + 2064N^2 + 1601N + 439}{96(N+1)^3} \left(S_1^2 + S_2 \right)$$

$$+ \frac{7\left(19N^3 + 18N^2 - 13N - 8\right)}{96(N+1)^2} \zeta_3 + \frac{32N^2 + 171N + 50}{96(N+1)} S_4 + \frac{1}{2} S_{4,1} - \frac{1}{4} S_{2,2,1}$$

$$+\left(\frac{229N^4 + 835N^3 + 1119N^2 + 665N + 160}{128(N+1)^3} - \frac{7}{8}\zeta_3\right)\zeta_2 + \frac{7}{4}S_{3,1,1} + \frac{1}{4}S_{2,1,1,1}$$

$$-\frac{5}{48}\zeta_2 S_3 + \frac{3}{8}\zeta_2 S_{2,1} + \left(\frac{7}{48}\zeta_3 - \frac{209}{144}S_3 + \frac{9}{8}S_{2,1} + \frac{2N^2 + 9N + 2}{32(N+1)}\zeta_2\right)S_2 - \frac{239}{20}\zeta_5$$

$$+\frac{19405}{768}N - \frac{455}{64(N+1)} - \frac{41}{32(N+1)^2} - \frac{1}{16(N+1)^3} + \frac{1}{12(N+1)^4} + \frac{5407}{192}$$

$$\left.\left.+\frac{1}{24(N+1)^5}\right]\right\}. \tag{3.122}$$

Note that instead of using Mellin-Barnes, we can also obtain the same result by applying the transformation in Eq. (3.63) to z and y, which maps $(1-yz)^{1+\frac{3}{2}\varepsilon}$ to $(1-z')^{1+\frac{3}{2}\varepsilon}$. At the same time the operator part becomes more complicated, but it can be brought into the form $(1-y'z')^N$. Here we can apply the binomial theorem and perform all integrations in terms of Beta functions. The resulting finite sum can be dealt with using `EvaluateMultiSums` and yields the same result as the approach via Mellin-Barnes.

3.3.4. Differential and difference equations

Another powerful method for solving master integrals is the differential equation method [264–268]. It is based on the fact that derivatives of dimensionally regularised Feynman integrals with respect to masses or external kinematic invariants are expressible as linear combinations of Feynman integrals where some of the propagators are raised to different powers, written schematically for a ℓ-loop integral with n propagators as

$$\frac{d}{dx}\int\frac{d^D k_1}{(2\pi)^D}\cdots\int\frac{d^D k_\ell}{(2\pi)^D}\frac{1}{P_1^{\nu_1}\ldots P_n^{\nu_n}} = \sum_{\vec{\nu}'}c_{\vec{\nu}'}\int\frac{d^D k_1}{(2\pi)^D}\cdots\int\frac{d^D k_\ell}{(2\pi)^D}\frac{1}{P_1^{\nu_1'}\ldots P_n^{\nu_n'}}, \tag{3.123}$$

where x denotes some kinematic invariant or mass, $P_i = (p_i^2 - m_i^2)$ are inverse propagators and the ν_i are the powers to which the propagators are raised. The sum over $\vec{\nu}'$ ranges over a finite number of propagator exponents. The coefficients $c_{\vec{\nu}'}$ are rational functions in the space-time dimension D and the kinematic invariants. This approach uses the property of dimensionally regularised integrals, that the differentiation with respect to external momenta and masses can be performed on the integrand, cf. for example [285, 389, 394]. If we take derivatives of master integrals, in general, the Feynman integrals on the right hand side will not be master integrals, but using integration-by-parts identities they can be reduced to master integrals again. In this way, we can derive coupled systems of linear, first-order ordinary differential equations. Together with suitable initial conditions, the integrals can now be obtained as solutions to the differential equations. In this subsection we will review how the method of differential equations can be applied to solve master integrals for the OMEs [268, 340, 395–397].

By construction, the systems of differential equations derived via IBP relations exhibit a hierarchical structure. As explained in Section 3.1, each master integral belongs to an integral family. The completeness property of integral families guarantees that all scalar products of internal and external momenta can be expressed as linear combinations of inverse propagators from that family. Taking derivatives with respect to masses or external kinematic invariants raises the powers of propagators and introduces scalar products of momenta in the numerator, which can be expressed as inverse propagators. Therefore, taking derivatives can only lower the power of propagators or introduce inverse propagators in the numerator, but it cannot introduce new propagators in the denominator. Thus, the integrals on the right-hand side must be from the same sector as the original integral or subsectors thereof – recall that the sector of an integral is defined by the set of propagators in its denominator. The Laporta algorithm presupposes an order on the

scalar integrals which orders the integrals by their "complexity." Upon inserting the reductions to master integrals on the right-hand side, this induces a hierarchical structure of the coupled systems: The linear combination on the right-hand side is spanned by master integrals from the same sector and "simpler" integrals according to the ordering. The corresponding homogeneous system is almost triangular, except for couplings within each sector. Schematically, the structure of the system can be illustrated as

$$
\begin{pmatrix} I_1' \\ I_2' \\ I_3' \\ I_4' \\ I_5' \\ I_6' \\ I_7' \\ \vdots \end{pmatrix} = \begin{pmatrix} \boxed{\begin{matrix} * & * \end{matrix}} & 0 & 0 & 0 & 0 & 0 & \\ \boxed{\begin{matrix} * & * \end{matrix}} & 0 & 0 & 0 & 0 & 0 & \\ * & * & \boxed{*} & 0 & 0 & 0 & 0 & \\ * & * & * & \boxed{\begin{matrix} * & * & * \end{matrix}} & 0 & \cdots \\ * & * & * & \boxed{\begin{matrix} * & * & * \end{matrix}} & 0 \\ * & * & * & \boxed{\begin{matrix} * & * & * \end{matrix}} & 0 \\ * & * & * & * & * & * & \boxed{*} \\ & & & \vdots & & & & \ddots \end{pmatrix} \begin{pmatrix} I_1 \\ I_2 \\ I_3 \\ I_4 \\ I_5 \\ I_6 \\ I_7 \\ \vdots \end{pmatrix} + \begin{pmatrix} R_1 \\ R_2 \\ R_3 \\ R_4 \\ R_5 \\ R_6 \\ R_7 \\ \vdots \end{pmatrix} , \tag{3.124}
$$

where we number the master integrals as $I_i, i \in \mathbb{N}$, the derivatives of the master integrals are denoted by I_i' and the asterisks denote possibly non-vanishing entries in the coefficient matrix. The $R_i, i \in \mathbb{N}$ are inhomogeneities which are linear combinations of already known master intgrals. For this example we assume that the master integrals are orderd according to their complexity and that they are grouped into sectors as $\{I_1, I_2\}$, $\{I_3\}$, $\{I_4, I_5, I_6\}$ and $\{I_7\}$. The boxes mark the homogeneous part of the subsystem of differential equations for each sector. Due to this hierarchical structure, the system can be solved sector by sector, solving the simplest sector first. For each sector we treat the integrals from simpler sectors, to the left of the marked boxes, as inhomogeneities in addition to the R_i.

To compute some Feynman diagrams up to the constant term in ε, we have to calculate the master integrals up to a certain order in ε, which can be higher than $\mathcal{O}(\varepsilon^0)$ if the coefficient of the master integral contains poles in ε. In addition, the required order for a master integral can be even higher, if it enters the differential equations of another master integral as an inhomogeneity and the corresponding coefficient also contains a pole in ε.

The master integrals for the OMEs depend on the heavy quark mass m^2 and the scalar product $\Delta.p$. However, the functional dependence on both variables is trivial, since they factor out for each integral

$$
I_i(m^2, \Delta.p, N) = (m^2)^{-\nu + \frac{3}{2}D}(\Delta.p)^N \tilde{I}_i(N) , \tag{3.125}
$$

where ν is the sum of powers of the propagators and $\tilde{I}_i(N)$ is independent of m^2 and $\Delta.p$. Differential equations with respect to either variable would only recover the dependence above and would require calculating the $\tilde{I}_i(N)$ for general N as initial conditions. But those functions are exactly what is difficult to calculate. Due to this trivial dependence, we will set both $m^2 = 1$ and $\Delta.p = 1$ for the discussions in this section. Their dependence can always be reconstructed according to Eq. (3.125). Taking derivatives with respect to the Mellin variable N would yield logarithms like

$$
\frac{\mathrm{d}}{\mathrm{d}N}(\Delta.k_i)^N = (\Delta.k_i)^N \ln(\Delta.k_i) \tag{3.126}
$$

in the integrand, so that the right-hand side cannot be reexpressed as Feynman integrals as discussed above. However, we can resort to the generating functions, which we already introduced in Eqs. (3.8) to (3.12) for deriving the IBP relations. The integrands of the master integrals in generating function representations contain linear propagators which depend on the tracing

variable t. Taking derivatives with respect to t raises the power of the linear propagators and introduces the scalar product into the numerator, as for example in

$$\frac{\mathrm{d}}{\mathrm{d}t} \frac{1}{1 - t\Delta.k_1} = \frac{\Delta.k_1}{(1 - t\Delta.k_1)^2} . \tag{3.127}$$

In this representation, we can apply the approach outlined above, reduce the right-hand side to master integrals and find solutions to the differential equations as functions of t. For practical calculations, we use the feature of `Reduze 2`, that the differential equations can be calculated directly by `Reduze 2`.

Instead of solving the differential equations directly, we will make use of the fact that the master integrals are power series in t by construction, and we will derive systems of difference equations, which we uncouple the system to a scalar recurrence and then solve using the algorithm worked out in [398] and implemented in the packages `Sigma` [241, 252, 253] and `SumProduction` [254–257]. As the result, we obtain the master integrals as functions of the Mellin variable N. In the following, we outline the steps of the approach and give some examples. First, we discuss how to deal with an individual sector, assuming that all master integrals from simpler sectors are already known and in a second step, we describe how to solve the hierarchical system sector by sector.

Solving a single sector

In general, if a sector contains more than one master integral, the differential equations for these master integrals are coupled. The right hand side of the differential equations also depend on master integrals from simpler sectors. Suppose that we have a sector containing n master integrals $I_1, \ldots I_n$. The differential equations can be written as

$$\frac{\mathrm{d}I_i(t,\varepsilon)}{\mathrm{d}t} = \sum_{j=1}^{n} A_{ij}(t,\varepsilon)I_j(t,\varepsilon) + \sum_{j=1}^{m} C_j(t,\varepsilon)B_j(t,\varepsilon), \quad i \in \{1, \ldots, n\}. \tag{3.128}$$

The coefficients $A_{ij}(t,\varepsilon)$ and $C_j(t,\varepsilon)$ are rational functions in the dimensional regulator ε and the tracing variable t. We will call the master integrals $I_i(t,\varepsilon)$ belonging to the sector under consideration *unknown integrals* and the master integrals $B_j(t,\varepsilon)$ from simpler sectors *base case integrals*. We assume that the base case integrals have already been solved before and we treat them as inhomogeneities of the differential equation.

To illustrate the discussion below, we will use a sector with three master integrals as an example. The integrals are

$$I_1(t,\varepsilon) = I^{\text{B3a}}_{010110110;100} = \int \frac{\mathrm{d}^D k_1}{(2\pi)^D} \frac{\mathrm{d}^D k_2}{(2\pi)^D} \frac{\mathrm{d}^D k_3}{(2\pi)^D} \frac{1}{P_2 P_4 P_5 P_7 P_8 P_{10}}, \tag{3.129}$$

$$I_2(t,\varepsilon) = I^{\text{B3a}}_{020110110;100} = \int \frac{\mathrm{d}^D k_1}{(2\pi)^D} \frac{\mathrm{d}^D k_2}{(2\pi)^D} \frac{\mathrm{d}^D k_3}{(2\pi)^D} \frac{1}{P_2^2 P_4 P_5 P_7 P_8 P_{10}}, \tag{3.130}$$

$$I_3(t,\varepsilon) = I^{\text{B3a}}_{010210110;100} = \int \frac{\mathrm{d}^D k_1}{(2\pi)^D} \frac{\mathrm{d}^D k_2}{(2\pi)^D} \frac{\mathrm{d}^D k_3}{(2\pi)^D} \frac{1}{P_2 P_4^2 P_5 P_7 P_8 P_{10}}. \tag{3.131}$$

The definition of the propagators of family B3a is given in Appendix C. Our goal is to compute the coefficients of their Laurent expansion in ε up to some order $\varepsilon^k, k \in \mathbb{Z}$. Here the integrals I_1, I_2 and I_3 are required up to $\mathcal{O}(\varepsilon^2)$, $\mathcal{O}(\varepsilon^3)$ and $\mathcal{O}(\varepsilon^3)$, respectively. The system of differential equations for this sector has the form

$$\frac{\mathrm{d}}{\mathrm{d}t} \begin{pmatrix} I_1(t,\varepsilon) \\ I_2(t,\varepsilon) \\ I_3(t,\varepsilon) \end{pmatrix} = A(t,\varepsilon) \begin{pmatrix} I_1(t,\varepsilon) \\ I_2(t,\varepsilon) \\ I_3(t,\varepsilon) \end{pmatrix} + \begin{pmatrix} R_1(t,\varepsilon) \\ R_2(t,\varepsilon) \\ -R_2(t,\varepsilon) \end{pmatrix}, \tag{3.132}$$

where coefficient matrix for the homogeneous part reads

$$A(t,\varepsilon) = \begin{pmatrix} \dfrac{1+\varepsilon-t}{(t-1)t} & \dfrac{-2}{(t-1)t} & 0 \\[2mm] \dfrac{\varepsilon(3\varepsilon+2)}{4(t-1)} & \dfrac{2+\varepsilon-3t-3\varepsilon t}{2(t-1)t} & -\dfrac{\varepsilon+1}{2(t-1)} \\[2mm] \dfrac{-\varepsilon(3\varepsilon+2)(t-2)}{4(t-1)t} & \dfrac{-2-5\varepsilon+t+3\varepsilon t}{2(t-1)t} & \dfrac{(-2\varepsilon-t+\varepsilon t)}{2(t-1)t} \end{pmatrix} \tag{3.133}$$

and the inhomogeneities are written in terms of the already known base case integrals $B_1(t,\varepsilon)$ to $B_4(t,\varepsilon)$,

$$R_1(t,\varepsilon) = \frac{B_4(t,\varepsilon)}{(t-1)t}, \tag{3.134}$$

$$R_2(t,\varepsilon) = -\frac{(\varepsilon+2)^3}{16(\varepsilon+1)(t-1)t}B_1(t,\varepsilon) + \frac{(\varepsilon+2)(3\varepsilon+4)\left(19\varepsilon^2+36\varepsilon+16\right)}{16\varepsilon(5\varepsilon+6)(t-1)t}B_2(t,\varepsilon)$$

$$+ \frac{(\varepsilon+1)^2(3\varepsilon+4)^2}{2\varepsilon(5\varepsilon+6)t}B_3(t,\varepsilon) + \frac{-24-50\varepsilon-25\varepsilon^2+8t+14\varepsilon t+6\varepsilon^2 t}{4(5\varepsilon+6)(t-1)t}B_4(t,\varepsilon). \tag{3.135}$$

Below, we will suppress the dependence on ε of the integrals to shorten the notation. In this example the base case integrals are

$$B_1 = I^{\text{B1a}}_{000011100;000}, \quad B_2 = I^{\text{B1a}}_{101001100;000}, \quad B_3 = I^{\text{B1a}}_{001001011;010}, \quad B_4 = I^{\text{B1a}}_{002001011;010}. \tag{3.136}$$

The first two integrals are constants, independent of t, since they do not have any linear propagator.

Since our goal is to apply the recurrence solver of `Sigma`, we aim for a scalar difference equation that carries the same information as the coupled system of differential equations. This requires two main steps: We have to translate differential equations into difference equations and we have to transform a coupled system of equations into a scalar equation. Two options arise for how to proceed.

1. Either we can first insert a power series ansatz for each master integral, derive a system of coupled difference equations and uncouple it to arrive at a scalar recurrence.

2. Or we can first uncouple the differential equation system into a single higher-order differential equation, insert the power series ansatz there and derive a scalar recurrence.

We will discuss the first approach in the following and only briefly comment on the second approach later on.

First, we insert the power series ansatz

$$I_i(t) = \sum_{N=0}^{\infty} t^N I_i(N), \tag{3.137}$$

for the unknown integrals $I_i(t)$ and an analogous ansatz for the base case integrals $B_i(t)$. Next, we take each differential equation of the system and clear the denominators of the right-hand side by multiplying the equation by the common denominator of all rational coefficients $A_{ij}(t,\varepsilon)$ and $C_j(t,\varepsilon)$. This way, we obtain polynomials in t and ε multiplying the power series for the master integrals. For the first equation of the example we get

$$t(t-1)\frac{\mathrm{d}}{\mathrm{d}t}\sum_{N=0}^{\infty} t^N I_1(N) = (1-t+\varepsilon)\sum_{N=0}^{\infty} t^N I_1(N) - 2\sum_{N=0}^{\infty} t^N I_2(N) + \sum_{N=0}^{\infty} t^N B_4(N). \tag{3.138}$$

3. Calculation of massive operator matrix elements

Differentiation and multiplication by monomials in t are simple operations on formal power series,

$$\frac{\mathrm{d}}{\mathrm{d}t} \sum_{N=0}^{\infty} t^N f(N) = \sum_{N=1}^{\infty} t^{N-1} N f(N) = \sum_{N=0}^{\infty} t^N (N+1) f(N+1) \tag{3.139}$$

$$t^k \sum_{N=0}^{\infty} t^N f(N) = \sum_{N=0}^{\infty} t^{N+k} f(N) = \sum_{N=k}^{\infty} t^N f(N-k) . \tag{3.140}$$

Thus, by comparing the coefficient of t^N of the differential equations with power series inserted, we obtain difference equations in N for the coefficients $I_i(N)$, which holds from some $n_0 \in \mathbb{Z}$ onwards. In our example we get

$$-(N + \varepsilon + 1)I_1(N) + NI_1(N-1) + 2I_2(N) = r_1(N) , \tag{3.141}$$

with

$$r_1(N) = B_4(N) . \tag{3.142}$$

Analogously, the other two equations of the system yield

$$\begin{aligned}
&- \varepsilon(3\varepsilon + 2)I_1(N-1) + 2(1 + 3\varepsilon + 2N)I_2(N-1) \\
&- 2(2 + \varepsilon + 2N)I_2(N) + 2(\varepsilon + 1)I_3(N-1) = r_2(N) ,
\end{aligned} \tag{3.143}$$

$$\begin{aligned}
&\varepsilon(3\varepsilon + 2)I_1(N-1) - 2\varepsilon(3\varepsilon + 2)I_1(N) \\
&- 2(3\varepsilon + 1)I_2(N-1) + 2(5\varepsilon + 2)I_2(N) \\
&- 2(1 + \varepsilon - 2N)I_3(N-1) + 4(\varepsilon - N)I_3(N) = r_3(N) ,
\end{aligned} \tag{3.144}$$

with the inhomogeneous parts given by

$$\begin{aligned}
r_2(N) = &- \frac{(\varepsilon + 2)^3}{4(\varepsilon + 1)} B_1(N) + \frac{(\varepsilon + 2)(3\varepsilon + 4)\left(19\varepsilon^2 + 36\varepsilon + 16\right)}{4\varepsilon(5\varepsilon + 6)} B_2(N) \\
&+ \frac{2(\varepsilon + 1)^2(3\varepsilon + 4)^2}{\varepsilon(5\varepsilon + 6)} B_3(N-1) - \frac{2(\varepsilon + 1)^2(3\varepsilon + 4)^2}{\varepsilon(5\varepsilon + 6)} B_3(N) \\
&+ \frac{2(\varepsilon + 1)(3\varepsilon + 4)}{5\varepsilon + 6} B_4(N-1) - (5\varepsilon + 4)B_4(N) ,
\end{aligned} \tag{3.145}$$

$$r_3(N) = - r_2(N) . \tag{3.146}$$

This is a system of first-order difference equations, where the inhomogeneities are linear combinations of the moments of the base case integrals $B_i(N)$ and their shifted versions. In this case, we directly obtained a first-order system, while in general, clearing the denominators can bring polynomials of higher order in t into the numerator which lead to higher shifts in N. Such a system, however, can always be written as a first-order system by introducing auxilliary functions. For example, the difference equation

$$a_3(N)I_1(N+3) + a_2(N)I_1(N+2) + a_1(N)I_1(N+1) + a_0(N)I_1(N) + \ldots = 0 \tag{3.147}$$

can be written as the system

$$a_3(N)h_2(N+1) + a_2(N)h_2(N) + a_1(N)h_1(N) + a_0(N)I_1(N) + \cdots = 0 , \tag{3.148}$$

$$h_1(N+1) - h_2(N) = 0 , \tag{3.149}$$

$$I_1(N+1) - h_1(N) = 0 , \tag{3.150}$$

with the definitions $h_1(N) = I_1(N+1)$ and $h_2(N) = I_1(N+2)$.

The first-order system can then be written as

$$
\begin{pmatrix} I_1(N+1) \\ I_2(N+1) \\ I_3(N+1) \end{pmatrix} = A(N) \begin{pmatrix} I_1(N) \\ I_2(N) \\ I_3(N) \end{pmatrix} + \begin{pmatrix} v_1(N) \\ v_2(N) \\ v_3(N) \end{pmatrix} \tag{3.151}
$$

by an appropriate shift in N such that the highest shift among the $I_i(N)$ is $N+1$ and solving for $I_i(N+1)$. If we had to introduce auxilliary functions, the system would of course be larger than the original differential equation system. For our example, the coefficient matrix is given by

$$
A(N) = \begin{pmatrix} \dfrac{(1-\varepsilon+N)(4+3\varepsilon+2N)}{(2+\varepsilon+N)(4+\varepsilon+2N)} & \dfrac{2(3+3\varepsilon+2N)}{(2+\varepsilon+N)(4+\varepsilon+2N)} & \dfrac{2(\varepsilon+1)}{(2+\varepsilon+N)(4+\varepsilon+2N)} \\ -\dfrac{\varepsilon(3\varepsilon+2)}{2(4+\varepsilon+2N)} & \dfrac{3+3\varepsilon+2N}{4+\varepsilon+2N} & \dfrac{\varepsilon+1}{4+\varepsilon+2N} \\ a(N) & b(N) & c(N) \end{pmatrix},
\tag{3.152}
$$

where the entries of the last row are

$$
a(N) = -\frac{\varepsilon(3\varepsilon+2)\left(-2-2\varepsilon+\varepsilon^2-3N-2\varepsilon N-N^2\right)}{2(-1+\varepsilon-N)(2+\varepsilon+N)(4+\varepsilon+2N)}, \tag{3.153}
$$

$$
b(N) = \frac{-2-3\varepsilon-\varepsilon^2+3\varepsilon^3-3N-5\varepsilon N-2\varepsilon^2 N-N^2-2\varepsilon N^2}{(-1+\varepsilon-N)(2+\varepsilon+N)(4+\varepsilon+2N)}, \tag{3.154}
$$

$$
c(N) = \frac{-6-5\varepsilon-\varepsilon^2+\varepsilon^3-13N-7\varepsilon N-2\varepsilon^2 N-9N^2-2\varepsilon N^2-2N^3}{(-1+\varepsilon-N)(2+\varepsilon+N)(4+\varepsilon+2N)} \tag{3.155}
$$

and the inhomogeneities read

$$
v_1(N) = -\frac{r_2(N+1)}{(2+\varepsilon+N)(4+\varepsilon+2N)} - \frac{r_1(N+1)}{2+\varepsilon+N}, \tag{3.156}
$$

$$
v_2(N) = -\frac{r_2(N+1)}{2(\varepsilon+2N+4)}, \tag{3.157}
$$

$$
v_3(N) = \frac{-\varepsilon(3\varepsilon+2)r_1(N+1)}{2(-1+\varepsilon-N)(2+\varepsilon+N)}
$$
$$
+ \frac{r_3(N+1)}{4(-1+\varepsilon-N)} + \frac{(-4-8\varepsilon+\varepsilon^2-2N-5\varepsilon N)r_2(N+1)}{4(1-\varepsilon+N)(2+\varepsilon+N)(4+\varepsilon+2N)}. \tag{3.158}
$$

The first-order system of difference equations now has to be uncoupled to a scalar recurrence. We use Zürcher's algorithm [382] which is implemented in the `Mathematica` package `OreSys` [383]. This algorithm returns a scalar linear recurrence for the system which is expressed in terms of only one of the integrals, say $I_1(N)$, and its shifted versions. Moreover, the algorithm provides expressions for the other unkown integrals of the system which can be evaluated trivially as soon as a solution for $I_1(N)$ is known. Solving the system now amounts to solving the scalar recurrence for $I_1(N)$. In general, it can happen that the uncoupling algorithm finds separate scalar recurrences for a coupled system. Each such scalar recurrence only depends on one unknown integral as well as the base case integrals. All remaining integrals are expressed as linear combinations of the solutions of the scalar recurrences and the base case integrals. As the

3. Calculation of massive operator matrix elements

recurrence for $I_1(N)$ of the example we obtain

$$
\begin{aligned}
2(N+1)&(N+2)(2+\varepsilon+N)I_1(N) \\
&+ (N+2)\big(-32 - 7\varepsilon + 2\varepsilon^2 - 28N - 5\varepsilon N - 6N^2\big)I_1(N+1) \\
&+ \big(120 + 3\varepsilon - 14\varepsilon^2 - \varepsilon^3 + 136N + 13\varepsilon N - 4\varepsilon^2 N + 50N^2 + 4\varepsilon N^2 + 6N^3\big)I_1(N+2) \\
&- (2 - \varepsilon + N)(4 + \varepsilon + N)(8 + \varepsilon + 2N)I_1(N+3) \\
&= 2(N+2)(2+\varepsilon+N)r_1(N+1) + \big(-24 - \varepsilon + \varepsilon^2 - 20N - \varepsilon N - 4N^2\big)r_1(N+2) \\
&+ (2 - \varepsilon + N)(8 + \varepsilon + 2N)r_1(N+3) + \frac{1}{2}(-3 + \varepsilon - 2N)r_2(N+2) \\
&+ (2 - \varepsilon + N)r_2(N+3) + \frac{1}{2}(\varepsilon+1)r_3(N+2)\,,
\end{aligned}
\tag{3.159}
$$

and the other two integrals can be expressed purely in terms of $I_1(N)$, its shifted versions and the base case integrals,

$$
\begin{aligned}
I_2(N) = {}& \frac{-8 + 2\varepsilon + 4\varepsilon^2 - 12N - \varepsilon N - 4N^2}{4(1+\varepsilon+N)}I_1(N) \\
&+ \frac{28 - 6\varepsilon - 10\varepsilon^2 - \varepsilon^3 + 54N + 5\varepsilon N - 4\varepsilon^2 N + 32N^2 + 4\varepsilon N^2 + 6N^3}{4(N+1)(1+\varepsilon+N)}I_1(N+1) \\
&- \frac{(1 - \varepsilon + N)(3 + \varepsilon + N)(6 + \varepsilon + 2N)}{4(N+1)(1+\varepsilon+N)}I_1(N+2) \\
&+ \frac{8 - \varepsilon^2 + 12N + \varepsilon N + 4N^2}{4(N+1)(1+\varepsilon+N)}r_1(N+1) - \frac{(1 - \varepsilon + N)(6 + \varepsilon + 2N)}{4(N+1)(1+\varepsilon+N)}r_1(N+2) \\
&+ \frac{1 - \varepsilon + 2N}{8(N+1)(1+\varepsilon+N)}r_2(N+1) - \frac{1 - \varepsilon + N}{4(N+1)(1+\varepsilon+N)}r_2(N+2) \\
&- \frac{\varepsilon+1}{8(N+1)(1+\varepsilon+N)}r_3(N+1)\,,
\end{aligned}
\tag{3.160}
$$

$$
\begin{aligned}
I_3(N) = {}& \frac{16 + 12\varepsilon - 10\varepsilon^2 - 6\varepsilon^3 + 32N + 23\varepsilon N - \varepsilon^2 N + 20N^2 + 8\varepsilon N^2 + 4N^3}{4(\varepsilon+1)(1+\varepsilon+N)}I_1(N) \\
&+ \frac{Q(N)}{4(\varepsilon+1)(N+1)(1+\varepsilon+N)}I_1(N+1) \\
&+ \frac{(1 - \varepsilon + N)(3 + \varepsilon + N)(6 + \varepsilon + 2N)(3 + 3\varepsilon + 2N)}{4(\varepsilon+1)(N+1)(1+\varepsilon+N)}I_1(N+2) \\
&+ \frac{-16 - 14\varepsilon + 5\varepsilon^2 + 3\varepsilon^3 - 32N - 23\varepsilon N + \varepsilon^2 N - 20N^2 - 8\varepsilon N^2 - 4N^3}{4(\varepsilon+1)(N+1)(1+\varepsilon+N)}r_1(N+1) \\
&+ \frac{(1 - \varepsilon + N)(6 + \varepsilon + 2N)(3 + 3\varepsilon + 2N)}{4(\varepsilon+1)(N+1)(1+\varepsilon+N)}r_1(N+2) \\
&+ \frac{(1 - \varepsilon + N)(3 + 3\varepsilon + 2N)}{4(\varepsilon+1)(N+1)(1+\varepsilon+N)}r_2(N+2) + \frac{3\varepsilon+1}{8(N+1)(1+\varepsilon+N)}r_2(N+1) \\
&+ \frac{3 + 3\varepsilon + 2N}{8(N+1)(1+\varepsilon+N)}r_3(N+1)\,,
\end{aligned}
\tag{3.161}
$$

with

$$
\begin{aligned}
Q(N) = {}& -68 - 38\varepsilon + 62\varepsilon^2 + 35\varepsilon^3 + 3\varepsilon^4 - 170N - 103\varepsilon N + 39\varepsilon^2 N + 16\varepsilon^3 N - 152N^2 \\
& - 74\varepsilon N^2 + 4\varepsilon^2 N^2 - 58N^3 - 16\varepsilon N^3 - 8N^4\,.
\end{aligned}
\tag{3.162}
$$

At this stage it is possible to analyse up to which order in ε the base case integrals have to be known and whether some of the unknown integrals have to be calculated to higher orders than

what is required by the diagrams. We start by considering the coefficients of $I_1(N)$ and its shifted versions in the expression for $I_2(N)$, Eq. (3.160). After factoring the numerator and denominator polynomials of the coefficients, we read off the exponent $p \in \mathbb{Z}$ of ε^{-p} for each coefficient. We take $p_{\max}$ to be the largest p across all coefficients. If we have to calculate $I_2(N)$ up to a certain order k, we need to calculate $I_1(N)$ up to order $k' = k + p_{\max}$. This order may be higher than the order required for the diagram. Similarly, we can determine the required order for the base case integrals. Next, we repeat the analysis for the expression for $I_3(N)$, Eq. (3.161), keeping track of the highest required order of each master integral. Finally, we analyse the requirements for the base case integrals in the recurrence for $I_1(N)$, Eq. (3.159), based on the previously determined required order of $I_1(N)$. The base case integrals are required to the highest order encountered during this analysis. For the example at hand, we find that the calculation of $I_2(N)$ and $I_3(N)$ up to $\mathcal{O}(\varepsilon^3)$ necessitates the calculation of $I_1(N)$ up to $\mathcal{O}(\varepsilon^3)$ as well, which is higher than what is required by the diagram. The base case integrals $B_1(N)$ to $B_4(N)$ have to be known up to order 3, 4, 4 and 3 respectively.

To fix the coefficients of the solutions to the homogeneous recurrence, we need n initial values, if the recurrence is of order n. Here we need three initial values for $I_1(N)$. We use the values of the unknown integrals for (small) fixed values of $N \in \mathbb{N}$ as initial values. They have to be obtained using other methods up to the same order in ε as we would like to calculate the unknown integral. Several options to calculate initial values exist:

- Up to $\mathcal{O}(\varepsilon^0)$, we can use the `MATAD` [217] setup developed for [193, 203]. It allows to calculate moments of scalar 3-loop integrals with operator insertions by mapping them to massive tadpole integrals. Up to $N = 14$ the required projectors are readily available in the setup.

- For some integrals a sum representation can be derived using the methods described in the previous sections. The calculation of these sums for fixed values of N is usually less complicated than the solution for general N. Therefore, the calculation of fixed moments is sometimes still feasible, even when the calculation for general N exceeds the available computing resources.

- The evaluation of the integrals for fixed N can also be performed using the α-representation, cf. e.g. [389, 399, 400], as it was worked out in [340]. The idea is to reexpress integrals with scalar products like $(\Delta.k_i)^N$ in the numerator in terms of integrals without numerators but in a different number of space-time dimensions. These integrals are again reduced to master integrals without operator insertions via IBP relations. It turns out, that only three operator-less master integrals appear in this approach. Once they are calculated to sufficient order in ε in different dimensions $D = n + \varepsilon$, the initial values for the original master integrals can be computed. For details on this approach, we refer to [340].

Instead of $I_1(N)$, we could also derive a scalar recurrence with respect to $I_2(N)$ or $I_3(N)$. However, the required order in ε for the base case integrals is higher in these cases. The steps up to the analysis of required orders are usually computationally inexpensive such that all avaiable options can be analysed and the optimal one selected. Here the scalar recurrence with respect to $I_1(N)$ is the optimal choice.

Once we have derived the scalar recurrence for one of the unknown integrals, we have to solve it. Since we are interested in the coefficients of the Laurent expansion in ε of the master integrals, we solve the recurrence order by order in ε. The highest pole that can occur for the master integrals of this project is of order ε^{-3}. Therefore, we insert a formal Laurent series ansatz in ε,

$$I_1(N, \varepsilon) = \frac{I_1^{(-3)}(N)}{\varepsilon^3} + \frac{I_1^{(-2)}(N)}{\varepsilon^2} + \frac{I_1^{(-1)}(N)}{\varepsilon} + I_1^{(0)}(N) + \varepsilon I_1^{(1)}(N) + \dots, \qquad (3.163)$$

3. Calculation of massive operator matrix elements

as well as analogous expressions for the base case integrals into the scalar recurrence. After expanding the rational coefficients in ε, we can compare coefficients to obtain separate recurrences at each order in ε. To lowest order in ε we obtain a scalar recurrence in N for the coefficient of the highest pole, $I_1^{(-3)}(N)$ with polynomial coefficients. The inhomogeneous part of the recurrence is given in terms of the Laurent expansion coefficients of the base case integrals and their shifted versions. According to our assumptions, the base case integrals have already been calculated and their result is known in terms of nested indefinite product-sum expressions, i.e. in our case harmonic sums and their generalisations. Inserting these results into the recurrence yields a recurrence which can be handled by the recurrence solving algorithms implemented in `Sigma`. Given such a recurrence, `Sigma` either returns a result in terms of nested indefinite product-sum expressions or aborts, which means that no such solution exists.

In our example, the recurrence for the triple pole reads

$$
(N+1)(N+2)^2 I_1^{(-3)}(N) - (3N+8)(N+2)^2 I_1^{(-3)}(N+1)
$$
$$
+ (N+3)(3N+10)(N+2) I_1^{(-3)}(N+2) - (N+4)^2(N+2) I_1^{(-3)}(N+3) = 0 \,. \qquad (3.164)
$$

Note, that the expansion of the right-hand side vanishes and we obtain a homogeneous recurrence. The routines implemented in `Sigma` now allow us to find three solutions to the homogeneous recurrence. The general solution must be a linear combination of these solutions with real coefficients c_1, c_2, c_3,

$$
I_1^{(-3)}(N) = c_1 \frac{1}{N+1} + c_2 \frac{N}{N+1} + c_3 \left(\frac{S_1}{N+1} - \frac{N}{(N+1)^2} \right) \,. \qquad (3.165)
$$

Given three initial values for $I_1(N)$,

$$
I_1^{(-3)}(0) = \frac{16}{3} \,, \qquad I_1^{(-3)}(1) = 5 \,, \qquad I_1^{(-3)}(2) = \frac{130}{27} \,, \qquad (3.166)
$$

we find that

$$
c_1 = \frac{16}{3} \,, \qquad c_2 = 4 \,, \qquad c_3 = \frac{4}{3} \,, \qquad (3.167)
$$

and therefore the result for the triple pole term of $I_1(N)$ is

$$
I_1^{(-3)}(N) = \frac{4(3N^2 + 6N + 4)}{3(N+1)^2} + \frac{4S_1}{3(N+1)} \,. \qquad (3.168)
$$

Once the result for the lowest order is known, it can be inserted into the recurrence of the next higher order and now belongs to its inhomogeneous part. We proceed order by order until the required order is reached.

For the master integral $I_1(N)$ from our example we obtain

$$
I_1(N) = \frac{1}{\varepsilon^3} \left[\frac{4(3N^2 + 6N + 4)}{3(N+1)^2} + \frac{4S_1}{3(N+1)} \right]
$$
$$
+ \frac{1}{\varepsilon^2} \left[-\frac{2(20N^3 + 58N^2 + 57N + 22)}{3(N+1)^3} + \frac{2(N+2)(2N-1)S_1}{3(N+1)^2} - \frac{S_1^2}{N+1} - \frac{S_2}{N+1} \right]
$$
$$
+ \frac{1}{\varepsilon} \left[\frac{89N^4 + 344N^3 + 495N^2 + 317N + 84}{3(N+1)^4} + \left(\frac{3N^2 + 6N + 4}{2(N+1)^2} + \frac{S_1}{2(N+1)} \right) \zeta_2 \right.
$$
$$
\left. + \left(\frac{-12N^3 - 39N^2 - 39N - 5}{3(N+1)^3} + \frac{S_2}{6(N+1)} \right) S_1 + \frac{(3N+4)S_1^2}{6(N+1)^2} \right.
$$

$$+ \frac{S_1^3}{18(N+1)} + \frac{(3N+4)S_2}{6(N+1)^2} + \frac{S_3}{9(N+1)} + \frac{2S_{2,1}}{N+1} \bigg] + \mathcal{O}(\varepsilon^0) \tag{3.169}$$

as the result up to the single pole term ε^{-1}. We calculate also the constant term and higher terms in the expansion up to $\mathcal{O}(\varepsilon^3)$. They can be expressed in terms of harmonic sums up to weight $w = 7$.

Finally, we insert the result for $I_1(N)$, Eq. (3.169), into Eqs. (3.160) and (3.161) to obtain also the solutions for $I_2(N)$ and $I_3(N)$. Up to the constant term in ε they read

$$I_2(N) = \frac{4}{3\varepsilon^3} - \frac{2}{\varepsilon^2} + \frac{1}{\varepsilon}\left[\frac{5N+7}{3(N+1)} + \frac{2}{3}S_1 - \frac{1}{3}S_1^2 - \frac{1}{3}S_2 + \frac{\zeta_2}{2} \right]$$
$$+ \frac{N^2 - 12N - 15}{6(N+1)^2} + \left(\frac{-7N-8}{3(N+1)} + \frac{(1-N)S_2}{2(N+1)} \right)S_1 + S_1^2 + \frac{(1-N)S_1^3}{6(N+1)}$$
$$+ S_2 + \frac{(1-N)S_3}{3(N+1)} - \frac{3\zeta_2}{4} + \frac{(5N+17)\zeta_3}{6(N+1)} + \mathcal{O}(\varepsilon), \tag{3.170}$$

$$I_3(N) = \frac{8}{3\varepsilon^3} + \frac{1}{\varepsilon^2}\left[-\frac{4(4N^2+7N+2)}{3(N+1)^2} + \frac{4(N+2)S_1}{3(N+1)} \right]$$
$$+ \frac{1}{\varepsilon}\left[\frac{2(12N^3 + 32N^2 + 25N + 2)}{3(N+1)^3} - \frac{2(4N^2 + 11N + 10)S_1}{3(N+1)^2} \right.$$
$$\left. + \frac{(N-2)S_1^2}{3(N+1)} + \frac{(N-2)S_2}{3(N+1)} + \zeta_2 \right]$$
$$+ \frac{-32N^4 - 116N^3 - 148N^2 - 69N + 2}{3(N+1)^4} + \left(\frac{-4N^2 - 7N - 2}{2(N+1)^2} + \frac{(N+2)S_1}{2(N+1)} \right)\zeta_2$$
$$+ \left(\frac{12N^3 + 44N^2 + 59N + 34}{3(N+1)^3} + \frac{(N-4)S_2}{6(N+1)} \right)S_1$$
$$+ \frac{(-4N^2 - 7N - 2)S_1^2}{6(N+1)^2} + \frac{(N-4)S_1^3}{18(N+1)} + \frac{(-4N^2 - 7N - 2)S_2}{6(N+1)^2}$$
$$+ \frac{(N-4)S_3}{9(N+1)} + \frac{2(N+2)S_{2,1}}{N+1} + \frac{(-N-7)\zeta_3}{3(N+1)} + \mathcal{O}(\varepsilon). \tag{3.171}$$

Similar expressions can be found for the expansion coefficients up to $\mathcal{O}(\varepsilon^3)$ in terms of harmonic sums up to weight $w = 7$.

As mentioned above, we can also use a slightly different approach to derive the scalar recurrences: Instead of deriving a coupled system of difference equations first and uncoupling the difference equations, we can uncouple the first-order differential equations to a scalar, higher-order differential equation and determine the scalar recurrence from there using the power series ansatz. The uncoupling of the system of differential equations leads to derivatives of the inhomogeneities and thus to derivatives of the base case integrals $B_i(t, \varepsilon)$. If we proceed as above and insert a formal power series ansatz for all integrals, we arrive at the same recurrences as above. However, the alternative approach has the advantage that we can calculate the derivatives of the base case integrals explicitly and express them again in terms of master integrals using the IBP relations. We observe in some cases, that this can reduce the order in ε to which the base case integrals are required to solve the scalar recurrences.

Solving the hierarchical system

The approach described above allows us to solve a single coupled sector of master integrals provided that we know the base case integrals up to the required orders in ε and that we can

3. Calculation of massive operator matrix elements

Table 3.1.: Example for a set of 32 master integrals which are required for the calculation of the V-diagram discussed in Chapter 6. The differential equations of these master integrals is hierachically structured as described by the dependecies on lower sectors. The last three columns give the scalar integral with respect to which the uncoupling was performed, the order of the derived scalar recurrence and the computing time required to solve the sector.

sector	unknown integrals	required up to ε^k	dependencies on lower sectors	scalar rec. in I_i	order of rec.	time used
1	I_1, I_2, I_3	$3, 3, 3$	–	I_1	3	$229\,\mathrm{s}$
2	I_4, I_5, I_6, I_7	$4, 3, 2, 3$	–	I_4	5	$125\,\mathrm{h}$
3	I_8	1	–	I_8	1	$12\,\mathrm{s}$
4	I_9	0	–	I_9	1	$8\,\mathrm{s}$
5	I_{10}, I_{11}	$2, 1$	1	$\begin{cases} I_{10} \\ I_{11} \end{cases}$	$\begin{cases} 3 \\ 1 \end{cases}$	$115\,\mathrm{s}$
6	I_{12}, I_{13}, I_{14}	$3, 1, 2$	–	I_{13}	1	$68\,\mathrm{s}$
7	I_{15}, I_{16}, I_{17}	$2, 1, 1$	–	I_{15}	5	$530\,\mathrm{s}$
8	I_{18}	3	2	I_{18}	2	$19.6\,\mathrm{h}$
9	I_{19}	3	2	I_{19}	1	$13.3\,\mathrm{h}$
10	I_{20}, I_{21}	$1, -1$	$1, 2$	I_{20}	5	$3754\,\mathrm{s}$
11	I_{22}, I_{23}	$1, 0$	$2, 6$	I_{22}	5	$22.5\,\mathrm{h}$
12	I_{24}	1	–	I_{24}	1	$17.5\,\mathrm{s}$
13	I_{25}	0	$1, 5$	I_{25}	2	$6\,\mathrm{s}$
14	I_{26}	1	1	I_{26}	3	$169\,\mathrm{s}$
15	I_{27}, I_{28}	$1, 0$	$1, 5, 6, 7$	$\begin{cases} I_{27} \\ I_{28} \end{cases}$	$\begin{cases} 5 \\ 1 \end{cases}$	$1852\,\mathrm{s}$
16	I_{29}	1	$1, 2, 6, 10, 11$	I_{29}	2	$1708\,\mathrm{s}$
17	I_{30}	0	$1, 5, 6, 7, 15$	I_{30}	1	$41\,\mathrm{s}$
18	I_{31}	1	$1, 2, 5, 6, 7, 10, 11, 15$	I_{31}	2	$2816\,\mathrm{s}$
19	I_{32}	1	$1, 5, 6, 7, 14, 15$	I_{32}	3	$953\,\mathrm{s}$

calculate a sufficient number of initial values. It is now relatively straightforward to extend this to hierarchically structured systems of differential equations. While, in principle, we can just treat the system of all required master integrals as a single coupled system, it is computationally advantageous to make use of the hierarchical structure explicitly. The idea is to solve each sector individually, starting with the simplest sector. In each step, we treat the master integrals of simpler sectors as additional base case integrals. After all, the presence of base case integrals only arises in the first place, because we have already solved some of the master integrals instead of considering them as part of the differential equation system.

As a prerequesite, we have to know the required order of the ε-expansion of the base case integrals and the number and required order of the initial values for the unknown integrals. Therefore, we use a two stage process: We first analyse the hierarchical system in a top-down direction, starting with the most complicated sector, and extract the information about the required orders in ε and the initial values. In the second step, we solve the system bottom-up, starting from the simplest sector.

We use a set of 32 master integrals, which are required for the calculation of a V-topology diagram discussed in Chapter 6, as an example. The information about these master integrals

can be found in Table 3.1. The integrals I_1, I_2 and I_3 from the previous example constitute the first sector of these 32 master integrals. The dependencies among the sectors are given in the fourth column: The integrals I_{10} and I_{11} depend on the integrals I_1, I_2 and I_3, etc.

We start the analysis with the list of expansion orders for the unknown integrals I_i and base case integrals B_i required by the diagrams. We then apply the following procedure for each sector in turn, starting with the most complicated sector, sector 19 in our example, and working towards simpler sectors: We derive the uncoupled, scalar recurrences and the relations for the remaining unknown integrals of the sector. Then we extract the required orders for the master integrals and the information about initial values as described above. If the required order for any of the integrals exceeds the order required so far, we update the list and move to the next sector using the updated list for the subsequent analysis. Along the way, we gather the information about the initial values. Moreover, we also keep the scalar recurrences and relations for the unknown integrals which we derived for this analysis to save computation time when we solve the systems later on.

If the analysis reveals that one of the base case integrals has to be expanded to higher orders than already available, we can either use the previously used method and try to calculate also the higher orders, or we can add the differential equation for the missing base case integral to the system of differential equations and repeat the analysis.

When all base case integrals and initial values are available, we start with the simplest sector and apply the procedure described above to solve the scalar recurrences and to calculate the remaining unknown integrals of each sector. We add the results to the database of available master integrals and move to the next, more complicated sector.

The approach outlined in this subsection can be put into an algorithmic form and implemented in `Mathematica`. Corresponding routines are available in the package `SumProduction` which uses `Sigma`, `HarmonicSums`, `EvaluateMultiSums` and `OreSys`. The implementation of these routines is not part of this thesis. For more information about the routines and the algorithmic details, we refer to [268, 395, 396, 398].

4. Non-singlet contributions to DIS

In this chapter, we discuss a first application of the calculational techniques described so far and calculate the non-singlet operator matrix element $A_{qq,Q}^{\text{NS}}$ at 3-loop order for even and odd values of the Mellin variable N. The renormalisation procedure of the OMEs allows us to extract the N_F-dependent part of the non-singlet anomalous dimensions from this calculation. The non-singlet OME enters the factorisation of the corresponding heavy flavour Wilson coefficients in the limit $Q^2 \gg m^2$ [201, 203]. The even moments are relevant for the unpolarised structure function for photon-mediated DIS, $F_2(x, Q^2)$, while the odd moments are applicable to polarised photon-mediated scattering in the structure function $g_1(x, Q^2)$ and to the structure function $xF_3(x, Q^2)$, which appears in W-boson mediated scattering. We discuss these applications in turn in the following sections. Additionally, we consider the influence of the heavy quark contributions to the polarised Bjorken sum rule [271] and the Gross-Llewellyn-Smith sum rule [401]. Moreover, the non-singlet OME also appears in the matching relations of the variable flavour number scheme [202, 203]. We give illustrations of the heavy flavour effects in the scheme change from a PDF scheme with N_F massless quarks and one massive quark to a scheme with N_F effectively massless quarks.

The results presented in this chapter are published as journal articles. The calculation of the OMEs and the unpolarised Wilson coefficient $L_{q,2}^{\text{NS}}$ is described in [358] and the polarised and charged-current Wilson coefficients are published in [402] and [403], respectively.

4.1. The non-singlet operator matrix element $A_{qq,Q}^{\text{NS},(3)}$

The massive non-singlet OME $A_{qq,Q}^{\text{NS}}$ is defined as the expectation value of the non-singlet light cone operator between on-shell massless quark states. Here we consider the case of one massive and N_F massless quarks. For deep-inelastic scattering at HERA, the heavy quark can be a charm or a bottom quark. Starting at 3-loop order, there are also diagrams with two massive quarks of different mass. We do not consider these diagrams here. The non-singlet contributions of two-mass diagrams have been calculated in [301, 302, 404].

The renormalisation and factorisation procedure allows to determine the structure of the 3-loop correction to the renormalised OME, which in Mellin N space is given by [203]

$$A_{qq,Q}^{\text{NS},(2)}(N) = \frac{\beta_{0,Q}\gamma_{qq}^{\text{NS},(0)}}{4} \ln^2\left(\frac{m^2}{\mu^2}\right) + \frac{\hat{\gamma}_{qq}^{\text{NS},(1)}}{2} \ln\left(\frac{m^2}{\mu^2}\right) + a_{qq,Q}^{\text{NS},(2)} - \frac{\beta_{0,Q}\gamma_{qq}^{\text{NS},(0)}}{4}\zeta_2 \,, \qquad (4.1)$$

$$A_{qq,Q}^{\text{NS},(3)}(N) = -\frac{\gamma_{qq}^{\text{NS},(0)}\beta_{0,Q}}{6}\left(\beta_0 + 2\beta_{0,Q}\right)\ln^3\left(\frac{m^2}{\mu^2}\right) + \frac{1}{4}\left\{2\gamma_{qq}^{\text{NS},(1)}\beta_{0,Q} - 2\hat{\gamma}_{qq}^{\text{NS},(1)}\left(\beta_0 + \beta_{0,Q}\right)\right.$$

$$\left. + \beta_{1,Q}\gamma_{qq}^{\text{NS},(0)}\right\}\ln^2\left(\frac{m^2}{\mu^2}\right) + \frac{1}{2}\left\{\hat{\gamma}_{qq}^{\text{NS},(2)} - \left(4a_{qq,Q}^{\text{NS},(2)} - \zeta_2\beta_{0,Q}\gamma_{qq}^{\text{NS},(0)}\right)\left(\beta_0 + \beta_{0,Q}\right)\right.$$

$$\left. + \gamma_{qq}^{\text{NS},(0)}\beta_{1,Q}^{(1)}\right\}\ln\left(\frac{m^2}{\mu^2}\right) + 4\overline{a}_{qq,Q}^{\text{NS},(2)}(\beta_0 + \beta_{0,Q}) - \gamma_{qq}^{\text{NS},(0)}\beta_{1,Q}^{(2)} - \frac{\gamma_{qq}^{\text{NS},(0)}\beta_0\beta_{0,Q}\zeta_3}{6}$$

$$- \frac{\gamma_{qq}^{\text{NS},(1)}\beta_{0,Q}\zeta_2}{4} + 2\delta m_1^{(1)}\beta_{0,Q}\gamma_{qq}^{(0)} + \delta m_1^{(0)}\hat{\gamma}_{qq}^{\text{NS},(1)} + 2\delta m_1^{(-1)}a_{qq,Q}^{\text{NS},(2)}$$

$$+ a_{qq,Q}^{\mathrm{NS},(3)} \, . \tag{4.2}$$

where $N \in \mathbb{N}$ denotes the Mellin variable. This representation applies to both the unpolarised and polarised case, if we consider even and odd values of N, respectively. The renormalisation of the coupling constant refers to the $\overline{\mathrm{MS}}$ scheme, while the mass renormalisation was performed in the OMS scheme. The logarithmic terms consist solely of quantities which are already known in the literature such as the coefficients of the β-function of QCD β_k and $\beta_{k,Q}$, see Eqs. (2.134), (2.135) and (2.144) to (2.146), the mass renormalisation constants δm_k, cf. Eqs. (2.127) and (2.129), and the non-singlet anomalous dimensions $\gamma_{qq}^{\mathrm{NS},(k)}$ [135]. Here the notation $\hat{\gamma}$ refers to the N_F prescription defined in Eq. (2.97). Moreover, the constant term $a_{qq,Q}^{\mathrm{NS},(2)}$ and the linear term $\overline{a}_{qq,Q}^{\mathrm{NS},(2)}$ of the ε expansion of the 2-loop OME enter [201, 205, 206]. To stay consistent with the conventions of [203], both $a_{qq,Q}^{\mathrm{NS},(2)}$ and $\overline{a}_{qq,Q}^{\mathrm{NS},(3)}$ refer to the unrenormalised OMEs *after* on-shell mass renormalisation. This convention was chosen in [203] to facilitate the comparison to earlier literature and is at variance with the default convention to denote by $a_{ij}^{(k)}$ the constant part of the ε expansion of the completely unrenormalised OME. We adhere to the latter convention for $a_{qq,Q}^{\mathrm{NS},(3)}$ above. Explicit expressions for $a_{qq,Q}^{\mathrm{NS},(2)}$ were obtained in [201, 205] and for the $\mathcal{O}(\varepsilon)$ term in [206]. In the following calculation, we complete the 3-loop non-singlet OME by calculating the constant term of the 3-loop OME $a_{qq,Q}^{\mathrm{NS},(3)}$.

As a by-product of this calculation, we recalculate certain parts of the anomalous dimensions. The 2-loop anomalous dimension can be completely recovered from the double pole (ε^{-2}) term – or equivalently from the L_M^2 term of the renormalised OME. By contrast, the single pole (ε^{-1}) term of the OME contains only the difference between $N_F + 1$ and N_F flavours of the 3-loop anomalous dimension. Therefore, we can extract just those terms of the anomalous dimension which are proportional to some power of N_F.

We calculate $A_{qq,Q}^{\mathrm{NS},(3)}$ both for even and odd moments. The former are relevant for unpolarised deep-inelastic scattering mediated by neutral currents, while the latter enter polarised neutral current and unpolarised charged current scattering. Moreover, we calculate the OME for transversity $A_{qq,Q}^{\mathrm{NS,TR},(3)}$ [215] since the same diagrams contribute and the calculations share much overlap.

For the polarised and charged current cases γ_5 enters the operator due to the additional axial coupling of these currents. We need to pay special attention to γ_5 since it is an inherently four dimensional object while we work in dimensional regularisation, which requires the continuation of all expressions to a continuous number of dimensions, see Section 2.7. In general, an additional renormalisation is required for the axial current in order to restore the axial Ward identity [129, 319]. In the present calculation, however, a Ward-Takahashi identity [320, 321] allows to map the vertex function at zero momentum insertion to the momentum derivative of the self-energy, which is free of γ_5. This allows us to use an anti-commuting definition of γ_5. Since γ_5 appears on the external quark line, which is massless, we can then anti-commute the γ_5 to the end of the line until it is adjacent to the γ_5 of the projector. Then $\gamma_5^2 = \mathbb{1}$ allows us to completely remove both matrices. Thus, the calculation is the same as in the unpolarised case, but instead of the even moments the odd moments are relevant.

4.1.1. Details on the calculation

The calculation proceeds along the lines outlined in Chapter 3. A total of 112 diagrams contribute to the non-singlet OME which were generated using `QGRAF` [347]. Figure 4.1 shows examples for the relevant diagrams. Since the external states of the OME are massless quarks, all diagrams have a massless quark line which is connected to the external legs. The operator insertion is located on this line. As we calculate the heavy flavour matrix elements, at least one closed heavy
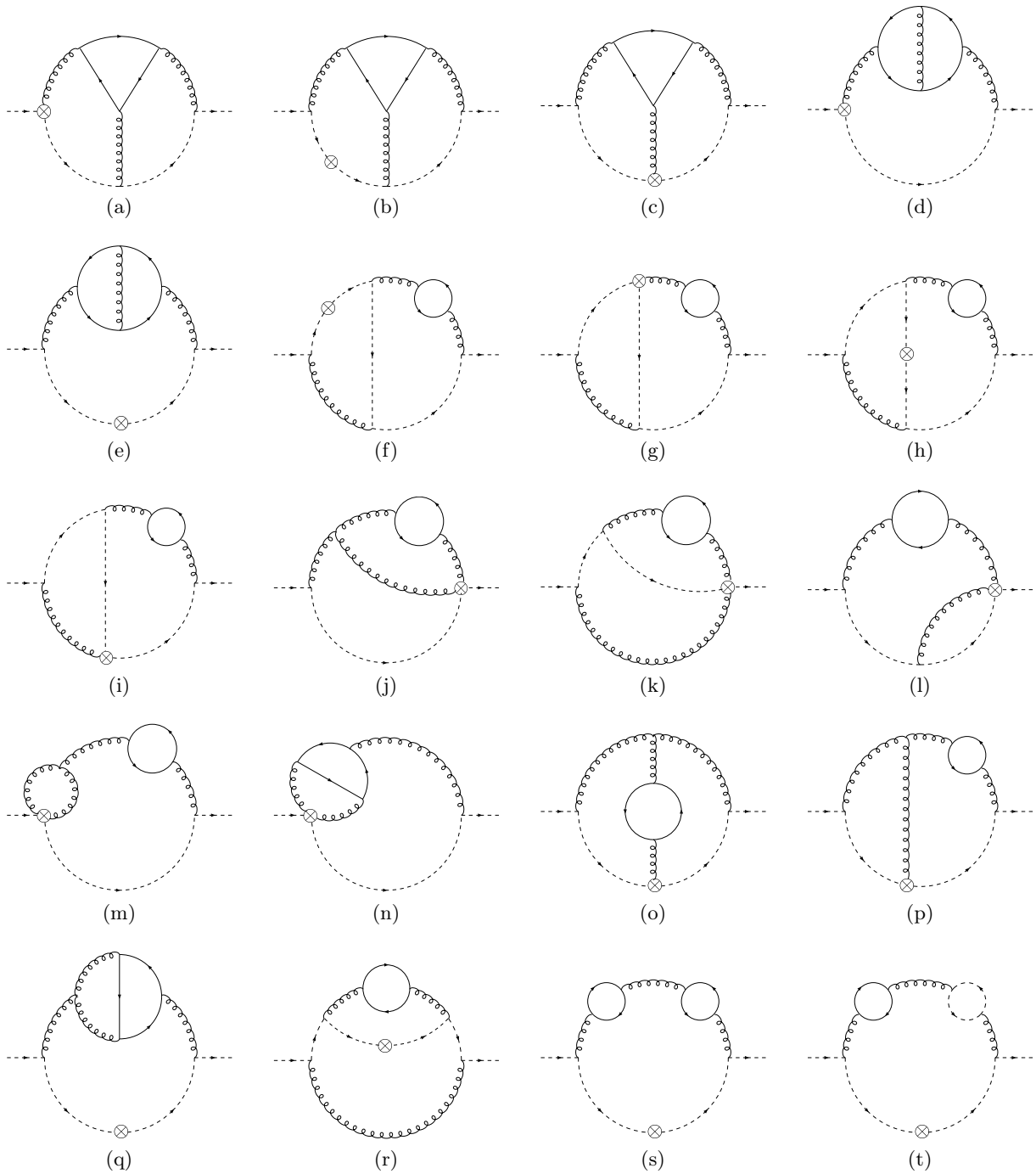
Figure 4.1.: Examples for the diagrams contributing to the non-singlet OME $A_{qq,Q}^{\mathrm{NS},(3)}$. Massless quarks are drawn as dashed arrow lines and massive quarks as solid arrow lines. Curly lines represent gluons and the operator insertion is marked by a circled cross.

quark loop has to be present. Together, these requirements limit the complexity of the topologies that can contribute. The most involved diagrams are related to the Benz topology, but no ladder or non-planar topologies enter here. As mentioned above, the same diagrams contribute to the transversity OME, but the Feynman rules for the operator insertions are different. Instead of the vector operator, transversity refers to the tensor operator. Therefore, $\slashed{\Delta}$ has to be replaced by $\sigma^{\mu\nu}\Delta_\nu$ in all Feynman rules.

The diagram description produced by QGRAF is then processed with the FORM [216] program which inserts the appropriate Feynman rules, carries out the Dirac and colour algebra simplifications and produces expressions for the diagrams in terms of scalar integrals. These scalar integrals have to be mapped to the integral families for which we have reductions to master integrals. Only three integral families appear among the scalar integrals. Most of the diagrams have only up to three different massive propagators and can be mapped to the families B1b and B1c. Only a few diagrams are mapped to the family B5a, which has more massive propagators.

This simplicity is also reflected in the set of master integrals which are required after applying the IBP identities. In total, 34 master integrals contribute. They have up to six propagators of which just three are massive for most integrals. Those integrals belong to the families B1b and B1c. Additionally, two master integrals from the family B5a with four massive propagators are required. Many of the integrals can be done in terms of Euler Beta functions or single sums over Beta functions. Such sums can be simplified using the programs EvaluateMultiSums [254–257] and Sigma [241, 252, 253]. More complicated master integrals require hypergeometric functions and their convergent series representations and yield multiple sums which can be handled using EvaluateMultiSums, Sigma and HarmonicSums [258–263]. In a few cases we also employed Mellin-Barnes integrals to derive sum representations. Details on these methods can be found in Section 3.3.

Since the renormalisation procedure in [203] refers to reducible diagrams, we have to include those in our result as well. In addition to the irreducible diagrams discussed above, we need to consider self-energy insertions on external lines. The unrenormalised third order term of the heavy quark contribution to the massless, on-shell quark self-energy reads [203]

$$
\begin{aligned}
\Sigma^{(3)}\left(0, \frac{m^2}{\mu^2}\right) =& \frac{1}{\varepsilon^3} C_F C_A T_F \frac{8}{3} + \frac{1}{\varepsilon^2}\left[C_F T_F^2\left(\frac{64}{9} + \frac{32}{9}N_F\right) - C_A C_F T_F \frac{40}{9} - C_F^2 T_F \frac{8}{3}\right] \\
& \frac{1}{\varepsilon}\left[C_F C_A T_F\left(\frac{454}{27} + \zeta_2\right) + C_F T_F^2\left(\frac{80}{27} + \frac{40}{27}N_F\right) - 26 C_F^2 T_F\right] \\
& + C_F C_A T_F\left(\frac{1879}{162} - \frac{5}{3}\zeta_2 + \frac{17}{3}\zeta_3\right) + C_F T_F^2\left[\frac{604}{81} + \frac{674}{81}N_F + \left(\frac{8}{3} + \frac{4}{3}N_F\right)\zeta_2\right] \\
& - C_F^2 T_F\left(\frac{335}{18} + \zeta_2 + 8\zeta_3\right) .
\end{aligned}
$$
(4.3)

To arrive at the result for the reducible diagrams, the unrenormalised self-energy has to be subtracted from the unrenormalised, irreducible part of the OME

$$
\hat{\hat{A}}_{qq,Q}^{\mathrm{NS},(3)} = \hat{\hat{A}}_{qq,Q}^{\mathrm{NS,irr},(3)} - \Sigma^{(3)}\left(0, \frac{m^2}{\mu^2}\right) .
$$
(4.4)

After this subtraction, the first moment of the vector OME vanishes due to fermion number conservation.

4.1.2. Non-singlet anomalous dimensions

The OMEs have ultraviolet and collinear divergences which need to be regularised and subsequently removed via renormalisation and factorisation. This involves, among other constants,

also the anomalous dimensions of the local operators. Therefore, the anomalous dimensions appear in the ε poles of the unrenormalised OMEs and after renormalisation they appear in the logarithmic terms proportional to powers of $L_M = \ln\left(m^2/\mu^2\right)$, cf. Eqs. (4.1) and (4.2). It is possible to reconstruct the 2-loop anomalous dimension $\gamma^{\mathrm{NS},(1)}$ from the ε^{-2} or the L_M^2 term, and the ε^{-1} or L_M term allows to extract the 3-loop quantity $\hat{\gamma}^{\mathrm{NS},(2)}$, i.e. the part of the 3-loop anomalous dimension which is proportional to N_F.

For the non-singlet anomalous dimensions there is a γ_+^{NS} and a γ_-^{NS} combination. They can be written as

$$\gamma_\pm^{\mathrm{NS}}(N) = \sum_{k=1}^{\infty} a_s^k \left[\gamma_{qq}^{\mathrm{NS},(k-1)}(N) + (-1)^N \gamma_{q\bar{q}}^{\mathrm{NS},(k-1)}(N) \right] . \tag{4.5}$$

The analytic continuation to complex values of N must be performed for either $\gamma_+^{\mathrm{NS}}(N)$, which is defined for even N, or for $\gamma_-^{\mathrm{NS}}(N)$, which is defined for odd N. The parts of the anomalous dimensions extracted here can be expressed in terms of harmonic sums up to weight $w = 4$.

Since our calculation encompasses the massive matrix elements of the vector as well as transversity non-singlet operators, we obtain the anomalous dimensions for both operators. Our result for the 2-loop non-singlet anomalous dimension of the vector operator reads

$$\gamma_{qq}^{\mathrm{NS},(1)}(N) = C_A C_F \left[-32 S_{-2,1} + \frac{536}{9} S_1 + 2 \left(16 S_1 - \frac{8}{N(N+1)} \right) S_{-2} \right.$$
$$\left. - \frac{P_1}{9N^3(N+1)^3} - \frac{88}{3} S_2 + 16[S_3 + S_{-3}] \right]$$
$$+ 4 C_F T_F N_F \left[\frac{3N^4 + 6N^3 + 47N^2 + 20N - 12}{9N^2(N+1)^2} - \frac{40}{9} S_1 + \frac{8}{3} S_2 \right]$$
$$+ C_F^2 \left[64 S_{-2,1} + 2 \left(\frac{8(2N+1)}{N^2(N+1)^2} - 16 S_2 \right) S_1 + \frac{8\left(3N^2 + 3N + 2\right)}{N(N+1)} S_2 \right.$$
$$\left. - \frac{P_2}{N^3(N+1)^3} + 2 \left(\frac{16}{N(N+1)} - 32 S_1 \right) S_{-2} - 32[S_3 + S_{-3}] \right], \tag{4.6}$$

$$\gamma_{q\bar{q}}^{\mathrm{NS},(1)}(N) = 16 C_F \left(\frac{C_A}{2} - C_F \right) \frac{2N^3 + 2N^2 + 2N + 1}{N^3(N+1)^3}, \tag{4.7}$$

where we abbreviated some polynomials as

$$P_1 = 51N^6 + 153N^5 + 757N^4 + 144(-1)^N N^3 + 995N^3 + 352N^2 + 12N + 72 \tag{4.8}$$
$$P_2 = 3N^6 + 9N^5 + 9N^4 - 32(-1)^N N^3 + 27N^3 + 8N^2 - 8. \tag{4.9}$$

We agree with the results in the literature [107, 108, 111, 115, 118]. At 3-loop order the N_F dependent part of the non-singlet anomalous dimension is

$$\gamma_{qq}^{\mathrm{NS},(2)}(N) = C_F T_F N_F \left\{ 4 T_F N_F \left[\frac{P_4}{27N^3(N+1)^3} - \frac{16}{27} S_1 - \frac{80}{27} S_2 + \frac{16}{9} S_3 \right] \right.$$
$$+ C_A \left\{ \frac{1}{2}(-1)^N \left[\frac{256(4N+1)}{9(N+1)^4} - \frac{128}{3(N+1)^3} S_1 \right] + \frac{1}{2} \left[-\frac{8 P_8}{27N^4(N+1)^4} + \left[\frac{128}{3} S_1 \right. \right. \right.$$
$$\left. - \frac{64\left(10N^2 + 10N + 3\right)}{9N(N+1)} \right] S_{-3} + \frac{5344}{27} S_2 + \left[\frac{64\left(16N^2 + 10N - 3\right)}{9N^2(N+1)^2} - \frac{1280}{9} S_1 \right]$$

$$+ \frac{256}{3} S_2 \Bigg] S_{-2} - \frac{32\left(14N^2 + 14N + 3\right)}{3N(N+1)} S_3 + \frac{320}{3} S_4 + \frac{256}{3} S_{-4} - \frac{128}{3} S_{2,-2}$$

$$- \frac{256}{3} S_{3,1} + \frac{128\left(10N^2 + 10N - 3\right)}{9N(N+1)} S_{-2,1} + \Bigg[-\frac{16P_6}{27N^3(N+1)^3} + 64S_3$$

$$+ \frac{256}{3} S_{-2,1} \Bigg] S_1 - \frac{512}{3} S_{-2,1,1} \Bigg] + \frac{1}{2} \Bigg[\frac{32\left(3N^2 + 3N + 2\right)}{N(N+1)} - 128S_1 \Bigg] \zeta_3 \Bigg\}$$

$$+ C_F \Bigg\{ \frac{1}{2} (-1)^N \Bigg[\frac{256}{3(N+1)^3} S_1 - \frac{512(4N+1)}{9(N+1)^4} \Bigg] + \frac{1}{2} \Bigg[-\frac{128}{3} S_2^2 - \frac{16P_3}{9N^2(N+1)^2} S_2$$

$$+ \frac{4P_7}{9N^4(N+1)^4} + \Bigg[\frac{128\left(10N^2 + 10N + 3\right)}{9N(N+1)} - \frac{256}{3} S_1 \Bigg] S_{-3}$$

$$+ \Bigg[-\frac{128\left(16N^2 + 10N - 3\right)}{9N^2(N+1)^2} + \frac{2560}{9} S_1 - \frac{512}{3} S_2 \Bigg] S_{-2} - \frac{512}{3} [S_4 + S_{-4}]$$

$$+ \frac{64\left(29N^2 + 29N + 12\right)}{9N(N+1)} S_3 + \frac{256}{3} [S_{2,-2} + S_{3,1}] + \Bigg[-\frac{8P_5}{9N^3(N+1)^3}$$

$$+ \frac{1280}{9} S_2 - \frac{512}{3} [S_3 + S_{-2,1}] \Bigg] S_1 - \frac{256\left(10N^2 + 10N - 3\right)}{9N(N+1)} S_{-2,1} + \frac{1024}{3} S_{-2,1,1} \Bigg]$$

$$+ \frac{1}{2} \Bigg[128S_1 - \frac{32\left(3N^2 + 3N + 2\right)}{N(N+1)} \Bigg] \zeta_3 \Bigg\} \Bigg\} , \tag{4.10}$$

$$\gamma_{q\bar{q}}^{\mathrm{NS},(2)}(N) = C_F T_F N_F \left(\frac{C_A}{2} - C_F \right) \Bigg[\frac{64\left(2N^3 + 2N^2 + 2N + 1\right)}{3N^3(N+1)^3} S_1 - \frac{16P_9}{9N^4(N+1)^4} \Bigg] , \tag{4.11}$$

with polynomials defined by

$$P_3 = 15N^4 + 30N^3 + 79N^2 + 16N - 24 \tag{4.12}$$

$$P_4 = 51N^6 + 153N^5 + 57N^4 + 35N^3 + 96N^2 + 16N - 24 \tag{4.13}$$

$$P_5 = 165N^6 + 495N^5 + 495N^4 + 421N^3 + 240N^2 - 16N - 48 \tag{4.14}$$

$$P_6 = 209N^6 + 627N^5 + 627N^4 + 209N^3 - 36N^2 - 36N - 18 \tag{4.15}$$

$$P_7 = 207N^8 + 828N^7 + 1467N^6 + 1707N^5 + 650N^4 - 163N^3 - 320N^2$$
$$- 80N + 24 \tag{4.16}$$

$$P_8 = 270N^8 + 1080N^7 + 365N^6 - 1417N^5 - 1087N^4 + 45N^3 - 128N^2$$
$$- 72N + 72 \tag{4.17}$$

$$P_9 = 3N^6 + 73N^5 + 86N^4 + 77N^3 + 39N^2 - 10N - 12 . \tag{4.18}$$

This independent calculation matches the available moments [131–134] and confirms the corresponding parts of the general N results of [135]. Here and in the following, we reduce the appearing harmonic sums to an algebraically independent basis [146].

Analogously, we obtain the transversity non-singlet anomalous dimension at 2-loop order

$$\gamma_{qq}^{\mathrm{NS,TR},(1)}(N) = - C_F \left(\frac{C_A}{2} - C_F \right) \Bigg[64S_{-2,1} + \frac{2\left(17N^2 + 17N - 12\right)}{3N(N+1)} - 64S_{-2}S_1 - \frac{1072}{9} S_1$$

$$+ \frac{176}{3} S_2 - 32S_3 - 32S_{-3} \Bigg] + C_F^2 \Bigg[S_1 \Bigg[\frac{1072}{9} - 32S_2 \Bigg] - \frac{104}{3} S_2 - \frac{43}{3} \Bigg]$$

$$+ C_F T_F N_F \left[-\frac{160}{9} S_1 + \frac{32}{3} S_2 + \frac{4}{3} \right], \tag{4.19}$$

$$\gamma_{q\bar{q}}^{\text{NS,TR},(1)}(N) = -C_F \left(\frac{C_A}{2} - C_F \right) \frac{8}{N(N+1)}, \tag{4.20}$$

which is in agreement with previous results in [405–407]. Finally, at 3-loop the N_F dependent part of the anomalous dimension for the transversity case is given by

$$
\begin{aligned}
\gamma_{qq}^{\text{NS,TR},(2)}(N) = {}& C_F^2 T_F N_F \left\{ \frac{256}{3} S_{3,1} + \left[-\frac{512}{3} S_{-2,1} + \frac{1280}{9} S_2 - \frac{512}{3} S_3 - \frac{440}{3} \right] S_1 - \frac{2560}{9} S_{-2,1} \right. \\
& - \frac{256}{3} S_{-2,2} + \frac{1024}{3} S_{-2,1,1} + \frac{4\left(207 N^3 + 414 N^2 + 311 N + 56\right)}{9 N (N+1)^2} - \frac{128}{3} S_2^2 \\
& - \frac{80}{3} S_2 + \left[\frac{1280}{9} - \frac{256}{3} S_1 \right] S_{-3} + \left[\frac{2560}{9} S_1 - \frac{256}{3} S_2 \right] S_{-2} + \frac{1856}{9} S_3 \\
& \left. - \frac{512}{3} S_4 - \frac{256}{3} S_{-4} + \left[128 S_1 - 96 \right] \zeta_3 \right\} \\
& + C_F C_A T_F N_F \left\{ \left[\frac{256}{3} S_{-2,1} - \frac{16\left(209 N^2 + 209 N - 9\right)}{27 N (N+1)} + 64 S_3 \right] S_1 - \frac{256}{3} S_{3,1} \right. \\
& + \frac{1280}{9} S_{-2,1} + \frac{128}{3} S_{-2,2} - \frac{512}{3} S_{-2,1,1} - \frac{16\left(15 N^3 + 30 N^2 + 12 N - 5\right)}{3 N (N+1)^2} \\
& + \left[\frac{128}{3} S_1 - \frac{640}{9} \right] S_{-3} + \frac{5344}{27} S_2 + \left[\frac{128}{3} S_2 - \frac{1280}{9} S_1 \right] S_{-2} - \frac{448}{3} S_3 + \frac{320}{3} S_4 \\
& \left. + \frac{128}{3} S_{-4} + \left[96 - 128 S_1 \right] \zeta_3 \right\} \\
& + C_F T_F^2 N_F^2 \left\{ \frac{8\left(17 N^2 + 17 N - 8\right)}{9 N (N+1)} - \frac{128}{27} S_1 - \frac{640}{27} S_2 + \frac{128}{9} S_3 \right\}, \tag{4.21}
\end{aligned}
$$

$$\gamma_{q\bar{q}}^{\text{NS,TR},(2)}(N) = \frac{32}{3} C_F T_F N_F \left(\frac{C_A}{2} - C_F \right) \left[\frac{13 N + 7}{3 N (N+1)^2} - \frac{2}{N(N+1)} S_1 \right]. \tag{4.22}$$

The result agrees with the moments given in [408–412]. However, we note a typo in the moment $N = 15$ published in [413].

4.1.3. Result for the non-singlet OME

A major new result of this calculation is $a_{qq,Q}^{\text{NS},(3)}$, the constant part of the unrenormalised non-singlet vector OME at 3-loop order. It is obtained as the constant term of the ε-expansion in dimensional regularisation. In contrast to the pole terms, it cannot be predicted from lower order results via the renormalisation group equations. For the presentation of the result we define the shorthand

$$\gamma_{qq}^{(0)} = 4 \left[2 S_1 - \frac{3 N^2 + 3 N + 2}{2 N (N+1)} \right], \tag{4.23}$$

which is the leading-order anomalous dimension up to its colour factor. The result for general values of N is given by

$$a_{qq,Q}^{\text{NS},(3)}(N) =$$

4. Non-singlet contributions to DIS

$$C_F^2 T_F \left\{ \left[\frac{128}{27} S_2 - \frac{16(2N+1)}{27N^2(N+1)^2} \right] S_1^3 + \left[-\frac{8P_{18}}{9N^3(N+1)^3} - \frac{64}{9N(N+1)} S_2 + \frac{64}{3} S_3 \right. \right.$$

$$- \frac{128}{9} S_{2,1} - \frac{256}{9} S_{-2,1} \right] S_1^2 + \left[-\frac{64}{9} S_2^2 + \frac{16P_{15}}{81N^2(N+1)^2} S_2 + \frac{8P_{30}}{81N^4(N+1)^4} + \frac{704}{9} S_4 \right.$$

$$- \frac{64(40N^2+40N+9)}{27N(N+1)} S_3 + \frac{128}{9N(N+1)} S_{2,1} - \frac{320}{9} S_{3,1} - \frac{256(10N^2+10N-3)}{27N(N+1)} S_{-2,1}$$

$$\left. - \frac{256}{9} S_{-2,2} + \frac{1024}{9} S_{-2,1,1} \right] S_1 - \frac{16(31N^2+31N-6)}{27N(N+1)} S_2^2 - \frac{8}{3} B_4 \gamma_{qq}^0 + \frac{P_{34}}{162N^5(N+1)^5}$$

$$+ \left[\frac{256}{9} S_1 - \frac{128(10N^2+10N+3)}{27N(N+1)} \right] S_{-4} + \left[\frac{128}{9} S_1^2 - \frac{128(10N^2+10N+3)}{27N(N+1)} S_1 \right.$$

$$+ \frac{64(112N^3+224N^2+169N+39)}{81N(N+1)^2} + \frac{128}{9} S_2 \right] S_{-3} + \frac{8P_{17}}{81N^2(N+1)^2} S_3$$

$$- \frac{176(17N^2+17N+6)}{27N(N+1)} S_4 + \frac{512}{9} S_5 + \frac{256}{9} S_{-5} + \left[\frac{256}{27} S_1^3 - \frac{128}{9N(N+1)} S_1^2 \right.$$

$$+ \frac{128P_{13}}{81N^2(N+1)^2} S_1 - \frac{64P_{14}}{81N^3(N+1)^3} - \frac{1280}{27} S_2 + \frac{512}{27} S_3 - \frac{512}{9} S_{2,1} \right] S_{-2}$$

$$+ \frac{16P_{11}}{9N^2(N+1)^2} S_{2,1} + \frac{256}{9} S_{2,3} - \frac{512}{9} S_{2,-3} + \frac{16(89N^2+89N+30)}{27N(N+1)} S_{3,1} - \frac{512}{9} S_{4,1}$$

$$- \frac{128(112N^3+112N^2-39N+18)}{81N^2(N+1)} S_{-2,1} + \left[-\frac{8P_{27}}{81N^3(N+1)^3} + \frac{256}{27} S_3 + \frac{256}{3} S_{-2,1} \right] S_2$$

$$- \frac{128(10N^2+10N-3)}{27N(N+1)} S_{-2,2} + \frac{512}{9} S_{-2,3} + \frac{512}{9} S_{2,1,-2} + \frac{256}{9} S_{3,1,1}$$

$$+ \frac{512(10N^2+10N-3)}{27N(N+1)} S_{-2,1,1} + \frac{512}{9} S_{-2,2,1} - \frac{2048}{9} S_{-2,1,1,1} + \left[\frac{P_{23}}{3N^3(N+1)^3} \right.$$

$$+ \frac{8P_{12}}{3N^2(N+1)^2} S_1 + \left[\frac{64}{3} S_1 - \frac{32}{3N(N+1)} \right] S_{-2} + \frac{32}{3} S_3 + \frac{32}{3} S_{-3} - \frac{64}{3} S_{-2,1} \right] \zeta_2$$

$$+ (-1)^N \left[\frac{64(2N^2+2N+1)}{9N^3(N+1)^3} S_1^2 - \frac{32P_{24}}{27N^4(N+1)^4} S_1 + \frac{16P_{28}}{81N^5(N+1)^5} \right.$$

$$+ \frac{64(2N^2+2N+1)}{9N^3(N+1)^3} S_2 + \frac{16(2N^2+2N+1)}{3N^3(N+1)^3} \zeta_2 \right]$$

$$+ \gamma_{qq}^0 \left[12\zeta_4 + \frac{8}{3} S_{2,1,1} + \frac{4}{3} S_2 \zeta_2 \right] + \left[\frac{2P_{16}}{9N^2(N+1)^2} - \frac{1208}{9} S_1 - \frac{64}{3} S_2 \right] \zeta_3 \right\}$$

$$+ C_F T_F^2 \left\{ -\frac{4P_{29}}{729N^4(N+1)^4} - \frac{19424}{729} S_1 + \frac{1856}{81} S_2 - \frac{640}{81} S_3 + \frac{128}{27} S_4 \right.$$

$$+ \left[\frac{8P_{10}}{27N^2(N+1)^2} - \frac{320}{27} S_1 + \frac{64}{9} S_2 \right] \zeta_2 - \frac{128}{27} \gamma_{qq}^0 \zeta_3 \right\}$$

$$+ C_F T_F^2 N_F \left\{ \frac{2P_{32}}{729N^4(N+1)^4} - \frac{55552}{729} S_1 + \frac{640}{27} S_2 - \frac{320}{81} S_3 + \frac{64}{27} S_4 \right.$$

$$+ \left[\frac{4P_{10}}{27N^2(N+1)^2} - \frac{160}{27} S_1 + \frac{32}{9} S_2 \right] \zeta_2 + \frac{56}{27} \gamma_{qq}^0 \zeta_3 \Bigg\}$$

$$+ C_F C_A T_F \Bigg\{ -\frac{64}{27} S_2 S_1^3 + \left[\frac{4P_{19}}{9N^3(N+1)^3} + \frac{32}{9N(N+1)} S_2 - \frac{80}{9} S_3 + \frac{128}{9} [S_{2,1} + S_{-2,1}] \right] S_1^2$$

$$+ \left[\frac{80(2N+1)^2}{9N(N+1)} S_3 + \frac{112}{9} S_2^2 + \frac{4P_{31}}{729N^4(N+1)^4} - \frac{16(N-1)(2N^3 - N^2 - N - 2)}{9N^2(N+1)^2} S_2 \right.$$

$$- \frac{208}{9} S_4 - \frac{8(9N^2 + 9N + 16)}{9N(N+1)} S_{2,1} + \frac{64}{3} S_{3,1} + \frac{128(10N^2 + 10N - 3)}{27N(N+1)} S_{-2,1} + \frac{128}{9} S_{-2,2}$$

$$\left. - \frac{512}{9} S_{-2,1,1} \right] S_1 - \frac{4(15N^2 + 15N + 14)}{9N(N+1)} S_2^2 + \frac{4}{3} B_4 \gamma_{qq}^0 + \frac{P_{33}}{1458N^5(N+1)^5}$$

$$+ \left[\frac{64(10N^2 + 10N + 3)}{27N(N+1)} - \frac{128}{9} S_1 \right] S_{-4} + \left[-\frac{64}{9} S_1^2 + \frac{64(10N^2 + 10N + 3)}{27N(N+1)} S_1 \right.$$

$$\left. - \frac{32(112N^3 + 224N^2 + 169N + 39)}{81N(N+1)^2} - \frac{64}{9} S_2 \right] S_{-3} - \frac{8P_{21}}{81N^2(N+1)^2} S_3$$

$$+ \frac{4(311N^2 + 311N + 78)}{27N(N+1)} S_4 - \frac{224}{9} S_5 - \frac{128}{9} S_{-5} - \frac{4(2N^3 - 35N^2 - 37N - 24)}{9N^3(N+1)^2} [S_1^2 + S_2]$$

$$- \frac{8P_{20}}{9N^2(N+1)^2} S_{2,1} + \left[-\frac{128}{27} S_1^3 + \frac{64}{9N(N+1)} S_1^2 - \frac{64P_{13}}{81N^2(N+1)^2} S_1 + \frac{32P_{14}}{81N^3(N+1)^3} \right.$$

$$\left. + \frac{640}{27} S_2 - \frac{256}{27} S_3 + \frac{256}{9} S_{2,1} \right] S_{-2} - \frac{128}{3} S_{2,3} + \frac{256}{9} S_{2,-3} - \frac{8(13N+4)(13N+9)}{27N(N+1)} S_{3,1}$$

$$+ \frac{256}{9} S_{4,1} + \left[-\frac{4P_{26}}{81N^3(N+1)^3} + \frac{496}{27} S_3 - \frac{64}{3} S_{2,1} - \frac{128}{3} S_{-2,1} \right] S_2$$

$$+ \frac{64(112N^3 + 112N^2 - 39N + 18)}{81N^2(N+1)} S_{-2,1} + \frac{64(10N^2 + 10N - 3)}{27N(N+1)} S_{-2,2} - \frac{256}{9} S_{-2,3}$$

$$+ \gamma_{qq}^0 \left[-12\zeta_4 - 4S_{2,1,1} \right] - \frac{256}{9} S_{2,1,-2} + \frac{64}{3} S_{2,2,1} - \frac{256}{9} S_{3,1,1} - \frac{256(10N^2 + 10N - 3)}{27N(N+1)} S_{-2,1,1}$$

$$- \frac{256}{9} S_{-2,2,1} + \frac{224}{9} S_{2,1,1,1} + \frac{1024}{9} S_{-2,1,1,1} + \left[\frac{P_{25}}{27N^3(N+1)^3} + \left[\frac{16}{3N(N+1)} - \frac{32}{3} S_1 \right] S_{-2} \right.$$

$$- \frac{16}{27} S_1 - \frac{88}{9} S_2 - \frac{16}{3} S_3 - \frac{16}{3} S_{-3} + \frac{32}{3} S_{-2,1} \bigg] \zeta_2 + (-1)^N \left[-\frac{32(2N^2 + 2N + 1)}{9N^3(N+1)^3} S_1^2 \right.$$

$$+ \frac{16P_{24}}{27N^4(N+1)^4} S_1 - \frac{8P_{28}}{81N^5(N+1)^5} - \frac{32(2N^2 + 2N + 1)}{9N^3(N+1)^3} S_2 - \frac{8(2N^2 + 2N + 1)}{3N^3(N+1)^3} \zeta_2 \bigg]$$

$$+ \left[-16S_1^2 + \frac{4(637N^2 + 637N + 108)}{27N(N+1)} S_1 + \frac{P_{22}}{27N^2(N+1)^2} + 16S_2 \right] \zeta_3 \Bigg\}, \tag{4.24}$$

where the polynomials P_i are given by

$$P_{10} = 3N^4 + 6N^3 + 47N^2 + 20N - 12 \tag{4.25}$$

$$P_{11} = 7N^4 + 14N^3 + 3N^2 - 4N - 4 \tag{4.26}$$

$$P_{12} = 15N^4 + 30N^3 + 15N^2 - 4N - 2 \tag{4.27}$$

4. Non-singlet contributions to DIS

$$P_{13} = 112N^4 + 224N^3 + 121N^2 + 9N + 9 \tag{4.28}$$

$$P_{14} = 181N^4 + 266N^3 + 82N^2 - 3N + 18 \tag{4.29}$$

$$P_{15} = 448N^4 + 896N^3 + 484N^2 + 54N + 45 \tag{4.30}$$

$$P_{16} = 561N^4 + 1122N^3 + 767N^2 + 302N + 48 \tag{4.31}$$

$$P_{17} = 1301N^4 + 2602N^3 + 2177N^2 + 492N - 84 \tag{4.32}$$

$$P_{18} = 2N^5 + 7N^4 + 3N^3 - 9N^2 - 7N + 2 \tag{4.33}$$

$$P_{19} = 3N^5 + 13N^4 - 23N^3 - 69N^2 - 54N - 16 \tag{4.34}$$

$$P_{20} = 12N^5 + 16N^4 + 18N^3 - 15N^2 - 5N - 8 \tag{4.35}$$

$$P_{21} = 27N^5 + 533N^4 + 913N^3 + 821N^2 + 144N - 36 \tag{4.36}$$

$$P_{22} = 648N^5 - 2235N^4 - 4542N^3 - 3725N^2 - 770N - 432 \tag{4.37}$$

$$P_{23} = -87N^6 - 261N^5 - 321N^4 - 183N^3 - 52N^2 - 8 \tag{4.38}$$

$$P_{24} = 3N^6 + 9N^5 + 70N^4 + 77N^3 + 39N^2 - 10N - 12 \tag{4.39}$$

$$P_{25} = 255N^6 + 765N^5 + 581N^4 + 151N^3 + 356N^2 + 276N + 72 \tag{4.40}$$

$$P_{26} = 364N^6 + 1227N^5 + 1191N^4 + 589N^3 + 621N^2 + 486N + 144 \tag{4.41}$$

$$P_{27} = 1014N^6 + 3042N^5 + 3757N^4 + 1703N^3 + 31N^2 + 93N + 162 \tag{4.42}$$

$$P_{28} = 39N^8 + 138N^7 + 847N^6 + 1371N^5 + 1283N^4 + 485N^3 + 101N^2$$
$$+ 132N + 72 \tag{4.43}$$

$$P_{29} = 417N^8 + 1668N^7 - 4822N^6 - 12384N^5 - 6507N^4 + 740N^3 + 216N^2$$
$$+ 144N + 432 \tag{4.44}$$

$$P_{30} = 2307N^8 + 9255N^7 + 13977N^6 + 7915N^5 - 350N^4 - 1456N^3 - 106N^2$$
$$- 138N - 108 \tag{4.45}$$

$$P_{31} = 6197N^8 + 24788N^7 + 39126N^6 + 28838N^5 + 9977N^4 - 702N^3 - 3240N^2$$
$$- 3456N - 1620 \tag{4.46}$$

$$P_{32} = 11751N^8 + 47004N^7 + 93754N^6 + 104364N^5 + 55287N^4 + 6256N^3 - 2448N^2$$
$$- 144N - 432 \tag{4.47}$$

$$P_{33} = -22989N^{10} - 114945N^9 - 199958N^8 - 99362N^7 + 179919N^6 + 291355N^5$$
$$+ 223828N^4 + 90936N^3 + 31680N^2 + 23760N + 10368 \tag{4.48}$$

$$P_{34} = -22293N^{10} - 111465N^9 - 252090N^8 - 310818N^7 - 225241N^6 - 77573N^5$$
$$- 8808N^4 - 352N^3 + 256N^2 + 672N - 288 \,. \tag{4.49}$$

In this result, only harmonic sums up to weight $w = 5$ appear. They have been reduced to an algebraically independent basis using the algorithms implemented in `HarmonicSums`. The constant B_4 is defined in Eq. (3.31).

After partial fractioning of the coefficients of the harmonic sums, there are still terms proportional to N left.

$$T_1 = \frac{8}{3}C_A C_F T_F N \left[9\zeta_3 - S_3(N) - 4S_{2,1}(N)\right] \tag{4.50}$$

Performing an inverse Mellin transformation on the expression yields terms which are proportional to $1/(1-x)^2$. In general, positive powers of N would require more singular distributions like the derivative of the δ-distribution. In the present case, however, these distributions cancel.

The asymptotic expansion of T_1,

$$T_1 \underset{N\to\infty}{\propto} \frac{32}{3}C_A C_F T_F \ln(\bar{N}),\tag{4.51}$$

shows that only a logarithmic instead of a linear divergence in the limit $N \to \infty$ remains and that, therefore, the $1/(1-x)^2$ terms behave like $1/(1-x)_+$ distributions. A similar behaviour had previously been observed in the massless Wilson coefficients where even higher powers of N appeared [138].

After renormalisation, cf. Eqs. (4.1) and (4.2), the non-singlet OME in the vector case can be expressed in N space as

$$
\begin{aligned}
A_{qq,Q}^{NS}(N) = 1 &+ a_s^2 C_F T_F \left\{ -\frac{\gamma_{qq}^{(0)}}{3}\ln^2\left(\frac{m^2}{\mu^2}\right) + \ln\left(\frac{m^2}{\mu^2}\right)\left[\frac{2P_{10}}{9N^2(N+1)^2} - \frac{80}{9}S_1 + \frac{16}{3}S_2\right] \right. \\
&+ \frac{P_{43}}{54N^3(N+1)^3} - \frac{224}{27}S_1 + \frac{40}{9}S_2 - \frac{8}{3}S_3 \Bigg\} \\
&+ a_s^3 \Bigg\{ C_F^2 T_F \left[\ln^2\left(\frac{m^2}{\mu^2}\right)\left[\frac{4P_{39}}{3N^3(N+1)^3} - \frac{8}{3}\frac{(N+2)(3N^3+3N+2)}{N^2(N+1)^2}S_1 \right.\right. \\
&+ \frac{8}{3}\gamma_{qq}^{(0)}S_2 + \frac{64}{3}S_3 + \left(-\frac{64}{3N(N+1)} + \frac{128}{3}S_1\right)S_{-2} + \frac{64}{3}S_{-3} - \frac{128}{3}S_{-2,1} \Bigg] \\
&+ \ln\left(\frac{m^2}{\mu^2}\right)\left[\frac{(N-1)P_{47}}{9N^4(N+1)^4} + \left(-\frac{8P_{40}}{9N^3(N+1)^3} + \frac{640}{9}S_2 - \frac{256}{3}S_3\right.\right. \\
&- \frac{256}{3}S_{-2,1}\right)S_1 - \frac{8P_3}{9N^2(N+1)^2}S_2 - \frac{64}{3}S_2^2 + \frac{32(29N^2+29N+12)}{9N(N+1)}S_3 \\
&- \frac{256}{3}S_4 + \left(-\frac{64(16N^2+10N-3)}{9N^2(N+1)^2} + \frac{1280}{9}S_1 - \frac{128}{3}S_2\right)S_{-2} \\
&+ \left(\frac{64(10N^2+10N+3)}{9N(N+1)} - \frac{128}{3}S_1\right)S_{-3} - \frac{128}{3}S_{-4} + \frac{128}{3}S_{3,1} - \frac{128}{3}S_{-2,2} \\
&- \frac{128(10N^2+10N-3)}{9N(N+1)}S_{-2,1} + \frac{512}{3}S_{-2,1,1} + 8\gamma_{qq}^{(0)}\zeta_3\right] + \frac{P_{53}}{81N^5(N+1)^5} \\
&- \frac{128}{81}\frac{(112N^3+112N^2-39N+18)}{N^2(N+1)}S_{-2,1} + \left(\frac{2P_{16}}{9N^2(N+1)^2} - \frac{1208}{9}S_1\right. \\
&- \frac{64}{3}S_2\right)\zeta_3 + (-1)^N\left[\ln^2\left(\frac{m^2}{\mu^2}\right)\frac{32}{3}\frac{(2N^2+2N+1)}{N^3(N+1)^3} + \frac{16P_{28}}{81N^5(N+1)^5}\right. \\
&+ \ln\left(\frac{m^2}{\mu^2}\right)\left[\frac{16P_{24}}{9N^4(N+1)^4} - \frac{64(2N^2+2N+1)}{3N^3(N+1)^3}S_1\right] - \frac{32P_{24}}{27N^4(N+1)^4}S_1 \\
&+ \frac{64(2N^2+2N+1)}{9N^3(N+1)^3}S_1^2 + \frac{64(2N^2+2N+1)}{9N^3(N+1)^3}S_2\right] + \gamma_{qq}^{(0)}\left(-\frac{8B_4}{3} + 12\zeta_4\right. \\
&+ \frac{8}{3}S_{2,1,1}\right) + \left(\frac{2P_{51}}{81N^4(N+1)^4} + \frac{16P_{15}}{81N^2(N+1)^2}S_2 - \frac{64}{9}S_2^2 + \frac{128}{9N(N+1)}S_{2,1}\right. \\
&- \frac{64(40N^2+40N+9)}{27N(N+1)}S_3 + \frac{704}{9}S_4 - \frac{320}{9}S_{3,1} - \frac{256}{9}S_{-2,2} + \frac{1024}{9}S_{-2,1,1} \\
&- \frac{256(10N^2+10N-3)}{27N(N+1)}S_{-2,1}\right)S_1 + \left(-\frac{8P_{18}}{9N^3(N+1)^3} - \frac{64}{9N(N+1)}S_2\right. \\
&+ \frac{64}{3}S_3 - \frac{128}{9}S_{2,1} - \frac{256}{9}S_{-2,1}\right)S_1^2 + \left(-\frac{16(2N+1)}{27N^2(N+1)^2} + \frac{128}{27}S_2\right)S_1^3
\end{aligned}
$$

$$
+ \left(-\frac{8P_{46}}{81N^3(N+1)^3} + \frac{256}{27}S_3 + \frac{256}{3}S_{-2,1} \right) S_2 - \frac{16\left(31N^2 + 31N - 6\right)}{27N(N+1)}S_2^2
$$

$$
+ \frac{8P_{35}}{81N^2(N+1)^2}S_3 - \frac{176\left(17N^2 + 17N + 6\right)}{27N(N+1)}S_4 + \frac{512}{9}S_5 + \left(-\frac{512}{9}S_{2,1} \right.
$$

$$
- \frac{64P_{14}}{81N^3(N+1)^3} + \frac{128P_{13}}{81N^2(N+1)^2}S_1 - \frac{128}{9N(N+1)}S_1^2 + \frac{256}{27}S_1^3 - \frac{1280}{27}S_2
$$

$$
+ \frac{512}{27}S_3 \bigg)S_{-2} + \left(\frac{64}{81}\frac{\left(112N^3 + 224N^2 + 169N + 39\right)}{N(N+1)^2} + \frac{128}{9}S_1^2 + \frac{128}{9}S_2 \right.
$$

$$
- \frac{128\left(10N^2 + 10N + 3\right)}{27N(N+1)}S_1 \bigg)S_{-3} + \left(-\frac{128\left(10N^2 + 10N + 3\right)}{27N(N+1)} + \frac{256}{9}S_1 \right)S_{-4}
$$

$$
+ \frac{256}{9}S_{-5} + \frac{16P_{11}}{9N^2(N+1)^2}S_{2,1} + \frac{256}{9}S_{2,3} - \frac{512}{9}S_{2,-3} - \frac{512}{9}S_{4,1} + \frac{512}{9}S_{-2,3}
$$

$$
+ \frac{16\left(89N^2 + 89N + 30\right)}{27N(N+1)}S_{3,1} - \frac{128\left(10N^2 + 10N - 3\right)}{27N(N+1)}S_{-2,2} + \frac{512}{9}S_{2,1,-2}
$$

$$
+ \frac{256}{9}S_{3,1,1} + \frac{512\left(10N^2 + 10N - 3\right)}{27N(N+1)}S_{-2,1,1} + \frac{512}{9}S_{-2,2,1} - \frac{2048}{9}S_{-2,1,1,1} \Bigg]
$$

$$
+ C_A C_F T_F \Bigg[\frac{22\gamma_{qq}^{(0)}}{27}\ln^3\left(\frac{m^2}{\mu^2}\right) + \ln^2\left(\frac{m^2}{\mu^2}\right)\left[\frac{2P_{41}}{9N^3(N+1)^3} - \frac{184}{9}S_1 - \frac{32}{3}S_3 \right.
$$

$$
+ \left(\frac{32}{3N(N+1)} - \frac{64}{3}S_1 \right)S_{-2} - \frac{32}{3}S_{-3} + \frac{64}{3}S_{-2,1} \Bigg]
$$

$$
+ \ln\left(\frac{m^2}{\mu^2}\right)\Bigg[\frac{P_{48}}{81N^4(N+1)^4} + \left(-\frac{8P_{42}}{81N^3(N+1)^3} + 32S_3 + \frac{128}{3}S_{-2,1} \right)S_1
$$

$$
+ \frac{1792}{27}S_2 - \frac{16\left(31N^2 + 31N + 9\right)}{9N(N+1)}S_3 + \frac{160}{3}S_4 + \left(\frac{32\left(16N^2 + 10N - 3\right)}{9N^2(N+1)^2} \right.
$$

$$
- \frac{640}{9}S_1 + \frac{64}{3}S_2 \bigg)S_{-2} + \left(-\frac{32\left(10N^2 + 10N + 3\right)}{9N(N+1)} + \frac{64}{3}S_1 \right)S_{-3} + \frac{64}{3}S_{-4}
$$

$$
- \frac{128}{3}S_{3,1} + \frac{64\left(10N^2 + 10N - 3\right)}{9N(N+1)}S_{-2,1} + \frac{64}{3}S_{-2,2} - \frac{256}{3}S_{-2,1,1} - 8\gamma_{qq}^{(0)}\zeta_3 \Bigg]
$$

$$
+ \frac{P_{54}}{729N^5(N+1)^5} + \frac{64}{81}\frac{\left(112N^3 + 112N^2 - 39N + 18\right)}{N^2(N+1)}S_{-2,1}
$$

$$
+ \left(\frac{P_{38}}{27N^2(N+1)^2} + \frac{4\left(593N^2 + 593N + 108\right)}{27N(N+1)}S_1 - 16S_1^2 + 16S_2 \right)\zeta_3
$$

$$
+ (-1)^N \Bigg[-\frac{\left(2N^2 + 2N + 1\right)}{N^3(N+1)^3}\frac{16}{3}\ln^2\left(\frac{m^2}{\mu^2}\right) + \ln\left(\frac{m^2}{\mu^2}\right)\left[-\frac{8P_{24}}{9N^4(N+1)^4} \right.
$$

$$
+ \frac{32\left(2N^2 + 2N + 1\right)}{3N^3(N+1)^3}S_1 \Bigg] - \frac{8P_{28}}{81N^5(N+1)^5} + \frac{16P_{24}}{27N^4(N+1)^4}S_1
$$

$$
- \frac{32\left(2N^2 + 2N + 1\right)}{9N^3(N+1)^3}S_1^2 - \frac{32\left(2N^2 + 2N + 1\right)}{9N^3(N+1)^3}S_2 \Bigg] + \gamma_{qq}^{(0)}\left(\frac{4B_4}{3} - 12\zeta_4 \right.
$$

$$
- 4S_{2,1,1} \bigg) + \left(-\frac{4P_{52}}{729N^4(N+1)^4} - \frac{16}{9}\frac{\left(N-1\right)\left(2N^3 - N^2 - N - 2\right)}{N^2(N+1)^2}S_2 \right.
$$

$$
+ \frac{112}{9}S_2^2 + \frac{80(2N+1)^2}{9N(N+1)}S_3 - \frac{208}{9}S_4 - \frac{8\left(9N^2 + 9N + 16\right)}{9N(N+1)}S_{2,1} + \frac{64}{3}S_{3,1}
$$

$$+ \frac{128(10N^2 + 10N - 3)}{27N(N+1)} S_{-2,1} + \frac{128}{9} S_{-2,2} - \frac{512}{9} S_{-2,1,1} \Bigg) S_1$$

$$+ \left(\frac{4P_{36}}{9N^3(N+1)^3} + \frac{32}{9N(N+1)} S_2 - \frac{80}{9} S_3 + \frac{128}{9} S_{2,1} + \frac{128}{9} S_{-2,1} \right) S_1^2$$

$$+ \left(\frac{4P_{45}}{81N^3(N+1)^3} + \frac{496}{27} S_3 - \frac{64}{3} S_{2,1} - \frac{128}{3} S_{-2,1} \right) S_2 - \frac{64}{27} S_1^3 S_2$$

$$- \frac{4(15N^2 + 15N + 14)}{9N(N+1)} S_2^2 + \frac{4(443N^2 + 443N + 78)}{27N(N+1)} S_4 - \frac{224}{9} S_5$$

$$- \frac{8P_{37}}{81N^2(N+1)^2} S_3 + \left(\frac{32P_{14}}{81N^3(N+1)^3} - \frac{64P_{13}}{81N^2(N+1)^2} S_1 + \frac{64}{9N(N+1)} S_1^2 \right.$$

$$\left. - \frac{128}{27} S_1^3 + \frac{640}{27} S_2 - \frac{256}{27} S_3 + \frac{256}{9} S_{2,1} \right) S_{-2} + \left(\frac{64(10N^2 + 10N + 3)}{27N(N+1)} S_1 \right.$$

$$- \frac{32}{81} \frac{(112N^3 + 224N^2 + 169N + 39)}{N(N+1)^2} - \frac{64}{9} S_1^2 - \frac{64}{9} S_2 \right) S_{-3} + \left(-\frac{128}{9} S_1 \right.$$

$$+ \frac{64(10N^2 + 10N + 3)}{27N(N+1)} \right) S_{-4} - \frac{128}{9} S_{-5} - \frac{8P_{20} S_{2,1}}{9N^2(N+1)^2} - \frac{128}{3} S_{2,3}$$

$$+ \frac{256}{9} S_{2,-3} - \frac{8(13N+4)(13N+9)}{27N(N+1)} S_{3,1} + \frac{256}{9} S_{4,1} - \frac{256}{9} S_{-2,3} - \frac{256}{9} S_{2,1,-2}$$

$$+ \frac{64(10N^2 + 10N - 3)}{27N(N+1)} S_{-2,2} + \frac{64}{3} S_{2,2,1} - \frac{256}{9} S_{3,1,1} - \frac{256}{9} S_{-2,2,1}$$

$$- \frac{256(10N^2 + 10N - 3)}{27N(N+1)} S_{-2,1,1} + \frac{224}{9} S_{2,1,1,1} + \frac{1024}{9} S_{-2,1,1,1} \Bigg]$$

$$+ C_F T_F^2 \left[-\frac{16\gamma_{qq}^{(0)}}{27} \ln^3 \left(\frac{m^2}{\mu^2} \right) + \ln^2 \left(\frac{m^2}{\mu^2} \right) \left[\frac{8P_{10}}{27N^2(N+1)^2} - \frac{320}{27} S_1 + \frac{64}{9} S_2 \right] \right.$$

$$- \frac{248\gamma_{qq}^{(0)}}{81} \ln \left(\frac{m^2}{\mu^2} \right) - \frac{2P_{50}}{729N^4(N+1)^4} + \frac{12064}{729} S_1 + \frac{64}{81} S_2 + \frac{320}{81} S_3 - \frac{64}{27} S_4$$

$$- \frac{112\gamma_{qq}^{(0)}}{27} \zeta_3 \right] + C_F N_F T_F^2 \left[-\frac{8\gamma_{qq}^{(0)} \ln^3 \left(\frac{m^2}{\mu^2} \right)}{27} + \ln \left(\frac{m^2}{\mu^2} \right) \left[\frac{4P_{44}}{81N^3(N+1)^3} \right. \right.$$

$$\left. - \frac{2176}{81} S_1 - \frac{320}{27} S_2 + \frac{64}{9} S_3 \right] + \frac{4P_{49}}{729N^4(N+1)^4} - \frac{24064}{729} S_1 + \frac{128}{81} S_2 + \frac{640}{81} S_3$$

$$\left. \left. - \frac{128}{27} S_4 + \frac{64\gamma_{qq}^{(0)}}{27} \zeta_3 \right] \right\}. \tag{4.52}$$

In addition to the polynomials which we already defined before in this chapter, we use

$$P_{35} = 977N^4 + 1954N^3 + 1853N^2 + 492N - 84 \tag{4.53}$$

$$P_{36} = 3N^5 + 11N^4 + 10N^3 + 3N^2 + 7N + 8 \tag{4.54}$$

$$P_{37} = 27N^5 + 863N^4 + 1573N^3 + 1151N^2 + 144N - 36 \tag{4.55}$$

$$P_{38} = 648N^5 - 2103N^4 - 4278N^3 - 3505N^2 - 682N - 432 \tag{4.56}$$

$$P_{39} = 6N^6 + 18N^5 + 21N^4 + 24N^3 + 7N^2 - 4 \tag{4.57}$$

$$P_{40} = 15N^6 + 45N^5 + 45N^4 + 143N^3 + 120N^2 - 8N - 24 \tag{4.58}$$

$$P_{41} = 51N^6 + 153N^5 + 223N^4 + 191N^3 + 118N^2 + 48N + 24 \tag{4.59}$$

4. Non-singlet contributions to DIS

$$P_{42} = 155N^6 + 465N^5 + 465N^4 + 155N^3 - 108N^2 - 108N - 54 \tag{4.60}$$

$$P_{43} = 219N^6 + 657N^5 + 1193N^4 + 763N^3 - 40N^2 - 48N + 72 \tag{4.61}$$

$$P_{44} = 525N^6 + 1575N^5 + 1535N^4 + 973N^3 + 536N^2 + 48N - 72 \tag{4.62}$$

$$P_{45} = 868N^6 + 2469N^5 + 2487N^4 + 940N^3 + 27N^2 + 63N + 72 \tag{4.63}$$

$$P_{46} = 906N^6 + 2718N^5 + 3433N^4 + 1595N^3 + 31N^2 + 93N + 162 \tag{4.64}$$

$$P_{47} = 9N^7 + 45N^6 + 279N^5 + 1263N^4 + 1348N^3 + 752N^2 + 112N - 48 \tag{4.65}$$

$$P_{48} = -4785N^8 - 19140N^7 - 18970N^6 + 672N^5 + 7683N^4 + 1004N^3 + 1272N^2 \\ + 72N - 864 \tag{4.66}$$

$$P_{49} = 3549N^8 + 14196N^7 + 23870N^6 + 25380N^5 + 15165N^4 + 1712N^3 - 2016N^2 \\ + 144N + 432 \tag{4.67}$$

$$P_{50} = 5487N^8 + 21948N^7 + 36370N^6 + 28836N^5 + 11943N^4 + 4312N^3 + 2016N^2 \\ - 144N - 432 \tag{4.68}$$

$$P_{51} = 7131N^8 + 28632N^7 + 43326N^6 + 23272N^5 - 3497N^4 - 5824N^3 - 424N^2 \\ - 552N - 432 \tag{4.69}$$

$$P_{52} = 10807N^8 + 43228N^7 + 62898N^6 + 39178N^5 + 7027N^4 + 702N^3 + 3240N^2 \\ + 3456N + 1620 \tag{4.70}$$

$$P_{53} = -6219N^{10} - 31095N^9 - 72513N^8 - 95154N^7 - 79721N^6 - 32383N^5 - 2307N^4 \\ + 3280N^3 + 1424N^2 + 336N - 144 \tag{4.71}$$

$$P_{54} = 165N^{10} + 825N^9 + 106856N^8 + 321746N^7 + 396657N^6 + 247433N^5 \\ + 126914N^4 + 51804N^3 + 6336N^2 + 4752N + 5184 \,. \tag{4.72}$$

The corresponding x space expression is obtained after an inverse Mellin transformation and is presented in Appendix E in Eqs. (E.3), (E.6) and (E.7).

The heavy quark mass in the expressions presented here is defined in the OMS scheme. The conversion from the OMS to the $\overline{\text{MS}}$ scheme involves the matching coefficients of this scheme change [329, 414–418]. The difference of the OMEs with masses renormalised in these schemes is given by

$$A_{qq,Q}^{\text{NS},\overline{\text{MS}}}(N) - A_{qq,Q}^{\text{NS,OMS}}(N) = $$
$$C_F^2 T_F \left\{ 4\gamma_{qq}^0 \ln^2\left(\frac{m^2}{\mu^2}\right) + \left[\frac{4(21N^4 + 42N^3 - 7N^2 - 4N + 12)}{3N^2(N+1)^2} + \frac{32}{3}S_1 \right. \right.$$
$$\left. \left. - 32S_2 \right] \ln\left(\frac{m^2}{\mu^2}\right) + \frac{16(3N^4 + 6N^3 + 47N^2 + 20N - 12)}{9N^2(N+1)^2} - \frac{640}{9}S_1 + \frac{128}{3}S_2 \right\}, \tag{4.73}$$

where we have symbolically identified the masses in the two schemes to shorten the expression. Similarly the formula in x space reads

$$A_{qq,Q}^{\text{NS},\overline{\text{MS}}}(x) - A_{qq,Q}^{\text{NS,OMS}}(x) = $$
$$C_F^2 T_F \left\{ \left(\frac{1}{1-x} \left[-32\ln^2\left(\frac{m^2}{\mu^2}\right) - 32\ln\left(\frac{m^2}{\mu^2}\right)\left(\frac{1}{3} + H_0\right) + \frac{640}{9} + \frac{128}{3}H_0 \right] \right)_+ \right.$$
$$\left. + \left[-24\ln^2\left(\frac{m^2}{\mu^2}\right) + 28\ln\left(\frac{m^2}{\mu^2}\right) + \frac{16}{3} \right] \delta(1-x) + 16\ln^2\left(\frac{m^2}{\mu^2}\right)(x+1) \right.$$

$$+ \ln\left(\frac{m^2}{\mu^2}\right)\left(16(x+1)H_0 + \frac{16}{3}(7x-5)\right) - \frac{64}{3}(x+1)H_0 - \frac{64}{9}(11x-1)\bigg\}. \tag{4.74}$$

The notation $(\dots)_+$ refers to the plus distributions defined in Eq. (3.44).

The leading asymptotic behaviour of the OME in the limits of large x ($x \to 1$) and small x ($x \to 0$) can be obtained from the asymptotic expansion in N space around $N \to \infty$ and the expansion around the rightmost pole – in the non-singlet case $N \to 0$. These expansions of the harmonic sums and their rational coefficients can be done, for example, using `HarmonicSums`. The leading behaviour in the limit $N \to \infty$ is proportional to $\ln^k(\bar{N})$, where $\bar{N} = N\exp(\gamma_E)$ and γ_E is the Euler-Mascheroni constant. These logarithms arise from powers of the harmonic sum $S_1(N)^k$ and correspond to plus distributions $(\ln^{k-1}(1-x)/(1-x))_+$ in x space. Poles around $N = 0$ of the form N^{-k} give rise to powers of logarithms $\ln^{k-1}(x)$ in the $x \to 0$ limit in x space.

In the limit of small x, i.e. $x \to 0$, the non-singlet OME continued from even N behaves like

$$A_{qq,Q}^{NS} \underset{x\to 0}{\propto} a_s^2 C_F T_F \frac{2}{3}\ln^2(x) + a_s^3 C_F^2 T_F \frac{14}{27}\ln^4(x), \tag{4.75}$$

while the same limit for a continuation from odd N reads

$$A_{qq,Q}^{NS} \underset{x\to 0}{\propto} a_s^2 C_F T_F \frac{2}{3}\ln^2(x) + a_s^3\left(C_A C_F T_F \frac{16}{27} - C_F^2 T_F \frac{2}{3}\right)\ln^4(x). \tag{4.76}$$

The asymptotic behaviour is determined by the rightmost pole in N space, which is located at $N = 0$ [419, 420].

For $x \to 1$, which corresponds to the limit $N \to \infty$, the leading behaviour of the non-singlet OME is given by

$$A_{qq,Q}^{NS,(2)} \underset{x\to 1}{\propto} C_F T_F \left[\frac{8}{3}\ln^2\left(\frac{m^2}{\mu^2}\right) + \frac{80}{9}\ln\left(\frac{m^2}{\mu^2}\right) + \frac{224}{27}\right]\left(\frac{1}{1-x}\right)_+, \tag{4.77}$$

$$\begin{aligned}
A_{qq,Q}^{NS,(3)} \underset{x\to 1}{\propto} &-C_F T_F \Bigg\{\left\{\frac{176}{27}C_A - \left[\frac{64}{27}N_F + \frac{128}{27}\right]T_F\right\}\ln^3\left(\frac{m^2}{\mu^2}\right) \\
&+ \left\{-8C_F - \frac{320}{27}T_F + C_A\left[-\frac{184}{9} + \frac{32}{3}\zeta_2\right]\right\}\ln^2\left(\frac{m^2}{\mu^2}\right) \\
&+ \left\{-\left[\frac{2176}{81}N_F + \frac{1984}{81}\right]T_F + C_A\left[-\frac{1240}{81} + \frac{320}{9}\zeta_2 - \frac{224}{3}\zeta_3\right]\right. \\
&\left. + C_F\left[-\frac{40}{3} + 64\zeta_3\right]\right\}\ln\left(\frac{m^2}{\mu^2}\right) \\
&+ \left\{C_F\left[-\frac{2}{27}(288B_4 - 2377) - \frac{1208}{9}\zeta_3 + 96\zeta_4\right] + T_F\left[\frac{12064}{729} - \frac{896}{27}\zeta_3\right. \right. \\
&\left. + N_F\left[-\frac{24064}{729} + \frac{512}{27}\zeta_3\right]\right] + C_A\left[\frac{4}{729}(1944B_4 - 8863) + \frac{3296}{81}\zeta_2\right. \\
&\left.\left. + 60\zeta_3 - \frac{352}{3}\zeta_4\right]\right\}\Bigg\}\left(\frac{1}{1-x}\right)_+.
\end{aligned} \tag{4.78}$$

The large x limit for the continuation from even and odd N is identical.

4.1.4. Results for the transversity OME

Analogously to the massive OME of the non-singlet vector operator, the corresponding matrix element for the transversity operator can be obtained from the same diagrams by just using slightly different Feynman rules for the local operator insertions: Each of the Feynman rules for operator insertions on fermion lines contains a factor $\slashed{\Delta}$, which has to be replaced by $\sigma^{\mu\nu}\Delta_\nu$ for the transversity operator.

The constant term in the ε expansion of the unrenormalised OME $a_{qq,Q}^{\mathrm{NS,TR},(3)}$ is

$$
a_{qq,Q}^{\mathrm{NS,TR},(3)}(N) =
$$

$$
C_F^2 T_F \Bigg\{ \frac{128}{27} S_2 S_1^3 + \Bigg[-\frac{16\big(N + 2(-1)^N + 1\big)}{9N(N+1)} + \frac{64}{3} S_3 - \frac{128}{9} S_{2,1} - \frac{256}{9} S_{-2,1} \Bigg] S_1^2
$$

$$
+ \Bigg[-\frac{64}{9} S_2^2 + \frac{7168}{81} S_2 + \frac{8P_{59}}{27 N^2(N+1)^2} - \frac{2560}{27} S_3 + \frac{704}{9} S_4 - \frac{320}{9} S_{3,1} - \frac{2560}{27} S_{-2,1}
$$

$$
- \frac{256}{9} S_{-2,2} + \frac{64}{3} S_{2,1,1} + \frac{1024}{9} S_{-2,1,1} \Bigg] S_1 - \frac{496}{27} S_2^2 + \frac{32(-1)^N \big(2N^2 + 2N + 1\big)}{9N^3(N+1)^3}
$$

$$
- \frac{2P_{62}}{81 N^3(N+1)^3} + B_4 \Big(16 - \frac{64 S_1}{3} \Big) + 2 \Big(\frac{128}{9} S_1 - \frac{640}{27} \Big) S_{-4} + \big(96 S_1 - 72\big)\zeta_4
$$

$$
+ 2 \Bigg[\frac{64}{9} S_1^2 - \frac{640}{27} S_1 + \frac{64}{9} S_2 + \frac{3584}{81} \Bigg] S_{-3} + \frac{10408}{81} S_3 - \frac{2992}{27} S_4 + \frac{256}{9}\big(S_{-5} + 2S_5\big)
$$

$$
+ \Bigg[\frac{256}{27} S_1^3 + \frac{14336}{81} S_1 - \frac{1280}{27} S_2 + \frac{512}{27} S_3 - \frac{512}{9} S_{2,1} - \frac{64}{9N(N+1)} \Bigg] S_{-2} + \frac{112}{9} S_{2,1}
$$

$$
+ \frac{256}{9} S_{2,3} - \frac{512}{9} S_{2,-3} + \frac{1424}{27} S_{3,1} - \frac{512}{9} S_{4,1} - \frac{14336}{81} S_{-2,1} + \Bigg[\frac{256}{27} S_3 + \frac{256}{3} S_{-2,1}
$$

$$
- \frac{16\big(169 N^2 + 169 N + 6(-1)^N + 6\big)}{27 N(N+1)} \Bigg] S_2 - \frac{1280}{27} S_{-2,2} + \frac{512}{9} S_{-2,3} - 16 S_{2,1,1}
$$

$$
+ \frac{512}{9} S_{2,1,-2} + \frac{256}{9} S_{3,1,1} + \frac{5120}{27} S_{-2,1,1} + \frac{512}{9} S_{-2,2,1} - \frac{2048}{9} S_{-2,1,1,1}
$$

$$
+ \Bigg[-\frac{2\big(45 N^2 + 45 N + 4(-1)^N - 4\big)}{3N(N+1)} + \frac{64}{3} S_{-2} S_1 - 8 S_2 + \Big(\frac{32}{3} S_2 + 40 \Big) S_1 + \frac{32}{3} S_3
$$

$$
+ \frac{32}{3} S_{-3} - \frac{64}{3} S_{-2,1} + 1 \Bigg]\zeta_2 + \Big(-\frac{1208}{9} S_1 - \frac{64}{3} S_2 + \frac{350}{3} + 8 \Big)\zeta_3 + \frac{335}{18} \Bigg\}
$$

$$
+ C_F T_F^2 \Bigg\{ N_F \Bigg[\frac{32 P_{57}}{243 N^2(N+1)^2} - \frac{55552}{729} S_1 + \frac{640}{27} S_2 - \frac{320}{81} S_3 + \frac{64}{27} S_4
$$

$$
+ \Big(-\frac{160}{27} S_1 + \frac{32}{9} S_2 + \frac{4}{9} \Big)\zeta_2 + \Big(\frac{448}{27} S_1 - \frac{112}{9} \Big)\zeta_3 - \frac{674}{81} \Bigg] + \frac{8 P_{56}}{243 N^2(N+1)^2}
$$

$$
- \frac{19424}{729} S_1 + \frac{1856}{81} S_2 - \frac{640}{81} S_3 + \frac{128}{27} S_4 + \Bigg[-\frac{320}{27} S_1 + \frac{64}{9} S_2 + \frac{8}{9} \Bigg]\zeta_2 + \Bigg[-\frac{1024}{27} S_1
$$

$$
+ \frac{256}{9} \Bigg]\zeta_3 - \frac{604}{81} \Bigg\} + C_A C_F T_F \Bigg\{ -\frac{64}{27} S_2 S_1^3 + \Bigg[\frac{4 P_{55}}{9N(N+1)^2(N+2)} - \frac{80}{9} S_3
$$

$$
+ \frac{128}{9}\big(S_{2,1} + S_{-2,1}\big) \Bigg] S_1^2 + \Bigg[\frac{112}{9} S_2^2 - \frac{16(N-2)(2N+3) S_2}{9(N+1)(N+2)} - \frac{208}{9} S_4 - 8 S_{2,1}
$$

$$
+ \frac{1280}{27} S_{-2,1} + \frac{4 P_{60}}{729 N(N+1)^2(N+2)} + \frac{320}{9} S_3 + \frac{64}{3} S_{3,1} + \frac{128}{9} S_{-2,2} - 32 S_{2,1,1}
$$

$$-\frac{512}{9}S_{-2,1,1}\Bigg]S_1 - \frac{20}{3}S_2^2 - \frac{16(-1)^N\big(2N^2+2N+1\big)}{9N^3(N+1)^3} + \frac{P_{61}}{243N^3(N+1)^3}$$

$$+ \big(72-96S_1\big)\zeta_4 + 2\Big(\frac{320}{27}-\frac{64}{9}S_1\Big)S_{-4} + B_4\Big(\frac{32}{3}S_1-8\Big) + 2\Big[-\frac{32}{9}S_1^2 + \frac{320}{27}S_1$$

$$-\frac{32}{9}S_2 - \frac{1792}{81}\Big]S_{-3} - \frac{8\big(27N^3+560N^2+1365N+778\big)}{81(N+1)(N+2)}S_3 + \frac{1244}{27}S_4 - \frac{224}{9}S_5$$

$$-\frac{128}{9}S_{-5} + \frac{8\big(2N^2-35N-54\big)}{9N(N+1)^2(N+2)}S_{1,1} - \frac{32\big(3N^3+7N^2+7N+6\big)}{9(N+1)(N+2)}S_{2,1}$$

$$+\Big[-\frac{128}{27}S_1^3 - \frac{7168}{81}S_1 + \frac{640}{27}S_2 - \frac{256}{27}S_3 + \frac{256}{9}S_{2,1} + \frac{32}{9N(N+1)}\Big]S_{-2}$$

$$-\frac{128}{3}S_{2,3} + \frac{256}{9}S_{2,-3} - \frac{1352}{27}S_{3,1} + \frac{256}{9}S_{4,1} + \Big[-\frac{4P_{58}}{81N(N+1)^2(N+2)}$$

$$+\frac{496}{27}S_3 - \frac{64}{3}S_{2,1} - \frac{128}{3}S_{-2,1}\Big]S_2 + \frac{7168}{81}S_{-2,1} + \frac{640}{27}S_{-2,2} - \frac{256}{9}S_{-2,3}$$

$$+24S_{2,1,1} - \frac{256}{9}\big(S_{2,1,-2}+S_{3,1,1}+S_{-2,2,1}\big) + \frac{64}{3}S_{2,2,1} - \frac{2560}{27}S_{-2,1,1} + \frac{224}{9}S_{2,1,1,1}$$

$$+\frac{1024}{9}S_{-2,1,1,1} + \Big[\frac{2\big(35N^2+35N+6(-1)^N-6\big)}{9N(N+1)} - \frac{32}{3}S_{-2}S_1 - \frac{16}{27}S_1 - \frac{88}{9}S_2$$

$$+\frac{16}{3}\big(2S_{-2,1}-S_3-S_{-3}\big) + \frac{5}{3}\Big]\zeta_2 + \Big[\frac{2\big(108N^3-239N^2-1137N-646\big)}{9(N+1)(N+2)}$$

$$-16S_1^2 + \frac{2548}{27}S_1 + 16S_2 - \frac{17}{3}\Big]\zeta_3 - \frac{1879}{162}\Bigg\}\,, \tag{4.79}$$

with the polynomials P_i given by

$$P_{55} = 3N^3 + 9N^2 + 47N + 58 + 4(-1)^N(N+1)(N+2) \tag{4.80}$$

$$P_{56} = 157N^4 + 314N^3 + 277N^2 - 24N - 72 \tag{4.81}$$

$$P_{57} = 308N^4 + 616N^3 + 323N^2 - 3N - 9 \tag{4.82}$$

$$P_{58} = 364N^4 + 1591N^3 + 2117N^2 + 593N - 450 - 36(-1)^N(N+1)(N+2) \tag{4.83}$$

$$P_{59} = 769N^4 + 1547N^3 + 787N^2 - 15N - 12 + 4(-1)^N N(13N+7) \tag{4.84}$$

$$P_{60} = (N+1)\big(6197N^3 + 18591N^2 + 15850N + 4320\big) - 108(-1)^N(N+2)(13N+7) \tag{4.85}$$

$$P_{61} = -1013N^6 - 3039N^5 - 5751N^4 - 2981N^3 + 1752N^2 + 1872N + 432$$
$$+ 24(-1)^N N\big(133N^3 + 188N^2 + 82N - 9\big) \tag{4.86}$$

$$P_{62} = 6327N^6 + 18981N^5 + 18457N^4 + 5687N^3 - 260N^2 + 144N + 144$$
$$+ 8(-1)^N N\big(133N^3 + 188N^2 + 82N - 9\big)\,. \tag{4.87}$$

Results for the moments $N = 1,\dots,13$ were given in [215] before.

The renormalisation proceeds along the same lines as for the vector matrix element, summarised in Eqs. (4.1) and (4.2), but using the anomalous dimensions for the transversity operator. We use the leading-order anomalous dimension for transversity without its colour factor as a shorthand

$$\tilde{\gamma}_{qq,\mathrm{NS,TR}}^{(0)} = 2\,[4S_1 - 3]\,. \tag{4.88}$$

After renormalisation the OME $A_{qq,Q}^{\mathrm{NS,TR}}$ at 2- and 3-loop order is given in N space by

$$A_{qq,Q}^{\mathrm{NS,TR},(2)}(N) =$$

4. Non-singlet contributions to DIS

$$C_F T_F \left\{ -\frac{1}{3} \tilde{\gamma}^0_{qq,\text{NS,TR}} \ln^2\left(\frac{m^2}{\mu^2}\right) + \left[-\frac{2}{9}(-3 - 24S_2) - \frac{80}{9}S_1 \right] \ln\left(\frac{m^2}{\mu^2}\right) \right.$$

$$\left. + \frac{73N^2 + 73N + 24}{18N(N+1)} - \frac{224}{27}S_1 + \frac{40}{9}S_2 - \frac{8}{3}S_3 \right\} \tag{4.89}$$

$$A^{\text{NS,TR},(3)}_{qq,Q}(N) =$$

$$C_F T_F \left\{ -\frac{8}{27}T_F(2 + N_F) + \frac{22}{27}C_A \right\} \tilde{\gamma}^0_{qq,\text{NS,TR}} \ln^3\left(\frac{m^2}{\mu^2}\right)$$

$$+ C_F \left\{ T_F^2 \left[\frac{8}{27}(3 + 24S_2) - \frac{320}{27}S_1 \right] + C_A T_F \left[\frac{34}{3} - \frac{184}{9}S_1 \right] \right.$$

$$- \frac{64}{3}S_{-2}S_1 - \frac{32}{3}S_3 - \frac{32}{3}S_{-3} + \frac{64}{3}S_{-2,1} \right] + C_F T_F \left[8 + \left(-8 + \frac{64}{3}S_2 \right)S_1 \right.$$

$$\left. + \frac{128}{3}S_{-2}S_1 - 16S_2 + \frac{64}{3}[S_3 + S_{-3}] - \frac{128}{3}S_{-2,1} \right] \right\} \ln^2\left(\frac{m^2}{\mu^2}\right)$$

$$+ \left\{ C_F \left\{ T_F^2 \left[\frac{496}{27} + N_F \left[\frac{4(175N^2 + 175N - 24)}{27N(N+1)} - \frac{2176}{81}S_1 - \frac{320}{27}S_2 \right. \right. \right. \right.$$

$$\left. + \frac{64}{9}S_3 \right] - \frac{1984}{81}S_1 \right] + C_A T_F \left[-\frac{11(145N^2 + 145N - 24)}{27N(N+1)} + \frac{1}{2}\left[-\frac{640}{9} + \frac{128}{3}S_1 \right]S_{-3} \right.$$

$$+ \left[-\frac{8(155N^2 + 155N + 27)}{81N(N+1)} + 32S_3 + \frac{128}{3}S_{-2,1} \right]S_1 + \frac{1792}{27}S_2 - \frac{496}{9}S_3 + \frac{160}{3}S_4$$

$$+ \left[-\frac{640}{9}S_1 + \frac{64}{3}S_2 \right]S_{-2} + \frac{64}{3}S_{-4} - \frac{128}{3}S_{3,1} + \frac{640}{9}S_{-2,1} + \frac{64}{3}S_{-2,2} - \frac{256}{3}S_{-2,1,1}$$

$$+ \frac{1}{2}\left[96 - 128S_1 \right]\zeta_3 \right] + C_F T_F \left[1 + \frac{1}{2}\left[\frac{1280}{9} - \frac{256}{3}S_1 \right]S_{-3} + \left[-\frac{8(5N^2 + 5N - 4)}{3N(N+1)} \right. \right.$$

$$+ \frac{640}{9}S_2 - \frac{256}{3}S_3 - \frac{256}{3}S_{-2,1} \right]S_1 - \frac{40}{3}S_2 - \frac{64}{3}S_2^2 + \frac{928}{9}S_3 - \frac{256}{3}S_4 + \left[\frac{1280}{9}S_1 \right.$$

$$\left. - \frac{128}{3}S_2 \right]S_{-2} - \frac{128}{3}S_{-4} + \frac{128}{3}S_{3,1} - \frac{1280}{9}S_{-2,1} - \frac{128}{3}S_{-2,2} + \frac{512}{3}S_{-2,1,1}$$

$$+ \frac{1}{2}\left[-96 + 128S_1 \right]\zeta_3 \right] \right\} \ln\left(\frac{m^2}{\mu^2}\right)$$

$$+ C_F \left\{ C_A T_F \left[-\frac{16(-1)^N(2N^2 + 2N + 1)}{9N^3(N+1)^3} - 12\zeta_4 + \frac{P_{69}}{243N^3(N+1)^3} \right. \right.$$

$$+ \frac{4(2N^2 - 35N - 54)}{9N(N+1)^2(N+2)}[S_1^2 + S_2] - \frac{32(3N^3 + 7N^2 + 7N + 6)}{9(N+1)(N+2)}S_{2,1}$$

$$- \frac{8(27N^3 + 890N^2 + 2355N + 1438)}{81(N+1)(N+2)}S_3 + 2\left[\frac{320}{27} - \frac{64}{9}S_1 \right]S_{-4}$$

$$+ \left[\frac{(216N^3 - 485N^2 - 2295N - 1306)}{9(N+1)(N+2)} + \frac{2372}{27}S_1 - 16[S_1^2 - S_2] \right]\zeta_3$$

$$+ \left[84 - 96 S_1\right] \zeta_4 + \left[-8 + \frac{32}{3} S_1\right] B_4 + \left[-\frac{4 P_{67}}{729 N(N+1)^2(N+2)}\right.$$

$$- \frac{16(N-2)(2N+3)}{9(N+1)(N+2)} S_2 + \frac{112}{9} S_2^2 + \frac{320}{9} S_3 - \frac{208}{9} S_4 - 8 S_{2,1} + \frac{64}{3} S_{3,1} + \frac{1280}{27} S_{-2,1}$$

$$+ \frac{128}{9} S_{-2,2} - 32 S_{2,1,1} - \frac{512}{9} S_{-2,1,1} \Bigg] S_1 + \left[\frac{4(3N^3 + 13N^2 + 59N + 66)}{9N(N+1)^2(N+2)} - \frac{80}{9} S_3\right.$$

$$+ \frac{128}{9} [S_{2,1} + S_{-2,1}] \Bigg] S_1^2 + \left[\frac{4 P_{63}}{81 N(N+1)^2(N+2)} + \frac{496}{27} S_3 - \frac{64}{3} S_{2,1} - \frac{128}{3} S_{-2,1}\right] S_2$$

$$- \frac{64}{27} S_1^3 S_2 - \frac{20}{3} S_2^2 + \frac{1772}{27} S_4 - \frac{224}{9} S_5 + \left[\frac{32}{9N(N+1)} - \frac{7168}{81} S_1 - \frac{128}{27} S_1^3\right.$$

$$+ \frac{640}{27} S_2 - \frac{256}{27} S_3 + \frac{256}{9} S_{2,1} \Bigg] S_{-2} + \left[2\left[-\frac{1792}{81} - \frac{32}{9} S_2\right] + \frac{640}{27} S_1 - \frac{64}{9} S_1^2\right] S_{-3}$$

$$- \frac{128}{9} S_{-5} - \frac{128}{3} S_{2,3} + \frac{256}{9} S_{2,-3} - \frac{1352}{27} S_{3,1} + \frac{256}{9} S_{4,1} + \frac{7168}{81} S_{-2,1} + \frac{640}{27} S_{-2,2}$$

$$- \frac{256}{9} S_{-2,3} + 24 S_{2,1,1} - \frac{256}{9} S_{2,1,-2} + \frac{64}{3} S_{2,2,1} - \frac{256}{9} S_{3,1,1} - \frac{2560}{27} S_{-2,1,1}$$

$$- \frac{256}{9} S_{-2,2,1} + \frac{224}{9} S_{2,1,1,1} + \frac{1024}{9} S_{-2,1,1,1} \Bigg]$$

$$+ T_F^2 \left[-\frac{2 P_{65}}{243 N^2(N+1)^2} + N_F \left[\frac{4 P_{64}}{243 N^2(N+1)^2} - \frac{24064}{729} S_1 + \frac{128}{81} S_2 + \frac{640}{81} S_3\right.\right.$$

$$- \frac{128}{27} S_4 + \left[-\frac{128}{9} + \frac{512}{27} S_1\right] \zeta_3 \Bigg] + \frac{12064}{729} S_1 + \frac{64}{81} S_2 + \frac{320}{81} S_3 - \frac{64}{27} S_4$$

$$+ \left[\frac{224}{9} - \frac{896}{27} S_1\right] \zeta_3 \Bigg]$$

$$+ C_F T_F \left[\frac{32(-1)^N(2N^2 + 2N + 1)}{9 N^3(N+1)^3} + \frac{P_{68}}{9 N^3(N+1)^3} + 2\left[-\frac{640}{27} + \frac{128}{9} S_1\right] S_{-4}\right.$$

$$+ \left[16 - \frac{64}{3} S_1\right] B_4 + \left[-72 + 96 S_1\right] \zeta_4 + \left[\frac{2 P_{66}}{27 N^2(N+1)^2}\right.$$

$$+ \frac{7168}{81} S_2 - \frac{64}{9} S_2^2 - \frac{2560}{27} S_3 + \frac{704}{9} S_4 - \frac{320}{9} S_{3,1} - \frac{2560}{27} S_{-2,1} - \frac{256}{9} S_{-2,2}$$

$$+ \frac{64}{3} S_{2,1,1} + \frac{1024}{9} S_{-2,1,1} \Bigg] S_1 + \left[-\frac{16(N+3)}{9N(N+1)} + \frac{64}{3} S_3 - \frac{128}{9} S_{2,1} - \frac{256}{9} S_{-2,1}\right] S_1^2$$

$$+ \left[-\frac{16(151 N^2 + 151 N + 12)}{27 N(N+1)} + \frac{256}{27} S_3 + \frac{256}{3} S_{-2,1}\right] S_2 + \frac{128}{27} S_1^3 S_2 - \frac{496}{27} S_2^2$$

$$+ \frac{7816}{81} S_3 - \frac{2992}{27} S_4 + \frac{512}{9} S_5 + \left[-\frac{64}{9N(N+1)} + \frac{14336}{81} S_1 + \frac{256}{27} S_1^3 - \frac{1280}{27} S_2\right.$$

$$+ \frac{512}{27} S_3 - \frac{512}{9} S_{2,1} \Bigg] S_{-2} + \left[2\left[\frac{3584}{81} + \frac{64}{9} S_2\right] - \frac{1280}{27} S_1 + \frac{128}{9} S_1^2\right] S_{-3}$$

$$+ \frac{256}{9} S_{-5} + \frac{112}{9} S_{2,1} + \frac{256}{9} S_{2,3} - \frac{512}{9} S_{2,-3} + \frac{1424}{27} S_{3,1} - \frac{512}{9} S_{4,1}$$

$$
-\frac{14336}{81}S_{-2,1} - \frac{1280}{27}S_{-2,2} + \frac{512}{9}S_{-2,3} - 16S_{2,1,1} + \frac{512}{9}S_{2,1,-2} + \frac{256}{9}S_{3,1,1}
$$

$$
+ \frac{5120}{27}S_{-2,1,1} + \frac{512}{9}S_{-2,2,1} - \frac{2048}{9}S_{-2,1,1,1} + \left[\frac{374}{3} - \frac{1208}{9}S_1 - \frac{64}{3}S_2\right]\zeta_3 \Bigg]\Bigg\}
$$

$$
- \tfrac{1}{2}\left[1 - (-1)^N\right]C_F T_F\left(\frac{C_A}{2} - C_F\right)\Bigg\{\frac{1}{N(N+1)}\frac{32}{3}\ln^2\left(\frac{m^2}{\mu^2}\right) + \Bigg[\frac{32(13N+7)}{9N(N+1)^2}
$$

$$
- \frac{64}{3N(N+1)}S_1\Bigg]\ln\left(\frac{m^2}{\mu^2}\right) + \frac{32(133N^3 + 188N^2 + 82N - 9)}{81N^2(N+1)^3} - \frac{64(13N+7)}{27N(N+1)^2}S_1
$$

$$
+ \frac{64}{9N(N+1)}[S_2 + S_1^2]\Bigg\} , \tag{4.90}
$$

where we abbreviated long polynomials by

$$
P_{63} = 868N^4 + 3337N^3 + 4079N^2 + 1979N + 522 \tag{4.91}
$$

$$
P_{64} = 1183N^4 + 2366N^3 + 943N^2 + 48N + 144 \tag{4.92}
$$

$$
P_{65} = 1829N^4 + 3658N^3 + 2069N^2 - 48N - 144 \tag{4.93}
$$

$$
P_{66} = 2377N^4 + 4790N^3 + 2657N^2 + 52N - 48 \tag{4.94}
$$

$$
P_{67} = 10807N^4 + 43228N^3 + 51983N^2 + 17402N - 2808 \tag{4.95}
$$

$$
P_{68} = -691N^6 - 2073N^5 - 2049N^4 - 595N^3 + 56N^2 - 16N - 32 \tag{4.96}
$$

$$
P_{69} = 55N^6 + 165N^5 + 4605N^4 + 5767N^3 + 552N^2 - 720N + 432 . \tag{4.97}
$$

Corresponding expressions in x space in terms of HPLs are presented in Eqs. (E.8) and (E.9). As above, the expressions are given in the OMS scheme for the heavy quark mass. The $\overline{\text{MS}}$ scheme can be obtained from the difference of the OME in the two schemes. In N space the difference is

$$
A_{qq,Q}^{\text{NS,TR},\overline{\text{MS}}}(N) - A_{qq,Q}^{\text{NS,TR,OMS}}(N) =
$$

$$
C_F^2 T_F\Bigg\{4\tilde{\gamma}_{qq,\text{NS,TR}}^0 \ln^2\left(\frac{m^2}{\mu^2}\right) + \ln\left(\frac{m^2}{\mu^2}\right)\left[\frac{32}{3}S_1 - 32S_2 + 28\right]
$$

$$
+ \frac{16}{3} - \frac{640}{9}S_1 + \frac{128}{3}S_2\Bigg\} , \tag{4.98}
$$

while in x space the same difference yields

$$
A_{qq,Q}^{\text{NS,TR},\overline{\text{MS}}}(x) - A_{qq,Q}^{\text{NS,TR,OMS}}(x) =
$$

$$
C_F^2 T_F\Bigg\{-\left(\frac{1}{1-x}\left[32\ln^2\left(\frac{m^2}{\mu^2}\right) + \left[32H_0 + \frac{32}{3}\right]\ln\left(\frac{m^2}{\mu^2}\right) - \frac{128}{3}H_0 - \frac{640}{9}\right]\right)_+
$$

$$
+ \left[-24\ln^2\left(\frac{m^2}{\mu^2}\right) + 28\ln\left(\frac{m^2}{\mu^2}\right) + \frac{16}{3}\right]\delta(1-x) + 32\ln^2\left(\frac{m^2}{\mu^2}\right)
$$

$$
+ \ln\left(\frac{m^2}{\mu^2}\right)\left[32H_0 + \frac{32}{3}\right] - \frac{128}{3}H_0 - \frac{640}{9}\Bigg\} . \tag{4.99}
$$

The massless Wilson coefficients for transversity have not yet been calculated to $\mathcal{O}(a_s^3)$ for any process. Therefore, the massive Wilson coefficients in the asymptotic limit currently cannot be given. However, once the massless Wilson coefficients are known to the required order, our results can be used to complete also the heavy flavour contributions.

4.2. Unpolarised neutral current DIS

As a first application of the result for the non-singlet OME obtained in the previous section, we consider the non-singlet heavy flavour Wilson coefficient $L_{q,2}^{\mathrm{NS}}$. This Wilson coefficient contributes to the structure function $F_2(x, Q^2)$ for unpolarised DIS as described by Eq. (2.90). The relevant part for the non-singlet contribution to be discussed here reads

$$
F_2^{\mathrm{h,NS}}(x, N_F + 1, Q^2, m^2) =
$$
$$
x \sum_{k=1}^{N_F} e_k^2 L_{q,2}^{\mathrm{NS}} \left(x, N_F + 1, \frac{Q^2}{\mu^2}, \frac{m^2}{\mu^2} \right) \otimes \left[f_k(x, \mu^2, N_F) + \bar{f}_k(x, \mu^2, N_F) \right], \qquad (4.100)
$$

where f_k and $\bar{f}_k$ denote the quark and anti-quark PDFs of the flavour k, respectively. The non-singlet operator arising from the flavour decomposition of the light-cone expansion actually corresponds to the PDF combination

$$
\Delta^{\mathrm{NS}}(x, \mu^2) = f_k(x, \mu^2) + \bar{f}_k(x, \mu^2) - \frac{\Sigma(x, \mu^2)}{N_F}, \qquad (4.101)
$$

where $\Sigma(x, \mu^2)$ is the singlet combination defined in Eq. (2.66). This PDF combination is a non-singlet quantity in the sense that its evolution decouples from the evolution of the singlet and gluon distributions. For historical reasons, however, we follow the convention [201, 202] to call the sum $f_k(x, \mu^2) + \bar{f}_k(x, \mu^2)$ the non-singlet combination here. This convention follows from the calculational point of view: The singlet Wilson coefficient receives contributions from diagrams which contribute to both the singlet and non-singlet Wilson coefficient as well as from diagrams which contribute only to the singlet Wilson coefficient. Diagrams in the former class are called *non-singlet diagrams* while those in the latter class are called *pure-singlet diagrams*. Merging the contributions from non-singlet diagrams to the singlet and non-singlet Wilson coefficients yields the contribution in Eq. (4.100). The remaining pure-singlet diagrams contribute only to the pure-singlet Wilson coefficient, which we discuss in the next chapter.

At $Q^2 \gg m^2$ the heavy flavour Wilson coefficient $L_{q,2}^{\mathrm{NS}}$ can be written in terms of renormalised massive OMEs and massless Wilson coefficients. By inserting perturbative expansions for the massless Wilson coefficients and OMEs into Eq. (2.91), we obtain [201, 203]

$$
L_{q,2}^{\mathrm{NS}}(N_F + 1) = a_s^2 \left[A_{qq,Q}^{\mathrm{NS},(2)}(N_F + 1) + \hat{C}_{q,2}^{\mathrm{NS},(2)}(N_F) \right]
$$
$$
+ a_s^3 \left[A_{qq,Q}^{\mathrm{NS},(3)}(N_F + 1) + A_{qq,Q}^{\mathrm{NS},(2)}(N_F + 1) C_{q,2}^{\mathrm{NS},(1)}(N_F + 1) + \hat{C}_{q,2}^{\mathrm{NS},(3)}(N_F) \right],
$$
$$
(4.102)
$$

where $C_{q,2}^{\mathrm{NS}}$ denotes the massless non-singlet Wilson coefficient, which is known to 3-loop order [138]. Again, the argument $N_F + 1$ of the massive OMEs and the heavy flavour Wilson coefficients symbolically stands for these quantities evaluated with N_F massless quarks and one massive quark. The argument of the massless Wilson coefficients, on the other hand, is to be read literally. The hat above the massless Wilson coefficient refers to the N_F prescription in Eq. (2.97). In the unpolarised case, which we consider here, the non-singlet OME $A_{qq,Q}^{\mathrm{NS}}$ must be analytically continued from even values of N. The massless Wilson coefficients are published for the scale choice $\mu^2 = Q^2$, which eliminates the logarithms $L_Q = \ln(Q^2/\mu^2)$. As discussed at the end of Section 2.4, terms which are proportional to powers of these logarithms are fully determined by the renormalisation group equations [293] in terms of lower order massless Wilson

4. Non-singlet contributions to DIS

coefficients, coefficients of the β-function and anomalous dimensions. Here the unpolarised non-singlet anomalous dimension $\gamma_+^{\rm NS}$ enters [135]. We reconstruct the logarithmic terms in this way, before inserting the massless Wilson coefficients into Eq. (4.102).

4.2.1. Analytic results

The unpolarised heavy flavour non-singlet Wilson coefficient in the asymptotic limit $Q^2 \gg m^2$ in N space reads

$$
L_{q,2}^{\rm NS}(N) = \tfrac{1}{2}\left[1 + (-1)^N\right]
$$

$$
\times \Bigg\{ a_s^2 C_F T_F \Bigg\{ -\frac{8}{9}S_1^3 - \frac{2(29N^2 + 29N - 6)}{9N(N+1)}S_1^2 + \left(\frac{8}{3}S_2 - \frac{2P_{78}}{27N^2(N+1)^2}\right)S_1
$$

$$
- \frac{1}{3}\gamma_{qq}^{(0)}\left(L_M^2 + L_Q^2\right) + \frac{P_{93}}{27N^3(N+1)^3} + \left(\frac{8}{3}S_1^2 + \frac{4(29N^2 + 29N - 6)}{9N(N+1)}S_1\right.
$$

$$
- 8S_2 - \frac{2P_{75}}{9N^2(N+1)^2}\Bigg)L_Q + \left(\frac{2P_{10}}{9N^2(N+1)^2} - \frac{80}{9}S_1 + \frac{16}{3}S_2\right)L_M
$$

$$
- \frac{112}{9}S_3 + \frac{16}{3}S_{2,1} + \frac{2(35N^2 + 35N - 2)}{3N(N+1)}S_2\Bigg\}
$$

$$
+ a_s^3\Bigg\{ C_F^2 T_F \Bigg\{ \left(\frac{128}{27}S_2 - \frac{16P_{72}}{27N^2(N+1)^2}\right)S_1^3 + \left(\frac{16(5N^2 + 5N - 4)}{9N(N+1)}S_2 + 16S_3\right.
$$

$$
- \frac{128}{9}S_{2,1} + \frac{P_{86}}{9N^3(N+1)^3} - \frac{256}{9}S_{-2,1}\Bigg)S_1^2 + \left(-\frac{64}{9}S_2^2 + \frac{8P_{82}}{81N^2(N+1)^2}S_2\right.
$$

$$
+ \frac{704}{9}S_4 + \frac{P_{98}}{162N^4(N+1)^4} - \frac{8(347N^2 + 347N + 54)}{27N(N+1)}S_3 + \frac{128}{9N(N+1)}S_{2,1}
$$

$$
- \frac{320}{9}S_{3,1} - \frac{256(10N^2 + 10N - 3)}{27N(N+1)}S_{-2,1} - \frac{256}{9}S_{-2,2} + \frac{1024}{9}S_{-2,1,1}\Bigg)S_1
$$

$$
- \frac{32(23N^2 + 23N - 3)}{27N(N+1)}S_2^2 + \frac{1}{6}\gamma_{qq}^{(0)2}\left(L_Q^3 + L_M^2 L_Q\right) + \frac{P_{99}}{162N^5(N+1)^5}
$$

$$
- \frac{16(2N^3 + 2N^2 + 2N + 1)}{3N^3(N+1)^3}\zeta_2 + \left(\frac{256}{9}S_1 - \frac{128(10N^2 + 10N + 3)}{27N(N+1)}\right)S_{-4}
$$

$$
+ L_M L_Q\left(\frac{320}{9}S_1^2 - \frac{80(3N^2 + 3N + 2)}{9N(N+1)}S_1\right) + \left(-\frac{128(10N^2 + 10N + 3)}{27N(N+1)}S_1\right.
$$

$$
+ \frac{128}{9}S_1^2 + \frac{64(112N^3 + 224N^2 + 169N + 39)}{81N(N+1)^2} + \frac{128}{9}S_2\Bigg)S_{-3}
$$

$$
+ \frac{(-1)^N}{(N+1)^3}\Bigg[-\frac{64}{3}L_M^2 + \left(\frac{128}{3}S_1 - \frac{256(4N+1)}{9(N+1)}\right)L_M + \frac{64(2N^2 + 2N + 1)}{9N^3}S_1^2
$$

$$
+ \frac{16P_{28}}{81N^5(N+1)^2} + \frac{64P_{100}}{45(N-2)(N-1)^2N^2(N+1)(N+2)^2(N+3)^3}L_Q
$$

$$
+ \frac{16}{3}(2N^3 + 2N^2 + 2N + 1)\frac{\zeta_2}{N^3} - \frac{32P_{24}}{27N^4(N+1)}S_1 + \frac{64(2N^2 + 2N + 1)}{9N^3}S_2
$$

$$
- \frac{64}{3}L_Q^2\Bigg] + \frac{8P_{83}}{81N^2(N+1)^2}S_3 - \frac{176(17N^2 + 17N + 6)}{27N(N+1)}S_4 + \frac{512}{9}S_5 + \frac{256}{9}S_{-5}
$$

$$
+ \left(\frac{256}{27}S_1^3 - \frac{128}{9N(N+1)}S_1^2 + \frac{128P_{13}}{81N^2(N+1)^2}S_1 - \frac{64P_{14}}{81N^3(N+1)^3} - \frac{1280}{27}S_2\right)
$$

$$+ \frac{512}{27}S_3 - \frac{512}{9}S_{2,1}\bigg)S_{-2} + \frac{16P_{11}}{9N^2(N+1)^2}S_{2,1} + \frac{16(89N^2 + 89N + 30)}{27N(N+1)}S_{3,1}$$

$$+ \frac{256}{9}S_{2,3} - \frac{512}{9}S_{2,-3} - \frac{512}{9}S_{4,1} + \bigg[-16S_1^3 - \frac{4(107N^2 + 107N - 54)}{9N(N+1)}S_1^2$$

$$+ \frac{2P_{79}}{9N^2(N+1)^2}S_1 - \frac{2P_{90}}{9N^3(N+1)^3} + \bigg(\frac{128}{3}S_1 - \frac{64}{3N(N+1)}\bigg)S_{-2} + \frac{64}{3}S_3$$

$$+ \frac{64}{3}S_{-3} - \frac{128}{3}S_{-2,1}\bigg]L_Q^2 + \bigg[-\frac{16}{3}S_1^3 - \frac{4(N-1)(N+2)}{N(N+1)}S_1^2 + \frac{2P_{73}}{3N^2(N+1)^2}S_1$$

$$- \frac{2P_{88}}{3N^3(N+1)^3} + S_{-2}\bigg(\frac{128}{3}S_1 - \frac{64}{3N(N+1)}\bigg) + \frac{64}{3}(S_3 + S_{-3} - 2S_{-2,1})\bigg]L_M^2$$

$$- \frac{128(112N^3 + 112N^2 - 39N + 18)}{81N^2(N+1)}S_{-2,1} + \bigg(\frac{P_{85}}{81N^3(N+1)^3} + \frac{400S_3}{27}$$

$$+ \frac{256}{3}S_{-2,1}\bigg)S_2 - \frac{128(10N^2 + 10N - 3)S_{-2,2}}{27N(N+1)} + \frac{512}{9}S_{-2,3} + \frac{512}{9}S_{2,1,-2}$$

$$+ \frac{256}{9}S_{3,1,1} + \frac{512(10N^2 + 10N - 3)}{27N(N+1)}S_{-2,1,1} + \bigg[\bigg(\frac{32}{3}S_2 - \frac{4P_{71}}{3N^2(N+1)^2}\bigg)S_1^2$$

$$- \frac{160}{9}S_1^3 + \bigg(\frac{2P_{91}}{9N^3(N+1)^3} + \frac{16(59N^2 + 59N - 6)}{9N(N+1)}S_2 - \frac{256}{3}S_3 - \frac{256}{3}S_{-2,1}\bigg)S_1$$

$$- 32S_2^2 + \frac{P_{97}}{9N^4(N+1)^4} + S_{-3}\bigg(\frac{64(10N^2 + 10N + 3)}{9N(N+1)} - \frac{128}{3}S_1\bigg) + \frac{128}{3}S_{3,1}$$

$$+ S_{-2}\bigg(-\frac{64(16N^2 + 10N - 3)}{9N^2(N+1)^2} + \frac{1280}{9}S_1 - \frac{128}{3}S_2\bigg) - \frac{4P_{76}}{9N^2(N+1)^2}S_2$$

$$+ \frac{32(29N^2 + 29N + 12)}{9N(N+1)}S_3 - \frac{256}{3}S_4 - \frac{128}{3}S_{-4} - \frac{128(10N^2 + 10N - 3)}{9N(N+1)}S_{-2,1}$$

$$- \frac{128}{3}S_{-2,2} + \frac{512}{3}S_{-2,1,1}\bigg]L_M + \frac{512}{9}S_{-2,2,1} - \frac{2048}{9}S_{-2,1,1,1} + \bigg(\frac{2P_{16}}{9N^2(N+1)^2}$$

$$- \frac{1208}{9}S_1 - \frac{64}{3}S_2\bigg)\zeta_3 + \gamma_{qq}^{(0)}\bigg[\frac{10}{3}S_2L_M^2 + \bigg(\frac{P_{70}}{9N^2(N+1)^2} - \frac{8}{3}S_2\bigg)L_QL_M$$

$$+ 8\zeta_3L_M - \frac{8}{3}B_4 + 12\zeta_4 + \frac{22}{3}L_Q^2S_2 + \frac{8}{3}S_{2,1,1}\bigg] + \bigg[\frac{32(4N-1)(4N+5)}{9N(N+1)}S_1^3$$

$$+ \frac{80}{9}S_1^4 + \bigg(\frac{2P_{81}}{27N^2(N+1)^2} - \frac{224}{3}S_2\bigg)S_1^2 + \bigg(-\frac{32(67N^2 + 67N - 21)}{9N(N+1)}S_2$$

$$- \frac{4P_{94}}{27N^3(N+1)^3} + \frac{640}{9}S_3 + \frac{64}{3}S_{2,1} + \frac{512}{3}S_{-2,1}\bigg)S_1 + 48S_2^2 + 64S_{-2}^2$$

$$+ \frac{4P_{102}}{135(N-1)^2N^4(N+1)^4(N+2)^2(N+3)^3} - \frac{32(53N^2 + 77N + 4)}{9N(N+1)}S_3$$

$$+ S_{-3}\bigg(\frac{256}{3}S_1 - \frac{64(10N^2 + 22N + 3)}{9N(N+1)}\bigg) + \frac{2P_{80}}{9N^2(N+1)^2}S_2 + \bigg(\frac{256}{3}(S_2 - S_1^2)$$

$$- \frac{128(10N^2 + 22N - 9)}{9N(N+1)}S_1 - \frac{64P_{87}}{9(N-2)N^2(N+1)^2(N+3)}\bigg)S_{-2} + \frac{352}{3}S_4$$

$$+ \frac{448}{3}S_{-4} + \frac{16(9N^2 + 9N - 2)}{3N(N+1)}S_{2,1} + 64S_{3,1} + \frac{128(10N^2 + 22N - 9)}{9N(N+1)}S_{-2,1}$$

$$- \frac{256}{3} S_{-3,1} - 64 S_{2,1,1} - \frac{512}{3} S_{-2,1,1} + \left(64 S_1 - \frac{16\left(9N^2 - 7N + 6\right)}{N(N+1)} \right) \zeta_3 \bigg] L_Q \bigg\}$$

$$+ C_F T_F^2 \Bigg\{ \left(\frac{8 P_{10}}{27 N^2 (N+1)^2} - \frac{320}{27} S_1 + \frac{64}{9} S_2 \right) L_M^2 - \frac{2 P_{50}}{729 N^4 (N+1)^4} + \frac{64}{81} S_2$$

$$+ \frac{12064}{729} S_1 + \left(\frac{32}{9} S_1^2 + \frac{16\left(29N^2 + 29N - 6\right)}{27 N(N+1)} S_1 - \frac{8 P_{75}}{27 N^2 (N+1)^2} - \frac{32}{3} S_2 \right) L_Q^2$$

$$+ \frac{320}{81} S_3 - \frac{64}{27} S_4 + \Bigg[- \frac{896}{27} S_3 - \frac{16\left(29N^2 + 29N - 6\right)}{27 N(N+1)} S_1^2 + \frac{8 P_{92}}{81 N^3 (N+1)^3}$$

$$- \frac{16 P_{77}}{81 N^2 (N+1)^2} S_1 + \frac{16\left(35N^2 + 35N - 2\right)}{9 N(N+1)} S_2 + \frac{64}{27} \left(6 S_{2,1} - S_1^3 + 3 S_1 S_2 \right) \Bigg] L_Q$$

$$+ \gamma_{qq}^{(0)} \left(- \frac{16}{27} L_M^3 - \frac{248}{81} L_M - \frac{8}{27} L_Q^3 - \frac{112}{27} \zeta_3 \right) \Bigg\} + N_F C_F T_F^2 \Bigg\{ \left(\frac{64}{9} S_1^2 - \frac{64}{3} S_2 \right.$$

$$- \frac{16 P_{75}}{27 N^2 (N+1)^2} + \frac{32\left(29N^2 + 29N - 6\right)}{27 N(N+1)} S_1 \right) L_Q^2 + \Bigg[\frac{16 P_{92}}{81 N^3 (N+1)^3} - \frac{128}{27} S_1^3$$

$$- \frac{32\left(29N^2 + 29N - 6\right)}{27 N(N+1)} S_1^2 + \left(\frac{128}{9} S_2 - \frac{32 P_{77}}{81 N^2 (N+1)^2} \right) S_1 - \frac{1792}{27} S_3$$

$$+ \frac{256}{9} S_{2,1} + \frac{32\left(35N^2 + 35N - 2\right)}{9 N(N+1)} S_2 \Bigg] L_Q + \frac{4 P_{49}}{729 N^4 (N+1)^4} - \frac{24064}{729} S_1$$

$$+ \frac{128}{81} S_2 + \frac{640}{81} S_3 + \left(\frac{4 P_{44}}{81 N^3 (N+1)^3} - \frac{2176}{81} S_1 - \frac{320}{27} S_2 + \frac{64}{9} S_3 \right) L_M$$

$$- \frac{128 S_4}{27} + \gamma_{qq}^{(0)} \left(- \frac{8}{27} L_M^3 - \frac{16}{27} L_Q^3 + \frac{64}{27} \zeta_3 \right) \Bigg\} + C_A C_F T_F \Bigg\{ \left(- \frac{80}{9} S_3 + \frac{128}{9} S_{2,1} \right.$$

$$+ \frac{32}{9 N(N+1)} S_2 + \frac{4 P_{36}}{9 N^3 (N+1)^3} + \frac{128}{9} S_{-2,1} \right) S_1^2 + \Bigg[\frac{80 S_3 (2N+1)^2}{9 N(N+1)} + \frac{112}{9} S_2^2$$

$$- \frac{4 P_{52}}{729 N^4 (N+1)^4} - \frac{16(N-1)\left(2N^3 - N^2 - N - 2\right)}{9 N^2 (N+1)^2} S_2 - \frac{208}{9} S_4 - \frac{512}{9} S_{-2,1,1}$$

$$- \frac{8\left(9N^2 + 9N + 16\right)}{9 N(N+1)} S_{2,1} + \frac{128\left(10N^2 + 10N - 3\right)}{27 N(N+1)} S_{-2,1} + \frac{128}{9} S_{-2,2}$$

$$+ \frac{64}{3} S_{3,1} \Bigg] S_1 - \frac{64}{27} S_2 S_1^3 - \frac{4\left(15N^2 + 15N + 14\right)}{9 N(N+1)} S_2^2 + \frac{P_{54}}{729 N^5 (N+1)^5}$$

$$+ \frac{8\left(2N^3 + 2N^2 + 2N + 1\right)}{3 N^3 (N+1)^3} \zeta_2 + S_{-4} \left(\frac{64\left(10N^2 + 10N + 3\right)}{27 N(N+1)} - \frac{128}{9} S_1 \right)$$

$$+ \left(- \frac{64}{9} S_1^2 + \frac{64\left(10N^2 + 10N + 3\right)}{27 N(N+1)} S_1 - \frac{32\left(112N^3 + 224N^2 + 169N + 39\right)}{81 N(N+1)^2} \right.$$

$$- \frac{64}{9} S_2 \right) S_{-3} + (-1)^N \Bigg[\frac{32}{3(N+1)^3} L_M^2 + \left(\frac{128(4N+1)}{9(N+1)^4} - \frac{64}{3(N+1)^3} S_1 \right) L_M$$

$$+ \frac{32}{3(N+1)^3} L_Q^2 - \frac{32 P_{100}}{45(N-2)(N-1)^2 N^2 (N+1)^4 (N+2)^2 (N+3)^3} L_Q$$

$$- \frac{8\left(2N^3 + 2N^2 + 2N + 1\right)}{3 N^3 (N+1)^3} \zeta_2 + \frac{16 P_{24}}{27 N^4 (N+1)^4} S_1 - \frac{32\left(2N^2 + 2N + 1\right)}{9 N^3 (N+1)^3} S_2$$

$$- \frac{32\left(2N^2 + 2N + 1\right)}{9 N^3 (N+1)^3} S_1^2 - \frac{8 P_{28}}{81 N^5 (N+1)^5} \Bigg] - \frac{8 P_{37}}{81 N^2 (N+1)^2} S_3 - \frac{128}{9} S_{-5}$$

$$- \frac{224}{9} S_5 + \frac{4\left(443N^2 + 443N + 78\right)}{27N(N+1)} S_4 - \frac{8P_{20}}{9N^2(N+1)^2} S_{2,1} + \left[-\frac{256}{27} S_3 \right.$$

$$+ \frac{256}{9} S_{2,1} - \frac{128}{27} S_1^3 + \frac{64}{9N(N+1)} S_1^2 - \frac{64P_{13}}{81N^2(N+1)^2} S_1 + \frac{32P_{14}}{81N^3(N+1)^3}$$

$$+ \frac{640}{27} S_2 \right] S_{-2} - \frac{128}{3} S_{2,3} + \frac{256}{9} S_{2,-3} - \frac{8(13N+4)(13N+9)}{27N(N+1)} S_{3,1} + \frac{256}{9} S_{4,1}$$

$$+ S_2 \left(\frac{4P_{45}}{81N^3(N+1)^3} + \frac{496}{27} S_3 - \frac{64}{3} S_{2,1} - \frac{128}{3} S_{-2,1} \right) + \left[-\frac{32}{3} S_3 - \frac{32}{3} S_{-3} \right.$$

$$+ \frac{64}{3} S_{-2,1} + \frac{2P_{74}}{9N(N+1)^3} + S_{-2} \left(\frac{32}{3N(N+1)} - \frac{64}{3} S_1 \right) - \frac{184}{9} S_1 \right] L_M^2$$

$$+ \frac{64\left(112N^3 + 112N^2 - 39N + 18\right)}{81N^2(N+1)} S_{-2,1} + \left[-\frac{16\left(194N^2 + 194N - 33\right)}{27N(N+1)} S_1 \right.$$

$$- \frac{176}{9} S_1^2 + \frac{2P_{84}}{27N^2(N+1)^3} + S_{-2} \left(\frac{32}{3N(N+1)} - \frac{64}{3} S_1 \right) + \frac{176}{3} S_2 - \frac{32}{3} S_3$$

$$- \frac{32}{3} S_{-3} + \frac{64}{3} S_{-2,1} \right] L_Q^2 + \frac{64\left(10N^2 + 10N - 3\right)}{27N(N+1)} S_{-2,2} - \frac{256}{9} S_{-2,3} - \frac{256}{9} S_{2,1,-2}$$

$$+ \frac{64}{3} S_{2,2,1} - \frac{256}{9} S_{3,1,1} + \left[S_{-2} \left(\frac{32\left(16N^2 + 10N - 3\right)}{9N^2(N+1)^2} - \frac{640}{9} S_1 + \frac{64}{3} S_2 \right) \right.$$

$$+ \frac{P_{96}}{81N^3(N+1)^4} + S_{-3} \left(\frac{64}{3} S_1 - \frac{32\left(10N^2 + 10N + 3\right)}{9N(N+1)} \right) + \frac{1792}{27} S_2 + \frac{160}{3} S_4$$

$$- \frac{16\left(31N^2 + 31N + 9\right)}{9N(N+1)} S_3 + \frac{64}{3} S_{-4} - \frac{128}{3} S_{3,1} + \frac{64\left(10N^2 + 10N - 3\right)}{9N(N+1)} S_{-2,1}$$

$$+ S_1 \left(-\frac{8P_{89}}{81N^3(N+1)^3} + 32 S_3 + \frac{128}{3} S_{-2,1} \right) + \frac{64}{3} S_{-2,2} - \frac{256}{3} S_{-2,1,1} \right] L_M$$

$$- \frac{256\left(10N^2 + 10N - 3\right)}{27N(N+1)} S_{-2,1,1} - \frac{256}{9} S_{-2,2,1} + \frac{224}{9} S_{2,1,1,1} + \frac{1024}{9} S_{-2,1,1,1}$$

$$+ \left(-16 S_1^2 + \frac{4\left(593N^2 + 593N + 108\right)}{27N(N+1)} S_1 + \frac{P_{38}}{27N^2(N+1)^2} + 16 S_2 \right) \zeta_3$$

$$+ \gamma_{qq}^{(0)} \left(\frac{22}{27} L_M^3 - 8\zeta_3 L_M + \frac{44}{27} L_Q^3 + \frac{4}{3} B_4 - 12\zeta_4 - 4 S_{2,1,1} \right) + \left[\frac{352}{27} S_1^3 - \frac{32}{3} S_2^2 \right.$$

$$+ \left(\frac{16\left(194N^2 + 194N - 33\right)}{27N(N+1)} + \frac{32}{3} S_2 \right) S_1^2 + \left(-\frac{32\left(11N^2 + 11N + 3\right)}{9N(N+1)} S_2 \right.$$

$$+ \frac{4P_{95}}{81N^3(N+1)^3} + 32 S_3 - \frac{128}{3} S_{2,1} - \frac{256}{3} S_{-2,1} \right) S_1 - 32 S_{-2}^2 + S_{-3} \left(-\frac{128}{3} S_1 \right.$$

$$+ \frac{32\left(10N^2 + 22N + 3\right)}{9N(N+1)} \right) - \frac{4P_{101}}{405(N-1)^2 N^3 (N+1)^4 (N+2)^2 (N+3)^3}$$

$$+ S_{-2} \left(\frac{128}{3} S_1^2 + \frac{64\left(10N^2 + 22N - 9\right)}{9N(N+1)} S_1 + \frac{32P_{87}}{9(N-2)N^2(N+1)^2(N+3)} \right.$$

$$- \frac{128}{3} S_2 \right) - \frac{16\left(230N^3 + 460N^2 + 213N - 11\right)}{9N(N+1)^2} S_2 - \frac{64\left(11N^2 + 11N - 3\right)}{9N(N+1)} S_{2,1}$$

$$+ \frac{16\left(368N^2 + 440N - 45\right)}{27N(N+1)} S_3 - \frac{224}{3} \left(S_4 + S_{-4} \right) - \frac{64\left(10N^2 + 22N - 9\right)}{9N(N+1)} S_{-2,1}$$

$$+ \frac{128}{3} S_{-3,1} + 64 S_{2,1,1} + \frac{256}{3} S_{-2,1,1} + \left(\frac{32\left(3N^2 - N + 2\right)}{N(N+1)} - 64 S_1 \right) \zeta_3$$

4. Non-singlet contributions to DIS

$$- \frac{64}{3} S_{3,1} \bigg] L_Q \bigg\} + \hat{c}_{q,2}^{\mathrm{NS},(3)}(N_F) \bigg\} \bigg\}, \tag{4.103}$$

with the polynomials defined before, as well as

$$P_{70} = -3N^4 - 6N^3 - 47N^2 - 20N + 12 \tag{4.104}$$

$$P_{71} = 19N^4 + 38N^3 - 9N^2 - 20N + 4 \tag{4.105}$$

$$P_{72} = 28N^4 + 56N^3 + 28N^2 + 2N + 1 \tag{4.106}$$

$$P_{73} = 33N^4 + 38N^3 - 15N^2 - 60N - 28 \tag{4.107}$$

$$P_{74} = 51N^4 + 153N^3 + 223N^2 + 143N + 70 \tag{4.108}$$

$$P_{75} = 57N^4 + 72N^3 + 29N^2 - 22N - 24 \tag{4.109}$$

$$P_{76} = 141N^4 + 198N^3 + 169N^2 - 32N - 84 \tag{4.110}$$

$$P_{77} = 235N^4 + 596N^3 + 319N^2 + 66N + 72 \tag{4.111}$$

$$P_{78} = 359N^4 + 844N^3 + 443N^2 + 66N + 72 \tag{4.112}$$

$$P_{79} = 501N^4 + 750N^3 + 325N^2 - 188N - 204 \tag{4.113}$$

$$P_{80} = 1131N^4 + 1926N^3 + 1019N^2 - 64N - 276 \tag{4.114}$$

$$P_{81} = 1139N^4 + 3286N^3 + 1499N^2 + 504N + 828 \tag{4.115}$$

$$P_{82} = 1199N^4 + 2398N^3 + 1181N^2 + 18N + 90 \tag{4.116}$$

$$P_{83} = 1220N^4 + 2251N^3 + 1772N^2 + 303N - 138 \tag{4.117}$$

$$P_{84} = 1407N^5 + 3297N^4 + 2891N^3 + 583N^2 - 802N - 528 \tag{4.118}$$

$$P_{85} = -11145N^6 - 30915N^5 - 33923N^4 - 11449N^3 + 3112N^2 + 120N - 1512 \tag{4.119}$$

$$P_{86} = -151N^6 - 469N^5 - 181N^4 + 305N^3 + 208N^2 + 40N + 8 \tag{4.120}$$

$$P_{87} = 6N^6 - 6N^5 - 25N^4 + 52N^3 - 46N^2 - 39N - 162 \tag{4.121}$$

$$P_{88} = 15N^6 + 24N^5 - 88N^3 - 79N^2 - 52N - 12 \tag{4.122}$$

$$P_{89} = 155N^6 + 465N^5 + 465N^4 - 61N^3 - 324N^2 - 324N - 162 \tag{4.123}$$

$$P_{90} = 216N^6 + 459N^5 + 417N^4 - 99N^3 - 317N^2 - 272N - 84 \tag{4.124}$$

$$P_{91} = 309N^6 + 647N^5 + 293N^4 - 975N^3 - 1102N^2 - 316N + 24 \tag{4.125}$$

$$P_{92} = 609N^6 + 1029N^5 + 613N^4 - 37N^3 - 74N^2 + 300N + 216 \tag{4.126}$$

$$P_{93} = 795N^6 + 1587N^5 + 1295N^4 + 397N^3 + 50N^2 + 300N + 216 \tag{4.127}$$

$$P_{94} = 1770N^6 + 4731N^5 + 4483N^4 + 749N^3 + 55N^2 + 1440N + 756 \tag{4.128}$$

$$P_{95} = 7531N^6 + 26121N^5 + 27447N^4 + 8815N^3 + 1110N^2 + 936N - 324 \tag{4.129}$$

$$P_{96} = -4785N^7 - 19140N^6 - 19186N^5 - 4584N^4 + 1491N^3 - 4540N^2 \\ - 1536N + 792 \tag{4.130}$$

$$P_{97} = -45N^8 - 138N^7 - 678N^6 + 836N^5 + 1615N^4 + 1702N^3 + 380N^2 \\ - 408N - 192 \tag{4.131}$$

$$P_{98} = 42591N^8 + 161388N^7 + 226272N^6 + 104062N^5 - 40175N^4 - 43450N^3 - 3928N^2 \\ - 1272N - 2160 \tag{4.132}$$

$$P_{99} = -18351N^{10} - 87156N^9 - 196947N^8 - 239766N^7 - 157693N^6 - 26288N^5 \\ + 17847N^4 + 7490N^3 + 2248N^2 + 1896N + 144 \tag{4.133}$$

$$P_{100} = 101N^{11} + 1268N^{10} + 4423N^9 + 908N^8 - 20681N^7 - 19546N^6 + 52505N^5$$
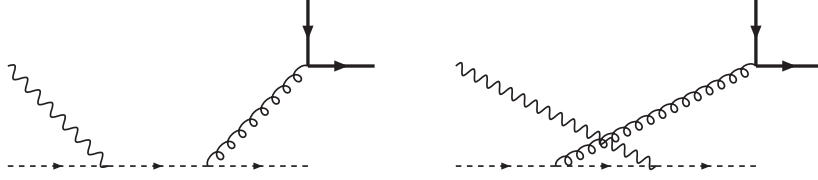
Figure 4.2.: Diagrams contributing to the tagged non-singlet heavy flavour production. The heavy quarks appear in the final state. Dashed lines denote massless quarks, massive quarks are draws as thick, solid lines, wavy lines are photons and curled lines denote gluons.

$$+ 83160N^4 - 4668N^3 - 38934N^2 - 2592N - 648 \tag{4.134}$$

$$P_{101} = 41370N^{14} + 571305N^{13} + 3141790N^{12} + 8395028N^{11} + 9302220N^{10} - 4510326N^9$$
$$- 22388388N^8 - 17101704N^7 + 7895114N^6 + 18219253N^5 + 4736406N^4$$
$$- 5978772N^3 - 1986336N^2 + 2361312N + 1283040 \tag{4.135}$$

$$P_{102} = 4140N^{15} + 54540N^{14} + 277575N^{13} + 634467N^{12} + 354380N^{11} - 1199584N^{10}$$
$$- 2051492N^9 + 733454N^8 + 4802206N^7 + 3686432N^6 - 1882531N^5 - 3693633N^4$$
$$- 1066014N^3 + 869508N^2 + 897480N + 233280 \,. \tag{4.136}$$

The 3-loop massless Wilson coefficient $\hat{c}_{q,2}^{\mathrm{NS},(3)}$ for $L_Q = 0$ is left symbolic in the expression above and can be found in [138]. The shorthand $\gamma_{qq}^{(0)}$ is given in Eq. (4.23). Harmonic sums up to weight $w = 5$ are necessary to express the result. All harmonic sums are reduced to an algebraically independent basis via quasi-shuffle relations. The corresponding expression in x can be found in Eq. (E.11), Appendix E. It is given in terms of HPLs up to weight $w = 5$ and has been reduced algebraically as well. In all these expressions the renormalisation and factorisation scales are set equal $\mu_R^2 = \mu_F^2$ and are denoted by μ^2.

Equation (4.103) appears to have poles at $N = 1$ and $N = 2$, but an expansion around these values shows that they are removable singularities. The rightmost pole is located at $N = 0$, which is consistent with the small x behaviour of the Wilson coefficient in x space.

While the result presented here deals with the heavy flavour contribution to the inclusive structure function, previous publications [201] treat heavy flavour production in DIS in the tagged case, by always requiring heavy quarks in the final state. The two cases differ by diagrams which contain heavy quarks as virtual particles. Such diagrams are omitted in the tagged case while they do contribute to the inclusive structure function. The non-singlet heavy flavour Wilson coefficient can be calculated analytically up to $\mathcal{O}(a_s^2)$ for any value of Q^2/m^2 [421]. Contributions to the tagged case come from the diagrams in Fig. 4.2 where the heavy quarks are explicitly present in the final state. There is no mass or collinear singularity from these diagrams since such divergences are regulated by the heavy quark mass. For the asymptotic region $Q^2 \gg m^2$, the authors of [201] give the following expression

$$L_{q,2}^{\mathrm{NS,tagged},(2)}(N_F + 1) = a_s^2 \left\{ \frac{1}{4} \beta_{0,Q} \gamma_{qq}^{\mathrm{NS},(0)} \ln^2\left(\frac{m^2}{\mu^2}\right) + \frac{1}{2} \hat{\gamma}_{qq}^{\mathrm{NS},(1)} \ln\left(\frac{m^2}{\mu^2}\right) - \frac{1}{4} \beta_{0,Q} \zeta_2 \gamma_{qq}^{\mathrm{NS},(0)} \right.$$
$$+ a_{qq,Q}^{\mathrm{NS},(2)} + \frac{1}{4} \beta_{0,Q} \gamma_{qq}^{\mathrm{NS},(0)} \ln^2\left(\frac{Q^2}{\mu^2}\right) - \left[\frac{1}{2} \hat{\gamma}_{qq}^{\mathrm{NS},(1)} + \beta_{0,Q} c_{q,2}^{\mathrm{NS},(1)}\right] \ln\left(\frac{Q^2}{\mu^2}\right)$$
$$\left. + \hat{c}_{q,2}^{\mathrm{NS},(2)} + \beta_{0,Q}\left[-\frac{1}{2} \gamma_{qq}^{\mathrm{NS},(0)} \ln\left(\frac{Q^2}{\mu^2}\right) + c_{q,2}^{\mathrm{NS},(1)}\right] \ln\left(\frac{m^2}{\mu^2}\right) \right\}$$
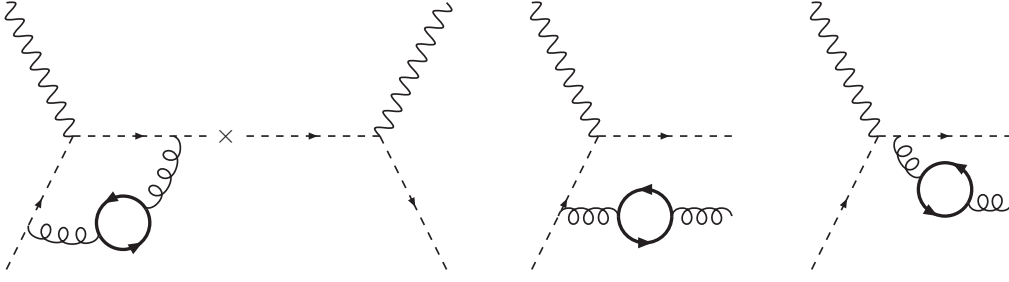
4. Non-singlet contributions to DIS

Figure 4.3.: Diagrams contributing to the inclusive non-singlet structure function. The heavy quarks (drawn as thick, solid lines) appear as virtual particles. In the final state, only massless partons are present.

$$
= a_s^2 \left\{ \frac{1}{4} \beta_{0,Q} \gamma_{qq}^{\mathrm{NS},(0)} \ln^2 \left(\frac{Q^2}{m^2} \right) - \left[\frac{1}{2} \hat{\gamma}_{qq}^{\mathrm{NS},(1)} + \beta_{0,Q} c_{q,2}^{\mathrm{NS},(1)} \right] \ln \left(\frac{Q^2}{m^2} \right) \right.
$$
$$
\left. + \hat{c}_{q,2}^{\mathrm{NS},(2)} + a_{qq,Q}^{\mathrm{NS},(2)} - \frac{1}{4} \beta_{0,Q} \zeta_2 \gamma_{qq}^{\mathrm{NS},(0)} \right\} . \tag{4.137}
$$

In the inclusive case treated by us, also the graphs depicted in Fig. 4.3 contribute. Here only massless partons appear in the final state and the heavy quarks enter as virtual particles. A definition of the tagged heavy flavour case beyond 2-loop order necessitates the introduction of jet cones as a non-inclusive quantity is dealt with. The inclusive heavy flavour contributions are instead defined as the difference between the inclusive structure function with massive and massless quarks and the inclusive structure function with just massless quarks. Then virtual corrections from heavy quarks do belong to the heavy flavour corrections. The difference between the two approaches at NLO in the asymptotic limit is given by

$$
- a_s^2 \beta_{0,Q} \ln \left(\frac{m^2}{\mu^2} \right) \left[-\frac{1}{2} \gamma_{qq}^{\mathrm{NS},(0)} \ln \left(\frac{Q^2}{\mu^2} \right) + c_{q,2}^{\mathrm{NS},(1)} \right] \tag{4.138}
$$

Taking this difference into account, we agree to the result of [201] for $L_{q,2}^{\mathrm{NS}}$ up to 2-loop order.

4.2.2. Numerical results

After having completed the Wilson coefficient $L_{q,2}^{\mathrm{NS}}$ we are now in the position to illustrate its impact on the structure function numerically. But before we do this, we would like to discuss the asymptotic behaviour of the Wilson coefficient in the small and large x limit. For the following discussions and illustrations we choose the scale $\mu^2 = Q^2$.

We would like to distinguish the part of the heavy flavour Wilson coefficient which involves massive OMEs and the part that is completely determined by the massless Wilson coefficient. The asymptotic behaviour of the former part in the small x limit ($x \to 0$) is given by

$$
L_{q,2}^{\mathrm{NS}}(N_F + 1) - \hat{C}_{q,2}^{\mathrm{NS}}(N_F) \underset{x \to 0}{\propto} a_s^2 C_F T_F \frac{2}{3} \ln^2(x) + a_s^3 C_F^2 T_F \frac{17}{27} \ln^4(x) , \tag{4.139}
$$

while for the latter part it reads [138]

$$
\hat{C}_{q,2}^{\mathrm{NS}}(N_F) \underset{x \to 0}{\propto} a_s^2 C_F T_F \frac{10}{3} \ln^2(x) + a_s^3 C_F^2 T_F \frac{91}{27} \ln^4(x) . \tag{4.140}
$$

By comparing the expressions above to the same limit of the OME in Eq. (4.75) we find that the small x behaviour of the heavy flavour Wilson coefficient receives contributions from both the

OMEs and the massless Wilson coefficient. This is in contrast to the large x limit: For Wilson coefficients it is given by

$$L_{q,2}^{\text{NS}}(N_F + 1) - \hat{C}_{q,2}^{\text{NS}}(N_F) \underset{x \to 1}{\propto} a_s^2 C_F T_F \left(\frac{8}{3} L_M^2 + \frac{80}{9} L_M + \frac{224}{27} \right) \left(\frac{1}{1 - x} \right)_+$$
$$+ a_s^3 C_F^2 T_F \left(16 L_M^2 + \frac{160}{3} L_M + \frac{448}{9} \right) \left(\frac{\ln^2(1 - x)}{1 - x} \right)_+ \quad (4.141)$$

and

$$\hat{C}_{q,2}^{\text{NS}}(N_F) \underset{x \to 1}{\propto} a_s^2 C_F T_F \frac{8}{3} \left(\frac{\ln^2(1 - x)}{1 - x} \right)_+ + a_s^3 C_F^2 T_F \frac{80}{9} \left(\frac{\ln^4(1 - x)}{1 - x} \right)_+ . \quad (4.142)$$

Comparing this again to the OME in this limit, cf. Eq. (4.78), we see that the massless Wilson coefficient exhibits much stronger soft singularities and dominates over the contributions from the OME. At 3-loop order it also becomes apparent that the mixed term in Eq. (4.102), which consists of the 2-loop OME and the 1-loop massless Wilson coefficient, has a more dominant behaviour in this asymptotic limit than the 3-loop OME.

Let us now proceed by numerically illustrating the impact of the heavy flavour Wilson coefficient on the structure function. Unless stated otherwise, we use the NNLO PDFs of [218] and we employ the LHAPDF library [422] to access the grids for the PDFs and the strong coupling constant provided by the fitting group. We consider three massless quarks ($N_F = 3$) and treat the charm quark as the heavy quark. Its mass in the OMS and $\overline{\text{MS}}$ scheme is taken to be [226]

$$m_c^{\text{OMS}} = 1.59 \, \text{GeV} \,, \qquad\qquad m_c^{\overline{\text{MS}}} = 1.24 \, \text{GeV} \,, \qquad (4.143)$$

respectively. For the numerical evaluation of the HPLs in Eq. (E.11) we use the weight $w = 5$ extension of the code described in [423]. The 3-loop part of the massless Wilson coefficient $\hat{c}_{q,2}^{\text{NS},(3)}$ is evaluated using the parametrisation presented in [138].

Figure 4.4 shows the contribution of $L_{q,2}^{\text{NS}}$ to the structure function $F_2(x, Q^2)$ for different values of Q^2. The higher order corrections to $L_{q,2}^{\text{NS}}$ are negative over the whole range of x that we consider. They grow as x becomes smaller, which originates from the singlet PDF, which enters due to the fact that we study the PDF combination $f_k + \bar{f}_k$ instead of $f_k + \bar{f} - \Sigma/N_F$. Moreover, the asymptotic heavy flavour corrections show a small peak at $x \approx 0.3$ for $Q^2 = 1000 \, \text{GeV}^2$, which shifts towards larger x and becomes more pronounced for lower Q^2. To compare the 2-loop and 3-loop effects coming from the Wilson coefficient, we keep the PDFs and the strong coupling constant at their NNLO values and only truncate the Wilson coefficient at 2- or 3-loop order, respectively. Going from $\mathcal{O}(a_s^2)$ to $\mathcal{O}(a_s^3)$, we observe an enhancement of the absolute value of the structure function by about 60 to 70%. The massive 3-loop corrections compared to the total non-singlet contribution of $F_2(x, Q^2)$ are below 1%. Currently the experimental precision for $F_2(x, Q^2)$ reaches order 1% and future experiments like the EIC [424, 425] might improve on that.

In Fig. 4.5 the same contribution is plotted at $\mathcal{O}(a_s^3)$ comparing the treatment of the heavy quark mass OMS and the $\overline{\text{MS}}$ scheme. The shapes as functions of x in both schemes are similar, but the absolute value of the heavy flavour contributions in the $\overline{\text{MS}}$ scheme is consistently larger by about 5 to 25% at all values of x and Q^2 considered here.

Figure 4.6 contains a comparison of the inclusive and the tagged case of the non-singlet contributions at 2-loop order. We use the NLO PDFs from [426] and the best fit value for the charm quark mass at NLO in the $\overline{\text{MS}}$ scheme $m_c = 1.15 \, \text{GeV}$ from [226]. Since we choose $\mu^2 = Q^2$, the L_Q term in Eq. (4.138) is absent. The contribution to the structure function is larger in the tagged case, except for large values of x.
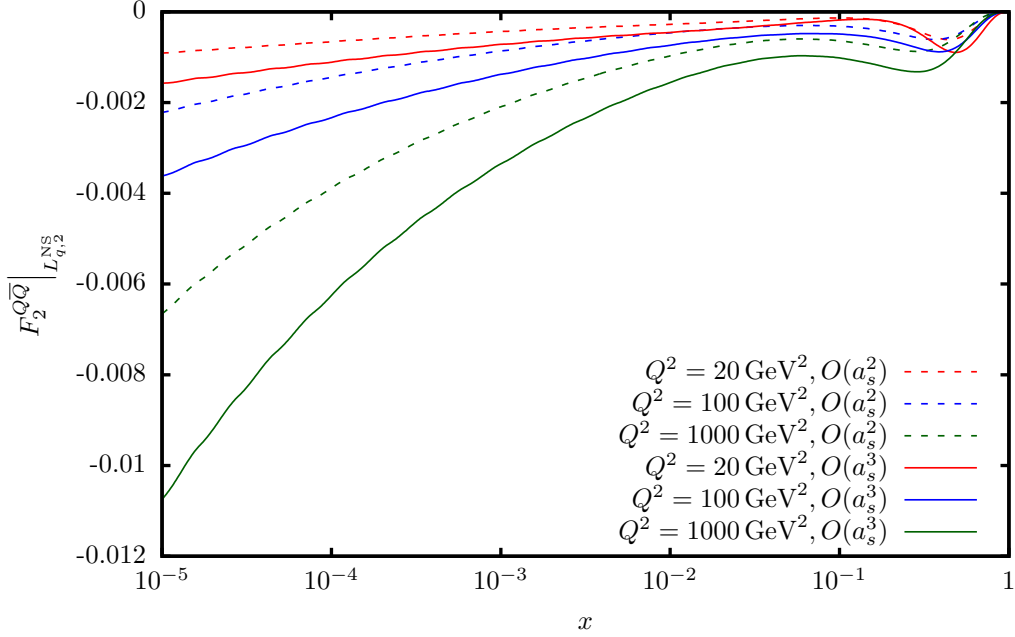
Figure 4.4.: Non-singlet charm contribution to the structure function $F_2(x, Q^2)$ from the Wilson coefficient $L_{q,2}^{\mathrm{NS}}$. The different curves show the corrections up to and including $\mathcal{O}\big(a_s^2\big)$ (dashed lines) and $\mathcal{O}\big(a_s^3\big)$ (solid lines) for different values of the virtuality Q^2. The PDFs are taken from [218] and the charm quark mass $m_c = 1.59\,\mathrm{GeV}$ [226] is treated in the OMS scheme. The $\mathcal{O}\big(a_s^0\big)$ term is not shown.

4.3. Polarised neutral current DIS

Given the odd moments of the non-singlet OME $A_{qq,Q}^{\mathrm{NS}}$, we can also complete the non-singlet heavy flavour Wilson coefficient L_{q,g_1}^{NS} in the asymptotic limit. It enters the heavy flavour component of the inclusive structure function $g_1(x, Q^2)$. In analogy to the unpolarised case in Eq. (2.90) the heavy flavour part $g_1^{\mathrm{h}}(x, Q^2)$ reads, cf. [191],

$$
\begin{aligned}
g_1^{\mathrm{h}}&(x, N_F + 1, Q^2, m^2) = \\
&\frac{1}{2}\Bigg\{ \sum_{k=1}^{N_F} e_k^2 \Bigg[L_{q,g_1}^{\mathrm{NS}}\left(x, N_F+1, \frac{Q^2}{\mu^2}, \frac{m^2}{\mu^2}\right) \otimes \left[\Delta f_k(x, \mu^2, N_F) + \Delta \bar{f}_k(x, \mu^2, N_F)\right] \\
&+ \frac{1}{N_F} L_{q,g_1}^{\mathrm{PS}}\left(x, N_F+1, \frac{Q^2}{m^2}, \frac{m^2}{\mu^2}\right) \otimes \Delta\Sigma(x, \mu^2, N_F) \\
&+ \frac{1}{N_F} L_{g,g_1}^{\mathrm{S}}\left(x, N_F+1, \frac{Q^2}{m^2}, \frac{m^2}{\mu^2}\right) \otimes \Delta G(x, \mu^2, N_F) \Bigg] \\
&+ e_Q^2 \Bigg[H_{q,g_1}^{\mathrm{PS}}\left(x, N_F+1, \frac{Q^2}{m^2}, \frac{m^2}{\mu^2}\right) \otimes \Delta\Sigma(x, \mu^2, N_F) \\
&+ H_{g,g_1}^{\mathrm{S}}\left(x, N_F+1, \frac{Q^2}{m^2}, \frac{m^2}{\mu^2}\right) \otimes \Delta G(x, \mu^2, N_F) \Bigg] \Bigg\},
\end{aligned}
\tag{4.144}
$$

where ΔG, Δf_k and $\Delta \bar{f}_k$ denote the polarised gluon, quark and anti-quark PDFs, respectively. We write $\Delta\Sigma = \sum_{k=1}^{N_F}[\Delta f_k + \Delta \bar{f}_k]$ for the polarised singlet PDF combination. In the limit
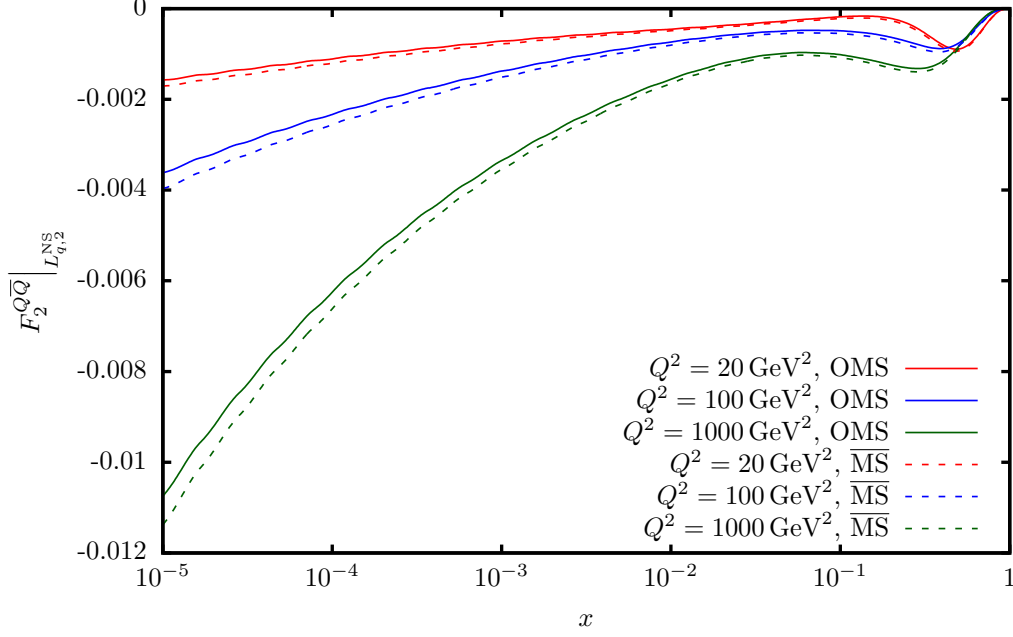
Figure 4.5.: Comparison of treating the charm quark mass in the OMS and $\overline{\text{MS}}$ scheme for the non-singlet charm contribution to the structure function $F_2(x, Q^2)$. The plot shows the contributions up to and including 3-loop effects, omitting however the $\mathcal{O}(a_s^0)$ term. The charm quark mass is $m_c = 1.59\,\text{GeV}$ in the OMS scheme and $m_c = 1.24\,\text{GeV}$ in the $\overline{\text{MS}}$ scheme.
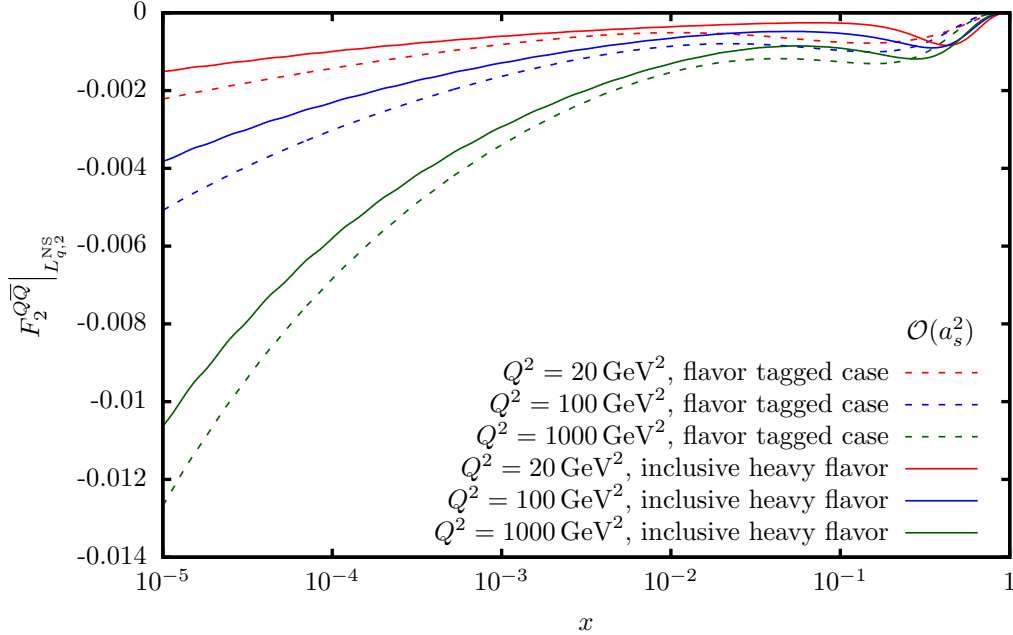

Figure 4.6.: Comparison of tagged charm (dashed lines) and inclusive charm (solid lines) cases for the contribution from $L_{q,2}^{\text{NS}}$ to $F_2(x, Q^2)$. The comparison is done at 2-loop order using the NLO PDFs from [426]. The charm mass is taken to be $m_c = 1.15\,\text{GeV}$ in the $\overline{\text{MS}}$ scheme.

4. Non-singlet contributions to DIS

$Q^2 \gg m^2$, the Wilson coefficient can be written in terms of massive OMEs $A_{qq,Q}^{\mathrm{NS}}$ and massless Wilson coefficients C_{q,g_1}^{NS}. In Mellin N space it can be written as, cf. [202, 203],

$$
L_{q,g_1}^{\mathrm{NS}}(N_F + 1) = a_s^2 \left[A_{qq,Q}^{\mathrm{NS},(2)}(N_F + 1) + \hat{C}_{q,g_1}^{\mathrm{NS},(2)}(N_F) \right]
$$

$$
+ a_s^3 \left[A_{qq,Q}^{\mathrm{NS},(3)}(N_F + 1) + A_{qq,Q}^{\mathrm{NS},(2)}(N_F + 1) C_{q,g_1}^{\mathrm{NS},(1)}(N_F + 1) + \hat{C}_{q,g_1}^{\mathrm{NS},(3)}(N_F) \right],
$$

(4.145)

where we have suppressed all dependence on N and the scales for better readability. Since non-trivial contributions to $A_{qq,Q}^{\mathrm{NS}}$ start at 2-loop order, the non-singlet Wilson coefficient also starts at $\mathcal{O}(a_s^2)$. Besides the renormalised non-singlet OME $A_{qq,Q}^{\mathrm{NS}}$ also the massless Wilson coefficient C_{q,g_1}^{NS} enters. It is known up to 3-loop order in the literature [106, 152, 153]. Up to $\mathcal{O}(a_s^2)$ it is identical to the charged current Wilson coefficient $C_{q,3}^{\mathrm{NS}}$. At $\mathcal{O}(a_s^3)$ the polarised Wilson coefficient $C_{q,g_1}^{\mathrm{NS},(3)}$ can be obtained from the charged current Wilson coefficient $C_{q,3}^{\mathrm{NS},(3)}$ by removing the terms proportional to the colour factor $d^{abc}d^{abc}$ [129, 153].

Equation (4.145) expresses L_{q,g_1}^{NS} in terms of renormalised massive OMEs and massless Wilson coefficients. As already discussed in the unpolarised case, the expressions for the massless Wilson coefficient [153] are published for the scale choice $\mu^2 = Q^2$ so that logarithms $\ln(Q^2/\mu^2)$ vanish. We reconstruct these terms using the renormalisation group, see also [293], in terms of the coefficients of the β-function and the polarised anomalous dimensions $\Delta\gamma_+^{\mathrm{NS},(k)}$, taken from [160], as well as the lower order Wilson coefficients.

At leading twist, the structure function $g_2(x, Q^2)$ can be obtained from the Wandzura-Wilczek relation [154] which, at the level of twist-2, reads

$$
g_2(x, Q^2) = -g_1(x, Q^2) + \int_x^1 \frac{\mathrm{d}y}{y} g_1(y, Q^2).
$$

(4.146)

This relation has also been derived in the covariant parton model for quarks [280, 427, 428] and for gluons in the initial state [190]. For target mass corrections [276, 429] and finite light quark masses [276] the relation is still valid. In [430] it was shown that it holds for non-forward scattering and in [431, 432] diffractive scattering, including target mass corrections, were considered.

4.3.1. Analytic Results

Since we have obtained the non-singlet OME $A_{qq,Q}^{\mathrm{NS}}$ to 3-loop order also for odd moments, cf. Section 4.1, we now have at hand all components required for the Wilson coefficient L_{q,g_1}^{NS}. Inserting the renormalised OME and Wilson coefficient into Eq. (4.145) we arrive at L_{q,g_1}^{NS} in N space. We define

$$
\Delta\gamma_{qq}^{(0)} = 4 \left[2S_1 - \frac{3N^2 + 3N + 2}{2N(N+1)} \right]
$$

(4.147)

as a shorthand for the leading-order non-singlet anomalous dimension up to its colour factor. The Wilson coefficient is then given by

$$
L_{q,g_1}^{\mathrm{NS}}(N) = \tfrac{1}{2} \left[1 - (-1)^N \right] \left\{ a_s^2 C_F T_F \left\{ -\frac{1}{3} [L_M^2 + L_Q^2] \Delta\gamma_{qq}^{(0)} + L_M \left[-\frac{2P_{70}}{9N^2(N+1)^2} - \frac{80}{9} S_1 \right. \right. \right.
$$

$$
\left. + \frac{16}{3} S_2 \right] + L_Q \left[-\frac{2P_{104}}{9N^2(N+1)^2} + \frac{4(29N^2 + 29N - 6)}{9N(N+1)} S_1 + \frac{8}{3} S_1^2 - 8 S_2 \right] + \frac{16}{3} S_{2,1}
$$

$$+ \frac{P_{121}}{27N^3(N+1)^3} + \left(-\frac{2P_{107}}{27N^2(N+1)^2} + \frac{8}{3}S_2\right)S_1 - \frac{2\left(29N^2 + 29N - 6\right)}{9N(N+1)}S_1^2$$

$$- \frac{8}{9}S_1^3 + \frac{2\left(35N^2 + 35N - 2\right)}{3N(N+1)}S_2 - \frac{112}{9}S_3\Bigg\}$$

$$+ a_s^3\Bigg\{C_F^2 T_F\Bigg[\frac{1}{6}\left[L_Q^3 + L_M^2 L_Q\right]\Delta\gamma_{qq}^{(0)2} + L_M^2\left[-\frac{2P_{116}}{3N^3(N+1)^3} - \frac{16}{3}S_1^3\right.$$

$$+ \frac{2P_{103}}{3N^2(N+1)^2}S_1 - \frac{4(N-1)(N+2)}{N(N+1)}S_1^2 + \frac{64}{3}S_3 + \frac{64}{3}S_{-3} - \frac{128}{3}S_{-2,1}$$

$$+ \left(-\frac{64}{3N(N+1)} + \frac{128}{3}S_1\right)S_{-2} + \frac{10}{3}\Delta\gamma_{qq}^{(0)}S_2\Bigg] + L_Q^2\Bigg[-\frac{2P_{118}}{9N^3(N+1)^3}$$

$$+ \frac{2P_{108}}{9N^2(N+1)^2}S_1 - \frac{4\left(107N^2 + 107N - 54\right)}{9N(N+1)}S_1^2 - 16S_1^3 + \frac{64}{3}\left[S_3 + S_{-3}\right]$$

$$+ \left(-\frac{64}{3N(N+1)} + \frac{128}{3}S_1\right)S_{-2} - \frac{128}{3}S_{-2,1} + \frac{22}{3}\Delta\gamma_{qq}^{(0)}S_2\Bigg]$$

$$+ L_M L_Q \Delta\gamma_{qq}^{(0)}\Bigg[\frac{P_{70}}{9N^2(N+1)^2} + \frac{40}{9}S_1 - \frac{8}{3}S_2\Bigg] + L_M\Bigg[\frac{P_{126}}{9N^4(N+1)^4}$$

$$+ \left(\frac{2P_{119}}{9N^3(N+1)^3} + \frac{16\left(59N^2 + 59N - 6\right)}{9N(N+1)}S_2 - \frac{256}{3}S_3 - \frac{256}{3}S_{-2,1}\right)S_1$$

$$+ \left(-\frac{4P_{71}}{3N^2(N+1)^2} + \frac{32}{3}S_2\right)S_1^2 - \frac{160}{9}S_1^3 - \frac{4P_{105}}{9N^2(N+1)^2}S_2 - 32S_2^2$$

$$+ \frac{32\left(29N^2 + 29N + 12\right)}{9N(N+1)}S_3 - \frac{256}{3}S_4 + \left(-\frac{64\left(16N^2 + 10N - 3\right)}{9N^2(N+1)^2} - \frac{128}{3}S_2\right.$$

$$+ \frac{1280}{9}S_1\right)S_{-2} + \left(\frac{64\left(10N^2 + 10N + 3\right)}{9N(N+1)} - \frac{128}{3}S_1\right)S_{-3} - \frac{128}{3}S_{-4}$$

$$+ \frac{128}{3}S_{3,1} - \frac{128\left(10N^2 + 10N - 3\right)}{9N(N+1)}S_{-2,1} - \frac{128}{3}S_{-2,2} + \frac{512}{3}S_{-2,1,1}$$

$$+ 8\Delta\gamma_{qq}^{(0)}\zeta_3\Bigg] + L_Q\Bigg[\frac{4P_{129}}{27N^4(N+1)^4(N+2)^3} + \left(-\frac{4P_{122}}{27N^3(N+1)^3} + \frac{640}{9}S_3\right.$$

$$- \frac{32\left(67N^2 + 67N - 21\right)}{9N(N+1)}S_2 + \frac{64}{3}S_{2,1} + \frac{512}{3}S_{-2,1}\right)S_1 + \left(\frac{2P_{110}}{27N^2(N+1)^2}\right.$$

$$- \frac{224}{3}S_2\right)S_1^2 + \frac{32(4N-1)(4N+5)}{9N(N+1)}S_1^3 + \frac{80}{9}S_1^4 + \frac{2P_{109}}{9N^2(N+1)^2}S_2 + 48S_2^2$$

$$- \frac{32\left(53N^2 + 53N + 16\right)}{9N(N+1)}S_3 + \frac{352}{3}S_4 + \left(-\frac{64P_{115}}{9(N-1)N^2(N+1)^2(N+2)}\right.$$

$$- \frac{128\left(10N^2 + 10N - 3\right)}{9N(N+1)}S_1 - \frac{256}{3}S_1^2 + \frac{256}{3}S_2\right)S_{-2} + 64S_{-2}^2 + \frac{448}{3}S_{-4}$$

$$+ \left(-\frac{64\left(10N^2 + 10N + 9\right)}{9N(N+1)} + \frac{256}{3}S_1\right)S_{-3} + \frac{16\left(9N^2 + 9N - 2\right)}{3N(N+1)}S_{2,1}$$

$$+ 64S_{3,1} + \frac{128\left(10N^2 + 10N - 3\right)}{9N(N+1)}S_{-2,1} - \frac{256}{3}S_{-3,1} - 64S_{2,1,1}$$

$$- \frac{512}{3}S_{-2,1,1} + \left(-\frac{16\left(9N^2 + 9N - 2\right)}{N(N+1)} + 64S_1\right)\zeta_3\Bigg] + \frac{P_{128}}{162N^5(N+1)^5}$$

$$- \frac{128\left(112N^3 + 112N^2 - 39N + 18\right)}{81N^2(N + 1)} S_{-2,1} + \left(\frac{P_{127}}{162N^4(N + 1)^4} - \frac{64}{9} S_2^2 \right.$$

$$+ \frac{8P_{82}}{81N^2(N + 1)^2} S_2 - \frac{8\left(347N^2 + 347N + 54\right)}{27N(N + 1)} S_3 + \frac{128}{9N(N + 1)} S_{2,1}$$

$$+ \frac{704}{9} S_4 - \frac{320}{9} S_{3,1} - \frac{256\left(10N^2 + 10N - 3\right)}{27N(N + 1)} S_{-2,1} + \frac{1024}{9} S_{-2,1,1}$$

$$\left. - \frac{256}{9} S_{-2,2} \right) S_1 + \left(\frac{P_{86}}{9N^3(N + 1)^3} + \frac{16\left(5N^2 + 5N - 4\right)}{9N(N + 1)} S_2 - \frac{128}{9} S_{2,1} \right.$$

$$+ 16S_3 - \frac{256}{9} S_{-2,1} \right) S_1^2 + \left(-\frac{16P_{72}}{27N^2(N + 1)^2} + \frac{128}{27} S_2 \right) S_1^3 + \left(\frac{400}{27} S_3 \right.$$

$$+ \frac{P_{114}}{81N^3(N + 1)^3} + \frac{256}{3} S_{-2,1} \right) S_2 - \frac{32\left(23N^2 + 23N - 3\right)}{27N(N + 1)} S_2^2 + \frac{512}{9} S_5$$

$$+ \frac{8P_{111}}{81N^2(N + 1)^2} S_3 - \frac{176\left(17N^2 + 17N + 6\right)}{27N(N + 1)} S_4 + \left(-\frac{64P_{14}}{81N^3(N + 1)^3} \right.$$

$$+ \frac{128P_{13}}{81N^2(N + 1)^2} S_1 - \frac{128}{9N(N + 1)} S_1^2 + \frac{256}{27} S_1^3 - \frac{1280}{27} S_2 + \frac{512}{27} S_3$$

$$\left. - \frac{512}{9} S_{2,1} \right) S_{-2} + \left(\frac{64\left(112N^3 + 224N^2 + 169N + 39\right)}{81N(N + 1)^2} + \frac{128}{9} S_1^2 \right.$$

$$+ \frac{128}{9} S_2 - \frac{128\left(10N^2 + 10N + 3\right)}{27N(N + 1)} S_1 \right) S_{-3} + \left(-\frac{128\left(10N^2 + 10N + 3\right)}{27N(N + 1)} \right.$$

$$+ \frac{256}{9} S_1 \right) S_{-4} + \frac{256}{9} S_{-5} + \frac{16P_{11}}{9N^2(N + 1)^2} S_{2,1} + \frac{256}{9} S_{2,3} - \frac{512}{9} S_{2,-3}$$

$$+ \frac{16\left(89N^2 + 89N + 30\right)}{27N(N + 1)} S_{3,1} - \frac{512}{9} S_{4,1} - \frac{128\left(10N^2 + 10N - 3\right)}{27N(N + 1)} S_{-2,2}$$

$$+ \frac{512}{9} S_{-2,3} + \frac{512}{9} S_{2,1,-2} + \frac{256}{9} S_{3,1,1} + \frac{512\left(10N^2 + 10N - 3\right)}{27N(N + 1)} S_{-2,1,1}$$

$$+ \frac{512}{9} S_{-2,2,1} - \frac{2048}{9} S_{-2,1,1,1} + \frac{16\left(2N^3 + 2N^2 + 2N + 1\right)}{3N^3(N + 1)^3} \zeta_2 + \left(-\frac{64}{3} S_2 \right.$$

$$+ \frac{2P_{16}}{9N^2(N + 1)^2} - \frac{1208}{9} S_1 \right) \zeta_3 + \left(\frac{8}{3} S_{2,1,1} - \frac{8}{3} B_4 + 12\zeta_4 \right) \Delta\gamma_{qq}^{(0)}$$

$$+ (-1)^N \left(-L_M^2 \frac{64}{3(N + 1)^3} - L_Q^2 \frac{64}{3(N + 1)^3} + L_M \left[-\frac{256(4N + 1)}{9(N + 1)^4} \right. \right.$$

$$\left. + \frac{128}{3(N + 1)^3} S_1 \right] + L_Q \frac{64P_{125}}{9(N - 1)N^2(N + 1)^4(N + 2)^3} + \frac{16P_{28}}{81N^5(N + 1)^5}$$

$$- \frac{32P_{24}}{27N^4(N + 1)^4} S_1 + \frac{64\left(2N^2 + 2N + 1\right)}{9N^3(N + 1)^3} S_1^2 + \frac{64\left(2N^2 + 2N + 1\right)}{9N^3(N + 1)^3} S_2$$

$$\left. + \frac{16\left(2N^3 + 2N^2 + 2N + 1\right)}{3N^3(N + 1)^3} \zeta_2 \right) \right] + \textcolor{blue}{C_A C_F T_F} \left[L_M^3 \frac{22}{27} \Delta\gamma_{qq}^{(0)} + L_Q^3 \frac{44}{27} \Delta\gamma_{qq}^{(0)} \right.$$

$$+ L_M^2 \left[\frac{2P_{112}}{9N^3(N + 1)^2} - \frac{184}{9} S_1 + \left(\frac{32}{3N(N + 1)} - \frac{64}{3} S_1 \right) S_{-2} - \frac{32}{3} \left[S_3 + S_{-3} \right] \right.$$

$$\left. + \frac{64}{3} S_{-2,1} \right] + L_Q^2 \left[\frac{2P_{113}}{27N^3(N + 1)^2} - \frac{16\left(194N^2 + 194N - 33\right)}{27N(N + 1)} S_1 - \frac{176}{9} S_1^2 \right.$$

$$+ \frac{176}{3} S_2 - \frac{32}{3} S_3 + \left(\frac{32}{3N(N+1)} - \frac{64}{3} S_1 \right) S_{-2} - \frac{32}{3} S_{-3} + \frac{64}{3} S_{-2,1} \Bigg]$$

$$+ L_M \Bigg[\frac{P_{124}}{81 N^4 (N+1)^3} + \left(-\frac{8 P_{117}}{81 N^3 (N+1)^3} + 32 S_3 + \frac{128}{3} S_{-2,1} \right) S_1$$

$$+ \frac{1792}{27} S_2 - \frac{16(31 N^2 + 31 N + 9)}{9 N (N+1)} S_3 + \frac{160}{3} S_4 + \left(\frac{32(16 N^2 + 10 N - 3)}{9 N^2 (N+1)^2} \right.$$

$$- \frac{640}{9} S_1 + \frac{64}{3} S_2 \right) S_{-2} + \left(-\frac{32(10 N^2 + 10 N + 3)}{9 N (N+1)} + \frac{64}{3} S_1 \right) S_{-3} + \frac{64}{3} S_{-4}$$

$$- \frac{128}{3} S_{3,1} + \frac{64(10 N^2 + 10 N - 3)}{9 N (N+1)} S_{-2,1} + \frac{64}{3} S_{-2,2} - \frac{256}{3} S_{-2,1,1} - 8 \Delta \gamma_{qq}^{(0)} \zeta_3 \Bigg]$$

$$+ L_Q \Bigg[-\frac{16(230 N^3 + 460 N^2 + 213 N - 11)}{9 N (N+1)^2} S_2 - \frac{4 P_{130}}{81 N^4 (N+1)^4 (N+2)^3}$$

$$+ \left(\frac{4 P_{123}}{81 N^3 (N+1)^3} - \frac{32(11 N^2 + 11 N + 3)}{9 N (N+1)} S_2 - \frac{128}{3} S_{2,1} - \frac{256}{3} S_{-2,1} \right.$$

$$+ 32 S_3 \right) S_1 + \left(\frac{16(194 N^2 + 194 N - 33)}{27 N (N+1)} + \frac{32}{3} S_2 \right) S_1^2 + \frac{352}{27} S_1^3 - \frac{32}{3} S_2^2$$

$$+ \frac{16(368 N^2 + 368 N - 9)}{27 N (N+1)} S_3 - \frac{224}{3} S_4 + \left(\frac{32 P_{115}}{9(N-1) N^2 (N+1)^2 (N+2)} \right.$$

$$+ \frac{64(10 N^2 + 10 N - 3)}{9 N (N+1)} S_1 + \frac{128}{3} S_1^2 - \frac{128}{3} S_2 \right) S_{-2} - 32 S_{-2}^2 + \left(-\frac{128}{3} S_1 \right.$$

$$+ \frac{32(10 N^2 + 10 N + 9)}{9 N (N+1)} \right) S_{-3} - \frac{224}{3} S_{-4} - \frac{64(11 N^2 + 11 N - 3)}{9 N (N+1)} S_{2,1}$$

$$- \frac{64}{3} S_{3,1} - \frac{64(10 N^2 + 10 N - 3)}{9 N (N+1)} S_{-2,1} + \frac{128}{3} S_{-3,1} + 64 S_{2,1,1} + \frac{256}{3} S_{-2,1,1}$$

$$+ \left(96 - 64 S_1 \right) \zeta_3 \Bigg] + \frac{64(112 N^3 + 112 N^2 - 39 N + 18)}{81 N^2 (N+1)} S_{-2,1}$$

$$+ \frac{P_{54}}{729 N^5 (N+1)^5} + \left(-\frac{16(N-1)(2 N^3 - N^2 - N - 2)}{9 N^2 (N+1)^2} S_2 + \frac{112}{9} S_2^2 \right.$$

$$- \frac{4 P_{52}}{729 N^4 (N+1)^4} + \frac{80(2 N + 1)^2}{9 N (N+1)} S_3 - \frac{208}{9} S_4 - \frac{8(9 N^2 + 9 N + 16)}{9 N (N+1)} S_{2,1}$$

$$+ \frac{64}{3} S_{3,1} + \frac{128(10 N^2 + 10 N - 3)}{27 N (N+1)} S_{-2,1} + \frac{128}{9} S_{-2,2} - \frac{512}{9} S_{-2,1,1} \right) S_1$$

$$+ \left(\frac{4 P_{36}}{9 N^3 (N+1)^3} + \frac{32}{9 N (N+1)} S_2 - \frac{80}{9} S_3 + \frac{128}{9} S_{2,1} + \frac{128}{9} S_{-2,1} \right) S_1^2$$

$$+ \left(\frac{4 P_{45}}{81 N^3 (N+1)^3} + \frac{496}{27} S_3 - \frac{64}{3} S_{2,1} - \frac{128}{3} S_{-2,1} \right) S_2 - \frac{64}{27} S_1^3 S_2$$

$$- \frac{4(15 N^2 + 15 N + 14)}{9 N (N+1)} S_2^2 - \frac{8 P_{37}}{81 N^2 (N+1)^2} S_3 + \frac{4(443 N^2 + 443 N + 78)}{27 N (N+1)} S_4$$

$$- \frac{224}{9} S_5 + \left(\frac{32 P_{14}}{81 N^3 (N+1)^3} - \frac{64 P_{13}}{81 N^2 (N+1)^2} S_1 + \frac{64}{9 N (N+1)} S_1^2 - \frac{128}{27} S_1^3 \right.$$

$$+ \frac{640}{27} S_2 - \frac{256}{27} S_3 + \frac{256}{9} S_{2,1} \right) S_{-2} + \left(-\frac{32(112 N^3 + 224 N^2 + 169 N + 39)}{81 N (N+1)^2} \right.$$

$$
\begin{aligned}
&+ \frac{64\left(10N^2 + 10N + 3\right)}{27N(N+1)} S_1 - \frac{64}{9} S_1^2 - \frac{64}{9} S_2 \Bigg) S_{-3} + \Bigg(\frac{64\left(10N^2 + 10N + 3\right)}{27N(N+1)} \\
&- \frac{128}{9} S_1 \Bigg) S_{-4} - \frac{128}{9} S_{-5} - \frac{8P_{20}}{9N^2(N+1)^2} S_{2,1} - \frac{8(13N+4)(13N+9)}{27N(N+1)} S_{3,1} \\
&+ \frac{256}{9} \left[S_{2,-3} + S_{4,1} - S_{-2,3} - S_{2,1,-2} - S_{3,1,1} - S_{-2,2,1} \right] - \frac{128}{3} S_{2,3} \\
&+ \frac{64}{3} S_{2,2,1} + \frac{64\left(10N^2 + 10N - 3\right)}{27N(N+1)} S_{-2,2} - \frac{256\left(10N^2 + 10N - 3\right)}{27N(N+1)} S_{-2,1,1} \\
&+ \frac{224}{9} S_{2,1,1,1} + \frac{1024}{9} S_{-2,1,1,1} - \frac{8\left(2N^3 + 2N^2 + 2N + 1\right)}{3N^3(N+1)^3} \zeta_2 \\
&+ \Bigg(\frac{P_{38}}{27N^2(N+1)^2} + \frac{4\left(593N^2 + 593N + 108\right)}{27N(N+1)} S_1 - 16S_1^2 + 16S_2 \Bigg) \zeta_3 \\
&+ \Bigg(\frac{4B_4}{3} - 4S_{2,1,1} - 12\zeta_4 \Bigg) \Delta\gamma_{qq}^{(0)} + (-1)^N \Bigg(L_M^2 \frac{32}{3(N+1)^3} + L_Q^2 \frac{32}{3(N+1)^3} \\
&+ L_M \left[\frac{128(4N+1)}{9(N+1)^4} - \frac{64}{3(N+1)^3} S_1 \right] - L_Q \frac{32P_{125}}{9(N-1)N^2(N+1)^4(N+2)^3} \\
&- \frac{8P_{28}}{81N^5(N+1)^5} + \frac{16P_{24}}{27N^4(N+1)^4} S_1 - \frac{32\left(2N^2 + 2N + 1\right)}{9N^3(N+1)^3} \left[S_1^2 + S_2 \right] \\
&- \frac{8\left(2N^3 + 2N^2 + 2N + 1\right)}{3N^3(N+1)^3} \zeta_2 \Bigg) \Bigg] + C_F T_F^2 \Bigg[-L_M^3 \frac{16}{27} \Delta\gamma_{qq}^{(0)} - L_Q^3 \frac{8}{27} \Delta\gamma_{qq}^{(0)} \\
&+ L_M^2 \left[-\frac{8P_{70}}{27N^2(N+1)^2} - \frac{320}{27} S_1 + \frac{64}{9} S_2 \right] + L_Q^2 \left[\frac{16\left(29N^2 + 29N - 6\right)}{27N(N+1)} S_1 \right. \\
&\left. - \frac{8P_{104}}{27N^2(N+1)^2} + \frac{32}{9} S_1^2 - \frac{32}{3} S_2 \right] - L_M \frac{248}{81} \Delta\gamma_{qq}^{(0)} + L_Q \left[\frac{8P_{120}}{81N^3(N+1)^3} \right. \\
&+ \left(-\frac{16P_{106}}{81N^2(N+1)^2} + \frac{64}{9} S_2 \right) S_1 - \frac{16\left(29N^2 + 29N - 6\right)}{27N(N+1)} S_1^2 - \frac{64}{27} S_1^3 \\
&\left. + \frac{16\left(35N^2 + 35N - 2\right)}{9N(N+1)} S_2 - \frac{896}{27} S_3 + \frac{128}{9} S_{2,1} \right] - \frac{2P_{50}}{729N^4(N+1)^4} + \frac{64}{81} S_2 \\
&+ \frac{12064}{729} S_1 + \frac{320}{81} S_3 - \frac{64}{27} S_4 - \frac{112}{27} \Delta\gamma_{qq}^{(0)} \zeta_3 \Bigg] + C_F N_F T_F^2 \Bigg[-L_M^3 \frac{8}{27} \Delta\gamma_{qq}^{(0)} \\
&- L_Q^3 \frac{16}{27} \Delta\gamma_{qq}^{(0)} + L_M \left[\frac{4P_{44}}{81N^3(N+1)^3} - \frac{2176}{81} S_1 - \frac{320}{27} S_2 + \frac{64}{9} S_3 \right] \\
&+ L_Q^2 \left[-\frac{16P_{104}}{27N^2(N+1)^2} + \frac{32\left(29N^2 + 29N - 6\right)}{27N(N+1)} S_1 + \frac{64}{9} S_1^2 - \frac{64}{3} S_2 \right] \\
&+ L_Q \left[\left(-\frac{32P_{106}}{81N^2(N+1)^2} + \frac{128}{9} S_2 \right) S_1 - \frac{32\left(29N^2 + 29N - 6\right)}{27N(N+1)} S_1^2 - \frac{128}{27} S_1^3 \right. \\
&\left. + \frac{16P_{120}}{81N^3(N+1)^3} + \frac{32\left(35N^2 + 35N - 2\right)}{9N(N+1)} S_2 - \frac{1792}{27} S_3 + \frac{256}{9} S_{2,1} \right] \\
&+ \frac{4P_{49}}{729N^4(N+1)^4} - \frac{24064}{729} S_1 + \frac{128}{81} S_2 + \frac{640}{81} S_3 - \frac{128}{27} S_4 + \frac{64}{27} \Delta\gamma_{qq}^{(0)} \zeta_3 \Bigg] \\
&+ \hat{c}_{q,g_1}^{\mathrm{NS},(3)}(N_F) \Bigg\} \Bigg\} ,
\end{aligned}
\tag{4.148}
$$

where the new polynomials P_i are

$$P_{103} = 33N^4 + 54N^3 + 9N^2 - 52N - 28 \tag{4.149}$$

$$P_{104} = 57N^4 + 96N^3 + 65N^2 - 10N - 24 \tag{4.150}$$

$$P_{105} = 141N^4 + 246N^3 + 241N^2 - 8N - 84 \tag{4.151}$$

$$P_{106} = 235N^4 + 524N^3 + 211N^2 + 30N + 72 \tag{4.152}$$

$$P_{107} = 359N^4 + 772N^3 + 335N^2 + 30N + 72 \tag{4.153}$$

$$P_{108} = 501N^4 + 894N^3 + 541N^2 - 116N - 204 \tag{4.154}$$

$$P_{109} = 1131N^4 + 2118N^3 + 1307N^2 + 32N - 276 \tag{4.155}$$

$$P_{110} = 1139N^4 + 2710N^3 + 635N^2 + 216N + 828 \tag{4.156}$$

$$P_{111} = 1220N^4 + 2359N^3 + 1934N^2 + 357N - 138 \tag{4.157}$$

$$P_{112} = 51N^5 + 102N^4 + 121N^3 + 118N^2 + 48N + 48 \tag{4.158}$$

$$P_{113} = 1407N^5 + 2418N^4 + 1793N^3 + 134N^2 - 384N + 144 \tag{4.159}$$

$$P_{114} = -11145N^6 - 32355N^5 - 37523N^4 - 14329N^3 + 2392N^2 + 120N - 1512 \tag{4.160}$$

$$P_{115} = 6N^6 + 18N^5 - N^4 - 20N^3 + 46N^2 + 29N - 6 \tag{4.161}$$

$$P_{116} = 15N^6 + 36N^5 + 30N^4 + 8N^3 + 3N^2 + 16N + 20 \tag{4.162}$$

$$P_{117} = 155N^6 + 465N^5 + 465N^4 + 371N^3 + 108N^2 + 108N + 54 \tag{4.163}$$

$$P_{118} = 216N^6 + 567N^5 + 687N^4 + 381N^3 + 37N^2 - 44N + 12 \tag{4.164}$$

$$P_{119} = 309N^6 + 807N^5 + 693N^4 - 271N^3 - 638N^2 + 68N + 216 \tag{4.165}$$

$$P_{120} = 609N^6 + 1485N^5 + 1393N^4 + 83N^3 - 422N^2 + 156N + 216 \tag{4.166}$$

$$P_{121} = 795N^6 + 2043N^5 + 2075N^4 + 517N^3 - 298N^2 + 156N + 216 \tag{4.167}$$

$$P_{122} = 1770N^6 + 4671N^5 + 4765N^4 + 1205N^3 - 227N^2 + 1044N + 756 \tag{4.168}$$

$$P_{123} = 7531N^6 + 23673N^5 + 23055N^4 + 7375N^3 + 1614N^2 + 936N - 324 \tag{4.169}$$

$$P_{124} = -4785N^7 - 14355N^6 - 4399N^5 + 10327N^4 + 3548N^3 + 3000N^2$$
$$+ 1080N - 1728 \tag{4.170}$$

$$P_{125} = 25N^7 + 138N^6 + 311N^5 + 464N^4 + 672N^3 + 670N^2 + 264N + 48 \tag{4.171}$$

$$P_{126} = -45N^8 - 162N^7 - 858N^6 - 1960N^5 - 1885N^4 - 1094N^3 - 804N^2$$
$$- 40N + 192 \tag{4.172}$$

$$P_{127} = 42591N^8 + 166764N^7 + 245088N^6 + 128254N^5 - 26735N^4 - 40762N^3$$
$$- 3928N^2 - 1272N - 2160 \tag{4.173}$$

$$P_{128} = -18351N^{10} - 89784N^9 - 208773N^8 - 267222N^7 - 192265N^6 - 46700N^5$$
$$+ 14565N^4 + 7730N^3 + 1240N^2 + 1464N + 144 \tag{4.174}$$

$$P_{129} = 828N^{11} + 7632N^{10} + 29217N^9 + 59592N^8 + 66844N^7 + 35738N^6 + 7405N^5$$
$$+ 16688N^4 + 27880N^3 + 11552N^2 - 3312N - 2304 \tag{4.175}$$

$$P_{130} = 8274N^{11} + 78519N^{10} + 313841N^9 + 686295N^8 + 881001N^7 + 638778N^6$$
$$+ 204948N^5 + 7992N^4 + 32296N^3 + 26544N^2 - 10656N - 8640. \tag{4.176}$$

The symbol $\hat{c}_{q,g_1}^{\text{NS},(3)}(N_F)$ refers to the 3-loop part of the massless non-singlet Wilson coefficient [153]. Contributions from lower order massless Wilson coefficients and the logarithmic terms of the 3-loop massless Wilson coefficient, proportional to powers of L_Q, are explicitly included in

the result above. The result is expressed in terms of harmonic sums up to weight $w = 5$. The corresponding expression in x space is obtained via an inverse Mellin transformation with the help of `HarmonicSums`. It is presented in Eq. (E.12), Appendix E, and is expressed in terms of HPLs which are reduced to an algebraically independent basis. Besides a regular part, the result features terms proportional to the distribution $\delta(1-x)$ and a part with plus distributions, cf. Eq. (3.44). At 3-loop order the plus distribution part contains terms proportional to $(1/(1-x)^2)_+$. They arise from the terms in the non-singlet OME which have coefficients with positive powers of N after partial fractioning, as discussed below Eq. (4.50). Our result agrees with the 2-loop result for $L_{q,g_1}^{\mathrm{NS},(2)}$ given in [191] if we accommodate for the differences between the inclusive case treated here and tagged flavour case; cf. also the discussion in Section 4.2.1. The massless Wilson coefficient C_{q,g_1}^{NS} can be compared to the 2-loop result published in [152]. We agree in all terms except the $\mathcal{O}(a_s^2 L_M C_F^2)$ and $\mathcal{O}(a_s^2 L_M C_A C_F)$ terms. Being of order a_s^2 and not proportional to N_F, these terms, however, do not enter the heavy flavour Wilson coefficient up to 3-loop order, cf. Eq. (4.145). All results are given in the on-shell scheme for the heavy quark mass. The transformations to the $\overline{\mathrm{MS}}$ scheme are identical to those in the unpolarised case, see Eq. (4.73) and Eq. (4.74).

4.3.2. Numerical results

Our results allow us to give numerical illustrations of the size of the non-singlet contribution to the structure function g_1. In what follows, we choose the renormalisation and factorisation scale $\mu^2 = Q^2$, unless stated otherwise.

In the small x region, the massive Wilson coefficient, stripped of the contribution from the massless Wilson coefficient $\hat{C}_{q,g_1}^{\mathrm{NS}}$, reads

$$L_{q,g_1}^{\mathrm{NS}}(N_F + 1) - \hat{C}_{q,g_1}^{\mathrm{NS}}(N_F) \underset{x \to 0}{\propto} a_s^2 \frac{2}{3} C_F T_F \ln^2(x) + a_s^3 \left[\frac{16}{27} C_A C_F T_F - \frac{5}{9} C_F^2 T_F \right] \ln^4(x). \quad (4.177)$$

The behaviour close to $x = 1$ is given by

$$
\begin{aligned}
L_{q,g_1}^{\mathrm{NS}}(N_F + 1) - \hat{C}_{q,g_1}^{\mathrm{NS}}(N_F) \underset{x \to 1}{\propto}{}& a_s^2 C_F T_F \left[\frac{8}{3} L_M^2 + \frac{80}{9} L_M + \frac{224}{27} \right] \left(\frac{1}{1-x} \right)_+ \\
&+ a_s^3 C_F^2 T_F \left[16 L_M^2 + \frac{160}{3} L_M + \frac{448}{9} \right] \left(\frac{\ln^2(1-x)}{1-x} \right)_+. \quad (4.178)
\end{aligned}
$$

For comparison, the contribution of the massless Wilson coefficient $\hat{C}_{q,g_1}^{\mathrm{NS}}$ to L_{q,g_1}^{NS} behaves in those limits like

$$\hat{C}_{q,g_1}^{\mathrm{NS}}(N_F) \underset{x \to 0}{\propto} a_s^2 \frac{10}{3} C_F T_F \ln^2(x) + a_s^3 \left[\frac{92}{27} C_A C_F T_F - \frac{31}{9} C_F^2 T_F \right] \ln^4(x) \quad (4.179)$$

and

$$\hat{C}_{q,g_1}^{\mathrm{NS}}(N_F) \underset{x \to 1}{\propto} a_s^2 \frac{8}{3} C_F T_F \left(\frac{\ln^2(1-x)}{1-x} \right)_+ + a_s^3 \frac{80}{9} C_F^2 T_F \left(\frac{\ln^4(1-x)}{1-x} \right)_+. \quad (4.180)$$

While the leading logarithms $\ln^k(x)$ in the $x \to 0$ limit receive contributions from both the massive OMEs and the massless Wilson coefficient, the massless soft singularities in the large x limit dominate over those of the massive OMEs, analogous to the situation in the unpolarised case discussed in Section 4.2. The small x behaviour can be compared to predictions for the non-singlet evolution kernels from a resummation of leading-order results [419, 420, 433, 434]. It
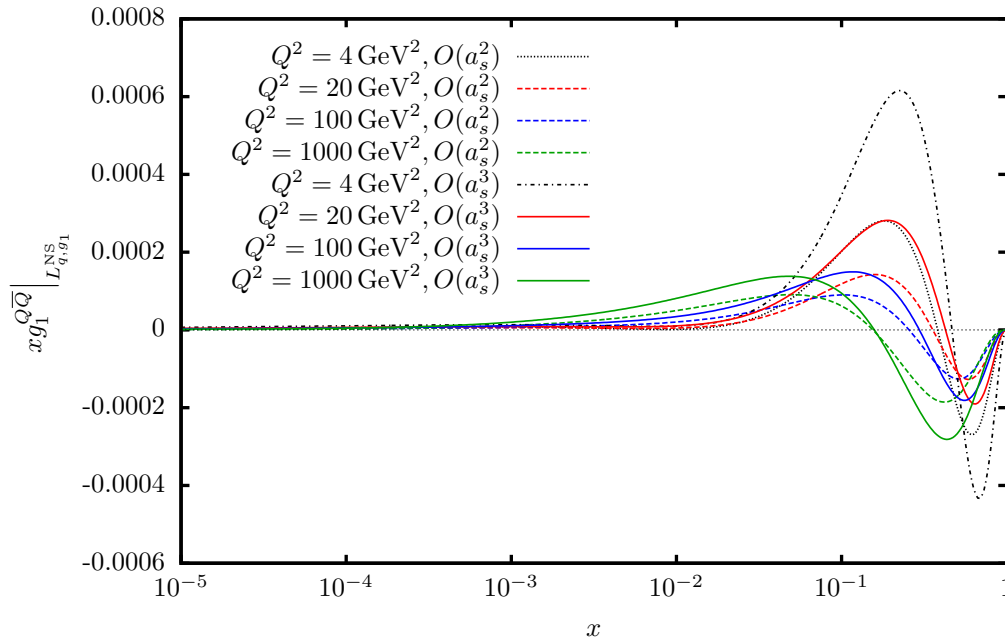
Figure 4.7.: The heavy flavour (charm) contribution from the asymptotic non-singlet Wilson coefficient L_{q,g_1}^{NS} to the structure function $xg_1(x,Q^2)$. Different values for the virtuality Q^2 are compared for the Wilson coefficient up to and including $\mathcal{O}(a_s^2)$ and $\mathcal{O}(a_s^3)$ corrections, respectively. We use $m_c = 1.59\,\mathrm{GeV}$ in the OMS scheme for the charm quark mass, $\alpha_s(M_Z^2) = 0.1132$ for the strong coupling constant and the NLO polarised PDFs from [435].

should be noted, however, that non-leading terms are partly numerically more relevant than the leading terms (in the physically relevant regions), cf. also [419, 420, 433].

Next, we present numerical illustrations for the contribution of L_{q,g_1}^{NS} to the structure function $g_1(x,Q^2)$. We assume three massless flavours ($N_F = 3$) and take the charm quark as the massive quark. The charm quark mass is treated in the OMS scheme and the pole mass $m_c = 1.59\,\mathrm{GeV}$ from [226] is used. For the PDFs we use the NLO polarised PDFs from [435]. A consistent treatment would require to use NNLO PDFs which are, however, not available for the polarised case so far. For the strong coupling constant we use $\alpha_s(M_Z^2) = 0.1132$ from the unpolarised NNLO analysis in [218]. To enable a comparison of the impact of the Wilson coefficients at different perturbative orders, we keep the settings for the strong coupling constant and the PDFs fixed, regardless of the order of a_s considered. For the 3-loop contribution from the massless Wilson coefficients, we use the approximate parametrisation given in [153]. The HPLs which appear in the result are evaluated numerically using the code presented in [423], extended to weight $w = 5$.

Figure 4.7 shows the contribution of the heavy quark non-singlet Wilson coefficient to $xg_1(x,Q^2)$ up to and including $\mathcal{O}(a_s^2)$ and $\mathcal{O}(a_s^3)$. The contribution is presented for different values of the virtuality Q^2 (4, 20, 100 and 1000 GeV^2). The plot also contains curves for $Q^2 = 4\,\mathrm{GeV}^2$ (dotted at $\mathcal{O}(a_s^2)$ and dash-dotted at $\mathcal{O}(a_s^3)$), which is clearly outside of the asymptotic region $Q^2 \gg m^2$. We include this formal extrapolation to the kinematic region where most experimental data for polarised DIS is available, noting that one cannot reasonably expect the power corrections to be negligible in this domain. For small values of x, the structure function $g_1(x,Q^2)$ grows as suggested also by the asymptotic limits discussed above. Plotting $xg_1(x,Q^2)$ allows to observe
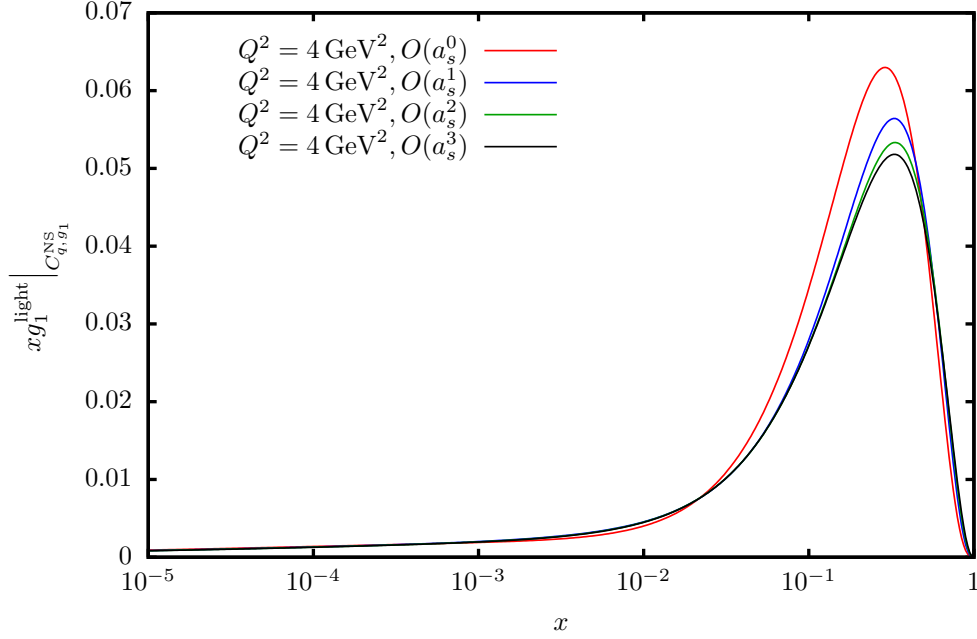
Figure 4.8.: The massless non-singlet part of the structure function $xg_1(x, Q^2)$ for $Q^2 = 4\,\mathrm{GeV}^2$, truncating the perturbative series at different orders of a_s. We use the same parameters and PDFs as in Fig. 4.7.
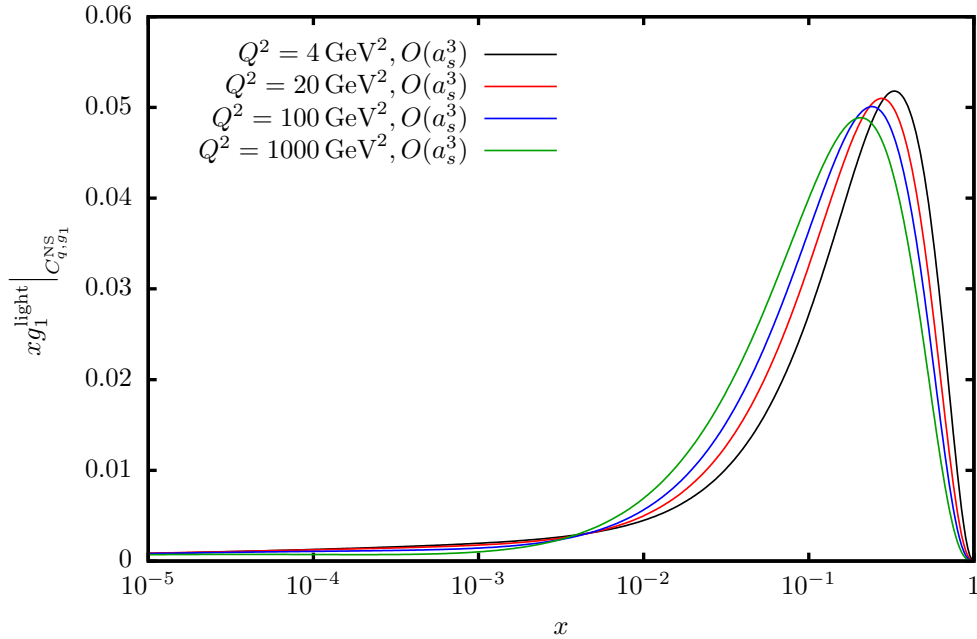

Figure 4.9.: The massless non-singlet part of the structure function $xg_1(x, Q^2)$ up to and including 3-loop contributions for different values of the virtuality Q^2. The parameters and PDFs are the same as in Fig. 4.7.
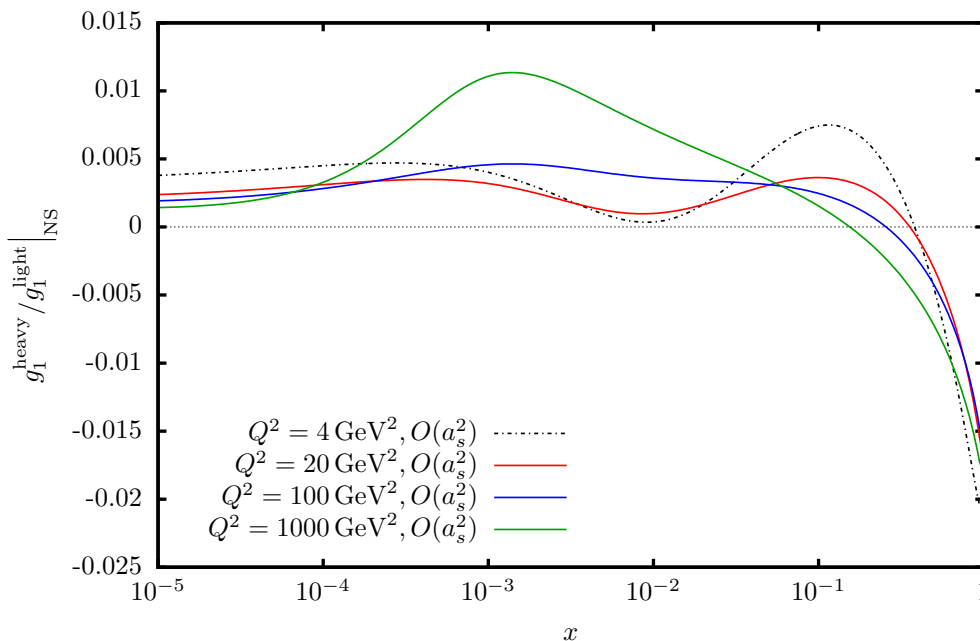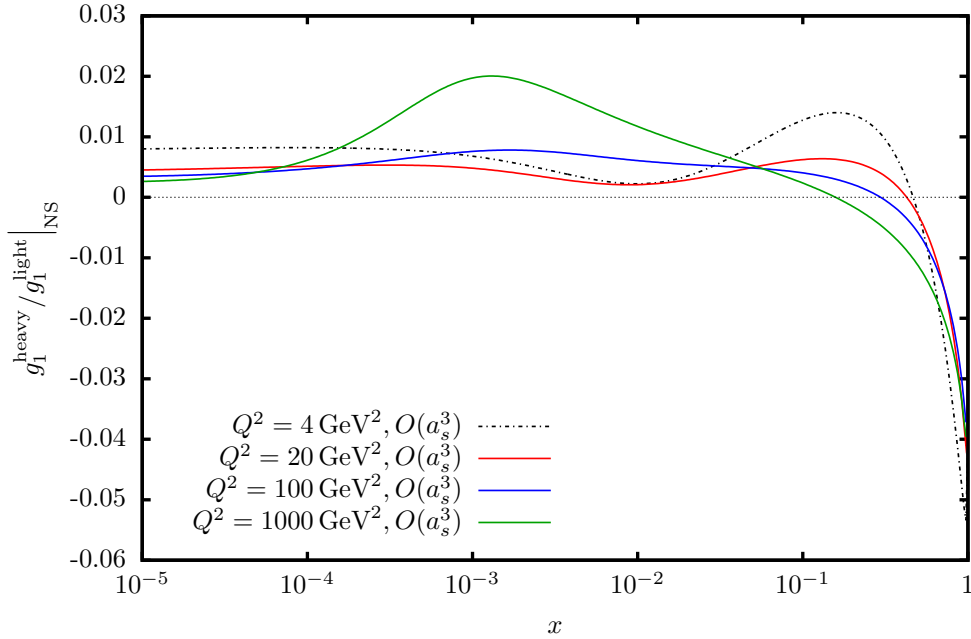
Figure 4.10.: The ratio of the heavy quark and massless non-singlet contributions to $g_1(x, Q^2)$ for different values of the virtuality Q^2, truncated at 2-loop order. The same parameters and PDFs as in Fig. 4.7 are used.

the features at large and medium x more clearly. There we note two extrema of the structure function. At $x = 1$ the contributions vanish and close to this value the heavy flavour corrections are negative. They cross zero between $x \approx 0.15$ and $x \approx 0.45$ depending on the value of Q^2. A maximum for $xg_1(x, Q^2)$ is attained around $x \approx 0.1$. At large x the value of $xg_1(x, Q^2)$ decreases for growing Q^2. From $Q^2 = 4\,\text{GeV}^2$, it goes through a minimum and increases again towards $Q^2 = 1000\,\text{GeV}^2$. Similarly, the absolute value of the minimum of $xg_1(x, Q^2)$ shows the same behaviour concerning the size, and the position of the minimum shifts towards smaller values of x. For medium values of x the structure function $xg_1(x, Q^2)$ diminishes for growing Q^2 as does the value of the maximum. The position of the maximum shifts towards smaller x. By including the 3-loop corrections, the value of the structure function is increased by a factor of approximately 0.5 to 1 compared to the 2-loop corrections.

In Fig. 4.8 we compare the contribution of the massless non-singlet Wilson coefficient C_{q,g_1}^{NS} to $xg_1(x, Q^2)$ at different orders in a_s for fixed $Q^2 = 4\,\text{GeV}^2$. Like the heavy flavour Wilson coefficient, the massless structure function $g_1(x, Q^2)$ grows towards small x and multiplying by x suppresses this growth in the plot. Around $x \approx 0.3$ there is a maximum in $xg_1(x, Q^2)$. By including higher orders in a_s, the maximum gets smaller and its position shifts to slightly larger values of x.

An illustration of the impact of varying the virtuality Q^2 can be found in Fig. 4.9, where we plot the same quantity as in the previous figure, but now for different Q^2 at 3-loop order. For larger Q^2 the value of the maximum in $xg_1(x, Q^2)$ decreases and its position is shifted towards smaller x.

For an easier comparison of heavy quark and massless contributions, Fig. 4.10 and Fig. 4.11 show the ratio of the heavy quark and massless non-singlet contributions $g_1^{\text{heavy}}(x, Q^2)/g_1^{\text{light}}(x, Q^2)$ for $\mathcal{O}(a_s^2)$ and $\mathcal{O}(a_s^3)$ respectively. The heavy flavour corrections at 2-loop order amount to $\mathcal{O}(0.5\%)$ effects for $Q^2 = 4$, 20 and $100\,\text{GeV}^2$ over most values of x, but larger effects occur for

Figure 4.11.: The ratio of the heavy quark and massless non-singlet contributions to $g_1(x, Q^2)$ for different values of the virtuality Q^2, truncated at 3-loop order. The same parameters and PDFs as in Fig. 4.7 are used.

$Q^2 = 1000 \, \text{GeV}^2$ around $x \approx 0.003$. The effects at 3-loop order are of similar shape, but roughly up to twice as large. Given the current experimental precision, the heavy flavour effects in the non-singlet part cannot be resolved experimentally. Nevertheless they may be relevant for future experiments like those planned at the EIC [424, 425].

To help assess the impact of varying the renormalisation and factorisation scale μ^2, Fig. 4.12 shows the scale variation of the sum of massless and massive non-singlet contributions to $xg_1(x, Q^2)$ for $Q^2 = 100 \, \text{GeV}^2$. The red curve represents the scale choice $\mu^2 = Q^2$, while the boundaries of the yellow band depict the values of $xg_1(x, Q^2)$ for $\mu^2 = Q^2/4$ and $\mu^2 = 4Q^2$. Similar results are obtained for $Q^2 = 20 \, \text{GeV}^2$. Moreover, the scale variation of the ratio $g_1^{\text{NS},(3)}/g_1^{\text{NS},(2)}$ can be found in Fig. 4.13. Here $g_1^{\text{NS},(k)}$ denotes the non-singlet part of the structure function g_1 up to and including $\mathcal{O}(a_s^k)$ corrections. The same conventions as in the previous figure apply also here. At small values of x up to $x \approx 0.3$, the ratio is slightly below 1 and grows towards $x = 1$ since the strength of the soft singularities increases with the loop order.

While interpreting the influence of varying the scale μ^2 one has to bear in mind several things: Ideally, the dependence of the structure functions on μ^2 would cancel exactly to the order of the perturbation series considered. In our case the remaining scale dependence would be an $\mathcal{O}(a_s^4)$ effect. This requires the evolution of the PDFs to be solved analytically in Mellin N space (cf. [436–438]). Such a procedure was carried out in the PDF analysis in [435] on which the illustrations are based. But since these are NLO PDFs and no NNLO polarised PDFs are available as of now, an exact cancellation at $\mathcal{O}(a_s^3)$ cannot be expected. Nevertheless, the effects of varying the scale μ^2 are below the current experimental accuracy.

The Wandzura-Wilczek relation, stated in Eq. (4.146), completely determines the twist-2 part of the structure function $g_2(x, Q^2)$ in terms of $g_1(x, Q^2)$. Therefore, we can also illustrate the behaviour of the non-singlet part of this structure function. Fig. 4.14 shows the heavy flavour contribution up to and including $\mathcal{O}(a_s^2)$ and $\mathcal{O}(a_s^3)$ effects. The overall behaviour is similar
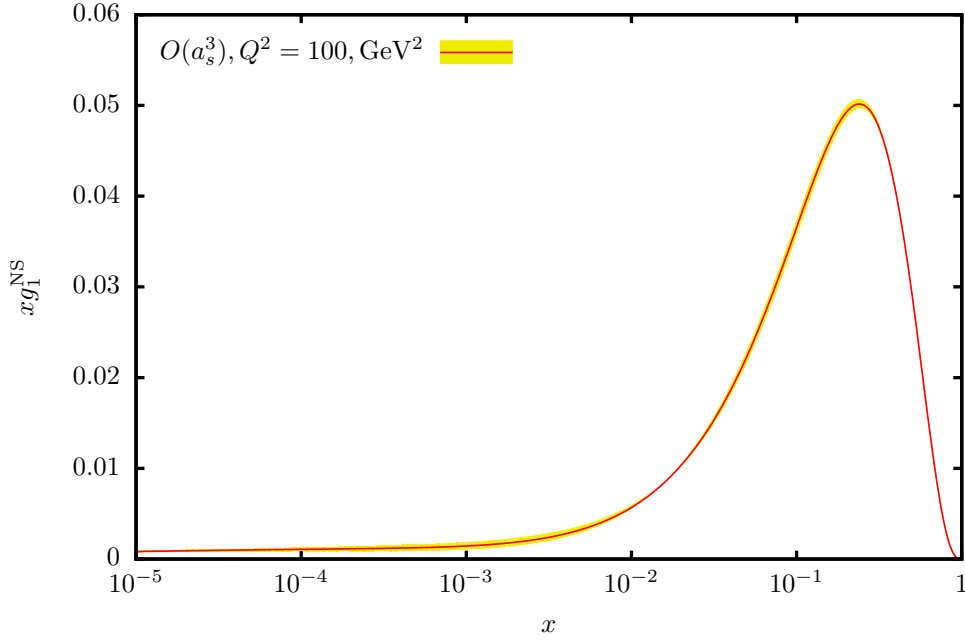
Figure 4.12.: Scale variation of the non-singlet contribution to $xg_1(x,Q^2)$. Massless and charm quark contributions up to and including $\mathcal{O}(a_s^3)$ are shown for $Q^2 = 100\,\mathrm{GeV}^2$. The red curve indicates the scale choice $\mu^2 = Q^2$ and the yellow band is delimited by the values of $xg_1(x,Q^2)$ for $\mu^2 = Q^2/4$ and $\mu^2 = 4Q^2$. The other parameters are identical to Fig. 4.7.
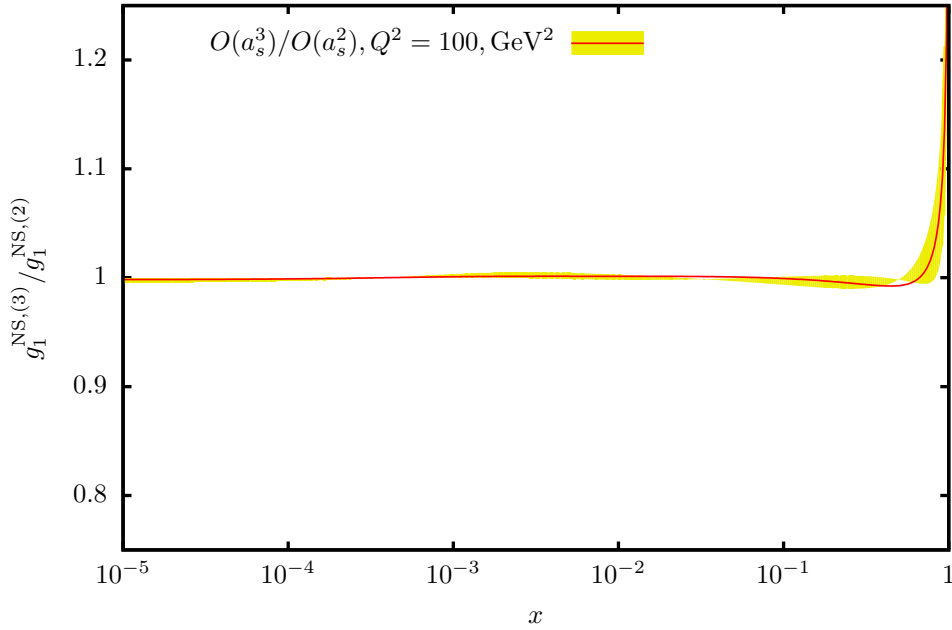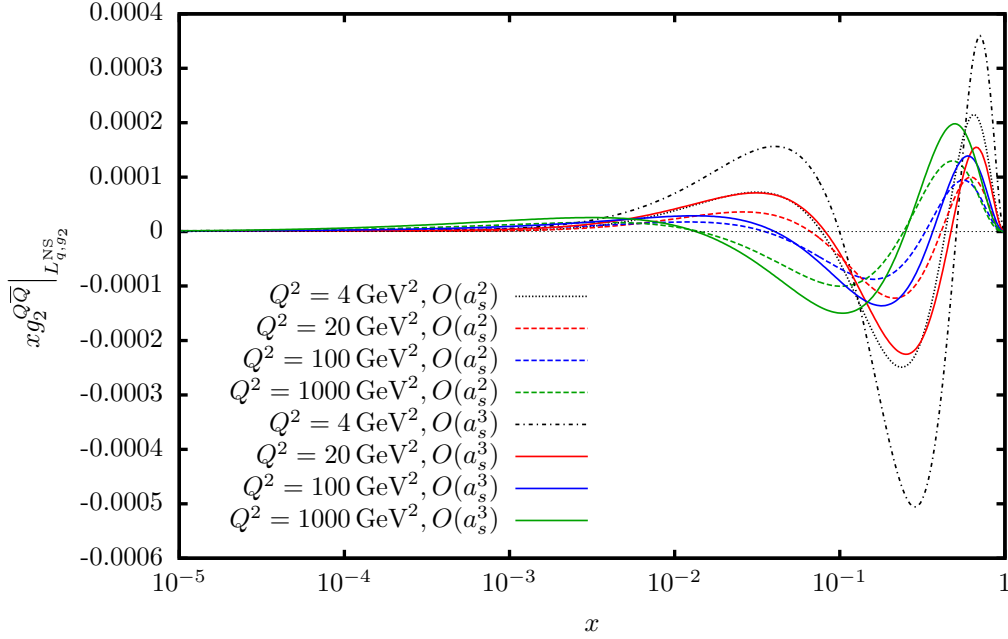

Figure 4.13.: Scale variation of the ratio of the non-singlet contributions to $g_1(x,Q^2)$ up to and including $\mathcal{O}(a_s^3)$ to those up to and including $\mathcal{O}(a_s^2)$ corrections. The red curve indicates the scale choice $\mu^2 = Q^2$ and the yellow band is delimited by the values of $xg_1(x,Q^2)$ for $\mu^2 = Q^2/4$ and $\mu^2 = 4Q^2$. The other parameters are identical to Fig. 4.7.

123

Figure 4.14.: The heavy flavour (charm) contributions of the asymptotic non-singlet Wilson coefficient L_{q,g_1}^{NS} to the structure function $xg_2(x, Q^2)$ as determined by the Wandzura-Wilczek relation, cf. Eq. (4.146). The 2- and 3-loop results are plotted for different values of Q^2. The parameters and PDFs are identical to those in Fig. 4.7.

to $xg_1(x, Q^2)$ up to a sign flip which is expected from the Wandzura-Wilczek relation. The oscillatory behaviour is more pronounced than it was for $xg_1(x, Q^2)$, producing one more crossing of zero.

For comparison, Figs. 4.15 and 4.16 show the contribution to $xg_2(x, Q^2)$ from the massless non-singlet Wilson coefficient. Contrary to $xg_1(x, Q^2)$ now $xg_2(x, Q^2)$ shows an oscillatory behaviour. The structure function $xg_2(x, Q^2)$ shrinks with increasing order in a_s at $Q^2 = 4\,\mathrm{GeV}^2$, and for growing Q^2 the shape of the structure function shifts towards larger x. The size of the heavy flavour corrections at 3-loop order is roughly 1% of the massless contribution.

4.3.3. Polarised Bjorken sum rule

The Bjorken sum rule for polarised structure functions [271] relates the difference of the structure functions $g_1(x, Q^2)$ for electron-proton and electron-neutron scattering to the ratio of the weak axial-vector and vector decay constants $g_A/g_V = -1.2767 \pm 0.0016$ [439]. It can be written as

$$\int_0^1 \mathrm{d}x \left[g_1^{ep}(x, Q^2) - g_1^{en}(x, Q^2) \right] = \frac{1}{6} \left| \frac{g_A}{g_V} \right| C_{\mathrm{pBj}}(\hat{a}_s), \qquad (4.181)$$

where $\hat{a}_s = \alpha_s/\pi$. The parton model predicts $C(\hat{a}_s) = 1$, but corrections to this sum rule can be calculated perturbatively in QCD. It has been calculated for massless quarks up to 4-loop order [129, 140, 440–442] and reads

$$C_{\mathrm{pBj}}(\hat{a}_s) = 1 - \hat{a}_s + \hat{a}_s^2(-4.58333 + 0.33333 N_F) + \hat{a}_s^3(-41.4399 + 7.60729 N_F - 0.17747 N_F^2)$$

$$+ \hat{a}_s^4(-479.448 + 123.391 N_F - 7.69747 N_F^2 + 0.10374 N_F^3)$$

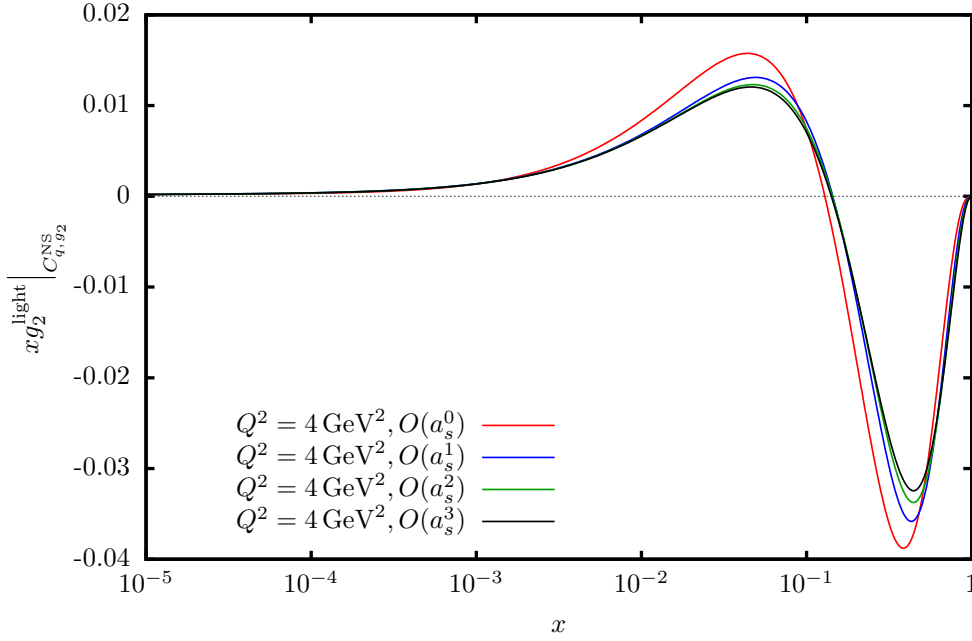$$+ \hat{a}_s^4(12.2222 - 0.740741 N_F) \sum_{k=1}^{N_F} e_k \qquad (4.182)$$

Figure 4.15.: Comparison of the different perturbative orders of the massless non-singlet part of $xg_2(x, Q^2)$ as given by the Wandzura-Wilczek relation. Parameters and PDFs used here are the same as in Fig. 4.7.
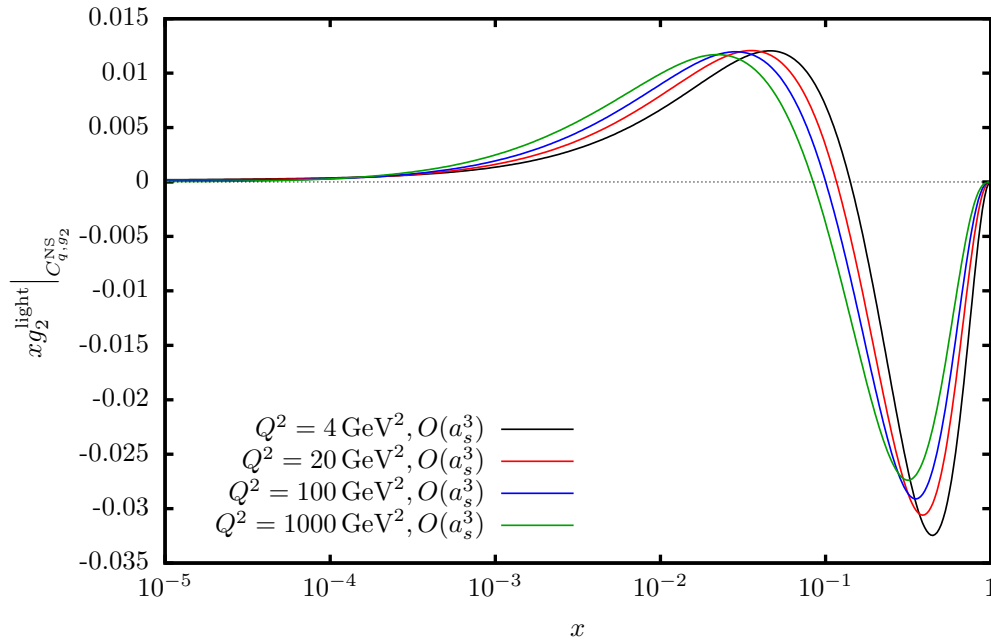

Figure 4.16.: Illustration of the effect of varying the virtuality Q^2 on the massless non-singlet part of $g_2(x, Q^2)$ according to the Wandzura-Wilczek relation. Parameters and PDFs used here are the same as in Fig. 4.7.

with the values of the colour factors of $SU(3)_c$ inserted. Again, the factorisation and renormalisation scales are set equal and chosen to be equal to the virtuality, $\mu^2 = Q^2$. The number of active light flavours is denoted by N_F. The last term in Eq. (4.182) is the singlet contribution to the sum rule, which starts at 4-loop order [140, 443]. It is proportional to the sum of charges e_k of the quarks and therefore vanishes for $N_F = 3$. For general N_F, however, it yields a finite contribution.

The heavy flavour corrections to the sum rule in the asymptotic limit $Q^2 \gg m^2$ can be obtained from the factorised heavy flavour Wilson coefficients. Since, however, the first moment of the non-singlet OME $A_{qq,Q}^{\mathrm{NS}}$ vanishes due to fermion number conservation, the only remaining contribution from Eq. (4.145) are the terms from $\hat{C}_{q,g_1}^{\mathrm{NS}}$. This amounts to adding one massless quark to the number of active flavours or equivalently to shifting N_F to $N_F + 1$ in Eq. (4.182). The above statements hold in the case of inclusive structure functions in the asymptotic limit $Q^2 \gg m^2$, which is considered here. For results in the tagged flavour case at $\mathcal{O}(a_s^2)$ see [191, 444] and for power corrections we refer to [306, 445] for the tagged case and to [421] for the inclusive case.

4.4. Unpolarised charged current DIS

Deep-inelastic scattering via charged currents occurs for example in neutrino-nucleon scattering, see Chapter 2. In addition to the structure functions that appear in unpolarised photon-mediated scattering, the parity violating couplings of the electro-weak W bosons allow for another independent structure function, $xF_3(x, Q^2)$, to contribute. Here we discuss the combination $xF_3^{W^+-W^-}(x, Q^2)$, which arises in the difference of the cross-sections for neutrino-nucleon and anti-neutrino-nucleon scattering, see Section 2.2. This structure function can be written in terms of CKM matrix elements V_{ij}, Wilson coefficients and PDFs as

$$
\begin{aligned}
F_3^{W^+-W^-}(x, Q^2) = {} & \\
2\Big\{ & \big[|V_{ud}|^2(d - \bar{d}) + |V_{us}|^2(s - \bar{s}) + V_u(u - \bar{u})\big] \otimes \Big[C_{q,3}^{\mathrm{NS},W^+-W^-} + L_{q,3}^{\mathrm{NS},W^+-W^-}\Big] \\
& + \big[|V_{cd}|^2(d - \bar{d}) + |V_{cs}|^2(s - \bar{s})\big] \otimes H_{q,3}^{\mathrm{NS},W^+-W^-} \Big\}.
\end{aligned}
$$
(4.183)

Here we use the shorthand $V_u = |V_{ud}|^2 + |V_{us}|^2$. The Mellin convolution, defined in Eq. (2.63), is denoted by the symbol $\otimes$ and $C_{q,3}^{\mathrm{NS},W^+-W^-}$ is the corresponding massless non-singlet Wilson coefficient. The heavy flavour Wilson coefficient $L_{q,3}^{\mathrm{NS},W^+-W^-}$ arises from diagrams in which heavy quark corrections are present but where the W boson couples only to light quarks. In contrast to the case of photon exchange, there are also non-singlet contributions from diagrams where the W boson couples to heavy quarks. They constitute the Wilson coefficient $H_{q,3}^{\mathrm{NS},W^+-W^-}$ and involve single flavour excitations of charm quarks like $s \to c$.

The PDF combinations appearing in the structure function above are valence distributions, frequently abbreviated by $q_v = q - \bar{q}$. Often, the sea quark valence distribution is assumed to vanish $s_v = 0$. Experiments probing targets with proton-neutron symmetry can be approximated by assuming an isoscalar target. For this, the PDFs have to be replaced in the following way

$$
u \to \tfrac{1}{2}(u + d), \qquad \bar{u} \to \tfrac{1}{2}(\bar{u} + \bar{d}), \qquad d \to \tfrac{1}{2}(u + d), \qquad \bar{d} \to \tfrac{1}{2}(\bar{u} + \bar{d}).
$$
(4.184)

Since we work with dimensional regularisation to regularise the Feynman integrals, the treatment of the Dirac matrix γ_5, which appears in the coupling of the W boson to fermions, requires care. In $L_{q,3}^{\mathrm{NS}}$ the γ_5 always appears in a chain of Dirac matrices belonging to a massless line. As discussed in Section 4.1, a Ward-Takahashi identity allows to work with an anti-commuting

definition of γ_5 in this case. In $H_{q,3}^{\mathrm{NS}}$, however, the vertex containing γ_5 can be attached to a massive line, when a flavour excitation like $s \to c$ happens. Nevertheless, the corresponding line has to be treated as massless since we disregard power corrections in the quark mass. Thus, the argument for anti-commuting γ_5 goes through as for the other non-singlet quantities. Therefore, we can use the odd moments of the non-singlet OME $A_{qq,Q}^{\mathrm{NS}}$ in both cases.

The charged current heavy flavour Wilson coefficients factorise in the limit $Q^2 \gg m^2$ into massless Wilson coefficients and massive OMEs [197–199]. In Mellin N space this can be written as

$$L_{q,3}^{\mathrm{NS},W^+-W^-}(N_F+1) = A_{qq,Q}^{\mathrm{NS}} C_{q,3}^{\mathrm{NS},W^+-W^-}(N_F+1) - C_{q,3}^{\mathrm{NS},W^+-W^-}(N_F) \qquad (4.185)$$

$$H_{q,3}^{\mathrm{NS},W^+-W^-}(N_F+1) = A_{qq,Q}^{\mathrm{NS}} C_{q,3}^{\mathrm{NS},W^+-W^-}(N_F+1), \qquad (4.186)$$

where we suppress the dependence on N and the scales for better readability. Expanding the factorised expressions in the strong coupling constant a_s up to third order yields

$$
\begin{aligned}
L_{q,3}^{\mathrm{NS},W^+-W^-}&(N_F+1) = \\
&a_s^2 \left[A_{qq,Q}^{\mathrm{NS},(2)} + \hat{C}_{q,3}^{\mathrm{NS},W^+-W^-,(2)}(N_F) \right] \\
&+ a_s^3 \left[A_{qq,Q}^{\mathrm{NS},(3)} + A_{qq,Q}^{\mathrm{NS},(2)} C_{q,3}^{\mathrm{NS},W^+-W^-,(1)}(N_F+1) + \hat{C}_{q,3}^{\mathrm{NS},W^+-W^-,(3)}(N_F) \right]
\end{aligned} \qquad (4.187)
$$

$$
\begin{aligned}
H_{q,3}^{\mathrm{NS},W^+-W^-}&(N_F+1) = \\
&1 + a_s C_{q,3}^{\mathrm{NS},W^+-W^-,(2)}(N_F+1) + a_s^2 \left[A_{qq,Q}^{\mathrm{NS},(2)} + C_{q,3}^{\mathrm{NS},W^+-W^-,(2)}(N_F+1) \right] \\
&+ a_s^3 \left[A_{qq,Q}^{\mathrm{NS},(3)} + A_{qq,Q}^{\mathrm{NS},(2)} C_{q,3}^{\mathrm{NS},W^+-W^-,(1)}(N_F+1) + C_{q,3}^{\mathrm{NS},W^+-W^-,(3)}(N_F+1) \right]
\end{aligned} \qquad (4.188)
$$

$$= L_{q,3}^{\mathrm{NS},W^+-W^-}(N_F+1) + C_{q,3}^{\mathrm{NS},W^+-W^-}(N_F). \qquad (4.189)$$

The result up to 3-loop order for the non-singlet OME $A_{qq,Q}^{\mathrm{NS}}$ is presented in Section 4.1 and the massless Wilson coefficient $C_{q,3}^{\mathrm{NS},W^+-W^-}$ is known up to 3-loop order as well [153]. We use a hat over the massless Wilson coefficient to denote its difference for N_F+1 and N_F flavours, see Eq. (2.97). In what follows, we will suppress the superscript W^+-W^- of the Wilson coefficients since we will only refer to this combination of structure functions.

Like for the Wilson coefficients in the preceding sections, the factorisation in Eqs. (4.187) and (4.188) is presented for renormalised OMEs and massless Wilson coefficients. We use a common scale μ^2 for the factorisation and renormalisation scales, $\mu^2 = \mu_R^2 = \mu_F^2$. The renormalised massless Wilson coefficients contain terms proportional to powers of $\ln(Q^2/\mu^2)$ which vanish for $\mu^2 = Q^2$. Results are usually published for this scale choice, since the logarithmic terms can be reconstructed using the renormalisation group, cf. [293]. We reconstruct the coefficients of the logarithms in terms of the coefficients of the β-function, lower order Wilson coefficients and the anomalous dimensions of the local operators, given in [135]. Here the valence anomalous dimensions $\gamma_{val}^{\mathrm{NS}} = \gamma_-^{\mathrm{NS}} + \gamma_s^{\mathrm{NS}}$ enter. The non-singlet sea anomalous dimensions γ_s^{NS} start at 3-loop order and are proportional to the colour factor $d^{abc}d^{abc}$, see [135].

4.4.1. Analytic results

Inserting the N space result for $A_{qq,Q}^{\mathrm{NS}}$ for odd values of N, given in Eq. (4.52), and the massless Wilson coefficient, given in [153], into Eq. (4.187) yields the N space expression for the heavy

4. Non-singlet contributions to DIS

flavour Wilson coefficient $L_{q,3}^{\text{NS}}$ in the asymptotic limit.

$$L_{q,3}^{\text{NS},W^+-W^-}(N) =$$

$$a_s^2 C_F T_F \Bigg\{ L_Q \left[-\frac{2P_{104}}{9N^2(N+1)^2} + \frac{4(29N^2+29N-6)}{9N(N+1)} S_1 + \frac{8}{3} S_1^2 - 8S_2 \right]$$

$$+ L_M \left[\frac{2P_{10}}{9N^2(N+1)^2} - \frac{80}{9} S_1 + \frac{16}{3} S_2 \right] - \frac{\gamma_{qq}^{(0)} L_M^2}{3} - \frac{\gamma_{qq}^{(0)} L_Q^2}{3} + \frac{P_{121}}{27N^3(N+1)^3}$$

$$+ \left(-\frac{2P_{107}}{27N^2(N+1)^2} + \frac{8}{3} S_2 \right) S_1 - \frac{2(29N^2+29N-6)}{9N(N+1)} S_1^2 - \frac{8}{9} S_1^3$$

$$+ \frac{2(35N^2+35N-2)}{3N(N+1)} S_2 - \frac{112}{9} S_3 + \frac{16}{3} S_{2,1} \Bigg\} + a_s^3 \Bigg\{ C_F^2 T_F \Bigg[\frac{1}{6} \gamma_{qq}^{(0)\,2} L_Q \big(L_Q^2$$

$$+ L_M^2 \big) + L_M^2 \Bigg[-\frac{2P_{137}}{3N^3(N+1)^3} + \frac{2P_{103}}{3N^2(N+1)^2} S_1 - \frac{4(N-1)(N+2)}{N(N+1)} S_1^2$$

$$- \frac{16}{3} S_1^3 + \frac{10}{3} \gamma_{qq}^{(0)} S_2 + \frac{64}{3} S_3 + \left(-\frac{64}{3N(N+1)} + \frac{128}{3} S_1 \right) S_{-2} + \frac{64}{3} S_{-3}$$

$$- \frac{128}{3} S_{-2,1} \Bigg] + L_Q^2 \Bigg[-\frac{2P_{139}}{9N^3(N+1)^3} + \frac{2P_{108}}{9N^2(N+1)^2} S_1 - \frac{4(107N^2+107N-54)}{9N(N+1)} S_1^2$$

$$- 16 S_1^3 + \frac{22}{3} \gamma_{qq}^{(0)} S_2 + \frac{64}{3} S_3 + \left(-\frac{64}{3N(N+1)} + \frac{128}{3} S_1 \right) S_{-2} + \frac{64}{3} S_{-3}$$

$$- \frac{128}{3} S_{-2,1} \Bigg] + \gamma_{qq}^{(0)} L_M L_Q \left[\frac{P_{70}}{9N^2(N+1)^2} + \frac{40}{9} S_1 - \frac{8}{3} S_2 \right] + L_Q \Bigg[\frac{80}{9} S_1^4 + \frac{448}{3} S_{-4}$$

$$+ \frac{4P_{151}}{27(N-1)N^4(N+1)^4(N+2)} + \left(-\frac{16(9N^2+9N-2)}{N(N+1)} + 64 S_1 \right) \zeta_3$$

$$+ \left(-\frac{4P_{122}}{27N^3(N+1)^3} - \frac{32(67N^2+67N-21)}{9N(N+1)} S_2 + \frac{640}{9} S_3 + \frac{64}{3} S_{2,1} + \frac{512}{3} S_{-2,1} \right) S_1$$

$$+ \left(\frac{2P_{110}}{27N^2(N+1)^2} - \frac{224}{3} S_2 \right) S_1^2 + \frac{32(4N-1)(4N+5)}{9N(N+1)} S_1^3 + \frac{2P_{109}}{9N^2(N+1)^2} S_2$$

$$+ 48 S_2^2 - \frac{32(53N^2+53N+16)}{9N(N+1)} S_3 + \frac{352}{3} S_4 + \left(-\frac{64P_{115}}{9(N-1)N^2(N+1)^2(N+2)} \right.$$

$$- \frac{128(10N^2+10N-3)}{9N(N+1)} S_1 - \frac{256}{3} S_1^2 + \frac{256}{3} S_2 \Bigg) S_{-2} + 64 S_{-2}^2 + 64 S_{3,1}$$

$$+ \left(-\frac{64(10N^2+10N+9)}{9N(N+1)} + \frac{256}{3} S_1 \right) S_{-3} + \frac{16(9N^2+9N-2)}{3N(N+1)} S_{2,1}$$

$$+ \frac{128(10N^2+10N-3)S_{-2,1}}{9N(N+1)} - \frac{256}{3} S_{-3,1} - 64 S_{2,1,1} - \frac{512}{3} S_{-2,1,1} \Bigg]$$

$$+ L_M \Bigg[\frac{P_{144}}{9N^4(N+1)^4} - 32 S_2^2 + \left(\frac{2P_{140}}{9N^3(N+1)^3} + \frac{16(59N^2+59N-6)}{9N(N+1)} S_2 - \frac{256}{3} S_3 \right.$$

$$- \frac{256}{3} S_{-2,1} \Bigg) S_1 + \left(-\frac{4P_{71}}{3N^2(N+1)^2} + \frac{32}{3} S_2 \right) S_1^2 - \frac{160}{9} S_1^3 - \frac{4P_{105}}{9N^2(N+1)^2} S_2$$

$$+ \frac{32(29N^2+29N+12)}{9N(N+1)} S_3 - \frac{256}{3} S_4 + \left(-\frac{64(16N^2+10N-3)}{9N^2(N+1)^2} + \frac{1280}{9} S_1 \right.$$

$$- \frac{128}{3} S_2 \Bigg) S_{-2} + \left(\frac{64(10N^2+10N+3)}{9N(N+1)} - \frac{128}{3} S_1 \right) S_{-3} - \frac{128}{3} S_{-4} + \frac{128}{3} S_{3,1}$$

128

$$
- \frac{128\left(10N^2 + 10N - 3\right)}{9N(N+1)} S_{-2,1} - \frac{128}{3} S_{-2,2} + \frac{512}{3} S_{-2,1,1} + 8\gamma_{qq}^{(0)} \zeta_3 \Bigg]
$$

$$
+ \frac{P_{149}}{162N^5(N+1)^5} - \frac{128\left(112N^3 + 112N^2 - 39N + 18\right)}{81N^2(N+1)} S_{-2,1}
$$

$$
+ \left(\frac{2P_{16}}{9N^2(N+1)^2} - \frac{1208}{9} S_1 - \frac{64}{3} S_2 \right) \zeta_3 + \gamma_{qq}^{(0)} \left(-\frac{8B_4}{3} + 12\zeta_4 + \frac{8}{3} S_{2,1,1} \right)
$$

$$
+ \left(\frac{P_{148}}{162N^4(N+1)^4} + \frac{8P_{82}}{81N^2(N+1)^2} S_2 - \frac{64}{9} S_2^2 - \frac{8\left(347N^2 + 347N + 54\right)S_3}{27N(N+1)} \right.
$$

$$
+ \frac{704}{9} S_4 + \frac{128}{9N(N+1)} S_{2,1} - \frac{320}{9} S_{3,1} - \frac{256\left(10N^2 + 10N - 3\right)}{27N(N+1)} S_{-2,1} - \frac{256}{9} S_{-2,2}
$$

$$
\left. + \frac{1024}{9} S_{-2,1,1} \right) S_1 + \left(\frac{P_{135}}{9N^3(N+1)^3} + \frac{16\left(5N^2 + 5N - 4\right)}{9N(N+1)} S_2 + 16S_3 - \frac{128}{9} S_{2,1} \right.
$$

$$
\left. - \frac{256}{9} S_{-2,1} \right) S_1^2 + \left(-\frac{16P_{72}}{27N^2(N+1)^2} + \frac{128}{27} S_2 \right) S_1^3 + \left(\frac{P_{134}}{81N^3(N+1)^3} + \frac{400}{27} S_3 \right.
$$

$$
\left. + \frac{256}{3} S_{-2,1} \right) S_2 - \frac{32\left(23N^2 + 23N - 3\right)}{27N(N+1)} S_2^2 + \frac{8P_{111}}{81N^2(N+1)^2} S_3 + \frac{512}{9} S_5
$$

$$
- \frac{176\left(17N^2 + 17N + 6\right)}{27N(N+1)} S_4 + \left(-\frac{64P_{14}}{81N^3(N+1)^3} + \frac{128P_{13}}{81N^2(N+1)^2} S_1 - \frac{1280}{27} S_2 \right.
$$

$$
\left. - \frac{128}{9N(N+1)} S_1^2 + \frac{256}{27} S_1^3 + \frac{512}{27} S_3 - \frac{512}{9} S_{2,1} \right) S_{-2} + \left(-\frac{128\left(10N^2 + 10N + 3\right)}{27N(N+1)} S_1 \right.
$$

$$
\left. + \frac{64\left(112N^3 + 224N^2 + 169N + 39\right)}{81N(N+1)^2} + \frac{128}{9} S_1^2 + \frac{128}{9} S_2 \right) S_{-3} + \left(\frac{256}{9} S_1 \right.
$$

$$
\left. - \frac{128\left(10N^2 + 10N + 3\right)}{27N(N+1)} \right) S_{-4} + \frac{256}{9} S_{-5} + \frac{16P_{11}S_{2,1}}{9N^2(N+1)^2} + \frac{256}{9} S_{2,3} - \frac{512}{9} S_{2,-3}
$$

$$
+ \frac{16\left(89N^2 + 89N + 30\right)}{27N(N+1)} S_{3,1} - \frac{512}{9} S_{4,1} - \frac{128\left(10N^2 + 10N - 3\right)}{27N(N+1)} S_{-2,2}
$$

$$
+ \frac{256}{9} \left(2S_{-2,3} + 2S_{2,1,-2} + S_{3,1,1} + 2S_{-2,2,1} \right) + \frac{512\left(10N^2 + 10N - 3\right)}{27N(N+1)} S_{-2,1,1}
$$

$$
- \frac{2048}{9} S_{-2,1,1,1} \Bigg]
$$

$$
+ C_A C_F T_F \Bigg[\frac{22\gamma_{qq}^{(0)}}{27} \left(L_M^3 + 2L_Q^3 \right) + L_M^2 \left[\frac{\gamma_{qq}^{(0)} P_{131}}{9N^2(N+1)^2} - \frac{16P_{132}}{3N^2(N+1)^2} S_1 - \frac{32}{3} S_3 \right.
$$

$$
\left. + \left(\frac{32}{3N(N+1)} - \frac{64}{3} S_1 \right) S_{-2} - \frac{32}{3} S_{-3} + \frac{64}{3} S_{-2,1} \right] + L_Q^2 \left[\frac{2P_{142}}{27N^3(N+1)^3} \right.
$$

$$
- \frac{16\left(194N^2 + 194N - 33\right)}{27N(N+1)} S_1 - \frac{176}{9} S_1^2 + \frac{176}{3} S_2 - \frac{32}{3} S_3 + \left(\frac{32}{3N(N+1)} \right.
$$

$$
\left. - \frac{64}{3} S_1 \right) S_{-2} - \frac{32}{3} S_{-3} + \frac{64}{3} S_{-2,1} \Bigg] + L_M \Bigg[\frac{P_{143}}{81N^4(N+1)^4} + \left(-\frac{8P_{138}}{81N^3(N+1)^3} \right.
$$

$$
\left. + 32S_3 + \frac{128}{3} S_{-2,1} \right) S_1 + \frac{1792}{27} S_2 - \frac{16\left(31N^2 + 31N + 9\right)}{9N(N+1)} S_3 + \frac{160}{3} S_4
$$

$$
+ \left(\frac{32\left(16N^2 + 10N - 3\right)}{9N^2(N+1)^2} - \frac{640}{9} S_1 + \frac{64}{3} S_2 \right) S_{-2} + \left(-\frac{32\left(10N^2 + 10N + 3\right)}{9N(N+1)} \right.
$$

$$+ \frac{64}{3}S_1 \Bigg) S_{-3} + \frac{64}{3}S_{-4} - \frac{128}{3}S_{3,1} + \frac{64\left(10N^2 + 10N - 3\right)}{9N(N+1)}S_{-2,1} + \frac{64}{3}S_{-2,2}$$

$$- \frac{256}{3}S_{-2,1,1} - 8\gamma_{qq}^{(0)}\zeta_3 \Bigg] + L_Q \Bigg[-\frac{16\left(230N^3 + 460N^2 + 213N - 11\right)}{9N(N+1)^2}S_2$$

$$- \frac{4P_{152}}{81(N-1)N^4(N+1)^4(N+2)} + \Bigg(\frac{4P_{123}}{81N^3(N+1)^3} - \frac{32\left(11N^2 + 11N + 3\right)}{9N(N+1)}S_2$$

$$+ 32S_3 - \frac{128}{3}S_{2,1} - \frac{256}{3}S_{-2,1} \Bigg) S_1 + \Bigg(\frac{16\left(194N^2 + 194N - 33\right)}{27N(N+1)} + \frac{32}{3}S_2 \Bigg) S_1^2$$

$$+ \frac{352}{27}S_1^3 - \frac{32}{3}S_2^2 + \frac{16\left(368N^2 + 368N - 9\right)}{27N(N+1)}S_3 + \Bigg(\frac{32P_{115}}{9(N-1)N^2(N+1)^2(N+2)}$$

$$+ \frac{64\left(10N^2 + 10N - 3\right)}{9N(N+1)}S_1 + \frac{128}{3}S_1^2 - \frac{128}{3}S_2 \Bigg) S_{-2} - \frac{224}{3}S_4 - 32S_{-2}^2$$

$$+ \Bigg(\frac{32\left(10N^2 + 10N + 9\right)}{9N(N+1)} - \frac{128}{3}S_1 \Bigg) S_{-3} - \frac{224}{3}S_{-4} - \frac{64\left(11N^2 + 11N - 3\right)}{9N(N+1)}S_{2,1}$$

$$- \frac{64}{3}S_{3,1} - \frac{64\left(10N^2 + 10N - 3\right)}{9N(N+1)}S_{-2,1} + \frac{128}{3}S_{-3,1} + 64S_{2,1,1} + \frac{256}{3}S_{-2,1,1}$$

$$+ \Bigg(96 - 64S_1 \Bigg)\zeta_3 \Bigg] + \frac{P_{150}}{729N^5(N+1)^5} + \frac{S_{-2,1}}{N^2(N+1)}\frac{64}{81}\left(112N^3 + 112N^2 - 39N\right.$$

$$+ 18) + \Bigg(\frac{P_{38}}{27N^2(N+1)^2} + \frac{4\left(593N^2 + 593N + 108\right)}{27N(N+1)}S_1 - 16S_1^2 + 16S_2 \Bigg)\zeta_3$$

$$+ \gamma_{qq}^{(0)}\Bigg(\frac{4B_4}{3} - 12\zeta_4 - 4S_{2,1,1} \Bigg) + \Bigg(-\frac{4P_{147}}{729N^4(N+1)^4} - \frac{16(N-1)}{9N^2(N+1)^2}S_2$$

$$\times \left(2N^3 - N^2 - N - 2\right) + \frac{112}{9}S_2^2 + \frac{80(2N+1)^2 S_3}{9N(N+1)} - \frac{208}{9}S_4 + \frac{64}{3}S_{3,1} + \frac{128}{9}S_{-2,2}$$

$$- \frac{8\left(9N^2 + 9N + 16\right)}{9N(N+1)}S_{2,1} + \frac{128\left(10N^2 + 10N - 3\right)}{27N(N+1)}S_{-2,1} - \frac{512}{9}S_{-2,1,1} \Bigg) S_1$$

$$+ \Bigg(\frac{4P_{133}}{9N^3(N+1)^3} + \frac{32}{9N(N+1)}S_2 - \frac{80}{9}S_3 + \frac{128}{9}S_{2,1} + \frac{128}{9}S_{-2,1} \Bigg) S_1^2 + \Bigg(\frac{496}{27}S_3$$

$$+ \frac{4P_{141}}{81N^3(N+1)^3} - \frac{64}{3}S_{2,1} - \frac{128}{3}S_{-2,1} \Bigg) S_2 - \frac{64}{27}S_1^3 S_2 - \frac{4\left(15N^2 + 15N + 14\right)}{9N(N+1)}S_2^2$$

$$- \frac{8P_{37}}{81N^2(N+1)^2}S_3 + \frac{4\left(443N^2 + 443N + 78\right)}{27N(N+1)}S_4 - \frac{224}{9}S_5 + \Bigg(\frac{32P_{14}}{81N^3(N+1)^3}$$

$$- \frac{64P_{13}}{81N^2(N+1)^2}S_1 + \frac{64}{9N(N+1)}S_1^2 - \frac{128}{27}S_1^3 + \frac{640}{27}S_2 - \frac{256}{27}S_3 + \frac{256}{9}S_{2,1} \Bigg) S_{-2}$$

$$+ \Bigg(-\frac{32\left(112N^3 + 224N^2 + 169N + 39\right)}{81N(N+1)^2} + \frac{64\left(10N^2 + 10N + 3\right)}{27N(N+1)}S_1$$

$$- \frac{64}{9}S_1^2 - \frac{64}{9}S_2 \Bigg) S_{-3} + \Bigg(\frac{64\left(10N^2 + 10N + 3\right)}{27N(N+1)} - \frac{128}{9}S_1 \Bigg) S_{-4} - \frac{128}{9}S_{-5}$$

$$- \frac{8P_{20}}{9N^2(N+1)^2}S_{2,1} - \frac{128}{3}S_{2,3} + \frac{256}{9}S_{2,-3} - \frac{8(13N+4)(13N+9)}{27N(N+1)}S_{3,1} + \frac{256}{9}S_{4,1}$$

$$+ \frac{64\left(10N^2 + 10N - 3\right)}{27N(N+1)}S_{-2,2} - \frac{256}{9}S_{-2,3} - \frac{256}{9}S_{2,1,-2} + \frac{64}{3}S_{2,2,1} - \frac{256}{9}S_{3,1,1}$$

$$-\frac{256\left(10N^2+10N-3\right)}{27N(N+1)}S_{-2,1,1}-\frac{256}{9}S_{-2,2,1}+\frac{224}{9}S_{2,1,1,1}+\frac{1024}{9}S_{-2,1,1,1}\Bigg]$$

$$+C_F T_F^2\Bigg[-\frac{8\gamma_{qq}^{(0)}}{27}\left(2L_M^3+L_Q^3\right)+L_Q^2\Bigg[-\frac{8P_{104}}{27N^2(N+1)^2}+\frac{32}{9}S_1^2-\frac{32}{3}S_2$$

$$+\frac{16\left(29N^2+29N-6\right)}{27N(N+1)}S_1\Bigg]+L_M^2\Bigg[\frac{8P_{10}}{27N^2(N+1)^2}-\frac{320}{27}S_1+\frac{64}{9}S_2\Bigg]-L_M\frac{248\gamma_{qq}^{(0)}}{81}$$

$$+L_Q\Bigg[\frac{8P_{120}}{81N^3(N+1)^3}+\left(-\frac{16P_{106}}{81N^2(N+1)^2}+\frac{64}{9}S_2\right)S_1-\frac{16\left(29N^2+29N-6\right)}{27N(N+1)}S_1^2$$

$$-\frac{64}{27}S_1^3+\frac{16\left(35N^2+35N-2\right)}{9N(N+1)}S_2-\frac{896}{27}S_3+\frac{128}{9}S_{2,1}\Bigg]-\frac{2P_{50}}{729N^4(N+1)^4}$$

$$+\frac{12064}{729}S_1+\frac{64}{81}S_2+\frac{320}{81}S_3-\frac{64}{27}S_4-\frac{112\gamma_{qq}^{(0)}\zeta_3}{27}\Bigg]$$

$$+C_F N_F T_F^2\Bigg[-\frac{8\gamma_{qq}^{(0)}}{27}\left(L_M^3+2L_Q^3\right)+L_Q^2\Bigg[-\frac{16P_{104}}{27N^2(N+1)^2}+\frac{64}{9}S_1^2-\frac{64}{3}S_2$$

$$+\frac{32\left(29N^2+29N-6\right)}{27N(N+1)}S_1\Bigg]+L_M\Bigg[\frac{4P_{44}}{81N^3(N+1)^3}-\frac{2176}{81}S_1-\frac{320}{27}S_2+\frac{64}{9}S_3\Bigg]$$

$$+L_Q\Bigg[\frac{16P_{120}}{81N^3(N+1)^3}+\left(-\frac{32P_{106}}{81N^2(N+1)^2}+\frac{128}{9}S_2\right)S_1-\frac{1792}{27}S_3$$

$$-\frac{32\left(29N^2+29N-6\right)}{27N(N+1)}S_1^2-\frac{128}{27}S_1^3+\frac{32\left(35N^2+35N-2\right)}{9N(N+1)}S_2+\frac{256}{9}S_{2,1}\Bigg]$$

$$+\frac{4P_{49}}{729N^4(N+1)^4}-\frac{24064}{729}S_1+\frac{128}{81}S_2+\frac{640}{81}S_3-\frac{128}{27}S_4+\frac{64\gamma_{qq}^{(0)}\zeta_3}{27}\Bigg]$$

$$+\frac{d^{abc}d^{abc}}{N_c}\frac{1}{2}L_Q\Bigg[-\frac{8P_{145}}{(N-1)N^5(N+1)^5(N+2)}+\frac{4P_{146}}{(N-1)N^4(N+1)^4(N+2)}S_1$$

$$+\frac{4\left(N^2+N+2\right)}{N^2(N+1)^2}S_3+\left(\frac{16\left(N^2+N+2\right)^2}{(N-1)N^2(N+1)^2(N+2)}S_1\right.$$

$$+\frac{8P_{136}}{(N-1)N^3(N+1)^3(N+2)}\Bigg)S_{-2}-\frac{8\left(N^2+N+2\right)}{N^2(N+1)^2}S_{-3}$$

$$+\frac{16\left(N^2+N+2\right)}{N^2(N+1)^2}S_{-2,1}\Bigg]+\hat{c}_{q,3}^{\mathrm{NS},W^+-W^-,(3)}(N_F)\Bigg\}\,,\tag{4.190}$$

with the additional polynomials

$$P_{131}=-17N^4-34N^3-29N^2-12N-24\tag{4.191}$$

$$P_{132}=N^4+2N^3-N^2-2N-4\tag{4.192}$$

$$P_{133}=3N^5+11N^4+10N^3+19N^2+23N+16\tag{4.193}$$

$$P_{134}=-11145N^6-32355N^5-37523N^4-14329N^3+1240N^2-1032N-2088\tag{4.194}$$

$$P_{135}=-151N^6-469N^5-181N^4+305N^3+80N^2-88N-56\tag{4.195}$$

$$P_{136}=N^6+3N^5-8N^4-21N^3-23N^2-12N-4\tag{4.196}$$

$$P_{137}=15N^6+36N^5+30N^4-24N^3+3N^2+16N+20\tag{4.197}$$

$$P_{138}=155N^6+465N^5+465N^4+155N^3+108N^2+108N+54\tag{4.198}$$

$$P_{139} = 216N^6 + 567N^5 + 687N^4 + 285N^3 + 37N^2 - 44N + 12 \tag{4.199}$$

$$P_{140} = 309N^6 + 807N^5 + 693N^4 - 463N^3 - 638N^2 + 68N + 216 \tag{4.200}$$

$$P_{141} = 868N^6 + 2469N^5 + 2487N^4 + 940N^3 + 171N^2 + 207N + 144 \tag{4.201}$$

$$P_{142} = 1407N^6 + 3825N^5 + 4211N^4 + 1783N^3 - 250N^2 - 240N + 144 \tag{4.202}$$

$$P_{143} = -4785N^8 - 19140N^7 - 18754N^6 + 1320N^5 + 12723N^4 + 6548N^3 + 4080N^2$$
$$- 648N - 1728 \tag{4.203}$$

$$P_{144} = -45N^8 - 162N^7 - 858N^6 - 936N^5 - 1629N^4 - 1094N^3 - 804N^2$$
$$- 40N + 192 \tag{4.204}$$

$$P_{145} = N^8 + 4N^7 + 13N^6 + 25N^5 + 57N^4 + 77N^3 + 55N^2 + 20N + 4 \tag{4.205}$$

$$P_{146} = 3N^8 + 12N^7 + 16N^6 + 6N^5 + 30N^4 + 64N^3 + 73N^2 + 40N + 12 \tag{4.206}$$

$$P_{147} = 10807N^8 + 43228N^7 + 63222N^6 + 40150N^5 + 14587N^4 + 9018N^3 + 7452N^2$$
$$+ 2376N + 324 \tag{4.207}$$

$$P_{148} = 42591N^8 + 166764N^7 + 245664N^6 + 129982N^5 - 13295N^4 - 25978N^3$$
$$+ 3560N^2 - 3192N - 4464 \tag{4.208}$$

$$P_{149} = -18351N^{10} - 89784N^9 - 210021N^8 - 271638N^7 - 219369N^6 - 90572N^5$$
$$- 26491N^4 - 7790N^3 - 1992N^2 - 2760N - 2160 \tag{4.209}$$

$$P_{150} = 165N^{10} + 825N^9 + 109664N^8 + 331682N^7 + 457641N^6 + 346145N^5$$
$$+ 219290N^4 + 86724N^3 + 13608N^2 + 14256N + 10368 \tag{4.210}$$

$$P_{151} = 828N^{10} + 3492N^9 + 4305N^8 - 2013N^7 - 8540N^6 - 3822N^5 - 1157N^4$$
$$- 3057N^3 - 4112N^2 - 324N + 576 \tag{4.211}$$

$$P_{152} = 8274N^{10} + 37149N^9 + 53630N^8 + 7538N^7 - 59902N^6 - 55159N^5$$
$$- 6994N^4 + 3272N^3 - 9048N^2 - 1656N + 2160 \,. \tag{4.212}$$

The 3-loop part of the massless Wilson coefficient $\hat{c}_{q,3}^{\mathrm{NS},(3)}$ was calculated in [153]. Logarithmic terms of the 3-loop massless Wilson coefficients, which are proportional to powers of L_Q, as well as lower order massless Wilson coefficients are explicitly included in Eq. (4.190). We use the shorthand $\gamma_{qq}^{(0)}$ defined in Eq. (4.23). The result is given in terms of of harmonic sums up to weight $w = 5$. The sums have been reduced to an algebraically independent basis. The result for $L_{q,3}^{\mathrm{NS}}$ in x space is obtained via an inverse Mellin transformation and can be found in Eq. (E.13), Appendix E. It is written in in terms of HPLs of up to weight $w = 5$ which were again reduced algebraically using shuffle relations.

The results contain the colour factor $d^{abc}d^{abc}$. It enters from the anomalous dimension γ_s^{NS} and the massless Wilson coefficient. The fact that this colour factor does not appear in the OME $A_{qq,Q}^{\mathrm{NS}}$ is discussed in Appendix D. The x space expression consists of three parts: A regular part, a part proportional to the distribution $\delta(1 - x)$ and a part which carries a plus prescription, see Eq. (3.44). As already in the unpolarised and polarised neutral current cases, the non-singlet OME contributes a term which, after partial fractioning, has coefficients with positive powers of N, cf. Eq. (4.50). Therefore, the plus function part of $L_{q,3}^{\mathrm{NS}}(x)$ has terms which are $\propto (1/(1-x)^2)_+$. The same discussion as below Eq. (4.50) applies here as well.

The result for the Wilson coefficient $H_{q,3}^{\mathrm{NS}}$ differs from $L_{q,3}^{\mathrm{NS}}$ only by the massless Wilson coefficient $C_{q,3}^{\mathrm{NS}}(N_F)$. We do not give explicit formulae here, but they can be easily obtained from Eq. (4.190) via Eq. (4.189).

Since the results for the massive OMEs refer to the heavy quark mass in the OMS scheme, a

scheme transformation is necessary if we want to treat the heavy quark mass in the $\overline{\text{MS}}$ scheme. It is, however, the same as in the unpolarised neutral current case and can be found in Eqs. (4.73) and (4.74).

4.4.2. Numerical results

For the numerical illustrations, we set the common factorisation and renormalisation scale to $\mu^2 = Q^2$ unless explicitly stated otherwise.

Before we present numerical illustrations, we would like to discuss the asymptotic behaviour of the Wilson coefficient in the limits $x \to 0$ and $x \to 1$. The heavy flavour Wilson coefficients stripped of the contribution from purely massless graphs ($L_{q,3}^{\text{NS}}(N_F+1) - \hat{C}_{q,3}^{\text{NS}}(N_F)$ and $H_{q,3}^{\text{NS}}(N_F+1) - C_{q,3}^{\text{NS}}(N_F+1)$) is the same as for L_{q,g_1}^{NS}, see Eqs. (4.177) and (4.178) respectively. This is obvious since the only difference between these Wilson coefficients stems from the contribution given by the massless Wilson coefficient, which is subtracted here.

The asymptotic behaviour of the massless Wilson coefficients, on the other hand, differs from that discussed in the polarised case. Obviously, the colour factor $d^{abc}d^{abc}$, which enters here at 3-loop order from purely massless graphs, is not present in the polarised case. Moreover, for $H_{q,3}^{\text{NS}}$ the massless Wilson coefficient $C_{q,3}^{\text{NS}}(N_F + 1)$ instead of the difference $\hat{C}_{q,3}^{\text{NS}}(N_F) = C_{q,3}^{\text{NS}}(N_F + 1) - C_{q,3}^{\text{NS}}(N_F)$ enters. In the region $x \to 0$ the massless Wilson coefficient behaves like

$$\hat{C}_{q,3}^{\text{NS}}(N_F) \underset{x\to 0}{\propto} a_s^2 \frac{10}{3} C_F T_F \ln^2(x) - a_s^3 \frac{2}{15} \frac{d^{abc}d^{abc}}{N_c} \ln^5(x)\,, \tag{4.213}$$

$$C_{q,3}^{\text{NS}}(N_F) \underset{x\to 0}{\propto} -a_s 2C_F \ln(x) + a_s^2 \left[\frac{7}{3} C_F^2 - 2C_A C_F \right] \ln^3(x)$$
$$+ a_s^3 \left[\frac{2}{5} C_A^2 C_F - \frac{29}{15} C_A C_F^2 + \frac{53}{30} C_F^3 - \frac{2}{15} \frac{d^{abc}d^{abc}}{N_c} N_F \right] \ln^5(x)\,, \tag{4.214}$$

while in the limit $x \to 1$ they behave like

$$\hat{C}_{q,3}^{\text{NS}}(N_F) \underset{x\to 1}{\propto} a_s^2 \frac{8}{3} C_F T_F \left(\frac{\ln^2(1-x)}{1-x} \right)_+ + a_s^3 \frac{80}{9} C_F^2 T_F \left(\frac{\ln^4(1-x)}{1-x} \right)_+\,, \tag{4.215}$$

$$C_{q,3}^{\text{NS}}(N_F) \underset{x\to 1}{\propto} a_s 4C_F \left(\frac{\ln(1-x)}{1-x} \right)_+ + a_s^2 8C_F^2 \left(\frac{\ln^3(1-x)}{1-x} \right)_+ + a_s^3 8C_F^3 \left(\frac{\ln^5(1-x)}{1-x} \right)_+\,. \tag{4.216}$$

Comparing Eqs. (4.215) and (4.216) to Eq. (4.178), we see that at large x the massless graphs exhibit stronger soft singularities than the massive ones. At 3-loop order in the small x region, the colour factor $d^{abc}d^{abc}$ contributes to the asymptotic behaviour, for $\hat{C}_{q,3}^{\text{NS},(3)}$ even dominating over other colour factors (compare Eq. (4.213) to Eq. (4.179)). The leading logarithms for $C_{q,3}^{\text{NS},(k)}$ are of the form $a_s^{k+1} \ln^{2k+1}(x)$. This can again be compared to predictions for non-singlet evolution kernels from leading-order resummation [419, 420, 433]. However, less singular terms numerically cancel the behaviour of the leading logarithms in the physically relevant regions, cf. also [420, 433].

The contributions of the heavy flavour Wilson coefficients to the charged current structure function can be illustrated numerically. We use the x space representations given in Eq. (E.13) and evaluate the occurring HPLs using an extension of the code presented in [423] to weight $w = 5$. For the 3-loop contribution to the massless Wilson coefficient $c_{q,3}^{\text{NS},(3)}$ we use the approximate parametrisation given in [153]. We assume three massless flavours ($N_F = 3$) and refer to the charm quark as the heavy quark. Its mass is treated in the OMS scheme and it is taken to
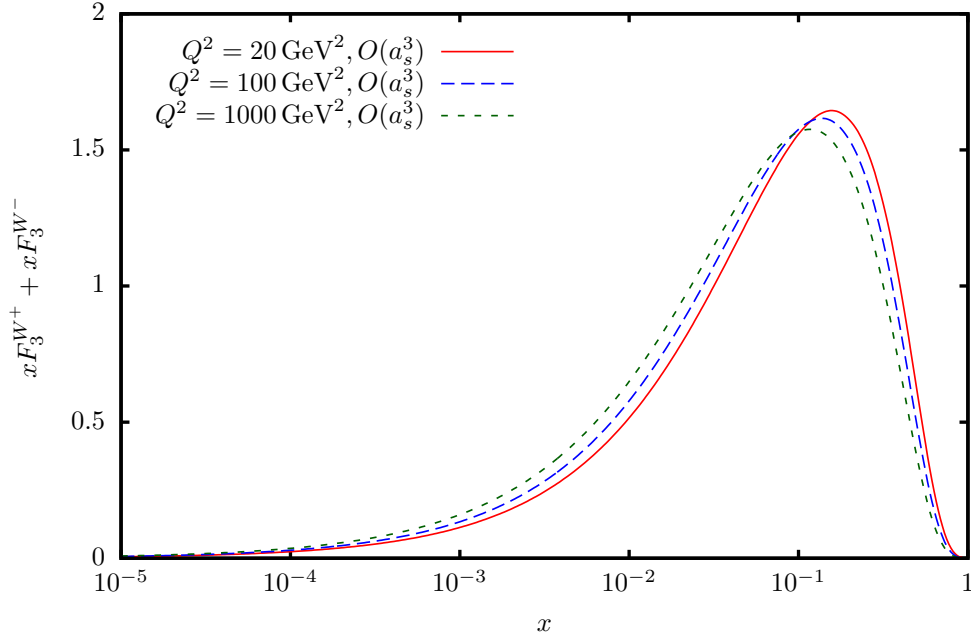
Figure 4.17.: The structure function combination $xF_3^{W^+-W^-}(x,Q^2)$ for a proton target with contributions from three massless as well as massive charm quarks, including corrections up to 3-loop order. The different curves correspond to different values for the virtuality Q^2 of the W boson. The charm quark is treated in the asymptotic approximation and its mass is taken to be $m_c = 1.59\,\mathrm{GeV}$ in the OMS scheme [226]. For the strong coupling constant $\alpha_s(M_Z^2) = 0.1132$ is used [218] and PDFs are taken from [218] as well.

be $m_c = 1.59\,\mathrm{GeV}$ [226]. We use the PDFs and the value of the strong coupling constant $\alpha_s(M_Z^2) = 0.1132$ from the NNLO analysis in [218] which are available through the LHAPDF library [422]. Like in the previous sections, we keep the settings for the strong coupling constant and the PDFs fixed when we plot different orders in α_s to facilitate a comparison of the influence of the Wilson coefficients. For the CKM matrix elements we use the values [37]

$$|V_{ud}| = 0.97425\,, \qquad |V_{us}| = 0.2253\,, \qquad |V_{cd}| = 0.225\,, \qquad |V_{cs}| = 0.986\,. \qquad (4.217)$$

In Fig. 4.17 the combination of structure functions $xF_3^{W^+-W^-}(x,Q^2)$ is plotted for a proton target up to and including 3-loop corrections. The plot includes contributions from three massless quarks and gluons as well as the charm corrections in the asymptotic limit. The structure functions vanish towards small and large values of x and show a maximum at $x \approx 0.1$. The shape is valence-like, as is suggested by the PDF combinations, cf. Eq. (4.183), and by the fact that the leading-order contribution of the massless Wilson coefficient is $\delta(1-x)$. By comparing different values of Q^2 we see that this maximum decreases for larger values of Q^2 and its position shifts towards smaller x.

Insight into the size of the heavy flavour corrections can be found in Fig. 4.18, which shows the ratio of structure functions containing the heavy flavour contributions from $L_{q,3}^{\mathrm{NS}}$ and $H_{q,3}^{\mathrm{NS}}$ to the purely massless contributions from $C_{q,3}^{\mathrm{NS}}$. The structure functions are truncated at 3-loop order and the different curves illustrate different values of Q^2. The corrections from heavy quarks increase the structure function by about 2% to 3% between $x = 10^{-5}$ and $x = 10^{-1}$ and become negative above $x \approx 0.5$, where they amount to up to -3.5% of the massless structure
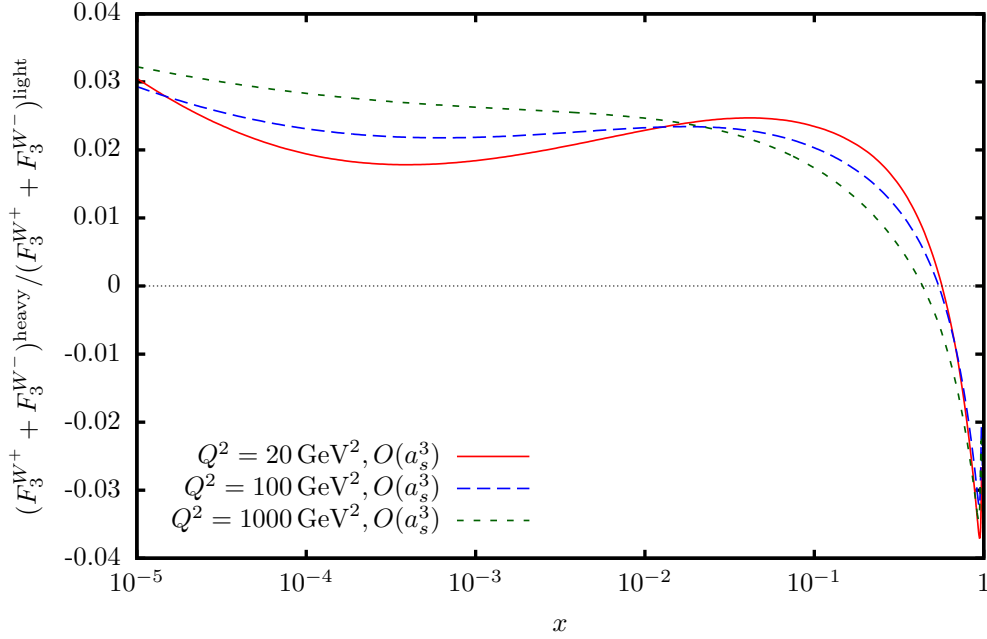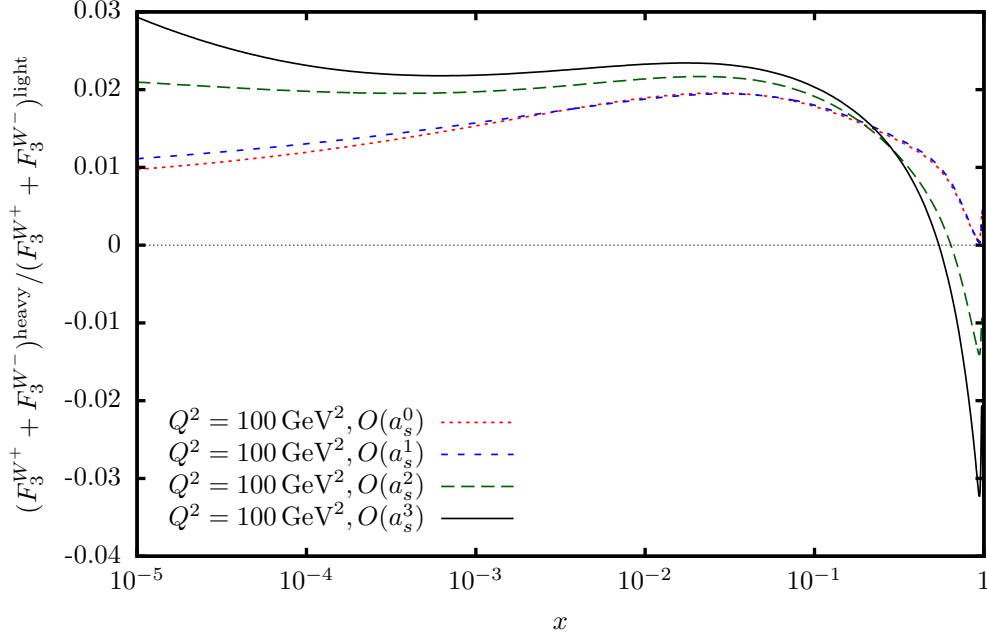
Figure 4.18.: Ratio of the contribution from charm quarks to the contribution of only three massless flavours to the combination of structure functions $xF_3^{W^+-W^-}(x,Q^2)$. The different curves compare different values of the virtuality Q^2 of the W boson. QCD corrections up to and including 3-loop order are included and a proton target is assumed. The PDFs and other parameters are the same as in Fig. 4.17.

function. With increasing Q^2 the corrections become more pronounced at small values of x and they decrease for $x \gtrsim 10^{-2}$.

The same ratio of structure functions is shown in Fig. 4.19 at fixed $Q^2 = 100\,\mathrm{GeV}^2$, comparing truncations of the perturbative series at different orders of a_s. As explained above, we do not change the PDFs or strong coupling constant across the different truncations. Increasing the order in a_s increases the size of the heavy flavour corrections at small x from 1% at tree level for $x = 10^{-5}$ to 3% at 3-loop order. At x close to 1 the higher order corrections drive the heavy flavour contribution negative.

Figure 4.20 addresses the sensitivity of the structure function to variations of the common renormalisation and factorisation scale μ^2. The borders of the yellow band correspond to the scale choices $\mu^2 = 4Q^2$ and $\mu^2 = Q^2/4$, normalised to the scale choice $\mu^2 = Q^2$. Here we plot the ratio for $Q^2 = 100\,\mathrm{GeV}^2$, but a similar behaviour is observed at other values of Q^2. The scale variation yields effects of order $\pm 1\%$ and is mostly flat in x, except for very small or large values of x.

Isoscalar targets can be described by making the replacements in Eq. (4.184) for the PDFs. The behaviour of $xF_3^{W^+-W^-}(x,Q^2)$ for a nucleon in an isoscalar target is almost indistinguishable form that of a proton target shown in Fig. 4.17. The reason for this can be seen from the difference of the structure function combinations for isoscalar and proton targets

$$F_3^{\mathrm{isoscalar}}(x,Q^2) - F_3^{\mathrm{proton}}(x,Q^2) = 2\left\{ |V_{us}|^2 \frac{d_v - u_v}{2} \otimes \left[C_{q,3}^{\mathrm{NS}}(N_F) + L_{q,3}^{\mathrm{NS}}(N_F + 1) \right] \right.$$
$$\left. - |V_{cd}|^2 \frac{d_v - u_v}{2} \otimes H_{q,3}^{\mathrm{NS}}(N_F + 1) \right\}, \qquad (4.218)$$

where u_v and d_v are the up and down quark valence distributions. Since the Wilson coefficient

Figure 4.19.: Ratio of the contribution from charm quarks to the contribution of only three massless flavours to the combination of structure functions $xF_3^{W^+-W^-}(x,Q^2)$. The different curves refer to the orders in a_s which are included in the ratio. For all curves a virtuality of $Q^2 = 100\,\mathrm{GeV}$ and a proton target is assumed. The PDFs and other parameters are the same as in Fig. 4.17.

$H_{q,3}^{\mathrm{NS}}(N_F+1)$ is structurally equivalent to $C_{q,3}^{\mathrm{NS}}(N_F)+L_{q,3}^{\mathrm{NS}}(N_F+1)$, cf. Eq. (4.189), the Wilson coefficients and the PDFs can be factored out. We find that the difference of the structure functions for isoscalar and proton targets is proportional to $|V_{us}|^2 - |V_{cd}|^2$, which is zero within the current experimental uncertainties [37].

4.4.3. Gross-Llewellyn-Smith sum rule

The first moment of the flavour non-singlet combination $F_3^{\bar{\nu}p} + F_3^{\nu p}$ fulfils the Gross-Llewellyn-Smith sum rule [401]

$$\int_0^1 \mathrm{d}x\,\left[F_3^{\bar{\nu}p}(x,Q^2) + F_3^{\nu p}(x,Q^2)\right] = 6C_{\mathrm{GLS}}(\hat{a}_s, N_F) \tag{4.219}$$

where $\hat{a}_s = \alpha_s/\pi$ and we idealise the CKM mixing by assuming unitarity of the two-flavour CKM submatrix. The massless QCD corrections to $C_{\mathrm{GLS}}(\hat{a}_s)$ have been calculated at 1-loop [105, 106, 446, 447], 2-loop [441], 3-loop [129] and 4-loop order [442, 448, 449]. They are given by

$$C_{\mathrm{GLS}}(\hat{a}_s, N_F) = 1 - \hat{a}_s + \hat{a}_s^2(-4.58333 + 0.33333N_F) + \hat{a}_s^3(-41.4399 + 8.02047N_F - 0.17747N_F^2)$$
$$+ \hat{a}_s^4(-479.448 + 129.193N_F - 7.93065N_F^2 + 0.10374N_F^3)\,. \tag{4.220}$$

For the colour factors the values of QCD $(\mathrm{SU}(3)_{\mathrm{c}})$ are assumed and we choose the factorisation and renormalisation scale as $\mu^2 = Q^2$. The number of massless quarks is denoted by N_F. The massless QCD corrections to the polarised Bjorken sum rule $C_{\mathrm{pBj}}(\hat{a}_s)$ are identical to those of the Gross-Llewellyn-Smith sum rule up to $\mathcal{O}(a_s^2)$, cf. Eq. (4.182). For the heavy quarks in the asymptotic limit, there are contributions from the heavy flavour Wilson coefficients $L_{q,3}^{\mathrm{NS}}$
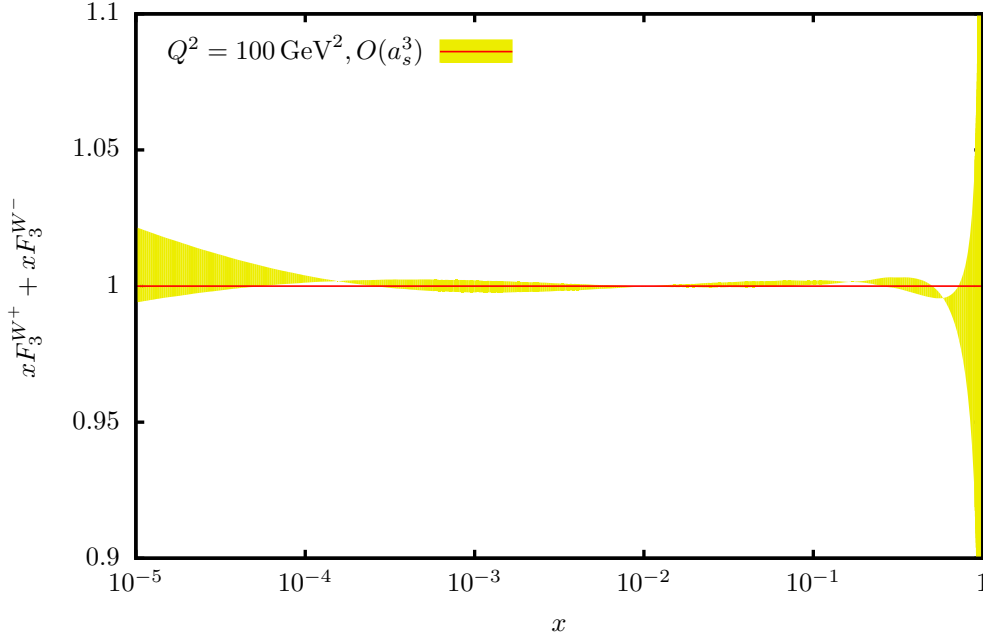
Figure 4.20.: The structure function combination $F_3^{W^+-W^-}(x, Q^2)$ for different choices of the renormalisation and factorisation scale μ^2, normalised to the choice $\mu^2 = Q^2$. The yellow band is delimited by the curves for the choices $\mu^2 = 4Q^2$ and $\mu^2 = Q^2/4$ respectively. Contributions from three massless flavours as well as from charm quarks are taken into account up to and including 3-loop order. The PDFs and other parameters are the same as in Fig. 4.17.

and $H_{q,3}^{\mathrm{NS}}$. The first moment of the massive OME $A_{qq,Q}^{\mathrm{NS}}$, however, vanishes due to fermion number conservation. Thus, the first moment receives contributions only from those parts of the heavy flavour Wilson coefficients which are determined by the massless Wilson coefficient. From $L_{q,3}^{\mathrm{NS}}(N_F + 1)$ we get $\hat{C}_{q,3}^{\mathrm{NS}}(N_F)$ as a contribution to the first moment, which effectively shifts $N_F \to N_F + 1$ in the massless Wilson coefficient. Moreover, the Wilson coefficient $H_{q,3}^{\mathrm{NS}}(N_F + 1)$ reduces to $C_{q,3}^{\mathrm{NS}}(N_F + 1)$, leaving us in the position to factor out the massless Wilson coefficient for $N_F + 1$ flavours. If we assume a vanishing valence distribution for the strange quarks $s_v = 0$ and neglect power corrections $(m^2/Q^2)^k$, the Gross-Llwellyn-Smith sum rule with charm quark contributions can be written as

$$\int_0^1 \mathrm{d}x \left[F_3^{\bar{\nu}p}(x, Q^2) + F_3^{\nu p}(x, Q^2) \right] =$$

$$2 \left[(|V_{ud}|^2 + |V_{us}|^2)\langle u_v \rangle + (|V_{ud}|^2 + |V_{cd}|^2)\langle d_v \rangle \right] \times C_{\mathrm{GLS}}(\hat{a}_s, N_F + 1) \qquad (4.221)$$

$$= 2 \left[2 \cdot 0.9999 + 0.9998 \right] C_{\mathrm{GLS}}(\hat{a}_s, N_F + 1), \qquad (4.222)$$

where N_F is the number of massless flavours and the first moment of the valence quark distribution is written as $\langle q_v \rangle = \int_0^1 \mathrm{d}x\, q_v(x)$. The experimental values of the CKM matrix elements amount to only a very small deviation from the factor 6, which is obtained in Eq. (4.221) for idealized CKM mixing. For isoscalar targets the result is practically identical. The difference between proton and isoscalar targets is again suppressed by $|V_{us}|^2 - |V_{cd}|^2$, cf. Eq. (4.218), and therefore consistent with zero at the current uncertainty of the CKM matrix elements [37].

Summarising the observations above, we can say that the asymptotic Wilson coefficients contribute to the Gross-Llewellyn-Smith sum rule only by shifting $N_F \to N_F + 1$ in C_{GLS} and if

we choose $\mu^2 = Q^2$, no logarithmic corrections appear in the inclusive case, which is considered here and in [198]. In the tagged heavy flavour case, on the other hand, logarithmic corrections do appear [197]. Power corrections to the tagged flavour case were considered in [306, 445] while the power corrections in the inclusive case were dealt with in [421].

4.5. Variable flavour number scheme

The variable flavour number scheme defined in [202] describes the transition from N_F massless and one massive quark to $N_F + 1$ effectively massless quarks, see also Section 2.6. Below a matching scale μ^2 the massive quark is regarded as being produced purely through radiative corrections and the massless evolution equations are used to describe the scale evolution of the PDFs of the N_F massless flavours. Above the matching scale the massive quark is regarded as effectively massless and a new PDF is assigned to this quark flavour. This distribution evolves using the standard massless evolution equations for $N_F + 1$ flavours. The PDFs in these two schemes are related through matching relations in which the massive OMEs appear as matching coefficients. To 2-loop order all necessary OMEs are known [201, 202, 205, 207]. At 3-loop order a number of fixed moments is known [193, 203] for all relevant OMEs. With the completion of the non-singlet OME $A_{qq,Q}^{\mathrm{NS}}$ to 3-loop order for general N, the matching relation for the PDF combination $f_k(N_F + 1, \mu^2) + \bar{f}_k(N_F + 1, \mu^2)$ is now completely known for general values of N. The relation reads

$$
f_k(N_F + 1, \mu^2) + \bar{f}_k(N_F + 1, \mu^2) =
$$
$$
A_{qq,Q}^{\mathrm{NS}} \otimes \left[f_k(N_F, \mu^2) + \bar{f}_k(N_F, \mu^2) \right] + \frac{1}{N_F} \left\{ A_{qq,Q}^{\mathrm{PS}} \otimes \Sigma(N_F, \mu^2) + A_{qg,Q} \otimes G(N_F, \mu^2) \right\} ,
$$
$$
(4.223)
$$

where $G(N_F, \mu^2)$ is the gluon PDF and $\Sigma(N_F, \mu^2)$ is the singlet PDF combination defined in Eq. (2.66). The Mellin convolution is denoted by $\otimes$. Since usually the PDFs are given as functions in x, the OMEs are needed in x space as well. The OMEs $A_{qq,Q}^{\mathrm{PS}}$ and $A_{qg,Q}$ have been obtained in [336] for general N to 3-loop order. In [450] the N and x space representations of the renormalised OMEs were given, including the logarithmic terms. This completes the first matching relation to $\mathcal{O}\!\left(a_s^3\right)$ for general values of N. Thus, we can give illustrations of the impact on the PDFs.

The choice of the matching scale μ^2 is process dependent and usually significantly larger than the heavy quark mass [306]. Scales close to threshold imply non-relativistic heavy quark production for which neglecting finite mass effects is generally not justified. It is interesting to note that the OMEs $A_{qq,Q}^{\mathrm{PS}}$ and $A_{qg,Q}$ start only at $\mathcal{O}\!\left(a_s^3\right)$ so that the gluon and singlet PDF combination mix into $f_k + \bar{f}_k$ only at this order.

Figure 4.21 demonstrates the size of the individual terms in Eq. (4.223) for the example of the $x(u + \bar{u})$ combination in the 4-flavour scheme. The term involving the non-singlet OME is small compared to the singlet and gluon terms and its shape as a function of x resembles that of the massive Wilson coefficient, which was discussed in the previous section. By comparison, the pure-singlet and gluon term are larger by about an order of magnitude and they grow towards small x. Only for $x \gtrsim 0.05$ is the non-singlet term of similar size as the other two terms. The relative difference in magnitude of the individual contributions is mainly driven by the magnitude of the corresponding PDF combinations in the 3-flavour scheme. The behaviour of the individual contributions to the down and strange combinations is similar.

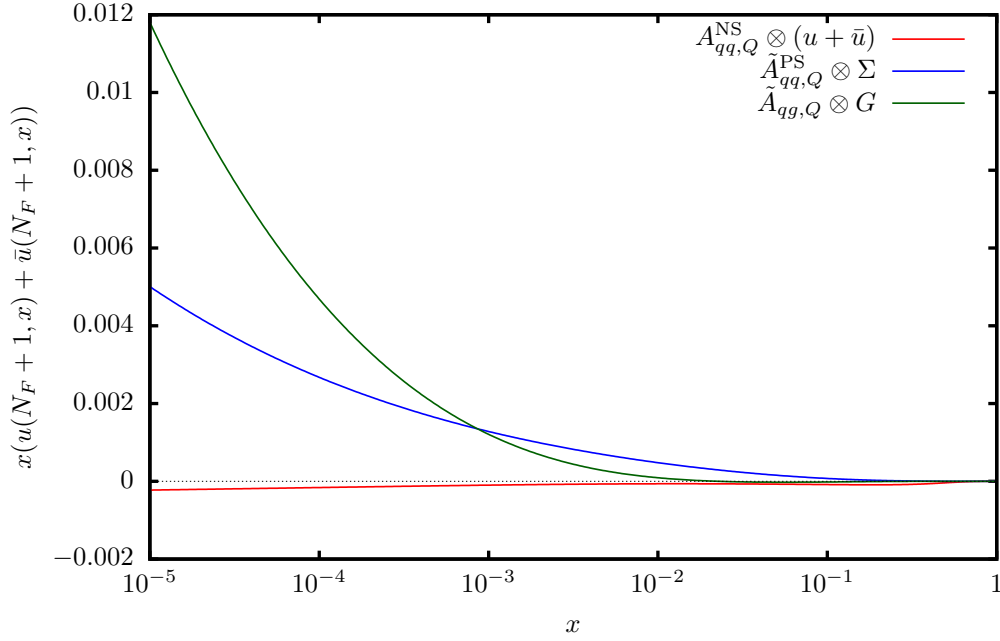The impact of the $\mathcal{O}\!\left(a_s^3\right)$ corrections to the matching relation Eq. (4.223) can be illustrated

Figure 4.21.: Individual contributions from the OMEs to the PDF combination $x(u+\bar{u})$ for four flavours in the variable flavour number scheme. Only the 3-loop terms are shown while lower order terms are not included in the plot. The matching scale is fixed at $\mu^2 = 20\,\mathrm{GeV}^2$ the PDFs are taken from [218]. The charm quark mass is treated in the OMS scheme and we use the value $m_c = 1.59\,\mathrm{GeV}$ [226].
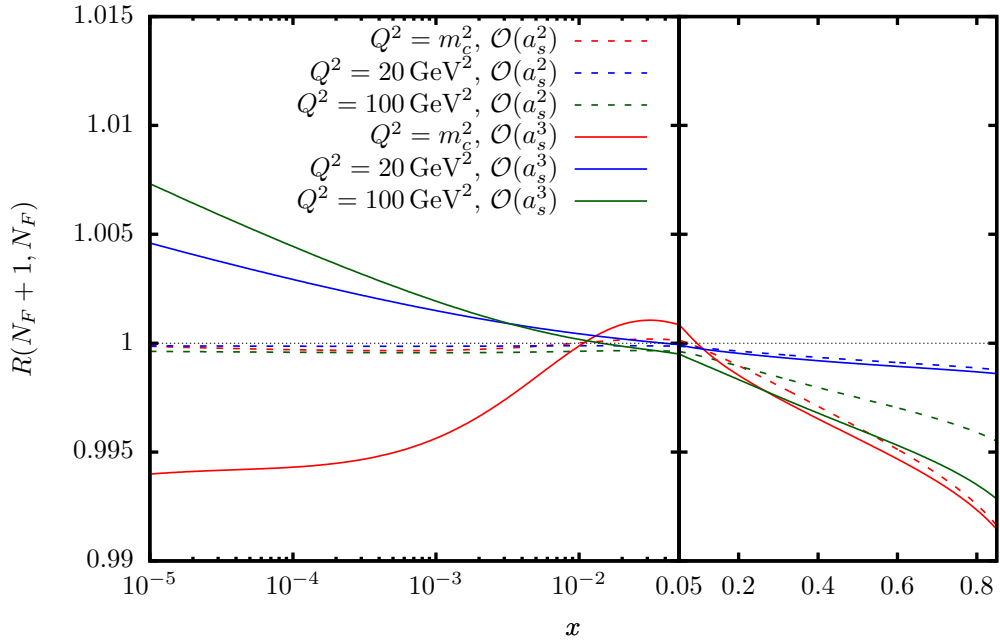

Figure 4.22.: Ratio of the distribution $x(u+\bar{u})$ at four flavours in the VFNS to the same distribution at three flavours. The dashed lines show the ratio up to and including 2-loop corrections and the solid lines also include 3-loop effects. Up to $x = 0.05$ the x axis has a logarithmic scale while the scale for $x \in [0.05, 0.85]$ is linear. The PDFs and the charm quark mass are the same as in Fig. 4.21.
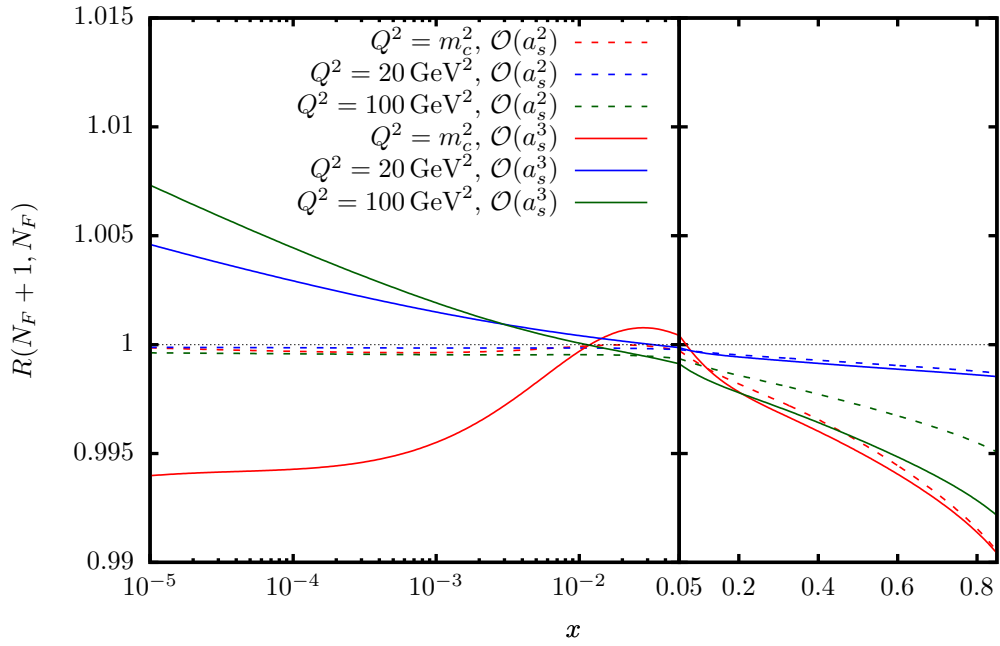
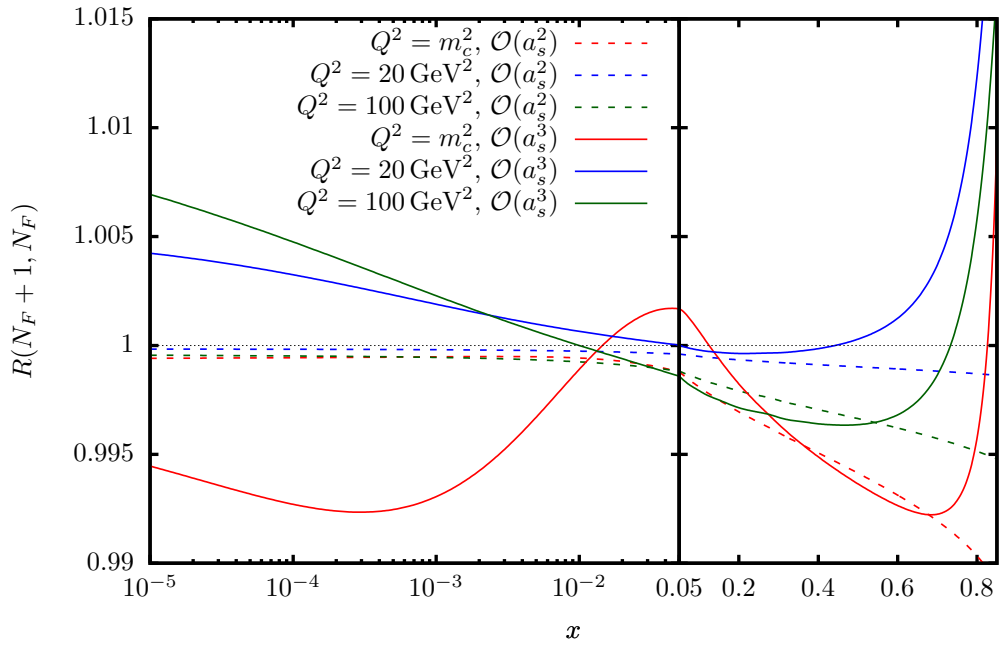Figure 4.23.: The same as Fig. 4.22 but for the PDF combination $x(d + \bar{d})$.

Figure 4.24.: The same as Fig. 4.22 but for the PDF combination $x(s + \bar{s})$.

by considering the ratio

$$R_k(N_F + 1, N_F) = \frac{f_k(N_F + 1, \mu^2) + \bar{f}_k(N_F + 1, \mu^2)}{f_k(N_F, \mu^2) + \bar{f}_k(N_F, \mu^2)}.$$
(4.224)

This ratio is plotted in Fig. 4.22 for the combination $x(u + \bar{u})$, in Fig. 4.23 for $x(d + \bar{d})$ and in Fig. 4.24 for $x(s + \bar{s})$. The figures show the ratio for $\mathcal{O}(a_s^2)$ and for $\mathcal{O}(a_s^3)$ as dashed and solid lines, respectively. Comparing the ratio at different orders, one observes the onset of mixing with the gluon and singlet combination at $\mathcal{O}(a_s^3)$ in the form of larger effects up to $\mathcal{O}(0.5\%)$ at small x. Given $\mathcal{O}(1\%)$ experimental precision for $F_2(x, Q^2)$ the effects from the matching are only slightly smaller. The behaviour of $d + \bar{d}$ is very similar to $u + \bar{u}$ – only with slightly larger effects at large x. Also the effects on the combination $s + \bar{s}$ are similar, though at large x the ratio shows a more pronounced behaviour.

5. Pure-singlet contributions to DIS

Considering contributions to deep-inelastic scattering from diagrams with a quark as the initial parton, we can distinguish two terms according to their transformation behaviour under the flavour group $\mathrm{SU}(N_F)$. Parts with a non-trivial transformation behaviour are called non-singlet contributions and have been dealt with in the previous chapter. Those terms which are invariant under flavour transformations are called singlet contributions and can be further split up due to the contributing diagrams. All non-singlet diagrams also contribute to the singlet terms, which suggests to isolate the *pure-singlet* part, i.e. all diagrams that are unique to the singlet part. At the level of massive OMEs, there are two pure-singlet OMEs, $A_{qq,Q}^{\mathrm{PS}}$ and A_{Qq}^{PS}. The former has the operator insertion on a light quark line and was calculated before in [336], whereas the diagrams of the latter have an operator insertion on a heavy quark line. In this chapter, we discuss the calculation of the pure-singlet OME A_{Qq}^{PS} and the associated heavy flavour Wilson coefficient $H_{q,2}^{\mathrm{PS}}$ for the unpolarised structure function $F_2(x, Q^2)$. We also extract the pure-singlet anomalous dimension, which enters the pole terms of the OME. In the results, we encounter generalised harmonic sums [261, 368] in N space and HPLs with generalised arguments in x space. The results of this chapter are published in [397].

5.1. The pure-singlet operator matrix element

Forming the matrix element of the singlet operator with heavy quark fields between massless, on-shell quark states yields the pure-singlet OME A_{Qq}^{PS}. The contributing diagrams have external massless, on-shell fermions and the operator insertion is carried by a heavy quark line. Contributions to this OME start at 2-loop order which can also be understood diagrammatically: The external particles are light quarks, which have to be connected due to fermion number conservation. The presence of the heavy quark introduces at least one closed fermion loop, and the requirement of one-particle irreducibility implies that we need at least two gluons to link the massive fermion loop to the external fermion line, which results in another loop. In contrast to the non-singlet OME, the pure-singlet OME up to 3-loop order does not receive contributions from reducible diagrams: Heavy quark corrections to the self-energy of external massless quarks start at 2-loop order and irreducible diagrams for the pure-singlet OME start at 2-loop order as well. Thus, reducible diagrams are expected only from 4-loop order onwards.

The structure of this OME can be derived from the renormalisation and factorisation procedure and reads [203]

$$
A_{Qq}^{\mathrm{PS},(2)}(N) = -\frac{\hat{\gamma}_{qg}^{(0)}\gamma_{gq}^{(0)}}{8}\ln^2\left(\frac{m^2}{\mu^2}\right) + \frac{\hat{\gamma}_{qq}^{\mathrm{PS},(1)}}{2}\ln\left(\frac{m^2}{\mu^2}\right) + \frac{\hat{\gamma}_{qg}^{(0)}\gamma_{gq}^{(0)}}{8}\zeta_2 + a_{Qq}^{\mathrm{PS},(2)}, \tag{5.1}
$$

$$
A_{Qq}^{\mathrm{PS},(3)}(N) = \frac{\hat{\gamma}_{qg}^{(0)}\gamma_{gq}^{(0)}}{48}\left\{\gamma_{gg}^{(0)} - \gamma_{qq}^{(0)} + 6\beta_0 + 16\beta_{0,Q}\right\}\ln^3\left(\frac{m^2}{\mu^2}\right) + \frac{1}{8}\left\{-4\hat{\gamma}_{qq}^{\mathrm{PS},(1)}\left(\beta_0 + \beta_{0,Q}\right)\right.
$$

$$
+ \hat{\gamma}_{qg}^{(0)}\left(\hat{\gamma}_{gq}^{(1)} - \gamma_{gq}^{(1)}\right) - \gamma_{gq}^{(0)}\hat{\gamma}_{qg}^{(1)}\left.\right\}\ln^2\left(\frac{m^2}{\mu^2}\right) + \frac{1}{16}\left\{8\hat{\gamma}_{qq}^{\mathrm{PS},(2)} - 8N_F\hat{\tilde{\gamma}}_{qq}^{\mathrm{PS},(2)}\right.
$$

$$
- 32a_{Qq}^{\mathrm{PS},(2)}(\beta_0 + \beta_{0,Q}) + 8\hat{\gamma}_{qg}^{(0)}a_{gq,Q}^{(2)} - 8\gamma_{gq}^{(0)}a_{Qg}^{(2)} - \hat{\gamma}_{qg}^{(0)}\gamma_{gq}^{(0)}\zeta_2\left(\gamma_{gg}^{(0)} - \gamma_{qq}^{(0)}\right)
$$

$$+ 6\beta_0 + 8\beta_{0,Q} \Bigg) \Bigg\} \ln\left(\frac{m^2}{\mu^2}\right) + 4(\beta_0 + \beta_{0,Q})\overline{a}_{Qq}^{\text{PS},(2)} + \gamma_{gq}^{(0)}\overline{a}_{Qg}^{(2)} - \hat{\gamma}_{qg}^{(0)}\overline{a}_{gq,Q}^{(2)}$$

$$+ \frac{\gamma_{gq}^{(0)}\hat{\gamma}_{qg}^{(0)}\zeta_3}{48}\left(\gamma_{gg}^{(0)} - \gamma_{qq}^{(0)} + 6\beta_0\right) + \frac{\hat{\gamma}_{qg}^{(0)}\gamma_{gq}^{(1)}\zeta_2}{16} - \delta m_1^{(1)}\hat{\gamma}_{qg}^{(0)}\gamma_{gq}^{(0)} + \delta m_1^{(0)}\hat{\gamma}_{qq}^{\text{PS},(1)}$$

$$+ 2\delta m_1^{(-1)}a_{Qq}^{\text{PS},(2)} + a_{Qq}^{\text{PS},(3)}, \tag{5.2}$$

The coefficients of renormalisation constants like the massless and massive β-function, β_k and $\beta_{k,Q}$, the mass renormalisation constants δm_k and the anomalous dimensions $\gamma_{ij}^{(k)}$ were already discussed in Chapter 2. The hat and tilde above the anomalous dimensions refer to the N_F prescriptions defined in Eqs. (2.96) and (2.97). The constant term of the ε expansion of the 2-loop OMEs $a_{ij}^{(2)}$ was obtained in [201] and recalculated in [205]. The corresponding linear terms $\overline{a}_{ij}^{(2)}$ are also known [206]. As discussed below Eq. (4.2), the 2-loop OMEs refer to the expressions *after* on-shell mass renormalisation, while the constant part of the 3-loop OME is taken to be completely unrenormalised.

The only unknown part of the expression above is the constant term of the 3-loop OME, which is what we will address in the calculation below. We give some details on the characteristics of the calculation in the next subsection, and we proceed by presenting results on the pure-singlet anomalous dimensions, which can be extracted from the pole terms or logarithmic terms. Finally, we present the result for the 3-loop OME.

5.1.1. Details on the calculation

An outline of the steps involved in the calculation is given in Section 3.1. Here we only comment on the characteristics which are particular to the pure-singlet OME. A sample of the diagrams, which are generated using `QGRAF` [347], can be found in Fig. 5.1. The topologically most involved diagrams are related to Benz diagrams with up to four massive propagators. Ladder diagrams or non-planar topologies do not contribute here.

The diagrams are then passed to the `FORM` [216] program [193, 203] which inserts the Feynman rules, applies the projectors, performs the simplifications of Dirac and colour algebra and finally yields a linear combination of scalar integrals for each diagram. Most diagrams yield scalar integrals which can be mapped to the B1a integral family. Only four diagrams, which have four distinct massive propagators and which are drawn in Figs. 5.1e to 5.1g and 5.1j, are mapped to the families B5a and B5c. Due to the structure of the Feynman rule for the 4-point operator insertion, diagrams with such an insertion consist of two parts whose scalar integrals may need to be mapped to different families.

After using the integration-by-parts relations to reduce the scalar integrals to master integrals, 66 master integrals are required to express all pure-singlet diagrams. Of these, 55 belong to the family B1a and 11 are from the family B5a. Unfortunately, there is almost no overlap with the master integrals which enter the non-singlet OME due to the placement of the operator insertion. Only the three master integrals which do not have an operator insertion occur in both OMEs. The scalar integrals of the family B5c are completely reduced to B5a master integrals. This is a peculiarity of the present OME and the way we choose the basis of master integrals. In general, other OMEs do have diagrams which are reduced to master integrals from the family B5c.

For the calculation of the master integrals we use several of the techniques described in Section 3.3. The simplest master integrals can be done by introducing Feynman parameters, performing the loop integrals and solving the Feynman parameter integrals in terms of Euler Beta functions. These results are valid to all orders of the dimensional parameter ε and their expansions up to the required order yields harmonic sums of depth one. Slightly more complicated master integrals can be done in terms of generalised hypergeometric functions evaluated at 1 or
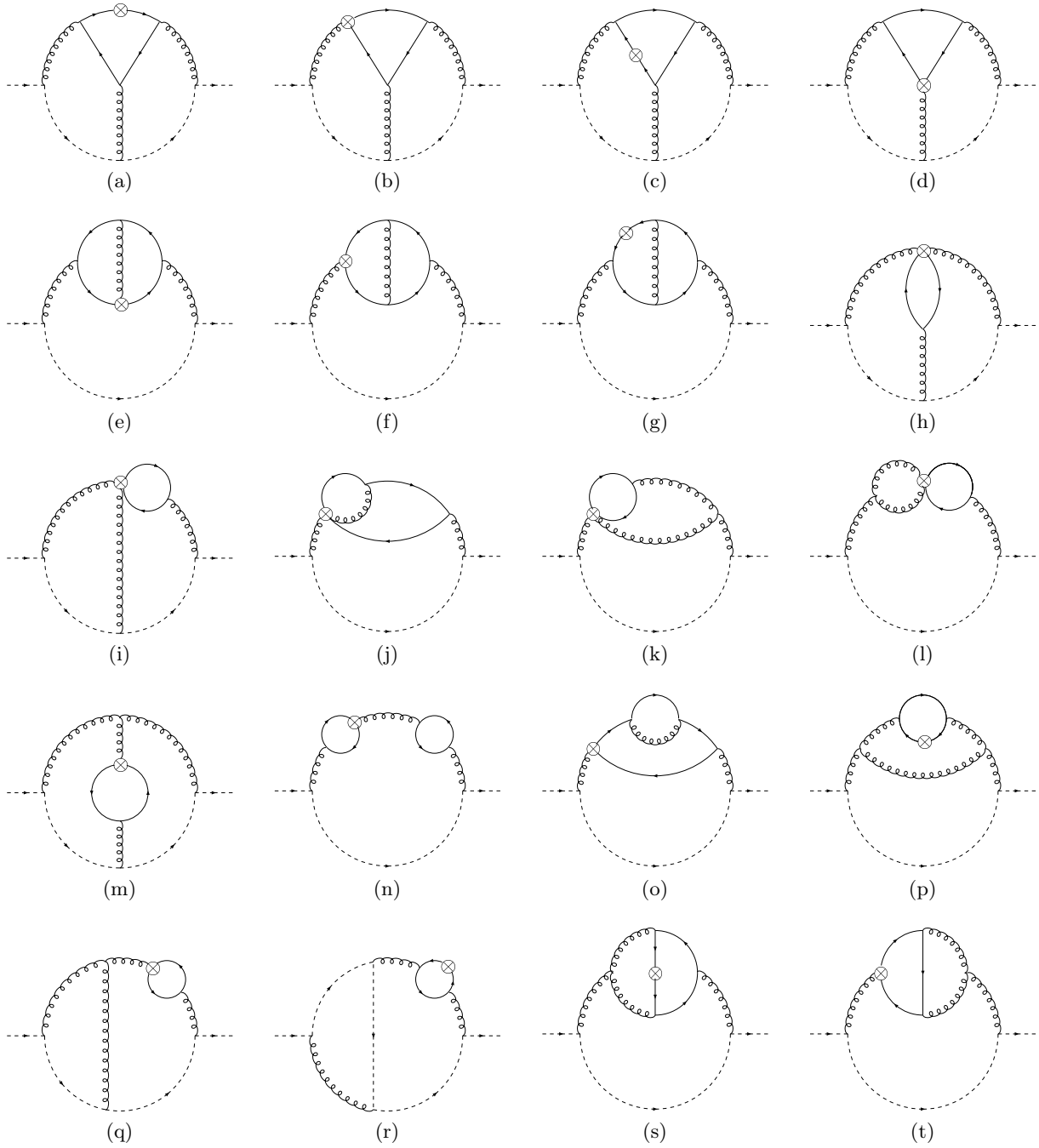
Figure 5.1.: Examples for the diagrams contributing to the pure-singlet OME $A_{qq,Q}^{\mathrm{PS},(3)}$. Massless quarks are drawn as dashed arrow lines and massive quarks as solid arrow lines. Curly lines represent gluons and the operator insertion is marked by a circled cross.

finite sums over these functions, where the summation indices appear in the parameters of the hypergeometric functions. Given appropriate convergence properties of the series representation of the hypergeometric function, we use this representation to arrive at a sum representation for the master integral which consists of several finite and infinite sums. The expression can then be simplified using the packages `Sigma` [241, 252, 253], `HarmonicSums` [258–263], `EvaluateMultiSums` and `SumProduction` [254–257] in terms of harmonic sums and generalised harmonic sums. For some integrals, in particular for those from the family B5a, we make use of Mellin-Barnes representations and the package `MB` [392] to derive a sum representation which could then be simplified using the packages mentioned above. Moreover, eleven master integrals from the family B1a are solved using the method of differential equations.

After completing all required master integrals, they can be written as generating functions and inserted into the expressions for the diagrams which leads to a result for the generating function of the diagram. The final step is then to extract the Nth Taylor coefficient from this generating function in order to obtain the result for the diagrams in N space.

All diagrams which contain a subdiagram with only two distinct propagators, called bubble diagrams, were calculated separately and their results were published in [338]. There, hypergeometric function techniques were used to derive sum representations which were subsequently simplified using the packages ρSum [451–453], `Sigma` [241, 252, 253], `EvaluateMultiSums` and `SumProduction` [254–257].

5.1.2. Anomalous dimension

Since the pure-singlet anomalous dimension enters in the pole terms of the unrenormalised OME A_{Qq}^{PS} and in the logarithmic terms after renormalisation, we can use our result for the pure-singlet OME to extract the pure-singlet anomalous dimensions. The double pole (ε^{-2}) term contains the 2-loop loop anomalous dimension $\gamma_{qq}^{\mathrm{PS},(1)}$. Equivalently it can be recovered from the term proportional to L_M^2 in the renormalised result. From the single pole (ε^{-1}) term or the L_M term, we extract the quantity $\hat{\gamma}_{qq}^{\mathrm{PS},(2)}$, which allows us to reconstruct all N_F-dependent terms of the 3-loop anomalous dimension. As the N_F-independent term is absent in the pure-singlet anomalous dimension, we obtain the complete result this way, which is the first recalculation of the result in [136] using a different observable and different methods.

We define the shorthand

$$F = \frac{(2 + N + N^2)^2}{(N-1)N^2(N+1)^2(N+2)} \, . \tag{5.3}$$

With this, the pure-singlet anomalous dimension at 2-loop order is given by

$$\gamma_{qq}^{\mathrm{PS},(1)}(N) = -\frac{1 + (-1)^N}{2} C_F T_F N_F \frac{16(N^2 + 5N + 2)(5N^3 + 7N^2 + 4N + 4)}{(N-1)N^3(N+1)^3(N+2)^2} \, . \tag{5.4}$$

At 3-loop order the result reads

$$
\gamma_{qq}^{\mathrm{PS},(2)}(N) = \frac{1 + (-1)^N}{2} \left\{ C_F^2 T_F N_F \left\{ -\frac{8(N^2 + N + 2)P_{153}}{(N-1)N^3(N+1)^3(N+2)} S_1^2 + 32F\left[\frac{1}{3}S_1^3 - S_2 S_1 \right.\right.\right.
$$
$$
\left.\left. - \frac{7}{3}S_3 + 2S_{2,1} + 6\zeta_3 \right] + \frac{32P_{160}}{(N-1)N^4(N+1)^4(N+2)^3} S_1 \right.
$$
$$
\left.\left. - \frac{8P_{164}}{(N-1)N^5(N+1)^5(N+2)^3} - \frac{8P_{158}}{(N-1)N^3(N+1)^3(N+2)^2} S_2 \right\}
$$

$$
+ C_F T_F^2 N_F^2 \Bigg\{ \frac{64 P_{159}}{9(N-1)N^3(N+1)^3(N+2)^2} S_1 - \frac{64 P_{161}}{27(N-1)N^4(N+1)^4(N+2)^3}
$$

$$
- F \frac{32}{3} [S_1^2 + S_2] \Bigg\} + C_F C_A T_F N_F \Bigg\{ \frac{8(N^2+N+2)P_{155}}{3(N-1)^2 N^3(N+1)^3(N+2)^2} S_1^2
$$

$$
- \frac{16 P_{163}}{9(N-1)^2 N^4(N+1)^4(N+2)^2} S_1 + \frac{16 P_{165}}{27(N-1)^2 N^5(N+1)^5(N+2)^4}
$$

$$
+ (-1)^N \Bigg[\frac{128 P_{154}}{3(N-1)N^2(N+1)^3(N+2)^3} S_1 - \frac{128 P_{162}}{9(N-1)N^3(N+1)^5(N+2)^4} \Bigg]
$$

$$
+ \frac{8(N^2+N+2)P_{156}}{3(N-1)^2 N^3(N+1)^3(N+2)^2} S_2 + \frac{16(N^2+N+2)(23N^2+23N+58)}{3(N-1)N^2(N+1)^2(N+2)} S_3
$$

$$
+ \frac{32 P_{157}}{(N-1)N^3(N+1)^3(N+2)^2} S_{-2} + \frac{32(N^2+N+2)(7N^2+7N+10)}{(N-1)N^2(N+1)^2(N+2)} S_{-3}
$$

$$
- \frac{64(N^2+N+2)(3N^2+3N+2)}{(N-1)N^2(N+1)^2(N+2)} S_{-2,1}
$$

$$
+ 32 F \Bigg[-\frac{1}{3} S_1^3 + S_2 S_1 + 2 S_{-2} S_1 - 2 S_{2,1} - 6\zeta_3 \Bigg] \Bigg\} \Bigg\}. \tag{5.5}
$$

Here we use the polynomials

$$
P_{153} = 5N^4 + 10N^3 + 25N^2 + 20N + 4 \tag{5.6}
$$

$$
P_{154} = 5N^6 + 29N^5 + 78N^4 + 118N^3 + 114N^2 + 72N + 16 \tag{5.7}
$$

$$
P_{155} = 17N^6 + 51N^5 + 99N^4 + 113N^3 - 32N^2 - 80N - 24 \tag{5.8}
$$

$$
P_{156} = 29N^6 + 99N^5 + 39N^4 + 65N^3 + 64N^2 - 128N - 24 \tag{5.9}
$$

$$
P_{157} = 2N^7 + 14N^6 + 37N^5 + 102N^4 + 155N^3 + 158N^2 + 132N + 40 \tag{5.10}
$$

$$
P_{158} = 5N^7 + 25N^6 + 11N^5 - 213N^4 - 420N^3 - 416N^2 - 352N - 112 \tag{5.11}
$$

$$
P_{159} = 8N^7 + 37N^6 + 68N^5 - 11N^4 - 86N^3 - 56N^2 - 104N - 48 \tag{5.12}
$$

$$
\begin{aligned}
P_{160} = {} & 9N^{10} + 69N^9 + 219N^8 + 345N^7 + 410N^6 + 724N^5 + 1124N^4 + 1116N^3 \\
& + 824N^2 + 400N + 96
\end{aligned} \tag{5.13}
$$

$$
\begin{aligned}
P_{161} = {} & 52N^{10} + 392N^9 + 1200N^8 + 1353N^7 - 317N^6 - 1689N^5 - 2103N^4 - 2672N^3 \\
& - 1496N^2 - 48N + 144
\end{aligned} \tag{5.14}
$$

$$
\begin{aligned}
P_{162} = {} & 77N^{10} + 646N^9 + 2553N^8 + 6903N^7 + 14498N^6 + 22898N^5 + 24861N^4 \\
& + 17068N^3 + 7040N^2 + 1760N + 192
\end{aligned} \tag{5.15}
$$

$$
\begin{aligned}
P_{163} = {} & 127N^{10} + 713N^9 + 1458N^8 + 78N^7 - 2360N^6 - 2352N^5 - 3663N^4 - 3359N^3 \\
& + 298N^2 + 924N + 72
\end{aligned} \tag{5.16}
$$

$$
\begin{aligned}
P_{164} = {} & 49N^{12} + 417N^{11} + 1619N^{10} + 3868N^9 + 6831N^8 + 10189N^7 + 13445N^6 \\
& + 14934N^5 + 12760N^4 + 8160N^3 + 4176N^2 + 1504N + 256
\end{aligned} \tag{5.17}
$$

$$
\begin{aligned}
P_{165} = {} & 731N^{14} + 8804N^{13} + 40614N^{12} + 90274N^{11} + 102402N^{10} + 67882N^9 \\
& + 23170N^8 - 120782N^7 - 357069N^6 - 421954N^5 - 293880N^4 - 183088N^3 \\
& - 109968N^2 - 42912N - 6912 \,.
\end{aligned} \tag{5.18}
$$

We suppress the argument N of the harmonic sums to shorten the notation. After reducing the harmonic sums to an algebraically independent basis [146], cf. also [149], seven harmonic sums

5. Pure-singlet contributions to DIS

up to weight three appear. The required sums read

$$S_1, S_2, S_{-2}, S_3, S_{-3}, S_{2,1}, S_{-2,1} \,. \tag{5.19}$$

Structural relations [147, 148] allow to reduce the number of independent sums even further until we reach the three sums

$$S_1, S_{2,1}, S_{-2,1} \,. \tag{5.20}$$

The corresponding results in x space are given in Eqs. (E.1) and (E.2) in Appendix E. It contains 15 HPLs up to weight $w = 4$ after algebraic reduction, which are

$$
\begin{aligned}
&H_0, H_1, H_{-1}, H_{0,1}, H_{0,-1}, H_{0,0,1}, H_{0,0,-1}, H_{0,1,1}, H_{0,-1,-1}, H_{0,-1,1}, H_{0,1,-1}, \\
&H_{0,0,0,1}, H_{0,0,0,-1}, H_{0,0,1,1}, H_{0,1,1,1} \,.
\end{aligned} \tag{5.21}
$$

Since $H_{0,-1,1}$ and $H_{0,1,-1}$ only appear as a sum, all HPLs can be represented as Nielsen integrals $\mathsf{S}_{n,p}(x)$ [378–380], cf. Eq. (3.43), if we allow for the more general arguments x, $-x$ and x^2, [147]. The required special functions are

$$
\begin{aligned}
&\ln(x), \ln(1-x), \ln(1+x), \mathrm{Li}_2(x), \mathrm{Li}_3(x), \mathrm{Li}_3(-x), \mathsf{S}_{1,2}(x), \mathsf{S}_{1,2}(-x), \mathsf{S}_{1,2}(x^2), \\
&\mathrm{Li}_4(x), \mathrm{Li}_4(-x), \mathsf{S}_{2,2}(x), \mathsf{S}_{1,3}(x) \,.
\end{aligned} \tag{5.22}
$$

It has been observed [147, 454] that all 3-loop splitting functions can be expressed in terms of Nielsen integrals with generalised arguments. The expressions in x space require a larger number of special functions compared to the result in N space. Our results in Eqs. (5.4) and (5.5) agree with the results in the literature [110, 112, 115, 117, 118, 136]. At 3-loop order, our result is the first independent recalculation.

5.1.3. The operator matrix element

A key objective of the present calculation is the missing constant term of the unrenormalised 3-loop pure-singlet OME. For the presentation of the results in this chapter, we define the shorthand

$$G = \frac{(N^2 + N + 2)}{(N-1)N^2(N+1)^2(N+2)} \,, \tag{5.23}$$

and we continue to use the shorthand F defined in Eq. (5.3). In N space $a_{Qq}^{\mathrm{PS},(3)}$ is given by

$$
\begin{aligned}
a_{Qq}^{\mathrm{PS},(3)}(N) = \\
C_F T_F^2 &\Bigg[\frac{32}{27(N-1)(N+3)(N+4)(N+5)} \Bigg(\frac{P_{179}}{N^3(N+1)^2(N+2)^2} S_2 \\
&- \frac{P_{183}}{N^3(N+1)^3(N+2)^2} S_1^2 + \frac{2 P_{192}}{3 N^4 (N+1)^4 (N+2)^3} S_1 - \frac{2 P_{196}}{9 N^5 (N+1)^4 (N+2)^4} \Bigg) \\
&- \frac{32 P_{168}}{9(N-1)N^3(N+1)^2(N+2)^2} \zeta_2 + \Bigg(\frac{32}{27} S_1^3 - \frac{160}{9} S_1 S_2 - \frac{512}{27} S_3 + \frac{128}{3} S_{2,1} \\
&+ \frac{32}{3} S_1 \zeta_2 - \frac{1024}{9} \zeta_3 \Bigg) F \Bigg] + C_F N_F T_F^2 \Bigg[\frac{16 P_{159}}{27(N-1)N^3(N+1)^3(N+2)^2} S_1^2 \\
&+ \frac{208 P_{159}}{27(N-1)N^3(N+1)^3(N+2)^2} S_2 - \frac{32 P_{185}}{81(N-1)N^4(N+1)^4(N+2)^3} S_1
\end{aligned}
$$

$$+ \frac{32P_{193}}{243(N-1)N^5(N+1)^5(N+2)^4} + \left(-\frac{16}{27}S_1^3 - \frac{208}{9}S_1S_2 - \frac{1760}{27}S_3 - \frac{16}{3}S_1\zeta_2\right.$$

$$\left.+ \frac{224}{9}\zeta_3\right)F + \frac{1}{(N-1)N^3(N+1)^3(N+2)^2}\frac{16P_{159}}{9}\zeta_2\Bigg]$$

$$+ C_F^2 T_F \Bigg[\frac{32P_{173}}{3(N-1)N^3(N+1)^3(N+2)^2}S_{2,1} - \frac{16P_{178}}{9(N-1)N^3(N+1)^3(N+2)^2}S_3$$

$$- \frac{4P_{181}}{3(N-1)N^4(N+1)^4(N+2)^3}S_1^2 + \frac{4P_{187}}{3(N-1)N^4(N+1)^4(N+2)^3}S_2$$

$$+ \frac{4P_{195}}{3(N-1)N^6(N+1)^6(N+2)^4} + \left(\left(\frac{2P_{170}}{N^2(N+1)^2} - \frac{4P_{166}}{N(N+1)}S_1\right)\zeta_2\right.$$

$$\left.- \frac{4P_{166}}{9N(N+1)}S_1^3\right)G + \left(\left(\frac{80}{9}S_3 - 64S_{2,1}\right)S_1 - \frac{2}{9}S_1^4 - \frac{20}{3}S_1^2S_2 + \frac{46}{3}S_2^2 + \frac{124}{3}S_4\right.$$

$$+ \frac{416}{3}S_{2,1,1} + 64\left(\left(S_3(2) - S_{1,2}(2,1) + S_{2,1}(2,1) - S_{1,1,1}(2,1,1)\right)S_1\left(\frac{1}{2}\right)\right.$$

$$- S_{1,3}\left(2,\frac{1}{2}\right) + S_{2,2}\left(2,\frac{1}{2}\right) - S_{3,1}\left(2,\frac{1}{2}\right) + S_{1,1,2}\left(2,\frac{1}{2},1\right) - S_{1,1,2}\left(2,1,\frac{1}{2}\right)$$

$$- S_{1,2,1}\left(2,\frac{1}{2},1\right) + S_{1,2,1}\left(2,1,\frac{1}{2}\right) - S_{2,1,1}\left(2,\frac{1}{2},1\right) - S_{2,1,1}\left(2,1,\frac{1}{2}\right)$$

$$+ S_{1,1,1,1}\left(2,\frac{1}{2},1,1\right) + S_{1,1,1,1}\left(2,1,\frac{1}{2},1\right) + S_{1,1,1,1}\left(2,1,1,\frac{1}{2}\right)\right) + \left(12S_2 - 4S_1^2\right)\zeta_2$$

$$+ \left(\frac{112}{3}S_1 - 448S_1\left(\frac{1}{2}\right)\right)\zeta_3 + 144\zeta_4 - 32B_4\right)F + \frac{32P_{167}2^{-N}}{(N-1)N^3(N+1)^2}\left(-S_3(2)\right.$$

$$+ S_{1,2}(2,1) - S_{2,1}(2,1) + S_{1,1,1}(2,1,1) + 7\zeta_3\right) + \left(-\frac{4P_{172}}{3(N-1)N^3(N+1)^3(N+2)^2}S_2\right.$$

$$+ \frac{8P_{191}}{3(N-1)N^5(N+1)^5(N+2)^4}\right)S_1 + \frac{1}{(N-1)N^3(N+1)^3(N+2)^2}\frac{4P_{180}}{3}\zeta_3\Bigg]$$

$$+ C_A C_F T_F \Bigg[-\frac{8P_{174}}{3(N-1)N^3(N+1)^3(N+2)^2}S_{2,1} + \frac{8P_{176}}{3(N-1)N^3(N+1)^3(N+2)^2}S_{-3}$$

$$+ \frac{16P_{177}}{3(N-1)N^3(N+1)^3(N+2)^2}S_{-2,1} + \frac{8P_{186}}{27(N-1)^2N^3(N+1)^3(N+2)^2}S_3$$

$$- \frac{4P_{188}}{27(N-1)^2N^4(N+1)^4(N+2)^3}S_1^2 - \frac{4P_{190}}{27(N-1)^2N^4(N+1)^4(N+2)^3}S_2$$

$$- \frac{8P_{197}}{243(N-1)^2N^6(N+1)^6(N+2)^5} + \left(\frac{4P_{169}}{27(N-1)N(N+1)(N+2)}S_1^3\right.$$

$$+ \left(\frac{8}{9}\left(137N^2 + 137N + 334\right)S_3 - \frac{16}{3}\left(35N^2 + 35N + 18\right)S_{-2,1}\right)S_1$$

$$+ \frac{8}{3}\left(69N^2 + 69N + 94\right)S_{-3}S_1 + \frac{64}{3}\left(7N^2 + 7N + 13\right)S_{-2}S_2 + \frac{2}{3}\left(29N^2 + 29N + 74\right)S_2^2$$

$$+ \frac{4}{3}\left(143N^2 + 143N + 310\right)S_4 - \frac{16}{3}\left(3N^2 + 3N - 2\right)S_{-2}^2 + \frac{16}{3}\left(31N^2 + 31N + 50\right)S_{-4}$$

$$- 8\left(7N^2 + 7N + 26\right)S_{3,1} - 64\left(3N^2 + 3N + 2\right)S_{-2,2} - \frac{32}{3}\left(23N^2 + 23N + 22\right)S_{-3,1}$$

$$+ \frac{64}{3}\left(13N^2 + 13N + 2\right)S_{-2,1,1} + \frac{4P_{169}}{3(N-1)N(N+1)(N+2)}S_1\zeta_2$$

5. Pure-singlet contributions to DIS

$$
-\frac{8}{3}\left(11N^2 + 11N + 10\right)S_1\zeta_3\bigg)G + \bigg(\frac{112}{3}S_{-2}S_1^2 + \frac{2}{9}S_1^4 + \frac{68}{3}S_1^2S_2 - \frac{80}{3}S_{2,1,1}
$$

$$
+ 32\bigg(\bigg(-S_3(2) + S_{1,2}(2,1) - S_{2,1}(2,1) + S_{1,1,1}(2,1,1)\bigg)S_1\left(\frac{1}{2}\right) + S_{1,3}\left(2,\frac{1}{2}\right)
$$

$$
- S_{2,2}\left(2,\frac{1}{2}\right) + S_{3,1}\left(2,\frac{1}{2}\right) - S_{1,1,2}\left(2,\frac{1}{2},1\right) + S_{1,1,2}\left(2,1,\frac{1}{2}\right) + S_{1,2,1}\left(2,\frac{1}{2},1\right)
$$

$$
- S_{1,2,1}\left(2,1,\frac{1}{2}\right) + S_{2,1,1}\left(2,\frac{1}{2},1\right) + S_{2,1,1}\left(2,1,\frac{1}{2}\right) - S_{1,1,1,1}\left(2,\frac{1}{2},1,1\right)
$$

$$
- S_{1,1,1,1}\left(2,1,\frac{1}{2},1\right) - S_{1,1,1,1}\left(2,1,1,\frac{1}{2}\right)\bigg) + \bigg(4S_1^2 + 12S_2 + 24S_{-2}\bigg)\zeta_2
$$

$$
+ 224S_1\left(\frac{1}{2}\right)\zeta_3 - 144\zeta_4 + 16B_4\bigg)F + \frac{16P_{167}2^{-N}}{(N-1)N^3(N+1)^2}\bigg(S_3(2) - S_{1,2}(2,1)
$$

$$
+ S_{2,1}(2,1) - S_{1,1,1}(2,1,1) - 7\zeta_3\bigg) + \bigg(\frac{4P_{175}}{9(N-1)^2N^3(N+1)^3(N+2)^2}S_2
$$

$$
+ \frac{4P_{194}}{81(N-1)^2N^5(N+1)^5(N+2)^4}\bigg)S_1 + \bigg(\frac{32P_{171}}{3(N-1)N^3(N+1)^3(N+2)^2}S_1
$$

$$
- \frac{8P_{182}}{3(N-1)N^4(N+1)^4(N+2)^3}\bigg)S_{-2} - \frac{4P_{189}}{9(N-1)^2N^4(N+1)^4(N+2)^3}\zeta_2
$$

$$
- \frac{8P_{184}}{9(N-1)^2N^3(N+1)^3(N+2)^2}\zeta_3\bigg], \tag{5.24}
$$

with B_4 as defined in Eq. (3.31) and the polynomials P_i given by those of the anomalous dimension as well as by

$$
P_{166} = 5N^4 + 4N^3 + N^2 - 10N - 8 \tag{5.25}
$$

$$
P_{167} = N^5 - N^3 + 10N^2 - 2N + 4 \tag{5.26}
$$

$$
P_{168} = 8N^6 + 29N^5 + 84N^4 + 193N^3 + 162N^2 + 124N + 24 \tag{5.27}
$$

$$
P_{169} = 17N^6 + 51N^5 + 27N^4 + 77N^3 + 76N^2 - 80N - 24 \tag{5.28}
$$

$$
P_{170} = 38N^6 + 108N^5 + 151N^4 + 106N^3 + 21N^2 - 28N - 12 \tag{5.29}
$$

$$
P_{171} = 3N^7 + 24N^6 + 49N^5 + 122N^4 + 154N^3 + 104N^2 + 120N + 32 \tag{5.30}
$$

$$
P_{172} = 81N^7 + 271N^6 + 229N^5 - 159N^4 - 530N^3 - 844N^2 - 904N - 288 \tag{5.31}
$$

$$
P_{173} = 6N^8 + 40N^7 + 84N^6 + 59N^5 + 114N^4 + 283N^3 + 250N^2 + 180N + 88 \tag{5.32}
$$

$$
P_{174} = 6N^8 + 48N^7 + 100N^6 - 5N^5 + 194N^4 + 763N^3 + 626N^2 + 356N + 152 \tag{5.33}
$$

$$
P_{175} = 269N^8 + 1064N^7 + 1342N^6 + 2552N^5 + 3273N^4 + 1896N^3 + 516N^2
$$
$$
- 2560N - 864 \tag{5.34}
$$

$$
P_{176} = 6N^9 + 39N^8 + 89N^7 + 148N^6 + 85N^5 + 147N^4 + 286N^3 + 248N^2
$$
$$
+ 440N + 112 \tag{5.35}
$$

$$
P_{177} = 6N^9 + 39N^8 + 105N^7 + 76N^6 - 91N^5 - 293N^4 - 338N^3 - 248N^2
$$
$$
- 264N - 80 \tag{5.36}
$$

$$
P_{178} = 36N^9 + 216N^8 + 478N^7 + 293N^6 - 663N^5 - 2063N^4 - 2859N^3 - 1074N^2
$$
$$
+ 444N + 56 \tag{5.37}
$$

$$
P_{179} = 40N^9 + 625N^8 + 3284N^7 + 5392N^6 - 7014N^5 - 33693N^4 - 47454N^3
$$
$$
- 46100N^2 - 26280N + 7200 \tag{5.38}
$$

$$P_{180} = 48N^9 + 192N^8 - 45N^7 - 1089N^6 - 1487N^5 - 3299N^4 - 7320N^3 - 4120N^2$$
$$- 1008N - 1072 \tag{5.39}$$

$$P_{181} = 3N^{10} + 75N^9 + 363N^8 + 735N^7 + 662N^6 + 490N^5 + 944N^4 + 840N^3$$
$$+ 176N^2 + 256N + 192 \tag{5.40}$$

$$P_{182} = 5N^{10} + 44N^9 + 82N^8 + 214N^7 + 259N^6 + 14N^5 - 346N^4 - 2096N^3$$
$$- 3680N^2 - 1952N - 416 \tag{5.41}$$

$$P_{183} = 8N^{10} + 133N^9 + 1095N^8 + 5724N^7 + 18410N^6 + 34749N^5 + 40683N^4$$
$$+ 37370N^3 + 22748N^2 - 3960N - 7200 \tag{5.42}$$

$$P_{184} = 9N^{10} - 229N^8 - 367N^7 + 1135N^6 - 472N^5 - 5661N^4 - 837N^3 + 1098N^2$$
$$+ 260N + 1032 \tag{5.43}$$

$$P_{185} = 25N^{10} + 176N^9 + 417N^8 + 30N^7 - 20N^6 + 1848N^5 + 2244N^4 + 1648N^3$$
$$+ 3040N^2 + 2112N + 576 \tag{5.44}$$

$$P_{186} = 135N^{10} + 702N^9 + 1745N^8 + 2039N^7 + 1345N^6 + 2618N^5 - 4923N^4$$
$$- 9939N^3 - 11598N^2 - 10516N - 2136 \tag{5.45}$$

$$P_{187} = 153N^{10} + 1049N^9 + 2811N^8 + 3411N^7 + 1084N^6 - 3976N^5 - 11660N^4$$
$$- 16088N^3 - 12272N^2 - 6240N - 1664 \tag{5.46}$$

$$P_{188} = 46N^{11} + 145N^{10} + 406N^9 + 1566N^8 + 1411N^7 - 4318N^6 - 12231N^5$$
$$- 14165N^4 - 6636N^3 + 3200N^2 + 4512N + 1872 \tag{5.47}$$

$$P_{189} = 127N^{11} + 856N^{10} + 2323N^9 + 2484N^8 - 317N^7 - 106N^6 + 4779N^5$$
$$+ 8470N^4 + 11112N^3 + 9680N^2 + 4656N + 864 \tag{5.48}$$

$$P_{190} = 1696N^{11} + 10993N^{10} + 27688N^9 + 26208N^8 - 773N^7 + 17000N^6$$
$$+ 62901N^5 + 81499N^4 + 114180N^3 + 106112N^2 + 55200N + 12240 \tag{5.49}$$

$$P_{191} = 12N^{13} + 151N^{12} + 819N^{11} + 2549N^{10} + 4893N^9 + 7260N^8 + 11172N^7$$
$$+ 15420N^6 + 16388N^5 + 16824N^4 + 16352N^3 + 10880N^2 + 4672N + 896 \tag{5.50}$$

$$P_{192} = 52N^{13} + 746N^{12} + 4658N^{11} + 20431N^{10} + 79990N^9 + 251778N^8$$
$$+ 553796N^7 + 837697N^6 + 886552N^5 + 599060N^4 + 155864N^3 - 82368N^2$$
$$- 76896N - 17280 \tag{5.51}$$

$$P_{193} = 158N^{13} + 1663N^{12} + 7714N^{11} + 23003N^{10} + 56186N^9 + 89880N^8 + 59452N^7$$
$$- 8896N^6 - 12856N^5 - 24944N^4 - 84608N^3 - 77952N^2 - 35712N - 6912 \tag{5.52}$$

$$P_{194} = 247N^{14} + 2518N^{13} + 12147N^{12} + 29936N^{11} + 47061N^{10} + 66314N^9$$
$$+ 15119N^8 - 144034N^7 + 1854N^6 + 528058N^5 + 571260N^4 + 113008N^3$$
$$- 61248N^2 - 22752N + 1728 \tag{5.53}$$

$$P_{195} = 88N^{15} + 978N^{14} + 4569N^{13} + 11443N^{12} + 18236N^{11} + 25694N^{10} + 41400N^9$$
$$+ 57974N^8 + 50675N^7 + 9415N^6 - 48500N^5 - 88676N^4 - 83504N^3$$
$$- 45232N^2 - 13504N - 1728 \tag{5.54}$$

$$P_{196} = 293N^{15} + 4670N^{14} + 32280N^{13} + 145948N^{12} + 559575N^{11} + 1871440N^{10}$$
$$+ 4877344N^9 + 9333994N^8 + 12958212N^7 + 12693884N^6 + 8472792N^5$$
$$+ 4514336N^4 + 3109248N^3 + 2192832N^2 + 1026432N + 207360 \tag{5.55}$$

5. Pure-singlet contributions to DIS

$$
\begin{aligned}
P_{197} = {} & 3244N^{17} + 40465N^{16} + 218915N^{15} + 671488N^{14} + 1331937N^{13} + 1654143N^{12} \\
& + 374900N^{11} - 2526162N^{10} - 3045065N^9 + 1320584N^8 + 6186057N^7 \\
& + 9141018N^6 + 12149124N^5 + 13312808N^4 + 10121520N^3 + 4812768N^2 \\
& + 1308096N + 155520 \,.
\end{aligned}
\tag{5.56}
$$

An interesting feature of the result is the appearance of generalised harmonic sums [261, 368] in the final result, see also Eq. (3.32). The non-singlet OME presented in Section 4.1 and previously published results on $A_{qq,Q}^{\text{PS}}$ and $A_{qg,Q}$ [336] as well as $A_{gq,Q}$ [339] do not require this class of sums for the final result. In [138] it has been observed that generalised harmonic sums were needed in intermediate results of the 3-loop massless Wilson coefficients for $F_2(x, Q^2)$, but they cancel in the final result. Similar observations were made in the calculation of the N_F dependent terms of the 3-loop OMEs [336]. Calculations of scalar prototype diagrams related to ladder topologies with local operator insertions [343] also required generalised harmonic sums, but to the best of our knowledge, this is the first instance where these sums remain in a physical result for a single scale quantity. In addition to the sums which are required for the anomalous dimensions, see Eq. (5.19), the following sums enter the 3-loop pure-singlet OME

$$
\begin{aligned}
& S_{-4}, S_4, S_{-3,1}, S_{3,1}, S_{-2,2}, S_{-2,1,1}, S_{2,1,1}, S_1\left(\frac{1}{2}\right), S_3(2), S_{1,3}\left(2, \frac{1}{2}\right), S_{1,2}(2,1), S_{2,1}(2,1), \\
& S_{2,2}\left(2, \frac{1}{2}\right), S_{3,1}\left(2, \frac{1}{2}\right), S_{1,1,1}(2,1,1), S_{1,1,2}\left(2, \frac{1}{2}, 1\right), S_{1,1,2}\left(2,1, \frac{1}{2}\right), S_{1,2,1}\left(2, \frac{1}{2}, 1\right), \\
& S_{1,2,1}\left(2,1, \frac{1}{2}\right), S_{2,1,1}\left(2, \frac{1}{2}, 1\right), S_{2,1,1}\left(2,1, \frac{1}{2}\right), S_{1,1,1,1}\left(2, \frac{1}{2}, 1, 1\right), S_{1,1,1,1}\left(2,1, \frac{1}{2}, 1\right), \\
& S_{1,1,1,1}\left(2,1,1, \frac{1}{2}\right).
\end{aligned}
\tag{5.57}
$$

Compared to the anomalous dimension, seven additional harmonic sums and 17 generalised harmonic sums enter. The generalised sums can be traced back to the diagrams depicted in Figs. 5.1e to 5.1g and those which are related to them by symmetry. Since the alphabet of parameters also includes the letter 2, individual sums may diverge in the limit $N \to \infty$. A simple example would be $S_3(2)$. Such a behaviour was in fact observed for individual scalar diagrams related to V-topologies in [344]. The combination of sums which appears in the physical result for the pure-singlet OME, however, is well-behaved in the limit $N \to \infty$ in the sense that it diverges at most like powers of $\ln(\bar{N})$, which is expected from the simple harmonic sum S_1. The asymptotic expansion of the result is given by

$$
\begin{aligned}
a_{Qq}^{\text{PS},(3)} \underset{N\to\infty}{\propto} {} & \frac{2}{9} C_F T_F (C_A - C_F) \frac{\ln^4(\bar{N})}{N^2} \\
& + \frac{4}{27} C_F T_F \left[17 C_A - 15 C_F + (8 - 4N_F) T_F\right] \frac{\ln^3(\bar{N})}{N^2} + \mathcal{O}\left(\frac{\ln^2(\bar{N})}{N^2}\right).
\end{aligned}
\tag{5.58}
$$

Performing the Mellin inversion of Eq. (5.24) leads to generalised harmonic polylogarithms [261] evaluated at argument x. The particular set of generalised HPLs that occur here can be reexpressed in terms of usual HPLs if we allow for the additional argument $1 - 2x$. The necessary transformations can be carried out using `HarmonicSums`. Referring only to usual HPL is advantageous for numerical applications since we can reuse existing implementations for the numerical evaluation of HPLs. In general, of course, it may not always be possible to restrict to usual HPLs and functions with support on only a subset of the interval $[0, 1]$ may occur. In intermediate steps of our calculation we observe functions with support on $[0, 1/2]$ or $[1/2, 1]$. While they can be combined into functions with support on the complete interval $[0, 1]$ for our

result, this may not always be possible. Mellin convolutions of functions with support on only parts of $[0, 1]$ with regular functions with support on the complete interval read

$$\left[A_1(x)\theta\left(\tfrac{1}{2} - x\right)\right] \otimes f(x) = \theta\left(\tfrac{1}{2} - x\right)\int_{2x}^{1}\frac{\mathrm{d}y}{y}A_1\left(\frac{x}{y}\right)f(y) \tag{5.59}$$

$$\left[A_2(x)\theta\left(x - \tfrac{1}{2}\right)\right] \otimes f(x) = \int_{x}^{1}\frac{\mathrm{d}y}{y}A_2\left(\frac{x}{y}\right)f(y) - \theta\left(\tfrac{1}{2} - x\right)\int_{2x}^{1}\frac{\mathrm{d}y}{y}A_2\left(\frac{x}{y}\right)f(y). \tag{5.60}$$

For the presentation of the result for $a_{Qq}^{\mathrm{PS},(3)}$ in x space, we split the result into a part which depends only on HPLs evaluated at x and a part where also HPLs evaluated at $1 - 2x$ enter.

$$a_{Qq}^{\mathrm{PS},(3)}(x) = a_{Qq}^{\mathrm{PS},\mathrm{a},(3)}(x) + a_{Qq}^{\mathrm{PS},\mathrm{b},(3)}(x). \tag{5.61}$$

Moreover, we introduce another shorthand notation for HPLs at this new argument

$$\tilde{H}_{\vec{a}} = H_{\vec{a}}(1 - 2x) \tag{5.62}$$

in addition to the usual shorthand $H_{\vec{a}} = H_{\vec{a}}(x)$. With these conventions, the result in x space can be written as

$$
\begin{aligned}
a_{Qq}^{\mathrm{PS},\mathrm{a},(3)}(x) =& \\
& C_F N_F T_F^2 \Bigg[\frac{16}{81}\frac{x-1}{x}\left(4x^2 + 7x + 4\right)H_1^3 + \frac{64}{729}\frac{x-1}{x}\left(5165x^2 - 2632x + 1736\right) - \frac{64}{243}\left(1350x^2\right. \\
& - 569x - 218\right)H_0 + \frac{64}{81}\left(111x^2 + 64x + 100\right)H_0^2 - \frac{128}{81}\left(6x^2 + 4x - 5\right)H_0^3 + \frac{64}{27}(x+1)H_0^4 \\
& + \left(\frac{64}{9}\frac{x-1}{x}\left(4x^2 + 7x + 4\right)H_0^2 - \frac{64}{27}\frac{x-1}{x}\left(74x^2 - 43x + 20\right)H_0 + \frac{64}{81}\frac{x-1}{x}\left(150x^2\right.\right. \\
& + 103x + 60\right)\right)H_1 + \left(-\frac{32}{9}\frac{x-1}{x}\left(4x^2 + 7x + 4\right)H_0 + \frac{16}{81}\frac{x-1}{x}\left(74x^2 - 43x + 20\right)\right)H_1^2 \\
& + \left(\frac{128}{9}\frac{1}{x}\left(2x^3 + x^2 - 2x + 4\right)H_0 + \frac{64}{81}\frac{1}{x}\left(111x^3 - 415x^2 + 89x - 60\right) - \frac{128}{3}(x+1)H_0^2\right) \\
& \times H_{0,1} + \left(-\frac{128}{27}\frac{2x+3}{x}\left(9x^2 - 8x + 4\right) + \frac{256}{3}(x+1)H_0\right)H_{0,0,1} + \left(\frac{64}{27}\frac{1}{x}\left(6x^3 + 5x^2\right.\right. \\
& - 4x - 12\right) + \frac{128}{3}(x+1)H_0\right)H_{0,1,1} - \frac{256}{9}(x+1)H_{0,0,0,1} - \frac{640}{9}(x+1)H_{0,0,1,1} \\
& - \frac{64}{9}(x+1)H_{0,1,1,1} + \left(\frac{80}{9}\frac{x-1}{x}\left(4x^2 + 7x + 4\right)H_1 + \frac{16}{81}\frac{1}{x}\left(666x^3 - 95x^2 + 589x - 60\right)\right. \\
& - \frac{224}{27}\left(6x^2 + 4x - 5\right)H_0 + \frac{224}{9}(x+1)H_0^2 - \frac{160}{3}(x+1)H_{0,1}\right)\zeta_2 + \left(\frac{32}{27}\frac{1}{x}\left(104x^3 + 67x^2\right.\right. \\
& - 89x + 28\right) - \frac{320}{3}(x+1)H_0\right)\zeta_3 + \frac{560}{3}(x+1)\zeta_4 \Bigg] \\
& + C_F T_F^2 \Bigg[-\frac{32}{81}\frac{x-1}{x}\left(4x^2 + 7x + 4\right)H_1^3 - \frac{128}{1215}\left(18x^4 - 171x^3 + 3006x^2 + 3502x + 775\right) \\
& \times H_0 - \frac{128}{3645}\frac{x-1}{x}\left(108x^4 - 918x^3 - 13889x^2 + 145x - 3035\right) + \frac{64}{405}\left(6x^5 - 60x^4 + 30x^3\right. \\
& + 630x^2 - 985x + 320\right)H_0^2 - \frac{128}{81}\left(6x^2 + 4x - 5\right)H_0^3 + \frac{64}{27}(x+1)H_0^4 + \left(\frac{64}{405}\frac{x-1}{x}\left(12x^4\right.\right.
\end{aligned}
$$

$$-102x^3 - 698x^2 - 255x - 290\Big) + \frac{64}{135}\frac{x-1}{x}\Big(4x^5 - 36x^4 - 16x^3 - 156x^2 - 431x$$

$$-100\Big)H_0\Big)H_1 + \Big(-\frac{32}{9}\frac{x-1}{x}\Big(4x^2 + 7x + 4\Big)H_0 - \frac{32}{405}\frac{x-1}{x}\Big(12x^5 - 108x^4 - 48x^3$$

$$+172x^2 - 2183x - 200\Big)\Big)H_1^2 + \Big(\frac{128}{9}\frac{x-1}{x}\Big(4x^2 + 7x + 4\Big)H_1 - \frac{256}{405}\frac{1}{x}\Big(6x^6 - 60x^5$$

$$+30x^4 - 1030x^2 + 122x + 75\Big) + \frac{128}{9}\Big(2x^2 + 11x + 8\Big)H_0\Big)H_{0,1} - \frac{128}{3}(x+1)H_{0,1}^2$$

$$-\frac{128}{27}\Big(6x^2 + 62x + 53\Big)H_{0,0,1} + \Big(-\frac{128}{27}\frac{3x-1}{x}\Big(4x^2 + 19x + 18\Big) + \frac{128}{3}(x+1)H_0\Big)H_{0,1,1}$$

$$-\frac{256}{9}(x+1)H_{0,0,0,1} + \frac{128}{9}(x+1)H_{0,0,1,1} + \frac{128}{9}(x+1)H_{0,1,1,1} + \Big(-\frac{32}{3}\frac{x-1}{x}\Big(4x^2$$

$$+7x + 4\Big)H_1 + \frac{32}{405}\frac{1}{x}\Big(24x^6 - 240x^5 + 120x^4 + 2250x^3 - 7265x^2 - 1145x - 600\Big)$$

$$-\frac{32}{27}\Big(60x^2 + 127x + 37\Big)H_0 + \frac{224}{9}(x+1)H_0^2 + 64(x+1)H_{0,1}\Big)\zeta_2 + \Big(\frac{64}{27}\frac{1}{x}\Big(64x^3$$

$$+251x^2 + 155x - 64\Big) - 128(x+1)H_0\Big)\zeta_3 - \frac{128}{3}(x+1)\zeta_4\Bigg]$$

$$+C_F^2 T_F\Bigg[\frac{2}{27}\frac{x-1}{x}\Big(4x^2 + 7x + 4\Big)H_1^4 - \frac{8}{81}\frac{x-1}{x}\Big(5400x^2 + 3811x + 4614\Big)$$

$$+\frac{4}{81}\Big(4376x^3 + 5311x^2 - 9879x + 840\Big)\frac{H_0^2}{1-x} + \frac{4}{81}\Big(11500x^2 - 1187x + 3989\Big)H_0$$

$$-\frac{2}{27}\Big(704x^2 - 313x + 151\Big)H_0^3 + \frac{4}{27}\Big(76x^2 + 15x + 33\Big)H_0^4 - \frac{6}{5}(x+1)H_0^5$$

$$+\Big(-\frac{80}{27}\frac{x-1}{x}\Big(4x^2 + 7x + 4\Big)H_0^3 + \frac{16}{81}\frac{x-1}{x}\Big(67x^2 - 1320x - 1490\Big) + \frac{4}{27}\frac{x-1}{x}\Big(904x^2$$

$$+2683x - 392\Big)H_0^2 - \frac{16}{81}\frac{x-1}{x}\Big(1312x^2 + 4357x - 722\Big)H_0\Big)H_1 + \Big(-\frac{16}{9}\frac{x-1}{x}\Big(4x^2$$

$$+7x + 4\Big)H_0^2 - \frac{8}{27}\frac{x-1}{x}\Big(122x^2 - 55x - 40\Big)H_0 + \frac{8}{81}\frac{x-1}{x}\Big(913x^2 + 3928x - 320\Big)\Big)$$

$$\times H_1^2 + \Big(-\frac{x-1}{x}\frac{16}{27}\Big(4x^2 + 7x + 4\Big)H_0 + \frac{x-1}{x}\frac{4}{27}\Big(40x^2 + 41x + 4\Big)\Big)H_1^3$$

$$+\Big(-\frac{32}{3}\frac{x-1}{x}\Big(4x^2 + 7x + 4\Big)H_1^2 - \frac{16}{9}\frac{1}{x}\Big(4x^3 + 225x^2 + 54x + 20\Big)H_0^2 - \frac{16}{27}\frac{1}{x}\Big(882x^3$$

$$+1527x^2 - 2364x + 196\Big)H_0 + \frac{16}{81}\frac{1}{x}\Big(3293x^3 + 8316x^2 - 5229x + 722\Big)$$

$$+\frac{160}{9}(x+1)H_0^3 + \Big(-\frac{448}{9}\frac{x-1}{x}\Big(4x^2 + 7x + 4\Big)H_0 + \frac{64}{9}\frac{1}{x}\Big(2x^3 - 102x^2 + 102x - 11\Big)\Big)$$

$$\times H_1\Big)H_{0,1} + \Big(-\frac{16}{9}\frac{1}{x}\Big(104x^3 - 39x^2 - 105x - 56\Big) + \frac{448}{3}(x+1)H_0\Big)H_{0,1}^2$$

$$+\Big(\frac{896}{9}\frac{x-1}{x}\Big(4x^2 + 7x + 4\Big)H_1 - \frac{32}{9}\frac{1}{x}\Big(28x^3 - 537x^2 - 123x - 20\Big)H_0 + \frac{8}{27}\frac{1}{x}\Big(1652x^3$$

$$+3273x^2 - 7665x + 392\Big) - 48(x+1)H_0^2 - \frac{1792}{3}(x+1)H_{0,1}\Big)H_{0,0,1} + \Big(\frac{608}{9}\frac{x-1}{x}\Big(4x^2$$

$$+7x + 4\Big)H_1 + \frac{32}{3}\frac{1}{x}\Big(36x^3 + 23x^2 - 32x - 40\Big)H_0 + \frac{32}{27}\frac{1}{x}\Big(209x^3 + 1743x^2 - 1572x$$

$$+ 152) + \frac{64}{3}(x+1)H_0^2 + 128(x+1)H_{0,1}\bigg)H_{0,1,1} + \bigg(\frac{32}{9}\frac{1}{x}\big(156x^3 - 876x^2 - 255x - 20\big)$$

$$+ \frac{640}{3}(x+1)H_0\bigg)H_{0,0,0,1} + \bigg(\frac{32}{9}\frac{1}{x}\big(8x^3 - 372x^2 - 81x + 120\big) - \frac{1792}{3}(x+1)H_0\bigg)$$

$$\times H_{0,0,1,1} + \bigg(-\frac{16}{9}\frac{1}{x}\big(300x^3 + 243x^2 - 219x - 304\big) + \frac{64}{3}(x+1)H_0\bigg)H_{0,1,1,1} - \frac{2560}{3}$$

$$\times (x+1)H_{0,0,0,0,1} + 3392(x+1)H_{0,0,0,1,1} + \frac{4288}{3}(x+1)H_{0,0,1,0,1} - 832(x+1)H_{0,0,1,1,1}$$

$$- \frac{1600}{3}(x+1)H_{0,1,0,1,1} - \frac{32}{3}(x+1)H_{0,1,1,1,1} + \bigg(\frac{124}{9}\frac{x-1}{x}\big(4x^2 + 7x + 4\big)H_1^2 - \frac{4}{81}\frac{1}{x}$$

$$\times \big(8896x^3 + 21003x^2 + 129x - 1620\big) + \frac{2}{9}\big(1536x^2 + 1879x + 1943\big)H_0 - \frac{8}{9}\big(68x^2 + 99x$$

$$- 57\big)H_0^2 + \frac{188}{9}(x+1)H_0^3 + \bigg(\frac{112}{9}\frac{x-1}{x}\big(4x^2 + 7x + 4\big)H_0 + \frac{4}{27}\frac{1}{x}\big(752x^3 + 4197x^2$$

$$- 5169x + 652\big)\bigg)H_1 + \bigg(\frac{8}{9}\frac{1}{x}\big(196x^3 - 327x^2 - 213x + 56\big) - \frac{224}{3}(x+1)H_0\bigg)H_{0,1}$$

$$- \frac{608}{3}(x+1)H_{0,0,1} - \frac{496}{3}(x+1)H_{0,1,1}\bigg)\zeta_2 + \frac{1024}{3}\zeta_2 \ln^3(2)(x+1) + \bigg(-\frac{592}{9}\frac{x-1}{x}$$

$$\times \big(4x^2 + 7x + 4\big)H_1 - \frac{4}{27}\frac{1}{x}\big(2824x^3 - 4125x^2 - 17331x + 1938\big) - \frac{16}{3}\big(76x^2 - 275x$$

$$- 112\big)H_0 + \frac{920}{3}(x+1)H_0^2 + \frac{1184}{3}(x+1)H_{0,1}\bigg)\zeta_3 + 1792(x+1)\zeta_3 \ln^2(2)$$

$$+ \bigg(-\frac{896}{3}\frac{1}{x}\big(4x^3 - 9x^2 - 6x - 2\big) + 1792(x+1)H_0\bigg)\zeta_3 \ln(2) + \bigg(-\frac{4}{9}\frac{1}{x}\big(628x^3 - 3669x^2$$

$$- 351x + 540\big) + \frac{928}{3}(x+1)H_0\bigg)\zeta_4 + 1664(x+1)\zeta_4 \ln(2) + \bigg(-\frac{32}{3}\frac{1}{x}\big(8x^3 - 30x^2$$

$$- 15x - 2\big) + 128(x+1)H_0\bigg)B_4 + 256(x+1)B_4 \ln(2) + \frac{944}{3}(x+1)\zeta_2\zeta_3$$

$$- 3544(x+1)\zeta_5 + 4096(x+1)\mathrm{Li}_5\bigg(\frac{1}{2}\bigg) - \frac{512}{15}\ln^5(2)(x+1)\bigg]$$

$$+ C_A C_F T_F\bigg[-\frac{2}{27}\frac{x-1}{x}\big(4x^2 + 7x + 4\big)H_1^4 - \frac{16}{9}\frac{x+1}{x}\big(32x^2 + 61x + 32\big)[H_{0,-1,-1,1}$$

$$+ H_{0,-1,1,-1} + H_{0,1,-1,-1}] - \frac{8}{729}\frac{x-1}{x}\big(1024228x^2 - 83309x + 274870\big) + \bigg(-\frac{112}{27}\frac{x+1}{x}$$

$$\times \big(4x^2 - 7x + 4\big)H_{-1}^3 + \frac{32}{27}\frac{x+1}{x}\big(188x^2 - 83x + 80\big)H_{-1}^2 - \frac{8}{27}\frac{x+1}{x}\big(4200x^2 - 1577x$$

$$+ 1236\big)H_{-1} + \frac{4}{243}\frac{1}{x}\big(503464x^3 + 110993x^2 + 171290x + 20992\big)\bigg)H_0 + \bigg(-\frac{2}{3}\frac{x+1}{x}$$

$$\times \big(40x^2 - 37x + 40\big)H_{-1}^2 + \frac{4}{27}\frac{1}{x}\big(202x^3 - 18x^2 + 9x + 256\big)H_{-1}\bigg)H_0^2 + \frac{4}{81}\frac{1}{(x+1)}$$

$$\times \big(22712x^4 - 5914x^3 - 9627x^2 + 5671x - 13652\big)\frac{H_0^2}{1-x} + \bigg(\frac{4}{81}\big(1290x^2 + 1213x + 1045\big)$$

$$+ \frac{28}{9}\frac{x+1}{x}\big(8x^2 - 11x + 8\big)H_{-1}\bigg)H_0^3 + \frac{2}{27}\big(95x - 172\big)H_0^4 - \frac{4}{15}\big(4x - 5\big)H_0^5 + \bigg(\frac{4}{27}\frac{x-1}{x}$$

$$\times \left(152x^2 + 203x + 152\right) H_0^3 - \frac{4}{243} \frac{x-1}{x} \left(6776x^2 + 15425x - 11926\right) + \frac{8}{81} \frac{x-1}{x} \left(21512x^2\right.$$

$$\left. - 1057x + 7436\right) H_0 - \frac{4}{9} \frac{1}{x} \left(936x^3 - 640x^2 + 379x - 684\right) H_0^2\right) H_1 + \left(-\frac{2}{9} \frac{x-1}{x} \left(136x^2\right.\right.$$

$$\left. + 283x + 136\right) H_0^2 + \frac{8}{27} \frac{x-1}{x} \left(481x^2 + 340x + 184\right) H_0 - \frac{4}{81} \frac{x-1}{x} \left(1754x^2 + 4169x\right.$$

$$\left.\left. - 658\right)\right) H_1^2 + \left(\frac{64}{27} \frac{x-1}{x} \left(4x^2 + 7x + 4\right) H_0 - \frac{4}{81} \frac{x-1}{x} \left(154x^2 + 163x + 46\right)\right) H_1^3$$

$$+ \left(-\frac{32}{9} \frac{x-1}{x} \left(4x^2 - 11x + 4\right) H_0 H_1 + \frac{112}{9} \frac{x+1}{x} \left(4x^2 - 7x + 4\right) H_{-1}^2 - \frac{64}{27} \frac{x+1}{x} \left(188x^2\right.\right.$$

$$\left. - 83x + 80\right) H_{-1} + \frac{8}{27} \frac{x+1}{x} \left(4200x^2 - 1577x + 1236\right) - \frac{4}{9} \frac{1}{x} \left(112x^3 - 27x^2 - 57x\right.$$

$$\left.\left. + 168\right) H_0^2 + \left(-\frac{8}{9} \frac{x+1}{x} \left(40x^2 - 151x + 40\right) H_{-1} + \frac{8}{27} \frac{1}{x} \left(1102x^3 - 2154x^2 + 765x - 256\right)\right)\right.$$

$$\left.\times H_0 + \frac{280}{9} (x-1) H_0^3\right) H_{0,-1} + \left(-\frac{8}{9} \frac{1}{x} \left(8x^3 + 81x^2 - 87x + 80\right) - \frac{152}{3} (x-1) H_0\right) H_{0,-1}^2$$

$$+ \left(-\frac{8}{9} \frac{x+1}{x} \left(32x^2 + 61x + 32\right) H_{-1}^2 - \frac{16}{27} \frac{1}{x} \left(82x^3 - 78x^2 - 267x - 80\right) H_{-1} - \frac{4}{9} \frac{1}{x} \left(144x^3\right.\right.$$

$$\left. - 555x^2 - 471x - 344\right) H_0^2 - \frac{8}{81} \frac{1}{x(x+1)} \left(20970x^4 + 2819x^3 - 10430x^2 + 857x - 6540\right)$$

$$+ \left(\frac{8}{9} \frac{1}{x} \left(154x^3 - 1068x^2 - 217x - 844\right) + 64 \frac{(x+1)}{x} \left(2x^2 - 3x + 2\right) H_{-1}\right) H_0$$

$$- \frac{248}{9} (x+1) H_0^3 + \left(\frac{8}{9} \frac{x-1}{x} \left(184x^2 + 349x + 184\right) H_0 - \frac{16}{27} \frac{1}{x} \left(167x^3 - 711x^2 + 657x\right.\right.$$

$$\left.\left. - 140\right)\right) H_1 + \left(-\frac{32}{9} \frac{x-1}{x} \left(4x^2 - 11x + 4\right) - \frac{64}{3} (x+1) H_0\right) H_{0,-1}\right) H_{0,1} + \left(\frac{4}{9} \frac{1}{x} \left(224x^3\right.\right.$$

$$\left. - 201x^2 - 105x - 112\right) - \frac{392}{3} (x+1) H_0\right) H_{0,1}^2 + \left(-\frac{224}{9} \frac{x+1}{x} \left(4x^2 - 7x + 4\right) H_{-1}\right.$$

$$+ \frac{64}{27} \frac{x+1}{x} \left(188x^2 - 83x + 80\right) + \frac{8}{9} \frac{1}{x} \left(56x^3 + 51x^2 - 285x + 200\right) H_0 - \frac{152}{3} (x-1) H_0^2$$

$$+ \frac{448}{3} (x-1) H_{0,-1}\right) H_{0,-1,-1} + \left(\frac{16}{9} \frac{x+1}{x} \left(32x^2 + 61x + 32\right) H_{-1} - \frac{32}{9} \frac{1}{x} \left(32x^3 - 3x^2\right.\right.$$

$$\left. - 33x + 40\right) H_0 + \frac{16}{27} \frac{1}{x} \left(82x^3 - 78x^2 - 267x - 80\right)\right) H_{0,-1,1} + \left(\frac{64}{9} \frac{x-1}{x} \left(4x^2 - 11x\right.\right.$$

$$\left. + 4\right) H_1 + \frac{8}{9} \frac{x+1}{x} \left(200x^2 - 413x + 200\right) H_{-1} - \frac{8}{3} \frac{1}{x} \left(8x^3 - 9x^2 + 27x - 56\right) H_0$$

$$- \frac{8}{27} \frac{1}{x} \left(2406x^3 - 4326x^2 + 1539x - 256\right) - \frac{32}{3} (15x - 17) H_0^2 + 304(x-1) H_{0,-1}$$

$$+ \frac{128}{3} (x+1) H_{0,1}\right) H_{0,0,-1} + \left(-\frac{8}{3} \frac{x+1}{x} \left(88x^2 - 169x + 88\right) H_{-1} - \frac{8}{9} \frac{x-1}{x} \left(296x^2\right.\right.$$

$$\left. + 491x + 296\right) H_1 + \frac{8}{9} \frac{1}{x} \left(136x^3 - 1605x^2 - 591x - 536\right) H_0 + \frac{8}{27} \frac{1}{x} \left(1936x^3 + 3913x^2\right.$$

$$\left. + 3019x + 3012\right) + \frac{16}{3} (69x + 25) H_0^2 - \frac{1136}{3} (x-1) H_{0,-1} + \frac{1136}{3} (x+1) H_{0,1}\right) H_{0,0,1}$$

$$+ \left(\frac{16}{9} \frac{x+1}{x} \left(32x^2 + 61x + 32\right) H_{-1} - \frac{32}{9} \frac{1}{x} \left(32x^3 - 3x^2 - 33x + 40\right) H_0 + \frac{16}{27} \frac{1}{x} \left(82x^3\right.\right.$$

$$- 78x^2 - 267x - 80\Big)\Big)H_{0,1,-1} + \Big(-\frac{176}{9}\frac{x-1}{x}\big(4x^2 + 7x + 4\big)H_1 - \frac{16}{9}\frac{1}{x}\big(148x^3 + 189x^2$$

$$- 45x - 140\big)H_0 - \frac{8}{27}\frac{1}{x}\big(356x^3 + 3725x^2 - 3469x + 272\big) + \frac{64}{9}\frac{x+1}{x}\big(2x^2 + x + 2\big)H_{-1}$$

$$+ 104(x+1)H_0^2\Big)H_{0,1,1} + \Big(\frac{224}{9}\frac{x+1}{x}\big(4x^2 - 7x + 4\big) - \frac{448}{3}(x-1)H_0\Big)H_{0,-1,-1,-1}$$

$$+ \Big(\frac{8}{9}\frac{1}{x}\big(136x^3 - 183x^2 - 75x + 104\big) + \frac{64}{3}(9x - 7)H_0\Big)H_{0,-1,0,1}$$

$$- \frac{64(x+1)\big(2x^2 + x + 2\big)}{9x}H_{0,-1,1,1} + \Big(-\frac{8}{9}\frac{x+1}{x}\big(200x^2 - 413x + 200\big) + 320(x-1)H_0\Big)$$

$$\times H_{0,0,-1,-1} + \Big(\frac{8}{3}\frac{x+1}{x}\big(88x^2 - 169x + 88\big) + \frac{128}{3}(x+1)H_0\Big)H_{0,0,-1,1} + \Big(\frac{8}{3}\frac{1}{x}\big(80x^3$$

$$- 33x^2 + 45x - 56\big) + \frac{1168}{3}(x-1)H_0\Big)H_{0,0,0,-1} + \Big(-\frac{16}{9}\frac{1}{x}\big(68x^3 - 1577x^2 - 260x - 364\big)$$

$$- 496(3x+1)H_0\Big)H_{0,0,0,1} + \Big(\frac{8}{3}\frac{x+1}{x}\big(88x^2 - 169x + 88\big) + \frac{128}{3}(x+1)H_0\Big)H_{0,0,1,-1}$$

$$+ \Big(\frac{16}{9}\frac{1}{x}\big(40x^3 + 617x^2 + 119x - 164\big) + \frac{16}{3}(35x + 37)H_0\Big)H_{0,0,1,1}$$

$$- \frac{64}{9}\frac{x+1}{x}\big(2x^2 + x + 2\big)[H_{0,1,-1,1} + H_{0,1,1,-1}] + \Big(\frac{16}{9}\frac{1}{x}\big(104x^3 + 101x^2 - 64x - 104\big)$$

$$- \frac{256}{3}(x+1)H_0\Big)H_{0,1,1,1} + \frac{160}{3}(x-1)H_{0,-1,-1,0,1} - \frac{896}{3}(x-1)H_{0,-1,0,-1,-1}$$

$$- \frac{1792}{3}(x-1)H_{0,0,-1,-1,-1} - 624(x-1)H_{0,0,-1,0,-1} + \frac{32}{3}(33x - 41)H_{0,0,-1,0,1}$$

$$- 1872(x-1)H_{0,0,0,-1,-1} + 16(63x - 79)H_{0,0,0,-1,1} - 128(3x - 1)H_{0,0,0,0,-1} + \frac{16}{3}(411x$$

$$+ 197)H_{0,0,0,0,1} + 16(63x - 79)H_{0,0,0,1,-1} - \frac{16}{3}(341x + 347)H_{0,0,0,1,1} + \frac{16}{3}(63x$$

$$- 79)H_{0,0,1,0,-1} - \frac{32}{3}(68x + 67)H_{0,0,1,0,1} + 160(x+1)H_{0,0,1,1,1} + \frac{352}{3}(x+1)H_{0,1,0,1,1}$$

$$+ \frac{32}{3}(x+1)H_{0,1,1,1,1} + \Big(\frac{16}{9}\frac{x+1}{x}\big(2x^2 + 55x + 2\big)H_{-1}^2 - \frac{20}{9}\frac{x-1}{x}\big(4x^2 + 7x + 4\big)H_1^2$$

$$+ \frac{16}{27}\frac{1}{x}\big(458x^3 + 132x^2 - 273x + 80\big)H_{-1} - \frac{8}{81}\frac{1}{x(x+1)}\big(5729x^4 + 3096x^3 + 1145x^2$$

$$+ 4805x + 703\big) + \Big(-\frac{8}{9}\frac{x+1}{x}\big(148x^2 - 97x + 148\big)H_{-1} + \frac{4}{27}\frac{1}{x}\big(1318x^3 - 2183x^2$$

$$- 275x + 240\big)\Big)H_0 + \frac{4}{9}\big(8x^2 + 23x - 211\big)H_0^2 - \frac{16}{9}(5x - 4)H_0^3 + \Big(-\frac{4}{27}\frac{1}{x}\big(214x^3$$

$$+ 3147x^2 - 3579x + 326\big) - \frac{32(x-1)\big(x^2 + x + 1\big)H_0}{3x}\Big)H_1 + \Big(\frac{8}{9}\frac{1}{x}\big(76x^3 + 135x^2$$

$$- 21x + 148\big) - \frac{304}{3}(x-1)H_0\Big)H_{0,-1} + \Big(-\frac{8}{3}\frac{1}{x}\big(32x^3 - 124x^2 - 55x + 24\big)$$

$$+ \frac{32}{3}(x+1)H_0\Big)H_{0,1} - 128(x-1)H_{0,-1,-1} + \frac{544}{3}(x-1)H_{0,0,-1} + \frac{16}{3}(7x + 3)H_{0,0,1}$$

$$+ \frac{80}{3}(x+1)H_{0,1,1}\Big)\zeta_2 - \frac{512}{3}(x+1)\zeta_2 \ln^3(2) + \Big(\frac{8}{9}\frac{x-1}{x}\big(88x^2 + 235x + 88\big)H_1$$

5. Pure-singlet contributions to DIS

$$
\begin{aligned}
&- \frac{16}{9}\frac{1}{x}\left(52x^3 + 819x^2 - 144x + 28\right)H_0 - \frac{4}{27}\frac{1}{x}\left(4612x^3 + 15262x^2 + 8524x + 2559\right)\\
&+ \frac{16(x-4)(x+1)(4x-1)H_{-1}}{x} + \frac{64}{3}(5x-6)H_0^2 + \frac{608}{3}(x-1)H_{0,-1} - \frac{496}{3}(x+1)\\
&\times H_{0,1}\Big)\zeta_3 - 896(x+1)\zeta_3\ln^2(2) + \left(\frac{448}{3}\frac{1}{x}\left(4x^3 - 9x^2 - 6x - 2\right) - 896(x+1)H_0\right)\\
&\times \zeta_3\ln(2) + \left(-\frac{2}{9}\frac{1}{x}\left(1752x^3 + 11325x^2 + 1401x + 1828\right) - \frac{76}{3}(17x-15)H_0\right)\zeta_4\\
&- 832(x+1)\zeta_4\ln(2) + \left(\frac{16}{3}\frac{1}{x}\left(8x^3 - 30x^2 - 15x - 2\right) - 64(x+1)H_0\right)B_4\\
&- 128(x+1)B_4\ln(2) + \frac{8}{3}(31x-127)\zeta_2\zeta_3 - 12(47x-145)\zeta_5 - 2048\,\mathrm{Li}_5\left(\frac{1}{2}\right)(x+1)\\
&+ \frac{256}{15}(x+1)\ln^5(2)\Bigg]
\end{aligned}
\tag{5.63}
$$

and

$$
\begin{aligned}
&a_{Qq}^{\mathrm{PS,b},(3)}(x) =\\
&\quad C_F T_F\left(\frac{C_A}{2} - C_F\right)\Bigg[-64(x+1)H_0^2\tilde{H}_{0,-1,-1} + \frac{64}{3}\frac{x-1}{x}\left(4x^2 + 7x + 4\right)H_1\tilde{H}_{0,-1,-1}\\
&\quad + \frac{16}{3}\frac{1}{x}\left(32x^3 + 200x^2 - 104x + 1\right)\tilde{H}_{0,-1,-1} + \frac{64}{3}\left(4x^2 - 21x - 9\right)H_0\tilde{H}_{0,-1,-1}\\
&\quad - 128(x+1)H_{0,1}\tilde{H}_{0,-1,-1} + \left(-\frac{64}{3}\frac{x-1}{x}\left(4x^2 + 7x + 4\right)H_1 - \frac{16}{3}\frac{1}{x}\left(32x^3 + 200x^2\right.\right.\\
&\quad \left.- 104x + 1\right) - \frac{64}{3}\left(4x^2 - 21x - 9\right)H_0 + 64(x+1)H_0^2 + 128(x+1)H_{0,1}\Big)\tilde{H}_{0,-1,1}\\
&\quad + \left(\frac{64}{3}\frac{x-1}{x}\left(4x^2 + 7x + 4\right)H_1 + \frac{16}{3}\frac{1}{x}\left(32x^3 + 200x^2 - 104x + 1\right) + \frac{64}{3}\left(4x^2 - 21x\right.\right.\\
&\quad \left.- 9\right)H_0 - 64(x+1)H_0^2 - 128(x+1)H_{0,1}\Big)\tilde{H}_{0,1,-1} + \left(-\frac{64}{3}\frac{x-1}{x}\left(4x^2 + 7x + 4\right)H_1\right.\\
&\quad - \frac{16}{3}\frac{1}{x}\left(32x^3 + 200x^2 - 104x + 1\right) - \frac{64}{3}\left(4x^2 - 21x - 9\right)H_0 + 64(x+1)H_0^2 + 128(x+1)\\
&\quad \times H_{0,1}\Big)\tilde{H}_{0,1,1} + \left(\frac{64(x-1)\left(4x^2 + 7x + 4\right)}{x} - 384(x+1)H_0\right)\tilde{H}_{0,-1,-1,-1} + \left(-\frac{64}{3}\frac{1}{x}\right.\\
&\quad \times \left(4x^3 + 27x^2 + 3x - 8\right) + 128(x+1)H_0\Big)\tilde{H}_{0,-1,-1,1} + \left(\frac{64}{3}\left(4x^2 - 21x - 9\right)\right.\\
&\quad - 128(x+1)H_0\Big)\tilde{H}_{0,-1,1,-1} + \left(-\frac{64}{3}\frac{1}{x}\left(12x^3 - 39x^2 - 21x - 4\right) + 384(x+1)H_0\right)\\
&\quad \times \tilde{H}_{0,-1,1,1} + \left(\frac{64}{3}\frac{1}{x}\left(12x^3 - 15x^2 - 15x - 8\right) - 384(x+1)H_0\right)\tilde{H}_{0,1,-1,-1} + \left(-\frac{64}{3}\frac{1}{x}\right.\\
&\quad \times (x-1)\left(4x^2 + 7x + 4\right) + 128(x+1)H_0\Big)\tilde{H}_{0,1,-1,1} + \left(\frac{64}{3}\frac{1}{x}\left(4x^3 - 45x^2 - 15x + 4\right)\right.\\
&\quad - 128(x+1)H_0\Big)\tilde{H}_{0,1,1,-1} + \left(-64\left(4x^2 - 21x - 9\right) + 384(x+1)H_0\right)\tilde{H}_{0,1,1,1}\\
&\quad - 384(x+1)\tilde{H}_{0,-1,-1,-1,1} - 256(x+1)\tilde{H}_{0,-1,-1,1,-1} + 384(x+1)\tilde{H}_{0,-1,-1,1,1}\\
&\quad - 128(x+1)\tilde{H}_{0,-1,1,-1,-1} - 384(x+1)\tilde{H}_{0,-1,1,1,-1} + 768(x+1)\tilde{H}_{0,-1,1,1,1}
\end{aligned}
$$

$$- 384(x+1)\tilde{H}_{0,1,-1,-1,1} - 256(x+1)\tilde{H}_{0,1,-1,1,-1} + 384(x+1)\tilde{H}_{0,1,-1,1,1}$$

$$- 128(x+1)\tilde{H}_{0,1,1,-1,-1} - 384(x+1)\tilde{H}_{0,1,1,1,-1} + 768(x+1)\tilde{H}_{0,1,1,1,1} + 64(x+1)$$

$$\times \left(\tilde{H}_{0,-1,-1} - \tilde{H}_{0,-1,1} + \tilde{H}_{0,1,-1} - \tilde{H}_{0,1,1} \right) \zeta_2 - 128(x+1)\left(\tilde{H}_{0,-1} + \tilde{H}_{0,1} \right) \zeta_2 \ln(2)$$

$$+ \left(-\frac{128}{3}\frac{x-1}{x}\left(4x^2 + 7x + 4 \right) H_1 \tilde{H}_{0,-1} - \frac{32}{3}\frac{1}{x}\left(32x^3 + 200x^2 - 104x + 1 \right) \tilde{H}_{0,-1} \right.$$

$$- \frac{128}{3}\left(4x^2 - 21x - 9 \right) H_0 \tilde{H}_{0,-1} + 128(x+1)H_0^2 \tilde{H}_{0,-1} + \left(-\frac{128}{3}\frac{x-1}{x}\left(4x^2 + 7x \right. \right.$$

$$\left. + 4 \right) H_1 - \frac{32}{3}\frac{1}{x}\left(32x^3 + 200x^2 - 104x + 1 \right) - \frac{128}{3}\left(4x^2 - 21x - 9 \right) H_0 + 128(x+1)H_0^2 \right) \tilde{H}_{0,1}$$

$$+ \left(256(x+1)\tilde{H}_{0,-1} + 256(x+1)\tilde{H}_{0,1} \right) H_{0,1} + \left(-\frac{128}{3}\frac{1}{x}\left(8x^3 + 18x^2 - 3x - 10 \right) \right.$$

$$\left. + 512(x+1)H_0 \right) \tilde{H}_{0,-1,-1} + \left(-\frac{128}{3}\frac{1}{x}\left(8x^3 - 30x^2 - 15x - 2 \right) + 512(x+1)H_0 \right) \tilde{H}_{0,-1,1}$$

$$+ \left(-\frac{128}{3}\frac{1}{x}\left(8x^3 - 6x^2 - 9x - 6 \right) + 512(x+1)H_0 \right) \tilde{H}_{0,1,-1} + \left(-\frac{128}{3}\frac{1}{x}\left(8x^3 - 54x^2 \right. \right.$$

$$\left. - 21x + 2 \right) + 512(x+1)H_0 \right) \tilde{H}_{0,1,1} - 384(x+1)\tilde{H}_{0,-1,-1,-1} + 640(x+1)\tilde{H}_{0,-1,-1,1}$$

$$+ 128(x+1)\tilde{H}_{0,-1,1,-1} + 1152(x+1)\tilde{H}_{0,-1,1,1} - 384(x+1)\tilde{H}_{0,1,-1,-1} + 640(x+1)\tilde{H}_{0,1,-1,1}$$

$$\left. + 128(x+1)\tilde{H}_{0,1,1,-1} + 1152(x+1)\tilde{H}_{0,1,1,1} \right) \ln(2) + \left(\frac{256\left(12x^2 + 3x - 2 \right)}{3x}[\tilde{H}_{0,-1} + \tilde{H}_{0,1}] \right.$$

$$\left. \left. + 512(x+1)[\tilde{H}_{0,-1,-1} + \tilde{H}_{0,-1,1} + \tilde{H}_{0,1,-1} + \tilde{H}_{0,1,1}] \right) \ln^2(2) \right]. \tag{5.64}$$

Beyond the HPLs that contributed to the anomalous dimension, cf. Eq. (5.21), here also the following HPLs occur

$$H_{0,-1,-1,-1}, H_{0,-1,-1,1}, H_{0,-1,0,1}, H_{0,-1,1,-1}, H_{0,-1,1,1}, H_{0,0,-1,-1}, H_{0,0,-1,1},$$
$$H_{0,0,1,-1}, H_{0,1,-1,-1}, H_{0,1,-1,1}, H_{0,1,1,-1}, H_{0,-1,-1,0,1}, H_{0,-1,0,-1,-1}, H_{0,0,-1,-1,-1},$$
$$H_{0,0,-1,0,-1}, H_{0,0,-1,0,1}, H_{0,0,0,-1,-1}, H_{0,0,0,-1,1}, H_{0,0,0,0,-1}, H_{0,0,0,0,1}, H_{0,0,0,1,-1},$$
$$H_{0,0,0,1,1}, H_{0,0,1,0,-1}, H_{0,0,1,0,1}, H_{0,0,1,1,1}, H_{0,1,0,1,1}, H_{0,1,1,1,1}, \tag{5.65}$$

along with a number of HPLs evaluated at $1 - 2x$,

$$\tilde{H}_{0,-1}, \tilde{H}_{0,1}, \tilde{H}_{0,-1,-1}, \tilde{H}_{0,-1,1}, \tilde{H}_{0,1,-1}, \tilde{H}_{0,1,1}, \tilde{H}_{0,-1,-1,-1}, \tilde{H}_{0,-1,-1,1}, \tilde{H}_{0,-1,1,-1},$$
$$\tilde{H}_{0,-1,1,1}, \tilde{H}_{0,1,-1,-1}, \tilde{H}_{0,1,-1,1}, \tilde{H}_{0,1,1,-1}, \tilde{H}_{0,1,1,1}, \tilde{H}_{0,-1,-1,-1,1}, \tilde{H}_{0,-1,-1,1,-1},$$
$$\tilde{H}_{0,-1,-1,1,1}, \tilde{H}_{0,-1,1,-1,-1}, \tilde{H}_{0,-1,1,1,-1}, \tilde{H}_{0,-1,1,1,1}, \tilde{H}_{0,1,-1,-1,1}, \tilde{H}_{0,1,-1,1,-1},$$
$$\tilde{H}_{0,1,-1,1,1}, \tilde{H}_{0,1,1,-1,-1}, \tilde{H}_{0,1,1,1,-1}, \tilde{H}_{0,1,1,1,1}. \tag{5.66}$$

While $a_{Qq}^{\mathrm{PS,a},(3)}$ and $a_{Qq}^{\mathrm{PS,b},(3)}$ individually take on non-vanishing values for $x = 1$, their sum cancels exactly. Moreover, $a_{Qq}^{\mathrm{PS,b},(3)}$ vanishes at $x = 1/2$.

Before moving on to the renormalisation of the OME, we would like to discuss the behaviour of the constant term for small and large values of x. Since the pure-singlet OME does not contain any distributions, like $\delta(1 - x)$ or plus distributions, the limits $x \to 0$ and $x \to 1$ can be taken
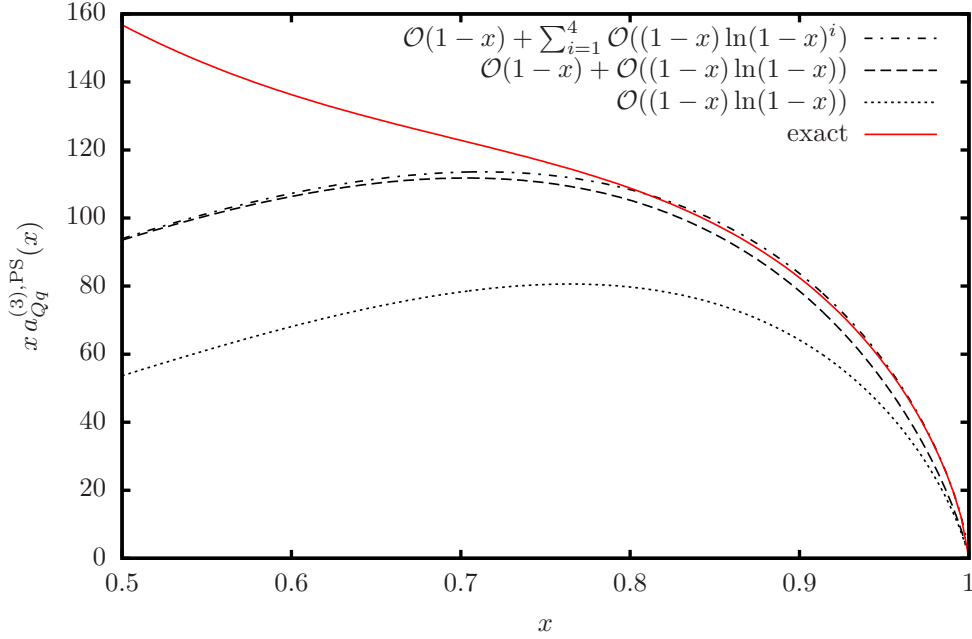
Figure 5.2.: Large x behaviour of $xa_{Qq}^{\mathrm{PS},(3)}(x)$ compared to different terms of its expansion around $x = 1$. The red, solid line depicts the exact result, while the dotted line gives the numerically leading term of the expansion. The dashed line includes also the numerically next to leading term and the dash-dotted line shows all terms of the form $(1 - x) \ln^k(1 - x)$.

directly in x space. For $x \to 1$ we get

$$a_{Qq}^{\mathrm{PS},(3)}(x) \underset{x \to 1}{\propto} C_F T_F (1-x) \left\{ \frac{2}{9}(C_A - C_F) \ln^4(1-x) \right.$$

$$\left. - \frac{4}{27}(23C_A - 21C_F + 4(2 - N_F)T_F) \ln^3(1-x) \right\} + \mathcal{O}\big((1-x)\ln^2(1-x)\big)$$

$$\propto (1-x) \Big[0.24691358 \ln^4(1-x) + (-4.44444444 + 0.19753086\, N_F) \ln^3(1-x)$$

$$+ (-2.28230742 + 0.98765432\, N_F) \ln^2(1-x)$$

$$+ (-357.426943 + 15.9385086\, N_F) \ln(1-x) + 116.478169 + 14.3167889\, N_F \Big]$$

$$+ \mathcal{O}\big((1-x)^2 \ln^3(1-x)\big). \tag{5.67}$$

For the numerical values we use the QCD values of the colour factors for $\mathrm{SU}(3)_\mathrm{c}$. We illustrate the contributions of terms of the form $(1 - x) \ln^k(1 - x)$ for k up to 4 in comparison to the exact function in Fig. 5.2. Formally, the $k = 4$ term dominates close to $x = 1$, but the large disparity of the numerical coefficients entails that it starts to be the largest contribution only very close to $x = 1$. With $N_F = 3$ this happens for $x \gtrsim 1 - 10^{-7}$. As it turns out, the $k = 1$ term is numerically most relevant, followed by the $k = 0$ term for values of x up to 0.99.

The expansion around $x = 0$ yields

$$a_{Qq}^{\mathrm{PS},(3)}(x) \underset{x \to 0}{\propto} \frac{64}{243} C_F T_F C_A \left[1312 + 135\zeta_2 - 189\zeta_3 \right] \frac{\ln(x)}{x}$$
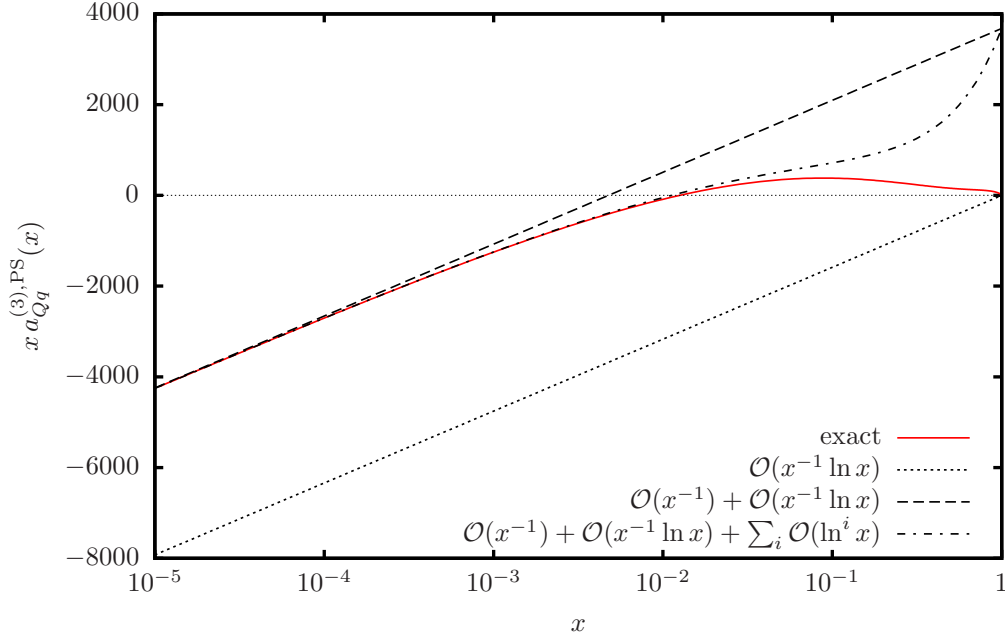
Figure 5.3.: Small x behaviour of $xa_{Qq}^{\mathrm{PS},(3)}(x)$ compared to different terms of the expansion of the OME. The red, solid line shows the exact expression and the dotted line illustrates the formally leading term $\propto \ln(x)/x$. Including the $\mathcal{O}(x^{-1})$ term yields the dashed line and the dash-dotted line also includes the logarithmic terms of the expansion.

$$
\begin{aligned}
&+ \left[C_F T_F C_A \left(\frac{2198960}{729} + \frac{64}{3} B_4 - \frac{5600}{9} \zeta_4 - \frac{3496}{9} \zeta_3 - \frac{5624}{81} \zeta_2 \right) \right.\\
&+ C_F^2 T_F \left(\frac{12304}{27} - \frac{128}{3} B_4 + 192 \zeta_4 - \frac{2416}{9} \zeta_3 + 80 \zeta_2 \right)\\
&+ C_F T_F^2 \left(-\frac{77696}{729} - \frac{4096}{27} \zeta_3 - \frac{1280}{27} \zeta_2 \right)\\
&+ \left. C_F T_F^2 N_F \left(-\frac{111104}{729} + \frac{896}{27} \zeta_3 - \frac{320}{27} \zeta_2 \right) \right] \frac{1}{x} + \mathcal{O}\left(\ln^5(x) \right)\\
\propto\; &688.39630 \frac{\ln(x)}{x} + (3812.8990 - 44.003690 N_F) \frac{1}{x} + 1.6 \ln^5(x)\\
&+ (-20.345679 + 0.7901235 N_F) \ln^4(x) + (165.11455 + 2.6337449 N_F) \ln^3(x)\\
&+ (-604.63554 + 30.502827 N_F) \ln^2(x) + (3524.9967 + 33.908944 N_F) \ln(x)\\
&+ \mathcal{O}\left(x^0 \right) . \tag{5.68}
\end{aligned}
$$

We plot the asymptotic behaviour in this limit in Fig. 5.3. Again, the formally leading term of the small x limit $\propto \ln(x)/x$ does not give a good description of the OME at finite values of x. This has also been observed in other small x studies, see for example [436, 455]. Including the x^{-1} term improves the description up to $x \approx 5 \cdot 10^{-3}$, but becomes insufficient for larger values of x. Adding also the $\mathcal{O}\left(\ln^k(x) \right)$ terms for $k = 1, \ldots, 5$ extends the region where the small x expansion describes the OME up to $x \approx 2 \cdot 10^{-2}$.

The authors of [456] gave a prediction for the constant term using the small x limit and the fixed moments of the pure-singlet OME calculated in [203]. In Fig. 5.4 we compare the exact
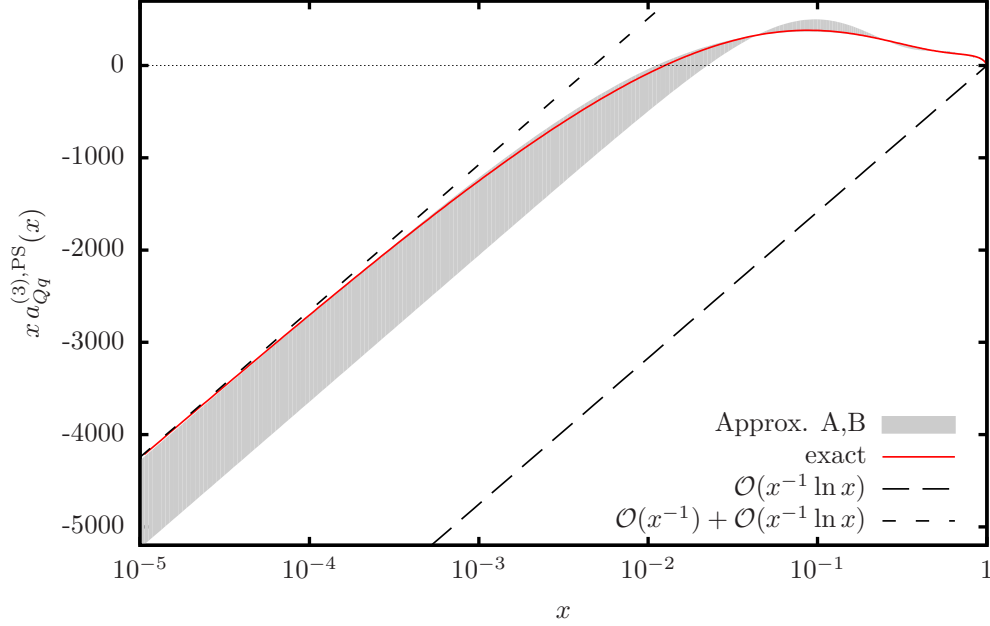
Figure 5.4.: Comparison of the prediction for $xa_{Qq}^{\mathrm{PS},(3)}(x)$ from [456], drawn as the shaded region, with the exact result which is given by the red, solid line. The dashed, black lines show the first terms of the small x expansion of the exact result.

result to the prediction of [456]. Our result is located at the edge of the range suggested by the prediction. For several values of x, the range of the prediction shrinks to a point which matches the exact result. This is enforced by the known fixed moments which were used in the prediction.

After applying the renormalisation and factorisation procedure outlined in [203], we arrive at the renormalised result in N space. Using the shorthands F and G defined in Eqs. (5.3) and (5.23), respectively, and denoting the logarithm of the scale ratio $L_M = \ln(m^2/\mu^2)$ the result reads

$$
\begin{aligned}
A_{Qq}^{\mathrm{PS}}(N) = a_s^2 C_F T_F & \left\{ -4F L_M^2 - L_M \frac{8(N^2 + 5N + 2)(5N^3 + 7N^2 + 4N + 4)}{(N-1)N^3(N+1)^3(N+2)^2} - 8F S_2 \right. \\
& \left. + \frac{4P_{218}}{(N-1)N^4(N+1)^4(N+2)^3} \right\} + a_s^3 \left\{ C_F T_F^2 \left[-L_M^3 \frac{128}{9} F + L_M^2 \left[\frac{32}{3} F S_1 \right. \right. \right. \\
& - \frac{32 P_{168}}{9(N-1)N^3(N+1)^2(N+2)^2} \right] + L_M \left[\frac{64 P_{209}}{9(N-1)N^3(N+1)^3(N+2)^2} S_1 \right. \\
& - \frac{64 P_{226}}{27(N-1)N^4(N+1)^4(N+2)^3} + \left(-\frac{32}{3} S_1^2 - 32 S_2 \right) F \right] \\
& + \frac{16}{27(N-1)N^3(N+1)^3(N+2)^2(N+3)(N+4)(N+5)} \left(P_{221} S_1^2 + P_{227} S_2 \right. \\
& - \frac{2 P_{235}}{3N(N+1)(N+2)} S_1 + \frac{2 P_{240}}{9N^2(N+1)^2(N+2)^2} \right) + \left(-\frac{16}{27} S_1^3 - \frac{208}{9} S_1 S_2 \right. \\
& \left. - \frac{32}{27} S_3 + \frac{128}{3} S_{2,1} - \frac{896}{9} \zeta_3 \right) F \right] + C_F N_F T_F^2 \left[-L_M^3 \frac{32}{9} F + L_M^2 \left[-\frac{32}{3} F S_1 \right. \right.
\end{aligned}
$$

$$+ \frac{32P_{209}}{9(N-1)N^3(N+1)^3(N+2)^2}\Bigg] + L_M\Bigg[\frac{32P_{159}}{9(N-1)N^3(N+1)^3(N+2)^2}S_1$$

$$- \frac{32P_{225}}{27(N-1)N^4(N+1)^4(N+2)^3} + \left(-\frac{16}{3}S_1^2 - \frac{80}{3}S_2\right)F\Bigg]$$

$$+ \frac{16}{27(N-1)N^3(N+1)^3(N+2)^2}\left(P_{159}S_1^2 + P_{211}S_2 - \frac{2P_{185}}{3N(N+1)(N+2)}S_1\right.$$

$$\left.+ \frac{2P_{236}}{9N^2(N+1)^2(N+2)^2}\right) + \left(-\frac{16}{27}S_1^3 - \frac{208}{9}S_1 S_2 - \frac{1184}{27}S_3 + \frac{256}{9}\zeta_3\right)F\Bigg]$$

$$+ C_F^2 T_F\Bigg[L_M^3 F\left[\frac{4\left(3N^2+3N+2\right)}{3N(N+1)} - \frac{16}{3}S_1\right] + L_M^2\left[\frac{4P_{202}}{N^2(N+1)^2}G + \left(16S_2\right.\right.$$

$$\left.\left.- \frac{8\left(5N^2+N-2\right)}{N(N+1)}S_1\right)F\right] + L_M\Bigg[-\frac{4\left(5N^3+4N^2+9N+6\right)}{N+1}S_1^2 G$$

$$- \frac{4P_{207}}{(N-1)N^3(N+1)^3(N+2)^2}S_2 + \frac{8P_{223}}{(N-1)N^4(N+1)^4(N+2)^3}S_1$$

$$- \frac{4P_{233}}{(N-1)N^5(N+1)^5(N+2)^3} + \left(\frac{8}{3}S_1^3 - 24S_1 S_2 - \frac{80}{3}S_3 + 32S_{2,1}\right.$$

$$\left.+ 96\zeta_3\right)F\Bigg] + \frac{4}{3(N-1)N^3(N+1)^3(N+2)^2}\left(8P_{212}S_{2,1} - \frac{2P_{217}}{3}S_3\right.$$

$$- \frac{2P_{219}}{N(N+1)(N+2)}S_1^2 + \frac{2P_{224}}{N(N+1)(N+2)}S_2 + \frac{P_{239}}{N^3(N+1)^3(N+2)^2}\right)$$

$$+ \left(\left(\frac{128}{9}S_3 - 32S_{2,1}\right)S_1 + \frac{4}{9}S_1^4 - \frac{8}{3}S_1^2 S_2 + \frac{52}{3}S_2^2 + \frac{88}{3}S_4 + \frac{224}{3}S_{2,1,1}\right.$$

$$+ 32S_{3,1} + \left(64S_3(2) - 64S_{1,2}(2,1) + 64S_{2,1}(2,1) - 64S_{1,1,1}(2,1,1)\right)S_1\left(\frac{1}{2}\right)$$

$$+ 64\left(-S_{1,3}\left(2,\frac{1}{2}\right) + S_{2,2}\left(2,\frac{1}{2}\right) - S_{3,1}\left(2,\frac{1}{2}\right) + S_{1,1,2}\left(2,\frac{1}{2},1\right)\right.$$

$$- S_{1,1,2}\left(2,1,\frac{1}{2}\right) - S_{1,2,1}\left(2,\frac{1}{2},1\right) + S_{1,2,1}\left(2,1,\frac{1}{2}\right) - S_{2,1,1}\left(2,\frac{1}{2},1\right)$$

$$- S_{2,1,1}\left(2,1,\frac{1}{2}\right) + S_{1,1,1,1}\left(2,\frac{1}{2},1,1\right) + S_{1,1,1,1}\left(2,1,\frac{1}{2},1\right)$$

$$+ S_{1,1,1,1}\left(2,1,1,\frac{1}{2}\right)\right) + \left(\frac{128}{3}S_1 - 448S_1\left(\frac{1}{2}\right)\right)\zeta_3 - 32B_4 + 144\zeta_4\right)F$$

$$+ 2^{-N}\frac{32P_{167}}{(N-1)N^3(N+1)^2}\left(7\zeta_3 - S_3(2) + S_{1,2}(2,1) - S_{2,1}(2,1) + S_{1,1,1}(2,1,1)\right)$$

$$+ \left(-\frac{4P_{210}}{3(N-1)N^3(N+1)^3(N+2)^2}S_2 + \frac{8P_{234}}{3(N-1)N^5(N+1)^5(N+2)^4}\right)S_1$$

$$+ \frac{32P_{214}}{3(N-1)N^3(N+1)^3(N+2)^2}\zeta_3 - \frac{4P_{198}}{9N(N+1)}S_1^3 G\Bigg]$$

$$+ C_A C_F T_F\Bigg[L_M^3 F\left[\frac{8P_{199}}{9(N-1)N(N+1)(N+2)} + \frac{16}{3}S_1\right]$$

$$+ L_M^2\Bigg[\frac{8P_{203}}{3(N-1)N(N+1)(N+2)}S_1 G - \frac{8P_{231}}{9(N-1)^2 N^4(N+1)^4(N+2)^3}$$

$$+ \left(16S_2 + 32S_{-2}\right)F\right] + L_M\left[\frac{16P_{206}}{(N-1)N^3(N+1)^3(N+2)^2}S_{-2}\right.$$

$$- \frac{8P_{229}}{9(N-1)^2N^4(N+1)^4(N+2)^2}S_1 + \frac{8P_{238}}{27(N-1)^2N^5(N+1)^5(N+2)^4}$$

$$+ \left(\frac{4P_{205}}{3(N-1)N(N+1)(N+2)}S_2 + \frac{4P_{200}}{3(N-1)N}S_1^2 + \frac{8}{3}\left(31N^2 + 31N + 74\right)S_3\right.$$

$$+ 64\left(2N^2 + 2N + 3\right)S_{-3} - 128\left(N^2 + N + 1\right)S_{-2,1}\right)G + \left(64S_{-2}S_1 - \frac{8}{3}S_1^3\right.$$

$$+ 40S_1S_2 - 32S_{2,1} - 96\zeta_3\right)F\right] + \frac{4}{3(N-1)N^3(N+1)^3(N+2)^2}\left(-2P_{174}S_{2,1}\right.$$

$$+ 2P_{215}S_{-3} + 4P_{216}S_{-2,1} + \frac{2P_{228}}{9(N-1)}S_3 - \frac{P_{230}}{9(N-1)N(N+1)(N+2)}S_1^2$$

$$- \frac{P_{232}}{9(N-1)N(N+1)(N+2)}S_2 - \frac{2P_{241}}{81(N-1)N^3(N+1)^3(N+2)^3}\right)$$

$$+ \left(\frac{4P_{204}}{27(N-1)N(N+1)(N+2)}S_1^3 + \left(\frac{8}{9}\left(77N^2 + 77N + 214\right)S_3\right.\right.$$

$$- \frac{16}{3}\left(23N^2 + 23N - 6\right)S_{-2,1}\right)S_1 + \frac{8}{3}\left(57N^2 + 57N + 70\right)S_{-3}S_1$$

$$+ \frac{32}{3}\left(11N^2 + 11N + 20\right)S_{-2}S_2 + \frac{4}{3}\left(13N^2 + 13N + 34\right)S_2^2$$

$$+ \frac{16}{3}\left(29N^2 + 29N + 64\right)S_4 - \frac{16}{3}\left(3N^2 + 3N - 2\right)S_{-2}^2$$

$$+ \frac{64}{3}\left(7N^2 + 7N + 11\right)S_{-4} - 8\left(5N^2 + 5N + 22\right)S_{3,1}$$

$$- 32\left(5N^2 + 5N + 2\right)S_{-2,2} - \frac{128}{3}\left(5N^2 + 5N + 4\right)S_{-3,1}$$

$$+ \frac{128}{3}\left(5N^2 + 5N - 2\right)S_{-2,1,1} - \frac{8}{3}\left(13N^2 + 13N + 14\right)S_1\zeta_3\right)G$$

$$+ \left(\frac{16}{3}S_{-2}S_1^2 - \frac{4}{9}S_1^4 + \frac{8}{3}S_1^2S_2 - \frac{32}{3}S_{2,1,1} + \left(-32S_3(2) + 32S_{1,2}(2,1)\right.\right.$$

$$- 32S_{2,1}(2,1) + 32S_{1,1,1}(2,1,1)\right)S_1\left(\frac{1}{2}\right) + 32\left(S_{1,3}\left(2,\frac{1}{2}\right)\right.$$

$$- S_{2,2}\left(2,\frac{1}{2}\right) + S_{3,1}\left(2,\frac{1}{2}\right) - S_{1,1,2}\left(2,\frac{1}{2},1\right) + S_{1,1,2}\left(2,1,\frac{1}{2}\right)$$

$$+ S_{1,2,1}\left(2,\frac{1}{2},1\right) - S_{1,2,1}\left(2,1,\frac{1}{2}\right) + S_{2,1,1}\left(2,\frac{1}{2},1\right) + S_{2,1,1}\left(2,1,\frac{1}{2}\right)$$

$$- S_{1,1,1,1}\left(2,\frac{1}{2},1,1\right) - S_{1,1,1,1}\left(2,1,\frac{1}{2},1\right) - S_{1,1,1,1}\left(2,1,1,\frac{1}{2}\right)$$

$$+ 7S_1\left(\frac{1}{2}\right)\zeta_3\right) + 16B_4 - 144\zeta_4\right)F + 2^{-N}\frac{16P_{167}}{(N-1)N^3(N+1)^2}\left(S_3(2)\right.$$

$$- S_{1,2}(2,1) + S_{2,1}(2,1) - S_{1,1,1}(2,1,1) - 7\zeta_3\right)$$

$$+ \left(\frac{4P_{213}}{9(N-1)^2N^3(N+1)^3(N+2)^2}S_2 - \frac{4P_{237}}{81(N-1)^2N^5(N+1)^5(N+2)^4}\right)S_1$$

$$+ \left(-\frac{8P_{220}}{3(N-1)N^4(N+1)^4(N+2)^3} + \frac{32P_{208}}{3(N-1)N^3(N+1)^3(N+2)^2}S_1\right)S_{-2}$$

$$-\frac{8P_{222}}{9(N-1)^2N^3(N+1)^3(N+2)^2}\zeta_3\Bigg]\Bigg\},\tag{5.69}$$

where we refer to the polynomials defined already for the constant part of the OME, and in addition we use

$$P_{198} = 5N^4 + 22N^3 + 49N^2 + 32N + 4\tag{5.70}$$

$$P_{199} = 11N^4 + 22N^3 - 23N^2 - 34N - 12\tag{5.71}$$

$$P_{200} = 17N^4 - 6N^3 + 41N^2 - 16N - 12\tag{5.72}$$

$$P_{201} = 3N^5 + 11N^3 + 14N^2 - 4N - 8\tag{5.73}$$

$$P_{202} = 7N^6 + 15N^5 + 7N^4 - 23N^3 - 26N^2 - 20N - 8\tag{5.74}$$

$$P_{203} = 17N^6 + 51N^5 + 51N^4 + 89N^3 + 40N^2 - 80N - 24\tag{5.75}$$

$$P_{204} = 17N^6 + 69N^5 + 153N^4 + 131N^3 - 86N^2 - 116N - 24\tag{5.76}$$

$$P_{205} = 73N^6 + 189N^5 + 45N^4 + 31N^3 - 238N^2 - 412N - 120\tag{5.77}$$

$$P_{206} = 2N^7 + 16N^6 + 37N^5 + 96N^4 + 143N^3 + 142N^2 + 132N + 40\tag{5.78}$$

$$P_{207} = 3N^7 - 15N^6 - 133N^5 - 449N^4 - 658N^3 - 500N^2 - 296N - 96\tag{5.79}$$

$$P_{208} = 3N^7 + 18N^6 + 49N^5 + 140N^4 + 190N^3 + 152N^2 + 120N + 32\tag{5.80}$$

$$P_{209} = 8N^7 + 37N^6 + 83N^5 + 85N^4 + 61N^3 + 58N^2 - 20N - 24\tag{5.81}$$

$$P_{210} = 81N^7 + 289N^6 + 331N^5 + 99N^4 - 128N^3 - 448N^2 - 688N - 240\tag{5.82}$$

$$P_{211} = 104N^7 + 481N^6 + 1064N^5 + 1009N^4 + 646N^3 + 640N^2 - 344N - 336\tag{5.83}$$

$$P_{212} = 6N^8 + 40N^7 + 87N^6 + 62N^5 + 93N^4 + 220N^3 + 148N^2 + 96N + 64\tag{5.84}$$

$$P_{213} = 269N^8 + 1010N^7 + 1558N^6 + 2984N^5 + 3633N^4 + 1950N^3 - 420N^2$$
$$- 2632N - 864\tag{5.85}$$

$$P_{214} = 6N^9 + 24N^8 - 6N^7 - 138N^6 - 191N^5 - 422N^4 - 927N^3 - 526N^2$$
$$- 132N - 136\tag{5.86}$$

$$P_{215} = 6N^9 + 39N^8 + 89N^7 + 136N^6 + 85N^5 + 183N^4 + 358N^3 + 344N^2$$
$$+ 440N + 112\tag{5.87}$$

$$P_{216} = 6N^9 + 39N^8 + 105N^7 + 88N^6 - 91N^5 - 329N^4 - 410N^3 - 344N^2$$
$$- 264N - 80\tag{5.88}$$

$$P_{217} = 72N^9 + 432N^8 + 965N^7 + 757N^6 - 729N^5 - 3193N^4 - 4848N^3 - 1968N^2$$
$$+ 528N + 16\tag{5.89}$$

$$P_{218} = N^{10} + 8N^9 + 29N^8 + 49N^7 - 11N^6 - 131N^5 - 161N^4 - 160N^3 - 168N^2$$
$$- 80N - 16\tag{5.90}$$

$$P_{219} = 3N^{10} + 39N^9 + 111N^8 - 27N^7 - 692N^6 - 1390N^5 - 1232N^4 - 636N^3$$
$$- 248N^2 + 80N + 96\tag{5.91}$$

$$P_{220} = 5N^{10} + 32N^9 + 46N^8 + 82N^7 - 137N^6 - 658N^5 - 1114N^4 - 2576N^3$$
$$- 3680N^2 - 1952N - 416\tag{5.92}$$

$$P_{221} = 8N^{10} + 133N^9 + 564N^8 - 720N^7 - 9202N^6 - 18333N^5 - 13074N^4$$
$$- 10744N^3 - 5512N^2 + 19440N + 14400\tag{5.93}$$

$$P_{222} = 9N^{10} - 218N^8 - 323N^7 + 1211N^6 - 398N^5 - 5724N^4 - 1035N^3 + 810N^2$$
$$+ 76N + 984\tag{5.94}$$

5. Pure-singlet contributions to DIS

$$P_{223} = 19N^{10} + 143N^9 + 427N^8 + 567N^7 + 454N^6 + 822N^5 + 1560N^4 + 1784N^3$$
$$+ 1488N^2 + 768N + 192 \tag{5.95}$$

$$P_{224} = 36N^{10} + 169N^9 + 33N^8 - 1407N^7 - 4051N^6 - 6392N^5 - 8176N^4 - 8212N^3$$
$$- 5560N^2 - 2736N - 736 \tag{5.96}$$

$$P_{225} = 43N^{10} + 320N^9 + 939N^8 + 912N^7 - 218N^6 - 510N^5 - 654N^4 - 1232N^3$$
$$+ 16N^2 + 672N + 288 \tag{5.97}$$

$$P_{226} = 43N^{10} + 320N^9 + 1059N^8 + 1914N^7 + 2431N^6 + 2874N^5 + 2379N^4 + 820N^3$$
$$+ 352N^2 + 336N + 144 \tag{5.98}$$

$$P_{227} = 104N^{10} + 1729N^9 + 10752N^8 + 31392N^7 + 48422N^6 + 57231N^5 + 75450N^4$$
$$+ 59408N^3 + 28136N^2 + 47376N + 31680 \tag{5.99}$$

$$P_{228} = 135N^{10} + 702N^9 + 1547N^8 + 1319N^7 + 553N^6 + 2150N^5 - 3213N^4 - 6735N^3$$
$$- 7854N^2 - 7492N - 1272 \tag{5.100}$$

$$P_{229} = 136N^{10} + 647N^9 + 1110N^8 - 438N^7 - 2555N^6 - 2106N^5 - 3105N^4 - 3167N^3$$
$$+ 418N^2 + 924N + 72 \tag{5.101}$$

$$P_{230} = 19N^{11} - 17N^{10} + 190N^9 + 1350N^8 + 1060N^7 - 4480N^6 - 12285N^5 - 13625N^4$$
$$- 5556N^3 + 2768N^2 + 4512N + 1872 \tag{5.102}$$

$$P_{231} = 118N^{11} + 793N^{10} + 2281N^9 + 3402N^8 + 2428N^7 + 1457N^6 + 1917N^5$$
$$+ 2476N^4 + 4392N^3 + 4976N^2 + 2832N + 576 \tag{5.103}$$

$$P_{232} = 1669N^{11} + 10399N^{10} + 26752N^9 + 36576N^8 + 33436N^7 + 39590N^6$$
$$+ 33039N^5 + 8815N^4 + 27708N^3 + 47504N^2 + 33312N + 8784 \tag{5.104}$$

$$P_{233} = 37N^{12} + 305N^{11} + 1107N^{10} + 2328N^9 + 3520N^8 + 5020N^7$$
$$+ 7642N^6 + 10519N^5 + 10938N^4 + 8248N^3 + 4656N^2 + 1712N + 288 \tag{5.105}$$

$$P_{234} = 18N^{13} + 193N^{12} + 900N^{11} + 2378N^{10} + 3486N^9 + 2817N^8 + 2052N^7 + 2256N^6$$
$$+ 2804N^5 + 7272N^4 + 12512N^3 + 10304N^2 + 4672N + 896 \tag{5.106}$$

$$P_{235} = 25N^{13} + 1016N^{12} + 11804N^{11} + 63190N^{10} + 184075N^9 + 321474N^8$$
$$+ 375092N^7 + 324832N^6 + 221884N^5 + 205760N^4 + 302240N^3 + 288576N^2$$
$$+ 153792N + 34560 \tag{5.107}$$

$$P_{236} = 158N^{13} + 1663N^{12} + 7309N^{11} + 17981N^{10} + 35774N^9 + 59586N^8 + 56374N^7$$
$$+ 23504N^6 + 25457N^5 + 30298N^4 - 11384N^3 - 30000N^2 - 18864N - 4320 \tag{5.108}$$

$$P_{237} = 77N^{14} + 1046N^{13} + 7131N^{12} + 35512N^{11} + 87723N^{10} + 89530N^9 + 46927N^8$$
$$+ 41002N^7 - 194958N^6 - 644698N^5 - 589404N^4 - 123376N^3 + 61248N^2$$
$$+ 22752N - 1728 \tag{5.109}$$

$$P_{238} = 686N^{14} + 6560N^{13} + 25572N^{12} + 43489N^{11} + 9045N^{10} - 72944N^9 - 125240N^8$$
$$- 156761N^7 - 206883N^6 - 241600N^5 - 250212N^4 - 225808N^3 - 150864N^2$$
$$- 56448N - 8640 \tag{5.110}$$

$$P_{239} = 100N^{15} + 1170N^{14} + 6234N^{13} + 20518N^{12} + 49217N^{11} + 94274N^{10}$$
$$+ 145788N^9 + 172682N^8 + 139145N^7 + 47068N^6 - 50228N^5 - 96416N^4$$
$$- 82448N^3 - 41536N^2 - 11968N - 1536 \tag{5.111}$$

$$
\begin{aligned}
P_{240} = {}& 158N^{16} + 6799N^{15} + 93011N^{14} + 633970N^{13} + 2547481N^{12} + 6605953N^{11} \\
& + 11841596N^{10} + 15808910N^9 + 17140651N^8 + 16081262N^7 + 12756671N^6 \\
& + 7253426N^5 + 1318688N^4 - 2323728N^3 - 2738448N^2 - 1334880N - 259200 \quad (5.112) \\
P_{241} = {}& 2272N^{17} + 27343N^{16} + 135485N^{15} + 332260N^{14} + 398250N^{13} + 111012N^{12} \\
& - 530356N^{11} - 1134420N^{10} - 86378N^9 + 3545573N^8 + 7139427N^7 + 8691144N^6 \\
& + 9505284N^5 + 9549872N^4 + 7324752N^3 + 3612672N^2 + 1017792N + 124416 \,.
\end{aligned}
$$

$$(5.113)$$

All nested sums which appear, can be continued to complex values of the argument N by performing the asymptotic expansion for $N \to \infty$ analytically, cf. [147, 261], and then using the recurrence relations for the sums. Expressions in x space can be derived by applying the inverse Mellin transformation, which results in the expressions presented in Eq. (E.10) in Appendix E.

The heavy quark mass m, which appears in the logarithms L_M in the result above, refers to the OMS scheme. If we reexpress the result in terms of the $\overline{\text{MS}}$ mass, we get a slightly different expression. The difference between the two schemes is given in N space by

$$
\begin{aligned}
A_{Qq}^{\text{PS},\overline{\text{MS}}}(N) - A_{Qq}^{\text{PS,OMS}}(N) = {}& \\
C_F^2 T_F \Bigg\{ & \frac{48\left(N^2 + N + 2\right)^2}{(N-1)N^2(N+1)^2(N+2)} \ln^2\left(\frac{m^2}{\mu^2}\right) \\
& - \frac{16\left(4N^7 + 20N^6 + 37N^5 - 4N^4 - 43N^3 - 34N^2 - 52N - 24\right)}{(N-1)N^3(N+1)^3(N+2)^2} \ln\left(\frac{m^2}{\mu^2}\right) \\
& - \frac{64\left(5N^3 + 7N^2 + 4N + 4\right)\left(N^2 + 5N + 2\right)}{(N-1)N^3(N+1)^3(N+2)^2} \Bigg\} \,,
\end{aligned}
$$

$$(5.114)$$

where we have identified the masses in both schemes symbolically to shorten the expression. Analogously, the difference in x space can be written as

$$
\begin{aligned}
A_{Qq}^{\text{PS},\overline{\text{MS}}}(x) - A_{Qq}^{\text{PS,OMS}}(x) = {}& C_F^2 T_F \Bigg\{ \left[\frac{16(1-x)\left(4x^2 + 7x + 4\right)}{x} + 96(x+1)H_0 \right] \ln^2\left(\frac{m^2}{\mu^2}\right) \\
& + \left[\frac{1}{x}\frac{32}{3}(1-x)(4x-1)(5x-2) + 16\left(8x^2 + 7x - 5\right)H_0 \right. \\
& \left. - 48(x+1)H_0^2 \right] \ln\left(\frac{m^2}{\mu^2}\right) - \frac{64}{3}\left(8x^2 + 15x + 3\right)H_0 \\
& + 64(x+1)H_0^2 - \frac{128(1-x)\left(28x^2 + x + 10\right)}{9x} \Bigg\} \,.
\end{aligned}
$$

$$(5.115)$$

We would like to discuss also the numerical behaviour of the pure-singlet OME as a function of x and Q^2. For the illustrations, we use the x space expressions from Eq. (E.10) and we employ the Mathematica package HPL-2.0 described in [457, 458] for the numerical evaluation of the HPLs. The value of the strong coupling constant $\alpha_s(\mu^2)$ is obtained using the LHAPDF library from the parametrisation of the NNLO analysis in [218]. We keep the value of $\alpha_s(\mu^2)$ the same for both NLO and NNLO illustrations since we would like to discuss the influence of just the OME itself. We consider the case of three massless quarks and a massive charm quark, whose mass in the OMS scheme we take to be $m_c = 1.59\,\text{GeV}$, as determined in [226].

Figure 5.5 shows the OME A_{Qq}^{PS} at 2- and 3-loop order for different choices of the scale μ^2 between $20\,\text{GeV}^2$ and $10\,000\,\text{GeV}^2$. At small values of x, the 2-loop term of the OME (dashed
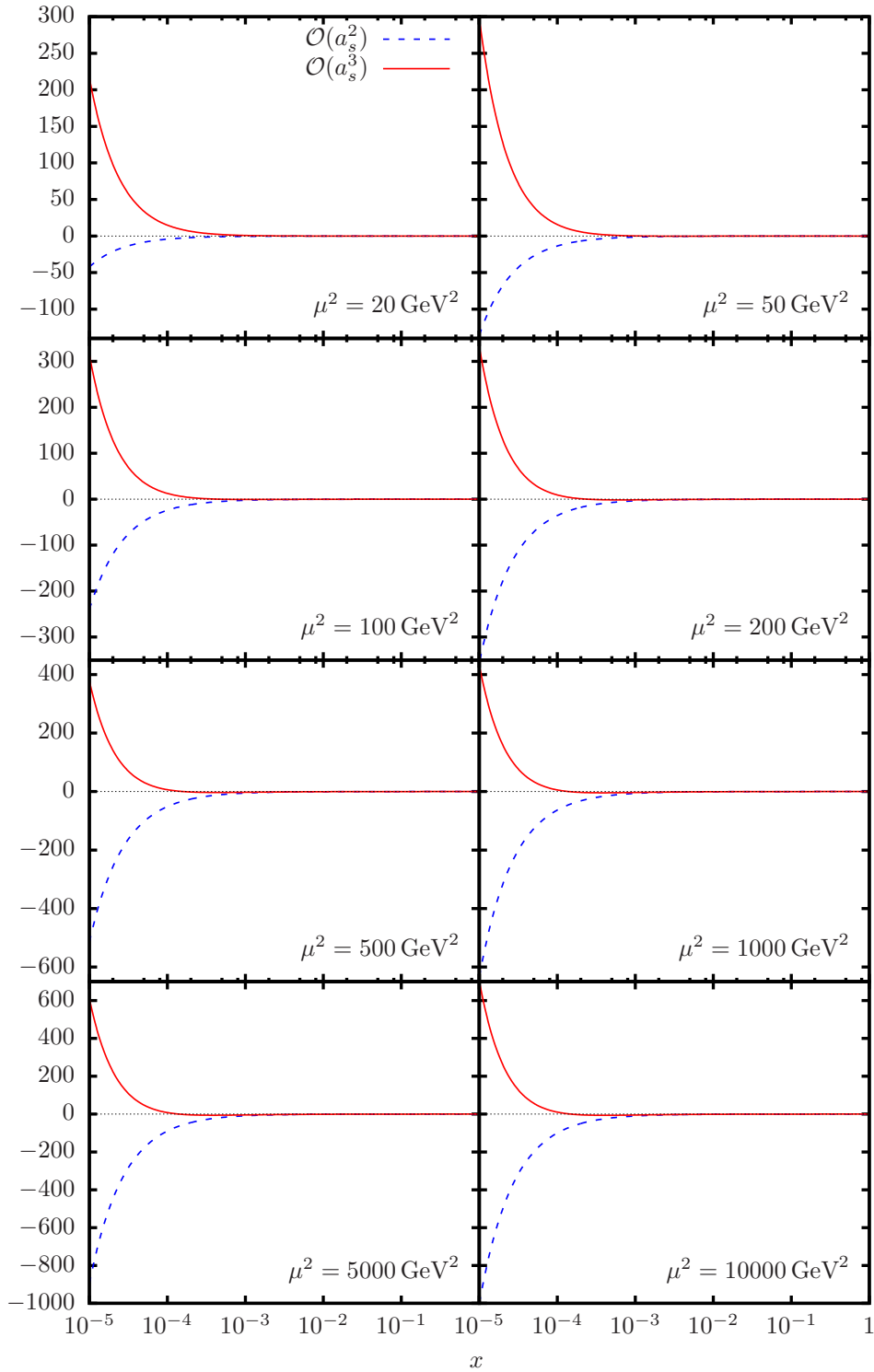
Figure 5.5.: Illustration of the pure-singlet OME A_{Qq}^{PS} for charm quarks at different values of the scale μ^2. The dashed line corresponds to the 2-loop term, while the solid line shows the sum of the 2-loop and 3-loop corrections. The charm quark mass $m_c = 1.59\,\mathrm{GeV}$ is treated in the OMS scheme [226].
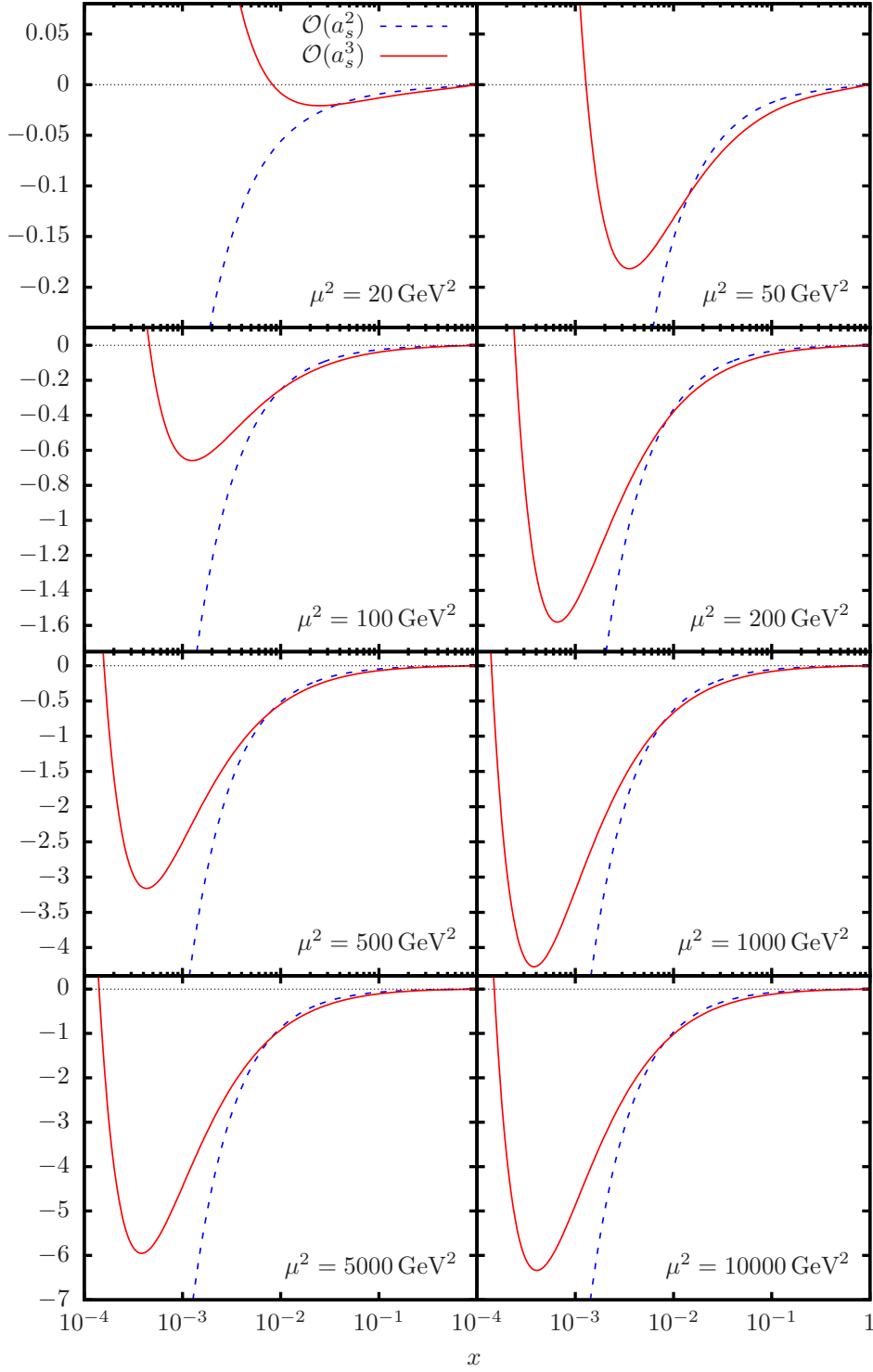
Figure 5.6.: The medium x behaviour of the pure-singlet OME A_{Qq}^{PS} for charm quarks. The dashed line corresponds to the 2-loop term, while the solid line shows the sum of the 2-loop and 3-loop corrections. The charm quark mass $m_c = 1.59\,\mathrm{GeV}$ is treated in the OMS scheme [226].

line) is negative, while the sum of the 2- and 3-loop correction (solid line) is of opposite sign. The overall size of the OME increases when μ^2 increases. Due to the rapid growth of the OME towards smaller values of x, an important feature is hidden in Fig. 5.5, which we demonstrate in Fig. 5.6. Despite being positive below $x \approx 10^{-4}$, the sum of the 2- and 3-loop terms is negative above some value of x and approaches zero from below for $x \to 1$. This fact will be important when we discuss the heavy flavour Wilson coefficient, since there, as well as for the matching relations of the variable flavour number scheme, we need to compute the Mellin convolution of the OME with the singlet PDF combination. This convolution receives contributions from all values of x and due to the sign flip of the OME, cancellations will occur. The value of x for which the OME changes sign shifts from $x \approx 8.3 \cdot 10^{-3}$ for $\mu^2 = 20\,\text{GeV}^2$ to $x \approx 1.5 \cdot 10^{-4}$ for $\mu^2 = 10\,000\,\text{GeV}^2$. The 2-loop term, on the other hand, remains negative over the whole range of x and for all values of μ^2 considered here. At around $x \approx 10^{-2}$ the 3-loop term also becomes negative, so that the sum of 2-loop and 3-loop corrections has a slightly larger absolute value than the 2-loop contribution alone.

The pure-singlet OME $A_{Qq}^{\text{PS},(3)}$ also enters the matching relations of the variable flavour number scheme. In particular, it enters in the relations for the new, heavy quark PDF combination $f_Q(x, N_F+1) + \bar{f}_Q(x, N_F+1)$ and the singlet combination $\Sigma(x, N_F+1)$. Both relations, however, also receive contributions from the OME $A_{Qg}^{(3)}$, which has not been completed yet. Therefore, we cannot yet present illustrations of the impact from the pure-singlet OME on these matching relations.

5.2. Contribution to unpolarised scattering

The structure function $F_2(x, Q^2)$ for unpolarised neutral current scattering receives contributions from the pure-singlet heavy flavour Wilson coefficient $H_{q,2}^{\text{PS}}$. The relevant part of the structure function, which is given in full in Eq. (2.90), reads

$$F_2^{\text{h,PS}}(x, N_F + 1, Q^2, m^2) = x e_Q^2 \left[H_{q,2}^{\text{PS}}\left(x, N_F + 1, \frac{Q^2}{\mu^2}, \frac{m^2}{\mu^2}\right) \otimes \Sigma(x, \mu^2, N_F) \right], \qquad (5.116)$$

where e_Q is the charge of the heavy quark and $\Sigma(x, \mu^2, N_F)$ denotes the singlet PDF combination in the fixed flavour number scheme, cf. Eq. (2.66).

The factorisation of the heavy flavour Wilson coefficients in the limit $m^2 \gg Q^2$ determines the structure of the Wilson coefficients in terms of massive OMEs and massless Wilson coefficients, cf. Eq. (2.94). The pure-singlet Wilson coefficient $H_{q,2}^{\text{PS}}$, expanded in a_s, can be written in this limit as

$$\begin{aligned} H_{q,2}^{\text{PS}}(N_F + 1) = {} & a_s^2 \left[A_{Qq}^{\text{PS},(2)}(N_F + 1) + \tilde{C}_{q,2}^{\text{PS},(2)}(N_F + 1) \right] \\ & + a_s^3 \Big[A_{Qq}^{\text{PS},(3)}(N_F + 1) + \tilde{C}_{q,2}^{\text{PS},(3)}(N_F + 1) + A_{gq,Q}^{(2)}(N_F + 1) \tilde{C}_{g,2}^{\text{S},(1)}(N_F + 1) \\ & + A_{Qq}^{\text{PS},(2)}(N_F + 1) C_{q,2}^{\text{NS},(1)}(N_F + 1) \Big]. \end{aligned} \qquad (5.117)$$

The pure-singlet OME at 2-loop order $A_{Qq}^{\text{PS},(2)}$ was calculated in [201, 205] and the 2-loop result for $A_{gq,Q}^{(2)}$ can be found in [202, 207]. For the massless Wilson coefficients $C_{q,2}^{\text{PS}}$, we refer to [106] for a collection of the 1-loop results, while the 2-loop corrections were published in [118–121]. Finally, also the 3-loop result is known [138]. The massless Wilson coefficients depend logarithmically on the scale ratio Q^2/μ^2. Terms proportional to logarithms of this scale ratio $L_Q = \ln(Q^2/m^2)$ vanish of course for the choice $\mu^2 = Q^2$, which is often used to present the results. These logarithmic

terms can, however, be fully recovered from the renormalisation group equations, as outlined for example in [293].

Referring to the shorthands F and G, see Eqs. (5.3) and (5.23), the assembly of all results according to Eq. (5.117) yields

$$
\begin{aligned}
H_{q,2}^{\mathrm{PS}}(N) = {} & a_s^2 C_F T_F \Bigg\{ -L_M^2 4F + L_Q^2 4F - L_M \frac{8\left(N^2 + 5N + 2\right)\left(5N^3 + 7N^2 + 4N + 4\right)}{(N-1)N^3(N+1)^3(N+2)^2} \\
& + L_Q \left[-\frac{8P_{248}}{(N-1)N^3(N+1)^3(N+2)^2} - 8S_1 F \right] + \left(4S_1^2 - 12S_2 \right) F \\
& + \frac{64}{(N-1)N(N+1)(N+2)} S_{-2} + \frac{8P_{248}}{(N-1)N^3(N+1)^3(N+2)^2} S_1 \\
& + \frac{8P_{258}}{(N-1)N^4(N+1)^4(N+2)^2} \Bigg\} + a_s^3 \Bigg\{ C_F T_F^2 \Bigg[-L_M^3 F \frac{128}{9} + L_Q^3 F \frac{32}{9} \\
& - L_M^2 \frac{32P_{244}}{9(N-1)N^2(N+1)^2(N+2)^2} - L_Q^2 \frac{32P_{253}}{9(N-1)N^3(N+1)^3(N+2)^2} \\
& + L_M^2 L_Q F \frac{32}{3} + L_M L_Q \left[\frac{64\left(8N^3 + 13N^2 + 27N + 16\right)1}{9(N+1)} G - \frac{64}{3} F S_1 \right] \\
& + L_M \left[\frac{64P_{248}}{3(N-1)N^3(N+1)^3(N+2)^2} S_1 + \left(\frac{32}{3} S_1^2 - 32 S_2 \right) F \right. \\
& \left. - \frac{64P_{266}}{27(N-1)N^4(N+1)^4(N+2)^3} \right] + L_Q \left[\frac{512}{3(N-1)N(N+1)(N+2)} S_{-2} \right. \\
& \left. + \frac{64P_{267}}{27(N-1)N^4(N+1)^4(N+2)^3} \right] + \left(-\frac{160}{27} S_1^3 - \frac{256}{9} S_1 S_2 - \frac{32}{27} S_3 \right. \\
& \left. + \frac{128}{3} S_{2,1} - \frac{896}{9} \zeta_3 \right) F + \left(-\frac{2P_{275}}{3N(N+1)(N+2)} S_1 - \frac{2P_{279}}{9N^2(N+1)^2(N+2)^2} \right. \\
& \left. + P_{264} S_1^2 + P_{268} S_2 \right) \frac{16}{27(N-1)N^3(N+1)^3(N+2)^2(N+3)(N+4)(N+5)} \Bigg] \\
& + C_F N_F T_F^2 \Bigg[-L_M^3 F \frac{32}{9} + L_Q^3 F \frac{32}{9} + L_M^2 \Bigg[\frac{32P_{209}}{9(N-1)N^3(N+1)^3(N+2)^2} \\
& - \frac{32}{3} S_1 F \Bigg] - L_Q^2 \frac{32P_{253}}{9(N-1)N^3(N+1)^3(N+2)^2} + L_M \left[\left(-\frac{16}{3} S_1^2 - \frac{80}{3} S_2 \right) F \right. \\
& + \frac{32P_{159}}{9(N-1)N^3(N+1)^3(N+2)^2} S_1 - \frac{32P_{225}}{27(N-1)N^4(N+1)^4(N+2)^3} \Bigg] \\
& + L_Q \left[\frac{512}{3(N-1)N(N+1)(N+2)} S_{-2} + \frac{32\left(8N^3 + 13N^2 + 27N + 16\right)}{9(N+1)} S_1 G \right. \\
& + \frac{32P_{270}}{27(N-1)N^4(N+1)^4(N+2)^3} + \left(-\frac{16}{3} S_1^2 - \frac{16}{3} S_2 \right) F \Bigg] \\
& + \frac{16}{27(N-1)N^3(N+1)^3(N+2)^2} \left(P_{159} S_1^2 + P_{211} S_2 - \frac{2P_{185}}{3N(N+1)(N+2)} S_1 \right. \\
& \left. + \frac{2P_{236}}{9N^2(N+1)^2(N+2)^2} \right) + \left(-\frac{16}{27} S_1^3 - \frac{208}{9} S_1 S_2 - \frac{1184}{27} S_3 + \frac{256\zeta_3}{9} \right) F \Bigg] \\
& + C_F^2 T_F \Bigg[L_M^3 F \left[\frac{4\left(3N^2 + 3N + 2\right)}{3N(N+1)} - \frac{16}{3} S_1 \right] + L_Q^3 F \left[\frac{8\left(3N^2 + 3N + 2\right)}{3N(N+1)} \right.
\end{aligned}
$$

$$-\frac{32}{3}S_1\Big] + L_M^2 L_Q F\left[-\frac{4\left(3N^2+3N+2\right)}{N(N+1)}+16S_1\right] + L_M^2\left[\frac{4P_{246}}{N^2(N+1)^2}G\right.$$

$$+ F\left(-\frac{4\left(13N^2+5N-6\right)}{N(N+1)}S_1 - 8S_1^2 + 24S_2\right)\right] + L_Q^2\left[\left(24S_1^2 - 24S_2\right)F\right.$$

$$+ \frac{8P_{251}}{(N-1)N^3(N+1)^3(N+2)^2}S_1 - \frac{4P_{260}}{(N-1)N^4(N+1)^4(N+2)^2}\right]$$

$$+ L_M L_Q\left[\frac{32\left(N^2+5N+2\right)\left(5N^3+7N^2+4N+4\right)}{(N-1)N^3(N+1)^3(N+2)^2}S_1\right.$$

$$- \frac{8\left(N^2+5N+2\right)\left(3N^2+3N+2\right)\left(5N^3+7N^2+4N+4\right)}{(N-1)N^4(N+1)^4(N+2)^2}\right]$$

$$+ L_M\left[\frac{4}{(N-1)N^3(N+1)^3(N+2)^2}\left(-P_{249}S_2 - P_{250}S_1^2\right.\right.$$

$$+ \frac{2P_{262}}{N(N+1)(N+2)}S_1 - \frac{P_{273}}{N^2(N+1)^2(N+2)}\right) + \left(\frac{8}{3}S_1^3 - 24S_1 S_2\right.$$

$$- \frac{80}{3}S_3 + 32S_{2,1} + 96\zeta_3\right)F\right] + L_Q\left[\frac{4}{(N-1)N^3(N+1)^3(N+2)^2}\left(P_{252}S_2\right.\right.$$

$$- P_{254}S_1^2 - \frac{2P_{263}}{N(N+1)(N+2)}S_1 + \frac{P_{276}}{(N-2)N^2(N+1)^2(N+2)(N+3)}\right)$$

$$+ \left(-\frac{16}{3}\left(N^2+N-22\right)S_3 + 128S_{-3} - 256S_{-2,1} - 384\zeta_3\right)G + \left(-\frac{56}{3}S_1^3\right.$$

$$+ 104S_1 S_2\right)F + \left(\frac{32P_{256}}{(N-2)(N-1)N^3(N+1)^3(N+2)(N+3)}\right.$$

$$+ \frac{512}{(N-1)N^2(N+1)^2(N+2)}S_1\right)S_{-2}\right] + \left(\frac{2\left[P_{265}S_2 - P_{259}S_1^2\right]}{N(N+1)(N+2)} + 8P_{212}S_{2,1}\right.$$

$$- \frac{2P_{217}}{3}S_3 + \frac{P_{278}}{N^3(N+1)^3(N+2)^2}\right)\frac{4}{3(N-1)N^3(N+1)^3(N+2)^2}$$

$$+ \left(\left(\frac{128}{9}S_3 - 32S_{2,1}\right)S_1 + \frac{4}{9}S_1^4 - \frac{56}{3}S_1^2 S_2 + \frac{100}{3}S_2^2 + \frac{88}{3}S_4 + 32S_{3,1}\right.$$

$$+ \frac{224}{3}S_{2,1,1} + 64\left(S_3(2) - S_{1,2}(2,1) + S_{2,1}(2,1) - S_{1,1,1}(2,1,1)\right)S_1\left(\frac{1}{2}\right)$$

$$+ 64\left(-S_{1,3}\left(2,\frac{1}{2}\right) + S_{2,2}\left(2,\frac{1}{2}\right) - S_{3,1}\left(2,\frac{1}{2}\right) + S_{1,1,2}\left(2,\frac{1}{2},1\right)\right.$$

$$- S_{1,1,2}\left(2,1,\frac{1}{2}\right) - S_{1,2,1}\left(2,\frac{1}{2},1\right) + S_{1,2,1}\left(2,1,\frac{1}{2}\right) - S_{2,1,1}\left(2,\frac{1}{2},1\right)$$

$$- S_{2,1,1}\left(2,1,\frac{1}{2}\right) + S_{1,1,1,1}\left(2,\frac{1}{2},1,1\right) + S_{1,1,1,1}\left(2,1,\frac{1}{2},1\right)$$

$$+ S_{1,1,1,1}\left(2,1,1,\frac{1}{2}\right)\right) + \left(\frac{128}{3}S_1 - 448S_1\left(\frac{1}{2}\right)\right)\zeta_3 - 32B_4 + 144\zeta_4\right)F$$

$$+ 2^{-N}\frac{32P_{167}}{(N-1)N^3(N+1)^2}\left(-S_3(2) + S_{1,2}(2,1)\right.$$

$$- S_{2,1}(2,1) + S_{1,1,1}(2,1,1) + 7\zeta_3\right) - \frac{4P_{198}}{9N(N+1)}S_1^3 G$$

$$+ \left(-\frac{4P_{255}}{3(N-1)N^3(N+1)^3(N+2)^2}S_2 + \frac{4P_{274}}{3(N-1)N^5(N+1)^5(N+2)^4}\right)S_1$$

$$+ \frac{32P_{214}}{3(N-1)N^3(N+1)^3(N+2)^2}\zeta_3 \bigg] + C_A C_F T_F \bigg[L_M^3 F \bigg[\frac{16}{3}S_1$$

$$+ \frac{8P_{199}}{9(N-1)N(N+1)(N+2)} \bigg] + L_Q^3 F \bigg[-\frac{8P_{199}}{9(N-1)N(N+1)(N+2)}$$

$$- \frac{16}{3}S_1 \bigg] + L_M^2 \bigg[-\frac{8P_{269}}{9(N-1)^2N^4(N+1)^3(N+2)^3} + \Big(16S_2 + 32S_{-2}\Big)F$$

$$+ \bigg(-\frac{16P_{243}}{N(N+1)^2(N+2)^2} + \frac{8P_{203}}{3(N-1)N(N+1)(N+2)}S_1\bigg)G\bigg]$$

$$+ L_Q^2 \bigg[\frac{16P_{243}}{N(N+1)^2(N+2)^2}G + \frac{8P_{271}}{9(N-1)^2N^4(N+1)^3(N+2)^3}$$

$$+ \bigg(-\frac{(5N^2-1)}{(N-1)N(N+1)}16S_1 + 16S_1^2 - 16S_2 - 32S_{-2}\bigg)F\bigg]$$

$$+ L_M \bigg[\bigg(64S_{-2}S_1 - \frac{8}{3}S_1^3 + 40S_1S_2 + 16S_{-3} - 32S_{2,1} - 96\zeta_3\bigg)F$$

$$+ \frac{16P_{157}}{(N-1)N^3(N+1)^3(N+2)^2}S_{-2} - \frac{8P_{229}}{9(N-1)^2N^4(N+1)^4(N+2)^2}S_1$$

$$+ \frac{8P_{238}}{27(N-1)^2N^5(N+1)^5(N+2)^4} + \bigg(\frac{4P_{205}}{3(N-1)N(N+1)(N+2)}S_2$$

$$+ \frac{4P_{200}}{3(N-1)N}S_1^2 + \frac{8}{3}\big(31N^2 + 31N + 74\big)S_3 + \frac{32N\big(N^2-N-4\big)}{(N+1)(N+2)}S_{-2}$$

$$+ 16\big(7N^2 + 7N + 10\big)S_{-3} - 128\big(N^2 + N + 1\big)S_{-2,1}\bigg)G\bigg]$$

$$+ L_Q \bigg[\frac{16P_{257}}{3(N-1)^2N^3(N+1)^3(N+2)^2}S_{-2} + \bigg(-\frac{40}{3}S_1^3 + 40S_1S_2$$

$$- 144S_{-3} + 96S_{-2,1}\bigg)F - \frac{8P_{272}}{9(N-1)^2N^4(N+1)^4(N+2)^3}S_1$$

$$- \frac{8P_{277}}{27(N-1)^2N^5(N+1)^5(N+2)^4} + \bigg(\frac{4\big[P_{245}S_1^2 + P_{247}S_2\big]}{3(N-1)N(N+1)(N+2)}$$

$$+ 32(N-1)(N+2)S_{-2}S_1 - \frac{8}{3}\big(13N^2 + 13N + 62\big)S_3$$

$$+ 48\big(N^2 + N + 6\big)\zeta_3\bigg)G\bigg] + \frac{4}{3(N-1)N^3(N+1)^3(N+2)^2}\bigg(-2P_{174}S_{2,1}$$

$$+ 2P_{176}S_{-3} + 4P_{216}S_{-2,1} + \frac{2P_{228}}{9(N-1)}S_3 - \frac{2P_{241}}{81(N-1)N^3(N+1)^3(N+2)^3}$$

$$- \frac{\big[P_{230}S_1^2 + P_{232}S_2\big]}{9(N-1)N(N+1)(N+2)}\bigg) + \bigg(\bigg(\frac{8}{9}\big(137N^2 + 137N + 334\big)S_3$$

$$- \frac{16}{3}\big(35N^2 + 35N + 18\big)S_{-2,1}\bigg)S_1 + \frac{4P_{204}}{27(N-1)N(N+1)(N+2)}S_1^3$$

$$+ \frac{2}{3}\big(29N^2 + 29N + 74\big)S_2^2 + \frac{4}{3}\big(143N^2 + 143N + 310\big)S_4$$

$$- \frac{16}{3}\big(3N^2 + 3N - 2\big)S_{-2}^2 + \bigg(\frac{32NP_{242}}{(N+1)^2(N+2)^2} - \frac{64N\big(N^2-N-4\big)}{(N+1)(N+2)}S_1$$

$$+ \frac{64}{3}\big(7N^2 + 7N + 13\big)S_2\bigg)S_{-2} + \bigg(\frac{8}{3}\big(69N^2 + 69N + 94\big)S_1$$

$$
\begin{aligned}
&- \frac{32N\left(N^2 - N - 4\right)}{(N+1)(N+2)}\Bigg) S_{-3} + \frac{16}{3}\left(31N^2 + 31N + 50\right) S_{-4} \\
&- 8\left(7N^2 + 7N + 26\right) S_{3,1} - 64\left(3N^2 + 3N + 2\right) S_{-2,2} \\
&- \frac{32}{3}\left(23N^2 + 23N + 22\right) S_{-3,1} + \frac{64}{3}\left(13N^2 + 13N + 2\right) S_{-2,1,1} \\
&+ \left(-\frac{24N\left(N^2 - N - 4\right)}{(N+1)(N+2)} - \frac{8}{3}\left(11N^2 + 11N + 10\right) S_1\right)\zeta_3\Bigg) G \\
&+ \Bigg(\left(\left(-\frac{160}{3} S_3 + 64 S_{-2,1}\right) S_1 - 32 S_{-3} S_1 - \frac{4}{9} S_1^4 + \frac{8}{3} S_1^2 S_2 - 2 S_2^2 - 36 S_4 \right. \\
&+ \left(\frac{16}{3} S_1^2 - 32 S_2\right) S_{-2} - 16 S_{-4} + 16 S_{3,1} + 32 S_{-2,2} + 32 S_{-3,1} - \frac{32}{3} S_{2,1,1} \\
&- 64 S_{-2,1,1} + 32\left(-S_3(2) + S_{1,2}(2,1) - S_{2,1}(2,1) + S_{1,1,1}(2,1,1)\right) S_1\left(\frac{1}{2}\right) \\
&+ 32\left(S_{1,3}\left(2,\frac{1}{2}\right) - S_{2,2}\left(2,\frac{1}{2}\right) + S_{3,1}\left(2,\frac{1}{2}\right) - S_{1,1,2}\left(2,\frac{1}{2},1\right)\right. \\
&+ S_{1,1,2}\left(2,1,\frac{1}{2}\right) + S_{1,2,1}\left(2,\frac{1}{2},1\right) - S_{1,2,1}\left(2,1,\frac{1}{2}\right) + S_{2,1,1}\left(2,\frac{1}{2},1\right) \\
&+ S_{2,1,1}\left(2,1,\frac{1}{2}\right) - S_{1,1,1,1}\left(2,\frac{1}{2},1,1\right) - S_{1,1,1,1}\left(2,1,\frac{1}{2},1\right) \\
&\left.\left. - S_{1,1,1,1}\left(2,1,1,\frac{1}{2}\right)\right) + \left(-\frac{16}{3} S_1 + 224 S_1\left(\frac{1}{2}\right)\right)\zeta_3 + 16 B_4 - 144\zeta_4\right) F \\
&+ 2^{-N}\frac{16 P_{167}}{(N-1)N^3(N+1)^2}\Big(S_3(2) - S_{1,2}(2,1) + S_{2,1}(2,1) \\
&- S_{1,1,1}(2,1,1) - 7\zeta_3\Big) + \left(\frac{4 P_{213}}{9(N-1)^2 N^3(N+1)^3(N+2)^2} S_2\right. \\
&- \frac{4 P_{237}}{81(N-1)^2 N^5(N+1)^5(N+2)^4}\right) S_1 + \left(\frac{32 P_{171}}{3(N-1)N^3(N+1)^3(N+2)^2} S_1\right. \\
&\left. - \frac{8 P_{182}}{3(N-1)N^4(N+1)^4(N+2)^3}\right) S_{-2} - \frac{8 P_{261}}{9(N-1)^2 N^3(N+1)^3(N+2)^2}\zeta_3\Bigg] \\
&+ \tilde{c}_{q,2}^{\mathrm{PS},(3)}(N_F + 1)\Bigg\},
\end{aligned}
\tag{5.118}
$$

where we abbreviate long polynomials as P_i. Those which did not yet appear in this chapter are given by

$$
\begin{aligned}
P_{242} &= N^4 + 2N^3 + 7N^2 + 22N + 20 &\tag{5.119}\\
P_{243} &= N^5 + 9N^4 + 24N^3 + 36N^2 + 32N + 8 &\tag{5.120}\\
P_{244} &= 11N^5 + 26N^4 + 57N^3 + 142N^2 + 84N + 88 &\tag{5.121}\\
P_{245} &= 5N^6 + 135N^5 + 327N^4 + 329N^3 + 220N^2 - 176N - 120 &\tag{5.122}\\
P_{246} &= 16N^6 + 35N^5 + 33N^4 - 11N^3 - 41N^2 - 36N - 12 &\tag{5.123}\\
P_{247} &= 17N^6 - 57N^5 - 213N^4 - 175N^3 - 140N^2 + 64N + 72 &\tag{5.124}\\
P_{248} &= N^7 - 15N^5 - 58N^4 - 92N^3 - 76N^2 - 48N - 16 &\tag{5.125}\\
P_{249} &= 3N^7 - 15N^6 - 153N^5 - 577N^4 - 854N^3 - 652N^2 - 408N - 128 &\tag{5.126}\\
P_{250} &= 5N^7 + 19N^6 + 61N^5 + 197N^4 + 266N^3 + 212N^2 + 136N + 32 &\tag{5.127}
\end{aligned}
$$

$$P_{251} = 7N^7 + 21N^6 + 5N^5 - 117N^4 - 244N^3 - 232N^2 - 192N - 80 \tag{5.128}$$

$$P_{252} = 9N^7 + 15N^6 - 103N^5 - 575N^4 - 998N^3 - 948N^2 - 696N - 256 \tag{5.129}$$

$$P_{253} = 11N^7 + 37N^6 + 53N^5 + 7N^4 - 68N^3 - 56N^2 - 80N - 48 \tag{5.130}$$

$$P_{254} = 25N^7 + 91N^6 + 101N^5 - 195N^4 - 546N^3 - 556N^2 - 520N - 224 \tag{5.131}$$

$$P_{255} = 99N^7 + 379N^6 + 553N^5 + 465N^4 + 232N^3 - 256N^2 - 688N - 336 \tag{5.132}$$

$$P_{256} = N^8 + 8N^7 + 8N^6 - 14N^5 - 53N^4 - 82N^3 + 60N^2 + 104N + 96 \tag{5.133}$$

$$P_{257} = 6N^8 - 42N^7 - 241N^6 - 579N^5 - 307N^4 + 477N^3 + 602N^2 + 492N + 168 \tag{5.134}$$

$$P_{258} = 2N^9 + 7N^8 + 17N^7 + 30N^6 + 83N^5 + 193N^4 + 220N^3 + 136N^2 + 64N + 16 \tag{5.135}$$

$$P_{259} = 15N^9 + 24N^8 - 174N^7 - 659N^6 - 997N^5 - 749N^4 - 156N^3 + 256N^2 \\ + 320N + 144 \tag{5.136}$$

$$P_{260} = 19N^9 + 86N^8 + 144N^7 - 38N^6 - 535N^5 - 1016N^4 - 1180N^3 - 872N^2 \\ - 416N - 96 \tag{5.137}$$

$$P_{261} = 9N^{10} - 218N^8 - 350N^7 + 1238N^6 - 317N^5 - 5643N^4 - 981N^3 + 594N^2 \\ + 76N + 984 \tag{5.138}$$

$$P_{262} = 19N^{10} + 143N^9 + 412N^8 + 426N^7 - N^6 + 159N^5 + 1066N^4 + 1552N^3 \\ + 1456N^2 + 848N + 224 \tag{5.139}$$

$$P_{263} = 20N^{10} + 111N^9 + 219N^8 - 3N^7 - 331N^6 + 920N^5 + 3712N^4 + 5080N^3 \\ + 4192N^2 + 2272N + 576 \tag{5.140}$$

$$P_{264} = 47N^{10} + 823N^9 + 5739N^8 + 21510N^7 + 53459N^6 + 105381N^5 + 160023N^4 \\ + 158774N^3 + 104300N^2 + 56664N + 18720 \tag{5.141}$$

$$P_{265} = 60N^{10} + 340N^9 + 594N^8 - 204N^7 - 2167N^6 - 4496N^5 - 7339N^4 - 8524N^3 \\ - 6112N^2 - 3024N - 784 \tag{5.142}$$

$$P_{266} = 67N^{10} + 383N^9 + 867N^8 + 696N^7 - 755N^6 - 2391N^5 - 3027N^4 - 2744N^3 \\ - 1256N^2 - 48N + 144 \tag{5.143}$$

$$P_{267} = 85N^{10} + 482N^9 + 1146N^8 + 1272N^7 + 532N^6 + 840N^5 + 2427N^4 + 2440N^3 \\ + 1768N^2 + 1248N + 432 \tag{5.144}$$

$$P_{268} = 95N^{10} + 1621N^9 + 10419N^8 + 32166N^7 + 55847N^6 + 78615N^5 + 111963N^4 \\ + 100934N^3 + 57980N^2 + 61560N + 36000 \tag{5.145}$$

$$P_{269} = 118N^{10} + 675N^9 + 1588N^8 + 1652N^7 + 326N^6 + 357N^5 + 876N^4 + 1672N^3 \\ + 3440N^2 + 2544N + 576 \tag{5.146}$$

$$P_{270} = 127N^{10} + 644N^9 + 1113N^8 - 372N^7 - 4016N^6 - 4578N^5 - 558N^4 + 2008N^3 \\ + 2848N^2 + 2496N + 864 \tag{5.147}$$

$$P_{271} = 151N^{10} + 708N^9 + 1156N^8 + 464N^7 - 967N^6 + 372N^5 + 3672N^4 + 5236N^3 \\ + 6152N^2 + 3792N + 864 \tag{5.148}$$

$$P_{272} = 118N^{11} + 649N^{10} + 1996N^9 + 5922N^8 + 14389N^7 + 26096N^6 + 33057N^5 \\ + 29305N^4 + 19668N^3 + 8048N^2 + 2016N + 432 \tag{5.149}$$

$$P_{273} = 37N^{12} + 305N^{11} + 1017N^{10} + 1462N^9 + 592N^8 + 408N^7 + 4064N^6 + 9645N^5 \\ + 12222N^4 + 10280N^3 + 6064N^2 + 2192N + 352 \tag{5.150}$$

5. Pure-singlet contributions to DIS

$$P_{274} = 45N^{13} + 485N^{12} + 2289N^{11} + 6064N^{10} + 8448N^9 + 4398N^8 - 1602N^7$$
$$- 2715N^6 - 584N^5 + 9300N^4 + 22624N^3 + 21232N^2 + 10112N + 1984 \tag{5.151}$$

$$P_{275} = 82N^{13} + 2471N^{12} + 27848N^{11} + 164605N^{10} + 597268N^9 + 1483293N^8$$
$$+ 2732000N^7 + 3846211N^6 + 4059946N^5 + 3144284N^4 + 1798280N^3$$
$$+ 756000N^2 + 222912N + 34560 \tag{5.152}$$

$$P_{276} = 83N^{14} + 636N^{13} + 1484N^{12} - 505N^{11} - 7588N^{10} - 8082N^9 + 12896N^8$$
$$+ 30199N^7 - 2799N^6 - 73072N^5 - 117444N^4 - 105808N^3 - 62992N^2$$
$$- 23424N - 4032 \tag{5.153}$$

$$P_{277} = 1790N^{14} + 13034N^{13} + 34014N^{12} + 16729N^{11} - 108615N^{10} - 261746N^9$$
$$- 246794N^8 - 165593N^7 - 316791N^6 - 606160N^5 - 724860N^4 - 602224N^3$$
$$- 352272N^2 - 124416N - 19008 \tag{5.154}$$

$$P_{278} = 73N^{15} + 867N^{14} + 4698N^{13} + 16255N^{12} + 43958N^{11} + 97502N^{10} + 165558N^9$$
$$+ 200747N^8 + 161729N^7 + 60265N^6 - 48800N^5 - 106628N^4 - 94640N^3$$
$$- 48016N^2 - 13696N - 1728 \tag{5.155}$$

$$P_{279} = 229N^{16} - 49N^{15} - 48956N^{14} - 530524N^{13} - 2816896N^{12} - 9419641N^{11}$$
$$- 22464935N^{10} - 41400392N^9 - 60928891N^8 - 70644896N^7 - 62314487N^6$$
$$- 39968930N^5 - 16753760N^4 - 2474640N^3 + 1995408N^2 + 1334880N + 259200 \,. \tag{5.156}$$

The corresponding expression in x space is given in Eq. (E.14). Alternatively, one can calculate the structure functions directly in N space and solve the evolution equations in N space, cf. [436]. Finally, one numerical contour integral around the poles of the problem is required. The necessary analytic continuation of the harmonic and generalised harmonic sums to complex argument N can be obtained from their asymptotic expansion and the shift relations [147, 261].

For the following illustrations of the pure-singlet Wilson coefficient and its contribution to the structure function $F_2(x, Q^2)$, we choose the factorisation and renormalisation scale $\mu^2 = Q^2$. To study the scale dependence in μ^2 properly, the gluonic contributions would have to be taken into account due to mixing in the scale evolution. Since the gluonic Wilson coefficient $H_{g,2}^{\mathrm{S}}$ requires the OME $A_{Qg}^{(3)}$, which is not completed yet, we restrict the discussion to the choice $\mu^2 = Q^2$ for now. The HPLs of the x space expressions are evaluated using an extension to weight $w = 5$ of the code described in [423]. For the contribution from the massless 3-loop Wilson coefficient $\tilde{c}_{q,2}^{\mathrm{PS},(3)}$ we use the parametrisation given in [138]. The PDFs refer to the NNLO sets from [218], which are available as grids for the library `LHAPDF` [422]. Like for the OME, we use the parametrisation of the strong coupling constant that belongs to this PDF set. Moreover, we use the same value of the coupling constant and PDFs for both the 2-loop and 3-loop curves in order to enable a better comparison of the impact from the Wilson coefficient. We consider the case of $N_F = 3$ massless quarks and a single massive quark in the fixed flavour number scheme. Unless stated otherwise, the massive quark is a charm quark for which we use $m_c = 1.59 \, \mathrm{GeV}$ in the OMS scheme [226].

Before discussing the contribution to the structure function $F_2(x, Q^2)$, we illustrate the Wilson coefficient $H_{q,2}^{\mathrm{PS}}$ in x space in Fig. 5.7. In contrast to the 2-loop OME, cf. Fig. 5.5, the 2-loop Wilson coefficient is positive at small x for $Q^2 = 20 \, \mathrm{GeV}^2$. Above $Q^2 = 50 \, \mathrm{GeV}^2$, it becomes negative as well. The overall shape of the Wilson coefficient at small x is similar to that of the OME, although the size of the sum of 2-loop and 3-loop contributions is larger than just the contributions from the OME alone. Figure 5.8 zooms in on the region of x where the 3-loop
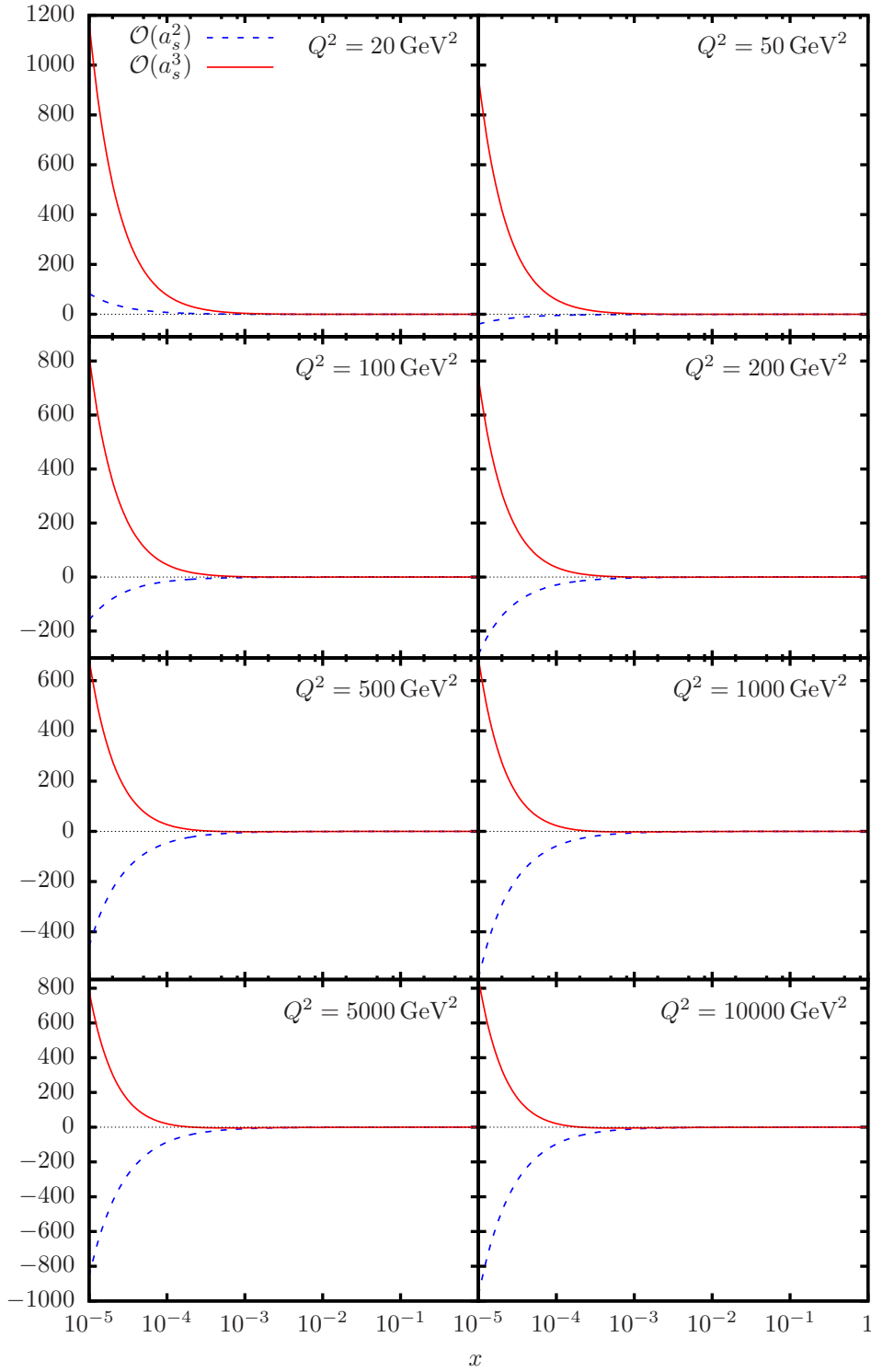
Figure 5.7.: The heavy flavour Wilson coefficient $H_{q,2}^{\mathrm{PS}}$ for different values of Q^2. We choose $\mu^2 = Q^2$ and refer to the charm quark as the heavy quark ($N_F = 3$) with a mass of $m_c = 1.59\,\mathrm{GeV}$ in the OMS scheme [226]. The dashed line shows the 2-loop contribution alone and the solid line gives the sum of the 2-loop and 3-loop terms.
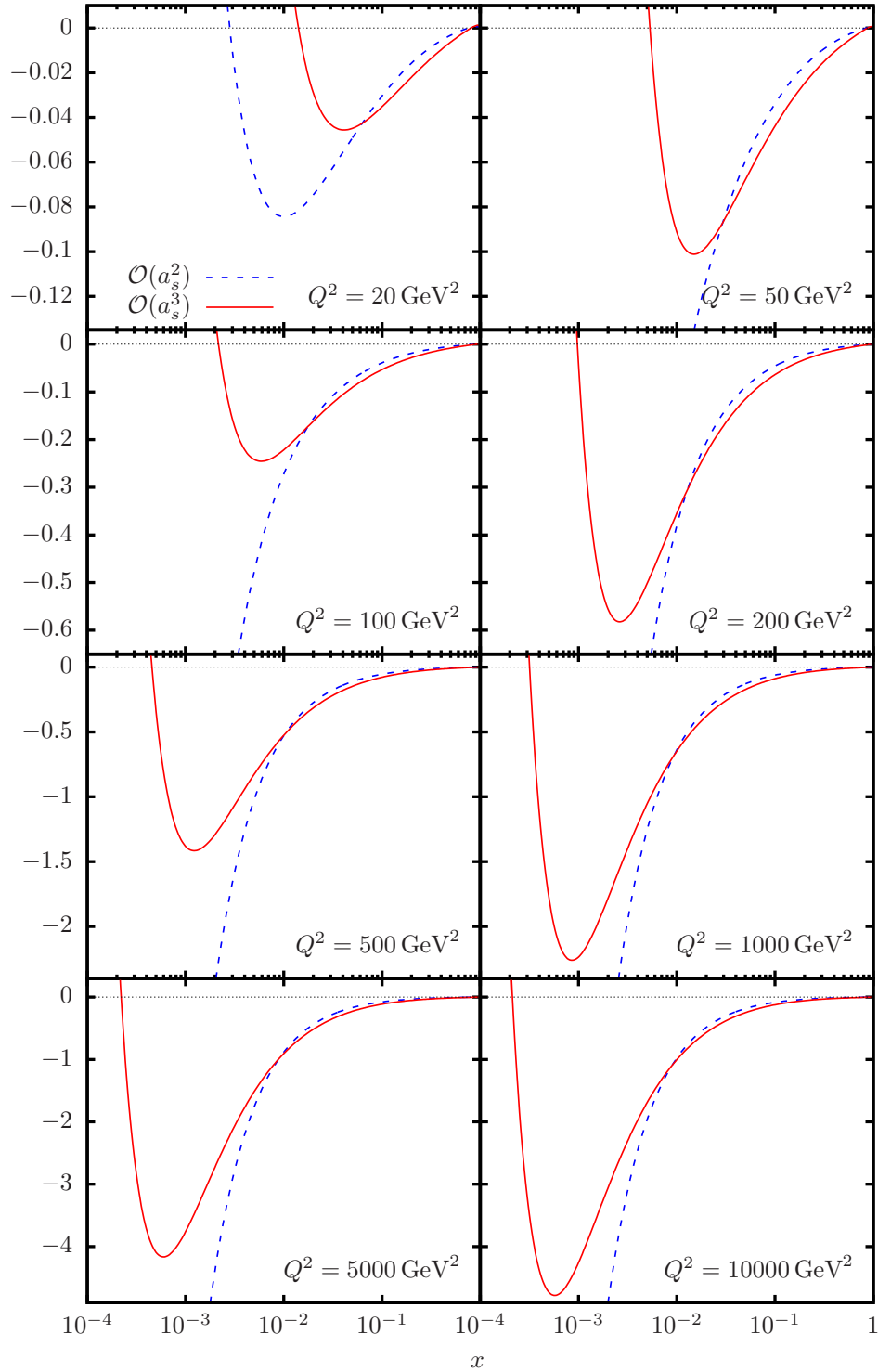
Figure 5.8.: Illustration of the Wilson coefficient $H_{q,2}^{\mathrm{PS}}$ near its sign change. The scale choice and charm quark mass are the same as in Fig. 5.7.

Table 5.1.: Charm contribution from $H_{q,2}^{\mathrm{PS}}$ at the lowest value of x which is kinematically accessible at HERA.

Q^2/GeV^2	x_0	$F_2^{\mathrm{h,PS}}(x_0, Q^2)$
20	0.0002	-0.013
100	0.001	-0.026
500	0.005	-0.023
1000	0.01	-0.019
5000	0.05	-0.007
10 000	0.1	-0.003

term of the Wilson coefficient becomes negative. The features observed in Fig. 5.6 for the OME remain qualitatively unaltered. The sum of the 2-loop and 3-loop terms is negative for x in the intervals $1.4 \cdot 10^{-2} \lesssim x \lesssim 0.8$ at $Q^2 = 20\,\mathrm{GeV}^2$ and $2 \cdot 10^{-4} \lesssim x < 1$ at $Q^2 = 10\,000\,\mathrm{GeV}^2$. Again, the 3-loop correction is negative for $x \gtrsim 0.01$ to 0.1, depending on Q^2, which makes the absolute value of the correction up to $\mathcal{O}(a_s^3)$ larger than the $\mathcal{O}(a_s^2)$ correction.

In Fig. 5.9 we plot the heavy flavour contribution from $H_{q,2}^{\mathrm{PS}}$ to $F_2(x, Q^2)$ for a charm quark. Moreover, the analogous plot for the contribution from bottom quarks is shown in Fig. 5.10, also assuming $N_F = 3$ in the fixed flavour number scheme to preserve additivity. The bottom quark mass in the OMS scheme is $m_b = 4.78\,\mathrm{GeV}$ [226]. Here we do not yet include contributions from diagrams with both charm and bottom quarks, which start to contribute at $\mathcal{O}(a_s^3)$. Contributions of this type are presented elsewhere. Both at 2-loop and 3-loop order the pure-singlet contribution to the structure function $F_2(x, Q^2)$ is negative. The fact that the structure function is negative, even at $x = 10^{-5}$, is a consequence of the negativity of the Wilson coefficient at medium values of x, which we discussed above. In the convolution integral, the positive contribution from x below 10^{-4} is cancelled by the negative contribution from medium values of x. At $x = 10^{-4}$ and $Q^2 = 100\,\mathrm{GeV}^2$ we get -0.026 for the $\mathcal{O}(a_s^3)$ charm correction to the pure-singlet structure function and -0.0015 for the bottom correction. The lowest attainable value of x for a given virtuality Q^2 is given by $x_0 = \frac{Q^2}{sy}$, where s is the centre-of-mass energy and $y \leq 1$ denotes the inelasticity, cf. Eq. (2.5). To get a rough estimate of the kinematic reach that is experimentally accessible, we can assume $s \approx 10^5\,\mathrm{GeV}^2$ for HERA. With these kinematic constraints, we get the values listed in Table 5.1 for the charm contribution at the smallest, kinematically allowed configuration. By comparison, the bottom quark contribution is about one order of magnitude smaller.
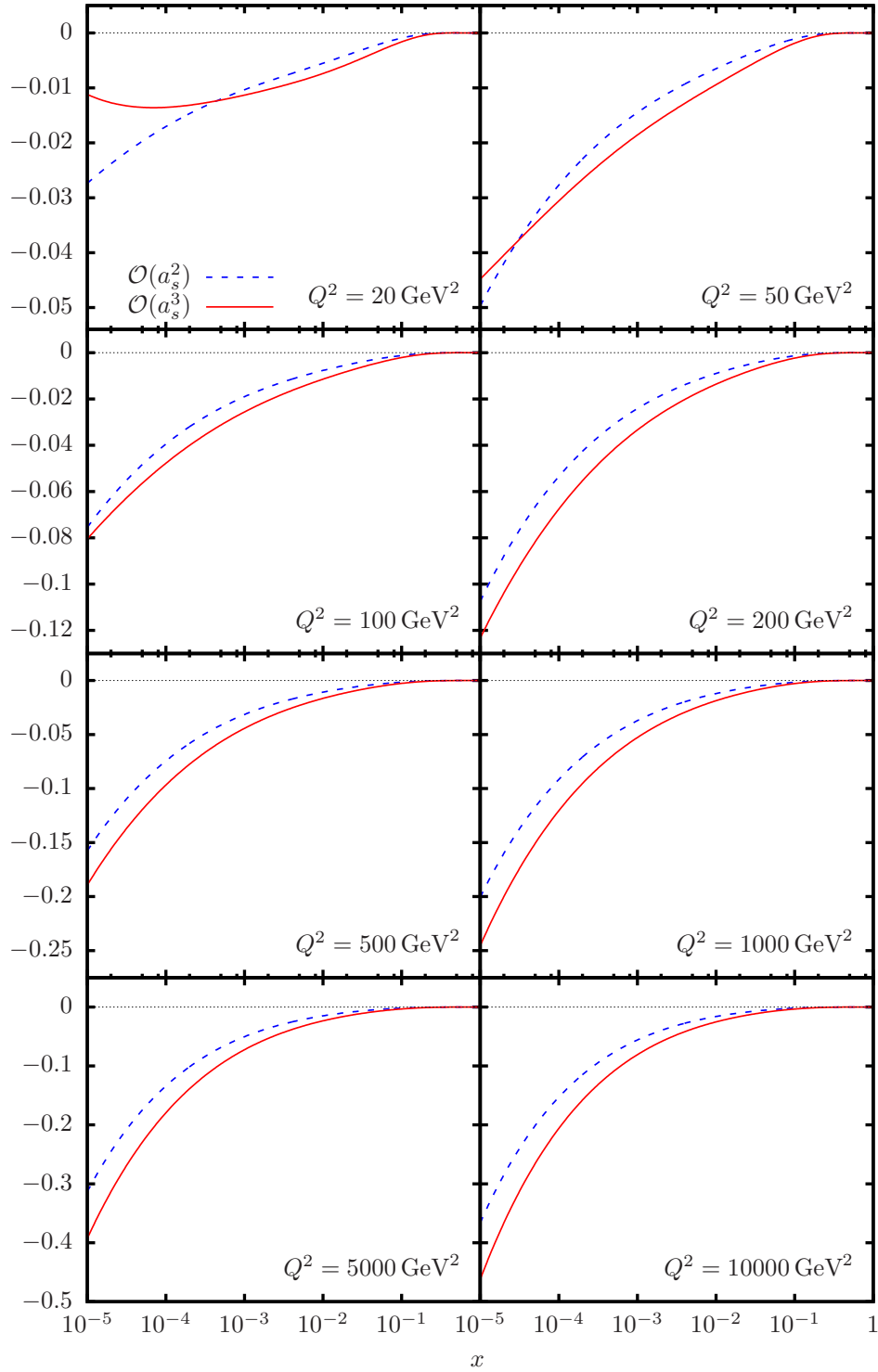
Figure 5.9.: The pure-singlet charm contribution from $H_{q,2}^{\mathrm{PS}}$ to the structure function $F_2(x, Q^2)$. The scale choice and charm quark mass are the same as in Fig. 5.7. For the PDFs we use the NNLO sets from [218]. The dashed line shows the 2-loop contribution alone and the solid line gives the sum of the 2-loop and 3-loop terms.
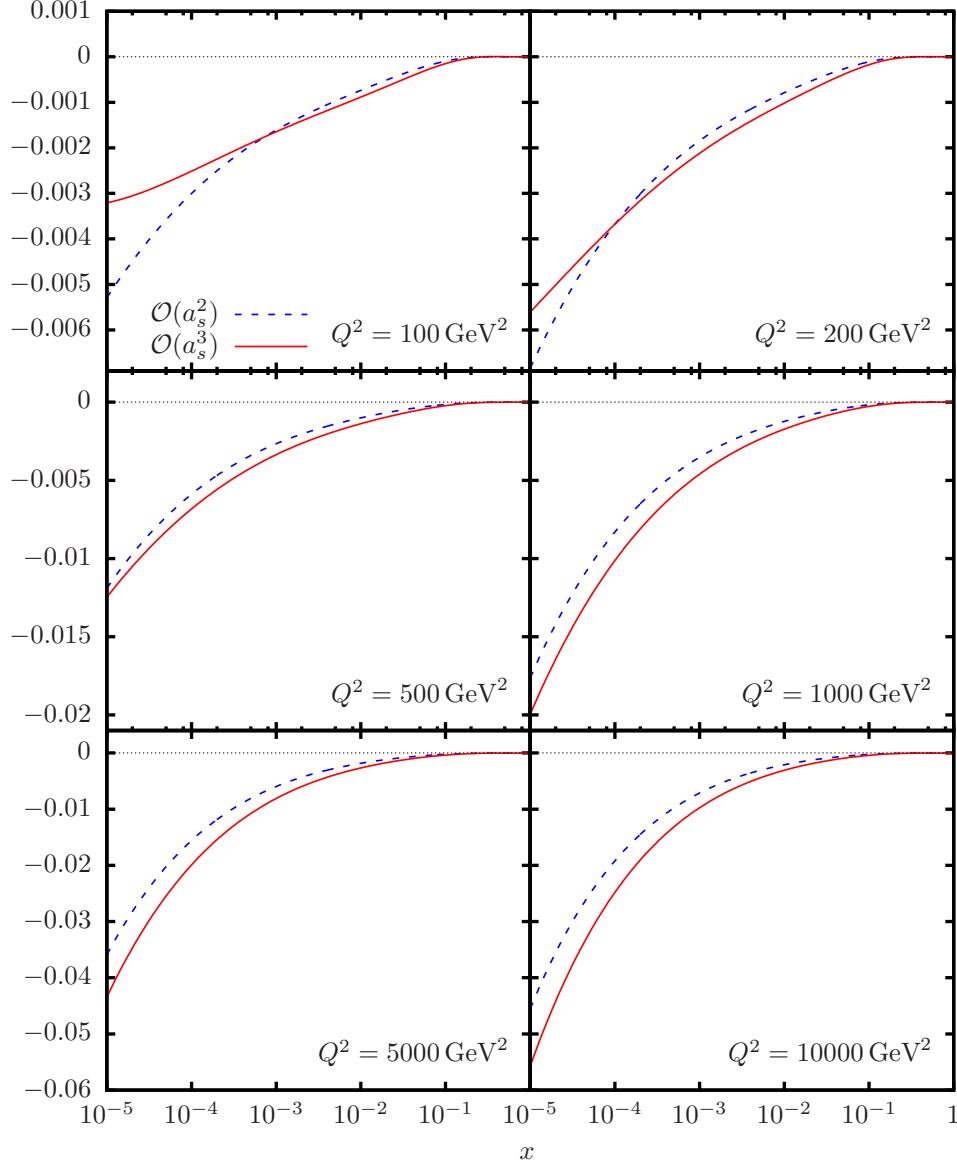
Figure 5.10.: The pure-singlet bottom contribution from $H_{q,2}^{\mathrm{PS}}$. The plot refers to the case of $N_F = 3$ massless quarks and one massive bottom quark. For the mass of the bottom quark we use $m_b = 4.78\,\mathrm{GeV}$ in the OMS scheme from [226]. All other settings are identical to Fig. 5.9.

6. Ladder- and V-diagrams for $A_{Qg}^{(3)}$

In this chapter, we turn to a collection of individual diagrams which contribute to the massive OME $A_{Qg}^{(3)}$. This OME is characterised by having external, on-shell gluon states and the operator insertion on a massive quark line. Contributions to this OME start at $\mathcal{O}(a_s)$ and its 3-loop term is relevant for the factorisation of the heavy flavour Wilson coefficients $H_{g,2}^{\mathrm{S}}$, see Eq. (2.95). Furthermore, it appears in the matching relations for $f_Q + f_{\bar{Q}}$, Eq. (2.112), and hence also for Σ, Eq. (2.114). Here we will discuss the calculation of physical diagrams with ladder- and V-topologies, which form an important class of diagrams in $A_{Qg}^{(3)}$. This is related to the calculations in [343] in the sense that we calculate the same diagrams (including some additional diagrams), but here we consider the full diagrams as they arise from the Feynman rules of QCD and the operator insertions instead of just the scalar prototypes considered in [343]. We chose to calculate these diagrams as a pilot calculation to test and develop our methods. Their complexity goes beyond that of the Benz diagrams which appear in the non-singlet and pure-singlet OMEs, discussed in the previous two chapters, see also [358, 397]. The results of these calculations are published in [268], where also the relevant methods are described.

Three-loop ladder diagrams appear in the OMEs $A_{qg,Q}^{(3)}$, $A_{gg,Q}^{(3)}$ and $A_{Qg}^{(3)}$. They have three loops, of which two loops have no propagator in common and where the external legs are connected to the two opposite loops. The loops can have different fields assigned, but the presence of a heavy quark requires at least one massive line. In contrast to the diagrams considered here, the ladder diagrams of $A_{qg,Q}^{(3)}$ must have both a massive and a massless quark and the operator must be on the massless quark line. This restricts the possible diagrams to configurations where we assign the quark lines to the two outer loops. Diagrams of this type were calculated in [336], since they are always proportional to $N_F T_F^2$. They are easier to calculate since they can contain at most three different massive propagators. A sample of ladder diagrams contributing to $A_{Qg}^{(3)}$ is depicted in Fig. 6.1. Compared to $A_{qg,Q}^{(3)}$ there is more freedom how to assign fields to the
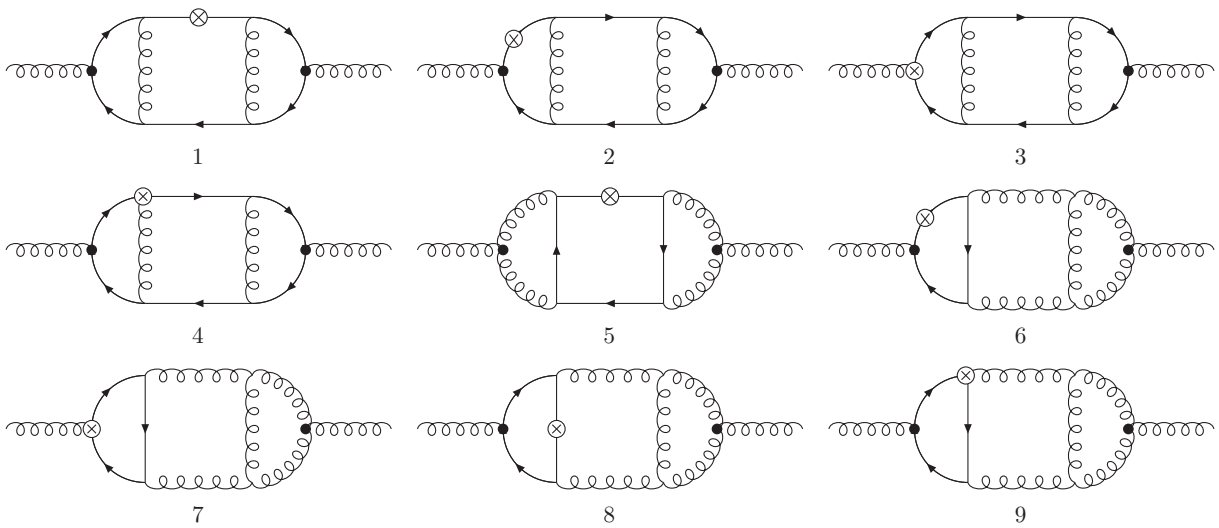

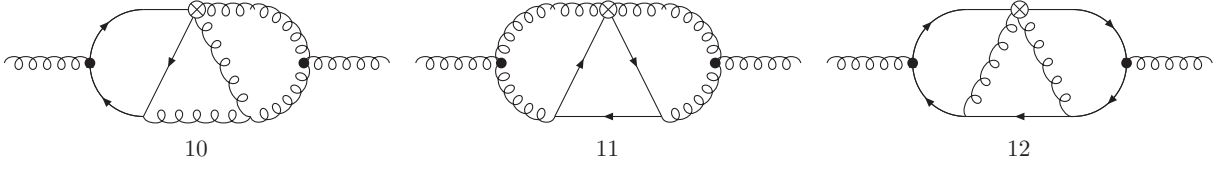Figure 6.1.: A sample of ladder diagrams which contribute to $A_{Qg}^{(3)}$.

Figure 6.2.: A sample of V-diagrams which contribute to $A_{Qg}^{(3)}$.

basic ladder topology. For $A_{Qg}^{(3)}$, the only requirements are that the external legs are gluons, that there is a massive quark line and that the operator is placed on that line. In principle, also two separate, massive quark lines can be present in a ladder diagram, but since their contribution is proportional to T_F^2, they again form separate colour factors and we exclude those diagrams from the present discussion. Analogous ladder diagrams also contribute to $A_{gg,Q}^{(3)}$, when the operator is placed on one of the gluon lines or vertices instead; see the discussion in the next chapter.

In addition to the ladder diagrams, the Feynman rules of the operator insertions also allow for an additional topology which contributes to $A_{Qg}^{(3)}$: V-diagrams are diagrams with a central triangle, which can occur due to the $q\bar{q}gg$ operator. Examples for such diagrams are shown in Fig. 6.2. V-diagrams can be obtained from ladder diagrams by contracting the upper or lower propagator of the central loop. Additionally, they can also be obtained from crossed box diagrams by contracting one of their upper or lower central propagators. These two ways to obtain a V-diagram are reflected by the two terms present in the Feynman rule of the $q\bar{q}gg$ operator,


$$g^2 \Delta^\mu \Delta^\nu \Delta\!\!\!/ \sum_{j=0}^{N-3} \sum_{l=j+1}^{N-2} (\Delta.p_1)^{N-l-2} (\Delta.p_2)^j$$

$$\times \left[(t^b t^a)_{ji} (\Delta.p_1 + \Delta.p_3)^{l-j-1} + (t^a t^b)_{ji} (\Delta.p_1 + \Delta.p_4)^{l-j-1} \right].$$

The scalar products of the first term can be brought into the form of $\mathrm{OP}_3^{(N-3)}(p_2, p_1, p_1 + p_3)$ and the second term can be written as $\mathrm{OP}_3^{(N-3)}(p_2, p_1, p_1 + p_4)$, where we refer to the definition of OP_3 in Eq. (3.6). Hence, the generating function for this operator involves three linear propagators which can be expressed graphically as

Here the dashed lines with blank arrows represent linear propagators and the direction of the arrows give the direction of momentum flow. The gluon momenta are taken to be incoming. As a result, the V-diagrams have two parts, correspondent to the two terms of the operator Feynman rule, which carry different combinations of momenta in their linear propagators. For diagram 12

of Fig. 6.2 the two terms can be drawn as
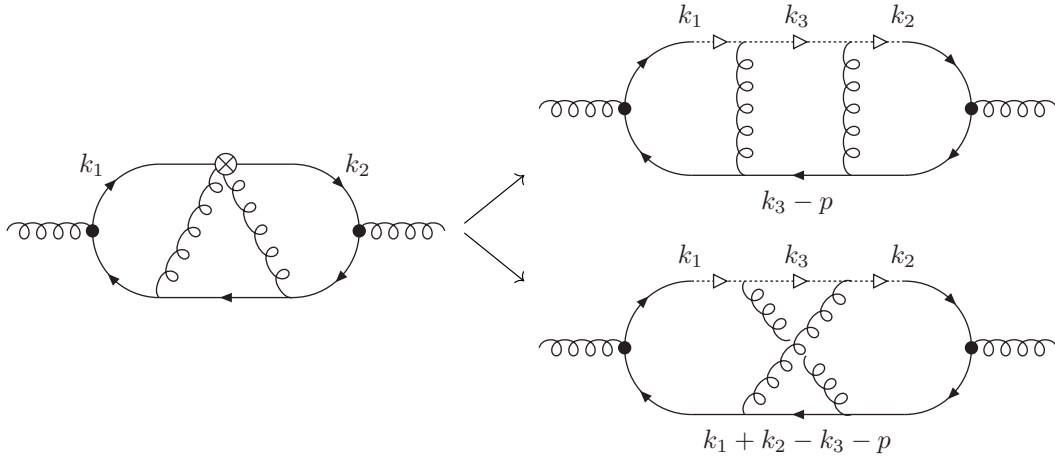
Here we have shifted the loop momenta such that the momentum flowing through the linear propagators is as simple as possible. On the other hand, the lower fermion propagator of the central triangle now carries $k_1 + k_2 - k_3 - p$. Note that, while the upper diagram is planar, the lower diagram has a non-planar structure. We map the scalar integrals of the former part to the planar integral family B3a, whereas we need the non-planar family C3a for the latter part. We see that, even though the original diagram is planar, the operator introduces "non-planarity" into the diagram. We will call the part of the diagram corresponding to the upper diagram the *planar* part and the part corresponding to the lower diagram to *non-planar* part. The difference in complexity also translates to different types of sums appearing in the results. As we will see below, the result of the upper diagram can be expressed purely in terms of harmonic sums, while the calculation of the lower diagram turns out to be particularly challenging and the result requires binomially weighted sums.

A similar discussion applies, in principle, also to diagrams 10 and 11 from Fig. 6.2: They have to be split into two parts, which are mapped to a planar and a non-planar integral family. However, the colour structure of the non-planar part simplifies exactly to zero, thereby eliminating the need to calculate this part of the diagram. Therefore, the complexity of the diagrams 10 and 11 is comparable to that of other ladder diagrams.

The calculation of the ladder- and V-diagrams again follows the procedure outlined in Section 3.1: The diagram description is generated using `QGRAF` [347] and treated with the `FORM` [216] programs developed for [193, 203] to insert Feynman rules, perform the Dirac and colour algebra and express all diagrams as scalar integrals from the families B1a, B3a and C3a. Those are reduced to master integrals via IBP relations computed using `Reduze 2` [353, 354]. In total, 157 master integrals are required to express the twelve diagrams. Table 6.1 lists the number of required master integrals for the individual diagrams. The largest number of master integrals is required by diagram 12 with 92 integrals. Besides the three families which already appeared among the scalar integrals, also the families B5a, B5b and B5c are present in the set of master integrals. Some of the integrals, in particular from the family B1a, appear also in the pure-singlet OME $A_{Qq}^{\mathrm{PS},(3)}$, so that their solutions can be reused or calculated to higher orders in ε, if necessary. We apply the techniques described in Section 3.3 to calculate the remaining master integrals. In particular the calculation via differential equations, see Section 3.3.4, is crucial for completing this task. The set of 32 master integrals, which are used as an example for a hierarchical system of differential equations in Table 3.1, are required for the calculation of diagram 12. They are solved via differential equations using the routines implemented in `SumProduction` [254–257], which uses `Sigma` [241, 252, 253], `HarmonicSums` [258–263] and `EvaluateMultiSums`

Diagram	# Master Integrals
D_1	28
D_2	43
D_3	43
D_4	72
D_5	16
D_6	13
D_7	13
D_8	8
D_9	19
D_{10}	46
D_{11}	39
$D_{12,a}$	61
$D_{12,b}$	80
D_{12}	92

Table 6.1.: Number of master integrals required for the individual diagrams of Figs. 6.1 and 6.2.

[254–257]. The system contains four master integrals from the non-planar family C3a, one of them being the scalar prototype of the non-planar part of diagram 12 itself. One sector of six master integrals was calculated using the multivariate Almkvist-Zeilberger algorithm [384, 385], which is implemented in the Mathematica package MultiIntegrate [259], see also [268]. Using these techniques, all master integrals required for the example diagrams can be calculated. By writing the results for the master integrals as formal power series in the tracing variable t, inserting them into the expression of the diagram, extracting the Nth coefficient in the expansion in t and simplifying the resulting sums, see Section 3.1, we obtain the results for the diagrams in N space.

As an example for one of the more involved ladder diagrams, we give the result for diagram 4 from Fig. 6.1,

$$
\begin{aligned}
D_4 = \left(\frac{C_A}{2} - C_F\right)^2 T_F \Bigg\{ & \frac{256}{\varepsilon^3} \frac{(1 - S_1)}{3(N + 1)(N + 2)} + \frac{16}{\varepsilon^2} \Bigg[\frac{2(7N^2 + 36N + 38)}{3(N + 1)^2(N + 2)^2} \\
& + \frac{(N - 1)(4N + 9)}{3N(N + 1)(N + 2)} S_2 + \frac{5N + 17}{3N(N + 1)(N + 2)} S_1^2 - \frac{P_{280} S_1}{3N^2(N + 1)^2(N + 2)^2} \Bigg] \\
& + \frac{4}{\varepsilon} \Bigg[-\frac{23N^2 - 57N + 198}{9N(N + 1)(N + 2)(N + 3)} S_1^3 - \frac{2(10N^2 + 13N + 40)}{3N(N + 1)(N + 2)} S_{2,1} \\
& + \frac{2(30N^3 + 289N^2 + 357N + 432)}{9N(N + 1)(N + 2)(N + 3)} S_3 - \frac{4P_{282}}{3(N + 1)^3(N + 2)^3(N + 3)} \\
& + \frac{P_{283} S_1^2 - P_{284} S_2}{3N^2(N + 1)^2(N + 2)^2(N + 3)} + \frac{8(1 - S_1)}{(N + 1)(N + 2)} \zeta_2 \\
& - \left(\frac{8N^3 + 47N^2 - 113N + 30}{3N(N + 1)(N + 2)(N + 3)} S_2 + \frac{2P_{292}}{3N^3(N + 1)^3(N + 2)^3(N + 3)} \right) S_1 \Bigg] \\
& + \frac{(-37N^2 + 38N - 345)}{9N(N + 1)(N + 2)(N + 3)} S_1^4 + \frac{4(26N^3 + 401N^2 + 2969N + 3408)}{3N(N + 1)(N + 2)(N + 3)} S_{3,1}
\end{aligned}
$$

$$
-\frac{2\left(86N^3+558N^2+2723N+2661\right)}{3N(N+1)(N+2)(N+3)}S_4-\frac{4P_{286}S_{2,1}}{3N^2(N+1)^2(N+2)^2(N+3)}
$$

$$
+\frac{\left(204N^3+885N^2+616N-537\right)}{3N(N+1)(N+2)(N+3)}S_2^2+\frac{4P_{287}S_1^3}{9N^2(N+1)^2(N+2)^2(N+3)^2}
$$

$$
-\frac{4\left(94N^3+505N^2+1513N+1236\right)}{3N(N+1)(N+2)(N+3)}S_{2,1,1}-\frac{4P_{290}S_3}{9N^2(N+1)^2(N+2)^2(N+3)^2}
$$

$$
+\frac{8P_{291}}{3(N+1)^4(N+2)^4(N+3)^2}-\frac{2P_{293}S_2}{3N^3(N+1)^3(N+2)^3(N+3)^2}
$$

$$
+\left(\frac{8\left(3N^3-193N^2-2221N-2829\right)}{9N(N+1)(N+2)(N+3)}S_3+\frac{4P_{289}S_2}{3N^2(N+1)^2(N+2)^2(N+3)^2}\right.
$$

$$
+\frac{4\left(52N^3+235N^2+661N+408\right)S_{2,1}}{3N(N+1)(N+2)(N+3)}+\frac{4P_{295}}{3N^4(N+1)^4(N+2)^4(N+3)^2}\Bigg)S_1
$$

$$
-\left(\frac{2\left(4N^3-41N^2-300N-207\right)}{3N(N+1)(N+2)(N+3)}S_2+\frac{2P_{294}}{3N^3(N+1)^3(N+2)^3(N+3)^2}\right)S_1^2
$$

$$
+\left(\frac{4\left(7N^2+36N+38\right)}{(N+1)^2(N+2)^2}+\frac{2(N-1)(4N+9)}{N(N+1)(N+2)}S_2+\frac{2(5N+17)}{N(N+1)(N+2)}S_1^2\right.
$$

$$
-\frac{2P_{280}S_1}{N^2(N+1)^2(N+2)^2}\Bigg)\zeta_2+\left(-\frac{16\left(21N^3+64N^2-147N-306\right)}{3N(N+1)(N+2)(N+3)}S_1\right.
$$

$$
+\frac{32P_{288}}{3N^2(N+1)^2(N+2)^2(N+3)^2}\Bigg)\zeta_3+(-1)^N\frac{8P_{285}\left(S_{-3}+2S_{-2,1}+2\zeta_3\right)}{N^2(N+1)^2(N+2)^2(N+3)^2}
$$

$$
+\frac{32(N^3+5N^2-2N-12)}{N(N+1)(N+2)(N+3)}\left[\left(S_{2,1}\left(1,\frac{1}{2}\right)-S_3\left(\frac{1}{2}\right)\right)S_1(2)-S_2S_{1,1}\left(2,\frac{1}{2}\right)\right.
$$

$$
+S_{3,1}\left(\frac{1}{2},2\right)-S_{2,1,1}\left(1,\frac{1}{2},2\right)-\frac{1}{2}S_{1,1,1,1}\left(2,\frac{1}{2},1,1\right)+S_1(2)\zeta_3\Bigg]
$$

$$
+\frac{2^N P_{281}}{N(N+1)^2(N+2)^2(N+3)^2}\left[8S_1^2S_1\left(\frac{1}{2}\right)+40S_2S_1\left(\frac{1}{2}\right)+32S_3\left(\frac{1}{2}\right)\right.
$$

$$
-16S_1S_{1,1}\left(1,\frac{1}{2}\right)+16S_{2,1}\left(\frac{1}{2},1\right)-48S_{2,1}\left(1,\frac{1}{2}\right)+16S_{1,1,1}\left(1,1,\frac{1}{2}\right)
$$

$$
-32\zeta_3\Bigg]\Bigg\}\,,\tag{6.1}
$$

where the polynomials are given by

$$
P_{280}=3N^4+61N^3+134N^2+80N+16 \tag{6.2}
$$

$$
P_{281}=N^5-N^4-27N^3-147N^2-290N-144 \tag{6.3}
$$

$$
P_{282}=22N^5+336N^4+1780N^3+4431N^2+5299N+2496 \tag{6.4}
$$

$$
P_{283}=25N^5-16N^4-154N^3-435N^2-704N-168 \tag{6.5}
$$

$$
P_{284}=69N^5+384N^4-258N^3-2455N^2-2048N-168 \tag{6.6}
$$

$$
P_{285}=N^6+18N^5+100N^4+256N^3+319N^2+210N+72 \tag{6.7}
$$

$$
P_{286}=10N^6+173N^5+922N^4+1196N^3+295N^2+1040N+600 \tag{6.8}
$$

$$
P_{287}=111N^6+415N^5-13N^4-1561N^3-2018N^2+150N+1332 \tag{6.9}
$$

$$
P_{288}=6N^7+8N^6-300N^5-1526N^4-2739N^3-1590N^2+423N+270 \tag{6.10}
$$

$$P_{289} = 16N^7 + 169N^6 + 43N^5 - 2819N^4 - 7717N^3 - 5562N^2 + 2250N + 2052 \qquad (6.11)$$

$$P_{290} = 156N^7 - 33N^6 - 12269N^5 - 60280N^4 - 109729N^3 - 82685N^2 - 24312N \\ - 4176 \qquad (6.12)$$

$$P_{291} = 33N^8 + 929N^7 + 9058N^6 + 45257N^5 + 132016N^4 + 235379N^3 + 255487N^2 \\ + 157641N + 43128 \qquad (6.13)$$

$$P_{292} = 94N^8 + 532N^7 + 607N^6 - 2110N^5 - 6389N^4 - 6022N^3 - 2064N^2 - 464N \\ - 96 \qquad (6.14)$$

$$P_{293} = 52N^9 - 320N^8 - 2503N^7 + 7573N^6 + 82014N^5 + 218117N^4 + 255071N^3 \\ + 134820N^2 + 33912N + 7344 \qquad (6.15)$$

$$P_{294} = 220N^9 + 1504N^8 + 2695N^7 - 5585N^6 - 31902N^5 - 54489N^4 - 41095N^3 \\ - 13260N^2 - 2664N + 432 \qquad (6.16)$$

$$P_{295} = 368N^{12} + 4462N^{11} + 20941N^{10} + 38782N^9 - 27919N^8 - 266895N^7 \\ - 523028N^6 - 498037N^5 - 240514N^4 - 53824N^3 - 4064N^2 + 1536N \\ + 576 \,. \qquad (6.17)$$

For fixed values of N, it agrees with the results obtained for this diagram in [193, 203] using
`MATAD` [217]. Besides harmonic sums up to weight $w = 4$, also generalised harmonic sums over
the alphabet $\{1/2, 1, 2\}$ are required. Since the letter 2 implies a growth proportional to 2^N
of individual sums and also an explicit factor 2^N appear, we have to explicitly check that the
asymptotic behaviour of the full diagram is at most logarithmic in the limit $N \to \infty$. In [344], a
massive scalar diagram was encountered which showed an exponential growth in that limit. The
asymptotic expansion, calculated using `HarmonicSums`, is given by

$$D_4 = \left(\frac{C_A}{2} - C_F\right)^2 T_F \left(\ln(\bar{N})^4 \left[-\frac{37}{9N^2} + \frac{260}{9N^3} - \frac{1498}{9N^4} + \frac{6350}{9N^5} - \frac{23182}{9N^6} + \frac{78230}{9N^7}\right.\right.$$

$$\left. - \frac{252478}{9N^8} + \frac{793430}{9N^9} - \frac{2452702}{9N^{10}}\right] + \ln(\bar{N})^3 \left[\frac{148}{3N^2} - \frac{3742}{9N^3} + \frac{56233}{27N^4} - \frac{237188}{27N^5}\right.$$

$$\left. + \frac{3030901}{90N^6} - \frac{364316}{3N^7} + \frac{1191908966}{2835N^8} - \frac{802611251}{567N^9} + \frac{7571739197}{1620N^{10}}\right]$$

$$+ \ln(\bar{N})^2 \left[-\frac{476}{3N^2} + \frac{3916}{3N^3} - \frac{37963}{6N^4} + \frac{487889}{18N^5} - \frac{115619381}{1080N^6} + \frac{214156793}{540N^7}\right.$$

$$\left. - \frac{10531100887}{7560N^8} + \frac{1953123301}{420N^9} - \frac{6574421070137}{453600N^{10}} + \zeta_2\left(-\frac{8}{3N} + \frac{160}{3N^2} - \frac{80}{3N^3}\right.\right.$$

$$\left.\left. - \frac{512}{3N^4} + \frac{2992}{3N^5} - \frac{11840}{3N^6} + \frac{41200}{3N^7} - \frac{134912}{3N^8} + \frac{427312}{3N^9} - \frac{1327040}{3N^{10}}\right)\right]$$

$$+ \ln(\bar{N}) \left[\frac{1568}{3N^2} - \frac{8678}{3N^3} + \frac{107683}{9N^4} - \frac{288043}{6N^5} + \frac{17224157}{90N^6} - \frac{794327263}{1080N^7}\right.$$

$$\left. + \frac{12708918931159}{4762800N^8} - \frac{21264661886953}{2381400N^9} + \frac{9733380027047}{381024N^{10}} + \zeta_3\left(\frac{88}{3N} - \frac{560}{9N^2}\right.\right.$$

$$\left. + \frac{5608}{9N^3} - \frac{27224}{9N^4} + \frac{105016}{9N^5} - \frac{364280}{9N^6} + \frac{1193848}{9N^7} - \frac{3786104}{9N^8} + \frac{11769976}{9N^9}\right.$$

$$\left.\left. - \frac{36135800}{9N^{10}}\right) + \zeta_2\left(\frac{64}{3N} - \frac{118}{3N^2} - \frac{7598}{9N^3} + \frac{44842}{9N^4} - \frac{304364}{15N^5} + \frac{222694}{3N^6}\right.\right.$$

$$\left.\left.\left. - \frac{48984386}{189N^7} + \frac{832600922}{945N^8} - \frac{2779325083}{945N^9} + \frac{1830552406}{189N^{10}}\right)\right] + \zeta_4\left(-\frac{148}{N} + \frac{1481}{6N^2}\right.\right.$$

$$- \frac{6998}{3N^3} + \frac{29773}{3N^4} - \frac{106103}{3N^5} + \frac{351103}{3N^6} - \frac{1118123}{3N^7} + \frac{3483223}{3N^8} - \frac{10706603}{3N^9}$$

$$+ \frac{32632903}{3N^{10}} \bigg) + \zeta_3 \bigg(-\frac{32}{N} - \frac{128}{3N^2} + \frac{2762}{3N^3} - \frac{87808}{27N^4} + \frac{1288903}{135N^5} - \frac{249484}{9N^6}$$

$$+ \frac{79258867}{945N^7} - \frac{107614439}{405N^8} + \frac{4928363147}{5670N^9} - \frac{1638402274}{567N^{10}} \bigg) + \zeta_2 \bigg(-\frac{256}{3N^2} + \frac{8477}{9N^3}$$

$$- \frac{105305}{18N^4} + \frac{3102209}{135N^5} - \frac{40907239}{540N^6} + \frac{168345925}{756N^7} - \frac{704036903}{1260N^8} + \frac{91944867169}{113400N^9}$$

$$+ \frac{18035424397}{4536N^{10}} \bigg) + \frac{632}{3N^2} + \frac{3767}{3N^3} - \frac{1025027}{162N^4} + \frac{6991955}{324N^5} - \frac{132245691}{2000N^6}$$

$$+ \frac{4030291117}{20250N^7} - \frac{6815103143399}{12348000N^8} + \frac{297957468833173}{333396000N^9} + \frac{6493831316846623}{1143072000N^{10}} \bigg)$$

$$+ \mathcal{O}\bigg(\frac{1}{N^{11}} \ln(\bar{N}) \bigg). \tag{6.18}$$

Here we use the abbreviation $\ln(\bar{N}) = \ln(N) + \gamma_{\mathrm{E}}$, where γ_{E} is the Euler-Mascheroni constant. The exponential growth cancels and only a logarithmic divergence, behaving like $\ln^4(\bar{N})$, remains. This corresponds to plus functions in x space and is expected. We obtain similar results for the other ladder diagrams of Fig. 6.1. Among the example diagrams, we observe that generalised harmonic sums only occur in diagrams with six massive propagators, i.e. diagrams 1 to 4. The results for the remaining diagrams can be expressed using only harmonic sums. For explicit results for the remaining ladder diagrams, we refer to the appendix of [268].

Diagram 12 is the most involved diagram among the examples, due to its non-planar component. The planar part $D_{12,a}$, which corresponds to a ladder topology, is expected to be much simpler than the non-planar part $D_{12,b}$. The scalar prototypes of this diagram, which are easier to compute, have been calculated in [344] and confirmed this expectation. Indeed, we find that also the diagram part $D_{12,a}$ with its full numerator structure requires just nested harmonic sums. It is given by

$$D_{12,a} = \left(\frac{C_A}{2} - C_F \right)^2 T_F \Bigg\{ \frac{1}{\varepsilon^3} \left[\frac{192 S_2 - 192 S_1^2 - 256}{3(N+1)(N+2)} + \frac{128(3N+1)S_1}{3(N+1)^2(N+2)} \right]$$

$$+ \frac{1}{\varepsilon^2} \left[-\frac{32\big(5N^3 + 53N^2 + 99N + 44\big)S_1^2}{3N(N+1)^2(N+2)^2} - \frac{32\big(5N^3 + 7N^2 - 5N - 4\big)S_2}{N(N+1)^2(N+2)^2} \right.$$

$$- \frac{64\big(9N^2 + 37N + 32\big)}{3(N+1)^2(N+2)^2} + \frac{64 S_1^3}{3(N+1)(N+2)} - \frac{64(4N+11)S_{2,1}}{3(N+1)(N+2)}$$

$$+ \frac{64(8N+15)S_3}{3(N+1)(N+2)} + \left(\frac{64 P_{296}}{3N(N+1)^3(N+2)^2} + \frac{64 S_2}{(N+1)(N+2)} \right) S_1 \bigg]$$

$$+ \frac{1}{\varepsilon} \left[\frac{32 P_{299}}{3(N+1)^3(N+2)^3} + \frac{20 S_1^4}{3(N+1)(N+2)} + \frac{32\big(26N^2 + 37N - 12\big)S_{2,1,1}}{3N(N+1)(N+2)} \right.$$

$$+ \frac{32 P_{301} S_{2,1}}{3N^2(N+1)^2(N+2)^2} - \frac{4\big(72N^2 + 93N - 16\big)S_2^2}{3N(N+1)(N+2)} - \frac{16 P_{302} S_2}{3N(N+1)^3(N+2)^3}$$

$$- \frac{32\big(15N^3 + 34N^2 - 19N - 42\big)S_1^3}{9N(N+1)^2(N+2)^2} - \frac{32\big(74N^2 + 115N - 20\big)S_{3,1}}{3N(N+1)(N+2)}$$

$$+ \left(\frac{16 P_{315}}{3N^3(N+1)^3(N+2)^3} + \frac{8 S_2}{(N+1)(N+2)} \right) S_1^2 + \frac{8\big(124N^2 + 225N - 24\big)S_4}{3N(N+1)(N+2)}$$

$$- \frac{32 P_{304} S_3}{9 N^2 (N+1)^2 (N+2)^2} + \left(\frac{32 P_{298} S_2}{3 N^2 (N+1)^2 (N+2)^2} + \frac{32 (28 N^2 + 41 N - 8) S_3}{3 N (N+1)(N+2)} \right.$$

$$- \frac{32 (14 N^2 + 33 N - 4) S_{2,1}}{3 N (N+1)(N+2)} - \frac{32 P_{313}}{3 N (N+1)^4 (N+2)^3} \bigg) S_1 + \left(- \frac{32}{(N+1)(N+2)} \right.$$

$$- \frac{24 S_1^2}{(N+1)(N+2)} + \frac{16 (3 N + 1) S_1}{(N+1)^2 (N+2)} + \frac{24 S_2}{(N+1)(N+2)} \bigg) \zeta_2$$

$$+ (-1)^N \left[\frac{640 S_{-3}}{(N+1)^2} - \frac{768 S_{-2,1}}{(N+1)^2} \right] \bigg] + \frac{16 P_{311}}{3 (N+1)^4 (N+2)^4} + \frac{8 S_1^5}{5 (N+1)(N+2)}$$

$$+ \frac{128 (6 N + 11) S_{-2} S_{-2,1}}{(N+1)(N+2)} - \frac{128 (6 N + 11) S_{-2,1,-2}}{(N+1)(N+2)} + \frac{64 (19 N + 22) S_{4,1}}{3 N (N+1)(N+2)}$$

$$- \frac{64 (105 N^2 + 126 N - 40) S_5}{15 N (N+1)(N+2)} - \frac{16 (116 N^2 + 289 N + 168) S_{2,2,1}}{3 N (N+1)(N+2)}$$

$$- \frac{16 (148 N^2 + 197 N - 72) S_{2,1,1,1}}{3 N (N+1)(N+2)} + \frac{16 (190 N^2 + 289 N + 28) S_{2,3}}{3 N (N+1)(N+2)}$$

$$+ \frac{16 (354 N^2 + 441 N - 284) S_{3,1,1}}{3 N (N+1)(N+2)} - \frac{2 (77 N^3 + 107 N^2 - 255 N - 292) S_1^4}{9 N (N+1)^2 (N+2)^2}$$

$$+ \frac{2 P_{306} S_2^2 + 16 P_{307} S_{3,1} - 16 P_{305} S_{2,1,1} - 4 P_{309} S_4}{3 N^2 (N+1)^2 (N+2)^2} + \frac{16 (P_{319} S_3 - 3 P_{318} S_{2,1})}{9 N^3 (N+1)^3 (N+2)^3}$$

$$+ \left(\frac{8 P_{316} S_2}{3 N^3 (N+1)^3 (N+2)^3} + \frac{16 P_{320}}{3 N (N+1)^5 (N+2)^4} - \frac{16 (35 N^2 + 44 N - 10) S_2^2}{3 N (N+1)(N+2)} \right.$$

$$+ \frac{16 (112 N^2 + 129 N - 32) S_{2,1,1}}{3 N (N+1)(N+2)} - \frac{16 (294 N^2 + 443 N - 84) S_{3,1}}{3 N (N+1)(N+2)}$$

$$+ \frac{16 (3 P_{303} S_{2,1} - P_{308} S_3)}{9 N^2 (N+1)^2 (N+2)^2} + \frac{8 (238 N^2 + 371 N - 68) S_4}{3 N (N+1)(N+2)} \bigg) S_1 + \left(\frac{32 S_2}{3 (N+1)(N+2)} \right.$$

$$+ \frac{8 P_{317}}{9 N^3 (N+1)^3 (N+2)^3} \bigg) S_1^3 - \frac{256 (N-1) S_{-2,-3}}{N (N+1)} + \left(\frac{8 P_{322}}{3 N^4 (N+1)^4 (N+2)^4} \right.$$

$$- \frac{32 (104 N^2 + 153 N - 36) S_3}{3 N (N+1)(N+2)} + \frac{8 (316 N^2 + 605 N + 88) S_{2,1}}{3 N (N+1)(N+2)} \bigg) S_2$$

$$+ \left(\frac{16 (56 N^2 + 87 N - 16) S_3}{3 N (N+1)(N+2)} - \frac{8 P_{321}}{3 N^4 (N+1)^4 (N+2)^4} - \frac{4 P_{297} S_2}{3 N^2 (N+1)^2 (N+2)^2} \right.$$

$$- \frac{8 (56 N^2 + 57 N - 16) S_{2,1}}{3 N (N+1)(N+2)} \bigg) S_1^2 + \left[- \frac{8 (9 N^2 + 37 N + 32)}{(N+1)^2 (N+2)^2} + \frac{8 S_1^3}{(N+1)(N+2)} \right.$$

$$- \frac{12 (5 N^3 + 7 N^2 - 5 N - 4) S_2}{N (N+1)^2 (N+2)^2} - \frac{4 (5 N^3 + 53 N^2 + 99 N + 44) S_1^2}{N (N+1)^2 (N+2)^2}$$

$$+ \left(\frac{8 P_{296}}{N (N+1)^3 (N+2)^2} + \frac{24 S_2}{(N+1)(N+2)} \right) S_1 + \frac{8 (8 N + 15) S_3}{(N+1)(N+2)}$$

$$- \frac{8 (4 N + 11) S_{2,1}}{(N+1)(N+2)} \bigg] \zeta_2 + \left[\frac{32 P_{300}}{3 N^2 (N+1)^3 (N+2)^2} - \frac{72 S_1^2}{(N+1)(N+2)} \right.$$

$$+ \frac{64 (3 N^2 + 8 N + 6) S_{-2}}{N (N+1)(N+2)} + \frac{8 (16 N^2 + 57 N + 32) S_2}{N (N+1)(N+2)} + \frac{16 (27 N + 17) S_1}{3 (N+1)^2 (N+2)} \bigg] \zeta_3$$

$$+ (-1)^N \left[\frac{32 (2 N + 3)}{(N+1)(N+2)} \Big(2 S_{-2} S_{2,1} - 2 S_{2,1,-2} - 4 S_{-2,2,1} - 5 S_{-3,1,1} + 6 S_2 S_{-2,1} \right.$$

$$+ 6S_{-2,1,1} - 2S_{-5} - S_{2,-3} + 3S_{-4,1}\right) + \left(-\frac{32P_{314}}{N^3(N+1)^3(N+2)^2} - \frac{576S_1}{(N+1)^2}\right.$$

$$\left.- \frac{32(2N+3)S_2}{(N+1)(N+2)}\right)S_{-3} - \frac{2176S_{-2,1,1}}{(N+1)^2} + \frac{896S_1S_{-2,1}}{(N+1)^2} + \frac{64P_{312}S_{-2,1}}{N^3(N+1)^3(N+2)^2}$$

$$- \frac{64(2N+3)S_{-2,3}}{(N+1)(N+2)} + \frac{1024S_{-2,2}}{(N+1)^2} - \frac{64S_{-4}}{(N+1)^2} + \frac{960S_{-3,1}}{(N+1)^2} + \left(\frac{64(2N+3)S_2}{(N+1)(N+2)}\right.$$

$$\left.\left.+ \frac{128S_1}{(N+1)^2} + \frac{64P_{310}}{N^3(N+1)^3(N+2)^2} + \frac{128(2N+3)S_{-2}}{(N+1)(N+2)}\right)\zeta_3\right]\right\}, \tag{6.19}$$

with the polynomials

$$P_{296} = 7N^4 + 53N^3 + 93N^2 + 53N + 16 \tag{6.20}$$

$$P_{297} = 9N^4 - 25N^3 - 131N^2 - 100N - 32 \tag{6.21}$$

$$P_{298} = 13N^4 + 92N^3 + 149N^2 + 66N + 16 \tag{6.22}$$

$$P_{299} = 17N^4 + 129N^3 + 351N^2 + 403N + 168 \tag{6.23}$$

$$P_{300} = N^5 - 56N^4 - 193N^3 - 232N^2 - 132N - 48 \tag{6.24}$$

$$P_{301} = 4N^5 + 39N^4 + 79N^3 + 31N^2 - 32N - 16 \tag{6.25}$$

$$P_{302} = 12N^5 + 167N^4 + 564N^3 + 807N^2 + 595N + 240 \tag{6.26}$$

$$P_{303} = 16N^5 - 31N^4 - 315N^3 - 467N^2 - 248N - 80 \tag{6.27}$$

$$P_{304} = 24N^5 + 105N^4 + 194N^3 + 139N^2 - 48N - 24 \tag{6.28}$$

$$P_{305} = 32N^5 + 3N^4 - 259N^3 - 283N^2 - 40N - 32 \tag{6.29}$$

$$P_{306} = 80N^5 + 151N^4 - 63N^3 - 77N^2 + 164N + 96 \tag{6.30}$$

$$P_{307} = 84N^5 + 167N^4 - 189N^3 - 453N^2 - 224N - 120 \tag{6.31}$$

$$P_{308} = 96N^5 + 101N^4 - 577N^3 - 831N^2 - 268N - 216 \tag{6.32}$$

$$P_{309} = 136N^5 + 467N^4 + 417N^3 - 153N^2 - 500N - 208 \tag{6.33}$$

$$P_{310} = 2N^6 + 2N^5 - 14N^4 - 43N^3 - 47N^2 - 20N - 4 \tag{6.34}$$

$$P_{311} = 7N^6 + 16N^5 - 139N^4 - 705N^3 - 1288N^2 - 1079N - 352 \tag{6.35}$$

$$P_{312} = 20N^6 + 104N^5 + 214N^4 + 197N^3 + 103N^2 + 76N + 20 \tag{6.36}$$

$$P_{313} = 22N^6 + 203N^5 + 632N^4 + 800N^3 + 280N^2 - 95N + 24 \tag{6.37}$$

$$P_{314} = 28N^6 + 168N^5 + 394N^4 + 443N^3 + 297N^2 + 180N + 44 \tag{6.38}$$

$$P_{315} = 26N^7 + 221N^6 + 624N^5 + 821N^4 + 555N^3 + 120N^2 - 112N - 32 \tag{6.39}$$

$$P_{316} = 30N^7 - 639N^6 - 3480N^5 - 5561N^4 - 2370N^3 + 1232N^2 + 1024N + 320 \tag{6.40}$$

$$P_{317} = 94N^7 + 457N^6 + 652N^5 + 131N^4 - 466N^3 - 760N^2 - 624N - 96 \tag{6.41}$$

$$P_{318} = 4N^8 + 16N^7 - 206N^6 - 1314N^5 - 3390N^4 - 4971N^3 - 4164N^2$$
$$- 1752N - 336 \tag{6.42}$$

$$P_{319} = 24N^8 + 157N^7 + 487N^6 - 14N^5 - 5221N^4 - 14311N^3 - 15376N^2$$
$$- 7056N - 1440 \tag{6.43}$$

$$P_{320} = 30N^8 + 378N^7 + 1635N^6 + 2867N^5 - 112N^4 - 8176N^3 - 11681N^2$$
$$- 5423N - 32 \tag{6.44}$$

$$P_{321} = 63N^{10} + 786N^9 + 3556N^8 + 8205N^7 + 10280N^6 + 4952N^5 - 4737N^4$$
$$- 9296N^3 - 6048N^2 - 1728N - 192 \tag{6.45}$$

6. Ladder- and V-diagrams for $A_{Qg}^{(3)}$

$$P_{322} = 83N^{10} + 1156N^9 + 5266N^8 + 11679N^7 + 15630N^6 + 16718N^5 + 16891N^4$$
$$+ 13040N^3 + 6240N^2 + 1728N + 192\,. \tag{6.46}$$

Its asymptotic expansion behaves only logarithmically $\propto \ln^5(\bar{N})$, as expected from the presence of $(S_1(N))^5$, see also [147].

The result for the non-planar part $D_{12,b}$ is more complicated and reads

$$
D_{12,b} = T_F\left(\frac{C_A}{2} - C_F\right)(C_A - C_F)\Bigg\{ \frac{1}{\varepsilon^3}\Bigg[-\frac{128(N^2 + N + 1)}{3N(N+1)^2(N+2)} + \frac{128(N+3)}{3(N+1)^2(N+2)}S_1
$$
$$
- \frac{64}{3(N+1)(N+2)}\left[3S_2 + S_1^2 + 4S_{-2}\right] + (-1)^N \frac{128}{3N(N+1)^2(N+2)}\Bigg]
$$
$$
+ \frac{1}{\varepsilon^2}\Bigg[-\frac{64 P_{324}}{3N(N+1)^3(N+2)^2} - \frac{32(2N+1)(4N^3 + 10N^2 + 17N + 20)}{3N(N+1)^2(N+2)^2}S_2
$$
$$
- \frac{32(2N^3 + 20N^2 + 35N + 12)}{3N(N+1)^2(N+2)^2}S_1^2 + (-1)^N \frac{64(4N^3 + 16N^2 + 28N + 21)}{3N(N+1)^3(N+2)^2}
$$
$$
+ \left(\frac{64 P_{325}}{3N(N+1)^3(N+2)^2} - \frac{96}{(N+1)(N+2)}S_2\right)S_1 + \frac{32}{3(N+1)(N+2)}S_1^3
$$
$$
- \frac{256(2N+5)}{3(N+1)(N+2)}S_3 + \left(-\frac{128 P_{323}}{3N(N+1)^2(N+2)^2} - \frac{512}{3(N+1)(N+2)}S_1\right)S_{-2}
$$
$$
+ \frac{256(N+4)}{3(N+1)(N+2)}S_{2,1} + \frac{512}{3(N+1)(N+2)}S_{-2,1}\Bigg] + \frac{1}{\varepsilon}\Bigg[-\frac{32 P_{350}}{3N(N+1)^4(N+2)^3}
$$
$$
+ \frac{128(N^2 - 5N + 2)}{3N(N+1)(N+2)}S_{-2,1,1} + \frac{16(10N^3 + 62N^2 + 111N + 60)}{9N(N+1)^2(N+2)^2}S_1^3
$$
$$
- \frac{128(N^2 - N + 2)}{3N(N+1)(N+2)}S_{-2,2} + \frac{128(N^2 + 4N + 2)}{3N(N+1)(N+2)}S_{-4} - \frac{64(3N^2 + N + 6)}{3N(N+1)(N+2)}S_{-3,1}
$$
$$
+ \frac{128(19N^2 + 37N - 4)}{3N(N+1)(N+2)}S_{3,1} + \frac{64 P_{330} S_{2,1}}{3N^2(N+1)^2(N+2)^2} - \frac{32 P_{340} S_3}{9N^2(N+1)^2(N+2)^2}
$$
$$
+ \frac{16 P_{351}}{3N(N+1)^3(N+2)^3}S_2 + (-1)^N\left(-\frac{64(4N^3 + 18N^2 + 29N + 16)}{N(N+1)^3(N+2)^3}S_2\right.
$$
$$
- \frac{32 P_{334}}{3N(N+1)^4(N+2)^3} - \frac{128(13N^3 + 59N^2 + 95N + 52)}{3N(N+1)^3(N+2)^3}S_{-2} - \frac{640}{(N+1)^2}S_{-3}
$$
$$
\left.+ \frac{768}{(N+1)^2}S_{-2,1} + \frac{16\zeta_2}{N(N+1)^2(N+2)}\right) - \frac{8(108N^2 + 127N - 56)}{3N(N+1)(N+2)}S_4
$$
$$
+ \frac{128(7N^3 + 4N^2 + 14N + 4)}{3N^2(N+1)(N+2)}S_{-2,1} + \left(-\frac{32(78N^2 + 187N - 36)}{9N(N+1)(N+2)}S_3\right.
$$
$$
+ \frac{32 P_{348}}{3N(N+1)^4(N+2)^3} - \frac{128(N^2 - 5N + 2)}{3N(N+1)(N+2)}S_{-2,1} + \frac{64(7N^2 + 19N - 2)}{3N(N+1)(N+2)}S_{2,1}
$$
$$
\left.- \frac{16 P_{338}}{3N^2(N+1)^2(N+2)^2}S_2\right)S_1 - \frac{28S_1^4}{9(N+1)(N+2)} + \left(-\frac{16 P_{336}}{3N(N+1)^3(N+2)^3}\right.
$$
$$
\left.+ \frac{8(4N^2 - 19N + 8)}{3N(N+1)(N+2)}S_2\right)S_1^2 + \frac{4(80N + 233)}{3(N+1)(N+2)}S_2^2 + \frac{512}{3(N+1)(N+2)}S_{-2}^2
$$
$$
+ \left(\frac{64 P_{349}}{3N(N+1)^3(N+2)^3} + \frac{64(N^2 - 5N + 2)}{3N(N+1)(N+2)}S_1^2 + \frac{64(N^2 + 9N + 2)}{3N(N+1)(N+2)}S_2\right.
$$

$$
-\frac{128\left(7N^3+4N^2+14N+4\right)}{3N^2(N+1)(N+2)}S_1\Bigg)S_{-2}+\Bigg(\frac{64\left(3N^2+N+6\right)}{3N(N+1)(N+2)}S_1
$$

$$
-\frac{64P_{329}}{3N^2(N+1)^2(N+2)^2}\Bigg)S_{-3}-\frac{512(2N+5)}{3(N+1)(N+2)}S_{2,1,1}+\Bigg(\frac{16(N+3)}{(N+1)^2(N+2)}S_1
$$

$$
-\frac{16\left(N^2+N+1\right)}{N(N+1)^2(N+2)}-\frac{8\left[S_1^2+3S_2+4S_{-2}\right]}{(N+1)(N+2)}\Bigg)\zeta_2\Bigg]
$$

$$
-\frac{P_{328}}{N^3(N+1)(N+2)(2N+1)(2N+3)\binom{2N}{N}}\Bigg[16\left(\sum_{i_1=1}^{N}(-2)^{i_1}\binom{2i_1}{i_1}\right)\zeta_3
$$

$$
+16\sum_{i_1=1}^{N}(-2)^{i_1}\binom{2i_1}{i_1}S_{1,2}\left(\frac{1}{2},1,i_1\right)+48\sum_{i_1=1}^{N}(-2)^{i_1}\binom{2i_1}{i_1}S_{1,2}\left(\frac{1}{2},-1,i_1\right)\Bigg]
$$

$$
+\frac{N^2+4N+2}{N(N+1)(N+2)}\Bigg[-192\sum_{i_1=1}^{N}(-2)^{i_1}\binom{2i_1}{i_1}\left(\sum_{i_2=1}^{i_1}\frac{1}{\binom{2i_2}{i_2}i_2^2}\right)S_{1,2}\left(\frac{1}{2},1,i_1\right)
$$

$$
-576\sum_{i_1=1}^{N}(-2)^{i_1}\binom{2i_1}{i_1}\left(\sum_{i_2=1}^{i_1}\frac{1}{\binom{2i_2}{i_2}i_2^2}\right)S_{1,2}\left(\frac{1}{2},-1,i_1\right)-32\sum_{i_1=1}^{N}\frac{\sum_{i_2=1}^{i_1}\frac{(-1)^{i_2}\binom{2i_2}{i_2}}{i_2^3}}{\binom{2i_1}{i_1}\left(1+i_1\right)}
$$

$$
+\left(192\sum_{i_1=1}^{N}(-2)^{i_1}\binom{2i_1}{i_1}S_{1,2}\left(\frac{1}{2},1,i_1\right)+576\sum_{i_1=1}^{N}(-2)^{i_1}\binom{2i_1}{i_1}S_{1,2}\left(\frac{1}{2},-1,i_1\right)\right)
$$

$$
\times\sum_{i_1=1}^{N}\frac{1}{\binom{2i_1}{i_1}i_1^2}-64\sum_{i_1=1}^{N}\frac{\sum_{i_2=1}^{i_1}\binom{2i_2}{i_2}\frac{S_1(i_2)}{i_2^2}}{\binom{2i_1}{i_1}\left(1+i_1\right)}+64\sum_{i_1=1}^{N}\frac{\sum_{i_2=1}^{i_1}\frac{(-1)^{i_2}\binom{2i_2}{i_2}S_2(i_2)}{i_2}}{\binom{2i_1}{i_1}\left(1+i_1\right)}
$$

$$
+96\sum_{i_1=1}^{N}\frac{\sum_{i_2=1}^{i_1}\frac{\binom{2i_2}{i_2}S_2(i_2)}{i_2}}{\binom{2i_1}{i_1}\left(1+i_1\right)}+96\sum_{i_1=1}^{N}\frac{\sum_{i_2=1}^{i_1}\frac{\binom{2i_2}{i_2}S_{-2}(i_2)}{i_2}}{\binom{2i_1}{i_1}\left(1+i_1\right)}+96\sum_{i_1=1}^{N}\frac{\sum_{i_2=1}^{i_1}\frac{\binom{2i_2}{i_2}S_{1,1}(i_2)}{i_2}}{\binom{2i_1}{i_1}\left(1+i_1\right)}
$$

$$
+192\sum_{i_1=1}^{N}\frac{\sum_{i_2=1}^{i_1}\frac{(-1)^{i_2}\binom{2i_2}{i_2}S_{-2}(i_2)}{i_2}}{\binom{2i_1}{i_1}\left(1+i_1\right)}-64S_{2,1,2}\left(-2,\frac{1}{2},1\right)-192S_{2,1,2}\left(-2,\frac{1}{2},-1\right)
$$

$$
+\left(192\sum_{i_1=1}^{N}\frac{\sum_{i_2=1}^{i_1}(-2)^{i_2}\binom{2i_2}{i_2}}{\binom{2i_1}{i_1}i_1^2}-256S_2(-2)\right)\zeta_3\Bigg]
$$

$$
+\frac{(3N^2+16)}{N(N+1)(N+2)}\Bigg[\frac{64}{3}\sum_{i_1=1}^{N}\frac{\sum_{i_2=1}^{i_1}\frac{(-1)^{i_2}\binom{2i_2}{i_2}}{i_2^3}}{\binom{2i_1}{i_1}\left(1+2i_1\right)}-128\sum_{i_1=1}^{N}\frac{\sum_{i_2=1}^{i_1}\frac{(-1)^{i_2}\binom{2i_2}{i_2}S_{-2}(i_2)}{i_2}}{\binom{2i_1}{i_1}\left(1+2i_1\right)}
$$

$$
+\frac{128}{3}\sum_{i_1=1}^{N}\frac{\sum_{i_2=1}^{i_1}\frac{\binom{2i_2}{i_2}S_1(i_2)}{i_2^2}}{\binom{2i_1}{i_1}\left(1+2i_1\right)}-64\sum_{i_1=1}^{N}\frac{\sum_{i_2=1}^{i_1}\frac{\binom{2i_2}{i_2}S_2(i_2)}{i_2}}{\binom{2i_1}{i_1}\left(1+2i_1\right)}-64\sum_{i_1=1}^{N}\frac{\sum_{i_2=1}^{i_1}\frac{\binom{2i_2}{i_2}S_{-2}(i_2)}{i_2}}{\binom{2i_1}{i_1}\left(1+2i_1\right)}
$$

$$
-\frac{128}{3}\sum_{i_1=1}^{N}\frac{\sum_{i_2=1}^{i_1}\frac{(-1)^{i_2}\binom{2i_2}{i_2}S_2(i_2)}{i_2}}{\binom{2i_1}{i_1}\left(1+2i_1\right)}-64\sum_{i_1=1}^{N}\frac{\sum_{i_2=1}^{i_1}\frac{\binom{2i_2}{i_2}S_{1,1}(i_2)}{i_2}}{\binom{2i_1}{i_1}\left(1+2i_1\right)}\Bigg]
$$

$$
+\frac{6N-5}{N(N+1)(N+2)}\Bigg[\left(-256\sum_{i_1=1}^{N}(-2)^{i_1}\binom{2i_1}{i_1}S_{1,2}\left(\frac{1}{2},1,i_1\right)\right)
$$

$$- 768 \sum_{i_1=1}^{N} (-2)^{i_1} \binom{2i_1}{i_1} S_{1,2}\left(\frac{1}{2}, -1, i_1\right)\Bigg) \sum_{i_1=1}^{N} \frac{1}{\binom{2i_1}{i_1} i_1}$$

$$+ 768 \sum_{i_1=1}^{N} (-2)^{i_1} \binom{2i_1}{i_1} \left(\sum_{i_2=1}^{i_1} \frac{1}{\binom{2i_2}{i_2} i_2}\right) S_{1,2}\left(\frac{1}{2}, -1, i_1\right)$$

$$+ 256 \sum_{i_1=1}^{N} (-2)^{i_1} \binom{2i_1}{i_1} \left(\sum_{i_2=1}^{i_1} \frac{1}{\binom{2i_2}{i_2} i_2}\right) S_{1,2}\left(\frac{1}{2}, 1, i_1\right)$$

$$+ \left(256 S_1(-2) - 256 \sum_{i_1=1}^{N} \frac{\sum_{i_2=1}^{i_1} (-2)^{i_2} \binom{2i_2}{i_2}}{\binom{2i_1}{i_1} i_1}\right) \zeta_3 \Bigg]$$

$$+ \frac{P_{343}}{N^3(N+1)^2(N+2)(2N+1)(2N+3)\binom{2N}{N}} \Bigg[\frac{32}{3} \sum_{i_1=1}^{N} \frac{(-1)^{i_1} \binom{2i_1}{i_1} S_2(i_1)}{i_1}$$

$$+ 32 \sum_{i_1=1}^{N} \frac{(-1)^{i_1} \binom{2i_1}{i_1} S_{-2}(i_1)}{i_1} - \frac{16}{3} \sum_{i_1=1}^{N} \frac{(-1)^{i_1} \binom{2i_1}{i_1}}{i_1^3} - \frac{32}{3} \sum_{i_1=1}^{N} \frac{\binom{2i_1}{i_1} S_1(i_1)}{i_1^2}$$

$$+ 16 \sum_{i_1=1}^{N} \frac{\binom{2i_1}{i_1} S_2(i_1)}{i_1} + 16 \sum_{i_1=1}^{N} \frac{\binom{2i_1}{i_1} S_{-2}(i_1)}{i_1} + 16 \sum_{i_1=1}^{N} \frac{\binom{2i_1}{i_1} S_{1,1}(i_1)}{i_1} \Bigg]$$

$$+ \frac{64(5N^2 - N + 10)}{3N(N+1)(N+2)} S_{-2,2,1} + \frac{2(34N^3 + 34N^2 - 119N - 108)}{9N(N+1)^2(N+2)^2} S_1^4$$

$$- \frac{64(5N^2 + 19N + 10)}{3N(N+1)(N+2)} S_{-4,1} - \frac{64(25N^3 + 4N^2 + 58N + 20)}{3N^2(N+1)(N+2)} S_{-2,1,1}$$

$$+ \frac{32(5N^2 + 57N + 10)}{3N(N+1)(N+2)} S_{2,-3} - \frac{64(7N^2 - 11N + 14)}{3N(N+1)(N+2)} S_{-2,1,1,1}$$

$$+ \frac{64(9N^2 - 7N + 18)}{3N(N+1)(N+2)} S_{2,1,-2} + \frac{32(19N^3 - 20N^2 + 62N + 28)}{3N^2(N+1)(N+2)} S_{-3,1}$$

$$+ \frac{64(9N^2 + 4N + 18)}{3N(N+1)(N+2)} S_{-2,3} + \frac{64(11N^3 - 4N^2 + 30N + 12)}{3N^2(N+1)(N+2)} S_{-2,2}$$

$$+ \frac{32(13N^2 + 7N + 26)}{3N(N+1)(N+2)} S_{-3,1,1} - \frac{64(13N^2 + 30N + 26)}{3N(N+1)(N+2)} S_{-5}$$

$$+ \frac{128(15N^2 + 10N - 6)}{3N(N+1)(N+2)} S_{-2,1,-2} - \frac{32(15N^2 + 412N + 530)}{15N(N+1)(N+2)} S_5$$

$$+ \frac{64(16N^2 + 43N + 16)}{3N(N+1)(N+2)} S_{2,2,1} + \frac{128(21N^2 + 58N + 18)}{3N(N+1)(N+2)} S_{-2,-3}$$

$$+ \frac{32(97N^2 + 167N + 10)}{3N(N+1)(N+2)} S_{2,1,1,1} - \frac{32(214N^2 + 335N - 68)}{3N(N+1)(N+2)} S_{3,1,1}$$

$$+ \frac{32(27N^2 + 14N + 10)}{3N(N+1)(N+2)} S_{4,1} - \frac{32(65N^2 + 50N - 46)}{3N(N+1)(N+2)} S_{2,3} - \frac{2 S_1^5}{5(N+1)(N+2)}$$

$$+ \frac{16 P_{363}}{9N^3(N+1)^3(N+2)^3} S_3 + \frac{1}{3N^2(N+1)^2(N+2)^2} \Big[-32 P_{333} S_{2,1,1} - 64 P_{339} S_{-2,1}$$

$$- 32 P_{332} S_{3,1} + 2 P_{345} S_2^2 + 4 P_{346} S_4\Big] - \frac{32 P_{359} S_{2,1}}{3N^3(N+1)^3(N+2)^3}$$

$$+ \left(-\frac{8 P_{355}}{9N^3(N+1)^3(N+2)^3} + \frac{4(28N^2 - 45N + 56)}{9N(N+1)(N+2)} S_2\right) S_1^3$$

$$+\left(\frac{32(11N-2)(13N+25)}{3N(N+1)(N+2)}S_{3,1}-\frac{64\big(5N^2-N+10\big)}{3N(N+1)(N+2)}S_{-2,2}\right.$$

$$+\frac{64\big(7N^2-11N+14\big)}{3N(N+1)(N+2)}S_{-2,1,1}-\frac{32\big(13N^2+7N+26\big)}{3N(N+1)(N+2)}S_{-3,1}$$

$$-\frac{64\big(28N^2+55N-8\big)}{3N(N+1)(N+2)}S_{2,1,1}+\frac{2\big(288N^2+759N-64\big)}{3N(N+1)(N+2)}S_2^2$$

$$-\frac{4\big(412N^2+461N-264\big)}{3N(N+1)(N+2)}S_4+\frac{64\big(25N^3+4N^2+58N+20\big)}{3N^2(N+1)(N+2)}S_{-2,1}$$

$$+\frac{64P_{326}S_{2,1}}{3N^2(N+1)^2(N+2)}-\frac{16P_{344}S_3}{9N^2(N+1)^2(N+2)^2}+\frac{8P_{361}S_2}{3N^3(N+1)^3(N+2)^3}$$

$$\left.-\frac{16P_{364}}{3N(N+1)^5(N+2)^4(2N+3)}\right)S_1+\left(\frac{8P_{362}}{3N(N+1)^4(N+2)^4(2N+3)}\right.$$

$$+\frac{128\big(3N^2+8N-2\big)}{3N(N+1)(N+2)}S_{2,1}-\frac{8\big(94N^2+213N-68\big)}{3N(N+1)(N+2)}S_3-\frac{4P_{342}S_2}{3N^2(N+1)^2(N+2)^2}$$

$$\left.-\frac{32\big(7N^2-11N+14\big)}{3N(N+1)(N+2)}S_{-2,1}\right)S_1^2+\frac{16P_{366}}{3N(N+1)^5(N+2)^4(2N+3)}$$

$$+\left(\frac{32\big(7N^2-47N+14\big)}{3N(N+1)(N+2)}S_{-2,1}-\frac{64\big(35N^2+75N+2\big)}{3N(N+1)(N+2)}S_{2,1}\right.$$

$$\left.+\frac{8\big(1054N^2+1245N-820\big)}{9N(N+1)(N+2)}S_3-\frac{8P_{367}}{3N(N+1)^4(N+2)^4(2N+3)}\right)S_2$$

$$+\left(\frac{32P_{358}}{3N^3(N+1)^3(N+2)^3}-\frac{128\big(3N^2+7N+6\big)}{N(N+1)(N+2)}S_{-2}+\frac{16\big(13N^2+7N+26\big)}{3N(N+1)(N+2)}S_1^2\right.$$

$$\left.-\frac{16\big(37N^2+67N+74\big)}{3N(N+1)(N+2)}S_2-\frac{32\big(19N^3-20N^2+62N+28\big)}{3N^2(N+1)(N+2)}S_1\right)S_{-3}$$

$$+\left(\frac{64P_{331}}{3N^2(N+1)^2(N+2)^2}+\frac{64\big(5N^2+19N+10\big)}{3N(N+1)(N+2)}S_1\right)S_{-4}$$

$$+\left(-\frac{64\big(5N^2-7N+10\big)}{3N(N+1)(N+2)}S_{2,1}-\frac{256\big(5N^2+14N+10\big)}{9N(N+1)(N+2)}S_3\right.$$

$$+\frac{32\big(7N^2-11N+14\big)}{9N(N+1)(N+2)}S_1^3-\frac{128\big(15N^2+32N-6\big)}{3N(N+1)(N+2)}S_{-2,1}$$

$$\left.-\frac{32\big(25N^3+4N^2+58N+20\big)}{3N^2(N+1)(N+2)}S_1^2+\frac{32P_{337}}{3N^2(N+1)^2(N+2)^2}S_2\right.$$

$$+\left(\frac{64P_{339}}{3N^2(N+1)^2(N+2)^2}+\frac{32\big(N^2+11N+2\big)}{N(N+1)(N+2)}S_2\right)S_1$$

$$\left.-\frac{32P_{365}}{3N(N+1)^4(N+2)^4(2N+3)}\right)S_{-2}+\left(\frac{64P_{327}}{3N(N+1)^2(N+2)^2}\right.$$

$$\left.+\frac{1024}{3(N+1)(N+2)}S_1\right)S_{-2}^2+\left[-\frac{4(2N+1)\big(4N^3+10N^2+17N+20\big)}{N(N+1)^2(N+2)^2}S_2\right.$$

$$-\frac{8P_{324}}{N(N+1)^3(N+2)^2}-\frac{4\big(2N^3+20N^2+35N+12\big)}{N(N+1)^2(N+2)^2}S_1^2+\left(-\frac{36S_2}{(N+1)(N+2)}\right.$$

$$\left.+\frac{8P_{325}}{N(N+1)^3(N+2)^2}\right)S_1+\frac{4}{(N+1)(N+2)}S_1^3-\frac{32(2N+5)}{(N+1)(N+2)}S_3$$

$$+\left(-\frac{16P_{323}}{N(N+1)^2(N+2)^2}-\frac{64}{(N+1)(N+2)}S_1\right)S_{-2}+\frac{32(N+4)}{(N+1)(N+2)}S_{2,1}$$

$$+\frac{64}{(N+1)(N+2)}S_{-2,1}\Bigg]\zeta_2+\Bigg[-\frac{136}{(N+1)(N+2)}S_2-\frac{16P_{335}}{3N^3(N+1)^3(N+2)}$$

$$+\frac{32\big(6N^2+19N+12\big)}{3N(N+1)(N+2)}S_{-2}+\frac{16(17N+27)}{3(N+1)^2(N+2)}S_1-\frac{136}{3(N+1)(N+2)}S_1^2\Bigg]\zeta_3$$

$$+(-1)^N\Bigg[-\frac{64\big(4N^3+18N^2+29N+16\big)}{N(N+1)^3(N+2)^3}S_{2,1}+\frac{32P_{347}}{3N^3(N+1)^3(N+2)^3}S_3$$

$$-\frac{64P_{354}}{N^3(N+1)^3(N+2)^3}S_{-2,1}+\frac{16P_{360}}{3N(N+1)^5(N+2)^4(2N+3)}+\left(-\frac{896S_{-2,1}}{(N+1)^2}\right.$$

$$+\frac{64\big(4N^3+18N^2+29N+16\big)}{N(N+1)^3(N+2)^3}S_2\Bigg)S_1+\left(-\frac{32P_{353}}{N(N+1)^4(N+2)^4(2N+3)}\right.$$

$$-\frac{192(2N+3)}{(N+1)(N+2)}S_{-2,1}\Bigg)S_2+\left(\frac{128\big(4N^3+18N^2+29N+16\big)}{N(N+1)^3(N+2)^3}S_1\right.$$

$$-\frac{32P_{356}}{3N(N+1)^4(N+2)^4(2N+3)}-\frac{64(2N+3)}{(N+1)(N+2)}S_{2,1}\Bigg)S_{-2}$$

$$+\left(\frac{32P_{357}}{3N^3(N+1)^3(N+2)^3}+\frac{576}{(N+1)^2}S_1+\frac{32(2N+3)}{(N+1)(N+2)}S_2\right)S_{-3}$$

$$+\frac{2N+3}{(N+1)(N+2)}\Big[64S_{-5}+32S_{2,-3}+64S_{-2,3}-96S_{-4,1}+64S_{2,1,-2}$$

$$+128S_{-2,2,1}+160S_{-3,1,1}-192S_{-2,1,1,1}\Big]+\frac{64}{(N+1)^2}\Big[S_{-4}-16S_{-2,2}-15S_{-3,1}$$

$$+34S_{-2,1,1}\Big]+\frac{8\big(4N^3+16N^2+28N+21\big)}{N(N+1)^3(N+2)^2}\zeta_2+\left(-\frac{16P_{352}}{3N^3(N+1)^3(N+2)^2}\right.$$

$$-\frac{128}{(N+1)^2}S_1-\frac{64(2N+3)}{(N+1)(N+2)}S_2-\frac{128(2N+3)}{(N+1)(N+2)}S_{-2}\Bigg)\zeta_3$$

$$+\frac{64P_{341}2^N}{3N^3(N+1)^2(N+2)^2(2N+3)}\left(S_{1,2}\left(\frac{1}{2},1\right)+3S_{1,2}\left(\frac{1}{2},-1\right)+\zeta_3\right)\Bigg]\Bigg\}. \qquad (6.47)$$

Here we use the polynomials

$$P_{323}=4N^4+16N^3+34N^2+41N+16 \qquad (6.48)$$

$$P_{324}=7N^4+37N^3+63N^2+49N+21 \qquad (6.49)$$

$$P_{325}=8N^4+37N^3+69N^2+52N+2 \qquad (6.50)$$

$$P_{326}=10N^4+23N^3+48N^2+41N+10 \qquad (6.51)$$

$$P_{327}=16N^4+67N^3+97N^2+71N+28 \qquad (6.52)$$

$$P_{328}=187N^4+284N^3+78N^2+114N+36 \qquad (6.53)$$

$$P_{329}=5N^5+7N^4-20N^3-12N^2+24N+8 \qquad (6.54)$$

$$P_{330}=6N^5+16N^4+20N^3+43N^2+52N+16 \qquad (6.55)$$

$$P_{331}=9N^5+57N^4+88N^3-3N^2-64N-24 \qquad (6.56)$$

$$P_{332}=10N^5+4N^4-293N^3-766N^2-564N-128 \qquad (6.57)$$

$$P_{333}=12N^5+98N^4+343N^3+521N^2+296N+56 \qquad (6.58)$$

$$P_{334}=16N^5+96N^4+234N^3+329N^2+327N+177 \qquad (6.59)$$

$$P_{335} = 17N^5 + 38N^4 + 66N^3 + 105N^2 + 60N + 24 \tag{6.60}$$

$$P_{336} = 19N^5 + 111N^4 + 253N^3 + 295N^2 + 203N + 76 \tag{6.61}$$

$$P_{337} = 27N^5 + 117N^4 + 172N^3 + 116N^2 + 32N - 8 \tag{6.62}$$

$$P_{338} = 28N^5 + 106N^4 + 206N^3 + 269N^2 + 148N + 32 \tag{6.63}$$

$$P_{339} = 29N^5 + 62N^4 - 88N^3 - 220N^2 - 44N + 48 \tag{6.64}$$

$$P_{340} = 42N^5 + 113N^4 + 70N^3 + 234N^2 + 408N + 96 \tag{6.65}$$

$$P_{341} = 77N^5 + 348N^4 + 532N^3 + 390N^2 + 192N + 72 \tag{6.66}$$

$$P_{342} = 100N^5 + 322N^4 + 542N^3 + 911N^2 + 716N + 160 \tag{6.67}$$

$$P_{343} = 103N^5 + 377N^4 + 514N^3 + 348N^2 + 150N + 36 \tag{6.68}$$

$$P_{344} = 138N^5 + 584N^4 + 1592N^3 + 2753N^2 + 1860N + 432 \tag{6.69}$$

$$P_{345} = 248N^5 + 1362N^4 + 2730N^3 + 2505N^2 + 948N + 64 \tag{6.70}$$

$$P_{346} = 296N^5 + 1466N^4 + 2014N^3 - 67N^2 - 1516N - 576 \tag{6.71}$$

$$P_{347} = 6N^6 + 110N^5 + 448N^4 + 787N^3 + 668N^2 + 264N + 48 \tag{6.72}$$

$$P_{348} = 12N^6 + 144N^5 + 563N^4 + 911N^3 + 560N^2 + 72N + 42 \tag{6.73}$$

$$P_{349} = 16N^6 + 94N^5 + 202N^4 + 175N^3 + 13N^2 - 65N - 24 \tag{6.74}$$

$$P_{350} = 31N^6 + 212N^5 + 551N^4 + 653N^3 + 259N^2 - 176N - 177 \tag{6.75}$$

$$P_{351} = 32N^6 + 195N^5 + 461N^4 + 491N^3 + 229N^2 + 131N + 132 \tag{6.76}$$

$$P_{352} = 48N^6 + 264N^5 + 595N^4 + 621N^3 + 314N^2 + 144N + 48 \tag{6.77}$$

$$P_{353} = 8N^7 + 65N^6 + 190N^5 + 128N^4 - 529N^3 - 1346N^2 - 1223N - 400 \tag{6.78}$$

$$P_{354} = 22N^7 + 167N^6 + 522N^5 + 839N^4 + 736N^3 + 408N^2 + 200N + 48 \tag{6.79}$$

$$P_{355} = 55N^7 + 535N^6 + 1873N^5 + 3245N^4 + 3365N^3 + 2516N^2 + 1344N + 384 \tag{6.80}$$

$$P_{356} = 64N^7 + 555N^6 + 1859N^5 + 2402N^4 - 1266N^3 - 7244N^2 - 7614N - 2664 \tag{6.81}$$

$$P_{357} = 78N^7 + 603N^6 + 1934N^5 + 3247N^4 + 3148N^3 + 2120N^2 + 1128N + 240 \tag{6.82}$$

$$P_{358} = 23N^8 + 71N^7 - 296N^6 - 1490N^5 - 1942N^4 - 342N^3 + 976N^2 + 624N + 96 \tag{6.83}$$

$$P_{359} = 30N^8 + 167N^7 + 269N^6 - 14N^5 - 170N^4 + 601N^3 + 1208N^2 + 696N + 144 \tag{6.84}$$

$$P_{360} = 112N^8 + 1112N^7 + 4488N^6 + 9374N^5 + 10942N^4 + 8442N^3 + 7578N^2 + 7338N + 3243 \tag{6.85}$$

$$P_{361} = 116N^8 + 565N^7 + 593N^6 - 1037N^5 - 2717N^4 - 2385N^3 - 1108N^2 - 288N - 192 \tag{6.86}$$

$$P_{362} = 142N^8 + 1555N^7 + 7455N^6 + 20242N^5 + 33670N^4 + 34794N^3 + 21892N^2 + 8089N + 1572 \tag{6.87}$$

$$P_{363} = 246N^8 + 1256N^7 + 635N^6 - 5665N^5 - 8519N^4 + 2968N^3 + 12124N^2 + 7008N + 1344 \tag{6.88}$$

$$P_{364} = 60N^9 + 1074N^8 + 7144N^7 + 24222N^6 + 45713N^5 + 46281N^4 + 18168N^3 - 5654N^2 - 4918N + 438 \tag{6.89}$$

$$P_{365} = 112N^9 + 1100N^8 + 4378N^7 + 8577N^6 + 6819N^5 - 3954N^4 - 13288N^3 - 11414N^2 - 4303N - 600 \tag{6.90}$$

$$P_{366} = 190N^9 + 2147N^8 + 10535N^7 + 29503N^6 + 52015N^5 + 59287N^4 + 41233N^3$$

$$+ 12273N^2 - 3909N - 3243 \tag{6.91}$$

$$P_{367} = 224N^9 + 2310N^8 + 10351N^7 + 25395N^6 + 34556N^5 + 21274N^4 - 1556N^3$$
$$- 4934N^2 + 3961N + 3516\,. \tag{6.92}$$

The binomial sums which appear in $D_{12,b}$ are simplified in such a way, that those sums which occurred in the scalar case in [344] are preferred over new sums. It turns out that the set of sums encountered there is sufficient also for the full, physical diagram. Since these sums were discussed in detail in [262], we do not need to derive any new relations here. The asymptotic expansion of the result is derived via the integral representation of the sums given in [262] and is given by

$$
\begin{aligned}
D_{12,b} = \left(\frac{C_A}{2} - C_F\right)(C_A - C_F)T_F \Bigg\{ &\ln(\bar{N})^5 \left[-\frac{2}{5N^2} + \frac{6}{5N^3} - \frac{14}{5N^4} + \frac{6}{N^5} - \frac{62}{5N^6}\right. \\
&+ \frac{126}{5N^7} - \frac{254}{5N^8} + \frac{102}{N^9} - \frac{1022}{5N^{10}}\bigg] + \ln(\bar{N})^4 \left[\frac{68}{9N^2} - \frac{349}{9N^3} + \frac{631}{6N^4} - \frac{4375}{18N^5}\right. \\
&+ \frac{94787}{180N^6} - \frac{66407}{60N^7} + \frac{2886593}{1260N^8} - \frac{1185505}{252N^9} + \frac{3462851}{360N^{10}}\bigg] + \ln(\bar{N})^3 \left[\zeta_2\left(\frac{32}{9N^2}\right.\right. \\
&- \frac{32}{3N^3} + \frac{224}{9N^4} - \frac{160}{3N^5} + \frac{992}{9N^6} - \frac{224}{N^7} + \frac{4064}{9N^8} - \frac{2720}{3N^9} + \frac{16352}{9N^{10}}\bigg) - \frac{568}{9N^2} - \frac{308}{9N^3} \\
&+ \frac{1925}{9N^4} - \frac{7282}{9N^5} + \frac{429499}{180N^6} - \frac{3454373}{540N^7} + \frac{45579011}{2835N^8} - \frac{217525589}{5670N^9} + \frac{2230906393}{25200N^{10}}\bigg] \\
&+ \ln(\bar{N})^2 \left[\zeta_3\left(-\frac{32}{N^2} + \frac{96}{N^3} - \frac{224}{N^4} + \frac{480}{N^5} - \frac{992}{N^6} + \frac{2016}{N^7} - \frac{4064}{N^8} + \frac{8160}{N^9}\right.\right. \\
&- \frac{16352}{N^{10}}\bigg) + \zeta_2\left(-\frac{16}{N^2} - \frac{184}{3N^3} + \frac{2824}{9N^4} - \frac{2848}{3N^5} + \frac{12076}{5N^6} - \frac{28348}{5N^7} + \frac{12055388}{945N^8}\right. \\
&- \frac{1765420}{63N^9} + \frac{8190218}{135N^{10}}\bigg) + \frac{376}{3N^2} - \frac{648}{N^3} + \frac{22174}{9N^4} - \frac{373883}{54N^5} + \frac{49074289}{2700N^6} \\
&- \frac{79605269}{1800N^7} + \frac{57961374941}{529200N^8} - \frac{5050028843}{19600N^9} + \frac{10982047297}{16800N^{10}}\bigg] + \ln(\bar{N})\left[\zeta_4\left(\frac{59}{N^2}\right.\right. \\
&- \frac{177}{N^3} + \frac{413}{N^4} - \frac{885}{N^5} + \frac{1829}{N^6} - \frac{3717}{N^7} + \frac{7493}{N^8} - \frac{15045}{N^9} + \frac{30149}{N^{10}}\bigg) + \zeta_3\left(\frac{1168}{9N^2}\right. \\
&- \frac{5264}{9N^3} + \frac{5008}{3N^4} - \frac{36736}{9N^5} + \frac{418456}{45N^6} - \frac{306376}{15N^7} + \frac{13849384}{315N^8} - \frac{5892536}{63N^9} \\
&+ \frac{8889164}{45N^{10}}\bigg) + \zeta_2\left(\frac{152}{N^2} - \frac{24}{N^3} - \frac{7136}{9N^4} + \frac{22748}{9N^5} - \frac{757274}{135N^6} + \frac{93404}{9N^7}\right. \\
&- \frac{17233624}{945N^8} + \frac{33655894}{945N^9} - \frac{2246721079}{28350N^{10}}\bigg) - \frac{672}{N^2} + \frac{2636}{3N^3} + \frac{58048}{81N^4} - \frac{172960}{27N^5} \\
&+ \frac{561942949}{27000N^6} - \frac{4643682457}{81000N^7} + \frac{20970432670037}{166698000N^8} - \frac{6200063134883}{20837250N^9} \\
&+ \frac{123812203727083}{266716800N^{10}}\bigg] + C_1\left(-\frac{2}{N} + \frac{14}{N^2} - \frac{166}{3N^3} + \frac{138}{N^4} - \frac{910}{3N^5} + \frac{634}{N^6} - \frac{3886}{3N^7}\right. \\
&+ \frac{2618}{N^8} - \frac{15790}{3N^9} + \frac{10554}{N^{10}}\bigg) + C_2\frac{\sqrt{N}}{2^{2N}}\left(-\frac{128}{N^3} + \frac{10448}{75N^4} - \frac{47827}{675N^5} - \frac{81793}{216N^6}\right. \\
&+ \frac{112032149}{57600N^7} - \frac{84661250029}{12441600N^8} + \frac{282488802823}{13271040N^9} - \frac{98593205185337}{1592524800N^{10}}\bigg) \\
&+ C_3\left(-\frac{2}{N^2} + \frac{23}{3N^3} - \frac{19}{N^4} + \frac{125}{3N^5} - \frac{87}{N^6} + \frac{533}{3N^7} - \frac{359}{N^8} + \frac{2165}{3N^9} - \frac{1447}{N^{10}}\right)
\end{aligned}
$$

$$+ C_4 \left(-\frac{2}{N} - \frac{2}{N^2} + \frac{6}{N^3} - \frac{14}{N^4} + \frac{30}{N^5} - \frac{62}{N^6} + \frac{126}{N^7} - \frac{254}{N^8} + \frac{510}{N^9} - \frac{1022}{N^{10}} \right)$$

$$+ \ln\left(\sqrt{5}-1\right)\zeta_2\left(-\frac{1536}{5N} + \frac{13312}{5N^2} - \frac{156928}{15N^3} + \frac{130304}{5N^4} - \frac{171776}{3N^5} + \frac{598272}{5N^6} \right.$$

$$\left. - \frac{3666688}{15N^7} + \frac{2470144}{5N^8} - \frac{2979584}{3N^9} + \frac{9957632}{5N^{10}} \right) + \zeta_5\left(-\frac{1034}{3N} - \frac{3878}{5N^2} + \frac{11634}{5N^3} \right.$$

$$\left. - \frac{27146}{5N^4} + \frac{11634}{N^5} - \frac{120218}{5N^6} + \frac{244314}{5N^7} - \frac{492506}{5N^8} + \frac{197778}{N^9} - \frac{1981658}{5N^{10}} \right)$$

$$+ \zeta_4\left(\frac{10502}{9N^2} - \frac{290539}{54N^3} + \frac{495337}{36N^4} - \frac{3328457}{108N^5} + \frac{2618423}{40N^6} - \frac{146561723}{1080N^7} \right.$$

$$\left. + \frac{233550391}{840N^8} - \frac{856245007}{1512N^9} + \frac{827962831}{720N^{10}} \right) + \zeta_2\zeta_3\left(\frac{29036}{45N} + \frac{14116}{45N^2} - \frac{14116}{15N^3} \right.$$

$$\left. + \frac{98812}{45N^4} - \frac{14116}{3N^5} + \frac{437596}{45N^6} - \frac{98812}{5N^7} + \frac{1792732}{45N^8} - \frac{239972}{3N^9} + \frac{7213276}{45N^{10}} \right)$$

$$+ \ln(2)\zeta_2\left(\frac{2176}{5N} - \frac{17792}{5N^2} + \frac{70016}{5N^3} - \frac{174464}{5N^4} + \frac{76672}{N^5} - \frac{801152}{5N^6} + \frac{1636736}{5N^7} \right.$$

$$\left. - \frac{3307904}{5N^8} + \frac{1330048}{N^9} - \frac{13334912}{5N^{10}} \right) + \zeta_3\left(-\frac{3328}{15N} + \frac{78128}{45N^2} - \frac{325864}{45N^3} \right.$$

$$\left. + \frac{799276}{45N^4} - \frac{364124}{9N^5} + \frac{1331092}{15N^6} - \frac{5163116}{27N^7} + \frac{1156829872}{2835N^8} - \frac{490844206}{567N^9} \right.$$

$$\left. + \frac{5764973003}{3150N^{10}} \right) + (-1)^N\zeta_3\left(\frac{80}{N^6} - \frac{400}{N^7} + \frac{1120}{N^8} - \frac{2400}{N^9} + \frac{5040}{N^{10}} \right) + \zeta_2\left(-\frac{160}{3N^2} \right.$$

$$\left. - \frac{1616}{3N^3} + \frac{17822}{3N^4} - \frac{618754}{27N^5} + \frac{3154276}{45N^6} - \frac{28040113}{150N^7} + \frac{284086748789}{595350N^8} \right.$$

$$\left. - \frac{229916539121}{198450N^9} + \frac{854848983379}{297675N^{10}} \right) + (-1)^N\zeta_2\left(\frac{40}{3N^6} - \frac{2968}{3N^7} + \frac{38504}{3N^8} \right.$$

$$\left. - \frac{128560}{N^9} + \frac{3754024}{3N^{10}} \right) + (-1)^N\left(-\frac{32}{N^5} - \frac{112}{N^6} + \frac{2304}{N^7} - \frac{222448}{9N^8} + \frac{51413552}{225N^9} \right.$$

$$\left. - \frac{476716016}{225N^{10}} \right) + \frac{656}{3N^2} - \frac{8614}{3N^3} + \frac{2690786}{243N^4} - \frac{30575645}{972N^5} + \frac{48619290341}{607500N^6}$$

$$- \frac{479063546623}{2430000N^7} + \frac{1856312420341649}{3889620000N^8} - \frac{3315935066084731}{2917215000N^9}$$

$$+ \frac{579849854424507841}{210039480000N^{10}} \Bigg\} + \mathcal{O}\left(\frac{\ln^5(\bar{N})}{N^{11}} \right). \tag{6.93}$$

Again, it grows at most logarithmically like $\ln^5(\bar{N})$. The exponential growth $\propto 2^N$ cancels, in contrast to the scalar prototype of this diagram, where 2^N-terms remain [344]. The asymptotic expansion involves new constants C_i which arise from binomial sums at infinity. They can be expressed as iterated integrals over root valued letters [262] at $x = 0$ or $x = 1$ and as Mellin transformations of iterated integrals at $N = 0$. In addition, multiple zeta values [361] and constants from infinite generalised harmonic and cyclotomic sums appear [260, 261]. The constant C_1 can be written as

$$C_1 = \frac{96}{\pi}\mathrm{M}^*\left[\frac{\mathrm{H}^*_{\mathsf{w}_2,\mathsf{w}_2,\mathsf{w}_1}(x)}{x - \frac{1}{4}}\right](0) + \frac{48}{\pi}\mathrm{M}^*\left[\frac{\mathrm{H}^*_{\mathsf{w}_2,\mathsf{w}_2,\mathsf{w}_1}(x)}{x + \frac{1}{4}}\right](0) + \frac{32}{\pi}\mathrm{H}^*_{\mathsf{r}_4,0,\mathsf{w}_1,1}(0)$$

$$- 64\mathrm{Li}_3\left(\frac{1}{2}\left(\sqrt{5}-1\right)\right) - \frac{64\pi^3}{9\sqrt{3}} + 64\ln^3(2) - 192\ln^2(2)\ln\left(\sqrt{5}-1\right)$$

$$+ 192 \ln(2) \ln^2\left(\sqrt{5} - 1\right) - 64 \ln^3\left(\sqrt{5} - 1\right) + \frac{32\pi}{3\sqrt{3}} \psi^{(1)}\left(\frac{1}{3}\right)$$

$$\simeq 101.3243556488913992 \tag{6.94}$$

and C_2 as

$$C_2 = -\frac{225}{32\sqrt{\pi}} \mathrm{M}^* \left[\frac{\sqrt{x}\mathrm{H}^*_{w_5,w_2,w_1}(x)}{\left(x - \frac{1}{4}\right)\sqrt{x+2}}\right](0) - \frac{75}{32\sqrt{\pi}} \mathrm{M}^* \left[\frac{\sqrt{x}\mathrm{H}^*_{w_6,w_1,w_1}(x)}{\sqrt{2-x}\left(x + \frac{1}{4}\right)}\right](0)$$

$$-\frac{75\zeta_2}{64\sqrt{\pi}} \mathrm{M}^* \left[\frac{\sqrt{x}\mathrm{H}^*_{w_6}(x)}{\sqrt{2-x}\left(x + \frac{1}{4}\right)}\right](0) + \frac{75}{16\sqrt{\pi}} \mathrm{M}^* \left[\frac{\mathrm{H}^*_{w_2,w_2,w_1}(x)}{x - \frac{1}{4}}\right](0)$$

$$+\frac{75}{32\sqrt{\pi}} \mathrm{M}^* \left[\frac{\mathrm{H}^*_{w_2,w_2,w_1}(x)}{x + \frac{1}{4}}\right](0) + \frac{25}{16\sqrt{\pi}}\mathrm{H}^*_{r_4,0,w_1,1}(0) - \frac{25\pi^{3/2}\zeta_2}{12\sqrt{3}} + \frac{65\sqrt{\pi}\zeta_3}{12}$$

$$-\frac{25}{8} \ln^3(\sqrt{5} - 1)\sqrt{\pi} + \frac{75}{8} \ln^2(\sqrt{5} - 1)\ln(2)\sqrt{\pi} + \frac{145}{16} \ln\left(\sqrt{5} - 1\right)\sqrt{\pi}\zeta_2$$

$$-\frac{75}{8} \ln\left(\sqrt{5} - 1\right) \ln^2(2)\sqrt{\pi} + \frac{25\ln^3(2)\sqrt{\pi}}{8} - \frac{195}{16} \ln(2)\sqrt{\pi}\zeta_2 + \frac{25\pi^{3/2}}{48\sqrt{3}}\psi^{(1)}\left(\frac{1}{3}\right)$$

$$-\frac{25\sqrt{\pi}}{8} \mathrm{Li}_3\left(\frac{1}{2}\left(\sqrt{5} - 1\right)\right)$$

$$< 10^{-53} . \tag{6.95}$$

The numerical evaluation suggests that this constant vanishes, which has, however, not yet been proven analytically. The remaining two constants are given by

$$C_3 = -128\pi^2 \mathrm{M}^* \left[\frac{\sqrt{x}\mathrm{H}^*_{w_{13}}(x)}{\sqrt{8-x}(x+1)}\right](0) - \frac{64\pi^2}{\sqrt{3}} \mathrm{M}^* \left[\frac{\sqrt{x}\mathrm{H}^*_{w_{25}}(x)}{\sqrt{8-x}(x+1)}\right](0) + \frac{512\mathrm{H}^*_{r_4,0,w_1,1}(0)}{3\sqrt{3}}$$

$$-\frac{3328\pi^3 \ln(2)}{15\sqrt{3}} + \frac{1024\pi \ln^3(2)}{3\sqrt{3}} + \frac{7424\pi^3 \ln\left(-1+\sqrt{5}\right)}{45\sqrt{3}} - \frac{1024\pi \ln^2(2) \ln\left(-1+\sqrt{5}\right)}{\sqrt{3}}$$

$$+\frac{1024\pi \ln(2) \ln^2\left(-1+\sqrt{5}\right)}{\sqrt{3}} - \frac{1024\pi \ln^3\left(-1+\sqrt{5}\right)}{3\sqrt{3}} + \frac{320}{27}\pi^2\psi^{(1)}\left(\frac{1}{3}\right)$$

$$-\frac{1024\pi}{3\sqrt{3}}\mathrm{Li}_3\left(\frac{1}{2}\left(-1+\sqrt{5}\right)\right) + \frac{26624\pi\zeta_3}{45\sqrt{3}} - \frac{32}{3}\pi^2 \mathrm{M}^* \left[\frac{x\mathrm{H}^*_{w_{14}}(x)}{\sqrt{x+\frac{1}{4}}(x+1)}\right](0)$$

$$- 1536\,\mathrm{M}^* \left[\frac{\sqrt{x}\mathrm{H}^*_{w_{13},1,0}(x)}{\sqrt{8-x}(x+1)}\right](0) - 64\,\mathrm{M}^* \left[\frac{x\mathrm{H}^*_{w_{14},0,0}(x)}{\sqrt{x+\frac{1}{4}}(x+1)}\right](0)$$

$$- 128\,\mathrm{M}^* \left[\frac{x\mathrm{H}^*_{w_{14},1,0}(x)}{\sqrt{x+\frac{1}{4}}(x+1)}\right](0) + 192\,\mathrm{M}^* \left[\frac{x\mathrm{H}^*_{w_{14},-1,0}(x)}{\sqrt{x+\frac{1}{4}}(x+1)}\right](0)$$

$$- 4608\,\mathrm{M}^* \left[\frac{\sqrt{x}\mathrm{H}^*_{w_{18},-1,0}(x)}{(x-1)\sqrt{x+8}}\right](0) + \frac{512}{\sqrt{3}} \mathrm{M}^* \left[\frac{\mathrm{H}^*_{w_2,w_2,w_1}(x)}{x - \frac{1}{4}}\right](0)$$

$$+ \frac{256}{\sqrt{3}} \mathrm{M}^* \left[\frac{\mathrm{H}^*_{w_2,w_2,w_1}(x)}{x + \frac{1}{4}}\right](0) - 768\sqrt{3}\,\mathrm{M}^* \left[\frac{\sqrt{x}\mathrm{H}^*_{w_{21},w_{20},w_{19}}(x)}{(x-1)\sqrt{x+8}}\right](0)$$

$$- 2304\,\mathrm{M}^* \left[\frac{\sqrt{x}\mathrm{H}^*_{w_{21},w_{23},0}(x)}{(x-1)\sqrt{x+8}}\right](0) - 256\sqrt{3}\,\mathrm{M}^* \left[\frac{\sqrt{x}\mathrm{H}^*_{w_{25},w_{19},w_{19}}(x)}{\sqrt{8-x}(x+1)}\right](0)$$

$$- 768\,\mathrm{M}^* \left[\frac{\sqrt{x}\mathrm{H}^*_{\mathrm{w25},\mathrm{w26},0}(x)}{\sqrt{8-x}(x+1)} \right](0) + 128\,\mathrm{M}^* \left[\frac{x\mathrm{H}^*_{\mathrm{w8},0,1}(x)}{(x-1)\sqrt{x-\frac{1}{4}}} \right](0)$$

$$- 192\,\mathrm{M}^* \left[\frac{x\mathrm{H}^*_{\mathrm{w8},1,0}(x)}{(x-1)\sqrt{x-\frac{1}{4}}} \right](0) + 192\,\mathrm{M}^* \left[\frac{x\mathrm{H}^*_{\mathrm{w8},1,1}(x)}{(x-1)\sqrt{x-\frac{1}{4}}} \right](0)$$

$$+ 384\,\mathrm{M}^* \left[\frac{x\mathrm{H}^*_{\mathrm{w8}-1,0}(x)}{(x-1)\sqrt{x-\frac{1}{4}}} \right](0)$$

$$\simeq\, -3.90077878750796324 \tag{6.96}$$

and

$$C_4 = \frac{64\pi^5}{81\sqrt{3}} + 8\pi^2\,\mathrm{M}^* \left[\frac{\sqrt{x}\mathrm{H}^*_{\mathrm{w12},0}(x)}{\sqrt{8-x}(x+1)} \right](0) + 8\pi^2\,\mathrm{M}^* \left[\frac{\sqrt{x}\mathrm{H}^*_{\mathrm{w12},2}(x)}{\sqrt{8-x}(x+1)} \right](0)$$

$$+ 8\pi^2\,\mathrm{M}^* \left[\frac{\sqrt{x}\mathrm{H}^*_{\mathrm{w25},\mathrm{w19}}(x)}{\sqrt{8-x}(x+1)} \right](0) - 32\mathrm{H}_{-1,0,2,1,0}(1) - 96\mathrm{H}_{0,-2,-1,0,1}(1) - 96\mathrm{H}_{0,-2,-1,1,0}(1)$$

$$- 96\mathrm{H}_{0,-2,1,-1,0}(1) - 96\mathrm{H}_{0,1,-2,-1,0}(1) + 2\pi^2\mathrm{H}^*_{1,\mathrm{w8},\mathrm{w8}}(0) - \frac{4}{3}\pi^2\mathrm{H}^*_{-1,\mathrm{w14},\mathrm{w14}}(0)$$

$$- \frac{32}{9}\pi\mathrm{H}^*_{\mathrm{r4},0,\mathrm{w1},1}(0) + \frac{187}{45}\pi^4\ln(2) + \frac{32}{9}\pi^2\ln^3(2) - 4\ln^5(2) - 12\pi^2\ln^2(2)\ln(3)$$

$$+ 4\pi^2\ln(2)\ln^2(3) - \frac{464}{135}\pi^4\ln\left(\sqrt{5}-1\right) + \frac{64}{3}\pi^2\ln(2)^2\ln\left(\sqrt{5}-1\right)$$

$$- \frac{64}{3}\pi^2\ln(2)\ln^2\left(\sqrt{5}-1\right) + \frac{64}{9}\pi^2\ln^3\left(\sqrt{5}-1\right) - \frac{32\pi^3}{27\sqrt{3}}\psi^{(1)}\left(\frac{1}{3}\right)$$

$$- 8\pi^2\ln(2)\mathrm{Li}_2\left(-\frac{1}{2}\right) - 8\pi^2\ln(3)\mathrm{Li}_2\left(-\frac{1}{2}\right) - 32\pi^2\mathrm{Li}_3\left(-\frac{1}{2}\right) - 4\pi^2\mathrm{Li}_3\left(\frac{3}{4}\right)$$

$$+ \frac{64}{9}\pi^2\mathrm{Li}_3\left(\frac{1}{2}\left(\sqrt{5}-1\right)\right) - 96\ln(2)\mathrm{Li}_4\left(\frac{1}{2}\right) - \frac{32}{3}\pi\,\mathrm{M}^* \left[\frac{\mathrm{H}^*_{\mathrm{w2},\mathrm{w2},\mathrm{w1}}(x)}{x-\frac{1}{4}} \right](0)$$

$$- \frac{16}{3}\pi\,\mathrm{M}^* \left[\frac{\mathrm{H}^*_{\mathrm{w2},\mathrm{w2},\mathrm{w1}}(x)}{x+\frac{1}{4}} \right](0) + 96\,\mathrm{M}^* \left[\frac{\sqrt{x}\mathrm{H}^*_{\mathrm{w12},0,1,0}(x)}{\sqrt{8-x}(x+1)} \right](0) + 96\,\mathrm{M}^* \left[\frac{\sqrt{x}\mathrm{H}^*_{\mathrm{w12},2,1,0}(x)}{\sqrt{8-x}(x+1)} \right](0)$$

$$+ 8\,\mathrm{M}^* \left[\frac{x\mathrm{H}^*_{\mathrm{w14},\mathrm{w14},0,0}(x)}{x+1} \right](0) + 16\,\mathrm{M}^* \left[\frac{x\mathrm{H}^*_{\mathrm{w14},\mathrm{w14},1,0}(x)}{x+1} \right](0) - 24\,\mathrm{M}^* \left[\frac{x\mathrm{H}^*_{\mathrm{w14},\mathrm{w14},-1,0}(x)}{x+1} \right](0)$$

$$+ 288\,\mathrm{M}^* \left[\frac{\sqrt{x}\mathrm{H}^*_{\mathrm{w17},0,-1,0}(x)}{(x-1)\sqrt{x+8}} \right](0) - 288\,\mathrm{M}^* \left[\frac{\sqrt{x}\mathrm{H}^*_{\mathrm{w17},-2,-1,0}(x)}{(x-1)\sqrt{x+8}} \right](0)$$

$$+ 288\,\mathrm{M}^* \left[\frac{\sqrt{x}\mathrm{H}^*_{\mathrm{w21},\mathrm{w20},0,0}(x)}{(x-1)\sqrt{x+8}} \right](0) - 288\,\mathrm{M}^* \left[\frac{\sqrt{x}\mathrm{H}^*_{\mathrm{w21},\mathrm{w20},-1,0}(x)}{(x-1)\sqrt{x+8}} \right](0)$$

$$+ 288\,\mathrm{M}^* \left[\frac{\sqrt{x}\mathrm{H}^*_{\mathrm{w21},\mathrm{w20},\mathrm{w19},\mathrm{w19}}(x)}{(x-1)\sqrt{x+8}} \right](0) + 96\,\mathrm{M}^* \left[\frac{\sqrt{x}\mathrm{H}^*_{\mathrm{w25},\mathrm{w19},0,0}(x)}{\sqrt{8-x}(x+1)} \right](0)$$

$$+ 96\,\mathrm{M}^* \left[\frac{\sqrt{x}\mathrm{H}^*_{\mathrm{w25},\mathrm{w19},1,0}(x)}{\sqrt{8-x}(x+1)} \right](0) + 96\,\mathrm{M}^* \left[\frac{\sqrt{x}\mathrm{H}^*_{\mathrm{w25},\mathrm{w19},\mathrm{w19},\mathrm{w19}}(x)}{\sqrt{8-x}(x+1)} \right](0)$$

$$- 16\,\mathrm{M}^* \left[\frac{x\mathrm{H}^*_{\mathrm{w8},\mathrm{w8},0,1}(x)}{x-1} \right](0) + 24\,\mathrm{M}^* \left[\frac{x\mathrm{H}^*_{\mathrm{w8},\mathrm{w8},1,0}(x)}{x-1} \right](0)$$

$$- 24\,\mathrm{M}^* \left[\frac{x\mathrm{H}^*_{\mathrm{w}_8,\mathrm{w}_8,1,1}(x)}{x-1} \right](0) - 48\,\mathrm{M}^* \left[\frac{x\mathrm{H}^*_{\mathrm{w}_8,\mathrm{w}_8,-1,0}(x)}{x-1} \right](0)$$

$$\simeq 278.9253246705036914\,. \tag{6.97}$$

Following [262], the iterated integrals H^* are defined as

$$\mathrm{H}^*_\emptyset(x) = 1 \tag{6.98}$$

$$\mathrm{H}^*_{a_1,\dots,a_k}(x) = \int_x^1 \mathrm{d}y\, a_1(y)\mathrm{H}^*_{a_2,\dots,a_k}(y)\,. \tag{6.99}$$

Note that this is similar to the definition of, for example, HPLs, but here the interval $[x,1]$ is used. The letters 0, 1 and -1 agree with those from the HPLs, see Eq. (3.38), and the letters 2, -2 and r_4 are defined by

$$f_2(x) = \frac{1}{2-x}\,, \qquad f_{-2}(x) = \frac{1}{2+x}\,, \qquad f_{r_4}(x) = \frac{4}{1-4x}\,. \tag{6.100}$$

The letters w_i contain square roots and we refer to [262] for their definition. The symbol $\mathrm{M}^*[f(x)](0)$ is used to denote the zeroth Mellin moment of the function $f(x)$,

$$\mathrm{M}^*[f(x)](0) = \int_0^1 \mathrm{d}x\, f(x)\,. \tag{6.101}$$

Again following [262], we use here the definition of the Mellin transform without a shift in N – contrary to the rest of this thesis, where we use Eq. (2.62). For both the iterated integrals and the Mellin transformation defined here, we use the star in the superscript to distinguish the definitions.

Since the non-planar parts of diagrams 10 and 11 vanish due to their colour structure, we obtain results similar to $D_{12,a}$ for them. They require only nested harmonic sums and their asymptotic expansion behaves at most logarithmically. Explicit expressions for their results can be found in [268].

The calculation of the ladder- and V-diagrams in this chapter is an important step towards the completion of the OME $A_{Qg}^{(3)}$. The same methods which are applied here, allow to calculate a large number of master integrals for similar diagrams in $A_{Qg}^{(3)}$. Among the diagrams which contribute to $A_{Qg}^{(3)}$, there are 100 ladder diagrams which do not have two separate massive fermion lines as well as 12 V-diagrams. All of these diagrams can be calculated using these methods and are completed by now. The same methods are also applicable to a large share of the remaining diagrams: We calculate 1128 of the 1358 diagrams for $A_{Qg}^{(3)}$. Of the remaining 230 diagrams, 120 fall into the category of diagrams with two separate massive quark lines and 110 are related to crossed box or Benz topologies with 4 or more massive propagators. The master integrals associated to these diagrams appear to require non-iterated integrals. Their calculation needs more advanced methods and will be dealt with elsewhere.

7. The gluonic operator matrix element $A_{gg,Q}^{(3)}$

The massive OME $A_{gg,Q}$ is defined as the expectation value of the gluonic light-cone operator between external, physical gluon states. It starts at $\mathcal{O}(a_s^0)$, but its contribution to the factorisation of the heavy flavour Wilson coefficients of the structure function $F_2(x,Q^2)$ is delayed by one order. It appears in the factorisation of the coefficients $L_{g,2}^{\mathrm{S}}$ and $H_{g,2}^{\mathrm{S}}$, cf. Eqs. (2.93) and (2.95), but to 3-loop order this OME only contributes up to its $\mathcal{O}(a_s^2)$ expansion since it is multiplied by the massless gluonic Wilson coefficient $C_{g,2}^{\mathrm{S}}$, which starts only at 1-loop order. However, the 3-loop term does appear in the matching relation of the gluon PDF in the variable flavour number scheme [202, 203], cf. Eq. (2.113).

In [202] the gluonic OME was calculated up to 2-loop order, which was later recalculated and corrected in [207]. The latter reference also extended the 2-loop results to $\mathcal{O}(\varepsilon)$, which enters the renormalisation of the 3-loop OME. A series of moments for $N = 2, 4, \ldots, 10$ was calculated at $\mathcal{O}(a_s^3)$ in [203]. Since then, there has been incremental progress on completing the 3-loop corrections for general values of N. The logarithmic terms have been reconstructed in [450] from the anomalous dimensions and known, lower-order quantities. Moreover, the terms proportional to the colour factors $C_A T_F^2 N_F$ and $C_F T_F^2 N_F$ have been computed in [337]. These colour factors encompass all diagrams with two closed quark loops of which one is massive and one is massless. The corresponding case of two closed massive quark loops yields the colour factors $C_A T_F^2$ and $C_F T_F^2$ and has been completed in [340]. All remaining diagrams which have two insertions of 1-loop self-energy insertions ("bubbles"), of which one is massless, have been calculated in [338]. In this chapter, we will deal with the calculation of the remaining colour factors of $A_{gg,Q}^{(3)}$ for general, even, integer values of N.

Starting at 3-loop order, there are also diagrams which contain two massive quarks with unequal masses. Fixed moments up to $N = 6$ are known for these diagrams [301, 302, 341, 342], and first progress towards the solution for general N has been made by calculating all scalar prototypes of the relevant diagrams [301, 404]. Here we restrict ourselves to the case of a single massive quark and N_F massless quark flavours.

The renormalisation of the massive OMEs has been derived up to $\mathcal{O}(a_s^3)$ in [203]. It allows to express the pole terms of the unrenormalised OME in terms of renormalisation group quantities. It is given by [203]

$$
\hat{\hat{A}}_{gg,Q}^{(3)} = \left(\frac{\hat{m}^2}{\mu^2}\right)^{3\varepsilon/2} \left[\frac{1}{\varepsilon^3}\left(-\frac{\gamma_{gq}^{(0)}\hat{\gamma}_{qg}^{(0)}}{6}\left[\gamma_{gg}^{(0)} - \gamma_{qq}^{(0)} + 6\beta_0 + 4N_F\beta_{0,Q} + 10\beta_{0,Q}\right]\right.\right.
$$

$$
\left.- \frac{2\gamma_{gg}^{(0)}\beta_{0,Q}}{3}\left[2\beta_0 + 7\beta_{0,Q}\right] - \frac{4\beta_{0,Q}}{3}\left[2\beta_0^2 + 7\beta_{0,Q}\beta_0 + 6\beta_{0,Q}^2\right]\right)
$$

$$
+ \frac{1}{\varepsilon^2}\left(\frac{\hat{\gamma}_{qg}^{(0)}}{6}\left[\gamma_{gq}^{(1)} - (2N_F - 1)\hat{\gamma}_{gq}^{(1)}\right] + \frac{\gamma_{gq}^{(0)}\hat{\gamma}_{qg}^{(1)}}{3} - \frac{\hat{\gamma}_{gg}^{(1)}}{3}\left[4\beta_0 + 7\beta_{0,Q}\right]\right.
$$

$$
+ \frac{2\beta_{0,Q}}{3}\left[\gamma_{gg}^{(1)} + \beta_1 + \beta_{1,Q}\right] + \frac{2\gamma_{gg}^{(0)}\beta_{1,Q}}{3} + \delta m_1^{(-1)}\left[-\hat{\gamma}_{qg}^{(0)}\gamma_{gq}^{(0)} - 2\beta_{0,Q}\gamma_{gg}^{(0)} - 10\beta_{0,Q}^2\right]
$$

$$
\left. - 6\beta_{0,Q}\beta_0 \right] \right) + \frac{1}{\varepsilon}\left(\frac{\hat{\gamma}_{gg}^{(2)}}{3} - 2(2\beta_0 + 3\beta_{0,Q})a_{gg,Q}^{(2)} - N_F\hat{\gamma}_{qg}^{(0)}a_{gq,Q}^{(2)} + \gamma_{gq}^{(0)}a_{Qg}^{(2)} + \beta_{1,Q}^{(1)}\gamma_{gg}^{(0)} \right.
$$

$$
+ \frac{\gamma_{gq}^{(0)}\hat{\gamma}_{qg}^{(0)}\zeta_2}{16}\left[\gamma_{gg}^{(0)} - \gamma_{qq}^{(0)} + 2(2N_F + 1)\beta_{0,Q} + 6\beta_0 \right] + \frac{\beta_{0,Q}\zeta_2}{4}\left[\gamma_{gg}^{(0)}\{2\beta_0 - \beta_{0,Q}\} + 4\beta_0^2 \right.
$$

$$
- 2\beta_{0,Q}\beta_0 - 12\beta_{0,Q}^2 \right] + \delta m_1^{(-1)}\left[-3\delta m_1^{(-1)}\beta_{0,Q} - 2\delta m_1^{(0)}\beta_{0,Q} - \hat{\gamma}_{gg}^{(1)} \right]
$$

$$
\left. + \delta m_1^{(0)}\left[-\hat{\gamma}_{qg}^{(0)}\gamma_{gq}^{(0)} - 2\gamma_{gg}^{(0)}\beta_{0,Q} - 4\beta_{0,Q}\beta_0 - 8\beta_{0,Q}^2 \right] + 2\delta m_2^{(-1)}\beta_{0,Q} \right) + a_{gg,Q}^{(3)} \right]. \quad (7.1)
$$

Here β_k denotes the kth order expansion coefficients of the β-function and $\beta_{k,Q}$ are the corresponding heavy quark contributions, see Eqs. (2.134), (2.134), (2.144) and (2.145). The constant term in the ε-expansion of the MOM-scheme coupling renormalisation constant Z_g at $\mathcal{O}(a_s^2)$ is written as $\beta_{Q,1}^{(1)}$ and given in Eq. (2.146). The mass renormalisation constant, expanded to order k in a_s, is called $\delta m_k^{(l)}$, where l labels the order in the ε-expansion. Moreover, the anomalous dimensions $\gamma_{ij}^{(k)}$ of the light-cone operator enter. They are known up to 3-loop order [136]. Finally, also the constant terms of the unrenormalised operator matrix elements, $a_{ij}^{(k)}$, contribute. Up to 2-loop order, explicit expressions for them can be found in [202, 207]. The expression for the constant term of the unrenormalised 3-loop OME $a_{gg,Q}^{(3)}$ will be the main result of this chapter. Before discussing the result for the constant term of the OME in Section 7.2, we give some details on the calculation in the next subsection.

7.1. Details on the calculation

In total 642 irreducible diagrams contribute to $A_{gg,Q}^{(3)}$, a sample of which can be found in Fig. 7.1. Of these 642 diagrams, 70 are covered by the colour factors $C_A T_F^2 N_F$ and $C_F T_F^2 N_F$ and another 36 by the colour factors $C_A T_F^2$ and $C_F T_F^2$. Another 71 diagrams fall into the category of bubble diagrams. The results for these diagrams have been obtained and published previously [337, 338, 340], which leaves 463 diagrams to be calculated. For completeness, however, we will include the previously known diagrams in the results discussed below.

In order to contribute to $A_{gg,Q}^{(3)}$, the diagrams need to have external gluons and the operator must be located on a gluon line or vertex. The topologies of the diagrams include Benz (e.g. Figs. 7.1g and 7.1h), ladder (e.g. Figs. 7.1a to 7.1c) and also crossed-box topologies (e.g. Figs. 7.1d to 7.1f).

The crossed-box diagrams are among the most complicated ones due to their non-planarity. In principle, there are 18 diagrams with this topology. However, all except for two of them vanish identically due to their colour structure. Only those two crossed-box diagrams in which both external gluons are connected to the heavy quark line remain, see Fig. 7.1d. Examples for the vanishing crossed-box diagrams are depicted in Figs. 7.1e and 7.1f.

Following the calculation procedure outlined in Section 3.1, the diagrams are generated using QGRAF [347] and subsequently Feynman rules are inserted using the FORM [216] program developed for [193, 203], which also applies the projector, carries out the Dirac matrix algebra and uses color.h [348] to simplify the colour structures. The resulting expressions for the diagrams contain scalar integrals, which can be mapped onto the integral families described in Section 3.1. The mapping we use involves the families B1a, B1b, B1c, B1d, B1e, B3c, B5a, B5f and C3b and yields a total of 67212 distinct scalar integrals for $A_{gg,Q}^{(3)}$. Applying then the reductions from IBP identities obtained with Reduze 2 [353, 354], the diagrams can be expressed in terms of 139 master integrals. Except for the family B1e, all families which appear in the mapping of the
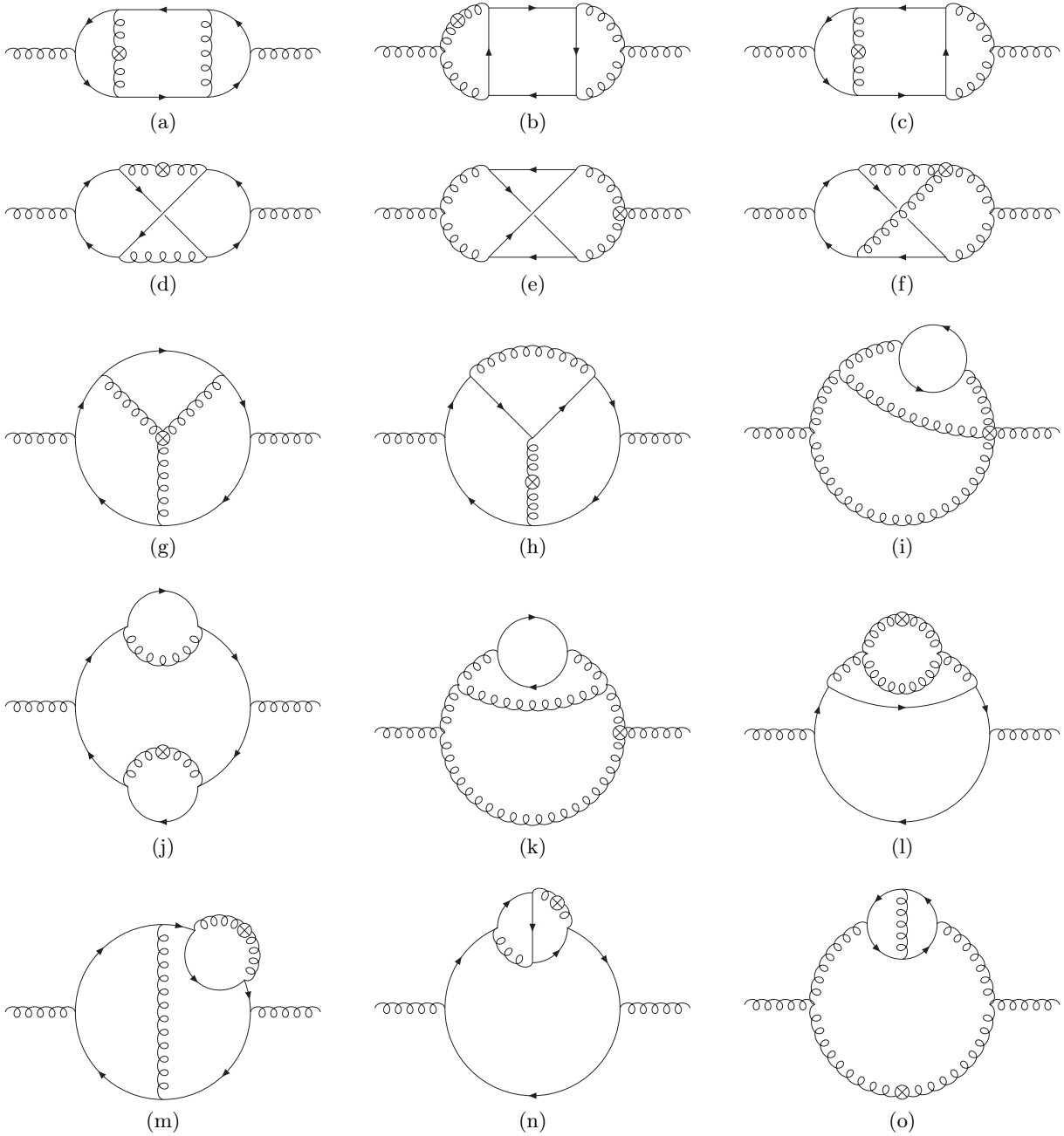
Figure 7.1.: Examples for the diagrams contributing to the gluonic OME $A_{gg,Q}^{(3)}$. Massive quarks are drawn as solid arrow lines. Curly lines represent gluons and the operator insertion is marked by a circled cross.

diagrams also appear among the master integrals.

Since the coefficients of the master integrals in the reductions contain poles in ε, some master integrals have to be evaluated to higher orders in ε. The highest required orders are encountered for two operator-less master integrals which are needed up to order ε^4. The lack of an operator insertion entails that these integrals evaluate to pure numbers and do not depend on N. Ten master integrals with operator insertions and therefore non-trivial N dependence are required to order ε^3. The crossed-box diagrams depend on two master integrals from the family C3b, which is the only non-planar family among the required families: $I_{1,1,1,1,1,0,1,1,0;1,0,0}^{\text{C3b}}$ and $I_{1,1,1,1,1,1,1,1,0;1,0,0}^{\text{C3b}}$. These two master integrals are required including their linear term in the ε-expansion. As mentioned previously, the required order of expansion depends on the choice of basis for the master integrals which is not unique. In this particular case, it can be shown that by eliminating the two integrals above in favour of $I_{1,1,1,1,1,-1,1,1,0;1,0,0}^{\text{C3b}}$ and $I_{1,1,1,1,1,1,1,1,-2;1,0,0}^{\text{C3b}}$ the required order of expansion can be lowered to the constant term for the two non-planar integrals. The trade-off is that irreducible scalar products are present in numerators of the latter integrals, as signalled by the negative indices. We will, nevertheless, use the original integrals for this calculation, since the amount of computation time required for this approach turns out to be still manageable and obtaining initial values for integrals with scalar products in the numerator would require additional steps. However, it may be useful to investigate this approach more systematically in future calculations.

About one quarter of the master integrals can be reused from calculations of other OMEs. In particular, there is an overlap with master integrals from the calculation of $A_{qq,Q}^{\text{NS},(3)}$ [358], described in Section 4.1, and of $A_{gq,Q}^{(3)}$, computed in [339]. At least about half of the diagrams are obtained using the method differential equations for master integrals. Six integrals require the use of the multivariate Almkvist-Zeilberger algorithm [384, 385] implemented in the `Mathematica` package `MultiIntegrate` [259], cf. also [268].

Our choice for the projector of the gluonic Green's functions onto the OMEs, cf. Eq. (2.104), necessitates the calculation of diagrams with external ghost lines in order to eliminate unphysical gluon polarisations. The 89 additional diagrams are topologically equivalent to those of $A_{gq,Q}^{(3)}$, see [339], if we replace the fermion line connected to the external massless quarks by ghost propagators. These diagrams lead to 924 scalar integrals which are reduced to 39 master integrals. However, no new master integrals need to be calculated since they are already required for the gluonic diagrams.

The renormalisation procedure of [203] is carried out for the reducible case. Therefore, we have to add self-energy diagrams to the external legs of the irreducible diagrams that we have discussed so far. For the 3-loop OME this leads to

$$\hat{\hat{A}}_{gg,Q}^{(3)} = \hat{\hat{A}}_{gg,Q}^{\text{irr},(3)} + \Pi^{(3)} + \hat{\hat{A}}_{gg,Q}^{\text{irr},(2)}\Pi^{(1)} + 2\hat{\hat{A}}_{gg,Q}^{(1)}\Pi^{(2)} + \hat{\hat{A}}_{gg,Q}^{(1)}\Pi^{(1)}\Pi^{(1)} , \qquad (7.2)$$

where $\Pi^{(k)}$ denotes the heavy quark contribution to the unrenormalised, k-loop gluon self-energy for on-shell (i.e. vanishing) external momentum and $\hat{\hat{A}}_{gg,Q}^{\text{irr},(k)}$ are the unrenormalised contributions to the OME from one-particle irreducible diagrams. The explicit expressions for $\Pi^{(k)}$ were given in [203].

7.2. The constant part of the unrenormalised OME

We are now in the position to discuss the result for the constant term $a_{gg,Q}^{(3)}$ of the unrenormalised gluonic OME. In order to shorten the expression, we define the following abbreviations

$$\tilde{\gamma}_{gq}^{(0)} = \frac{N^2 + N + 2}{(N-1)N(N+1)} , \qquad \tilde{\gamma}_{qg}^{(0)} = \frac{N^2 + N + 2}{N(N+1)(N+2)} , \qquad (7.3)$$

which are the N-dependent parts of the leading-order gq and qg anomalous dimensions. The constant term in the ε-expansion for even, integer $N \in \mathbb{N}$ is given by

$$
\begin{aligned}
a_{gg,Q}^{(3)} = \frac{1+(-1)^N}{2} &\left\{ C_F^2 T_F \left[\frac{16(N^2+N+2)}{N^2(N+1)^2} \sum_{i=1}^{N} \frac{\binom{2i}{i}\left(\sum_{j=1}^{i} \frac{4^j S_1(j-1)}{\binom{2j}{j}j^2} - 7\zeta_3\right)}{4^i(i+1)^2} \right.\right.\\
&+ \frac{16 P_{458}\binom{2N}{N}4^{-N}\left(\sum_{i=1}^{N}\frac{4^i S_1(i-1)}{\binom{2i}{i}i^2}-7\zeta_3\right)}{15(N-3)(N-2)(N-1)^2 N^3(N+1)^4(N+2)} - \frac{4P_{436}S_1^2}{3(N-1)N^4(N+1)^4(N+2)}\\
&+ \frac{64 P_{429}\left[S_{2,-1}-S_{-2,-1}-S_{-1}S_2\right]}{15(N-3)(N-2)(N-1)^2 N^2(N+1)^3} + \tilde{\gamma}_{gq}^{(0)}\left(\frac{128\left[S_{-4}-S_{-3}S_1+S_{-3,1}+2S_{-2,2}\right]}{3N(N+1)(N+2)}\right.\\
&+ \frac{4(5N^2+5N-22)S_1^2 S_2}{3N(N+1)(N+2)} + \frac{64S_{-2}^2-256S_{-2,1,1}}{N(N+1)(N+2)} + \frac{4P_{379}S_1^3}{9N^2(N+1)^2(N+2)}\\
&- \frac{32(7N^2+7N-10)S_{2,1,1}}{3N(N+1)(N+2)} + \frac{4(13N^2+13N-102)S_4}{3N(N+1)(N+2)} - \frac{2(31N^2+31N+30)S_2^2}{3N(N+1)(N+2)}\\
&+ \left(\frac{256S_{-2,1}}{N(N+1)(N+2)} + \frac{32(3N^2+3N-2)S_{2,1}}{3N(N+1)(N+2)} + \frac{16(13N^2+13N-46)S_3}{9N(N+1)(N+2)}\right)S_1\\
&\left.- \frac{256S_2 S_{-2}+384S_1^2 S_{-2}}{3N(N+1)(N+2)}\right) + \frac{32P_{445}S_{-2,1}-16P_{444}S_{-3}}{3(N-3)(N-2)(N-1)^2 N^3(N+1)^3(N+2)}\\
&- \frac{16P_{446}S_{2,1}}{15(N-3)(N-2)(N-1)^2 N^3(N+1)^3} + \tilde{\gamma}_{gq}^{(0)}\tilde{\gamma}_{qg}^{(0)}\left(\frac{2}{9}S_1^4 + \frac{32}{3}S_{3,1}\right)\\
&+ \frac{4P_{459}S_2}{15(N-3)(N-2)(N-1)^2 N^4(N+1)^4(N+2)} + \left(\frac{4P_{414}S_2}{3(N-1)N^3(N+1)^3(N+2)}\right.\\
&\left.+ \frac{8P_{465}}{15(N-3)(N-2)(N-1)N^5(N+1)^5(N+2)}\right)S_1 + \frac{32(N^2+N+2)}{N^2(N+1)^2}B_4\\
&+ \frac{2P_{483}}{45(N-3)(N-2)(N-1)N^6(N+1)^6(N+2)} - \frac{144(N^2+N+2)}{N^2(N+1)^2}\zeta_4\\
&+ \left(\frac{1}{(N-3)(N-2)(N-1)N^2(N+1)^3}\left(-\frac{32P_{445}S_1}{3(N-1)N(N+2)}+\frac{64P_{429}S_{-1}}{15(N-1)}\right.\right.\\
&\left.\left.+ \frac{32P_{451}}{15N^2(N+1)(N+2)}\right)\right)S_{-2} + \frac{16P_{447}S_3}{45(N-3)(N-2)(N-1)^2 N^3(N+1)^3(N+2)}\\
&+ \left(\tilde{\gamma}_{gq}^{(0)}\left(-\frac{2P_{420}}{N^3(N+1)^3(N+2)}+\frac{4P_{380}S_1}{N^2(N+1)^2(N+2)}\right)+\tilde{\gamma}_{gq}^{(0)}\tilde{\gamma}_{qg}^{(0)}\left(4S_1^2-12S_2\right)\right)\zeta_2\\
&\left.+ \left(-\frac{16(N^2+N-118)S_1}{3N(N+1)(N+2)}\tilde{\gamma}_{gq}^{(0)}+\frac{P_{461}}{15(N-3)(N-2)(N-1)^2 N^3(N+1)^3(N+2)}\right)\zeta_3\right]\\
&+ C_A C_F T_F \left[\frac{16P_{409}}{3(N-1)N^2(N+1)^2(N+2)}\sum_{i=1}^{N}\frac{\binom{2i}{i}\left(\sum_{j=1}^{i}\frac{4^j S_1(j-1)}{\binom{2j}{j}j^2}-7\zeta_3\right)}{4^i(i+1)^2}\right.
\end{aligned}
$$

7. The gluonic operator matrix element $A_{gg,Q}^{(3)}$

$$+ \frac{4P_{473}\binom{2N}{N}4^{-N}\left(\sum_{i=1}^{N}\frac{4^i S_1(i-1)}{\binom{2i}{i}i^2} - 7\zeta_3\right)}{15(N-3)(N-2)(N-1)^2 N^3(N+1)^4(N+2)^2} + \frac{32P_{369}S_{-2,2}}{(N-1)N^2(N+1)^2(N+2)}$$

$$+ \frac{32\left(N^2-8N-1\right)\left(N^2+10N+8\right)S_{-3,1}}{3(N-1)N^2(N+1)^2(N+2)} - \frac{64P_{381}S_{-2,1,1}}{3(N-1)N^2(N+1)^2(N+2)}$$

$$- \frac{16P_{390}S_{-4}}{3(N-1)N^2(N+1)^2(N+2)} - \frac{16P_{406}S_{3,1}}{3(N-2)(N-1)N^2(N+1)^2(N+2)}$$

$$- \frac{16P_{428}S_{2,1,1}}{3(N-2)(N-1)N^2(N+1)^2(N+2)} + \frac{4P_{430}S_4}{3(N-2)(N-1)N^2(N+1)^2(N+2)}$$

$$+ \frac{32P_{437}\left[S_{-1}S_2 - S_{2,-1} + S_{-2,-1}\right]}{5(N-3)(N-2)(N-1)^2 N^2(N+1)^3(N+2)} + \tilde{\gamma}_{gq}^{(0)}\left(-\frac{32\left(2N^2+2N+13\right)S_{-2}^2}{3N(N+1)(N+2)}\right)$$

$$+ \frac{2\left(5N^2+5N-6\right)S_2^2}{N(N+1)(N+2)} - \frac{4P_{418}S_1^3}{27(N-1)N^2(N+1)^2(N+2)^2}\right)$$

$$+ \left(\frac{64P_{382}S_{-2,1}}{3(N-1)N^2(N+1)^2(N+2)} + \frac{8P_{485}}{405(N-3)(N-2)(N-1)^2 N^5(N+1)^5(N+2)^4}\right.$$

$$+ \frac{32P_{404}S_3}{9(N-2)(N-1)N^2(N+1)^2(N+2)} + \frac{4P_{450}S_2}{3(N-2)(N-1)^2 N^3(N+1)^3(N+2)^2}$$

$$\left.+ \frac{32P_{410}S_{2,1}}{3(N-1)N^2(N+1)^2(N+2)}\right)S_1 - \frac{16P_{448}S_{-2,1}}{3(N-3)(N-2)(N-1)^2 N^3(N+1)^3(N+2)^2}$$

$$+ \frac{8P_{468}S_3}{135(N-3)(N-2)(N-1)^2 N^3(N+1)^3(N+2)^2} + \left(-\frac{4P_{393}S_2}{3(N-1)N^2(N+1)^2(N+2)}\right.$$

$$+ \frac{4P_{460}}{27(N-2)(N-1)^2 N^3(N+1)^4(N+2)^3}\right)S_1^2 - \frac{2}{9}\tilde{\gamma}_{gq}^{(0)}\tilde{\gamma}_{qg}^{(0)}S_1^4$$

$$- \frac{8P_{472}S_{2,1}}{15(N-3)(N-2)(N-1)^2 N^3(N+1)^3(N+2)^2} - \left(\frac{32P_{383}S_1^2}{3(N-1)N^2(N+1)^2(N+2)}\right.$$

$$+ \frac{1}{(N-3)(N-2)(N-1)^2 N^2(N+1)^3(N+2)}\left(\frac{32P_{437}S_{-1}}{5} + \frac{16P_{449}S_1}{3N(N+2)}\right.$$

$$\left.+ \frac{16P_{479}}{15(N-2)N^2(N+1)(N+2)^2}\right) + \frac{32P_{396}S_2}{3(N-2)(N-1)N^2(N+1)^2(N+2)}\right)S_{-2}$$

$$+ \frac{4P_{482}S_2}{45(N-3)(N-2)^2(N-1)^2 N^4(N+1)^4(N+2)^3} + \left(-\frac{32P_{368}S_1}{3(N-1)N^2(N+1)^2(N+2)}\right.$$

$$+ \frac{8P_{452}}{3(N-3)(N-2)(N-1)^2 N^3(N+1)^3(N+2)^2}\right)S_{-3} + \left(\tilde{\gamma}_{gq}^{(0)}\tilde{\gamma}_{qg}^{(0)}\left(-4S_1^2 - 12S_2\right.\right.$$

$$\left.- 24S_{-2}\right) + \frac{4P_{454}S_1}{3(N-1)^2 N^3(N+1)^3(N+2)^2} + \frac{4P_{471}}{9(N-1)^2 N^4(N+1)^4(N+2)^3}\right)\zeta_2$$

$$+ \frac{P_{488}}{2430(N-3)(N-2)^2(N-1)^2 N^6(N+1)^6(N+2)^5} + \left(96S_1\right.$$

$$- \frac{48\left(N^2+N+4\right)\left(N^2+N+6\right)}{(N-1)N^2(N+1)^2(N+2)}\right)\zeta_4 + \left(-\frac{8P_{433}S_1}{9(N-2)(N-1)N^2(N+1)^2(N+2)}\right.$$

$$
+\frac{P_{477}}{180(N-3)(N-2)(N-1)^2N^3(N+1)^3(N+2)^2}\Bigg)\zeta_3+\Bigg(-\frac{64}{3}S_1
$$

$$
+\frac{32\big(N^2+N+4\big)\big(N^2+N+6\big)}{3(N-1)N^2(N+1)^2(N+2)}\Bigg)B_4\Bigg]
$$

$$
+C_A^2T_F\Bigg[-\frac{4P_{413}}{3(N-1)N^2(N+1)^2(N+2)}\sum_{i=1}^{N}\frac{\binom{2i}{i}\left(\sum_{j=1}^{i}\frac{4^jS_1(j-1)}{\binom{2j}{j}j^2}-7\zeta_3\right)}{4^i\big(i+1\big)^2}
$$

$$
-\frac{2P_{474}\binom{2N}{N}4^{-N}\left(\sum_{i=1}^{N}\frac{4^iS_1(i-1)}{\binom{2i}{i}i^2}-7\zeta_3\right)}{15(N-3)(N-2)(N-1)^2N^3(N+1)^4(N+2)^2}+\frac{256P_{372}S_{-2,2}}{9(N-1)N^2(N+1)^2(N+2)}
$$

$$
+\frac{32P_{397}S_{-2,1,1}+16P_{402}S_{-3,1}+16P_{411}S_{-4}}{9(N-1)N^2(N+1)^2(N+2)}+\frac{8P_{425}S_{3,1}}{9(N-2)(N-1)N^2(N+1)^2(N+2)}
$$

$$
+\frac{16P_{419}S_{-2}^2}{27(N-1)N^2(N+1)^2(N+2)}+\frac{16P_{439}S_{2,-1}}{15(N-3)(N-2)(N-1)^2N^2(N+1)^3(N+2)}
$$

$$
-\frac{16P_{427}S_{2,1,1}}{3(N-2)(N-1)N^2(N+1)^2(N+2)}-\frac{4P_{431}S_4}{9(N-2)(N-1)N^2(N+1)^2(N+2)}
$$

$$
+\frac{8P_{403}S_2^2}{9(N-1)N^2(N+1)^2}-\frac{16P_{439}S_{-2,-1}}{15(N-3)(N-2)(N-1)^2N^2(N+1)^3(N+2)}
$$

$$
+\frac{8P_{467}S_{-3}}{81(N-3)(N-2)(N-1)^2N^3(N+1)^3(N+2)^2}+\Bigg(-\frac{32P_{399}S_{-2,1}}{9(N-1)N^2(N+1)^2(N+2)}
$$

$$
+\frac{8P_{417}S_{2,1}-16P_{401}S_{-3}}{9(N-1)N^2(N+1)^2(N+2)}+\frac{16P_{463}S_{-2}}{81(N-3)(N-2)(N-1)^2N^3(N+1)^3(N+2)}
$$

$$
-\frac{16P_{432}S_3}{27(N-2)(N-1)N^2(N+1)^2(N+2)}+\frac{4P_{464}S_2}{81(N-2)(N-1)^2N^3(N+1)^3(N+2)^2}
$$

$$
+\frac{2P_{486}}{3645(N-3)(N-2)(N-1)^2N^5(N+1)^5(N+2)^4}+\frac{16}{9}S_2^2+\frac{592}{9}S_4-\frac{64}{9}S_{-2}^2
$$

$$
+\frac{64}{9}S_{-4}-\frac{832}{9}S_{3,1}-\frac{128}{9}S_{-2,2}-\frac{128}{9}S_{-3,1}+\frac{32}{3}S_{2,1,1}+\frac{256}{9}S_{-2,1,1}\Bigg)S_1
$$

$$
-\frac{4P_{475}S_3}{405(N-3)(N-2)(N-1)^2N^3(N+1)^3(N+2)^2}+\Bigg(\frac{4P_{398}S_2}{9(N-1)N^2(N+1)^2(N+2)}
$$

$$
+\frac{16P_{400}S_{-2}}{9(N-1)N^2(N+1)^2(N+2)}+\frac{P_{466}}{27(N-2)(N-1)^2N^4(N+1)^3(N+2)^3}+\frac{272}{9}S_3
$$

$$
+\frac{32}{9}\left[2S_{-3}-S_{2,1}-4S_{-2,1}\right]\Bigg)S_1^2+\frac{P_{487}}{14580(N-3)(N-2)^2(N-1)^2N^5(N+1)^5(N+2)^5}
$$

$$
+\Bigg(-\frac{64(2N+1)P_{371}}{27(N-1)^2N^2(N+1)^2(N+2)^2}+\frac{64}{27}S_2+\frac{128}{27}S_{-2}\Bigg)S_1^3+\Bigg(\frac{32P_{377}S_{-3}}{9N(N+1)}
$$

$$
+\frac{P_{484}}{405(N-3)(N-2)^2(N-1)^2N^4(N+1)^4(N+2)^3}-\frac{16P_{394}S_3}{27N(N+1)}\Bigg)S_2-\frac{16P_{391}S_5}{9N(N+1)}
$$

$$
+\Bigg(\frac{16P_{481}}{405(N-3)(N-2)^2(N-1)^2N^4(N+1)^4(N+2)^3}-\frac{16P_{389}S_{-3}}{9N(N+1)}-\frac{320}{27}S_3
$$

7. The gluonic operator matrix element $A_{gg,Q}^{(3)}$

$$
+ \frac{16 P_{426} S_2}{9(N-2)(N-1)N^2(N+1)^2(N+2)} \Bigg) S_{-2} + \frac{32 P_{376} S_{-5}}{9N(N+1)} + \frac{16 P_{392} S_{2,3}}{9N(N+1)}
$$

$$
+ \frac{16 P_{439} \left[S_{-2} - S_2 \right] S_{-1}}{15(N-3)(N-2)(N-1)^2 N^2 (N+1)^3 (N+2)} + \left(-\frac{80}{9} S_2 + \frac{64 P_{378} S_{-2}}{9N(N+1)} \right.
$$

$$
- \frac{2 P_{476}}{45(N-3)(N-2)(N-1)^2 N^3 (N+1)^3 (N+2)^2} \Bigg) S_{2,1} + \frac{16 P_{388} S_{2,-3}}{9N(N+1)} - 96 S_{4,1}
$$

$$
+ \left(-\frac{16 P_{462}}{81(N-3)(N-2)(N-1)^2 N^3 (N+1)^3 (N+2)} - \frac{64 P_{370} S_2}{3N(N+1)} + \frac{64}{9} S_{-2} \right) S_{-2,1}
$$

$$
- \frac{16 P_{373} S_{-2,3}}{3N(N+1)} + \frac{64 P_{386} S_{-2,-3}}{9N(N+1)} - \frac{16 P_{374} S_{-4,1}}{3N(N+1)} - \frac{32 P_{385} S_{2,1,-2}}{9N(N+1)} + 16 S_{2,2,1} + \frac{416}{3} S_{3,1,1}
$$

$$
- \frac{32 P_{387} S_{-2,1,-2}}{9N(N+1)} + \frac{128}{9} S_{-2,2,1} + \frac{128}{9} S_{-3,1,1} - \frac{160}{9} S_{2,1,1,1} - \frac{256}{9} S_{-2,1,1,1} + \left(\frac{16}{3} S_3 \right.
$$

$$
- \frac{64 \left(N^2 + N + 1 \right) S_2}{3(N-1)N(N+1)(N+2)} - \frac{4 P_{457}}{27(N-1)^2 N^3 (N+1)^3 (N+2)^3} + \frac{16}{3} S_{-3} + \left(\frac{32}{3} S_2 \right.
$$

$$
- \frac{16 P_{435}}{27(N-1)^2 N^2 (N+1)^2 (N+2)^2} \Bigg) S_1 + \left(-\frac{64 \left(N^2 + N + 1 \right)}{3(N-1)N(N+1)(N+2)} + \frac{32}{3} S_1 \right) S_{-2}
$$

$$
- \frac{32}{3} S_{-2,1} \Bigg) \zeta_2 + \left(\frac{4 P_{434} S_1}{27(N-2)(N-1)N^2 (N+1)^2 (N+2)} - \frac{80}{3} S_1^2 - \frac{32 P_{370} S_2}{3N(N+1)} \right.
$$

$$
- \frac{32 P_{373} S_{-2}}{3N(N+1)} + \frac{P_{478}}{1080(N-3)(N-2)(N-1)^2 N^3 (N+1)^3 (N+2)^2} \Bigg) \zeta_3
$$

$$
+ \left(\frac{96 P_{375}}{(N-1)N^2 (N+1)^2 (N+2)} - 96 S_1 \right) \zeta_4 + \left(-\frac{8 P_{384}}{3(N-1)N^2 (N+1)^2 (N+2)} \right.
$$

$$
+ \frac{32}{3} S_1 \Bigg) B_4 \Bigg] + C_F T_F^2 \left[-\frac{16 P_{415} \binom{2N}{N} 4^{-N} \left(\sum_{i=1}^{N} \frac{4^i S_1(i-1)}{\binom{2i}{i} i^2} - 7\zeta_3 \right)}{3(N-1)N(N+1)^2 (N+2)(2N-3)(2N-1)} \right.
$$

$$
- \frac{32 P_{453} S_1}{81(N-1)N^4 (N+1)^4 (N+2)(2N-3)(2N-1)} + \frac{16 P_{412} S_1^2}{27(N-1)N^3 (N+1)^3 (N+2)}
$$

$$
- \frac{16 P_{412} S_2}{9(N-1)N^3 (N+1)^3 (N+2)} - \frac{2 P_{480}}{243(N-1)N^5 (N+1)^5 (N+2)(2N-3)(2N-1)}
$$

$$
+ \tilde{\gamma}_{gq}^{(0)} \tilde{\gamma}_{qg}^{(0)} \left(\frac{16}{27} S_1^3 - \frac{16}{3} S_1 S_2 - \frac{352}{27} S_3 + \frac{64}{3} S_{2,1} \right) + \left(-\frac{8 P_{440}}{9(N-1)N^3 (N+1)^3 (N+2)} \right.
$$

$$
+ \frac{16}{3} \tilde{\gamma}_{gq}^{(0)} \tilde{\gamma}_{qg}^{(0)} S_1 \Bigg) \zeta_2 + \frac{P_{408}}{9(N-1)N^2 (N+1)^2 (N+2)} \zeta_3 \Bigg]
$$

$$
+ C_A T_F^2 \left[-\frac{4 P_{441} \binom{2N}{N} 4^{-N} \left(\sum_{i=1}^{N} \frac{4^i S_1(i-1)}{\binom{2i}{i} i^2} - 7\zeta_3 \right)}{45(N-1)N(N+1)^2 (N+2)(2N-3)(2N-1)} \right.
$$

$$
- \frac{8 P_{456} S_1}{3645(N-1)N^3 (N+1)^3 (N+2)(2N-3)(2N-1)} - \frac{16 \left(4N^3 + 4N^2 - 7N + 1 \right) S_3}{15(N-1)N(N+1)}
$$

$$
+ \frac{16 \left(4N^3 + 4N^2 - 7N + 1 \right) S_{2,1}}{15(N-1)N(N+1)} + \frac{P_{470}}{3645(N-1)N^4 (N+1)^4 (N+2)(2N-3)(2N-1)}
$$

$$+ \frac{4\left[P_{424}S_2 - P_{407}S_1^2\right]}{135(N-1)N^2(N+1)^2(N+2)} + \left(\frac{4P_{423}}{27(N-1)N^2(N+1)^2(N+2)} - \frac{560}{27}S_1\right)\zeta_2$$

$$+ \left(-\frac{7P_{395}}{270(N-1)N(N+1)(N+2)} - \frac{1120}{27}S_1\right)\zeta_3\Bigg]$$

$$+ C_A N_F T_F^2 \Bigg[\frac{4\left[P_{421}S_2 - P_{405}S_1^2\right]}{27(N-1)N^2(N+1)^2(N+2)} - \frac{8P_{443}S_1}{729(N-1)N^3(N+1)^3(N+2)}$$

$$- \frac{2P_{455}}{729(N-1)N^4(N+1)^4(N+2)} + \left(\frac{4P_{416}}{27(N-1)N^2(N+1)^2(N+2)} - \frac{160}{27}S_1\right)\zeta_2$$

$$+ \left(-\frac{896\left(N^2 + N + 1\right)}{27(N-1)N(N+1)(N+2)} + \frac{448}{27}S_1\right)\zeta_3\Bigg]$$

$$+ C_F N_F T_F^2 \Bigg[-\frac{16P_{412}S_2}{9(N-1)N^3(N+1)^3(N+2)} + \frac{16P_{422}S_1^2}{27(N-1)N^3(N+1)^3(N+2)}$$

$$- \frac{32P_{442}S_1}{81(N-1)N^4(N+1)^4(N+2)} + \tilde{\gamma}_{gq}^{(0)}\tilde{\gamma}_{qg}^{(0)}\left(-\frac{112}{27}S_1^3 - \frac{16}{3}S_1S_2 + \frac{160}{27}S_3 - \frac{448}{9}\zeta_3\right.$$

$$\left.- \frac{16}{3}S_1\zeta_2\right) - \frac{2P_{469}}{243(N-1)N^5(N+1)^5(N+2)} - \frac{4P_{438}}{9(N-1)N^3(N+1)^3(N+2)}\zeta_2\Bigg]$$

$$+ T_F^3 \frac{64}{27}\zeta_3\Bigg\}, \tag{7.4}$$

with the polynomials P_i given by

$$P_{368} = N^4 + 2N^3 - 61N^2 - 62N - 8 \tag{7.5}$$

$$P_{369} = N^4 + 2N^3 - 23N^2 - 24N - 4 \tag{7.6}$$

$$P_{370} = N^4 + 2N^3 - N^2 - 2N + 3 \tag{7.7}$$

$$P_{371} = N^4 + 2N^3 + 3N^2 + 2N - 2 \tag{7.8}$$

$$P_{372} = N^4 + 2N^3 + 17N^2 + 16N + 3 \tag{7.9}$$

$$P_{373} = 2N^4 + 4N^3 - 3N^2 - 5N + 6 \tag{7.10}$$

$$P_{374} = 2N^4 + 4N^3 - N^2 - 3N + 6 \tag{7.11}$$

$$P_{375} = 2N^4 + 4N^3 + 7N^2 + 5N + 6 \tag{7.12}$$

$$P_{376} = 3N^4 + 6N^3 - 11N^2 - 14N + 9 \tag{7.13}$$

$$P_{377} = 3N^4 + 6N^3 - 8N^2 - 11N + 9 \tag{7.14}$$

$$P_{378} = 3N^4 + 6N^3 - 4N^2 - 7N + 9 \tag{7.15}$$

$$P_{379} = 5N^4 - 8N^3 - 23N^2 - 22N - 8 \tag{7.16}$$

$$P_{380} = 5N^4 + 4N^3 + N^2 - 10N - 8 \tag{7.17}$$

$$P_{381} = 5N^4 + 10N^3 - 65N^2 - 70N - 16 \tag{7.18}$$

$$P_{382} = 5N^4 + 10N^3 - 29N^2 - 34N - 16 \tag{7.19}$$

$$P_{383} = 5N^4 + 10N^3 - N^2 - 6N - 16 \tag{7.20}$$

$$P_{384} = 5N^4 + 10N^3 + 25N^2 + 20N + 36 \tag{7.21}$$

$$P_{385} = 6N^4 + 12N^3 - 7N^2 - 13N + 18 \tag{7.22}$$

7. The gluonic operator matrix element $A_{gg,Q}^{(3)}$

$$P_{386} = 6N^4 + 12N^3 - N^2 - 7N + 18 \tag{7.23}$$

$$P_{387} = 6N^4 + 12N^3 + N^2 - 5N + 18 \tag{7.24}$$

$$P_{388} = 6N^4 + 12N^3 + 5N^2 - N + 18 \tag{7.25}$$

$$P_{389} = 6N^4 + 12N^3 + 7N^2 + N + 18 \tag{7.26}$$

$$P_{390} = 11N^4 + 22N^3 - 5N^2 - 16N + 68 \tag{7.27}$$

$$P_{391} = 18N^4 + 36N^3 + 19N^2 + N + 54 \tag{7.28}$$

$$P_{392} = 18N^4 + 36N^3 + 41N^2 + 23N + 54 \tag{7.29}$$

$$P_{393} = 29N^4 + 58N^3 + 49N^2 + 20N + 20 \tag{7.30}$$

$$P_{394} = 36N^4 + 72N^3 + 103N^2 + 67N + 108 \tag{7.31}$$

$$P_{395} = 1287N^4 + 3726N^3 - 3047N^2 - 7214N - 2624 \tag{7.32}$$

$$P_{396} = N^5 - 12N^4 - 11N^3 - 54N^2 - 52N - 8 \tag{7.33}$$

$$P_{397} = 3N^5 - 7N^4 - 25N^3 - 269N^2 - 254N - 72 \tag{7.34}$$

$$P_{398} = 3N^5 - 5N^4 - 21N^3 - 79N^2 - 66N - 24 \tag{7.35}$$

$$P_{399} = 3N^5 - 4N^4 - 19N^3 - 146N^2 - 134N - 60 \tag{7.36}$$

$$P_{400} = 3N^5 - N^4 - 13N^3 - 47N^2 - 38N - 48 \tag{7.37}$$

$$P_{401} = 3N^5 + 16N^4 + 21N^3 + 194N^2 + 186N - 12 \tag{7.38}$$

$$P_{402} = 3N^5 + 25N^4 + 39N^3 + 275N^2 + 258N + 24 \tag{7.39}$$

$$P_{403} = 9N^5 + 18N^4 - 19N^3 - 30N^2 - 20N + 18 \tag{7.40}$$

$$P_{404} = 13N^5 + 36N^4 + 55N^3 + 60N^2 + 116N - 176 \tag{7.41}$$

$$P_{405} = 16N^5 + 41N^4 + 2N^3 + 47N^2 + 70N + 32 \tag{7.42}$$

$$P_{406} = 59N^5 + 72N^4 - 13N^3 + 78N^2 + 196N - 184 \tag{7.43}$$

$$P_{407} = 70N^5 + 95N^4 - 223N^3 - 751N^2 - 629N - 142 \tag{7.44}$$

$$P_{408} = -63N^6 - 189N^5 - 431N^4 - 547N^3 - 1714N^2 - 1472N - 1472 \tag{7.45}$$

$$P_{409} = 2N^6 + 8N^5 + 3N^4 - 14N^3 - 5N^2 + 6N + 24 \tag{7.46}$$

$$P_{410} = 2N^6 + 8N^5 + 9N^4 - 2N^3 + 7N^2 + 12N + 36 \tag{7.47}$$

$$P_{411} = 3N^6 + 3N^5 - 5N^4 + 17N^3 - 64N^2 - 86N + 60 \tag{7.48}$$

$$P_{412} = 4N^6 + 3N^5 - 50N^4 - 129N^3 - 100N^2 - 56N - 24 \tag{7.49}$$

$$P_{413} = 4N^6 + 16N^5 + 9N^4 - 22N^3 - 7N^2 + 12N + 36 \tag{7.50}$$

$$P_{414} = 9N^6 - 15N^5 - 89N^4 - 177N^3 + 36N^2 + 28N - 16 \tag{7.51}$$

$$P_{415} = 9N^6 + 9N^5 - 53N^4 + 47N^3 + 44N^2 - 104N - 80 \tag{7.52}$$

$$P_{416} = 9N^6 + 27N^5 + 161N^4 + 277N^3 + 358N^2 + 224N + 48 \tag{7.53}$$

$$P_{417} = 15N^6 + 60N^5 + 43N^4 - 76N^3 - 112N^2 - 38N - 132 \tag{7.54}$$

$$P_{418} = 17N^6 + 33N^5 - 27N^4 + 59N^3 + 130N^2 - 44N - 24 \tag{7.55}$$

$$P_{419} = 29N^6 + 78N^5 + 71N^4 + 90N^3 + 206N^2 + 138N + 180 \tag{7.56}$$

$$P_{420} = 38N^6 + 108N^5 + 151N^4 + 106N^3 + 21N^2 - 28N - 12 \tag{7.57}$$

$$P_{421} = 40N^6 + 112N^5 - 3N^4 - 166N^3 - 301N^2 - 210N - 96 \tag{7.58}$$

$$P_{422} = 44N^6 + 123N^5 + 386N^4 + 543N^3 + 520N^2 + 248N + 24 \tag{7.59}$$

$$P_{423} = 99N^6 + 297N^5 + 631N^4 + 767N^3 + 1118N^2 + 784N + 168 \tag{7.60}$$

$$P_{424} = 220N^6 + 550N^5 - 135N^4 - 883N^3 - 1621N^2 - 1329N - 462 \tag{7.61}$$

$$P_{425} = 3N^7 - 18N^6 + 334N^5 + 358N^4 - 649N^3 - 232N^2 + 492N - 144 \tag{7.62}$$

$$P_{426} = 3N^7 + 3N^6 - 21N^5 - 31N^4 - 64N^3 - 122N^2 - 104N + 72 \tag{7.63}$$

$$P_{427} = 5N^7 + 10N^6 - 15N^5 - 42N^4 - 4N^3 + 86N^2 + 32N + 72 \tag{7.64}$$

$$P_{428} = 8N^7 + 16N^6 - 57N^5 - 104N^4 + 87N^3 - 26N^2 - 28N - 248 \tag{7.65}$$

$$P_{429} = 15N^7 - 25N^6 - 192N^5 + 442N^4 + 107N^3 + 2391N^2 + 1030N + 1032 \tag{7.66}$$

$$P_{430} = 16N^7 + 32N^6 + 27N^5 + 32N^4 + 219N^3 + 398N^2 + 628N - 856 \tag{7.67}$$

$$P_{431} = 18N^7 + 15N^6 + 395N^5 + 305N^4 - 545N^3 - 584N^2 + 252N - 768 \tag{7.68}$$

$$P_{432} = 38N^7 + 20N^6 + 77N^5 + 104N^4 - 385N^3 - 466N^2 + 36N - 216 \tag{7.69}$$

$$P_{433} = 199N^7 + 247N^6 - 785N^5 - 1091N^4 + 1510N^3 - 56N^2 + 888N - 5424 \tag{7.70}$$

$$P_{434} = 421N^7 - 11N^6 - 881N^5 + 775N^4 + 172N^3 - 3356N^2 + 2880N - 10368 \tag{7.71}$$

$$P_{435} = N^8 + 4N^7 + 2N^6 + 64N^5 + 173N^4 + 292N^3 + 256N^2 - 72N - 72 \tag{7.72}$$

$$P_{436} = 5N^8 + 41N^7 + 41N^6 + 25N^5 - 14N^4 - 54N^3 - 84N^2 - 72N - 16 \tag{7.73}$$

$$P_{437} = 15N^8 - 252N^6 + 228N^5 + 631N^4 + 1780N^3 + 3822N^2 + 1032N + 744 \tag{7.74}$$

$$P_{438} = 15N^8 + 60N^7 + 4N^6 - 162N^5 - 311N^4 - 186N^3 - 220N^2 - 80N + 48 \tag{7.75}$$

$$P_{439} = 30N^8 - 5N^7 - 514N^6 + 626N^5 + 902N^4 + 2735N^3 + 5654N^2 + 4N + 168 \tag{7.76}$$

$$P_{440} = 33N^8 + 132N^7 + 106N^6 - 108N^5 - 74N^4 + 282N^3 + 245N^2 + 148N + 84 \tag{7.77}$$

$$P_{441} = 100N^8 + 539N^7 + 283N^6 - 2094N^5 + 452N^4 + 219N^3 - 1495N^2 + 712N + 996 \tag{7.78}$$

$$P_{442} = 205N^8 + 856N^7 + 3169N^6 + 6484N^5 + 7310N^4 + 4722N^3 + 1534N^2 + 48N - 72 \tag{7.79}$$

$$P_{443} = 6944N^8 + 26480N^7 + 23321N^6 - 15103N^5 - 39319N^4 - 27001N^3 - 11178N^2 \\ - 2016N + 864 \tag{7.80}$$

$$P_{444} = 5N^9 + 3N^8 - 66N^7 - 82N^6 + 469N^5 + 1099N^4 + 2392N^3 + 1092N^2 + 656N + 192 \tag{7.81}$$

$$P_{445} = 7N^9 - 3N^8 - 78N^7 - 46N^6 + 439N^5 + 1285N^4 + 2112N^3 + 1068N^2 + 592N + 384 \tag{7.82}$$

$$P_{446} = 40N^9 - 65N^8 - 545N^7 + 902N^6 + 1818N^5 - 2437N^4 + 8779N^3 + 8080N^2 + 1908N \\ + 720 \tag{7.83}$$

$$P_{447} = 215N^9 - 660N^8 - 1409N^7 + 4346N^6 + 4217N^5 + 9360N^4 + 31989N^3 + 24274N^2 \\ + 17788N - 3720 \tag{7.84}$$

$$P_{448} = N^{10} + 37N^9 - 10N^8 - 634N^7 + 81N^6 + 5157N^5 + 12472N^4 + 9408N^3 + 896N^2 \\ + 4272N + 2880 \tag{7.85}$$

$$P_{449} = 3N^{10} - 29N^9 - 62N^8 + 538N^7 + 251N^6 - 4533N^5 - 13200N^4 - 11384N^3 - 432N^2 \\ - 3408N - 2304 \tag{7.86}$$

$$P_{450} = 8N^{10} - 51N^9 - 96N^8 + 508N^7 + 458N^6 - 1601N^5 - 2194N^4 + 152N^3 - 464N^2 \\ - 976N + 224 \tag{7.87}$$

$$P_{451} = 15N^{10} + 10N^9 - 238N^8 + 88N^7 + 2647N^6 + 9610N^5 + 17712N^4 + 13108N^3 \\ + 5128N^2 - 1872N - 1440 \tag{7.88}$$

$$P_{452} = 15N^{10} + 19N^9 - 238N^8 - 358N^7 + 1087N^6 + 4483N^5 + 10400N^4 + 9536N^3$$

$$+ 2176N^2 + 5328N + 2880 \tag{7.89}$$

$$P_{453} = 23N^{10} + 136N^9 - 221N^8 + 388N^7 + 1470N^6 + 2206N^5 + 2192N^4 + 2564N^3$$
$$+ 2082N^2 + 1008N + 216 \tag{7.90}$$

$$P_{454} = 30N^{10} + 150N^9 + 163N^8 - 248N^7 - 562N^6 - 296N^5 + 33N^4 - 30N^3 - 48N^2$$
$$+ 184N + 48 \tag{7.91}$$

$$P_{455} = 7209N^{10} + 36045N^9 - 52924N^8 - 417598N^7 - 794647N^6 - 770095N^5 - 388726N^4$$
$$- 63040N^3 - 576N^2 - 25344N - 12096 \tag{7.92}$$

$$P_{456} = 96020N^{10} + 180403N^9 - 293651N^8 - 563492N^7 + 196513N^6 + 478087N^5$$
$$- 194200N^4 - 207066N^3 - 7470N^2 - 38880N - 12960 \tag{7.93}$$

$$P_{457} = 27N^{11} + 189N^{10} + 631N^9 + 1356N^8 + 2155N^7 + 2207N^6 + 211N^5 - 4984N^4$$
$$- 8400N^3 - 5824N^2 - 2544N - 576 \tag{7.94}$$

$$P_{458} = 50N^{11} + 40N^{10} - 780N^9 - 655N^8 + 4020N^7 + 5924N^6 + 14686N^5 + 37651N^4$$
$$+ 34968N^3 + 14640N^2 + 3936N + 720 \tag{7.95}$$

$$P_{459} = 75N^{11} - 35N^{10} + 624N^9 - 7558N^8 + 12763N^7 + 46561N^6 + 91954N^5 + 198152N^4$$
$$+ 119160N^3 + 5280N^2 - 4256N - 1920 \tag{7.96}$$

$$P_{460} = 76N^{11} + 875N^{10} + 3212N^9 + 4756N^8 + 1408N^7 - 5169N^6 - 12976N^5 - 12806N^4$$
$$+ 112N^3 + 3392N^2 - 1984N - 1632 \tag{7.97}$$

$$P_{461} = 475N^{11} + 330N^{10} - 1215N^9 - 19480N^8 - 26863N^7 + 159682N^6 + 88639N^5$$
$$+ 425740N^4 + 1245588N^3 + 901568N^2 + 296576N + 154560 \tag{7.98}$$

$$P_{462} = 502N^{11} - 1112N^{10} - 4284N^9 + 6519N^8 + 14409N^7 - 12978N^6 - 17866N^5$$
$$- 12913N^4 - 38013N^3 + 7524N^2 - 6588N - 12960 \tag{7.99}$$

$$P_{463} = 502N^{11} - 1112N^{10} - 4248N^9 + 6609N^8 + 13113N^7 - 11466N^6 - 14842N^5$$
$$- 12427N^4 - 51441N^3 + 8028N^2 - 2700N - 7776 \tag{7.100}$$

$$P_{464} = 1936N^{11} + 5826N^{10} - 8779N^9 - 34974N^8 + 5532N^7 + 59112N^6 - 4333N^5$$
$$- 41196N^4 + 21988N^3 + 34344N^2 + 6336N - 4320 \tag{7.101}$$

$$P_{465} = 30N^{12} + 25N^{11} + 120N^{10} - 1204N^9 - 2904N^8 - 8041N^7 - 11950N^6 - 3528N^5$$
$$+ 6536N^4 + 4620N^3 - 520N^2 - 1520N - 480 \tag{7.102}$$

$$P_{466} = 266N^{12} + 983N^{11} - 1576N^{10} - 9928N^9 - 6696N^8 + 7669N^7 - 954N^6 - 5380N^5$$
$$+ 16080N^4 + 10832N^3 - 2656N^2 + 8640N + 6912 \tag{7.103}$$

$$P_{467} = 394N^{12} - 36N^{11} - 4636N^{10} - 2733N^9 + 18141N^8 + 12348N^7 - 27010N^6$$
$$- 32985N^5 - 61373N^4 - 57162N^3 - 18828N^2 - 49032N - 20736 \tag{7.104}$$

$$P_{468} = 855N^{12} + 630N^{11} - 18415N^{10} - 10880N^9 + 121581N^8 + 49518N^7 - 276181N^6$$
$$- 145296N^5 - 95256N^4 - 452548N^3 - 141544N^2 + 70416N + 113760 \tag{7.105}$$

$$P_{469} = 2913N^{12} + 17478N^{11} + 6253N^{10} - 121030N^9 - 399973N^8 - 664606N^7$$
$$- 829641N^6 - 867778N^5 - 563504N^4 - 110240N^3 + 67728N^2 + 45504N + 12096 \tag{7.106}$$

$$P_{470} = 149796N^{12} + 481788N^{11} + 4037555N^{10} + 6431215N^9 - 710852N^8 - 14957774N^7$$
$$- 21164117N^6 - 11167685N^5 + 2360450N^4 + 2452488N^3 - 1225440N^2$$

$$- 518400N + 181440 \tag{7.107}$$

$$P_{471} = 33N^{13} + 264N^{12} + 574N^{11} - 470N^{10} - 2978N^9 - 912N^8 + 8524N^7 + 14408N^6$$
$$+ 9543N^5 + 4750N^4 + 4440N^3 + 3344N^2 + 2544N + 864 \tag{7.108}$$

$$P_{472} = 40N^{13} + 135N^{12} - 370N^{11} - 2695N^{10} - 280N^9 + 16269N^8 + 7142N^7 - 39049N^6$$
$$- 45084N^5 - 65764N^4 - 78472N^3 - 15456N^2 - 6816N - 11520 \tag{7.109}$$

$$P_{473} = 140N^{13} + 75N^{12} - 2625N^{11} - 1865N^{10} + 18485N^9 + 10075N^8 - 71219N^7$$
$$- 146799N^6 - 280833N^5 - 360790N^4 - 178316N^3 - 47896N^2 - 32832N - 11520$$
$$\tag{7.110}$$

$$P_{474} = 140N^{13} + 175N^{12} - 2345N^{11} - 3265N^{10} + 14055N^9 + 15495N^8 - 43291N^7$$
$$- 93731N^6 - 146787N^5 - 140250N^4 - 9164N^3 + 18536N^2 - 15648N - 8640 \tag{7.111}$$

$$P_{475} = 270N^{13} - 2725N^{12} + 3150N^{11} + 19615N^{10} - 62280N^9 - 19653N^8 + 318066N^7$$
$$+ 69493N^6 - 711822N^5 - 691882N^4 + 92904N^3 + 512832N^2 + 364032N + 142560$$
$$\tag{7.112}$$

$$P_{476} = 510N^{13} + 285N^{12} - 7310N^{11} - 8775N^{10} + 41670N^9 + 46959N^8 - 122258N^7$$
$$- 86309N^6 + 330156N^5 + 386896N^4 - 29072N^3 - 232496N^2 - 43776N + 46080$$
$$\tag{7.113}$$

$$P_{477} = 7680N^{13} + 10185N^{12} - 49440N^{11} - 285845N^{10} - 271990N^9 + 2253579N^8$$
$$+ 1796772N^7 - 7046779N^6 - 14683494N^5 - 29740484N^4 - 26073512N^3$$
$$- 3990016N^2 - 8326656N - 5575680 \tag{7.114}$$

$$P_{478} = 51840N^{13} - 27105N^{12} - 652320N^{11} - 373235N^{10} + 3654470N^9 + 3091437N^8$$
$$- 12027204N^7 - 3820797N^6 + 45087798N^5 + 61437668N^4 + 10569064N^3$$
$$- 30448128N^2 + 7229952N + 14100480 \tag{7.115}$$

$$P_{479} = 95N^{14} + 125N^{13} - 1134N^{12} - 2050N^{11} + 6499N^{10} + 26893N^9 + 38472N^8$$
$$- 55832N^7 - 205660N^6 - 56080N^5 + 145792N^4 + 53472N^3 - 6144N^2 - 88448N$$
$$- 42240 \tag{7.116}$$

$$P_{480} = 8868N^{14} + 35472N^{13} - 9409N^{12} - 152862N^{11} + 61883N^{10} + 593774N^9$$
$$- 379547N^8 - 1672874N^7 - 807075N^6 + 89818N^5 - 325576N^4 - 407328N^3$$
$$- 167688N^2 - 21600N + 18144 \tag{7.117}$$

$$P_{481} = 540N^{15} - 6940N^{14} - 6255N^{13} + 92984N^{12} + 99855N^{11} - 389419N^{10} - 647943N^9$$
$$+ 663238N^8 + 1833777N^7 - 126095N^6 - 1116630N^5 + 69928N^4 - 480432N^3$$
$$- 718416N^2 - 1212192N - 570240 \tag{7.118}$$

$$P_{482} = 420N^{16} + 540N^{15} - 8300N^{14} - 15615N^{13} + 49927N^{12} + 148830N^{11} - 80392N^{10}$$
$$- 672719N^9 - 625021N^8 + 156216N^7 + 823430N^6 + 3125340N^5 + 4621504N^4$$
$$+ 2625824N^3 + 429792N^2 + 87744N + 46080 \tag{7.119}$$

$$P_{483} = 685N^{16} + 1370N^{15} - 9010N^{14} - 19290N^{13} + 26146N^{12} + 91966N^{11} - 14748N^{10}$$
$$- 149230N^9 + 45035N^8 + 174316N^7 - 271314N^6 - 505068N^5 - 281130N^4$$
$$- 52080N^3 + 16080N^2 + 17280N + 4320 \tag{7.120}$$

$$P_{484} = 12180N^{16} + 8370N^{15} - 256195N^{14} - 157950N^{13} + 1778081N^{12} + 1177830N^{11}$$
$$- 4307281N^{10} - 3049362N^9 + 3710647N^8 + 11089008N^7 + 11202520N^6$$

$$- 23576760N^5 - 52089008N^4 - 32240448N^3 - 12305664N^2 - 7993728N - 1866240 \tag{7.121}$$

$$\begin{aligned}
P_{485} = {}& 10455N^{18} + 59490N^{17} - 15790N^{16} - 741440N^{15} - 1390120N^{14} + 1428397N^{13} \\
&+ 7150867N^{12} + 5281630N^{11} - 7138741N^{10} - 8816137N^9 + 10256689N^8 \\
&+ 16683860N^7 - 3484864N^6 - 12146200N^5 - 502576N^4 + 5909760N^3 \\
&+ 4302720N^2 + 2851200N + 829440 \tag{7.122}
\end{aligned}$$

$$\begin{aligned}
P_{486} = {}& 40100N^{18} + 99255N^{17} - 727380N^{16} - 3314430N^{15} - 1772040N^{14} + 14821596N^{13} \\
&+ 48888776N^{12} + 98029290N^{11} + 59157432N^{10} - 330544971N^9 - 879181188N^8 \\
&- 779917140N^7 - 105697492N^6 + 173719200N^5 + 551952N^4 - 97381440N^3 \\
&- 68610240N^2 - 34525440N - 8398080 \tag{7.123}
\end{aligned}$$

$$\begin{aligned}
P_{487} = {}& 1213695N^{20} + 7525170N^{19} - 6722900N^{18} - 132732760N^{17} - 180657906N^{16} \\
&+ 706987500N^{15} + 1986194496N^{14} - 505023504N^{13} - 7245869189N^{12} \\
&- 7460329438N^{11} + 6529524348N^{10} + 22209128904N^9 + 18794760144N^8 \\
&- 4187656992N^7 - 23855002304N^6 - 26274133120N^5 - 18561813504N^4 \\
&- 9634314240N^3 - 2690703360N^2 + 136028160N + 199065600 \tag{7.124}
\end{aligned}$$

$$\begin{aligned}
P_{488} = {}& 196275N^{22} + 1397685N^{21} - 1454770N^{20} - 30923820N^{19} - 41291522N^{18} \\
&+ 225466098N^{17} + 630395612N^{16} - 373372336N^{15} - 3171331361N^{14} \\
&- 2650077679N^{13} + 4908510270N^{12} + 10281951044N^{11} + 3751227016N^{10} \\
&- 6343664096N^9 - 8882356992N^8 - 5272720448N^7 + 530329472N^6 \\
&+ 4243436032N^5 + 2879400960N^4 + 137687040N^3 - 705024000N^2 \\
&- 525864960N - 149299200 \,. \tag{7.125}
\end{aligned}$$

As before, we suppress the argument of harmonic sums if it is N. Besides nested harmonic sums up to weight $w = 5$, also binomially weighted sums [262] emerge[1]. After simplifications using the quasi-shuffle relations of the nested sums, cf. Eq. (3.35), only two objects involving binomial coefficients enter the result. They are given by

$$b_1(N) = \binom{2N}{N}\frac{1}{4^N}\left(\sum_{i=1}^{N}\frac{4^i S_1(i-1)}{\binom{2i}{i}i^2} - 7\zeta_3\right), \tag{7.126}$$

$$b_2(N) = \sum_{i=1}^{N}\frac{\binom{2i}{i}\left(\sum_{j=1}^{i}\frac{4^j S_1(j-1)}{\binom{2j}{j}j^2} - 7\zeta_3\right)}{4^i\left(i+1\right)^2}. \tag{7.127}$$

The object $b_1(N)$ was already encountered in the T_F^2 terms in [340], but it also occurs in other colour factors. Obviously, the second binomial object $b_2(N)$ contains $b_1(i)$ in its summand. We note, that in contrast to, for example, the pure-singlet OME, no generalised harmonic sums (without binomial weights) occur in the result.

The expression in Eq. (7.4) is valid for even integers N. The result agrees with the fixed even moments of the constant term calculated in [193, 203]. For odd values of N, the operator matrix element has to vanish identically due to the crossing symmetry of the Compton amplitude $T^{\mu\nu}$ to which the light-cone expansion is applied. In order to verify the agreement at $N = 2$, an expansion around that value has to be performed since the result contains terms proportional

---

[1]See [369–371] for related binomial sums.

to $(N-2)^{-1}$ and $(N-2)^{-2}$. These poles can be shown to cancel: Since $b_1(N)$ occurs in the coefficient of $(N-2)^{-1}$, we also need its derivative with respect to N evaluated at $N=2$, $b_1'(2)$. This requires its analytic continuation, which was worked out in [262, 340]. The sum can be written as a Mellin transformation of an iterated integral over root-valued letters,

$$a(N) = \sum_{i=1}^{N} \frac{4^i S_1(i-1)}{\binom{2i}{i} i^2} \qquad = \int_0^1 dx \frac{x^N - 1}{x-1} \int_x^1 dy \frac{1}{y\sqrt{1-y}} \left[\ln(1-y) - \ln(y) + 2\ln(2)\right] . \tag{7.128}$$

Taking the derivative with respect to N in the integrand at setting $N=2$ afterwards, leads to

$$a'(2) = \int_0^1 dx \frac{x^2 \ln(x)}{x-1} \int_x^1 dy \frac{1}{y\sqrt{1-y}} \left[\ln(1-y) - \ln(y) + 2\ln(2)\right] , \tag{7.129}$$

which can be simplified to

$$a'(2) = -B_4 - \frac{23}{6}\zeta_2 - 14\ln(2)\zeta_3 + \frac{4}{3}\ln(2) + \frac{53}{4}\zeta_4 - \frac{19}{9} \tag{7.130}$$

using the routines of `HarmonicSums`. Writing the binomial coefficient in terms of Γ-functions, we can obtain the required expansion

$$\frac{b_1(N)}{N-2} = \frac{\frac{3}{8}a(2) - \frac{21}{8}\zeta_3}{N-2} + \frac{1}{16}\left([7 - 12\ln(2)]a(2) - [49 - 84\ln(2)]\zeta_3 + 6a'(2)\right) + \mathcal{O}(N-2)$$

$$= \frac{\frac{1}{4} - \frac{21}{8}\zeta_3}{N-2} - \frac{1}{2} - \frac{23}{16}\zeta_2 - \frac{49}{16}\zeta_3 + \frac{159}{32}\zeta_4 - \frac{3}{8}B_4 + \mathcal{O}(N-2) . \tag{7.131}$$

Together with the remaining sums, we can now verify that – after the cancellation of the poles – the expression in Eq. (7.4) agrees with the fixed moment for $N=2$ from [203]. As was already noted in [340], the T_F^2 terms have spurious poles at $N=3/2$ and $N=1/2$, which were shown to cancel. Outside of the T_F^2 colour factor, no such spurious poles arise at half integer values. The analytic continuation of the complete expression Eq. (7.4) to complex values $N \in \mathbb{C}$ still requires clarification of the behaviour at $N=3$ since naively stripping the prefactor $(1 + (-1)^N)/2$ introduces a pole at $N=3$ with non-vanishing residue. We conclude that a nested product-sum representation has been obtained for even integers N, which seems to still need a generalisation to allow for an analytic continuation.

The result for $a_{gg,Q}^{(3)}(N)$ is an important step towards the completion of the gluonic OME $A_{gg,Q}^{(3)}$. All logarithmic terms of the renormalised OME $A_{gg,Q}^{(3)}$ as well as those parts of the constant term which are determined by the renormalisation procedure, are known and were presented in [450]. Together with the constant term $a_{gg,Q}^{(3)}(N)$, the renormalised OME can be assembled. In order to check that the moments grow at most like powers of $\ln(\bar{N}) = \ln(N) + \gamma_E$, the asymptotic expansion of the OME around $N \to \infty$ has to be calculated analytically. The asymptotic expansion of the harmonic sums in known [147, 148, 259] and can be computed automatically with `HarmonicSums`. The expansion of the binomial objects can be obtained from their Mellin representations, see [262].[2] These remaining aspects will be discussed elsewhere.

---

[2]See also [340] for the asymptotic expansion of $b_1(N)$.

8. Remaining Wilson coefficients and OMEs

The heavy flavour Wilson coefficients $L_{q,2}^{\mathrm{NS}}$ and $H_{q,2}^{\mathrm{PS}}$ in the asymptotic limit $Q^2 \gg m^2$ have already been discussed in Section 4.2 and Section 5.2, respectively. There are three additional heavy flavour Wilson coefficients which contribute to the structure function $F_2(x, Q^2)$: $L_{q,2}^{\mathrm{PS}}$, $L_{g,2}^{\mathrm{S}}$ and $H_{g,2}^{\mathrm{S}}$. The former two depend, up to 3-loop order, on the OMEs $A_{qq,Q}^{\mathrm{PS},(3)}$ and $A_{qg,Q}^{(3)}$, which were published in [336]. The explicit 3-loop results for the Wilson coefficients $L_{q,2}^{\mathrm{PS}}$ and $L_{g,2}^{\mathrm{S}}$ were presented in [450]. The Wilson coefficient $H_{g,2}^{\mathrm{S}}$, on the other hand, depends on $A_{Qg}^{(3)}$, which has not been completed to 3-loop order for general values of N as of now.

To give a more complete picture of the heavy flavour contributions to $F_2(x, Q^2)$, we discuss the relative impact of the individual Wilson coefficients in this chapter. For $L_{q,2}^{\mathrm{PS}}$ and $L_{g,2}^{\mathrm{S}}$ we present numerical illustrations based on the x space representations given in [450]. The overall comparison of the five Wilson coefficients is based on the known fixed moments [203]. Moreover, we compare the contributions of the OMEs to the matching relations in the variable flavour number scheme based on the same moments. The discussions of this chapter are also published in [450].

For the following illustrations, we choose $\mu^2 = Q^2$ and we consider the case of a massive charm quark and three massless quarks ($N_F = 3$). The charm quark mass $m_c = 1.59\,\mathrm{GeV}$ [226] refers to the OMS scheme. We use the NNLO PDFs and strong coupling constant from [218] which are available through the library `LHAPDF` [422]. The HPLs are evaluated using the code presented in [423] and for the terms given by the massless 3-loop Wilson coefficients we use the parametrisation given in [138]. As before, we use the NNLO PDFs and strong coupling constant also for the 2-loop term to facilitate assessing the impact from the Wilson coefficients.

The pure-singlet Wilson coefficient $L_{q,2}^{\mathrm{PS}}$, where the photon couples to a light quark, starts at $\mathcal{O}\left(a_s^3\right)$. Its contribution to the structure function $F_2(x, Q^2)$ is illustrated in Fig. 8.1.

Figures 8.2 and 8.3 demonstrate the contribution from the Wilson coefficient $L_{g,2}^{\mathrm{S}}$ to $F_2(x, Q^2)$ at 2-loop order and up to 3-loop order, respectively. By comparing Fig. 8.1 to Fig. 8.3 we see that the contribution from $L_{g,2}^{\mathrm{S}}$ is larger by about a factor 2 to 3 in the small x region than the contribution from $L_{q,2}^{\mathrm{PS}}$. This is mainly due to the stronger rise of the gluon PDF compared to the singlet PDF combination. Moreover, we note that, in the small x limit, the 3-loop contribution far exceeds the 2-loop contribution of $L_{g,2}^{\mathrm{S}}$, despite the suppression by another power of the coupling constant a_s. This can be understood from the fact that the 3-loop term has terms proportional to $1/x$ while such terms are missing in the 2-loop term: In order to contribute to $L_{g,2}^{\mathrm{S}}$, the scattering must be initiated by a gluon, have a virtual heavy quark in one of the loops and the photon must couple to a light quark. At 2-loop order, these requirements prevent the exchange of gluons in the t-channel, which would give rise to an $1/x$ behaviour.

The moments for the 3-loop OMEs completed in 2009 in [203] allow us to compare the relative size of the impact from the different Wilson coefficients on the structure function $x^{-1} F_2^{\mathrm{h}}(x, Q^2)$. We split up the heavy flavour contribution to the structure function according to the individual terms in Eq. (2.90) and normalise it to the moments of $x^{-1} F_2^{\mathrm{h}}(x, Q^2)$. For the discussion, we treat each perturbative order in a_s independently. We introduce abbreviations for the Mellin moments of the normalisation

$$F(N) = \mathrm{M}\left[x^{-1} F_2^{\mathrm{h}}(x, Q^2)\right](N) = \int_0^1 \mathrm{d}x \; x^{N-2} F_2^{\mathrm{h}}(x, Q^2) = \mathrm{M}\left[F_2^{\mathrm{h}}(x, Q^2)\right](N-1) \qquad (8.1)$$
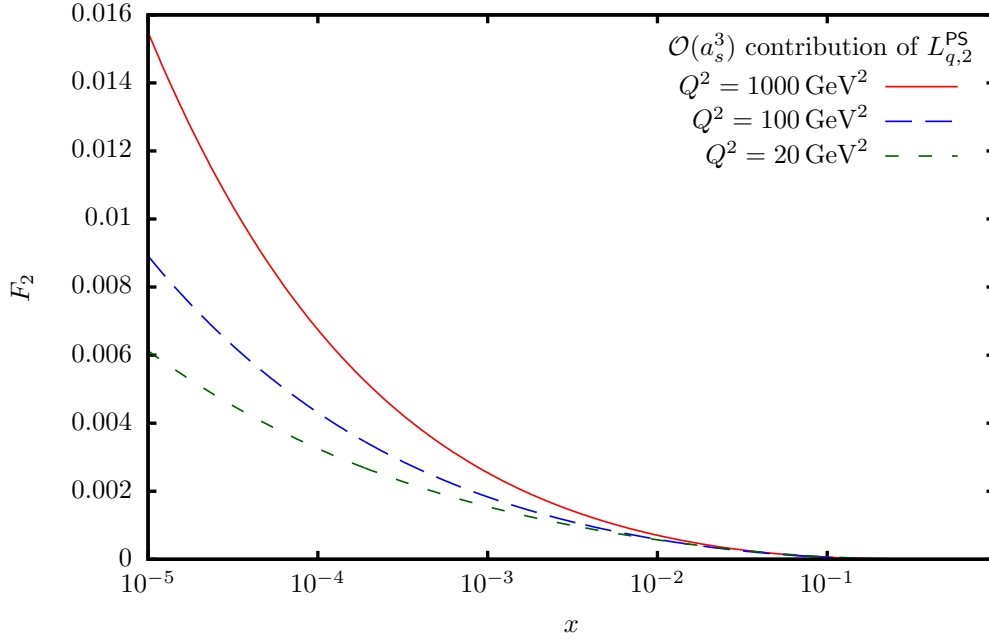
Figure 8.1.: Charm contribution from $L_{q,2}^{\mathrm{PS}}$ to the structure function $F_2(x, Q^2)$. We treat the charm quark mass in the OMS scheme and use $m_c = 1.59\,\mathrm{GeV}$ [226]. We use the NNLO PDFs and strong coupling constant from [218].
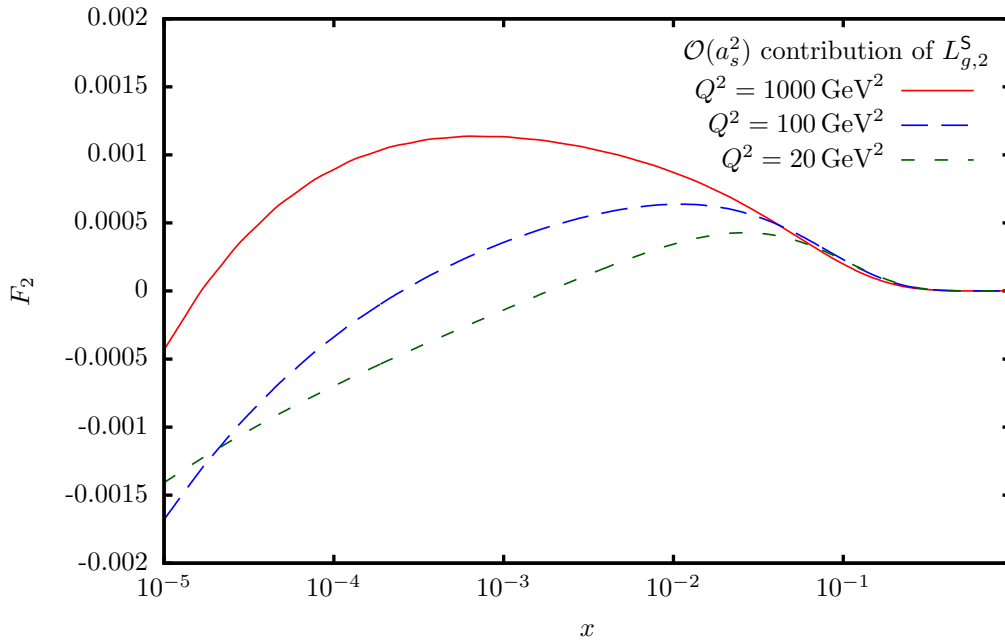

Figure 8.2.: Charm contribution from $L_{g,2}^{\mathrm{S}}$ to the structure function $F_2(x, Q^2)$ at 2-loop order. The charm quark, PDFs and strong coupling constant are treated as in Fig. 8.1.
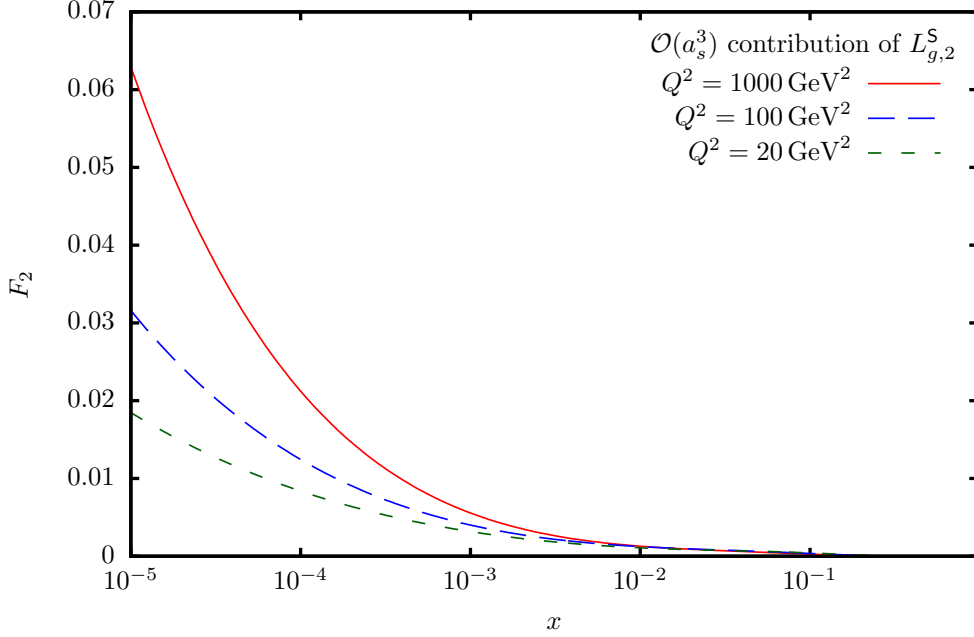
Figure 8.3.: Charm contribution from $L_{g,2}^{\mathrm{S}}$ to the structure function $F_2(x, Q^2)$ up to and including 3-loop corrections. The charm quark, PDFs and strong coupling constant are treated as in Fig. 8.1.

and for the normalised Mellin moments of the individual contributions from the Wilson coefficients

$$F[L_{q,2}^{\mathrm{PS}}](N) = \frac{\frac{1}{N_F}\sum_{k=1}^{N_F} e_k^2 L_{q,2}^{\mathrm{PS}}(N)\Sigma(N)}{F(N)} \tag{8.2}$$

$$F[L_{g,2}^{\mathrm{S}}](N) = \frac{\frac{1}{N_F}\sum_{k=1}^{N_F} e_k^2 L_{g,2}^{\mathrm{S}}(N)G(N)}{F(N)} \tag{8.3}$$

$$F[L_{q,2}^{\mathrm{NS}}](N) = \frac{\sum_{k=1}^{N_F} e_k^2 L_{q,2}^{\mathrm{NS}}(N)\left[f_k(N) + \bar{f}_k(N)\right]}{F(N)} \tag{8.4}$$

$$F[H_{q,2}^{\mathrm{PS}}](N) = \frac{e_Q^2 H_{q,2}^{\mathrm{PS}}(N)\Sigma(N)}{F(N)} \tag{8.5}$$

$$F[H_{g,2}^{\mathrm{S}}](N) = \frac{e_Q^2 H_{g,2}^{\mathrm{S}}(N)G(N)}{F(N)} \, , \tag{8.6}$$

where e_k is the electric charge of the kth quark flavour and e_Q is the charge of the heavy quark flavour. The Mellin moments of the quark and anti-quark number density PDFs are denoted $f_k(N)$ and $\bar{f}_k(N)$, respectively, and we write $\Sigma(N)$ for the moments of the singlet PDF combination and $G(N)$ for the gluon PDF.

For the numerical comparison, we assume $N_F = 3$ light quarks and set $e_Q = 2/3$. The strong coupling constant $a_s(\mu^2)$ and the moments of the PDFs are computed from the NNLO analysis in [218] which are available through the LHAPDF library. The charm quark mass is $m_c = 1.59\,\mathrm{GeV}$ in the OMS scheme [226]. We choose the renormalisation and factorisation scale $\mu^2 = Q^2$. The logarithmic terms of the Wilson coefficients have been published in [358] for the non-singlet Wilson coefficient and in [450] for the others. The moments of the massless Wilson coefficients are taken from [132, 133] and those of the constant part of the OMEs from [203].

Table 8.1.: Moments of the contributions to the structure function $x^{-1}F_2^{\mathrm{h}}(x,Q^2)$.

N	2	4	6	8	10
			$Q^2 = 20\,\mathrm{GeV}^2$		
$\mathcal{O}(a_s)$	$2.78 \cdot 10^{-3}$	$5.93 \cdot 10^{-7}$	$-3.05 \cdot 10^{-7}$	$-5.47 \cdot 10^{-8}$	$-1.26 \cdot 10^{-8}$
$\mathcal{O}(a_s^2)$	$7.37 \cdot 10^{-4}$	$-5.60 \cdot 10^{-5}$	$-1.98 \cdot 10^{-5}$	$-8.17 \cdot 10^{-6}$	$-3.89 \cdot 10^{-6}$
$\mathcal{O}(a_s^3)$	$5.79 \cdot 10^{-4}$	$-3.49 \cdot 10^{-5}$	$-1.58 \cdot 10^{-5}$	$-7.51 \cdot 10^{-6}$	$-3.97 \cdot 10^{-6}$
			$Q^2 = 100\,\mathrm{GeV}^2$		
$\mathcal{O}(a_s)$	$5.19 \cdot 10^{-3}$	$1.29 \cdot 10^{-5}$	$3.47 \cdot 10^{-7}$	$2.22 \cdot 10^{-8}$	$1.79 \cdot 10^{-9}$
$\mathcal{O}(a_s^2)$	$1.20 \cdot 10^{-3}$	$-4.31 \cdot 10^{-5}$	$-1.44 \cdot 10^{-5}$	$-5.53 \cdot 10^{-6}$	$-2.50 \cdot 10^{-6}$
$\mathcal{O}(a_s^3)$	$5.71 \cdot 10^{-4}$	$-2.66 \cdot 10^{-5}$	$-1.01 \cdot 10^{-5}$	$-4.29 \cdot 10^{-6}$	$-2.11 \cdot 10^{-6}$
			$Q^2 = 1000\,\mathrm{GeV}^2$		
$\mathcal{O}(a_s)$	$7.58 \cdot 10^{-3}$	$2.02 \cdot 10^{-5}$	$7.66 \cdot 10^{-7}$	$7.93 \cdot 10^{-8}$	$1.41 \cdot 10^{-8}$
$\mathcal{O}(a_s^2)$	$1.47 \cdot 10^{-3}$	$-4.65 \cdot 10^{-5}$	$-1.38 \cdot 10^{-5}$	$-4.88 \cdot 10^{-6}$	$-2.07 \cdot 10^{-6}$
$\mathcal{O}(a_s^3)$	$5.54 \cdot 10^{-4}$	$-2.92 \cdot 10^{-5}$	$-9.01 \cdot 10^{-6}$	$-3.39 \cdot 10^{-6}$	$-1.52 \cdot 10^{-6}$

In Table 8.1 we collect the moments of $x^{-1}F_2^{\mathrm{h}}(x,Q^2)$ to which we normalise. The normalised moments of the contributions from the individual Wilson coefficients are presented in Table 8.2. For the interpretation, we have to recall that the integral kernel of the Mellin transformation x^{N-1} places more and more weight on values close to $x = 1$ when we go to higher moments N. The gluon PDF is rather small close to $x = 1$ so that its higher moments are small compared to those of the singlet or non-singlet PDF combinations. As a consequence, the moments $F(N)$ (Table 8.1) decrease faster at $\mathcal{O}(a_s)$ than at higher orders since only the gluonic Wilson coefficient $H_{g,2}^{\mathrm{S}}$ contributes at lowest order. At higher orders, also singlet and in particular non-singlet Wilson coefficients yield a substantial contribution. The moment $F(10)$, for example, increases by two to three orders of magnitude when going from $\mathcal{O}(a_s)$ to $\mathcal{O}(a_s^2)$. Moreover, we note that the moments at $\mathcal{O}(a_s^2)$ and $\mathcal{O}(a_s^3)$ are negative, except for $N = 2$. This can be understood by looking at the contributions from the individual Wilson coefficients, as collected in Table 8.2.

For the second moment, the gluonic Wilson coefficient $H_{g,2}^{\mathrm{S}}$ yields the largest contribution for all values of Q^2 and at all orders of a_s considered here. The singlet and non-singlet Wilson coefficients, $H_{q,2}^{\mathrm{PS}}$ and $L_{q,2}^{\mathrm{NS}}$, contribute with the opposite sign, and the magnitude of their second moments is roughly a third to a quarter of the gluonic Wilson coefficient. The remaining two Wilson coefficients, $L_{g,2}^{\mathrm{S}}$ and $L_{q,2}^{\mathrm{PS}}$, give only minor contributions of a few percent. Starting with the fourth moment, the non-singlet term dominates the structure function. Since the Wilson coefficient is negative for all x, see Fig. 4.4, all its moments are negative as well. This explains the change of sign of $F(N)$ for $N \geq 4$. The reason for the relative size of the non-singlet contribution is twofold: As mentioned above, the moments of the non-singlet PDF outgrow the moments of the gluon PDF, which contributes to the suppression of the gluonic term. Moreover, the non-singlet Wilson coefficient contains plus distributions. These give rise to an asymptotic growth of the moments proportional to powers of $\ln(\bar{N}) = \ln(N) + \gamma_{\mathrm{E}}$, while the other Wilson coefficients have at most a constant asymptotic behaviour. Given these observations, we have to keep in mind, however, that even though the entirety of the integer moments determines also the small x behaviour through the pole structure of its analytic continuation, it is usually impossible to determine from just a few fixed moments. However, given a large but finite number of moments, the complete expression can be guessed from the moments [149].

Since the OMEs also enter the matching relations of the variable flavour number scheme, we can try to assess their impact using the available fixed moments. The matching relation for the PDF

Table 8.2.: Moments of the contributions to the structure function $F_2^{\mathrm{h}}(N, Q^2)$ from individual Wilson coefficients, normalised to their sum. The perturbative orders in a_s are considered separately.

N		2	4	6	8	10
		$Q^2 = 20\,\mathrm{GeV}^2$				
$\mathcal{O}(a_s^2)$	$F[L_{g,2}^{\mathrm{S}}](N)$	0.0688	−0.0129	−0.002 13	−0.000 632	−0.000 259
	$F[L_{q,2}^{\mathrm{NS}}](N)$	−0.384	1.08	1.01	1.00	1.00
	$F[H_{q,2}^{\mathrm{PS}}](N)$	−0.459	0.0289	−0.002 50	−0.003 94	−0.003 22
	$F[H_{g,2}^{\mathrm{S}}](N)$	1.77	−0.0957	−0.001 25	0.002 44	0.001 87
$\mathcal{O}(a_s^3)$	$F[L_{q,2}^{\mathrm{PS}}](N)$	0.0594	−0.0143	−0.005 18	−0.003 24	−0.002 37
	$F[L_{g,2}^{\mathrm{S}}](N)$	0.113	−0.0271	−0.004 59	−0.001 41	−0.000 593
	$F[L_{q,2}^{\mathrm{NS}}](N)$	−0.222	1.13	1.02	1.01	1.01
	$F[H_{q,2}^{\mathrm{PS}}](N)$	−0.306	0.0475	−0.002 35	−0.005 26	−0.004 57
	$F[H_{g,2}^{\mathrm{S}}](N)$	1.36	−0.137	−0.006 92	0.000 563	0.000 996
		$Q^2 = 100\,\mathrm{GeV}^2$				
$\mathcal{O}(a_s^2)$	$F[L_{g,2}^{\mathrm{S}}](N)$	0.0506	−0.0165	−0.003 01	−0.001 06	−0.000 505
	$F[L_{q,2}^{\mathrm{NS}}](N)$	−0.261	1.17	1.02	1.00	1.00
	$F[H_{q,2}^{\mathrm{PS}}](N)$	−0.402	0.0900	0.0153	0.004 35	0.001 41
	$F[H_{g,2}^{\mathrm{S}}](N)$	1.61	−0.240	−0.0281	−0.006 66	−0.002 09
$\mathcal{O}(a_s^3)$	$F[L_{q,2}^{\mathrm{PS}}](N)$	0.0559	−0.009 51	−0.003 17	−0.002 05	−0.001 57
	$F[L_{g,2}^{\mathrm{S}}](N)$	0.0879	−0.0215	−0.004 56	−0.001 73	−0.000 863
	$F[L_{q,2}^{\mathrm{NS}}](N)$	−0.287	1.15	1.02	1.01	1.00
	$F[H_{q,2}^{\mathrm{PS}}](N)$	−0.504	0.130	0.0223	0.005 90	0.001 52
	$F[H_{g,2}^{\mathrm{S}}](N)$	1.65	−0.251	−0.0315	−0.007 90	−0.002 70
		$Q^2 = 1000\,\mathrm{GeV}^2$				
$\mathcal{O}(a_s^2)$	$F[L_{g,2}^{\mathrm{S}}](N)$	0.0429	−0.0128	−0.002 64	−0.001 04	−0.000 540
	$F[L_{q,2}^{\mathrm{NS}}](N)$	−0.304	1.19	1.02	1.01	1.00
	$F[H_{q,2}^{\mathrm{PS}}](N)$	−0.499	0.124	0.0283	0.0113	0.005 68
	$F[H_{g,2}^{\mathrm{S}}](N)$	1.76	−0.304	−0.0497	−0.0169	−0.007 85
$\mathcal{O}(a_s^3)$	$F[L_{q,2}^{\mathrm{PS}}](N)$	0.0666	−0.006 03	−0.001 55	−0.000 921	−0.000 714
	$F[L_{g,2}^{\mathrm{S}}](N)$	0.0720	−0.0113	−0.003 11	−0.001 39	−0.000 782
	$F[L_{q,2}^{\mathrm{NS}}](N)$	−0.458	1.14	1.01	1.00	1.00
	$F[H_{q,2}^{\mathrm{PS}}](N)$	−0.815	0.170	0.0419	0.0169	0.008 34
	$F[H_{g,2}^{\mathrm{S}}](N)$	2.13	−0.289	−0.0521	−0.0182	−0.008 62

Table 8.3.: Ratio of the moments of the PDFs Σ/G for different values of the scale μ^2.

N	2	4	6	8	10
$\mu^2 = 20\,\text{GeV}^2$	1.18	8.00	25.8	58.0	103
$\mu^2 = 100\,\text{GeV}^2$	1.07	7.75	22.8	44.7	69.9
$\mu^2 = 1000\,\text{GeV}^2$	0.982	7.59	21.0	38.2	56.9

combination $f_k + \bar{f}_k$ was already discussed in detail in Section 4.5, so we restrict the discussion here to the remaining matching relations. We define the following ratios of moments in analogy to the combinations of OMEs and PDFs which occur in the matching relations Eqs. (2.112) to (2.114):

$$R(A_{gg,Q}, A_{Qg}) = \frac{A_{gg,Q}\,G}{A_{Qg}\,G}\,, \qquad\qquad R(A_{Qq}^{\text{PS}}, A_{Qg}) = \frac{A_{Qq}^{\text{PS}}\,\Sigma}{A_{Qg}\,G}\,, \qquad (8.7)$$

$$R(A_{qq,Q}^{\text{NS}}, A_{Qg}) = \frac{A_{qq,Q}^{\text{PS}}\,\Sigma}{A_{Qg}\,G}\,, \qquad\qquad R(A_{gq,Q}, A_{Qg}) = \frac{A_{gq,Q}\,\Sigma}{A_{Qg}\,G}\,, \qquad (8.8)$$

$$R(A_{qg,Q}, A_{Qg}) = \frac{A_{qg,Q}\,G}{A_{Qg}\,G}\,, \qquad\qquad R(A_{qq,Q}^{\text{PS}}, A_{Qg}) = \frac{A_{qq,Q}^{\text{PS}}\,\Sigma}{A_{Qg}\,G}\,. \qquad (8.9)$$

Table 8.4 lists numerical values for these ratios at different perturbative orders and for different scales μ^2. For reference we also give the ratio of just the singlet PDF combination to the gluon PDF Σ/G in Table 8.3. The same comments as for the Wilson coefficients apply for the interpretation of these ratios: Higher moments probe regions closer to $x = 1$ and the ratios of higher moments indicate the relative importance of the individual terms in the large x region. Due to the shape of the PDFs the ratio Σ/G increases for larger N. This enhances contributions which are proportional to the singlet PDF compared to the gluon contributions. We note that the relative importance of the OMEs is roughly stable across different perturbative orders and scale choices. Therefore, we will discuss the impact of the individual terms cumulatively for the scales and orders.

Only the OMEs A_{Qq}^{PS} and A_{Qg} contribute to the matching relation for $f_Q + f_{\bar{Q}}$, cf. Eq. (2.112). Their relative importance can be seen directly from the ratio $R(A_{Qq}^{\text{PS}}, A_{Qg})$. For the second moment, the magnitude of the pure-singlet contribution ranges from approximately 12% to 37% of that from A_{Qg}. However, its relative importance grows to up to about twice the size of the contribution from A_{Qg} for $N = 10$. The two contributions have opposite signs for all moments. One has to keep in mind though, that A_{Qg} already starts at $\mathcal{O}(a_s)$ while the pure-singlet OME only starts at $\mathcal{O}(a_s^2)$. Therefore, the overall PDF combination $f_Q + f_{\bar{Q}}$ is still dominated by the leading-order A_{Qg} contribution.

The matching relation of the gluon density, Eq. (2.113), receives contributions from the OMEs $A_{gg,Q}$, weighted by the gluon PDF, and by $A_{gq,Q}$, weighted by the singlet PDF. The latter OME starts at $\mathcal{O}(a_s^2)$ and has the opposite sign compared to the gluonic contribution, which starts at $\mathcal{O}(a_s)$. For the lowest moment $N = 2$ the gluonic contribution dominates at each order and the $A_{gq,Q}$ term has approximately 14% to 59% the size of the $A_{gg,Q}$ term. The ratio of the PDF moments enhances the singlet term towards higher moments, such that the singlet term is larger than the gluonic term by a factor 1.5 to 5.5 for $N = 10$, especially for low scales.

The singlet PDF for $N_F + 1$ massless quarks at the matching scale arises from the singlet PDF for N_F massless quarks, weighted by the OMEs $A_{qq,Q}^{\text{NS}}$, $A_{qq,Q}^{\text{PS}}$ and A_{Qq}^{PS} as well as the gluon PDF for N_F massless quarks, weighted by A_{Qg} and $A_{gg,Q}$, cf. Eq. (2.114). The size of the A_{Qq}^{PS}

Table 8.4.: Moments of the OMEs, weighted by the PDFs as they appear in the VFNS matching relations for $Q + \bar{Q}$, G and Σ and normalised to the contribution of A_{Qg}. The perturbative orders in a_s are considered separately.

N		2	4	6	8	10
		$\mu^2 = 20\,\mathrm{GeV}^2$				
$\mathcal{O}(a_s)$	$R(A_{gg,Q}, A_{Qg})$	-1.00	-1.82	-2.55	-3.24	-3.93
$\mathcal{O}(a_s^2)$	$R(A_{gg,Q}, A_{Qg})$	-1.00	-1.64	-2.38	-3.18	-4.03
	$R(A_{Qq}^{\mathrm{PS}}, A_{Qg})$	-0.126	-0.366	-0.782	-1.33	-1.94
	$R(A_{qq,Q}^{\mathrm{NS}}, A_{Qg})$	-0.0584	-1.13	-6.32	-20.7	-49.5
	$R(A_{gq,Q}, A_{Qg})$	0.184	1.14	4.00	9.81	19.0
$\mathcal{O}(a_s^3)$	$R(A_{gg,Q}, A_{Qg})$	-1.01	-1.34	-1.85	-2.43	-3.09
	$R(A_{Qq}^{\mathrm{PS}}, A_{Qg})$	-0.160	-0.484	-0.963	-1.54	-2.13
	$R(A_{qq,Q}^{\mathrm{NS}}, A_{Qg})$	-0.0404	-0.583	-2.94	-9.18	-21.4
	$R(A_{gq,Q}, A_{Qg})$	0.147	1.13	3.80	8.99	17.0
	$R(A_{gg,Q}, A_{Qg})$	$0.005\,13$	-0.0202	-0.0326	-0.0445	-0.0567
	$R(A_{qq,Q}^{\mathrm{PS}}, A_{Qg})$	0.0534	0.109	0.246	0.468	0.762
		$\mu^2 = 100\,\mathrm{GeV}^2$				
$\mathcal{O}(a_s)$	$R(A_{gg,Q}, A_{Qg})$	-1.00	-1.82	-2.55	-3.24	-3.93
$\mathcal{O}(a_s^2)$	$R(A_{gg,Q}, A_{Qg})$	-1.00	-1.77	-2.64	-3.58	-4.58
	$R(A_{Qq}^{\mathrm{PS}}, A_{Qg})$	-0.188	-0.425	-0.763	-1.09	-1.35
	$R(A_{qq,Q}^{\mathrm{NS}}, A_{Qg})$	-0.125	-2.44	-12.4	-35.5	-74.5
	$R(A_{gq,Q}, A_{Qg})$	0.313	1.39	3.91	7.77	12.6
$\mathcal{O}(a_s^3)$	$R(A_{gg,Q}, A_{Qg})$	-1.00	-1.61	-2.32	-3.07	-3.87
	$R(A_{Qq}^{\mathrm{PS}}, A_{Qg})$	-0.280	-0.581	-0.947	-1.25	-1.46
	$R(A_{qq,Q}^{\mathrm{NS}}, A_{Qg})$	-0.177	-2.87	-13.7	-37.9	-77.9
	$R(A_{gq,Q}, A_{Qg})$	0.392	1.41	3.41	6.05	8.93
	$R(A_{gg,Q}, A_{Qg})$	$0.004\,76$	-0.0375	-0.0491	-0.0580	-0.0657
	$R(A_{qq,Q}^{\mathrm{PS}}, A_{Qg})$	0.0646	0.0984	0.173	0.255	0.332
		$\mu^2 = 1000\,\mathrm{GeV}^2$				
$\mathcal{O}(a_s)$	$R(A_{gg,Q}, A_{Qg})$	-1.00	-1.82	-2.55	-3.24	-3.93
$\mathcal{O}(a_s^2)$	$R(A_{gg,Q}, A_{Qg})$	-1.00	-2.01	-3.02	-4.06	-5.14
	$R(A_{Qq}^{\mathrm{PS}}, A_{Qg})$	-0.255	-0.452	-0.700	-0.885	-1.01
	$R(A_{qq,Q}^{\mathrm{NS}}, A_{Qg})$	-0.205	-3.71	-17.0	-44.0	-85.9
	$R(A_{gq,Q}, A_{Qg})$	0.460	1.54	3.58	6.13	8.89
$\mathcal{O}(a_s^3)$	$R(A_{gg,Q}, A_{Qg})$	-1.01	-1.75	-2.50	-3.26	-4.03
	$R(A_{Qq}^{\mathrm{PS}}, A_{Qg})$	-0.373	-0.628	-0.907	-1.09	-1.19
	$R(A_{qq,Q}^{\mathrm{NS}}, A_{Qg})$	-0.293	-4.16	-17.5	-43.4	-82.1
	$R(A_{gq,Q}, A_{Qg})$	0.593	1.51	2.97	4.51	5.94
	$R(A_{gg,Q}, A_{Qg})$	$0.005\,42$	-0.0469	-0.0561	-0.0624	-0.0675
	$R(A_{qq,Q}^{\mathrm{PS}}, A_{Qg})$	0.0726	0.0901	0.134	0.172	0.201

term was already discussed in the context of the $f_Q + f_{\bar{Q}}$ matching relation above. The second moment receives its main contribution from A_{Qg}, followed by A_{Qq}^{PS} and $A_{qq,Q}^{\text{NS}}$. Towards higher moments, the ratio of the PDF moments again changes the relative importance of the terms. Additionally, the asymptotic behaviour of the non-singlet OME leads to a significant growth this term: Its relative size compared to the A_{Qg} term increases from 5% to 29% for $N = 2$ to up to 86 times the size of A_{Qg} for $N = 10$. This even lets the non-singlet term dominate the moment $N = 10$ if we take the suppression by a_s into account.

9. Conclusions

Deep-inelastic scattering experiments have a long history in establishing and testing QCD and allow us to extract important parameters of the Standard Model like the strong coupling constant a_s, the heavy quark masses m_c and m_b and the PDFs. Due to the precision of the current world data, modern analyses have to include theoretical predictions at least up to NNLO. At this level, a complete description of heavy quark contributions is still missing. Therefore, a long-term project was started in order to extend the description of the heavy quark contributions to NNLO. It relies on the factorisation of the heavy flavour Wilson coefficients into massless Wilson coefficients and massive operator matrix elements in the asymptotic region $Q^2 \gg m^2$ [201, 203], which is most relevant for experiments like HERA in the case of the structure function $F_2(x, Q^2)$. After the extension of the renormalisation procedure to $\mathcal{O}(a_s^3)$ and the calculation of a series of fixed Mellin moments up to $N = 10(14)$ in [193, 203, 302], the main focus of the project has shifted to the calculation of the massive OMEs for general values of N. This thesis constitutes a part of this effort and a number of steps towards the goal of the project have been accomplished here.

We obtain the non-singlet OME $A_{qq,Q}^{\mathrm{NS},(3)}$ in Chapter 4 for general values of N and confirm the N_F dependent part of the 3-loop non-singlet anomalous dimension $\gamma_{qq}^{\mathrm{NS},(2)}$. The calculation is performed by reducing the arising Feynman integrals to master integrals via integration-by-parts relations and calculating the master integrals using hypergeometric function techniques and Mellin-Barnes representations in combination with the summation algorithms and special function tools implemented in `Sigma` [241, 252, 253], `HarmonicSums` [258–263], `EvaluateMultiSums` and `SumProduction` [254–257]. In a similar calculation, we also obtain the result for the non-singlet OME for transversity $A_{qq,Q}^{\mathrm{NS,TR},(3)}$ and compute the anomalous dimension for transversity. Due to a Ward-Takahashi identity of the non-singlet Green's function, the renormalisation of the axial charge becomes trivial in this case and we are provided with even and odd moments for the non-singlet OME. The even moments correspond to the case of a vector coupling and the odd moments to the case of an axial-vector coupling. We combine the result for the even moments of the OME with the known unpolarised massless Wilson coefficient [138] to obtain the asymptotic heavy flavour Wilson coefficient $L_{q,2}^{\mathrm{NS}}$ for the unpolarised structure function $F_2(x, Q^2)$. This result allows us to give first illustrations of the impact of the non-singlet Wilson coefficient on the structure function $F_2(x, Q^2)$. The odd moments of $A_{qq,Q}^{\mathrm{NS},(3)}$ constitute the OME for the non-singlet operator with an axial-vector coupling, which enters the non-singlet Wilson coefficient for the polarised structure function $g_1(x, Q^2)$. Here we also illustrate the influence on the structure function and also give the twist-2 contribution to $g_2(x, Q^2)$ which is related to $g_1(x, Q^2)$ via the Wandzura-Wilczek relation. Moreover, we discuss the heavy flavour contributions to the polarised Bjorken sum rule. Since the first moment of the non-singlet OME vanishes, the only effect of the heavy quark is to increase the number of active quarks N_F by one in the massless contributions. Furthermore, we also apply the odd moments for the non-singlet OME to the charged current structure function $xF_3(x, Q^2)$. While the results for $L_{q,3}^{\mathrm{NS}}$ are structurally identical to the polarised case, up to terms proportional to the colour factor $d^{abc}d^{abc}$, there is a second non-singlet Wilson coefficient, $H_{q,3}^{\mathrm{NS}}$, which arises due to flavour excitation processes. Again, we illustrate the impact on the structure functions and discuss heavy flavour effects in the Gross-Llewellyn-Smith sum rule. Together with the OMEs $A_{qq,Q}^{\mathrm{PS},(3)}$ and $A_{qg,Q}^{(3)}$, which were

9. Conclusions

calculated in [336], the non-singlet OME completes the first matching relation of the variable flavour number scheme [202, 203]. It allows to express the PDF combinations $f_k + f_{\bar{k}}$ in the scheme with $N_F + 1$ flavours in terms of PDFs in the N_F flavour scheme. The overall effect of this scheme change is of the order of 0.5%. Since the OMEs $A_{qq,Q}^{\mathrm{PS},(3)}$ and $A_{qg,Q}^{(3)}$ start only at 3-loop order, the singlet and gluon PDFs begin to mix into the $f_k + f_{\bar{k}}$ combination at this order. Therefore, going from 2-loop to 3-loop order in this matching relation, changes the shape of the small x behaviour.

In Chapter 5, we calculate the pure-singlet OME $A_{Qq}^{\mathrm{PS},(3)}$. As a by-product, we obtain the pure-singlet anomalous dimension $\gamma_{qq}^{\mathrm{PS},(2)}$ in a first independent complete recalculation since it was computed in [136] in massless DIS. In addition to the techniques used for the non-singlet OME, we also employ differential equations to calculate some of the master integrals. Beyond nested harmonic sums and harmonic polylogarithms, which were sufficient to express the previous results of this project, here also generalised harmonic sums and HPLs with non-standard argument occur. Using the result for the pure-singlet OME and the corresponding massless Wilson coefficient [138], we complete the heavy flavour Wilson coefficient $H_{q,2}^{\mathrm{PS}}$. Our illustrations of the pure-singlet Wilson coefficients show that their largest contribution is expected in the region of small x, where one, however, has to keep in mind the kinematic restrictions of DIS experiments.

The calculation of a set of Feynman diagrams with ladder- and V-topologies, which we present in Chapter 6, is an important step for the calculation of the remaining OMEs. These diagrams contribute to $A_{Qg}^{(3)}$ and are examples for an important class of diagrams. Their calculation is possible due to a refinement of the computer algebra tools and the systematic use of differential and difference equations to calculate the large number of master integrals which are required. The differential equations, which are derived from the IBP relations, are written as difference equations via a formal power series ansatz and then decoupled into a scalar recurrence using the uncoupling algorithms [382] implemented in `OreSys` [383]. The scalar recurrences can be solved with `Sigma` and related packages and the results are simplified using `HarmonicSums`. One diagram with a V-topology turns out to be especially complicated due to its relation to non-planar diagrams induced by the operator insertion. Its solution requires also binomially weighted iterated sums, which give rise to new constants in its asymptotic expansion. Using the same methods, a large share of the diagrams which contribute to $A_{Qg}^{(3)}$ are computed as well. The remaining diagrams depend on master integrals which require more advanced methods and point towards non-iterative integrals.

The gluonic OME $A_{gg,Q}^{(3)}$ enters the matching relation of the gluon PDF in the VFNS. In Chapter 7, we discuss the calculation of the $\mathcal{O}(\varepsilon^0)$ term of the unrenormalised OME, $a_{gg,Q}^{(3)}$. We greatly benefit from the techniques and master integrals discussed for the ladder- and V-diagrams. As previously observed in [340] for diagrams with two massive fermion lines, binomial sums occur in the results. After simplifying the sums using quasi-shuffle relations only two objects involving binomial sums remain. The result agrees with the fixed moments calculated in [193, 203] and is valid for even integers N. Building on this intermediate result, the OME $A_{gg,Q}^{(3)}$ will be completed in a future publication.

Of the five heavy flavour Wilson coefficients that contribute to $F_2(x, Q^2)$, the non-singlet and pure-singlet coefficients have been discussed in connection with the respective OMEs. Two more Wilson coefficients, $L_{q,2}^{\mathrm{PS}}$ and $L_{g,2}^{\mathrm{S}}$, were completed in [450] based on the OMEs calculated in [336]. We give numerical illustrations of those two Wilson coefficients in Chapter 8 and compare the relative size of all Wilson coefficients based on the fixed moments from [193, 203]. Moreover, we use the fixed moments to compare the importance of the individual OMEs in the matching relations of the VFNS. The comparison underlines the importance of completing the two remaining OMEs $A_{gg,Q}^{(3)}$ and $A_{Qg}^{(3)}$ in order to fully assess the size of the $\mathcal{O}(a_s^3)$ heavy flavour corrections to deep-inelastic scattering.

The calculations performed in the present project demonstrate the strong need to extend the mathematical and computer-algebraic technologies for single mass, 3-loop problems, compared to various previous massless calculations. We encounter generalised harmonic and cyclotomic sums and finite sums with (inverse) binomial weights as well as their associated iterated integrals like generalised harmonic polylogarithms and the iterated integrals over square-root valued letters. The interplay of quantum field theory calculations and computer algebra in this project has led to extensions of summation theory and packages and both sides have mutually benefited from each other significantly. A number of techniques, ranging from hypergeometric functions to differential equations had to be developed further and employed to tackle the master integrals encountered here. Yet this is not the end on the side of technology, since the remaining master integrals which have to be solved next point towards non-iterative integrals. Further developments are necessary in this respect. The results of these calculations will finally allow to cope with the current precision measurements in collider physics, for a final interpretation of the precision data at HERA and precision measurements at the LHC.

Acknowledgements

A PhD thesis is written by one person, but many people have their parts in the path that leads there. I would like to take the opportunity to express my gratitude towards all of these people.

First of all, I would like to thank Prof. Johannes Blümlein for offering me the opportunity to work on this topic, for his support and numerous discussions and for providing contact to the scientific community through the schools and conferences I could attend during my time as a PhD student. Moreover, I would like to thank Prof. Gudrun Hiller for accepting the responsibility to act as a referee for this thesis as well as for the hospitality extended to me during several stays at Dortmund.

I am indebted to PD Carsten Schneider and Jakob Ablinger for their help with the use of their `Mathematica` packages, many interesting exchanges about related topics and their hospitality during two stays at RISC in Hagenberg. I have enjoyed countless discussions and fruitful collaboration with Abilio De Freitas, Giulio Falcioni, Alexander Hasselhuhn, Andreas von Manteuffel, Clemens Raab, Mark Round and Fabian Wißbrock. Thank you for sharing your insights and for your support. For further useful discussions and their interest in this project, I would like to thank Sergey Alekhin, Prof. Einan Gardi, Prof. Mark van Hoeij and Prof. Ewald Reya. I would also like to thank the members of the Theory and NIC groups at DESY Zeuthen for creating a motivating and pleasant atmosphere. For helpful comments and remarks on the manuscript, I am grateful to Margarete Behring, Katharina Diekmann, Giulio Falcioni, Alexander Hasselhuhn, Philipp Krah and Abilio De Freitas.

Moreover, I would like to thank my family and friends, in particular my parents, for their constant support and encouragement throughout the years. I cannot overstate my gratitude towards Katharina, whose patience, love and support means everything to me and keeps me going. Thank you!

A. Notation and conventions

Throughout the thesis we use natural units

$$\hbar = 1\,, \qquad\qquad c = 1\,, \qquad\qquad \varepsilon_0 = 1\,, \qquad\qquad \text{(A.1)}$$

where $\hbar$ is Planck's constant, c denotes the speed of light in vacuum and ε_0 is the permittivity of vacuum. Therefore, energies and momenta are given in electron volt (eV) and distances have the unit eV^{-1}.

In dimensional regularisation the dimension of space-time is assumed to be $D = 4 + \varepsilon$. Accordingly, Lorentz indices run from 0 to D and the metric of Minkowski space is

$$g_{\mu\nu} = \text{diag}(1, -1, \ldots, -1)\,. \qquad\qquad \text{(A.2)}$$

We use the notation

$$p.q = p_\mu q^\mu = \sum_{\mu=0}^{D-1} p_\mu q^\mu \qquad\qquad \text{(A.3)}$$

to denote the Minkowski product and we assume Einstein's summation convention unless stated otherwise.

The Dirac matrices γ_μ fulfil the anti-commutation relations

$$\{\gamma_\mu, \gamma_\nu\} = 2g_{\mu\nu} \qquad\qquad \text{(A.4)}$$

where the Lorentz indices and the Minkowski metric are of course assumed to be D-dimensional.

For the logarithms of the scale ratios we use the symbols

$$L_M = \ln\left(\frac{m^2}{\mu^2}\right)\,, \qquad\qquad L_Q = \ln\left(\frac{Q^2}{\mu^2}\right)\,, \qquad\qquad \text{(A.5)}$$

where m is the heavy quark mass, Q^2 is the virtuality of the exchanged gauge boson and μ^2 is the common renormalisation and factorisation scale.

The gauge structure introduces the generators of the Lie algebra associated to the gauge group into the Feynman rules. The Lie algebra is defined by the commutation relation of its generators [75]

$$[t^a, t^b] = if^{abc}t^c\,, \qquad\qquad \text{(A.6)}$$

where f^{abc} are the structure constants and they are totally anti-symmetric. For QCD the gauge group is SU(3), but we give the results for a general gauge group. For SU(N) one can define the anti-commutation relations by totally symmetric structure constants d^{abc}

$$\{t^a, t^b\} = \frac{\delta^{ab}}{N_c} + d^{abc}t^c\,. \qquad\qquad \text{(A.7)}$$

The simplification of the colour structures yields the following invariants

$$f^{abc}f^{abd} = C_A\delta^{cd} \qquad\qquad \text{(A.8)}$$

$$t_{ij}^a t_{jl}^a = C_F\delta_{il} \qquad\qquad \text{(A.9)}$$

$$t_{ij}^a t_{ji}^b = T_F\delta^{ab} \qquad\qquad \text{(A.10)}$$

which take the values $C_A = 3$, $C_F = 4/3$ and $T_F = 1/2$ for QCD. Another colour structure appears, based on the symmetric structure constants is $d^{abc}d^{abc}$ which takes the value $40/3$ for QCD.

B. Feynman rules

The Feynman rules for QCD employed in this thesis are those of [193, 203], which follow the conventions of [76]. For convenience, we repeat them in this appendix in Fig. B.1. We denote the D-dimensional momenta by p_i whose direction is marked by the arrows along the lines. We use Greek letters to label Lorentz indices, $a, b, \ldots$ for colour indices in the adjoint representation and $i, j, \ldots$ for colour indices in the fundamental representation. Fermions are drawn as solid lines, gluons as curled lines and ghosts as dashed lines. A factor of (-1) has to be included for each closed ghost- or fermion loop.

$$ig_s\gamma_\mu t^a_{ji}$$

$$-g_s f^{abc}[(p_1 - p_2)_\rho g_{\mu\nu} + (p_2 - p_3)_\mu g_{\nu\rho} + (p_3 - p_1)_\nu g_{\mu\rho}]$$

$$-g_s f^{abc} p_\mu$$

$$-ig_s^2 \sum_e \left\{ f^{abe} f^{cde}[g_{\mu\rho}g_{\nu\sigma} - g_{\mu\sigma}g_{\nu\rho}] \right.$$
$$+ f^{ace} f^{bde}[g_{\mu\nu}g_{\rho\sigma} - g_{\mu\sigma}g_{\nu\rho}]$$
$$\left. + f^{ade} f^{cbe}[g_{\mu\rho}g_{\nu\sigma} - g_{\mu\nu}g_{\rho\sigma}] \right\}$$

$$\frac{i}{\not{p}-m+i0}\delta_{ij}$$

$$\frac{i}{p^2+i0}(-g_{\mu\nu} + \xi p_\mu p_\nu/(p^2 + i0))\delta_{ab}$$

$$\frac{i}{p^2+i0}\delta_{ab}$$
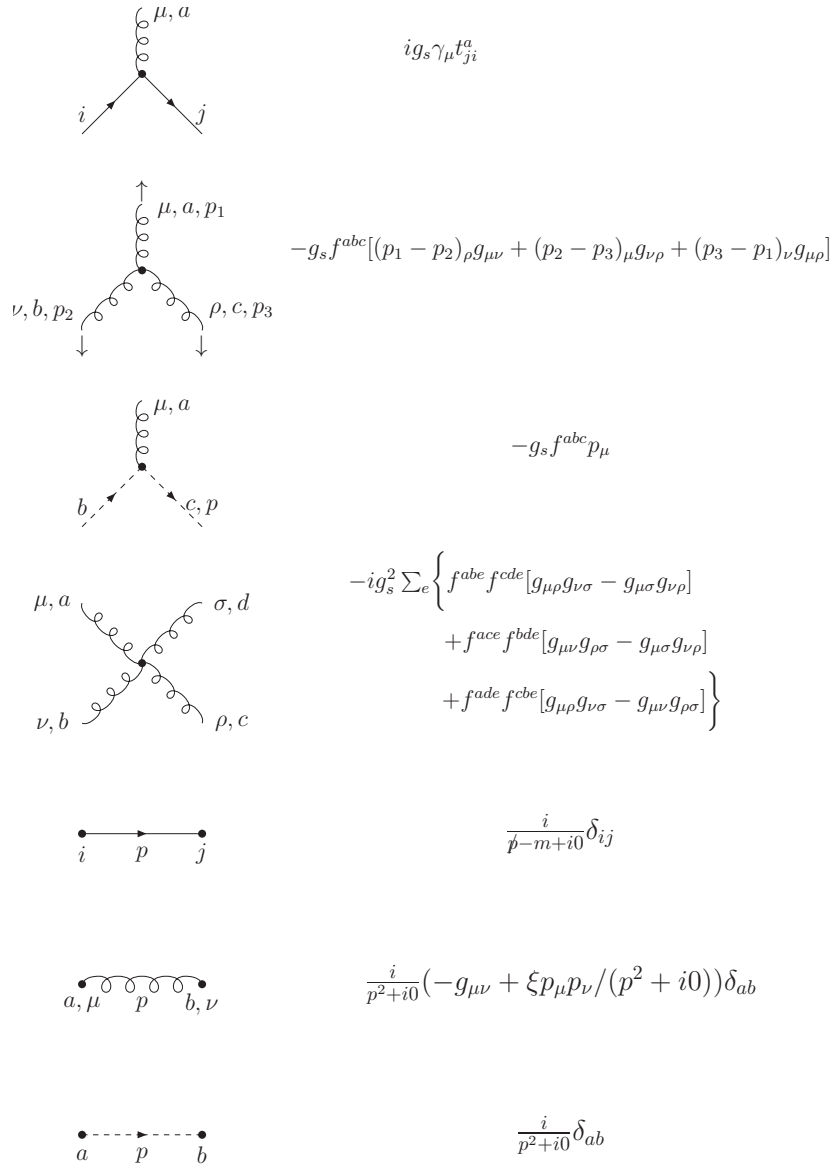
Figure B.1.: Feynman rules for QCD; from [203].
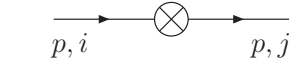
$$\delta^{ij}\slashed{\Delta}\gamma_\pm(\Delta\cdot p)^{N-1}\ ,\quad N\geq 1$$
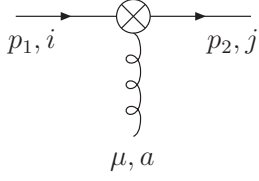
$$gt^a_{ji}\Delta^\mu\slashed{\Delta}\gamma_\pm\sum_{j=0}^{N-2}(\Delta\cdot p_1)^j(\Delta\cdot p_2)^{N-j-2}\ ,\quad N\geq 2$$
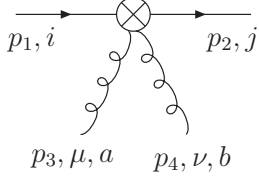
$$g^2\Delta^\mu\Delta^\nu\slashed{\Delta}\gamma_\pm\sum_{j=0}^{N-3}\sum_{l=j+1}^{N-2}(\Delta p_2)^j(\Delta p_1)^{N-l-2}$$
$$\left[(t^at^b)_{ji}(\Delta p_1+\Delta p_4)^{l-j-1}+(t^bt^a)_{ji}(\Delta p_1+\Delta p_3)^{l-j-1}\right]\ ,$$
$$N\geq 3$$
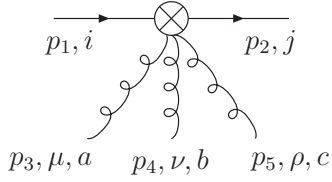
$$g^3\Delta^\mu\Delta^\nu\Delta^\rho\slashed{\Delta}\gamma_\pm\sum_{j=0}^{N-4}\sum_{l=j+1}^{N-3}\sum_{m=l+1}^{N-2}(\Delta.p_2)^j(\Delta.p_1)^{N-m-2}$$
$$\Big[\ (t^at^bt^c)_{ji}(\Delta.p_4+\Delta.p_5+\Delta.p_1)^{l-j-1}(\Delta.p_5+\Delta.p_1)^{m-l-1}$$
$$+(t^at^ct^b)_{ji}(\Delta.p_4+\Delta.p_5+\Delta.p_1)^{l-j-1}(\Delta.p_4+\Delta.p_1)^{m-l-1}$$
$$+(t^bt^at^c)_{ji}(\Delta.p_3+\Delta.p_5+\Delta.p_1)^{l-j-1}(\Delta.p_5+\Delta.p_1)^{m-l-1}$$
$$+(t^bt^ct^a)_{ji}(\Delta.p_3+\Delta.p_5+\Delta.p_1)^{l-j-1}(\Delta.p_3+\Delta.p_1)^{m-l-1}$$
$$+(t^ct^at^b)_{ji}(\Delta.p_3+\Delta.p_4+\Delta.p_1)^{l-j-1}(\Delta.p_4+\Delta.p_1)^{m-l-1}$$
$$+(t^ct^bt^a)_{ji}(\Delta.p_3+\Delta.p_4+\Delta.p_1)^{l-j-1}(\Delta.p_3+\Delta.p_1)^{m-l-1}\Big]\ ,$$
$$N\geq 4$$

$\gamma_+=1\ ,\quad \gamma_-=\gamma_5\ .$ For transversity, one has to replace: $\slashed{\Delta}\gamma_\pm\ \to\ \sigma^{\mu\nu}\Delta_\nu$.

Figure B.2.: Feynman rules for quarkonic operator insertions; from [203].

The quarkonic operator insertions require the Feynman rules given in Fig. B.2. They are also taken from [193, 203], cf. also [107, 157], and they use the same conventions as before. In addition $\gamma_\pm$ is used to distinguish the unpolarised $(+)$ and polarised $(-)$ case. All gluon momenta are considered as incoming and Δ is a light-like, D-dimensional vector $(\Delta^2=0)$. The corresponding Feynman rules for gluonic operator insertions are listed in Fig. B.3. They were derived in [193, 203] and compared to earlier results [104, 116].

$$\frac{1+(-1)^N}{2}\delta^{ab}(\Delta\cdot p)^{N-2}$$
$$\left[g_{\mu\nu}(\Delta\cdot p)^2 - (\Delta_\mu p_\nu + \Delta_\nu p_\mu)\Delta\cdot p + p^2\Delta_\mu\Delta_\nu\right]\,,\quad N\geq 2$$
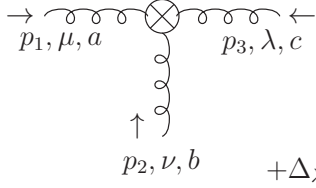
$$-ig\frac{1+(-1)^N}{2}f^{abc}\Bigg($$
$$\left[(\Delta_\nu g_{\lambda\mu}-\Delta_\lambda g_{\mu\nu})\Delta\cdot p_1 + \Delta_\mu(p_{1,\nu}\Delta_\lambda - p_{1,\lambda}\Delta_\nu)\right](\Delta\cdot p_1)^{N-2}$$
$$+\Delta_\lambda\left[\Delta\cdot p_1\,p_{2,\mu}\Delta_\nu + \Delta\cdot p_2\,p_{1,\nu}\Delta_\mu - \Delta\cdot p_1\,\Delta\cdot p_2\,g_{\mu\nu} - p_1\cdot p_2\,\Delta_\mu\Delta_\nu\right]$$
$$\times\sum_{j=0}^{N-3}(-\Delta\cdot p_1)^j(\Delta\cdot p_2)^{N-3-j}$$
$$+\left\{{}^{\,p_1\to p_2\to p_3\to p_1}_{\,\mu\to\nu\to\lambda\to\mu}\right\}+\left\{{}^{\,p_1\to p_3\to p_2\to p_1}_{\,\mu\to\lambda\to\nu\to\mu}\right\}\Bigg)\,,\quad N\geq 2$$
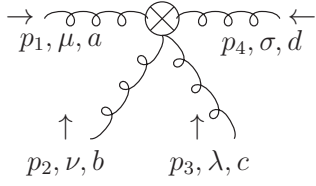
$$g^2\frac{1+(-1)^N}{2}\Bigg(f^{abe}f^{cde}O_{\mu\nu\lambda\sigma}(p_1,p_2,p_3,p_4)$$
$$+f^{ace}f^{bde}O_{\mu\lambda\nu\sigma}(p_1,p_3,p_2,p_4)+f^{ade}f^{bce}O_{\mu\sigma\nu\lambda}(p_1,p_4,p_2,p_3)\Bigg)\,,$$
$$O_{\mu\nu\lambda\sigma}(p_1,p_2,p_3,p_4)=\Delta_\nu\Delta_\lambda\Bigg\{-g_{\mu\sigma}(\Delta\cdot p_3+\Delta\cdot p_4)^{N-2}$$
$$+[p_{4,\mu}\Delta_\sigma - \Delta\cdot p_4\,g_{\mu\sigma}]\sum_{i=0}^{N-3}(\Delta\cdot p_3+\Delta\cdot p_4)^i(\Delta\cdot p_4)^{N-3-i}$$
$$-[p_{1,\sigma}\Delta_\mu - \Delta\cdot p_1\,g_{\mu\sigma}]\sum_{i=0}^{N-3}(-\Delta\cdot p_1)^i(\Delta\cdot p_3+\Delta\cdot p_4)^{N-3-i}$$
$$+[\Delta\cdot p_1\,\Delta\cdot p_4\,g_{\mu\sigma}+p_1\cdot p_4\,\Delta_\mu\Delta_\sigma - \Delta\cdot p_4\,p_{1,\sigma}\Delta_\mu - \Delta\cdot p_1\,p_{4,\mu}\Delta_\sigma]$$
$$\times\sum_{i=0}^{N-4}\sum_{j=0}^{i}(-\Delta\cdot p_1)^{N-4-i}(\Delta\cdot p_3+\Delta\cdot p_4)^{i-j}(\Delta\cdot p_4)^j\Bigg\}$$
$$-\left\{{}^{\,p_1\leftrightarrow p_2}_{\,\mu\leftrightarrow\nu}\right\}-\left\{{}^{\,p_3\leftrightarrow p_4}_{\,\lambda\leftrightarrow\sigma}\right\}+\left\{{}^{\,p_1\leftrightarrow p_2,\ p_3\leftrightarrow p_4}_{\,\mu\leftrightarrow\nu,\ \lambda\leftrightarrow\sigma}\right\}\,,\quad N\geq 2$$

Figure B.3.: Feynman rules for gluonic operator insertions; from [203].

C. Integral families

Here we collect the definitions of propagators of the individual integral families. Each family consists of twelve propagators of which nine are standard propagators that depend quadratically on the momenta and three are linear propagators. The nine standard propagators are based on one of six integral families for operator-less two-point diagrams. We therefore first list the propagators of the operator-less families,

Family B1	Family B3	Family B5
$P_1 = k_1^2$	$P_1 = k_1^2 - m^2$	$P_1 = k_1^2 - m^2$
$P_2 = (k_1 - p)^2$	$P_2 = (k_1 - p)^2 - m^2$	$P_2 = (k_1 - p)^2 - m^2$
$P_3 = k_2^2$	$P_3 = k_2^2 - m^2$	$P_3 = k_2^2 - m^2$
$P_4 = (k_2 - p)^2$	$P_4 = (k_2 - p)^2 - m^2$	$P_4 = (k_2 - p)^2 - m^2$
$P_5 = k_3^2 - m^2$	$P_5 = k_3^2 - m^2$	$P_5 = k_3^2$
$P_6 = (k_1 - k_3)^2 - m^2$	$P_6 = (k_1 - k_3)^2$	$P_6 = (k_1 - k_3)^2 - m^2$
$P_7 = (k_2 - k_3)^2 - m^2$	$P_7 = (k_2 - k_3)^2$	$P_7 = (k_2 - k_3)^2 - m^2$
$P_8 = (k_1 - k_2)^2$	$P_8 = (k_1 - k_2)^2$	$P_8 = (k_1 - k_2)^2$
$P_9 = (k_3 - p)^2 - m^2$	$P_9 = (k_3 - p)^2 - m^2$	$P_9 = (k_3 - p)^2$

Family C1	Family C2	Family C3
$P_1 = k_1^2$	$P_1 = k_1^2 - m^2$	$P_1 = k_1^2 - m^2$
$P_2 = (k_1 - p)^2$	$P_2 = (k_1 - p)^2 - m^2$	$P_2 = (k_1 - p)^2 - m^2$
$P_3 = k_2^2$	$P_3 = k_2^2$	$P_3 = k_2^2 - m^2$
$P_4 = (k_2 - p)^2$	$P_4 = (k_2 - p)^2$	$P_4 = (k_2 - p)^2 - m^2$
$P_5 = k_3^2 - m^2$	$P_5 = k_3^2$	$P_5 = k_3^2 - m^2$
$P_6 = (k_1 - k_3)^2 - m^2$	$P_6 = (k_1 - k_3)^2 - m^2$	$P_6 = (k_1 - k_3)^2$
$P_7 = (k_2 - k_3)^2 - m^2$	$P_7 = (k_2 - k_3)^2$	$P_7 = (k_2 - k_3)^2$
$P_8 = (k_1 + k_2 - k_3 - p)^2 - m^2$	$P_8 = (k_1 + k_2 - k_3 - p)^2 - m^2$	$P_8 = (k_1 + k_2 - k_3 - p)^2 - m^2$
$P_9 = (k_3 - p)^2 - m^2$	$P_9 = (k_3 - p)^2$	$P_9 = (k_3 - p)^2 - m^2 \,.$

The families starting with the letter "B" correspond to planar diagrams and cover topologies related to Benz and ladder diagrams. Non-planar topologies are covered by the three families starting with the letter "C." The digit distinguishes different assignments of massive and massive lines. The linear propagators of the families based on B1 are given by

Family B1a	Family B1b	Family B1c
$P_{10} = 1 - t\Delta.(k_3 - k_1)$	$P_{10} = 1 - t\Delta.k_1$	$P_{10} = 1 - t\Delta.(p - k_1)$
$P_{11} = 1 - t\Delta.k_3$	$P_{11} = 1 - t\Delta.k_3$	$P_{11} = 1 - t\Delta.(k_2 - k_1)$
$P_{12} = 1 - t\Delta.(k_3 - k_2)$	$P_{12} = 1 - t\Delta.k_2$	$P_{12} = 1 - t\Delta.k_3$

C. Integral families

Family B1d	**Family B1e**	
$P_{10} = 1 + t\Delta.k_1$	$P_{10} = 1 + t\Delta.k_1$	
$P_{11} = 1 - t\Delta.(p - k_2)$	$P_{11} = 1 - t\Delta.(k_2 - k_1)$	
$P_{12} = 1 - t\Delta.k_3$	$P_{12} = 1 - t\Delta.k_3$.	

The families based on B3 are supplemented by

Family B3a	**Family B3b**	**Family B3c**
$P_{10} = 1 - t\Delta.k_1$	$P_{10} = 1 - t\Delta.(k_1 - p)$	$P_{10} = 1 - t\Delta.(k_1 - k_3)$
$P_{11} = 1 - t\Delta.k_3$	$P_{11} = 1 - t\Delta.k_3$	$P_{11} = 1 - t\Delta.(k_2 - k_3)$
$P_{12} = 1 - t\Delta.k_2$	$P_{12} = 1 - t\Delta.(k_2 - p)$	$P_{12} = 1 - t\Delta.k_3$,

and the linear propagators of the B5 families read

Family B5a	**Family B5b**	**Family B5c**
$P_{10} = 1 - t\Delta.k_1$	$P_{10} = 1 - t\Delta.(k_3 - k_1)$	$P_{10} = 1 - t\Delta.k_1$
$P_{11} = 1 - t\Delta.k_3$	$P_{11} = 1 - t\Delta.k_3$	$P_{11} = 1 - t\Delta.(k_1 - k_3)$
$P_{12} = 1 - t\Delta.k_2$	$P_{12} = 1 - t\Delta.(k_3 - k_2)$	$P_{12} = 1 - t\Delta.(k_2 - k_3)$
Family B5d	**Family B5e**	**Family B5f**
$P_{10} = 1 - t\Delta.k_1$	$P_{10} = 1 - t\Delta.(k_1 - p)$	$P_{10} = 1 - t\Delta.k_1$
$P_{11} = 1 - t\Delta.(k_1 - k_3)$	$P_{11} = 1 - t\Delta.(k_1 - k_3)$	$P_{11} = 1 - t\Delta.(k_1 - k_3)$
$P_{12} = 1 - t\Delta.(k_2 - p)$	$P_{12} = 1 - t\Delta.(k_2 - p)$	$P_{12} = 1 - t\Delta.(k_1 - k_2)$.

For the non-planar families based on C1, we have the linear propagators

Family C1a	**Family C1b**
$P_{10} = 1 - t\Delta.(k_3 - k_1)$	$P_{10} = 1 - t\Delta.k_1$
$P_{11} = 1 - t\Delta.k_3$	$P_{11} = 1 - t\Delta.k_3$
$P_{12} = 1 - t\Delta.(k_3 - k_2)$	$P_{12} = 1 - t\Delta.k_2$,

while those for C2 are given by

Family C2a	**Family C2b**
$P_{10} = 1 - t\Delta.k_1$	$P_{10} = 1 - t\Delta.k_1$
$P_{11} = 1 - t\Delta.(k_1 - k_3)$	$P_{11} = 1 - t\Delta.k_3$
$P_{12} = 1 - t\Delta.(k_1 + k_2 - k_3 - p)$	$P_{12} = 1 - t\Delta.k_2$
Family C2c	**Family C2d**
$P_{10} = 1 - t\Delta.k_1$	$P_{10} = 1 - t\Delta.k_1$
$P_{11} = 1 - t\Delta.k_3$	$P_{11} = 1 - t\Delta.k_3$
$P_{12} = 1 - t\Delta.(k_2 - p)$	$P_{12} = 1 - t\Delta.(k_3 - k_2)$.

Finally, families based on C3 have the following propagators:

Family C3a	**Family C3b**
$P_{10} = 1 - t\Delta.k_1$	$P_{10} = 1 - t\Delta.(k_3 - k_1)$
$P_{11} = 1 - t\Delta.k_3$	$P_{11} = 1 - t\Delta.k_3$

$P_{12} = 1 - t\Delta.k_2$

$P_{12} = 1 - t\Delta.(k_3 - k_2)$

Family C3c

Family C3d

$P_{10} = 1 - t\Delta.k_1$

$P_{10} = 1 - t\Delta.(k_1 - p)$

$P_{11} = 1 - t\Delta.k_3$

$P_{11} = 1 - t\Delta.k_3$

$P_{12} = 1 - t\Delta.(k_1 + k_2 - k_3 - p)$

$P_{12} = 1 - t\Delta.k_2 \,.$

D. The colour factor $d^{abc}d^{abc}$

The massless Wilson coefficients and anomalous dimensions for $xF_3(x, Q^2)$ contain a new colour factor proportional to $d^{abc}d^{abc}$ ($= 40/3$ in QCD) [135, 153]. This colour factor does not appear in the massive operator matrix elements at 3-loop order. It does, however, arise in individual diagrams contributing to the OMEs but it cancels in the complete result. The cancellation can be seen as follows.

The colour factor can appear when there are two separate fermion lines connected by three gluons. One fermion line connected to three gluons yields the colour structure

$$\text{Tr}\left[t^a t^b t^c\right] = \frac{T_F}{2}(if^{abc} + d^{abc}).$$ (D.1)

Thus, two fermion lines connected by three individual gluon propagators produce the colour structure

$$\text{Tr}\left[t^a t^b t^c\right]\delta^{aa'}\delta^{bb'}\delta^{cc'}\text{Tr}\left[t^{a'} t^{b'} t^{c'}\right] = \frac{T_F^2}{4}(-f^{abc}f^{abc} + d^{abc}d^{abc}).$$ (D.2)

For each such diagram there is a corresponding diagram with the fermion flow along the closed fermion loop reversed. An example of a pair of diagrams is given in Fig. D.1. The closed loop has to have three quark-gluon vertices in order to produce the colour factor and therefore the loop must have three fermion propagators. Keeping the direction of the momenta fixed, the reversal of the fermion flow entails a change of the sign of the momentum $\displaystyle{\not}p_i$ in the numerator of each fermion propagator,

$$\frac{i({\not}p_i + m)}{p_i^2 - m^2} \to \frac{i(-{\not}p_i + m)}{p_i^2 - m^2} \ .$$ (D.3)

Since traces over an odd number of Dirac matrices vanish, this sign can be factored out and yields a global factor (-1). Besides that, the reversal of the fermion flow also reverses the order of the colour generators $t^{a'} t^{b'} t^{c'}$ in Eq. (D.2) which flips the sign in front of the $f^{abc}f^{abc}$ term, but leaves the $d^{abc}d^{abc}$ term unchanged. We see that each pair of such diagrams has exactly the same integrand, but the sign in front of the $d^{abc}d^{abc}$ colour factor is changed. Therefore, this colour factor cancels in the sum for each pair of diagrams.
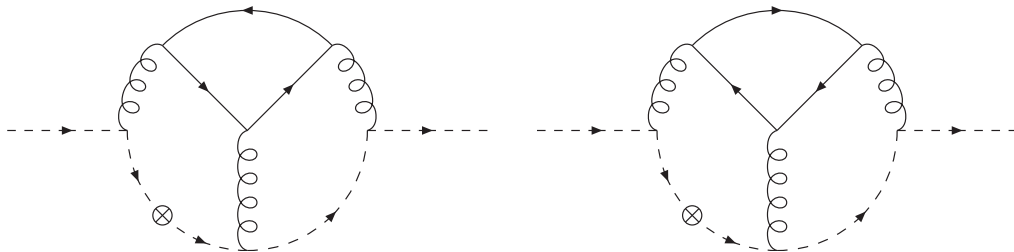
Figure D.1.: Example of a pair of diagrams which each contain a term proportional to the colour factor $d^{abc}d^{abc}$.

E. Results in x space

The results obtained in Mellin N space in terms of nested sums are related to iterated integrals in x space via a Mellin transformation. In this chapter, we collect the results for the anomalous dimensions, the OMEs and the heavy flavour Wilson coefficients in x space. For the HPLs we suppress the argument x to shorten the notation and write $H_{\vec{a}} = H_{\vec{a}}(x)$. All HPLs are reduced to an algebraically independent basis [143, 144, 146, 147] using `HarmonicSums` [258–263].

E.1. Anomalous dimensions

We have obtained the pure-singlet anomalous dimensions in Section 5.1.2 from the renormalisation procedure of the pure-singlet OME. The NLO term of the anomalous dimension appears in the double pole (ε^{-2}) term and its x space representation reads

$$\gamma_{qq}^{\mathrm{PS},(1)}(x) = C_F T_F N_F \left\{ 16(x+1)H_0^2 - \frac{16}{3}\left(8x^2 + 15x + 3\right)H_0 + \frac{32(x-1)\left(28x^2 + x + 10\right)}{9x} \right\}.$$

$$(\mathrm{E.1})$$

From the ε^{-1} term, we extract the NNLO pure-singlet anomalous dimension,

$$\gamma_{qq}^{\mathrm{PS},(2)}(x) =$$

$$C_F^2 T_F N_F \left\{ \frac{32}{3}(x+1)H_0^4 - \frac{16}{9}\left(44x^2 + 15x + 9\right)H_0^3 + \left[\frac{8}{3}\left(88x^2 - 53x + 128\right) - 192(x+1)\zeta_2\right] \right.$$

$$\times H_0^2 + \left[\frac{8}{27}\left(52x^2 - 8229x - 2265\right) + \frac{64}{3}\left(16x^2 + 9x - 6\right)\zeta_2\right]H_0 - \frac{32(x-1)\left(4x^2 + 7x + 4\right)}{9x}H_1^3$$

$$+ \left[\frac{8(x-1)\left(16x^2 + 23x + 16\right)}{3x} - \frac{32(x-1)\left(4x^2 + 7x + 4\right)}{3x}H_0\right]H_1^2 - 64(x+1)H_{0,1}^2$$

$$+ \frac{8(x-1)\left(3924x^2 + 2255x + 990\right)}{27x} + 592(x+1)\zeta_4 + \left[\frac{16(x-1)\left(4x^2 + 7x + 4\right)}{3x}H_0^2\right.$$

$$+ \frac{64(x-1)\left(50x^2 - x + 23\right)}{9x}H_0 + \frac{16(x-1)\left(242x^2 - 2017x - 523\right)}{27x}\right]H_1 + \left[-32(x+1)H_0^2\right.$$

$$- \frac{32\left(28x^3 + 45x^2 + 9x - 4\right)}{3x}H_0 - \frac{16\left(88x^3 - 249x^2 - 516x - 92\right)}{9x}$$

$$+ \frac{64(x-1)\left(4x^2 + 7x + 4\right)}{3x}H_1\right]H_{0,1} + \left[\frac{32\left(20x^3 + 69x^2 + 33x - 4\right)}{3x} + 384(x+1)H_0\right]H_{0,0,1}$$

$$+ \left[128(x+1)H_0 - \frac{64\left(8x^3 + 15x^2 + 6x - 4\right)}{3x}\right]H_{0,1,1} - 576(x+1)H_{0,0,0,1}$$

$$+ 64(x+1)H_{0,0,1,1} + 128(x+1)H_{0,1,1,1} - \frac{16}{9}\left(112x^2 + 45x + 612\right)\zeta_2 + \left[448(x+1)H_0\right.$$

$$-\frac{128\left(8x^3+15x^2-6\right)}{3x}\Bigg]\zeta_3\Bigg\}$$

$$+C_FT_F^2N_F\Bigg\{-\frac{64}{9}(x+1)H_0^3-\frac{928}{9}(x+1)H_0^2+\left[\frac{128}{27}\left(57x^2+35x-37\right)-\frac{256}{3}(x+1)\zeta_2\right]H_0$$

$$+\frac{32(x-1)\left(4x^2+7x+4\right)}{9x}H_1^2-\frac{64(x-1)\left(100x^2-85x-8\right)}{27x}+\frac{64(x-1)\left(74x^2-43x+20\right)}{27x}H_1$$

$$-\frac{128}{9}\left(6x^2+4x-5\right)H_{0,1}+\frac{256}{3}(x+1)H_{0,0,1}-\frac{128}{3}(x+1)H_{0,1,1}+\frac{128}{9}\left(6x^2+4x-5\right)\zeta_2$$

$$-\frac{128}{3}(x+1)\zeta_3\Bigg\}$$

$$+C_FC_AT_FN_F\Bigg\{\frac{8}{3}(3x-4)H_0^4-\frac{16}{9}(31x-29)H_0^3+\bigg[-\frac{8}{9}\left(498x^2-397x+269\right)$$

$$+\frac{16(x+1)\left(16x^2-19x+16\right)}{3x}H_{-1}+16(x-1)\zeta_2\bigg]H_0^2+\left[\frac{32(x+1)\left(4x^2-7x+4\right)}{3x}H_{-1}^2\right.$$

$$-\frac{128(x+1)\left(53x^2-2x+26\right)}{9x}H_{-1}+\frac{16\left(4598x^3+3304x^2+3565x+224\right)}{27x}$$

$$+\frac{16}{3}\left(8x^2-7x+59\right)\zeta_2\bigg]H_0+\frac{32(x-1)\left(4x^2+7x+4\right)}{9x}H_1^3+\bigg[\frac{32(x-1)\left(4x^2+7x+4\right)}{3x}H_0$$

$$-\frac{8(x-1)\left(4x^2+31x+4\right)}{9x}\bigg]H_1^2-64(x-1)H_{0,-1}^2+64(x+1)H_{0,1}^2-8(117x+107)\zeta_4$$

$$-\frac{16(x-1)\left(20558x^2+3494x+6761\right)}{81x}-\frac{16\left(112x^3+226x^2-479x+128\right)}{9x}\zeta_2$$

$$-\frac{32(x+1)\left(4x^2+11x+4\right)}{3x}\zeta_2H_{-1}+\bigg[-\frac{8(x-1)\left(8x^2+17x+8\right)}{x}H_0^2$$

$$+\frac{32(x-1)\left(27x^2+22x+9\right)}{3x}H_0-\frac{16(x-1)\left(302x^2-1882x-571\right)}{27x}$$

$$+\frac{32(x-1)\left(4x^2+7x+4\right)}{3x}\zeta_2\bigg]H_1+\bigg[\frac{64(x+1)\left(4x^2-7x+4\right)}{3x}+128(x-1)H_0\bigg]H_{0,-1,-1}$$

$$-\frac{128(x+1)\left(2x^2+x+2\right)}{3x}H_{0,-1,1}+\bigg[-\frac{32\left(32x^3-75x^2+21x-16\right)}{3x}-64(5x-1)H_0\bigg]$$

$$\times H_{0,0,-1}+\bigg[-\frac{32\left(8x^3+19x^2+4x-12\right)}{3x}-448(x+1)H_0\bigg]H_{0,0,1}$$

$$-\frac{128(x+1)\left(2x^2+x+2\right)}{3x}H_{0,1,-1}+\bigg[\frac{32\left(12x^3+23x^2+5x-12\right)}{3x}-128(x+1)H_0\bigg]H_{0,1,1}$$

$$+384(x+1)H_{0,0,0,-1}+704(x+1)H_{0,0,0,1}-64(x+1)H_{0,0,1,1}-128(x+1)H_{0,1,1,1}$$

$$+H_{0,-1}\bigg[96(x-1)H_0^2+\frac{128\left(2x^3-9x^2+3x-4\right)}{3x}H_0+\frac{128(x+1)\left(53x^2-2x+26\right)}{9x}$$

$$-\frac{64(x+1)\left(4x^2-7x+4\right)}{3x}H_{-1}+64(x-1)\zeta_2\bigg]+H_{0,1}\bigg[112(x+1)H_0^2$$

$$+ \frac{16\left(16x^3 - 3x^2 - 39x - 24\right)}{3x} H_0 - \frac{16\left(50x^3 + 152x^2 + 401x + 26\right)}{9x}$$

$$+ \frac{128(x+1)\left(2x^2 + x + 2\right)}{3x} H_{-1} - \frac{64(x-1)\left(4x^2 + 7x + 4\right)}{3x} H_1 - 64(x+1)\zeta_2 \Bigg]$$

$$+ \left[\frac{32\left(52x^3 - 31x^2 + 2x - 36\right)}{3x} - 64(9x + 13)H_0 \right] \zeta_3 \Bigg\} . \tag{E.2}$$

E.2. Operator matrix elements

The operator matrix elements for the non-singlet and pure-singlet operators were discussed in Section 4.1 and Section 5.1, respectively. Here we give their x space representations.

E.2.1. Non-singlet operator matrix element

Since we calculate the non-singlet OME for even and odd values of N, we have to distinguish two cases for their Mellin inversion. The analytic continuation from the even moments yields an x space representation of the OME for the non-singlet vector operator, which corresponds to the unpolarised situation. The analytic continuation from the odd moments, on the other hand, leads to an x space representation of the axial-vector non-singlet OME, which finds its application in the polarised and charged current cases. These different continuations actually start to differ at the 3-loop level. Therefore, we define the following notation to distinguish the two cases:

$$A_{qq,Q}^{\text{NS}}(x) = A_{qq,Q}^{\text{NS,a}}(x) + (-1)^N A_{qq,Q}^{\text{NS,b}}(x) \tag{E.3}$$

$$A_{qq,Q}^{\text{NS,even}}(x) = A_{qq,Q}^{\text{NS,a}}(x) + A_{qq,Q}^{\text{NS,b}}(x) \tag{E.4}$$

$$A_{qq,Q}^{\text{NS,odd}}(x) = A_{qq,Q}^{\text{NS,a}}(x) - A_{qq,Q}^{\text{NS,b}}(x) \tag{E.5}$$

Vector case

For the renormalised OME of the vector operator we obtain the expressions

$$A_{qq,Q}^{\text{NS,a}}(x) = \delta(1-x) + a_s^2 \Bigg\{ \left(\frac{1}{1-x} C_F T_F \left[\ln^2\left(\frac{m^2}{\mu^2}\right)\frac{8}{3} + \ln\left(\frac{m^2}{\mu^2}\right)\left[\frac{16H_0}{3} + \frac{80}{9}\right] \right.\right.$$

$$\left.\left. + \frac{4}{3}H_0^2 + \frac{40}{9}H_0 + \frac{224}{27} \right] \right)_+ + \delta(1-x)C_F T_F \left[\ln^2\left(\frac{m^2}{\mu^2}\right)2 + \ln\left(\frac{m^2}{\mu^2}\right)\frac{2}{3} + \frac{73}{18} \right]$$

$$+ C_F T_F \left[-\ln^2\left(\frac{m^2}{\mu^2}\right)\frac{4}{3}(x+1) - \ln\left(\frac{m^2}{\mu^2}\right)\left[\frac{8}{3}(x+1)H_0 + \frac{8}{9}(11x-1)\right] \right.$$

$$\left. - \frac{2}{3}(x+1)H_0^2 - \frac{4}{9}(11x-1)H_0 - \frac{4}{27}(67x-11) \right] \Bigg\}$$

$$+ a_s^3 \Bigg\{ \left(\frac{1}{(1-x)^2} C_A C_F T_F \left[\frac{32}{3}H_{0,1} - \frac{4}{3}H_0^2 - \frac{32}{3}\zeta_2 \right] \right.$$

$$+ \frac{1}{1-x}\Bigg\{ C_F^2 T_F \left[\ln^2\left(\frac{m^2}{\mu^2}\right)\left[\frac{64}{3}H_1 H_0 - 16H_0 + 8\right] + \ln\left(\frac{m^2}{\mu^2}\right)\left[\frac{32}{9}H_0^3 \right.\right.$$

$$\left.\left. - 16H_0^2 - \frac{128}{3}H_{0,1}H_0 - \frac{64}{3}\zeta_2 H_0 - \frac{40}{3}H_0 + \left(\frac{128}{3}H_0^2 + \frac{640}{9}H_0\right)H_1 \right.$$

247

$$+ \frac{128}{3} H_{0,0,1} - \frac{320}{3} \zeta_3 + \frac{40}{3} \Big] + \frac{8}{9} H_0^4 + \frac{32}{81} H_0^3 - \frac{32}{9} H_1^2 H_0^2 - 4 H_0^2$$

$$+ \frac{128}{27} H_1^3 H_0 - \frac{2416}{27} H_0 + \frac{32}{9} H_{0,1}^2 + \frac{64}{3} B_4 - \frac{544}{9} \zeta_4 + \Big(\frac{256}{27} H_0^3 + \frac{1280}{27} H_0^2 $$

$$+ \frac{7168}{81} H_0 \Big) H_1 + \Big(-\frac{32}{3} H_0^2 + \frac{256}{9} H_1 H_0 - \frac{1568}{27} H_0 - \frac{128}{9} H_1^2 + \frac{112}{9} \Big) H_{0,1}$$

$$+ \Big(\frac{128}{9} H_0 - \frac{448}{9} H_1 + \frac{1712}{27} \Big) H_{0,0,1} + \Big(-\frac{64}{3} H_0 + \frac{64}{3} H_1 - 16 \Big) H_{0,1,1}$$

$$- \frac{128}{9} H_{0,0,0,1} + \frac{64}{3} H_{0,0,1,1} + \Big(-\frac{32}{9} H_0^2 + \frac{64}{3} H_1 H_0 - \frac{496}{27} H_0 + \frac{128}{9} H_1^2 $$

$$- \frac{128}{9} H_{0,1} - \frac{112}{9} \Big) \zeta_2 + \Big(-\frac{128}{9} H_0 + \frac{256}{9} H_1 + \frac{2344}{27} \Big) \zeta_3 - \frac{4754}{27} \Big]$$

$$+ C_F T_F^2 N_F \Big[\ln^3 \Big(\frac{m^2}{\mu^2} \Big) \frac{64}{27} + \ln \Big(\frac{m^2}{\mu^2} \Big) \Big[-\frac{32}{9} H_0^2 - \frac{320}{27} H_0 + \frac{2176}{81} \Big] \Big]$$

$$- \frac{64}{81} H_0^3 - \frac{320}{81} H_0^2 + \frac{128}{81} H_0 - \frac{512}{27} \zeta_3 + \frac{24064}{729} \Big] + C_F T_F^2 \Big[\ln^3 \Big(\frac{m^2}{\mu^2} \Big) \frac{128}{27} $$

$$+ \ln^2 \Big(\frac{m^2}{\mu^2} \Big) \Big[\frac{64}{9} H_0 + \frac{320}{27} \Big] + \ln \Big(\frac{m^2}{\mu^2} \Big) \frac{1984}{81} - \frac{32}{81} H_0^3 - \frac{160}{81} H_0^2 + \frac{64}{81} H_0 $$

$$+ \frac{896}{27} \zeta_3 - \frac{12064}{729} \Big] + C_A C_F T_F \Big[- \ln^3 \Big(\frac{m^2}{\mu^2} \Big) \frac{176}{27} + \ln^2 \Big(\frac{m^2}{\mu^2} \Big) \Big[\frac{16}{3} H_0^2 $$

$$- \frac{32}{3} \zeta_2 + \frac{184}{9} \Big] + \ln \Big(\frac{m^2}{\mu^2} \Big) \Big[\frac{32}{9} H_0^3 - 16 H_1 H_0^2 + \frac{248}{9} H_0^2 + 32 H_{0,1} H_0 $$

$$+ \frac{1792}{27} H_0 - \frac{64}{3} H_{0,0,1} + \Big(-\frac{64}{3} H_0 - \frac{320}{9} \Big) \zeta_2 + 96 \zeta_3 + \frac{1240}{81} \Big] + \frac{16}{27} H_0^4 $$

$$+ \frac{496}{81} H_0^3 + \frac{8}{9} H_1^2 H_0^2 + \frac{3200}{81} H_0^2 - \frac{64}{27} H_1^3 H_0 + \frac{3256}{81} H_0 - \frac{32}{9} H_{0,1}^2 - \frac{32}{3} B_4 $$

$$+ \frac{296}{3} \zeta_4 + \Big(-\frac{112}{27} H_0^3 - \frac{160}{9} H_0^2 - \frac{32}{9} H_0 + \frac{32}{3} \Big) H_1 + \Big(\frac{16}{3} H_0^2 + \frac{368}{9} H_0 $$

$$+ \frac{128}{9} H_1^2 + \Big(-\frac{128}{9} H_0 - 8 \Big) H_1 - \frac{32}{9} \Big) H_{0,1} + \Big(\frac{160}{9} H_0 - 32 H_1 + 24 \Big) H_{0,1,1}$$

$$+ \Big(\frac{32}{9} H_0 + \frac{320}{9} H_1 - \frac{1072}{27} \Big) H_{0,0,1} - \frac{224}{9} H_{0,0,1,1} + \frac{224}{9} H_{0,1,1,1}$$

$$+ \Big(-\frac{112}{9} H_0^2 - \frac{496}{27} H_0 - \frac{128}{9} H_1^2 + \Big(8 - \frac{160}{9} H_0 \Big) H_1 + \frac{32}{9} H_{0,1} - \frac{3008}{81} \Big) \zeta_2 $$

$$+ \Big(\frac{160}{9} H_0 - \frac{32}{9} H_1 - \frac{1196}{27} \Big) \zeta_3 + \frac{43228}{729} \Big] \Big\} \Big)_+$$

$$+ \delta(1-x) \Big\{ C_A C_F T_F \Big[- \ln^3 \Big(\frac{m^2}{\mu^2} \Big) \frac{44}{9} + \ln^2 \Big(\frac{m^2}{\mu^2} \Big) \Big[\frac{34}{3} - \frac{16}{3} \zeta_3 \Big] $$

$$+ \ln \Big(\frac{m^2}{\mu^2} \Big) \Big[\frac{272}{9} \zeta_3 + \frac{68}{3} \zeta_4 - \frac{1595}{27} \Big] - 8 B_4 - \frac{16}{9} \zeta_2 \zeta_3 - \frac{10045}{81} \zeta_3 + \frac{2624}{27} \zeta_4 $$

$$- \frac{176}{9} \zeta_5 + \frac{55}{243} \Big] + C_F^2 T_F \Big[\ln^2 \Big(\frac{m^2}{\mu^2} \Big) \Big[\frac{32}{3} \zeta_3 + 8 \Big] + \ln \Big(\frac{m^2}{\mu^2} \Big) \Big[-\frac{112}{9} \zeta_3 $$

$$- \frac{136}{3} \zeta_4 + 1 \Big] + 16 B_4 + \frac{32}{9} \zeta_2 \zeta_3 + \frac{13682}{81} \zeta_3 + \frac{352}{9} \zeta_5 - \frac{3304}{27} \zeta_4 - \frac{691}{9} \Big]$$

$$+ C_F N_F T_F^2 \Big[\ln^3 \left(\frac{m^2}{\mu^2} \right) \frac{16}{9} + \ln \left(\frac{m^2}{\mu^2} \right) \frac{700}{27} - \frac{128}{9} \zeta_3 + \frac{4732}{243} \Big]$$

$$+ C_F T_F^2 \Big[\ln^3 \left(\frac{m^2}{\mu^2} \right) \frac{32}{9} + \ln^2 \left(\frac{m^2}{\mu^2} \right) \frac{8}{9} + \ln \left(\frac{m^2}{\mu^2} \right) \frac{496}{27} + \frac{224}{9} \zeta_3 - \frac{3658}{243} \Big] \Big\}$$

$$+ C_F^2 T_F \Big[\ln^2 \left(\frac{m^2}{\mu^2} \right) \Big[-\frac{8}{3} (x+1) H_0^2 - \frac{32}{3} x H_0 - \frac{32}{3} (x+1) H_1 H_0$$

$$+ \frac{4}{3} (17x - 23) \Big] + \ln \left(\frac{m^2}{\mu^2} \right) \Big[-\frac{40}{9} (x+1) H_0^3 - \frac{32}{9} (7x+1) H_0^2$$

$$- \frac{8}{9} (37x + 45) H_0 + \frac{64}{3} (x+1) H_{0,1} H_0 + \frac{32}{3} (x+1) \zeta_2 H_0 + \frac{4}{9} (149x - 179)$$

$$+ \left(-\frac{64}{3} (x+1) H_0^2 - \frac{128}{9} (4x+1) H_0 \right) H_1 - \frac{64}{3} (x+1) H_{0,0,1}$$

$$+ \frac{160}{3} (x+1) \zeta_3 \Big] - \frac{26}{27} (x+1) H_0^4 - \frac{16}{81} (49x + 13) H_0^3 - \frac{4}{81} (575x + 221) H_0^2$$

$$- \frac{64}{27} (x+1) H_1^3 H_0 - \frac{56}{81} (7x - 18) H_0 + \left(\frac{16}{9} (x+1) H_0^2 - \frac{32}{9} (x-1) H_0 \right.$$

$$+ \frac{16}{9} (11x - 12) \left. \right) H_1^2 - \frac{16}{9} (x+1) H_{0,1}^2 - \frac{32}{3} B_4 (x+1) + \frac{1}{81} (19187x - 4925)$$

$$+ \frac{272}{9} (x+1) \zeta_4 + \left(-\frac{128}{27} (x+1) H_0^3 - \frac{16}{27} (61x + 19) H_0^2 + \frac{8}{9} (31x - 28) \right.$$

$$- \frac{16}{81} (263x + 194) H_0 \left. \right) H_1 + \left(\frac{16}{3} (x+1) H_0^2 + \frac{32}{27} (17x + 11) H_0 \right.$$

$$+ \frac{64}{9} (x+1) H_1^2 - \frac{16}{9} x + \left(\frac{64}{9} (x-1) - \frac{128}{9} (x+1) H_0 \right) H_1 \left. \right) H_{0,1}$$

$$+ \left(-\frac{64}{27} (4x + 7) + \frac{32}{9} (x+1) \left(7 H_1 - 2 H_0 \right) \right) H_{0,0,1} + \left(-\frac{64}{3} x \right.$$

$$+ \frac{32}{3} (x+1) \left(H_0 - H_1 \right) \left. \right) H_{0,1,1} + \frac{32}{3} (x+1) \left(\frac{2}{3} H_{0,0,0,1} - H_{0,0,1,1} \right)$$

$$+ \left(\frac{16}{9} (x+1) H_0^2 + \frac{64}{27} (8x + 5) H_0 - \frac{64}{9} (x+1) H_1^2 - \frac{32}{9} (7x - 8) \right.$$

$$+ \left(-\frac{64}{9} (x-1) - \frac{32}{3} (x+1) H_0 \right) H_1 + \frac{64}{9} (x+1) H_{0,1} \left. \right) \zeta_2$$

$$+ \left(-\frac{4}{27} (101x + 485) + \frac{64}{9} (x+1) H_0 - \frac{128}{9} (x+1) H_1 \right) \zeta_3 \Big]$$

$$+ C_F T_F^2 \Big[-\ln^3 \left(\frac{m^2}{\mu^2} \right) \frac{64}{27} (x+1) + \ln^2 \left(\frac{m^2}{\mu^2} \right) \Big[-\frac{32}{27} (11x - 1)$$

$$- \frac{32}{9} (x+1) H_0 \Big] - \ln \left(\frac{m^2}{\mu^2} \right) \frac{992}{81} (x+1) + \frac{16}{81} (x+1) H_0^3 + \frac{16}{81} (11x - 1) H_0^2$$

$$+ \frac{16}{729} (431x + 323) + \frac{64}{81} (6x - 7) H_0 - \frac{448}{27} (x+1) \zeta_3 \Big]$$

E. Results in x space

$$
+ C_F T_F^2 N_F \left[-\ln^3\left(\frac{m^2}{\mu^2}\right) \frac{32}{27}(x+1) + \ln\left(\frac{m^2}{\mu^2}\right) \left[\frac{16}{9}(x+1)H_0^2 \right. \right.
$$

$$
\left. + \frac{32}{27}(11x-1)H_0 + \frac{32}{81}(5x-73) \right] + \frac{32}{81}(x+1)H_0^3 + \frac{32}{81}(11x-1)H_0^2
$$

$$
\left. - \frac{64}{729}(161x+215) + \frac{128}{81}(6x-7)H_0 + \frac{256}{27}(x+1)\zeta_3 \right]
$$

$$
+ C_A C_F T_F \left[\ln^3\left(\frac{m^2}{\mu^2}\right) \frac{88}{27}(x+1) + \ln^2\left(\frac{m^2}{\mu^2}\right) \left[-\frac{4}{9}(59x-13) \right. \right.
$$

$$
\left. + \frac{8}{3}(x+1)\left(-H_0^2 + 2H_0 + 2\zeta_2\right) \right] + \ln\left(\frac{m^2}{\mu^2}\right) \left[-\frac{16}{9}(x+1)H_0^3 \right.
$$

$$
- \frac{4}{9}(19x+13)H_0^2 - \frac{8}{27}(181x-95)H_0 - \frac{4}{81}(3479x-3169)
$$

$$
+ \left(8(x+1)H_0^2 - \frac{32}{3}(x-1) \right) H_1 + \left(\frac{16}{3}(x+1) - 16(x+1)H_0 \right) H_{0,1}
$$

$$
\left. + \frac{32}{3}(x+1)H_{0,0,1} + \left(\frac{16}{9}(13x+1) + \frac{32}{3}(x+1)H_0 \right) \zeta_2 - 48(x+1)\zeta_3 \right]
$$

$$
+ \frac{8}{27}(x+1)\left(4H_1^3 H_0 - H_0^4\right) - \frac{8}{81}(16x+13)H_0^3 - \frac{4}{81}(268x-65)H_0^2
$$

$$
- \frac{4}{81}(2115x-1687)H_0 + \left(-\frac{4}{9}(x+1)H_0^2 - \frac{8}{9}(2x+5)H_0 - \frac{4}{3}(9x-10) \right) H_1^2
$$

$$
+ \frac{16}{9}(7x+1)H_{0,1}^2 + \frac{16}{3}B_4(x+1) - \frac{2}{729}(79747x-58133) - \frac{4}{3}(65x+37)\zeta_4
$$

$$
+ \left(\frac{56}{27}(x+1)H_0^3 + \frac{8}{9}(14x+3)H_0^2 + \frac{8}{9}(9x+4)H_0 - \frac{8}{27}(187x-151) \right) H_1
$$

$$
+ \left(-\frac{8}{3}(x+1)H_0^2 - \frac{16}{9}(13x+6)H_0 - \frac{64}{9}(x+1)H_1^2 - \frac{8}{27}(61x-80) \right)
$$

$$
+ \left(\frac{8}{9}(11x+20) + \frac{64}{9}(x+1)H_0 \right) H_1 \right) H_{0,1} + \left(\frac{8}{27}(85x+88) \right)
$$

$$
- \frac{16}{9}(7x+1)H_0 - \frac{160}{9}(x+1)H_1 \right) H_{0,0,1} + \left(-\frac{16}{9}(11x+5)H_0 \right.
$$

$$
\left. - \frac{16}{9}(5x+11) + 16(x+1)H_1 \right) H_{0,1,1} + \frac{128}{3}x H_{0,0,0,1} - \frac{16}{9}(5x-7)H_{0,0,1,1}
$$

$$
- \frac{112}{9}(x+1)H_{0,1,1,1} + \left(\frac{8}{9}(x+7)H_0^2 + \frac{8}{27}(25x-32)H_0 + \frac{64}{9}(x+1)H_1^2 \right.
$$

$$
+ \frac{16}{81}(250x-113) + \left(\frac{80}{9}(x+1)H_0 - \frac{8}{9}(3x+14) \right) H_1 - \frac{16}{9}(7x+1)H_{0,1} \right) \zeta_2
$$

$$
+ \left(\frac{2}{27}(209x+797) + \frac{16}{9}(13x-5)H_0 + \frac{16}{9}(x+1)H_1 \right) \zeta_3 \right] \Bigg\} , \tag{E.6}
$$

and

$$
A_{qq,Q}^{\mathrm{NS,b}}(x) = a_s^3 \left(\frac{C_A}{2} - C_F \right) C_F T_F \left[\ln^2\left(\frac{m^2}{\mu^2}\right) \left[-\frac{32}{3}(x+1)H_0 + \frac{64}{3}(x-1) \right. \right.
$$

$$
\left. + \frac{16(x^2+1)}{3(x+1)}\left(-H_0^2 + 4H_{-1}H_0 - 4H_{0,-1} + 2\zeta_2 \right) \right]
$$

250

$$+ \ln\left(\frac{m^2}{\mu^2}\right)\left[\frac{16\left(x^2+x+1\right)}{3(x+1)}\left(-6H_0^2 + 16H_0H_{-1} - 16H_{0,-1}\right)\right.$$

$$-\frac{656}{9}(x+1)H_0 + \frac{976}{9}(x-1) - \frac{128}{3}(x-1)H_1 + \frac{64}{3}(x+1)H_{0,1}$$

$$+\frac{16\left(x^2+1\right)}{3(x+1)}\left(-\frac{2}{3}H_0^3 - \frac{1}{3}H_0^2 + 2H_{-1}H_0^2 + \frac{16}{3}H_0H_{-1} - \frac{16}{3}H_{0,-1}\right.$$

$$-8H_{-1}H_{0,1} + 8H_{0,-1,1} - 4H_{0,0,-1} + 4H_{0,0,1} + 8H_{0,1,-1} - 6\zeta_3$$

$$\left.+\left(8H_{-1} - 2H_0 + \frac{20}{3}\right)\zeta_2\right)\right] + \frac{16}{9}(x-1)\left(8H_1^2 - \frac{122}{3}H_1 + \frac{793}{9}\right)$$

$$+\frac{32}{9}(x+1)\left(-\frac{280}{9}H_0 - 2H_0H_{-1}^2 + 4H_{-1}H_{0,-1} + \frac{41}{3}H_{0,1} - 4H_{0,-1,-1}\right.$$

$$\left.- 4H_{0,1,1}\right) + \frac{16\left(x^2+x+1\right)}{3(x+1)}\left(-\frac{4}{3}H_0^3 - 11H_0^2 + 4H_0^2H_{-1} + \frac{232}{9}H_0H_{-1}\right.$$

$$-\frac{232}{9}H_{0,-1} - \frac{32}{3}H_{-1}H_{0,1} + \frac{32}{3}H_{0,-1,1} - 8H_{0,0,-1} + 8H_{0,0,1}$$

$$\left.+\frac{32}{3}H_{0,1,-1} + \left(8H_{-1} - 4H_0 - \frac{16}{3}\right)\zeta_2 - \frac{8}{3}\zeta_3\right)$$

$$+\frac{16\left(x^2+1\right)}{9(x+1)}\left(-\frac{1}{3}H_0^4 - \frac{2}{9}H_0^3 + \frac{73}{18}H_0^2 + \frac{8}{3}H_{-1}^3H_0 + \frac{21}{2}\zeta_4 - 2H_0^2H_{-1}^2\right.$$

$$+\frac{4}{3}H_0^3H_{-1} + \frac{2}{3}H_0^2H_{-1} + \frac{100}{9}H_0H_{-1} - 8H_{-1}^2H_{0,-1} - \frac{100}{9}H_{0,-1}$$

$$-\frac{32}{3}H_{-1}H_{0,1} + 16H_{-1}H_{0,-1,-1} + \frac{32}{3}H_{0,-1,1} + 8H_{-1}H_{0,0,-1}$$

$$-\frac{4}{3}H_{0,0,-1} - 8H_{-1}H_{0,0,1} + \frac{4}{3}H_{0,0,1} + \frac{32}{3}H_{0,1,-1} + 16H_{-1}H_{0,1,1}$$

$$-16H_{0,-1,-1,-1} - 16H_{0,-1,1,1} - 8H_{0,0,-1,-1} + 8H_{0,0,-1,1} - 8H_{0,0,0,-1}$$

$$+ 8H_{0,0,0,1} + 8H_{0,0,1,-1} - 8H_{0,0,1,1} - 16H_{0,1,-1,1} - 16H_{0,1,1,-1}$$

$$+\left(4H_{-1}^2 + \frac{44}{3}H_{-1} - 2H_0^2 + 4H_{-1}H_0 - \frac{2}{3}H_0 + \frac{296}{9}\right)\zeta_2$$

$$+\left(-16H_{-1} + 2H_0 - 16\right)\zeta_3\right)\right]. \tag{E.7}$$

Transversity

Using an analogous notation as in Eq. (E.3), the renormalised non-singlet OME for transversity can we written in x space as

$$A_{qq,Q}^{\text{NS,TR,a}}(x) = \delta(1-x) + a_s^2\left\{\left(\frac{1}{1-x}C_FT_F\left[\frac{8}{3}\ln^2\left(\frac{m^2}{\mu^2}\right) + \left[\frac{80}{9} + \frac{16}{3}H_0\right]\ln\left(\frac{m^2}{\mu^2}\right) + \frac{224}{27}\right.\right.$$

$$\left.\left.+ \frac{40}{9}H_0 + \frac{4}{3}H_0^2\right]\right)_+ + C_FT_F\left[2\ln^2\left(\frac{m^2}{\mu^2}\right) + \frac{2}{3}\ln\left(\frac{m^2}{\mu^2}\right) + \frac{73}{18}\right]\delta(1-x)$$

$$+ C_FT_F\left[-\frac{8}{3}\ln^2\left(\frac{m^2}{\mu^2}\right) - \frac{4}{27}(9x+47) - \frac{4}{27}\ln\left(\frac{m^2}{\mu^2}\right)\left(60 + 36H_0\right)\right.$$

$$\left.\left.- \frac{40}{9}H_0 - \frac{4}{3}H_0^2\right]\right\}$$

$$+ a_s^3 \Bigg\{ \Bigg(\frac{1}{(1-x)^2} C_A C_F T_F \Big\{ -\frac{4}{3} H_0^2 + \frac{32}{3} H_{0,1} - \frac{32}{3} \zeta_2 \Big\}$$

$$+ \frac{1}{1-x} \Bigg\{ C_F N_F T_F^2 \Bigg[\frac{64}{27} \ln^3 \left(\frac{m^2}{\mu^2} \right) + \ln \left(\frac{m^2}{\mu^2} \right) \left[\frac{2176}{81} - \frac{320}{27} H_0 - \frac{32}{9} H_0^2 \right]$$

$$+ \frac{24064}{729} + \frac{128}{81} H_0 - \frac{320}{81} H_0^2 - \frac{64}{81} H_0^3 - \frac{512}{27} \zeta_3 \Bigg] + C_F T_F^2 \Bigg[\frac{128}{27} \ln^3 \left(\frac{m^2}{\mu^2} \right)$$

$$+ \ln^2 \left(\frac{m^2}{\mu^2} \right) \left[\frac{320}{27} + \frac{64}{9} H_0 \right] + \frac{1984}{81} \ln \left(\frac{m^2}{\mu^2} \right) - \frac{12064}{729} + \frac{64}{81} H_0 - \frac{160}{81} H_0^2$$

$$- \frac{32}{81} H_0^3 + \frac{896}{27} \zeta_3 \Bigg] + C_A C_F T_F \Bigg[-\frac{176}{27} \ln^3 \left(\frac{m^2}{\mu^2} \right) + \ln^2 \left(\frac{m^2}{\mu^2} \right) \left[\frac{184}{9} + \frac{16}{3} H_0^2 \right]$$

$$- \frac{32}{3} \zeta_2 \Bigg] + \ln \left(\frac{m^2}{\mu^2} \right) \left[\frac{1240}{81} + \frac{1792}{27} H_0 + \frac{248}{9} H_0^2 + \frac{32}{9} H_0^3 - 16 H_0^2 H_1 \right.$$

$$+ 32 H_0 H_{0,1} - \frac{64}{3} H_{0,0,1} + \left(-\frac{320}{9} - \frac{64}{3} H_0 \right) \zeta_2 + 96 \zeta_3 \Bigg] + \frac{43228}{729} + \frac{3256}{81} H_0$$

$$+ \frac{3200}{81} H_0^2 + \frac{496}{81} H_0^3 + \frac{16}{27} H_0^4 + \left(\frac{32}{3} - \frac{32}{9} H_0 - \frac{160}{9} H_0^2 - \frac{112}{27} H_0^3 \right) H_1$$

$$+ \frac{8}{9} H_0^2 H_1^2 - \frac{64}{27} H_0 H_1^3 + \left(-\frac{32}{9} + \frac{368}{9} H_0 + \frac{16}{3} H_0^2 - \left(8 + \frac{128}{9} H_0 \right) H_1 \right)$$

$$+ \frac{128}{9} H_1^2 \Bigg) H_{0,1} - \frac{32}{9} H_{0,1}^2 + \left(-\frac{1072}{27} + \frac{32}{9} H_0 + \frac{320}{9} H_1 \right) H_{0,0,1} + \left(\frac{160}{9} H_0 \right.$$

$$+ 24 - 32 H_1 \Bigg) H_{0,1,1} - \frac{224}{9} H_{0,0,1,1} + \frac{224}{9} H_{0,1,1,1} + \left(-\frac{3008}{81} - \frac{112}{9} H_0^2 \right.$$

$$- \frac{496}{27} H_0 + \left(8 - \frac{160}{9} H_0 \right) H_1 - \frac{128}{9} H_1^2 + \frac{32}{9} H_{0,1} \right) \zeta_2 + \left(-\frac{1196}{27} + \frac{160}{9} H_0 \right.$$

$$- \frac{32}{9} H_1 \Bigg) \zeta_3 + \frac{296}{3} \zeta_4 - \frac{32}{3} B_4 \Bigg] + C_F^2 T_F \Bigg[\ln^2 \left(\frac{m^2}{\mu^2} \right) \left[8 - 16 H_0 + \frac{64}{3} H_0 H_1 \right]$$

$$+ \ln \left(\frac{m^2}{\mu^2} \right) \left[\frac{40}{3} - \frac{40}{3} H_0 - 16 H_0^2 + \frac{32}{9} H_0^3 + \left(\frac{640}{9} H_0 + \frac{128}{3} H_0^2 \right) H_1 \right.$$

$$- \frac{128}{3} H_0 H_{0,1} + \frac{128}{3} H_{0,0,1} - \frac{64}{3} H_0 \zeta_2 - \frac{320}{3} \zeta_3 \right] - \frac{4754}{27} - \frac{2416}{27} H_0 - 4 H_0^2$$

$$+ \frac{32}{81} H_0^3 + \frac{8}{9} H_0^4 + \left(\frac{7168}{81} H_0 + \frac{1280}{27} H_0^2 + \frac{256}{27} H_0^3 \right) H_1 - \frac{32}{9} H_0^2 H_1^2$$

$$+ \frac{128}{27} H_0 H_1^3 + \left(\frac{112}{9} - \frac{1568}{27} H_0 - \frac{32}{3} H_0^2 + \frac{256}{9} H_0 H_1 - \frac{128}{9} H_1^2 \right) H_{0,1}$$

$$+ \left(\frac{1712}{27} + \frac{128}{9} H_0 - \frac{448}{9} H_1 \right) H_{0,0,1} - \left(16 + \frac{64}{3} H_0 - \frac{64}{3} H_1 \right) H_{0,1,1} + \frac{32}{9} H_{0,1}^2$$

$$- \frac{128}{9} H_{0,0,0,1} + \frac{64}{3} H_{0,0,1,1} + \left(-\frac{112}{9} - \frac{496}{27} H_0 - \frac{32}{9} H_0^2 + \frac{128}{9} H_1^2 - \frac{128}{9} H_{0,1} \right.$$

$$+ \frac{64}{3} H_0 H_1 \Bigg) \zeta_2 + \left(\frac{2344}{27} - \frac{128}{9} H_0 + \frac{256}{9} H_1 \right) \zeta_3 - \frac{544}{9} \zeta_4 + \frac{64}{3} B_4 \Bigg] \Bigg\} \Bigg)_+$$

$$+ \delta(1-x) \Bigg\{ C_F N_F T_F^2 \Bigg[\frac{16}{9} \ln^3 \left(\frac{m^2}{\mu^2} \right) + \frac{700}{27} \ln \left(\frac{m^2}{\mu^2} \right) + \frac{4732}{243} - \frac{128}{9} \zeta_3 \Bigg]$$

$$+ C_F T_F^2 \left[\frac{32}{9} \ln^3 \left(\frac{m^2}{\mu^2} \right) + \frac{8}{9} \ln^2 \left(\frac{m^2}{\mu^2} \right) + \frac{496}{27} \ln \left(\frac{m^2}{\mu^2} \right) - \frac{3658}{243} + \frac{224}{9} \zeta_3 \right]$$

$$+ C_A C_F T_F \left[-\frac{44}{9} \ln^3 \left(\frac{m^2}{\mu^2} \right) + \ln^2 \left(\frac{m^2}{\mu^2} \right) \left[\frac{34}{3} - \frac{16}{3} \zeta_3 \right] + \ln \left(\frac{m^2}{\mu^2} \right) \left[-\frac{1595}{27} \right. \right.$$

$$\left. + \frac{272}{9} \zeta_3 + \frac{68}{3} \zeta_4 \right] + \frac{55}{243} - \frac{10045}{81} \zeta_3 + \frac{2624}{27} \zeta_4 - 8 B_4 - \frac{16}{9} \zeta_2 \zeta_3 - \frac{176}{9} \zeta_5 \right]$$

$$+ C_F^2 T_F \left[\ln^2 \left(\frac{m^2}{\mu^2} \right) \left[8 + \frac{32}{3} \zeta_3 \right] + \ln \left(\frac{m^2}{\mu^2} \right) \left[1 - \frac{136}{3} \zeta_4 - \frac{112}{9} \zeta_3 \right] - \frac{691}{9} \right.$$

$$\left. \left. + \frac{13682}{81} \zeta_3 - \frac{3304}{27} \zeta_4 + 16 B_4 + \frac{32}{9} \zeta_2 \zeta_3 + \frac{352}{9} \zeta_5 \right] \right\} + C_F T_F^2 \left[-\frac{128}{27} \ln^3 \left(\frac{m^2}{\mu^2} \right) \right.$$

$$+ \ln^2 \left(\frac{m^2}{\mu^2} \right) \left[-\frac{320}{27} - \frac{64}{9} H_0 \right] - \frac{1984}{81} \ln \left(\frac{m^2}{\mu^2} \right) + \frac{32}{729} (45x + 332) + \frac{160}{81} H_0^2$$

$$+ \frac{32}{81} (3x - 5) H_0 + \frac{32}{81} H_0^3 - \frac{896}{27} \zeta_3 \right] + C_F N_F T_F^2 \left[-\frac{64}{27} \ln^3 \left(\frac{m^2}{\mu^2} \right) \right.$$

$$+ \ln \left(\frac{m^2}{\mu^2} \right) \left[\frac{32}{81} (9x - 77) + \frac{320}{27} H_0 + \frac{32}{9} H_0^2 \right] + \frac{64}{729} (45x - 421) + \frac{320}{81} H_0^2$$

$$+ \frac{64}{81} (3x - 5) H_0 + \frac{64}{81} H_0^3 + \frac{512}{27} \zeta_3 \right] + C_F^2 T_F \left[\ln^2 \left(\frac{m^2}{\mu^2} \right) \left[16 H_0 - \frac{64}{3} H_0 H_1 \right. \right.$$

$$\left. - \frac{8}{3} (2x + 1) \right] + \ln \left(\frac{m^2}{\mu^2} \right) \left[-\frac{8}{9} (14x + 1) - \frac{16}{9} \frac{3x + 1}{x + 1} H_0^3 \right.$$

$$+ 16 H_0^2 - \frac{128}{3} H_{0,0,1} + \frac{64}{3} H_0 \zeta_2 + \frac{320}{3} \zeta_3 - \frac{8}{3} (4x - 5) H_0 - \frac{16(1 - x) H_0^3}{9(x + 1)}$$

$$+ \left(-\frac{640}{9} H_0 - \frac{128}{3} H_0^2 \right) H_1 + \frac{128}{3} H_0 H_{0,1} \right] - \frac{2}{81} (476x - 7607)$$

$$+ \frac{1 - x}{x + 1} \left(\frac{64}{9} H_{0,0,0,1} + \frac{16}{9} H_0^2 \zeta_2 \right) + \frac{3x + 1}{x + 1} \left(\frac{64}{9} H_{0,0,0,1} + \frac{16}{9} H_0^2 \zeta_2 \right)$$

$$- \frac{4}{9} (12x - 5) H_0^2 - \frac{32}{81} H_0^3 - \frac{8}{9} H_0^4 - \frac{16}{27} (17x - 139) H_0 - \frac{64}{3} H_{0,0,1,1}$$

$$+ \left(\frac{8}{3} - \frac{16}{81} (18x + 439) H_0 - \frac{1280}{27} H_0^2 - \frac{256}{27} H_0^3 \right) H_1 + \left(-\frac{16}{9} + \frac{32}{9} H_0^2 \right) H_1^2$$

$$- \frac{128}{27} H_0 H_1^3 + \left(-\frac{32}{3} + \frac{1568}{27} H_0 + \frac{32}{3} H_0^2 - \frac{256}{9} H_0 H_1 + \frac{128}{9} H_1^2 \right) H_{0,1}$$

$$- \frac{32}{9} H_{0,1}^2 + \left(-\frac{1712}{27} - \frac{128}{9} H_0 + \frac{448}{9} H_1 \right) H_{0,0,1} + \left(16 + \frac{64}{3} H_0 \right.$$

$$\left. - \frac{64}{3} H_1 \right) H_{0,1,1} + \left(\frac{112}{9} + \frac{496}{27} H_0 - \frac{64}{3} H_0 H_1 - \frac{128}{9} H_1^2 + \frac{128}{9} H_{0,1} \right) \zeta_2$$

$$+ \left(-\frac{2344}{27} + \frac{128}{9} H_0 - \frac{256}{9} H_1 \right) \zeta_3 + \frac{544}{9} \zeta_4 - \frac{64}{3} B_4 \right]$$

$$+ C_A C_F T_F \left[\frac{176}{27} \ln^3 \left(\frac{m^2}{\mu^2} \right) + \ln^2 \left(\frac{m^2}{\mu^2} \right) \left[\frac{8}{9} (3x - 26) - \frac{16}{3} H_0^2 + \frac{32}{3} \zeta_2 \right] \right.$$

$$+ \ln\left(\frac{m^2}{\mu^2}\right)\left[-\frac{8}{81}(36x + 119) + \frac{8}{27}(9x - 224)H_0 + \frac{8}{3}(1-x)H_1 - \frac{248}{9}H_0^2\right.$$

$$+ 16H_0^2 H_1 - \frac{32}{9}H_0^3 - 32H_0 H_{0,1} + \frac{64}{3}H_{0,0,1} + \left(\frac{320}{9} + \frac{64}{3}H_0\right)\zeta_2 - 96\zeta_3\bigg]$$

$$- \frac{4}{729}(2016x + 8791) + \frac{4}{81}(9x - 755)H_0^2 - \frac{496}{81}H_0^3 - \frac{16}{27}H_0^4 + \frac{224}{9}H_{0,0,1,1}$$

$$- \frac{8}{81}(135x + 332)H_0 + \left(-\frac{32}{27}(10x - 1) + \frac{8}{9}(7x + 6)H_0 + \frac{160}{9}H_0^2\right.$$

$$+ \frac{112}{27}H_0^3\bigg)H_1 + \left(\frac{4(x+2)}{9} - \frac{8}{9}x(4x+3)H_0 - \frac{8}{9}H_0^2\right)H_1^2 + \frac{64}{27}H_0 H_1^3$$

$$+ \left(-\frac{16}{9}(7x + 5) - \frac{16}{9}(4x^2 + 3x + 23)H_0 - \frac{16}{3}H_0^2 + \left(\frac{128}{9}H_0\right.\right.$$

$$+ \frac{8}{9}(16x^2 + 12x + 9)\bigg)H_1 - \frac{128}{9}H_1^2\bigg)H_{0,1} + \left(\frac{16}{27}(36x^2 + 27x + 67)\right.$$

$$- \frac{32}{9}H_0 - \frac{320}{9}H_1\bigg)H_{0,0,1} + \frac{32}{9}H_{0,1}^2 + \left(-\frac{8}{3}(8x^2 + 6x + 9) - \frac{160}{9}H_0\right.$$

$$+ 32H_1\bigg)H_{0,1,1} - \frac{224}{9}H_{0,1,1,1} + \left(\frac{8}{81}(81x + 466) - \frac{16}{27}(12x^2 + 9x - 31)H_0\right.$$

$$- \frac{8}{9}(8x^2 + 6x + 9)H_1 + \frac{112}{9}H_0^2 + \frac{160}{9}H_0 H_1 + \frac{128}{9}H_1^2 - \frac{32}{9}H_{0,1}\bigg)\zeta_2$$

$$+ \left(\frac{4}{27}(144x^2 + 108x + 299) - \frac{160}{9}H_0 + \frac{32}{9}H_1\right)\zeta_3 - \frac{296}{3}\zeta_4 + \frac{32}{3}B_4\bigg]\bigg\}, \quad \text{(E.8)}$$

and

$$A_{qq,Q}^{\mathrm{NS,TR,b}}(x) = a_s^3\bigg\{C_F T_F\left(\frac{C_A}{2} - C_F\right)\bigg[\ln^2\left(\frac{m^2}{\mu^2}\right)\left[-\frac{16}{3}(x-1) + \frac{x}{x+1}\left(-\frac{128}{3}H_{-1}H_0\right.\right.$$

$$+ \frac{32}{3}H_0^2 + \frac{128}{3}H_{0,-1} - \frac{64}{3}\zeta_2\bigg)\bigg] + \ln\left(\frac{m^2}{\mu^2}\right)\left[(1-x)\left(\frac{112}{9} - \frac{32}{3}H_1\right)\right.$$

$$+ \frac{x}{x+1}\left(-\frac{1280}{9}H_{-1}H_0 + \left(\frac{320}{9} - \frac{64}{3}H_{-1}\right)H_0^2 + \frac{64}{9}H_0^3 + \frac{1280}{9}H_{0,-1}\right.$$

$$+ \frac{256}{3}H_{-1}H_{0,1} - \frac{256}{3}H_{0,-1,1} + \frac{128}{3}H_{0,0,-1} - \frac{128}{3}H_{0,0,1} - \frac{256}{3}H_{0,1,-1}$$

$$+ \left(-\frac{640}{9} - \frac{256}{3}H_{-1} + \frac{64}{3}H_0\right)\zeta_2 + 64\zeta_3\bigg)\bigg] + (1-x)\left(\frac{1168}{81} - \frac{224}{27}H_1\right.$$

$$+ \frac{32}{9}H_1^2\bigg) - \frac{16}{9}(x+1)H_0 + \frac{1}{x+1}\left(\left(\frac{64}{81}(9x^2 - 206x + 9)H_0 - \frac{640}{27}xH_0^2\right.\right.$$

$$- \frac{128}{27}xH_0^3\bigg)H_{-1} - \frac{256}{27}xH_{-1}^3 H_0 - \frac{16}{81}(9x^2 - 206x + 9)H_0^2 + \frac{64}{9}xH_{-1}^2 H_0^2$$

$$+ \frac{640}{81}xH_0^3 + \frac{32}{27}xH_0^4 + \left(-\frac{64}{81}(9x^2 - 206x + 9) + \frac{256}{9}xH_{-1}^2\right)H_{0,-1}$$

$$+ \frac{2560}{27}xH_{-1}H_{0,1} - \frac{512}{9}xH_{-1}H_{0,-1,-1} - \frac{2560}{27}xH_{0,-1,1} + \left(\frac{1280}{27}x\right.$$

$$- \frac{256}{9}xH_{-1}\bigg)H_{0,0,-1} + \left(-\frac{1280}{27}x + \frac{256}{9}xH_{-1}\right)H_{0,0,1} - \frac{2560}{27}xH_{0,1,-1}$$

$$- \frac{512}{9}xH_{-1}H_{0,1,1} + \frac{512}{9}xH_{0,-1,-1,-1} + \frac{512}{9}xH_{0,-1,1,1} + \frac{256}{9}xH_{0,0,-1,-1}$$

$$- \frac{256}{9} x H_{0,0,-1,1} + \frac{256}{9} x H_{0,0,0,-1} - \frac{256}{9} x H_{0,0,0,1} - \frac{256}{9} x H_{0,0,1,-1}$$

$$+ \frac{256}{9} x H_{0,0,1,1} + \frac{512}{9} x H_{0,1,-1,1} + \frac{512}{9} x H_{0,1,1,-1} + \left(\frac{32}{81} \left(9x^2 - 206x + 9 \right) \right.$$

$$- \frac{2560}{27} x H_{-1} - \frac{128}{9} x H_{-1}^2 + \left(\frac{640}{27} x - \frac{128}{9} x H_{-1} \right) H_0 + \frac{64}{9} x H_0^2 \right) \zeta_2$$

$$+ \left. \left(\frac{640}{9} x + \frac{512}{9} x H_{-1} - \frac{64}{9} x H_0 \right) \zeta_3 - \frac{112}{3} x \zeta_4 \right) \bigg] \bigg\} . \tag{E.9}$$

E.2.2. Pure-singlet operator matrix element

As already discussed in Section 5.1.3, the generalised harmonic sums appearing in the N space result for the pure-singlet OME can be expressed in terms of usual HPLs evaluated at argument $1-2x$. The x space representation of the constant term of the unrenormalised OME has already been given in Eqs. (5.63) and (5.64). The renormalised OME reads

$$A_{Qq}^{\mathrm{PS}}(x) = a_s^2 C_F T_F \left[L_M^2 \left[- \frac{4}{3} \frac{4x^2 + 7x + 4}{x} (1-x) - 8(1+x) H_0 \right] + L_M \left[8(1+x) H_0^2 \right. \right.$$

$$- \frac{16}{9} \frac{28x^2 + x + 10}{x} (1-x) - \frac{8}{3} \left(8x^2 + 15x + 3 \right) H_0 \right] + \left(- \frac{4}{3} H_0^3 + 16 H_0 H_{0,1} \right.$$

$$- 32 H_{0,0,1} \bigg) (1+x) + \left(- \frac{4}{27} \frac{400x^2 + 121x + 112}{x} + \frac{8}{3} \frac{4x^2 + 7x + 4}{x} H_0 H_1 \right.$$

$$- \frac{8}{3} \frac{4x^2 + 7x + 4}{x} H_{0,1} \bigg) (1-x) - \frac{8}{9} \left(56x^2 + 33x + 21 \right) H_0 + 32(1+x) \zeta_3$$

$$+ \frac{2}{3} \left(8x^2 + 15x + 3 \right) H_0^2 \right] + a_s^3 \bigg\{ C_A C_F T_F \left[L_M^3 \left[\left(\frac{8}{9} \frac{44x^2 - x + 44}{x} \right. \right. \right.$$

$$+ \frac{16}{9} \frac{4x^2 + 7x + 4}{x} H_1 \bigg) (1-x) + \frac{32}{3} (1+x) H_{0,1} + \frac{16}{9} \frac{8x^2 + 11x + 4}{x} H_0$$

$$+ \frac{16}{3} \left(2x - 1 \right) H_0^2 - \frac{32}{3} (1+x) \zeta_2 \right] + L_M^2 \left[\left(\frac{8}{27} \frac{1864x^2 - 485x + 694}{x} \right. \right.$$

$$+ \frac{32}{3} H_0^3 + \left(\frac{8}{9} \frac{104x^2 + 119x + 32}{x} - \frac{16}{3} \frac{4x^2 + 7x + 4}{x} H_0 \right) H_1 + 64 H_0 H_{0,-1}$$

$$- 128 H_{0,0,-1} \bigg) (1-x) + \left(- \frac{32}{3} \frac{4x^2 - 7x + 4}{x} H_{-1} H_0 - 32 H_0 H_{0,1} + 32 H_{0,0,1} \right.$$

$$+ \frac{32}{3} \frac{4x^2 - 7x + 4}{x} H_{0,-1} \bigg) (1+x) + \frac{8}{9} \frac{272x^3 + 103x^2 + 139x + 40}{x} H_0$$

$$+ \frac{8}{3} \left(16x - 17 \right) H_0^2 + \frac{32}{3} \left(10x + 7 \right) H_{0,1} + \left(- \frac{16}{3} \frac{4x^3 + 17x^2 + 11x + 4}{x} \right.$$

$$+ 32(1-x) H_0 \bigg) \zeta_2 - 64 \left(2x - 1 \right) \zeta_3 \right] + L_M \left[\left(\frac{8}{27} \frac{11542x^2 + 399x + 3892}{x} \right. \right.$$

$$+ \frac{8}{9} \frac{210x^2 - 559x - 186}{x} H_1 + \frac{4}{3} \frac{20x^2 + 21x + 2}{x} H_1^2 - \frac{8}{9} \frac{4x^2 + 7x + 4}{x} H_1^3$$

$$+ \left(- \frac{16}{9} \frac{203x^2 + 47x + 140}{x} H_1 - 8 \frac{4x^2 + 7x + 4}{x} H_1^2 \right) H_0 + 64 H_{0,-1}^2$$

$$+ \left(4 \frac{8x^2 + 17x + 8}{x} H_1 - 32 H_{0,-1} \right) H_0^2 + \frac{32}{3} \frac{4x^2 + 7x + 4}{x} H_1 H_{0,1}$$

$$
\begin{aligned}
&\left. - 128 H_0 H_{0,-1,-1} - 32\frac{x-2}{x}H_{0,0,-1}\right)(1-x) + \left(32x H_{-1}H_0^2\right. \\
&+\left(-\frac{32}{9}\frac{125x^2-20x+62}{x}H_{-1} + \frac{32}{3}\frac{4x^2-7x+4}{x}H_{-1}^2\right)H_0 \\
&+\left(\frac{32}{9}\frac{125x^2-20x+62}{x} - \frac{64}{3}\frac{4x^2-7x+4}{x}H_{-1}\right)H_{0,-1} + \left(56 H_0^2\right. \\
&+\frac{64}{3}\frac{2x^2+x+2}{x}H_{-1}\right)H_{0,1} + 32 H_{0,1}^2 + \frac{64}{3}\frac{4x^2-7x+4}{x}H_{0,-1,-1} \\
&-\frac{64}{3}\frac{2x^2+x+2}{x}H_{0,-1,1} - \frac{64}{3}\frac{2x^2+x+2}{x}H_{0,1,-1} - 96 H_0 H_{0,1,1} + 32 H_{0,0,1,1} \\
&\left. - 32 H_{0,1,1,1}\right)(1+x) + \frac{16}{27}\frac{3729x^3+2093x^2+2330x+224}{x}H_0 \\
&+ 32\frac{(1+x)(1-x)}{x}H_{-1}H_0^2 - \frac{4}{9}\left(606x^2-346x+377\right)H_0^2 - \frac{8}{9}\left(35x-46\right)H_0^3 \\
&+\left(\frac{8}{3}\frac{16x^3-41x^2-77x-40}{x}H_0 - \frac{8}{9}\frac{274x^3-205x^2+659x-200}{x}\right)H_{0,1} \\
&+\frac{4}{3}\left(4x-5\right)H_0^4 + 16\frac{4x^3-13x^2+3x-4}{x}H_0 H_{0,-1} - \left(192(x-2)x\right. \\
&\left. + 32\left(3x+1\right)H_0\right)H_{0,0,-1} + 96\left(x+3\right)H_{0,0,0,-1} + 32\left(23x+5\right)H_{0,0,0,1} \\
&+\left(-\frac{32}{3}\frac{4x^3-11x^2-17x-14}{x} - 32\left(11x+5\right)H_0\right)H_{0,0,1} \\
&+\frac{16}{3}\frac{8x^3+23x^2+5x-8}{x}H_{0,1,1} + \left(\left(-8H_0^2 - \frac{16}{3}\frac{4x^2+7x+4}{x}H_1\right.\right. \\
&\left. - 64 H_{0,-1}\right)(1-x) - \frac{8}{9}\frac{132x^3+313x^2-473x+168}{x} + \left(-96 H_{-1}\right. \\
&\left. - 32 H_{0,1}\right)(1+x) + \frac{8}{3}\left(8x^2-13x+59\right)H_0\right)\zeta_2 + \left(-32\left(16x+9\right)H_0\right. \\
&\left. + \frac{16}{3}\frac{52x^3-78x^2-33x-48}{x}\right)\zeta_3 - 4\left(209x+87\right)\zeta_4\right] \\
&+\left(\frac{4}{729}\frac{1368812x^2-97732x+353855}{x} - \frac{4}{243}\frac{724x^2-7160x+17239}{x}H_1\right. \\
&-\frac{4}{27}\frac{152x^2+203x+152}{x}H_0^3 H_1 + \frac{4}{81}\frac{770x^2+3230x-859}{x}H_1^2 \\
&+\frac{2}{9}\frac{112x^2+241x+112}{x}H_0^2 H_1^2 - \frac{4}{81}\frac{14x^2-67x-40}{x}H_1^3 \\
&-\frac{4}{27}\frac{4x^2+7x+4}{x}H_1^4 + \left(-\frac{8}{81}\frac{12284x^2-313x+3392}{x}H_1\right. \\
&\left. - \frac{8}{27}\frac{367x^2+244x+124}{x}H_1^2 - \frac{16}{27}\frac{4x^2+7x+4}{x}H_1^3\right)H_0 + \left(-\frac{232}{9}H_0^3\right. \\
&\left. + \frac{32}{9}\frac{4x^2-11x+4}{x}H_0 H_1\right)H_{0,-1} + \left(-\frac{8}{9}\frac{112x^2+223x+112}{x}H_0 H_1\right. \\
&\left. + \frac{32}{9}\frac{4x^2-11x+4}{x}H_{0,-1}\right)H_{0,1} + \left(\frac{248}{3}H_0^2 - \frac{64}{3}H_{0,-1}\right)H_{0,-1,-1}
\end{aligned}
$$

$$+ \frac{56}{3} H_0 H_{0,-1}^2 + \left(-\frac{64}{9} \frac{4x^2 - 11x + 4}{x} H_1 - 240 H_{0,-1} \right) H_{0,0,-1} + \left(\frac{752}{3} H_{0,-1} \right.$$

$$+ \frac{8}{9} \frac{176x^2 + 281x + 176}{x} H_1 \right) H_{0,0,1} + \frac{128}{9} \frac{4x^2 + 7x + 4}{x} H_1 H_{0,1,1}$$

$$+ \frac{64}{3} H_0 H_{0,-1,-1,-1} - 320 H_0 H_{0,0,-1,-1} - \frac{880}{3} H_0 H_{0,0,0,-1} - \frac{160}{3} H_{0,-1,-1,0,1}$$

$$+ \frac{128}{3} H_{0,-1,0,-1,-1} + \frac{256}{3} H_{0,0,-1,-1,-1} + 560 H_{0,0,-1,0,-1}$$

$$+ 1680 H_{0,0,0,-1,-1} \right) (1-x) + \left(\left(-\frac{8}{27} \frac{3472x^2 - 1089x + 1048}{x} H_{-1} \right. \right.$$

$$+ \frac{32}{27} \frac{131x^2 - 35x + 50}{x} H_{-1}^2 - \frac{16}{27} \frac{4x^2 - 7x + 4}{x} H_{-1}^3 \right) H_0$$

$$- \frac{2}{3} \frac{56x^2 - 65x + 56}{x} H_{-1}^2 H_0^2 + \frac{4}{3} \frac{16x^2 - 21x + 16}{x} H_{-1} H_0^3$$

$$+ \left(\frac{8}{27} \frac{3472x^2 - 1089x + 1048}{x} - \frac{64}{27} \frac{131x^2 - 35x + 50}{x} H_{-1} \right.$$

$$+ \frac{16}{9} \frac{4x^2 - 7x + 4}{x} H_{-1}^2 + \frac{8}{9} \frac{8x^2 + 67x + 8}{x} H_{-1} H_0 \right) H_{0,-1} - \frac{248}{3} H_0 H_{0,1}^2$$

$$+ \left(-\frac{8}{9} \frac{32x^2 + 61x + 32}{x} H_{-1}^2 + \frac{32}{3} \frac{8x^2 - 11x + 8}{x} H_{-1} H_0 - \frac{64}{3} H_0 H_{0,-1} \right.$$

$$- \frac{248}{9} H_0^3 \right) H_{0,1} + \left(\frac{64}{27} \frac{131x^2 - 35x + 50}{x} - \frac{32}{9} \frac{4x^2 - 7x + 4}{x} H_{-1} \right) H_{0,-1,-1}$$

$$+ \frac{16}{9} \frac{32x^2 + 61x + 32}{x} H_{-1} H_{0,-1,1} + \left(\frac{8}{9} \frac{152x^2 - 329x + 152}{x} H_{-1} \right.$$

$$+ \frac{128}{3} H_{0,1} \right) H_{0,0,-1} + \left(-\frac{8}{3} \frac{(7x - 8)(8x - 7)}{x} H_{-1} + \frac{656}{3} H_{0,1} \right) H_{0,0,1}$$

$$+ \frac{16}{9} \frac{32x^2 + 61x + 32}{x} H_{-1} H_{0,1,-1} + \left(\frac{64}{9} \frac{2x^2 + x + 2}{x} H_{-1} + 88 H_0^2 \right) H_{0,1,1}$$

$$+ \left(\frac{8}{3} \frac{(7x - 8)(8x - 7)}{x} + \frac{128}{3} H_0 \right) H_{0,0,-1,1} + \frac{32}{9} \frac{4x^2 - 7x + 4}{x} H_{0,-1,-1,-1}$$

$$- \frac{16}{9} \frac{32x^2 + 61x + 32}{x} [H_{0,-1,-1,1} + H_{0,-1,1,-1}] - \frac{64}{9} \frac{2x^2 + x + 2}{x} H_{0,-1,1,1}$$

$$- \frac{8}{9} \frac{152x^2 - 329x + 152}{x} H_{0,0,-1,-1} - \frac{16}{9} \frac{32x^2 + 61x + 32}{x} H_{0,1,-1,-1}$$

$$+ \left(\frac{8}{3} \frac{(7x - 8)(8x - 7)}{x} + \frac{128}{3} H_0 \right) H_{0,0,1,-1} - \frac{64}{3} H_0 H_{0,1,1,1}$$

$$- \frac{64}{9} \frac{2x^2 + x + 2}{x} [H_{0,1,-1,1} + H_{0,1,1,-1}] + 32 H_{0,0,1,1,1} + \frac{256}{3} H_{0,1,0,1,1}$$

$$- \frac{64}{3} H_{0,1,1,1,1} \right) (1+x) + \frac{16}{243} \frac{85213x^3 + 20744x^2 + 30011x + 3280}{x} H_0$$

$$+ \frac{4}{81} \frac{16316x^4 - 3871x^3 - 5796x^2 + 3628x - 11087}{1+x} \frac{H_0^2}{1-x}$$

$$+ \frac{4}{81} \left(966x^2 + 790x + 721 \right) H_0^3 - \frac{4}{9} \frac{692x^3 - 358x^2 + 115x - 458}{x} H_0^2 H_1$$

$$+ \frac{2}{27}(83x - 121)H_0^4 + \left(\frac{8}{27} \frac{874x^3 - 1866x^2 + 837x - 376}{x} H_0 \right.$$

$$- \frac{4}{9} \frac{88x^3 - 9x^2 - 39x + 144}{x} H_0^2 \right) H_{0,-1} - \frac{8}{9} \frac{8x^3 + 81x^2 - 87x + 80}{x} H_{0,-1}^2$$

$$- \frac{4}{15}(3x - 4)H_0^5 - \frac{8}{81} \frac{12078x^4 + 4106x^3 - 4355x^2 + 797x - 2496}{(1 + x)x} H_{0,1}$$

$$+ \left(\frac{8}{9} \frac{262x^3 - 306x^2 - 181x - 538}{x} H_0 - \frac{4}{9} \frac{144x^3 - 441x^2 - 357x - 296}{x} H_0^2 \right.$$

$$\left. - \frac{16}{27} \frac{167x^3 - 711x^2 + 657x - 140}{x} H_1 \right) H_{0,1} + \frac{4}{9} \frac{176x^3 - 237x^2 - 69x - 64}{x} H_{0,1}^2$$

$$+ \left(\frac{4}{27} \frac{430x^3 + 18x^2 - 63x + 376}{x} H_0^2 - \frac{16}{27} \frac{82x^3 - 78x^2 - 267x - 80}{x} H_{0,1} \right) H_{-1}$$

$$+ \frac{8}{9} \frac{8x^3 + 87x^2 - 249x + 152}{x} H_0 H_{0,-1,-1} + \left(\frac{16}{27} \frac{82x^3 - 78x^2 - 267x - 80}{x} \right.$$

$$\left. - \frac{64}{9} \frac{10x^3 + 3x^2 - 12x + 14}{x} H_0 \right) H_{0,-1,1} + \left(-\frac{8}{3} \frac{16x^3 - 15x^2 + 21x - 48}{x} H_0 \right.$$

$$\left. - \frac{64}{3}(6x - 7)H_0^2 - \frac{8}{27} \frac{2178x^3 - 3714x^2 + 1611x - 376}{x} \right) H_{0,0,-1}$$

$$+ \left(\frac{8}{27} \frac{556x^3 + 187x^2 + 2011x + 1854}{x} + \frac{16}{3}(57x + 31)H_0^2 \right.$$

$$\left. + \frac{8}{9} \frac{136x^3 - 1365x^2 - 567x - 440}{x} H_0 \right) H_{0,0,1} + \left(\frac{16}{27} \frac{82x^3 - 78x^2 - 267x - 80}{x} \right.$$

$$\left. - \frac{64}{9} \frac{10x^3 + 3x^2 - 12x + 14}{x} H_0 \right) H_{0,1,-1} + \left(-\frac{128}{9} \frac{11x^3 + 18x^2 - 10}{x} H_0 \right.$$

$$\left. - \frac{8}{27} \frac{188x^3 + 4040x^2 - 3271x + 392}{x} \right) H_{0,1,1} + \left(\frac{8}{9} \frac{88x^3 - 147x^2 - 39x + 56}{x} \right.$$

$$\left. + \frac{128}{3}(3x - 2)H_0 \right) H_{0,-1,0,1} + \frac{8}{3} \frac{88x^3 - 39x^2 + 39x - 48}{x} H_{0,0,0,-1}$$

$$+ \left(-\frac{16}{9} \frac{68x^3 - 1388x^2 - 395x - 292}{x} - 16(73x + 39)H_0 \right) H_{0,0,0,1}$$

$$+ \left(-\frac{16}{9} \frac{20x^3 - 563x^2 - 164x + 104}{x} + \frac{16}{3}(11x + 13)H_0 \right) H_{0,0,1,1}$$

$$+ \frac{16}{9} \frac{92x^3 + 83x^2 - 46x - 92}{x} H_{0,1,1,1} + \frac{32}{3}(21x - 29)H_{0,0,-1,0,1}$$

$$+ 16(39x - 55)H_{0,0,0,-1,1} - 256xH_{0,0,0,0,-1} + \frac{16}{3}(315x + 221)H_{0,0,0,0,1}$$

$$+ 16(39x - 55)H_{0,0,0,1,-1} - \frac{16}{3}(179x + 185)H_{0,0,0,1,1} - \frac{32}{3}(41x + 40)H_{0,0,1,0,1}$$

$$+ \frac{16}{3}(39x - 55)H_{0,0,1,0,-1} + \left(\left(\frac{8}{3} \frac{8x^2 + 11x + 8}{x} H_0 H_1 + \frac{8}{9} \frac{4x^2 + 7x + 4}{x} H_1^2 \right. \right.$$

$$\left. + \frac{160}{3} H_0 H_{0,-1} + 64 H_{0,-1,-1} - \frac{256}{3} H_{0,0,-1} \right)(1 - x) + \left(\frac{32}{9} \frac{7x^2 + 17x + 7}{x} H_{-1}^2 \right.$$

$$\left. - \frac{16}{9} \frac{56x^2 - 17x + 56}{x} H_{-1}H_0 - \frac{8}{9}H_0^3 + \frac{80}{3}H_0 H_{0,1} + \frac{32}{3}H_{0,1,1} \right)(1 + x)$$

$$
-\frac{16}{81}\frac{103x^4 + 1365x^3 + 1306x^2 + 1330x + 1124}{(1+x)x} - \frac{8}{27}\left(52x^2 + 1273x + 580\right)H_0
$$

$$
+\frac{16}{27}\frac{344x^3 + 114x^2 - 237x + 20}{x}H_{-1} + \frac{4}{9}\left(8x^2 - 37x - 109\right)H_0^2
$$

$$
+\frac{16}{27}\frac{62x^3 - 780x^2 + 807x - 116}{x}H_1 + \frac{16}{9}\frac{20x^3 + 81x^2 + 3x + 56}{x}H_{0,-1}
$$

$$
-\frac{8}{3}\frac{32x^3 - 101x^2 - 41x + 24}{x}H_{0,1} + \frac{64}{3}xH_{0,0,1}\Bigg)\zeta_2 - \frac{512}{3}(1+x)\ln^3(2)\zeta_2
$$

$$
+\left(-\left(160H_{-1} + 112H_{0,1}\right)(1+x) - \frac{4}{27}\frac{4x^3 + 8314x^2 + 4402x + 2103}{x}\right.
$$

$$
-\left(\frac{8}{3}\frac{16x^2 + 55x + 16}{x}H_1 + \frac{320}{3}H_{0,-1}\right)(1-x) + \frac{16}{3}\left(6x - 11\right)H_0^2
$$

$$
-\frac{16}{9}\frac{52x^3 + 806x^2 + 71x + 32}{x}H_0\Bigg)\zeta_3 + \left(\frac{448}{3}\frac{4x^3 - 9x^2 - 6x - 2}{x}\right.
$$

$$
-896(1+x)H_0\Bigg)\ln(2)\zeta_3 - 896(1+x)\ln^2(2)\zeta_3 + \frac{16}{3}\left(37x - 45\right)\zeta_2\zeta_3
$$

$$
+\left(-\frac{2}{9}\frac{1632x^3 + 9285x^2 + 2223x + 916}{x} - \frac{20}{3}\left(19x - 51\right)H_0\right)\zeta_4
$$

$$
-832(1+x)\ln(2)\zeta_4 - 4\left(x - 375\right)\zeta_5 + \left(\frac{16}{3}\frac{8x^3 - 30x^2 - 15x - 2}{x}\right.
$$

$$
-64(1+x)H_0\Bigg)B_4 - 2048(1+x)\,\mathrm{Li}_5\left(\frac{1}{2}\right) - 128(1+x)B_4\ln(2)
$$

$$
+\frac{256}{15}(1+x)\ln^5(2)\Bigg] + C_F^2 T_F\left[L_M^3\left[\left(-\frac{92}{9} - \frac{16}{9}\frac{4x^2 + 7x + 4}{x}H_1\right)(1-x)\right.\right.
$$

$$
+\left(-\frac{8}{3}H_0^2 - \frac{32}{3}H_{0,1}\right)(1+x) + \frac{16}{9}\left(4x + 3\right)xH_0 + \frac{32}{3}(1+x)\zeta_2\Bigg]
$$

$$
+L_M^2\left[\left(\frac{8}{3}\left(32x - 31\right)H_0 - \frac{16}{3}H_0^3 - 32H_0H_{0,1} + 32H_{0,0,1}\right)(1+x)\right.
$$

$$
+\frac{8}{3}\left(4x^2 - 9x - 3\right)H_0^2 + \left(-\frac{4}{3}\frac{32x^2 + 81x + 12}{x} - \frac{8}{3}\frac{32x^2 + 35x + 8}{x}H_1\right.
$$

$$
-\frac{16}{3}\frac{4x^2 + 7x + 4}{x}H_0H_1\Bigg)(1-x) - \frac{16}{3}\frac{4x^3 + 21x^2 + 9x - 4}{x}H_{0,1}
$$

$$
+\left(32(1+x)H_0 + 32\left(3x + 2\right)\right)\zeta_2 - 32(1+x)\zeta_3\Bigg] + L_M\left[-\frac{128}{3}x^2H_0^3\right.
$$

$$
+\left(-\frac{4}{27}\frac{3204x^2 + 1625x + 180}{x} - \frac{16}{27}\frac{229x^2 - 1175x - 239}{x}H_1\right.
$$

$$
-\frac{4}{3}\frac{28x^2 + 21x + 4}{x}H_1^2 + \frac{8}{9}\frac{4x^2 + 7x + 4}{x}H_1^3 - \frac{32}{3}\frac{4x^2 + 7x + 4}{x}H_1H_{0,1}
$$

$$
+\left(-\frac{8}{9}\frac{140x^2 - 127x + 104}{x}H_1 + \frac{16}{3}\frac{4x^2 + 7x + 4}{x}H_1^2\right)H_0\Bigg)(1-x)
$$

$$
+\left(-\frac{32}{3}H_0^3 + 6H_0^4 - 32H_{0,1}^2 + 96H_0H_{0,0,1} + 64H_0H_{0,1,1} - 96H_{0,0,0,1}\right.
$$

$$
+32H_{0,1,1,1}\Bigg)(1+x) + \left(\frac{8}{9}\frac{8x^3 + 303x^2 + 363x + 104}{x}\right.
$$

$$
\begin{aligned}
&-32\big(4x^2+3x+1\big)H_0\Big)H_{0,1}+\frac{8}{27}\big(242x^2-3984x-633\big)H_0\\
&+\frac{2}{3}\big(136x^2-111x+213\big)H_0^2-\frac{16}{3}\frac{12x^3+27x^2+3x-8}{x}H_{0,1,1}\\
&+\frac{32}{3}\big(8x^2+15\big)H_{0,0,1}+\bigg(\frac{32}{3}\big(2x+3\big)\big(8x-3\big)H_0-96(1+x)H_0^2\\
&-\frac{16}{9}\big(74x^2+18x+297\big)\bigg)\zeta_2+\bigg(192(1+x)H_0-16\frac{12x^3-x^2+x-8}{x}\bigg)\zeta_3\\
&+144(1+x)\zeta_4\bigg]+\bigg(\frac{4}{81}\frac{4464x^2+260x+7131}{x}+\bigg(\frac{4}{81}\frac{1892x^2+393x+5717}{x}\\
&+\frac{8}{81}\frac{3056x^2+7553x+338}{x}H_0-\frac{8}{27}\frac{362x^2+1157x-178}{x}H_0^2\\
&+\frac{104}{27}\frac{4x^2+7x+4}{x}H_0^3\bigg)H_1+\bigg(\frac{8}{27}\frac{122x^2-55x-40}{x}H_0+\frac{16}{9}\frac{4x^2+7x+4}{x}H_0^2\\
&-\frac{4}{81}\frac{1178x^2+8207x-1099}{x}\bigg)H_1^2+\bigg(\frac{16}{27}\frac{4x^2+7x+4}{x}H_0\\
&-\frac{4}{27}\frac{4x^2+47x+40}{x}\bigg)H_1^3+\frac{4}{27}\frac{4x^2+7x+4}{x}\Big[\big(36H_1+264H_0\big)H_{0,1}+H_1^3\\
&-528H_{0,0,1}-312H_{0,1,1}\big]H_1\bigg)(1-x)+\bigg(-\frac{16}{15}H_0^5+\frac{208}{9}H_0^3H_{0,1}+\frac{352}{3}H_0H_{0,1}^2\\
&-\bigg(96H_0^2+\frac{1408}{3}H_{0,1}\bigg)H_{0,0,1}+\bigg(\frac{64}{3}H_0^2+64H_{0,1}\bigg)H_{0,1,1}+\frac{1120}{3}H_0H_{0,0,0,1}\\
&-\frac{1408}{3}H_0H_{0,0,1,1}+\frac{64}{3}H_0H_{0,1,1,1}-\frac{3136}{3}H_{0,0,0,0,1}+2624H_{0,0,0,1,1}\\
&+\frac{3328}{3}H_{0,0,1,0,1}-416H_{0,0,1,1,1}-\frac{1024}{3}H_{0,1,0,1,1}+\frac{64}{3}H_{0,1,1,1,1}\bigg)(1+x)\\
&+\frac{2}{81}\big(4432x^3+9785x^2-11442x-1479\big)\frac{H_0^2}{1-x}+\frac{4}{81}\big(700x^2+2458x-2005\big)H_0\\
&+\bigg(\frac{8}{81}\frac{6370x^3+13932x^2-8163x-338}{x}-\frac{16}{27}\frac{792x^3+1518x^2-2247x+178}{x}H_0\\
&+\frac{8}{9}\frac{4x^3-369x^2-99x-52}{x}H_0^2\bigg)H_{0,1}-\frac{4}{27}\big(412x^2+67x+248\big)H_0^3\\
&+\frac{32}{9}\frac{4x^3-207x^2+207x-22}{x}H_1H_{0,1}+\frac{2}{27}\big(140x^2+39x+57\big)H_0^4\\
&-\frac{16}{9}\frac{80x^3-75x^2-105x-44}{x}H_{0,1}^2+\bigg(\frac{16}{27}\frac{736x^3+2064x^2-3639x+178}{x}\\
&-\frac{16}{9}\frac{44x^3-975x^2-201x-52}{x}H_0\bigg)H_{0,0,1}+\bigg(\frac{8}{27}\frac{728x^3+7179x^2-6090x+608}{x}\\
&+\frac{32}{3}\frac{28x^3+17x^2-26x-32}{x}H_0\bigg)H_{0,1,1}+\frac{16}{9}\frac{252x^3-1689x^2-411x-52}{x}H_{0,0,0,1}\\
&+\frac{32}{9}\frac{8x^3-381x^2-126x+96}{x}H_{0,0,1,1}-\frac{32}{9}\frac{120x^3+99x^2-69x-116}{x}H_{0,1,1,1}\\
&+\bigg(-\frac{64}{9}\frac{4x^2+7x+4}{x}\big[H_0H_1+H_1^2\big](1-x)+\bigg(\frac{224}{9}H_0^3-\frac{128}{3}H_0H_{0,1}-\frac{512}{3}H_{0,0,1}
\end{aligned}
$$

$$-\frac{256}{3}H_{0,1,1}\Big)(1+x)-\frac{8}{81}\left(3314x^2+9435x-948\right)+\frac{16}{9}\left(162x^2+59x+160\right)H_0$$

$$+\frac{16}{27}\frac{98x^3+1065x^2-1227x+172}{x}H_1+\frac{32}{9}\frac{40x^3-93x^2-60x+8}{x}H_{0,1}$$

$$-\frac{16}{9}\left(40x^2+45x-33\right)H_0^2\Big)\zeta_2+\left(\frac{416}{9}\frac{4x^2+7x+4}{x}(1-x)H_1+\left(\frac{832}{3}H_0^2\right.$$

$$+\frac{832}{3}H_{0,1}\Big)(1+x)-\frac{8}{27}\frac{1304x^3-849x^2-8448x+969}{x}$$

$$-\frac{32}{9}\left(92x^2-438x-159\right)H_0\Big)\zeta_3+\frac{1024}{3}(1+x)\ln^3(2)\zeta_2+\Big(1792(1+x)H_0$$

$$-\frac{896}{3}\frac{4x^3-9x^2-6x-2}{x}\Big)\ln(2)\zeta_3+1792(1+x)\ln^2(2)\zeta_3+288(1+x)\zeta_2\zeta_3$$

$$+\left(\frac{256}{3}(1+x)H_0-\frac{16}{9}\frac{16x^3-897x^2-9x+135}{x}\right)\zeta_4+1664(1+x)\ln(2)\zeta_4$$

$$-3384(1+x)\zeta_5+\left(128(1+x)H_0-\frac{32}{3}\frac{8x^3-30x^2-15x-2}{x}\right)B_4$$

$$+4096(1+x)\mathrm{Li}_5\left(\frac{1}{2}\right)+256(1+x)B_4\ln(2)-\frac{512}{15}(1+x)\ln^5(2)\bigg]$$

$$+C_FT_F^2\Bigg[L_M^3\bigg[-\frac{128}{27}\frac{4x^2+7x+4}{x}(1-x)-\frac{256}{9}(1+x)H_0\bigg]$$

$$+L_M^2\bigg[\left(-\frac{32}{27}\frac{94x^2+49x+40}{x}+\frac{32}{9}\frac{4x^2+7x+4}{x}H_1\right)(1-x)+\left(\frac{32}{3}H_0^2\right.$$

$$+\frac{64}{3}H_{0,1}\Big)(1+x)-\frac{32}{9}\left(12x^2+37x+19\right)H_0-\frac{64}{3}(1+x)\zeta_2\bigg]$$

$$+L_M\bigg[\left(-\frac{64}{9}H_0^3+\frac{128}{3}H_0H_{0,1}-\frac{128}{3}H_{0,0,1}-\frac{128}{3}H_{0,1,1}\right)(1+x)$$

$$+\left(-\frac{256}{81}\frac{40x^2+79x+31}{x}+\frac{32}{9}\frac{4x^2+7x+4}{x}\left[2H_0H_1-H_1^2\right]\right.$$

$$-\frac{64}{3}\left(2x-5\right)H_1\Big)(1-x)-\frac{64}{27}\left(18x^2+65x+101\right)H_0+\frac{32}{9}\left(4x^2-7x-13\right)H_0^2$$

$$+\frac{128}{9}\frac{5x^2+5x-2}{x}H_{0,1}+\left(-\frac{128}{3}(1+x)H_0+\frac{64}{9}\left(4x^2-7x-13\right)\right)\zeta_2$$

$$+\frac{256}{3}(1+x)\zeta_3\bigg]+\left(\frac{64}{3645}\frac{216x^4-1836x^3-1063x^2+8375x+3770}{x}\right.$$

$$+\left(\frac{32}{9}\frac{4x^2+7x+4}{x}H_0^2-\frac{64}{405}\frac{12x^4-102x^3-148x^2+385x-10}{x}\right.$$

$$-\frac{64}{135}\left(4x^4-36x^3-16x^2+124x-421\right)H_0\Big)H_1+\left(\frac{32}{9}\frac{4x^2+7x+4}{x}H_0\right.$$

$$+\frac{16}{405}\frac{24x^5-216x^4-96x^3+914x^2-3661x-100}{x}\Big)H_1^2-\frac{16}{81}\frac{4x^2+7x+4}{x}H_1^3$$

$$-\frac{128}{9}\frac{4x^2+7x+4}{x}H_1H_{0,1}\Big)(1-x)+\left(\frac{40}{27}H_0^4+\frac{64}{3}H_0^2H_{0,1}-\frac{128}{3}H_{0,1}^2\right.$$

$$-\frac{128}{3}H_0H_{0,0,1}+\frac{128}{3}H_0H_{0,1,1}-\frac{256}{9}H_{0,0,0,1}+\frac{128}{9}H_{0,0,1,1}-\frac{64}{9}H_{0,1,1,1}\Big)(1+x)$$

E. Results in x space

$$-\frac{16}{81}\left(24x^2-13x-49\right)H_0^3-\frac{32}{1215}\left(72x^4-684x^3-3276x^2+3553x-6005\right)H_0$$

$$+\left(-\frac{64}{405}\left(24x^5-240x^4+120x^3+1125x^2-3925x+1403\right)\right.$$

$$+\left.\frac{128}{9}\frac{5x^2+5x-2}{x}H_0\right)H_{0,1}+\frac{64}{27}\frac{24x^3-43x^2-79x+12}{x}H_{0,0,1}$$

$$+\frac{32}{405}\left(12x^5-120x^4+60x^3+420x^2-2465x+325\right)H_0^2$$

$$-\frac{64}{27}\frac{18x^3+73x^2+46x-36}{x}H_{0,1,1}+\left(\frac{64}{9}\frac{4x^2+7x+4}{x}(1-x)H_1+\left(\frac{128}{9}H_0^2\right.\right.$$

$$+\left.\left.\frac{128}{3}H_{0,1}\right)(1+x)+\frac{64}{405}\left(12x^5-120x^4+60x^3+705x^2-2290x+140\right)\right.$$

$$-\left.\frac{128}{27}\left(6x^2+4x-5\right)H_0\right)\zeta_2+\left(\frac{64}{27}\frac{2x^3+122x^2+119x-56}{x}\right.$$

$$-\left.\frac{128}{9}(1+x)H_0\right)\zeta_3+32(1+x)\zeta_4\Bigg]+C_FN_FT_F^2\Bigg[L_M^3\left[-\frac{64}{9}(1+x)H_0\right.$$

$$-\left.\frac{32}{27}\frac{4x^2+7x+4}{x}(1-x)\right]+L_M^2\left[\left(-\frac{32}{3}\left(2x-5\right)-\frac{32}{9}\frac{4x^2+7x+4}{x}H_1\right)(1-x)\right.$$

$$+\left.\left(\frac{32}{3}H_0^2-\frac{64}{3}H_{0,1}\right)(1+x)-\frac{32}{9}\left(4x^2-7x-13\right)H_0+\frac{64}{3}(1+x)\zeta_2\right]$$

$$+L_M\Bigg[\left(-\frac{64}{9}H_0^3+\frac{128}{3}H_0H_{0,1}-\frac{128}{3}H_{0,0,1}-\frac{64}{3}H_{0,1,1}\right)(1+x)$$

$$+\frac{64}{27}\left(x^2+2x-58\right)H_0+\left(-\frac{128}{81}\frac{25x^2+94x+34}{x}-\frac{32}{27}\frac{74x^2-43x+20}{x}H_1\right.$$

$$+\left.\frac{16}{9}\frac{4x^2+7x+4}{x}\left[4H_0H_1-H_1^2\right]\right)(1-x)+\frac{32}{9}\left(4x^2-7x-13\right)H_0^2$$

$$-\frac{64}{9}\frac{2x^3+x^2-2x+4}{x}H_{0,1}+\left(-\frac{128}{3}(1+x)H_0+\frac{64}{9}\left(6x^2+4x-5\right)\right)\zeta_2$$

$$+64(1+x)\zeta_3\Bigg]+\left(-\frac{64}{729}\frac{1697x^2-2023x+752}{x}-\frac{64}{81}\frac{150x^2+103x+60}{x}H_1\right.$$

$$-\frac{32}{9}\frac{4x^2+7x+4}{x}H_0^2H_1-\frac{16}{81}\frac{74x^2-43x+20}{x}H_1^2-\frac{16}{81}\frac{4x^2+7x+4}{x}H_1^3$$

$$+\left.\left(\frac{64}{3}\left(2x-5\right)H_1+\frac{32}{9}\frac{4x^2+7x+4}{x}H_1^2\right)H_0\right)(1-x)+\left(\frac{40}{27}H_0^4-\frac{64}{3}H_0^2H_{0,1}\right.$$

$$+\frac{128}{3}H_0H_{0,0,1}+\frac{128}{3}H_0H_{0,1,1}-\frac{256}{9}H_{0,0,0,1}-\frac{640}{9}H_{0,0,1,1}-\left.\frac{64}{9}H_{0,1,1,1}\right)(1+x)$$

$$+\left(\frac{64}{81}\left(111x^2+64x+100\right)-\frac{64}{9}\frac{4x^2+7x+4}{x}(1-x)H_1+\left(\frac{128}{9}H_0^2\right.\right.$$

$$-\left.\frac{128}{3}H_{0,1}\right)(1+x)-\frac{128}{27}\left(6x^2+4x-5\right)H_0\right)\zeta_2-\frac{32}{243}\left(300x^2-967x-769\right)H_0$$

$$+\frac{32}{81}\left(54x^2+29x+137\right)H_0^2-\frac{16}{81}\left(24x^2-13x-49\right)H_0^3-\left(\frac{64}{81}\left(57x^2+253x-35\right)\right.$$

$$+\left.\frac{128}{9}\frac{5x^2+5x-2}{x}H_0\right)H_{0,1}+\left(-\frac{128}{9}(1+x)H_0+\frac{64}{27}\frac{2x^3-58x^2-61x+16}{x}\right)\zeta_3$$

$$+ \frac{64}{27}\frac{59x^2 + 59x - 12}{x}H_{0,0,1} + \frac{64}{27}\frac{6x^3 + 5x^2 - 4x - 12}{x}H_{0,1,1} + 160(1+x)\zeta_4 \Bigg]$$

$$+ a_{Qq}^{\mathrm{PS,b,(3)}} \Bigg\}, \tag{E.10}$$

where $a_{Qq}^{\mathrm{PS,b,(3)}}$ refers to the term containing HPLs with non-standard argument, given in Eq. (5.64).

E.3. Wilson coefficients

For several cases, we have calculated the heavy flavour Wilson coefficients in the asymptotic limit $Q^2 \gg m^2$.

E.3.1. The unpolarised Wilson coefficient $L_{q,2}^{\mathsf{NS}}$

The non-singlet Wilson coefficient for the unpolarised structure function $F_2(x, Q^2)$ is given in x space by

$$
\begin{aligned}
L_{q,2}^{\mathrm{NS}}(x) = a_s^2 \Bigg\{ &\left(\frac{1}{1-x}C_F T_F \left[L_M^2 \frac{8}{3} + L_Q^2 \frac{8}{3} + L_M \left[\frac{16}{3}H_0 + \frac{80}{9} \right] + L_Q \left[-\frac{32}{3}H_0 \right.\right.\right. \\
&\left. -\frac{16}{3}H_1 - \frac{116}{9} \right] + \frac{8}{3}H_1^2 + \frac{16}{3}H_{0,1} + 8H_0^2 + \frac{268}{9}H_0 + \left(\frac{16}{3}H_0 + \frac{116}{9} \right)H_1 \\
&\left.\left. + \frac{718}{27} - \frac{32}{3}\zeta_2 \right] \right)_+ + \delta(1-x)C_F T_F \left[2L_M^2 + 2L_Q^2 + L_M\frac{2}{3} - L_Q\frac{38}{3} + \frac{265}{9} \right] \\
&+ C_F T_F \left[-L_M^2 \frac{4}{3}(x+1) - L_Q^2 \frac{4}{3}(x+1) + L_M \left[-\frac{8}{9}(11x-1) \right.\right. \\
&\left. -\frac{8}{3}(x+1)H_0 \right] + L_Q \left[\frac{8}{9}(17x+8) + (x+1)\left(\frac{16}{3}H_0 + \frac{8}{3}H_1 \right) \right] \\
&+ (x+1)\left(-\frac{4}{3}H_1^2 - \frac{8}{3}H_{0,1} - 4H_0^2 - \frac{8}{3}H_1 H_0 + \frac{16}{3}\zeta_2 \right) \\
&\left.\left. -\frac{8}{9}(17x+8)H_1 - \frac{4}{27}(311x+68) - \frac{8}{9}(34x+19)H_0 \right] \right\} \\
&+ a_s^3 \Bigg\{ \left(\frac{1}{(1-x)^2}C_A C_F T_F \left[\frac{32}{3}H_{0,1} - \frac{4}{3}H_0^2 - \frac{32}{3}\zeta_2 \right] \right. \\
&+ \frac{1}{1-x}\left\{ C_F T_F^2 N_F \left[L_M^3 \frac{64}{27} + L_Q^3 \frac{128}{27} + L_Q^2 \left[-\frac{256}{9}H_0 - \frac{128}{9}H_1 - \frac{928}{27} \right] \right.\right. \\
&+ L_M \left[-\frac{32}{9}H_0^2 - \frac{320}{27}H_0 + \frac{2176}{81} \right] + L_Q \left[\frac{128}{3}H_0^2 + \left(\frac{256}{9}H_0 + \frac{1856}{27} \right)H_1 \right] \\
&+ \frac{128}{9}H_1^2 + \frac{256}{9}H_{0,1} + \frac{4288}{27}H_0 - \frac{512}{9}\zeta_2 + \frac{7520}{81} \right] - \frac{64}{81}H_0^3 - \frac{320}{81}H_0^2 \\
&\left. + \frac{128}{81}H_0 + \frac{24064}{729} - \frac{512}{27}\zeta_3 \right] + C_A C_F T_F \left[-L_M^3 \frac{176}{27} - L_Q^3 \frac{352}{27} \right. \\
&+ L_M^2 \left[\frac{16}{3}H_0^2 - \frac{32}{3}\zeta_2 + \frac{184}{9} \right] + L_Q^2 \left[\frac{16}{3}H_0^2 + \frac{352}{9}H_1 + \frac{704}{9}H_0 - \frac{32}{3}\zeta_2 \right.
\end{aligned}
$$

$$+ \frac{3104}{27} \Bigg] + L_M \Bigg[\frac{248}{9} H_0^2 + \frac{1792}{27} H_0 + \frac{32}{9} H_0^3 - 16 H_0^2 H_1 + 32 H_0 H_{0,1}$$

$$- \frac{64}{3} H_{0,0,1} + \left(-\frac{64}{3} H_0 - \frac{320}{9} \right) \zeta_2 + 96 \zeta_3 + \frac{1240}{81} \Bigg] + L_Q \Bigg[-\frac{80}{9} H_0^3$$

$$- \frac{1216}{9} H_0^2 + \left(-\frac{16}{3} H_0^2 - \frac{704}{9} H_0 - \frac{6208}{27} \right) H_1 + \left(\frac{32}{3} H_0 - \frac{352}{9} \right) H_1^2$$

$$+ \left(\frac{32}{3} H_0 - \frac{128}{3} H_1 - \frac{704}{9} \right) H_{0,1} - 64 H_0 H_{0,-1} + 128 H_{0,0,-1}$$

$$- \frac{128}{3} H_{0,0,1} + 64 H_{0,1,1} - \frac{14144}{27} H_0 + \left(\frac{128}{3} H_0 + 64 H_1 + 192 \right) \zeta_2$$

$$- \frac{256}{3} \zeta_3 - \frac{30124}{81} \Bigg] + \frac{43228}{729} + \frac{3256}{81} H_0 + \frac{496}{81} H_0^3 + \frac{3200}{81} H_0^2$$

$$+ \left(-\frac{112}{27} H_0^3 - \frac{160}{9} H_0^2 - \frac{32}{9} H_0 + \frac{32}{3} \right) H_1 + \frac{8}{9} H_0^2 H_1^2 - \frac{64}{27} H_0 H_1^3$$

$$+ \left(\frac{16}{3} H_0^2 + \frac{368}{9} H_0 - \frac{32}{9} + \frac{128}{9} H_1^2 + \left(-\frac{128}{9} H_0 - 8 \right) H_1 \right) H_{0,1}$$

$$+ \left(\frac{32}{9} H_0 + \frac{320}{9} H_1 - \frac{1072}{27} \right) H_{0,0,1} + \left(\frac{160}{9} H_0 - 32 H_1 + 24 \right) H_{0,1,1}$$

$$+ \frac{224}{9} H_{0,1,1,1} - \frac{224}{9} H_{0,0,1,1} + \frac{16}{27} H_0^4 - \frac{32}{9} H_{0,1}^2 + \left(-\frac{112}{9} H_0^2 - \frac{496}{27} H_0 \right.$$

$$- \frac{3008}{81} + \left(8 - \frac{160}{9} H_0 \right) H_1 - \frac{128}{9} H_1^2 + \frac{32}{9} H_{0,1} \left. \right) \zeta_2 + \left(\frac{160}{9} H_0 \right.$$

$$- \frac{32}{9} H_1 - \frac{1196}{27} \left. \right) \zeta_3 + \frac{296}{3} \zeta_4 - \frac{32}{3} B_4 \Bigg] + C_F T_F^2 \Bigg[L_M^3 \frac{128}{27} + L_Q^3 \frac{64}{27}$$

$$+ L_M^2 \left[\frac{64}{9} H_0 + \frac{320}{27} \right] + L_Q^2 \left[-\frac{128}{9} H_0 - \frac{64}{9} H_1 - \frac{464}{27} \right] + L_M \frac{1984}{81}$$

$$+ L_Q \Bigg[\frac{64}{3} H_0^2 + \left(\frac{128}{9} H_0 + \frac{928}{27} \right) H_1 + \frac{64}{9} H_1^2 + \frac{128}{9} H_{0,1} + \frac{2144}{27} H_0$$

$$- \frac{256}{9} \zeta_2 + \frac{3760}{81} \Bigg] - \frac{12064}{729} - \frac{32}{81} H_0^3 - \frac{160}{81} H_0^2 + \frac{64}{81} H_0 + \frac{896}{27} \zeta_3 \Bigg]$$

$$+ C_F^2 T_F \Bigg[L_M^2 L_Q \left[-\frac{32}{3} H_0 - \frac{64}{3} H_1 + 16 \right] + L_Q^3 \left[-\frac{32}{3} H_0 - \frac{64}{3} H_1 + 16 \right]$$

$$+ L_M^2 \Bigg[16 H_1^2 + \left(\frac{128}{3} H_0 + 8 \right) H_1 + \frac{16}{3} H_0^2 - 16 H_0 - \frac{64}{3} \zeta_2 - 22 \Bigg]$$

$$+ L_M L_Q \Bigg[\left(-\frac{64}{3} H_0 - \frac{640}{9} \right) H_1 - \frac{32}{3} H_0^2 - \frac{176}{9} H_0 + \frac{64}{3} \zeta_2 + \frac{88}{3} \Bigg]$$

$$+ L_Q^2 \Bigg[48 H_1^2 + \frac{80}{3} H_0^2 + \left(\frac{320}{3} H_0 + \frac{856}{9} \right) H_1 + \frac{32}{9} H_0 - \frac{256}{3} \zeta_2 - \frac{334}{3} \Bigg]$$

$$+ L_M \Bigg[\left(\frac{160}{3} H_0^2 + \frac{1424}{9} H_0 + \frac{152}{3} \right) H_1 + \left(\frac{32}{3} H_0 + \frac{160}{3} \right) H_1^2 + \frac{64}{9} H_0^3$$

$$- \frac{64}{3} H_0 H_{0,1} + \frac{88}{9} H_0^2 - \frac{112}{3} H_0 + \left(-\frac{128}{3} H_0 - \frac{64}{3} H_1 - \frac{784}{9} \right) \zeta_2$$

$$- 64 \zeta_3 - \frac{206}{3} \Bigg] + L_Q \Bigg[\left(-128 H_0 - \frac{512}{3} \right) H_1^2 + \left(-128 H_0^2 - \frac{3680}{9} H_0 \right.$$

$$-\frac{4556}{27}\Big)H_1 - \frac{224}{9}H_0^3 + 128H_0H_{0,-1} + \Big(-\frac{64}{3}H_0 + \frac{64}{3}H_1 + 48\Big)H_{0,1}$$

$$-256H_{0,0,-1} - 64H_{0,1,1} - \frac{320}{9}H_1^3 - \frac{160}{3}H_0^2 + \frac{4508}{27}H_0 + \Big(\frac{832}{3}H_0$$

$$+\frac{448}{3}H_1 + \frac{2608}{9}\Big)\zeta_2 + 320\zeta_3 + \frac{2360}{9}\Big] - \frac{3262}{27}H_0 - \frac{14197}{54} + \frac{380}{81}H_0^3$$

$$+\frac{196}{27}H_0^2 + \frac{4}{3}H_0^4 + \Big(\frac{304}{27}H_0^3 + \frac{1628}{27}H_0^2 + \frac{13624}{81}H_0 + \frac{302}{9}\Big)H_1$$

$$+\Big(-\frac{8}{9}H_0^2 + \frac{80}{9}H_0 + \frac{448}{9}\Big)H_1^2 + \Big(-\frac{32}{3}H_0^2 - \frac{1304}{27}H_0 + \frac{160}{9}H_0H_1$$

$$-\frac{128}{9}H_1^2 + \frac{112}{9}\Big)H_{0,1} - \frac{16}{9}H_{0,1}^2 + \Big(\frac{128}{9}H_0 - \frac{256}{9}H_1 + \frac{1184}{27}\Big)H_{0,0,1}$$

$$+\Big(-\frac{32}{3}H_0 + \frac{64}{3}H_1 - 16\Big)H_{0,1,1} + \frac{64}{3}H_{0,0,1,1} - \frac{128}{9}H_{0,0,0,1}$$

$$+\frac{128}{27}H_0H_1^3 + \Big(-\frac{80}{9}H_0^2 - \frac{1192}{27}H_0 - \frac{2488}{27} + \Big(\frac{32}{3}H_0 - \frac{160}{9}\Big)H_1$$

$$+\frac{128}{9}H_1^2 - \frac{32}{9}H_{0,1}\Big)\zeta_2 + \Big(-\frac{128}{9}H_0 + \frac{160}{9}H_1 + \frac{3088}{27}\Big)\zeta_3 + \frac{64}{3}B_4$$

$$-\frac{664}{9}\zeta_4\Big]\Big\}\Big)_+ + \delta(1-x)\Big\{C_AC_FT_F\Big[-L_M^3\frac{44}{9} - L_Q^3\frac{88}{9} + L_M^2\Big[\frac{34}{3} - \frac{16}{3}\zeta_3\Big]$$

$$+L_Q^2\Big[\frac{938}{9} - \frac{16}{3}\zeta_3\Big] + L_M\Big[-\frac{1595}{27} + \frac{68}{3}\zeta_4 + \frac{272}{9}\zeta_3\Big] + L_Q\Big[-\frac{11032}{27}$$

$$-\frac{32}{3}\zeta_2 + \frac{1024}{9}\zeta_3 - \frac{196}{3}\zeta_4\Big] + \frac{55}{243} - \frac{10045}{81}\zeta_3 + \frac{2624}{27}\zeta_4 - 8B_4 - \frac{16}{9}\zeta_2\zeta_3$$

$$-\frac{176}{9}\zeta_5\Big] + C_F^2T_F\Big[6L_M^2L_Q + 6L_Q^3 + L_M^2\Big[\frac{32}{3}\zeta_3 - 10\Big] + L_Q^2\Big[\frac{32}{3}\zeta_3 - 48\Big]$$

$$+2L_ML_Q + L_M\Big[-5 - \frac{112}{9}\zeta_3 - \frac{136}{3}\zeta_4\Big] + L_Q\Big[\frac{368}{3} + \frac{64}{3}\zeta_2 - \frac{1616}{9}\zeta_3$$

$$+\frac{392}{3}\zeta_4\Big] - \frac{2039}{18} + \frac{13682}{81}\zeta_3 - \frac{3304}{27}\zeta_4 + \frac{32}{9}\zeta_2\zeta_3 + \frac{352}{9}\zeta_5 + 16B_4\Big]$$

$$+C_FT_F^2N_F\Big[L_M^3\frac{16}{9} + L_Q^3\frac{32}{9} - L_Q^2\frac{304}{9} + L_M\frac{700}{27} + L_Q\frac{3248}{27} + \frac{4732}{243}$$

$$-\frac{128}{9}\zeta_3\Big] + C_FT_F^2\Big[L_M^3\frac{32}{9} + L_Q^3\frac{16}{9} + L_M^2\frac{8}{9} - L_Q^2\frac{152}{9} + L_M\frac{496}{27}$$

$$+L_Q\frac{1624}{27} - \frac{3658}{243} + \frac{224}{9}\zeta_3\Big]\Big\} + C_FT_F^2\Big[-L_M^3\frac{64}{27}(x+1) - L_Q^3\frac{32}{27}(x+1)$$

$$+L_M^2\Big[-\frac{32}{27}(11x-1) - \frac{32}{9}(x+1)H_0\Big] + L_Q^2\Big[(x+1)\Big(\frac{64}{9}H_0 + \frac{32}{9}H_1\Big)$$

$$+\frac{32}{27}(17x+8)\Big] - L_M\frac{992}{81}(x+1) + L_Q\Big[-\frac{32}{81}(280x+37)$$

$$-\frac{64}{27}(34x+19)H_0 + (x+1)\Big(-\frac{32}{9}H_1^2 - \frac{64}{9}H_0H_1 - \frac{64}{9}H_{0,1} - \frac{32}{3}H_0^2$$

$$+ \frac{128}{9}\zeta_2\Big) - \frac{64}{27}(17x+8)H_1\bigg] + \frac{16}{729}(431x+323) + \frac{16}{81}(11x-1)H_0^2$$

$$+ \frac{64}{81}(6x-7)H_0 + (x+1)\Big(\frac{16}{81}H_0^3 - \frac{448}{27}\zeta_3\Big)\bigg]$$

$$+ C_F T_F^2 N_F\bigg[-L_M^3\frac{32}{27}(x+1) - L_Q^3\frac{64}{27}(x+1) + L_Q^2\Big[\frac{64}{27}(17x+8)$$

$$+ (x+1)\Big(\frac{128}{9}H_0 + \frac{64}{9}H_1\Big)\Big] + L_M\Big[\frac{16}{9}(x+1)H_0^2 + \frac{32}{81}(5x-73)$$

$$+ \frac{32}{27}(11x-1)H_0\Big] + L_Q\Big[-\frac{64}{81}(280x+37) - \frac{128}{27}(34x+19)H_0$$

$$- \frac{128}{27}(17x+8)H_1 + (x+1)\Big(-\frac{64}{9}H_1^2 - \frac{128}{9}H_0H_1 - \frac{128}{9}H_{0,1} - \frac{64}{3}H_0^2$$

$$+ \frac{256}{9}\zeta_2\Big)\Big] + \frac{128}{81}(6x-7)H_0 - \frac{64}{729}(161x+215) + \frac{32}{81}(11x-1)H_0^2$$

$$+ (x+1)\Big(\frac{32}{81}H_0^3 + \frac{256}{27}\zeta_3\Big)\bigg] + C_A C_F T_F\bigg[L_M^3\frac{88}{27}(x+1) + L_Q^3\frac{176}{27}(x+1)$$

$$+ L_M^2\bigg[\frac{1}{x+1}\Big(-\frac{16}{3}H_0^2 - \frac{64}{3}H_{0,-1} + \frac{64}{3}H_{-1}H_0 + \frac{32}{3}\zeta_2\Big) - \frac{16}{3}xH_0^2$$

$$- \frac{4}{9}(35x+11) + (1-x)\Big(\frac{32}{3}H_{0,-1} - \frac{32}{3}H_{-1}H_0\Big) + \frac{32x}{3}\zeta_2\bigg]$$

$$+ L_Q^2\bigg[\frac{1}{x+1}\Big(-\frac{16}{3}H_0^2 - \frac{64}{3}H_{0,-1} + \frac{64}{3}H_{-1}H_0 + \frac{32}{3}\zeta_2\Big) - \frac{16}{3}xH_0^2$$

$$+ (x+1)\Big(-\frac{352}{9}H_0 - \frac{176}{9}H_1\Big) + (1-x)\Big(\frac{32}{3}H_{0,-1} - \frac{32}{3}H_{-1}H_0\Big)$$

$$- \frac{4}{27}(853x+385) + \frac{32x}{3}\zeta_2\bigg] + L_M\bigg[\frac{1}{x+1}\Big(\Big(\frac{32}{3}H_{-1} - \frac{160}{9}\Big)H_0^2 - \frac{32}{9}H_0^3$$

$$+ \frac{640}{9}H_{-1}H_0 - \frac{640}{9}H_{0,-1} + \frac{128}{3}H_{0,-1,1} - \frac{128}{3}H_{-1}H_{0,1} + \frac{64}{3}H_{0,0,1}$$

$$- \frac{64}{3}H_{0,0,-1} + \frac{128}{3}H_{0,1,-1} + \Big(\frac{128}{3}H_{-1} - \frac{32}{3}H_0 + \frac{320}{9}\Big)\zeta_2 - 32\zeta_3\Big)$$

$$+ \frac{128}{9}(4x-1)H_{-1}H_0 - \frac{32}{27}(76x+7)H_0 - \frac{32}{9}xH_0^3 - \frac{4}{9}(57x+11)H_0^2$$

$$+ (x+1)\Big(8H_1H_0^2 + \Big(16 - 16H_0\Big)H_{0,1}\Big) - \frac{128}{9}(4x-1)H_{0,-1}$$

$$+ (1-x)\Big(32H_1 + \frac{64}{3}H_{-1}H_{0,1} + \frac{32}{3}H_{0,0,-1} - \frac{64}{3}H_{0,-1,1} - \frac{64}{3}H_{0,1,-1}$$

$$- \frac{16}{3}H_{-1}H_0^2 - \frac{64}{3}H_{-1}\zeta_2\Big) + \frac{64}{3}xH_{0,0,1} - \frac{4}{81}(2381x-2071)$$

$$+ \Big(\frac{16}{9}(23x-9) + \frac{16}{3}(x+3)H_0\Big)\zeta_2 - 32(2x+1)\zeta_3\bigg]$$

$$+ L_Q\bigg[-\frac{4\big(3888x^3 - 83347x^2 - 7873x + 432\big)}{405x} + \frac{1}{x+1}\Big(\frac{128}{3}H_0H_{-1}^2$$

$$+ \frac{64}{3}H_0 + \Big(-64H_0^2 - \frac{640}{9}H_0\Big)H_{-1} + \frac{80}{9}H_0^3 + \frac{160}{9}H_0^2 + \Big(-\frac{256}{3}H_{-1}$$

$$+ \frac{128}{3}H_0 + \frac{640}{9}\right)H_{0,-1} + \frac{256}{3}H_{0,-1,-1} + \frac{128}{3}H_{0,0,-1} + \left(\frac{128}{3}H_{-1} - \frac{32}{3}H_0\right.$$

$$- \frac{320}{9}\right)\zeta_2 - \frac{128}{3}\zeta_3\right) + \frac{32}{3}(7x-1)H_{-1}^2 H_0 - \frac{8}{45}\left(108x^3 - 595x - 330\right)H_0^2$$

$$+ \frac{80}{9}xH_0^3 + \left(\frac{32\left(54x^5 - 155x^3 - 115x^2 - 6\right)}{45x^2}H_0 - \frac{16}{3}(11x-5)H_0^2\right)H_{-1}$$

$$+ \left(\frac{8}{3}(11x-1)H_0^2 + \frac{8}{27}(1195x+169)\right)H_1 + \left(\frac{320}{3}xH_0 - \frac{64}{3}(7x-1)H_{-1}\right.$$

$$- \frac{32\left(54x^5 - 155x^3 - 115x^2 - 6\right)}{45x^2}\right)H_{0,-1} - \frac{16}{3}(11x-1)H_0 H_{0,1}$$

$$+ \frac{64}{3}(7x-1)H_{0,-1,-1} - \frac{32}{3}(9x+5)H_{0,0,-1} + (x+1)\left(\left(\frac{176}{9} - \frac{16}{3}H_0\right)H_1^2\right.$$

$$+ \frac{352}{9}H_0 H_1 + \left(\frac{64}{3}H_1 + \frac{208}{9}\right)H_{0,1} - 32H_{0,1,1}\right) + \frac{32}{3}(7x+1)H_{0,0,1}$$

$$- \frac{32\left(162x^3 - 2641x^2 - 1051x - 18\right)}{135x}H_0 + \left(\frac{16}{45}\left(108x^3 - 485x - 175\right)\right.$$

$$+ \frac{32}{3}(7x-1)H_{-1} - \frac{16}{3}(5x+3)H_0 - \frac{64}{3}(4x+1)H_1\right)\zeta_2 - \frac{64}{3}(4x-3)\zeta_3\Bigg]$$

$$+ (1-x)\left(\frac{16}{9}H_{-1}^2 H_0^2 - \frac{32}{27}H_{-1}H_0^3 + \frac{64}{9}H_{-1}^2 H_{0,-1} - \frac{128}{9}H_{-1}H_{0,-1,-1}\right.$$

$$+ \frac{64}{9}H_{-1}H_{0,0,1} - \frac{64}{9}H_{-1}H_{0,0,-1} + \frac{128}{9}H_{0,-1,-1,-1} - \frac{128}{9}H_{-1}H_{0,1,1}$$

$$+ \frac{128}{9}H_{0,-1,1,1} + \frac{64}{9}H_{0,0,-1,-1} + \frac{64}{9}H_{0,0,0,-1} - \frac{64}{9}H_{0,0,-1,1} + \frac{128}{9}H_{0,1,-1,1}$$

$$- \frac{64}{9}H_{0,0,1,-1} + \frac{128}{9}H_{0,1,1,-1} - \frac{64}{27}H_{-1}^3 H_0 + \left(-\frac{32}{9}H_{-1}^2 - \frac{32}{9}H_0 H_{-1}\right)\zeta_2$$

$$+ \frac{128}{9}H_{-1}\zeta_3\right) + \frac{1}{x+1}\left(\left(-\frac{32}{9}H_{-1}^2 + \frac{320}{27}H_{-1} - \frac{1792}{81}\right)H_0^2 + \left(\frac{64}{27}H_{-1}\right.\right.$$

$$- \frac{320}{81}\right)H_0^3 + \left(\frac{128}{27}H_{-1}^3 + \frac{7168}{81}H_{-1}\right)H_0 + \left(-\frac{128}{9}H_{-1}^2 - \frac{7168}{81}\right)H_{0,-1}$$

$$+ \frac{256}{9}H_{-1}H_{0,-1,-1} - \frac{1280}{27}H_{-1}H_{0,1} + \frac{1280}{27}H_{0,-1,1} + \left(\frac{128}{9}H_{-1}\right.$$

$$- \frac{640}{27}\right)H_{0,0,-1} + \left(\frac{640}{27} - \frac{128}{9}H_{-1}\right)H_{0,0,1} + \frac{1280}{27}H_{0,1,-1} - \frac{256}{9}H_{0,-1,-1,-1}$$

$$+ \frac{256}{9}H_{-1}H_{0,1,1} - \frac{256}{9}H_{0,-1,1,1} + \frac{128}{9}H_{0,0,-1,1} - \frac{128}{9}H_{0,0,-1,-1}$$

$$+ \frac{128}{9}H_{0,0,0,1} - \frac{128}{9}H_{0,0,0,-1} + \frac{128}{9}H_{0,0,1,-1} - \frac{128}{9}H_{0,0,1,1} - \frac{256}{9}H_{0,1,-1,1}$$

$$- \frac{256}{9}H_{0,1,1,-1} - \frac{16}{27}H_0^4 + \left(\frac{64}{9}H_{-1}^2 + \frac{1280}{27}H_{-1} + \frac{3584}{81} - \frac{32}{9}H_0^2\right.$$

$$+ \left(\frac{64}{9}H_{-1} - \frac{320}{27}\right)H_0\right)\zeta_2 + \left(-\frac{256}{9}H_{-1} + \frac{32}{9}H_0 - \frac{320}{9}\right)\zeta_3 + \frac{56}{3}\zeta_4\right)$$

$$+ (x+1)\left(-\frac{32}{9}H_{-1}^2 H_0 + \frac{32}{27}H_0 H_1^3 - \frac{4}{9}H_0^2 H_1^2 + \frac{64}{9}H_{-1}H_{0,-1} - \frac{64}{9}H_{0,-1,-1}\right.$$

$$+ \left(-\frac{64}{9}H_1^2 + \frac{64}{9}H_0 H_1 - \frac{8}{3}H_0^2\right)H_{0,1} - \frac{160}{9}H_1 H_{0,0,1} + 16H_1 H_{0,1,1}$$

$$+ \frac{56}{27} H_1 H_0^3 - \frac{112}{9} H_{0,1,1,1} + \left(\frac{64}{9} H_1^2 + \frac{80}{9} H_0 H_1 \right) \zeta_2 + \frac{16}{9} H_1 \zeta_3 + \frac{16}{3} B_4 \Bigg)$$

$$- \frac{4}{81} (3235x - 567) H_0 + \left(\frac{16}{27} (19x - 1) H_0^2 + \frac{32}{81} (199x - 25) H_0 \right) H_{-1}$$

$$- \frac{8}{81} (54x + 11) H_0^3 - \frac{4}{81} (789x + 8) H_0^2 + \left(\frac{8}{9} (14x + 3) H_0^2 + \frac{8}{9} (9x + 4) H_0 \right.$$

$$\left. - \frac{8}{9} (103x - 91) \right) H_1 - \frac{32}{81} (199x - 25) H_{0,-1} + \left(-\frac{4}{9} (11x - 14) \right.$$

$$\left. - \frac{8}{9} (2x + 5) H_0 \right) H_1^2 + \left(\frac{8}{9} (7x + 54) - \frac{256}{27} (4x - 1) H_{-1} + \frac{8}{9} (11x + 20) H_1 \right.$$

$$\left. - \frac{16}{9} (13x + 6) H_0 \right) H_{0,1} + \frac{16}{9} (7x + 1) H_{0,1}^2 + \frac{256}{27} (4x - 1) H_{0,-1,1}$$

$$- \frac{32}{27} (19x - 1) H_{0,0,-1} + \left(\frac{56}{27} (23x + 12) - \frac{16}{9} (7x + 1) H_0 \right) H_{0,0,1}$$

$$+ \frac{256}{27} (4x - 1) H_{0,1,-1} + \left(-\frac{16}{3} (3x + 5) - \frac{16}{9} (11x + 5) H_0 \right) H_{0,1,1}$$

$$+ \frac{64}{9} (7x - 1) H_{0,0,0,1} - \frac{16}{9} (9x - 11) H_{0,0,1,1} - \frac{2}{729} (51199x - 29585)$$

$$- \frac{16}{27} x H_0^4 + \left(\frac{16}{81} (326x - 261) + \frac{32}{27} (29x - 11) H_{-1} - \frac{8}{9} (x - 9) H_0^2 \right.$$

$$\left. - \frac{8}{27} (13x + 30) H_0 - \frac{8}{9} (3x + 14) H_1 - \frac{16}{9} (7x + 1) H_{0,1} \right) \zeta_2$$

$$+ \left(\frac{32}{9} (7x - 3) H_0 - \frac{2}{27} (79x - 989) \right) \zeta_3 - \frac{8}{3} (29x + 22) \zeta_4 \Bigg]$$

$$+ C_F^2 T_F \left[(L_M^2 + L_Q^2) L_Q \left[(x + 1) \left(8 H_0 + \frac{32}{3} H_1 \right) - \frac{8(x + 5)}{3} \right] \right.$$

$$+ L_M^2 \left[\frac{1}{x + 1} \left(\frac{32}{3} H_0^2 + \frac{128}{3} H_{0,-1} - \frac{128}{3} H_{-1} H_0 - \frac{64}{3} \zeta_2 \right) - \frac{4}{3} (x + 9) H_0^2 \right.$$

$$- \frac{16}{3} (2x - 1) H_0 + (1 - x) \left(\frac{64}{3} H_{-1} H_0 - \frac{64}{3} H_{0,-1} \right) - \frac{16}{3} (3x + 2) H_1$$

$$\left. + (x + 1) \left(-8 H_1^2 - \frac{64}{3} H_0 H_1 - \frac{8}{3} H_{0,1} \right) + \frac{4}{3} (13x + 14) + \frac{8}{3} (x + 9) \zeta_2 \right]$$

$$+ L_M L_Q \left[\frac{4}{9} (19x - 85) + \frac{8}{3} (13x + 1) H_0 + (x + 1) \left(8 H_0^2 + \frac{32}{3} H_1 H_0 - \frac{32}{3} \zeta_2 \right) \right.$$

$$\left. + \frac{128}{9} (4x + 1) H_1 \right] + L_Q^2 \left[\frac{1}{x + 1} \left(\frac{32}{3} H_0^2 + \frac{128}{3} H_{0,-1} - \frac{128}{3} H_{-1} H_0 - \frac{64}{3} \zeta_2 \right) \right.$$

$$- \frac{4}{3} (13x + 21) H_0^2 - \frac{8}{3} (25x + 3) H_0 + (1 - x) \left(\frac{64}{3} H_{-1} H_0 - \frac{64}{3} H_{0,-1} \right)$$

$$- \frac{16}{9} (59x + 26) H_1 + (x + 1) \left(-24 H_1^2 - \frac{160}{3} H_0 H_1 - 8 H_{0,1} \right) + \frac{92}{9} (4x + 11)$$

$$\left. + \frac{8}{3} (15x + 23) \zeta_2 \right] + L_M \left[(1 - x) \left(\frac{128}{3} H_{0,-1,1} - \frac{128}{3} H_{-1} H_{0,1} + \frac{128}{3} H_{0,1,-1} \right. \right.$$

$$\left. - \frac{64}{3} H_{0,0,-1} + \frac{32}{3} H_{-1} H_0^2 + \frac{128}{3} H_{-1} \zeta_2 \right) + (x + 1) \left(\left(\frac{32}{3} H_0 - \frac{104}{9} \right) H_{0,1} \right.$$

$$- \frac{16}{3} H_0 H_1^2 - \frac{80}{3} H_0^2 H_1 + \frac{32}{3} H_1 \zeta_2 \bigg) + \frac{4}{9}(7x + 61) H_0 - \frac{256}{9}(4x - 1) H_{-1} H_0$$

$$- \frac{32}{9}(x + 3) H_0^3 - \frac{4}{9}(49x + 57) H_0^2 + \frac{256}{9}(4x - 1) H_{0,-1} - \frac{16}{3}(7x + 3) H_1^2$$

$$+ \bigg(-\frac{4}{9}(135x + 119) - \frac{32}{9}(38x + 17) H_0 \bigg) H_1 + \frac{1}{x+1} \bigg(\frac{1280}{9} H_{0,-1}$$

$$+ \frac{256}{3} H_{-1} H_{0,1} + \frac{128}{3} H_{0,0,-1} - \frac{256}{3} H_{0,-1,1} - \frac{128}{3} H_{0,0,1} - \frac{256}{3} H_{0,1,-1}$$

$$+ \frac{64}{9} H_0^3 + \bigg(\frac{320}{9} - \frac{64}{3} H_{-1} \bigg) H_0^2 + \bigg(-\frac{256}{3} H_{-1} + \frac{64}{3} H_0 - \frac{640}{9} \bigg) \zeta_2 + 64 \zeta_3$$

$$- \frac{1280}{9} H_{-1} H_0 \bigg) - \frac{16}{3}(5x - 3) H_{0,0,1} + \frac{20}{9}(5x + 28) + \frac{16}{3}(13x + 1) \zeta_3$$

$$+ \bigg(\frac{8}{9}(37x + 81) + \frac{16}{3}(7x + 3) H_0 \bigg) \zeta_2 \bigg] + L_Q \bigg[(x + 1) \bigg(\frac{160}{9} H_1^3 + 64 H_0 H_1^2$$

$$+ 48 H_{0,1,1} - \frac{32}{3} H_1 H_{0,1} \bigg) + \frac{8 \big(1296 x^3 - 4489 x^2 - 5156 x + 144 \big)}{135 x}$$

$$- \frac{64}{3}(7x - 1) H_{-1}^2 H_0 + \frac{4}{45} \big(432 x^3 + 845 x + 945 \big) H_0^2 + \frac{32}{9}(4x + 9) H_0^3$$

$$+ \bigg(-\frac{64 \big(54 x^5 - 155 x^3 - 115 x^2 - 6 \big)}{45 x^2} H_0 + \frac{32}{3}(11x - 5) H_0^2 \bigg) H_{-1}$$

$$+ \bigg(\frac{32}{3}(x + 7) H_0^2 + \frac{8}{27}(425 x + 434) + \frac{16}{9}(193 x + 121) H_0 \bigg) H_1$$

$$+ \bigg(\frac{64 \big(54 x^5 - 155 x^3 - 115 x^2 - 6 \big)}{45 x^2} + \frac{128}{3}(7x - 1) H_{-1} - \frac{640}{3} x H_0 \bigg) H_{0,-1}$$

$$+ \bigg(\frac{16}{9}(61x + 13) + \frac{16}{3}(25x + 1) H_0 \bigg) H_{0,1} + \frac{1}{x+1} \bigg(-\frac{160}{9} H_0^3 - \frac{320}{9} H_0^2$$

$$+ \bigg(128 H_0^2 + \frac{1280}{9} H_0 \bigg) H_{-1} + \bigg(\frac{512}{3} H_{-1} - \frac{256}{3} H_0 - \frac{1280}{9} \bigg) H_{0,-1}$$

$$- \frac{512}{3} H_{0,-1,-1} - \frac{256}{3} H_{0,0,-1} - \frac{256}{3} H_0 H_{-1}^2 - \frac{128}{3} H_0 + \bigg(-\frac{256}{3} H_{-1} + \frac{64}{3} H_0$$

$$+ \frac{640}{9} \bigg) \zeta_2 + \frac{256}{3} \zeta_3 \bigg) - \frac{128}{3}(7x - 1) H_{0,-1,-1} + \frac{64}{3}(9x + 5) H_{0,0,-1}$$

$$- \frac{16}{3}(19x - 5) H_{0,0,1} + \frac{32}{3}(15x + 8) H_1^2 + \frac{8 \big(432 x^3 - 766 x^2 - 611 x - 48 \big)}{45 x} H_0$$

$$+ \bigg(-\frac{32}{45} \big(108 x^3 + 325 x + 335 \big) - \frac{64}{3}(7x - 1) H_{-1} - \frac{16}{3}(31x + 35) H_0$$

$$+ 32(x - 3) H_1 \bigg) \zeta_2 + \frac{224}{3}(x - 3) \zeta_3 \bigg] + \frac{1}{x+1} \bigg(\bigg(-\frac{256}{27} H_{-1}^3 - \frac{14336}{81} H_{-1} \bigg) H_0$$

$$+ \bigg(\frac{64}{9} H_{-1}^2 - \frac{640}{27} H_{-1} + \frac{3584}{81} \bigg) H_0^2 + \bigg(\frac{640}{81} - \frac{128}{27} H_{-1} \bigg) H_0^3 + \bigg(\frac{256}{9} H_{-1}^2$$

$$+ \frac{14336}{81} \bigg) H_{0,-1} + \frac{2560}{27} H_{-1} H_{0,1} - \frac{512}{9} H_{-1} H_{0,-1,-1} - \frac{2560}{27} H_{0,-1,1}$$

$$- \frac{2560}{27} H_{0,1,-1} + \bigg(\frac{1280}{27} - \frac{256}{9} H_{-1} \bigg) \big(H_{0,0,-1} - H_{0,0,1} \big) - \frac{512}{9} H_{-1} H_{0,1,1}$$

$$+ \frac{512}{9} H_{0,-1,-1,-1} + \frac{512}{9} H_{0,-1,1,1} + \frac{256}{9} H_{0,0,-1,-1} - \frac{256}{9} H_{0,0,-1,1}$$

$$+ \frac{256}{9} H_{0,0,0,-1} - \frac{256}{9} H_{0,0,0,1} + \frac{256}{9} H_{0,0,1,1} - \frac{256}{9} H_{0,0,1,-1} + \frac{512}{9} H_{0,1,-1,1}$$

$$+ \frac{512}{9} H_{0,1,1,-1} + \frac{32}{27} H_0^4 + \left(-\frac{128}{9} H_{-1}^2 - \frac{2560}{27} H_{-1} - \frac{7168}{81} + \frac{64}{9} H_0^2 \right.$$

$$+ \left(\frac{640}{27} - \frac{128}{9} H_{-1} \right) H_0 \right) \zeta_2 + \left(\frac{512}{9} H_{-1} - \frac{64}{9} H_0 + \frac{640}{9} \right) \zeta_3 - \frac{112}{3} \zeta_4 \right)$$

$$+ \frac{1}{81} (7761x + 8921) H_0 + \left(-\frac{32}{27} (19x - 1) H_0^2 - \frac{64}{81} (199x - 25) H_0 \right) H_{-1}$$

$$+ \frac{2}{81} (61x - 636) H_0^2 - \frac{10}{81} (59x + 51) H_0^3 + \left(-\frac{32}{81} (319x + 190) H_0 \right.$$

$$- \frac{40}{27} (31x + 16) H_0^2 - \frac{1}{27} (x + 2401) \right) H_1 + \frac{64}{81} (199x - 25) H_{0,-1}$$

$$+ \left(-\frac{8}{9} (35x + 23) - \frac{8}{9} (9x + 1) H_0 \right) H_1^2 + \left(\frac{512}{27} (4x - 1) H_{-1} - \frac{4}{9} (115x + 63) \right.$$

$$+ \frac{16}{27} (19x + 52) H_0 \right) H_{0,1} + \frac{64}{27} (19x - 1) H_{0,0,-1} - \frac{512}{27} (4x - 1) H_{0,-1,1}$$

$$- \frac{28}{27} (41x + 33) H_{0,0,1} - \frac{512}{27} (4x - 1) H_{0,1,-1} + (x + 1) \left(\frac{64}{9} H_{-1}^2 H_0 \right.$$

$$+ \frac{4}{9} H_0^2 H_1^2 - \frac{64}{27} H_0 H_1^3 + \left(\frac{64}{9} H_1^2 + \frac{16}{3} H_0^2 - \frac{80}{9} H_0 H_1 \right) H_{0,1} - \frac{128}{9} H_{-1} H_{0,-1}$$

$$+ \frac{128}{9} H_{0,-1,-1} + \left(\frac{128}{9} H_1 - \frac{64}{9} H_0 \right) H_{0,0,1} + \left(\frac{16}{3} H_0 - \frac{32}{3} H_1 \right) H_{0,1,1} + \frac{8}{9} H_{0,1}^2$$

$$- \frac{152}{27} H_1 H_0^3 + \left(-\frac{64}{9} H_1^2 - \frac{16}{3} H_0 H_1 + \frac{16}{9} H_{0,1} \right) \zeta_2 - \frac{80}{9} H_1 \zeta_3 - \frac{32}{3} B_4 \right)$$

$$- \frac{32}{9} (5x - 7) H_{0,1,1} - \frac{8}{9} (11x - 21) H_{0,0,0,1} + (1 - x) \left(\frac{64}{27} H_{-1} H_0^3 - \frac{32}{9} H_{-1}^2 H_0^2 \right.$$

$$- \frac{128}{9} H_{0,-1} H_{-1}^2 - \frac{64}{9} H_1 H_{0,1} + \frac{256}{9} H_{-1} H_{0,-1,-1} + \frac{128}{9} H_{-1} H_{0,0,-1}$$

$$+ \frac{256}{9} H_{-1} H_{0,1,1} - \frac{128}{9} H_{-1} H_{0,0,1} - \frac{256}{9} H_{0,-1,-1,-1} - \frac{256}{9} H_{0,-1,1,1}$$

$$+ \frac{128}{9} H_{0,0,-1,1} - \frac{128}{9} H_{0,0,-1,-1} + \frac{128}{9} H_{0,0,1,-1} - \frac{128}{9} H_{0,0,0,-1} - \frac{256}{9} H_{0,1,-1,1}$$

$$- \frac{256}{9} H_{0,1,1,-1} + \frac{128}{27} H_{-1}^3 H_0 + \left(\frac{64}{9} H_{-1}^2 + \frac{64}{9} H_0 H_{-1} \right) \zeta_2 - \frac{256}{9} H_{-1} \zeta_3 \right)$$

$$+ \frac{32}{9} (x - 7) H_{0,0,1,1} + \frac{1}{81} (10693x + 12902) + \frac{1}{27} (-19x - 51) H_0^4$$

$$+ \left(\frac{4}{81} (403x + 2087) - \frac{64}{27} (29x - 11) H_{-1} + \frac{4}{9} (21x + 5) H_0^2 + \frac{16}{9} (x + 9) H_1 \right.$$

$$+ \frac{4}{27} (451x + 135) H_0 \right) \zeta_2 + \left(\frac{8}{27} (53x - 361) + \frac{8}{9} (7x + 15) H_0 \right) \zeta_3$$

$$+ \frac{4}{9} (47x + 131) \zeta_4 \right] + \hat{c}_{q,2}^{\text{NS},(3)}(N_F) \Bigg\} , \tag{E.11}$$

where $\hat{c}_{q,2}^{\text{NS},(3)}(N_F)$ refers to the constant term of the renormalised massless Wilson coefficient [138] and the N_F prescription in Eq. (2.97).

E.3.2. The polarised Wilson coefficient L_{q,g_1}^{NS}

The polarised structure function $g_1(x, Q^2)$ receives contributions from the non-singlet heavy flavour Wilson coefficient L_{q,g_1}^{NS}, for which we obtain in x space

$$
\begin{aligned}
L_{q,g_1}^{\mathrm{NS}}(x) = a_s^2 &\Bigg\{ \Bigg(\frac{1}{1-x} C_F T_F \Bigg[\frac{8}{3} \big[L_Q^2 + L_M^2 \big] + L_M \Big[\frac{80}{9} + \frac{16}{3} H_0 \Big] + L_Q \Big[-\frac{116}{9} - \frac{32}{3} H_0 \\
&- \frac{16}{3} H_1 \Big] + \frac{718}{27} + \frac{268}{9} H_0 + 8 H_0^2 + \Big(\frac{116}{9} + \frac{16}{3} H_0 \Big) H_1 + \frac{8}{3} H_1^2 + \frac{16}{3} H_{0,1} \\
&- \frac{32}{3} \zeta_2 \Bigg] \Bigg)_+ + \delta(1-x) \Bigg(C_F T_F \Bigg[2 \big[L_M^2 + L_Q^2 \big] + L_M \frac{2}{3} - L_Q \frac{38}{3} + \frac{265}{9} \Bigg] \Bigg) \\
&+ C_F T_F \Bigg[-\frac{4}{3}(x+1) \big[L_Q^2 + L_M^2 \big] + L_M \Big[-\frac{8}{9}(11x-1) - \frac{8}{3}(x+1) H_0 \Big] \\
&+ L_Q \Big[\frac{8}{9}(14x+5) + \frac{16}{3}(x+1) H_0 + \frac{8}{3}(x+1) H_1 \Big] - \frac{4}{27}(218x+47) \\
&- \frac{8}{9}(28x+13) H_0 - 4(x+1) H_0^2 + \Big(-\frac{8}{9}(14x+5) - \frac{8}{3}(x+1) H_0 \Big) H_1 \\
&- \frac{4}{3}(x+1) H_1^2 - \frac{8}{3}(x+1) H_{0,1} + \frac{16}{3}(x+1)\zeta_2 \Bigg] \Bigg\} \\
+ a_s^3 &\Bigg\{ \Bigg(\frac{1}{(1-x)^2} C_A C_F T_F \Bigg[-\frac{4}{81}(800x-773) H_0^2 + \frac{32}{81}(94x-121)\zeta_2 \\
&+ \frac{32}{9}(x+2) H_{0,1} \Bigg] + \frac{1}{1-x} \Bigg(C_A C_F T_F \Bigg[-L_M^3 \frac{176}{27} - L_Q^3 \frac{352}{27} + L_M^2 \Bigg[\frac{184}{9} \\
&+ \frac{16}{3} H_0^2 - \frac{32}{3}\zeta_2 \Bigg] + L_Q^2 \Bigg[\frac{3104}{27} + \frac{704}{9} H_0 + \frac{16}{3} H_0^2 + \frac{352}{9} H_1 - \frac{32}{3}\zeta_2 \Bigg] \\
&+ L_M \Bigg[\frac{1240}{81} + \frac{1792}{27} H_0 + \frac{248}{9} H_0^2 + \frac{32}{9} H_0^3 - 16 H_0^2 H_1 + 32 H_0 H_{0,1} - \frac{64}{3} H_{0,0,1} \\
&+ \Big(-\frac{320}{9} - \frac{64}{3} H_0 \Big) \zeta_2 + 96\zeta_3 \Bigg] + L_Q \Bigg[-\frac{80}{9} H_0^3 - \frac{30124}{81} - \frac{14144}{27} H_0 - \frac{1216}{9} H_0^2 \\
&+ \Big(-\frac{6208}{27} - \frac{704}{9} H_0 - \frac{16}{3} H_0^2 \Big) H_1 + \Big(-\frac{352}{9} + \frac{32}{3} H_0 \Big) H_1^2 - 64 H_0 H_{0,-1} \\
&+ \Big(-\frac{704}{9} + \frac{32}{3} H_0 - \frac{128}{3} H_1 \Big) H_{0,1} - \frac{128}{3} H_{0,0,1} + 128 H_{0,0,-1} + 64 H_{0,1,1} \\
&+ \Big(192 + \frac{128}{3} H_0 + 64 H_1 \Big) \zeta_2 - \frac{256}{3}\zeta_3 \Bigg] + \frac{43228}{729} + \frac{3256}{81} H_0 + \frac{496}{81} H_0^3 + \frac{16}{27} H_0^4 \\
&+ \Big(\frac{32}{3} - \frac{32}{9} H_0 - \frac{160}{9} H_0^2 - \frac{112}{27} H_0^3 \Big) H_1 + \frac{8}{9} H_0^2 H_1^2 - \frac{64}{27} H_0 H_1^3 + \Big(\frac{368}{9} H_0 \\
&+ \frac{16}{3} H_0^2 + \Big(-8 - \frac{128}{9} H_0 \Big) H_1 + \frac{128}{9} H_1^2 \Big) H_{0,1} - \frac{32}{9} H_{0,1}^2 + \Big(-\frac{1072}{27} + \frac{32}{9} H_0 \\
&+ \frac{320}{9} H_1 \Big) H_{0,0,1} + \frac{224}{9} \big[H_{0,1,1,1} - H_{0,0,1,1} \big] + \Big(\frac{160}{9} H_0 - 32 H_1 + 24 \Big) H_{0,1,1} \\
&+ \Big(-\frac{496}{27} H_0 - \frac{112}{9} H_0^2 + \Big(8 - \frac{160}{9} H_0 \Big) H_1 - \frac{128}{9} H_1^2 + \frac{32}{9} H_{0,1} \Big) \zeta_2 + \Big(-\frac{1196}{27}
\end{aligned}
$$

$$
+ \frac{160}{9} H_0 - \frac{32}{9} H_1 \Big) \zeta_3 + \frac{296}{3} \zeta_4 - \frac{32}{3} B_4 \Bigg] + C_F^2 T_F \Bigg[L_Q^3 \Big[16 - \frac{32}{3} H_0 - \frac{64}{3} H_1 \Big]
$$

$$
+ L_M^2 L_Q \Big[16 - \frac{32}{3} H_0 - \frac{64}{3} H_1 \Big] + L_M^2 \Big[-22 - 16 H_0 + \Big(8 + \frac{128}{3} H_0 \Big) H_1
$$

$$
+ \frac{16}{3} H_0^2 + 16 H_1^2 - \frac{64}{3} \zeta_2 \Big] + L_Q^2 \Big[-\frac{334}{3} + \frac{32}{9} H_0 + \Big(\frac{856}{9} + \frac{320}{3} H_0 \Big) H_1
$$

$$
+ \frac{80}{3} H_0^2 + 48 H_1^2 - \frac{256}{3} \zeta_2 \Big] + L_M L_Q \Big[\frac{88}{3} - \frac{176}{9} H_0 + \Big(-\frac{640}{9} - \frac{64}{3} H_0 \Big) H_1
$$

$$
- \frac{32}{3} H_0^2 + \frac{64}{3} \zeta_2 \Big] + L_M \Big[-\frac{206}{3} - \frac{112}{3} H_0 + \frac{88}{9} H_0^2 + \Big(\frac{160}{3} + \frac{32}{3} H_0 \Big) H_1^2
$$

$$
+ \frac{64}{9} H_0^3 + \Big(\frac{152}{3} + \frac{1424}{9} H_0 + \frac{160}{3} H_0^2 \Big) H_1 - \frac{64}{3} H_0 H_{0,1} + \Big(-\frac{784}{9} - \frac{128}{3} H_0
$$

$$
- \frac{64}{3} H_1 \Big) \zeta_2 - 64 \zeta_3 \Big] + L_Q \Big[\frac{2360}{9} + \frac{4508}{27} H_0 - \frac{160}{3} H_0^2 - \frac{224}{9} H_0^3 - \frac{320}{9} H_1^3
$$

$$
+ \Big(-\frac{4556}{27} - \frac{3680}{9} H_0 - 128 H_0^2 \Big) H_1 + \Big(-\frac{512}{3} - 128 H_0 \Big) H_1^2 + 128 H_0 H_{0,-1}
$$

$$
+ \Big(48 - \frac{64}{3} H_0 + \frac{64}{3} H_1 \Big) H_{0,1} - 256 H_{0,0,-1} - 64 H_{0,1,1} + \Big(\frac{2608}{9} + \frac{832}{3} H_0
$$

$$
+ \frac{448}{3} H_1 \Big) \zeta_2 + 320 \zeta_3 \Big] - \frac{14197}{54} - \frac{3262}{27} H_0 + \frac{4}{3} H_0^4 + \frac{196}{27} H_0^2 + \frac{380}{81} H_0^3
$$

$$
+ \Big(\frac{302}{9} + \frac{13624}{81} H_0 + \frac{1628}{27} H_0^2 + \frac{304}{27} H_0^3 \Big) H_1 + \Big(\frac{448}{9} + \frac{80}{9} H_0 - \frac{8}{9} H_0^2 \Big) H_1^2
$$

$$
+ \frac{128}{27} H_0 H_1^3 + \Big(\frac{112}{9} - \frac{1304}{27} H_0 - \frac{32}{3} H_0^2 + \frac{160}{9} H_0 H_1 - \frac{128}{9} H_1^2 \Big) H_{0,1}
$$

$$
+ \Big(\frac{1184}{27} + \frac{128}{9} H_0 - \frac{256}{9} H_1 \Big) H_{0,0,1} + \Big(-16 - \frac{32}{3} H_0 + \frac{64}{3} H_1 \Big) H_{0,1,1}
$$

$$
- \frac{16}{9} H_{0,1}^2 - \frac{128}{9} H_{0,0,0,1} + \frac{64}{3} H_{0,0,1,1} + \Big(-\frac{2488}{27} - \frac{1192}{27} H_0 - \frac{80}{9} H_0^2 + \Big(-\frac{160}{9}
$$

$$
+ \frac{32}{3} H_0 \Big) H_1 + \frac{128}{9} H_1^2 - \frac{32}{9} H_{0,1} \Big) \zeta_2 + \Big(\frac{3088}{27} - \frac{128}{9} H_0 + \frac{160}{9} H_1 \Big) \zeta_3 + \frac{64}{3} B_4
$$

$$
- \frac{664}{9} \zeta_4 \Big] + C_F T_F^2 \Big[L_M^3 \frac{128}{27} + L_Q^3 \frac{64}{27} + L_M^2 \Big[\frac{320}{27} + \frac{64}{9} H_0 \Big] + L_Q^2 \Big[-\frac{464}{27}
$$

$$
- \frac{128}{9} H_0 - \frac{64}{9} H_1 \Big] + L_M \frac{1984}{81} + L_Q \Big[\frac{3760}{81} + \frac{2144}{27} H_0 + \Big(\frac{928}{27} + \frac{128}{9} H_0 \Big) H_1
$$

$$
+ \frac{64}{3} H_0^2 + \frac{64}{9} H_1^2 + \frac{128}{9} H_{0,1} - \frac{256}{9} \zeta_2 \Big] - \frac{12064}{729} + \frac{64}{81} H_0 - \frac{160}{81} H_0^2 - \frac{32}{81} H_0^3
$$

$$
+ \frac{896}{27} \zeta_3 \Big] + C_F N_F T_F^2 \Big[L_M^3 \frac{64}{27} + L_Q^3 \frac{128}{27} + L_Q^2 \Big[-\frac{928}{27} - \frac{256}{9} H_0 - \frac{128}{9} H_1 \Big]
$$

$$
+ L_M \Big[\frac{2176}{81} - \frac{320}{27} H_0 - \frac{32}{9} H_0^2 \Big] + L_Q \Big[\frac{7520}{81} + \frac{4288}{27} H_0 + \frac{128}{3} H_0^2 + \Big(\frac{1856}{27}
$$

$$
+ \frac{256}{9} H_0 \Big) H_1 + \frac{128}{9} H_1^2 + \frac{256}{9} H_{0,1} - \frac{512}{9} \zeta_2 \Big] + \frac{24064}{729} + \frac{128}{81} H_0 - \frac{320}{81} H_0^2
$$

$$
-\frac{64}{81}H_0^3 - \frac{512}{27}\zeta_3\Bigg]\Bigg)\Bigg)_+ + \delta(1-x)\Bigg(C_A C_F T_F\Bigg[-L_M^3\frac{44}{9} - L_Q^3\frac{88}{9} + L_M^2\bigg[\frac{34}{3}
$$

$$
-\frac{16}{3}\zeta_3\bigg] + L_Q^2\bigg[\frac{938}{9} - \frac{16}{3}\zeta_3\bigg] + L_M\bigg[-\frac{1595}{27} + \frac{272}{9}\zeta_3 + \frac{68}{3}\zeta_4\bigg] + L_Q\bigg[-\frac{11032}{27}
$$

$$
-\frac{32}{3}\zeta_2 + \frac{1024}{9}\zeta_3 - \frac{196}{3}\zeta_4\bigg] + \frac{55}{243} - \frac{10045}{81}\zeta_3 - \frac{16}{9}\zeta_2\zeta_3 + \frac{2624}{27}\zeta_4 - \frac{176}{9}\zeta_5
$$

$$
-8B_4\bigg] + C_F^2 T_F\bigg[L_Q^3 6 + L_M^2 L_Q 6 + L_M^2\bigg[-10 + \frac{32}{3}\zeta_3\bigg] + L_Q^2\bigg[-48 + \frac{32}{3}\zeta_3\bigg]
$$

$$
+ L_M L_Q 2 + L_M\bigg[-5 - \frac{112}{9}\zeta_3 - \frac{136}{3}\zeta_4\bigg] + L_Q\bigg[\frac{368}{3} + \frac{64}{3}\zeta_2 - \frac{1616}{9}\zeta_3
$$

$$
+ \frac{392}{3}\zeta_4\bigg] - \frac{2039}{18} + \frac{13682}{81}\zeta_3 + \frac{32}{9}\zeta_2\zeta_3 - \frac{3304}{27}\zeta_4 + 16B_4 + \frac{352}{9}\zeta_5\bigg]
$$

$$
+ C_F T_F^2\bigg[L_M^3\frac{32}{9} + L_Q^3\frac{16}{9} + L_M^2\frac{8}{9} - L_Q^2\frac{152}{9} + L_M\frac{496}{27} + L_Q\frac{1624}{27} - \frac{3658}{243}
$$

$$
+ \frac{224}{9}\zeta_3\bigg] + C_F N_F T_F^2\bigg[L_M^3\frac{16}{9} + L_Q^3\frac{32}{9} - L_Q^2\frac{304}{9} + L_M\frac{700}{27} + L_Q\frac{3248}{27} + \frac{4732}{243}
$$

$$
- \frac{128}{9}\zeta_3\bigg]\Bigg) + C_A C_F T_F\bigg[L_M^3\frac{88}{27}(x+1) + L_Q^3\frac{176}{27}(x+1) + L_M^2\bigg[-\frac{4}{9}(83x-37)
$$

$$
+ \frac{32}{3}(x+1)H_0 + \frac{32}{3}\frac{x^2+1}{x+1}\big[H_{0,-1} - H_{-1}H_0\big] + \frac{16}{3}\frac{x}{x+1}\big[2\zeta_2 - H_0^2\big]\bigg]
$$

$$
+ L_Q^2\bigg[-\frac{4}{27}(865x+109) - \frac{256}{9}(x+1)H_0 + \frac{32}{3}\frac{x^2+1}{x+1}\big[H_{0,-1} - H_{-1}H_0\big]
$$

$$
- \frac{176}{9}(x+1)H_1 + \frac{16}{3}\frac{x}{x+1}\big[2\zeta_2 - H_0^2\big]\bigg] + L_M\bigg[-\frac{4}{81}(4577x-4267)
$$

$$
- \frac{16}{27}(29x-109)H_0 + \frac{4}{9}\frac{19x^2+4x+25}{x+1}H_0^2 - \frac{32}{9}\frac{x}{x+1}H_0^3 + \bigg(\frac{32}{3}(x-1)
$$

$$
+ 8(x+1)H_0^2\bigg)H_1 + \frac{128}{9}\frac{4x^2+3x+4}{x+1}H_{0,-1} + \bigg(-\frac{16}{3} - 16H_0\bigg)(x+1)H_{0,1}
$$

$$
+ \bigg(-\frac{128}{9}\frac{4x^2+3x+4}{x+1}H_0 + \frac{16}{3}\frac{x^2+1}{x+1}\big[4H_{0,1} - H_0^2\big]\bigg)H_{-1} + \frac{64}{3}\frac{x}{x+1}H_{0,0,1}
$$

$$
+ \frac{32}{3}\frac{x^2+1}{x+1}\big[H_{0,0,-1} - 2H_{0,-1,1} - 2H_{0,1,-1}\big] + \bigg(\frac{16}{9}\frac{3x^2+14x-9}{x+1}
$$

$$
- \frac{64}{3}\frac{x^2+1}{x+1}H_{-1} + \frac{16}{3}\frac{3x^2+4x+3}{x+1}H_0\bigg)\zeta_2 - 32\frac{x^2+3x+1}{x+1}\zeta_3\bigg]
$$

$$
+ L_Q\bigg[\frac{4}{81}(12329x-577) + \bigg(\frac{64}{27}\frac{181x^2+239x+49}{x+1} - \frac{32}{3}\frac{(x-1)^2}{x+1}H_{-1}^2
$$

$$
+ \frac{32}{9}\frac{6x^4+25x^3+18x^2+25x+6}{(x+1)x}H_{-1}\bigg)H_0 + \bigg(-\frac{8}{9}\frac{12x^3-21x^2-77x-24}{x+1}
$$

$$
+ \frac{16}{3}\frac{5x^2-2x+5}{x+1}H_{-1}\bigg)H_0^2 + \frac{80}{9}\frac{x}{x+1}H_0^3 + \bigg(\frac{8}{27}(703x+253) - \frac{8}{3}(x-3)H_0^2
$$

$$+ \frac{352}{9}(x+1)H_0 \bigg) H_1 + \left(\frac{176}{9}(x+1) - \frac{16}{3}(x+1)H_0 \right) H_1^2 + \left(\frac{64}{3}\frac{3x+1}{x+1}H_0 \right.$$

$$- \frac{32}{9}\frac{6x^4 + 25x^3 + 18x^2 + 25x + 6}{(x+1)x} + \frac{64}{3}\frac{(x-1)^2}{x+1}H_{-1} \bigg) H_{0,-1} + \left(\frac{208}{9}(x+1) \right.$$

$$+ \frac{16}{3}(x-3)H_0 + \frac{64}{3}(x+1)H_1 \bigg) H_{0,1} + \frac{32}{3}(x+3)H_{0,0,1} - 32(x+1)H_{0,1,1}$$

$$- \frac{64}{3}\frac{(x-1)^2}{x+1}H_{0,-1,-1} - \frac{32}{3}\frac{5x^2 + 10x + 9}{x+1}H_{0,0,-1} + \left(-\frac{64}{3}(x+2)H_1 \right.$$

$$+ \frac{16}{9}\frac{12x^3 - 23x^2 - 72x - 17}{x+1} - \frac{32}{3}\frac{(x-1)^2}{x+1}H_{-1} - \frac{16}{3}\frac{3x^2 + 8x + 3}{x+1}H_0 \bigg) \zeta_2$$

$$+ \frac{64}{3}\frac{3x^2 + 3x + 2}{x+1}\zeta_3 \bigg] - \frac{2}{729}(108295x - 86681) + \left(-\frac{4}{81}(995x - 2807) \right.$$

$$- \frac{32}{81}\frac{199x^2 + 174x + 199}{x+1}H_{-1} + \frac{32}{9}(x+1)H_{-1}^2 - \frac{64}{27}\frac{x^2+1}{x+1}H_{-1}^3 \bigg) H_0$$

$$+ \left(\frac{4}{81}\frac{253x^2 + 391x + 586}{x+1} - \frac{16}{27}\frac{19x^2 + 18x + 19}{x+1}H_{-1} + \frac{16}{9}\frac{x^2+1}{x+1}H_{-1}^2 \right) H_0^2$$

$$+ \left(\frac{8}{81}\frac{22x^2 + 7x + 25}{x+1} - \frac{32}{27}\frac{x^2+1}{x+1}H_{-1} \right) H_0^3 - \frac{16}{27}\frac{x}{x+1}H_0^4 + \left(\frac{8}{9}(9x+4)H_0 \right.$$

$$- \frac{8}{27}(65x - 29) + \frac{8}{9}(14x+3)H_0^2 + \frac{56}{27}(x+1)H_0^3 \bigg) H_1 + \left(-\frac{4}{9}(43x - 46) \right.$$

$$- \frac{8}{9}(2x+5)H_0 - \frac{4}{9}(x+1)H_0^2 \bigg) H_1^2 + \frac{32}{27}(x+1)H_0 H_1^3 + \left(-\frac{64}{9}(x+1)H_{-1} \right.$$

$$+ \frac{32}{81}\frac{199x^2 + 174x + 199}{x+1} + \frac{64}{9}\frac{x^2+1}{x+1}H_{-1}^2 \bigg) H_{0,-1} + \left(\frac{256}{27}\frac{4x^2 + 3x + 4}{x+1}H_{-1} \right.$$

$$- \frac{8}{27}(143x + 2) - \frac{16}{9}(13x+6)H_0 - \frac{8}{3}(x+1)H_0^2 + \left(\frac{8}{9}(11x + 20) \right.$$

$$+ \frac{64}{9}(x+1)H_0 \bigg) H_1 - \frac{64}{9}(x+1)H_1^2 \bigg) H_{0,1} + \frac{16}{9}(7x+1)H_{0,1}^2 + \left(\frac{64}{9}(x+1) \right.$$

$$- \frac{128}{9}\frac{x^2+1}{x+1}H_{-1} \bigg) H_{0,-1,-1} - \frac{256}{27}\frac{4x^2 + 3x + 4}{x+1}H_{0,-1,1} + \left(-\frac{64}{9}\frac{x^2+1}{x+1}H_{-1} \right.$$

$$+ \frac{32}{27}\frac{19x^2 + 18x + 19}{x+1} \bigg) H_{0,0,-1} + \left(\frac{8}{27}\frac{9x^2 + 101x + 12}{x+1} + \frac{64}{9}\frac{x^2+1}{x+1}H_{-1} \right.$$

$$- \frac{16}{9}(7x+1)H_0 - \frac{160}{9}(x+1)H_1 \bigg) H_{0,0,1} - \frac{256}{27}\frac{4x^2 + 3x + 4}{x+1}H_{0,1,-1}$$

$$+ \left(-\frac{16}{9}(x+7) - \frac{128}{9}\frac{x^2+1}{x+1}H_{-1} - \frac{16}{9}(11x + 5)H_0 + 16(x+1)H_1 \right) H_{0,1,1}$$

$$+ \frac{64}{9}\frac{x^2+1}{x+1}\big[2H_{0,-1,-1,-1} + 2H_{0,-1,1,1} + H_{0,0,-1,-1} - H_{0,0,-1,1} + H_{0,0,0,-1}$$

$$- H_{0,0,1,-1} + 2H_{0,1,-1,1} + 2H_{0,1,1,-1} \big] + \frac{64}{9}\frac{5x^2 + 6x - 1}{x+1}H_{0,0,0,1}$$

$$- \frac{16}{9}\frac{x^2 - 2x - 11}{x+1}H_{0,0,1,1} - \frac{112}{9}(x+1)H_{0,1,1,1} + \left(\frac{16}{81}\frac{174x^2 + 209x - 189}{x+1} \right.$$

$$- \frac{32}{27}\frac{29x^2 + 18x + 29}{x+1}H_{-1} + \left(-\frac{8}{9}(3x + 14) + \frac{80}{9}(x+1)H_0 \right) H_1$$

$$
+ \left(\frac{8}{27} \frac{63x^2 + 29x + 6}{x + 1} - \frac{32}{9} \frac{x^2 + 1}{x + 1} H_{-1} \right) H_0 - \frac{32}{9} \frac{x^2 + 1}{x + 1} H_{-1}^2 + \frac{64}{9} (x + 1) H_1^2
$$

$$
+ \frac{8}{9} \frac{3x^2 + 8x + 9}{x + 1} H_0^2 - \frac{16}{9} (7x + 1) H_{0,1} \bigg) \zeta_2 + \left(\frac{2}{27} \frac{497x^2 + 1102x + 1085}{x + 1} \right.
$$

$$
+ \frac{128}{9} \frac{x^2 + 1}{x + 1} H_{-1} + \frac{32}{9} \frac{6x^2 + 4x - 3}{x + 1} H_0 + \frac{16}{9} (x + 1) H_1 \bigg) \zeta_3 + \frac{16}{3} (x + 1) B_4
$$

$$
- \frac{8}{3} \frac{36x^2 + 51x + 22}{x + 1} \zeta_4 \bigg] + C_F^2 T_F \Bigg[\left[L_Q^3 + L_M^2 L_Q \right] \left[-\frac{8}{3} (x + 5) + \frac{32}{3} (x + 1) H_1 \right.
$$

$$
+ 8(x + 1) H_0 \bigg] + L_M^2 \Bigg[28(2x - 1) + \left(-\frac{8}{3} (11x + 5) + \frac{64}{3} \frac{x^2 + 1}{x + 1} H_{-1} \right) H_0
$$

$$
- \frac{4}{3} \frac{9x^2 + 10x + 9}{x + 1} H_0^2 + \left(-\frac{16}{3} (2x + 1) - \frac{64}{3} (x + 1) H_0 \right) H_1 - \frac{8}{3} (x + 1) H_{0,1}
$$

$$
- 8(x + 1) H_1^2 - \frac{64}{3} \frac{x^2 + 1}{x + 1} H_{0,-1} + \frac{8}{3} \frac{9x^2 + 10x + 9}{x + 1} \zeta_2 \Bigg] + L_Q^2 \Bigg[\frac{4}{9} (161x + 130)
$$

$$
+ \left(-\frac{16}{3} (15x + 4) + \frac{64}{3} \frac{x^2 + 1}{x + 1} H_{-1} \right) H_0 - 24(x + 1) H_1^2 + \left(-\frac{16}{9} (50x + 17) \right.
$$

$$
- \frac{160}{3} (x + 1) H_0 \bigg) H_1 - \frac{4}{3} \frac{21x^2 + 34x + 21}{x + 1} H_0^2 + \frac{8}{3} \frac{23x^2 + 38x + 23}{x + 1} \zeta_2
$$

$$
- \frac{64}{3} \frac{x^2 + 1}{x + 1} H_{0,-1} - 8(x + 1) H_{0,1} \bigg] + L_M L_Q \Bigg[\frac{4}{9} (19x - 85) + \frac{8}{3} (13x + 1) H_0
$$

$$
+ 8(x + 1) H_0^2 + \left(\frac{128}{9} (4x + 1) + \frac{32}{3} (x + 1) H_0 \right) H_1 - \frac{32}{3} (x + 1) \zeta_2 \bigg]
$$

$$
+ L_M \Bigg[-\frac{4}{9} (337x + 235) H_0 - \frac{4}{9} \frac{195x^2 + 238x + 123}{x + 1} H_0^2 - \frac{32}{9} \frac{3x^2 + 4x + 3}{x + 1} H_0^3
$$

$$
+ \left(-\frac{4}{9} (287x - 113) - \frac{224}{9} (5x + 2) H_0 - \frac{80}{3} (x + 1) H_0^2 \right) H_1 + \frac{4}{3} (178x - 125)
$$

$$
+ \left(-\frac{16}{3} (7x + 3) - \frac{16}{3} (x + 1) H_0 \right) H_1^2 + \left(\frac{184}{9} (x + 1) + \frac{32}{3} (x + 1) H_0 \right) H_{0,1}
$$

$$
- \frac{256}{9} \frac{4x^2 + 3x + 4}{x + 1} H_{0,-1} + \frac{16}{3} \frac{3x^2 - 2x + 3}{x + 1} H_{0,0,1} + \left(\frac{256}{9} \frac{4x^2 + 3x + 4}{x + 1} H_0 \right.
$$

$$
+ \frac{32}{3} \frac{x^2 + 1}{x + 1} \left[H_0^2 - 4 H_{0,1} \right] \bigg) H_{-1} + \frac{64}{3} \frac{x^2 + 1}{x + 1} \left[2 H_{0,-1,1} - H_{0,0,-1} + 2 H_{0,1,-1} \right]
$$

$$
+ \left(\frac{8}{9} \frac{117x^2 + 118x + 81}{x + 1} + \frac{128}{3} \frac{x^2 + 1}{x + 1} H_{-1} + \frac{16}{3} \frac{(x + 3)(3x + 1)}{x + 1} H_0 \right.
$$

$$
+ \frac{32}{3} (x + 1) H_1 \bigg) \zeta_2 + \frac{16}{3} \frac{x^2 + 14x + 1}{x + 1} \zeta_3 \Bigg] + L_Q \Bigg[-\frac{8}{27} (557x + 652)
$$

$$
+ \left(\frac{8}{9} \frac{115x^2 + 99x + 32}{x + 1} - \frac{64}{9} \frac{6x^4 + 25x^3 + 18x^2 + 25x + 6}{(x + 1)x} H_{-1} \right.
$$

$$
+ \frac{64}{3} \frac{(x - 1)^2}{x + 1} H_{-1}^2 \bigg) H_0 + \frac{32}{9} \frac{9x^2 + 13x + 9}{x + 1} H_0^3 + \left(-\frac{32}{3} \frac{5x^2 - 2x + 5}{x + 1} H_{-1} \right.
$$

$$
+ \frac{4}{9} \frac{48x^3 + 519x^2 + 706x + 315}{x + 1} \bigg) H_0^2 + \left(\frac{8}{27} (908x - 19) + \frac{16}{9} (169x + 97) H_0 \right.
$$

$$+ \frac{32}{3}(7x+5)H_0^2\Big)H_1 + \Big(\frac{32}{3}(13x+6) + 64(x+1)H_0\Big)H_1^2 + \frac{160}{9}(x+1)H_1^3$$

$$+ \Big(\frac{64}{9}(13x+1) + \frac{16}{3}(x+9)H_0 - \frac{32}{3}(x+1)H_1\Big)H_{0,1} + \Big(-\frac{128}{3}\frac{3x+1}{x+1}H_0$$

$$+ \frac{64}{9}\frac{6x^4+25x^3+18x^2+25x+6}{(x+1)x} - \frac{128}{3}\frac{(x-1)^2}{x+1}H_{-1}\Big)H_{0,-1}$$

$$+ \frac{128}{3}\frac{(x-1)^2}{x+1}H_{0,-1,-1} + \frac{64}{3}\frac{5x^2+10x+9}{x+1}H_{0,0,-1} + \frac{16}{3}(5x-3)H_{0,0,1}$$

$$+ 48(x+1)H_{0,1,1} + \Big(-\frac{16}{9}\frac{24x^3+245x^2+318x+137}{x+1} + \frac{64}{3}\frac{(x-1)^2}{x+1}H_{-1}$$

$$- \frac{16}{3}\frac{35x^2+66x+35}{x+1}H_0 - \frac{32}{3}(9x+5)H_1\Big)\zeta_2 - \frac{32}{3}\frac{21x^2+30x+17}{x+1}\zeta_3\Big]$$

$$+ \frac{1}{27}(12332x-4905) + \Big(-\frac{64}{9}(x+1)H_{-1}^2 + \frac{64}{81}\frac{199x^2+174x+199}{x+1}H_{-1}$$

$$+ \frac{1}{81}\big(-10999x-8399\big) + \frac{128}{27}\frac{x^2+1}{x+1}H_{-1}^3\Big)H_0 + \Big(\frac{32}{27}\frac{19x^2+18x+19}{x+1}H_{-1}$$

$$- \frac{32}{9}\frac{x^2+1}{x+1}H_{-1}^2 - \frac{2}{81}\frac{4179x^2+5255x+2868}{x+1}\Big)H_0^2 + \Big(\frac{64}{27}\frac{x^2+1}{x+1}H_{-1}$$

$$- \frac{10}{81}\frac{177x^2+218x+105}{x+1}\Big)H_0^3 - \frac{1}{27}\frac{51x^2+70x+51}{x+1}H_0^4 + \Big(-\frac{152}{27}(x+1)H_0^3$$

$$+ \frac{1}{27}\big(-3457x+1951\big) - \frac{16}{81}(593x+335)H_0 - \frac{8}{27}(146x+71)H_0^2\Big)H_1$$

$$+ \Big(-\frac{8}{9}(3x+55) - \frac{8}{9}(9x+1)H_0 + \frac{4}{9}(x+1)H_0^2\Big)H_1^2 - \frac{64}{27}(x+1)H_0H_1^3$$

$$+ \Big(-\frac{64}{81}\frac{199x^2+174x+199}{x+1} + \frac{128}{9}(x+1)H_{-1} - \frac{128}{9}\frac{x^2+1}{x+1}H_{-1}^2\Big)H_{0,-1}$$

$$+ \Big(\frac{4}{27}(251x+407) + \frac{16}{27}(10x+43)H_0 + \frac{16}{3}(x+1)H_0^2 + \Big(\frac{64}{9}(x-1)$$

$$- \frac{80}{9}(x+1)H_0\Big)H_1 - \frac{512}{27}\frac{4x^2+3x+4}{x+1}H_{-1} + \frac{64}{9}(x+1)H_1^2\Big)H_{0,1}$$

$$+ \frac{8}{9}(x+1)H_{0,1}^2 + \frac{512}{27}\frac{4x^2+3x+4}{x+1}H_{0,-1,1} + \Big(\frac{256}{9}\frac{x^2+1}{x+1}H_{-1}$$

$$- \frac{128}{9}(x+1)\Big)H_{0,-1,-1} + \Big(-\frac{64}{27}\frac{19x^2+18x+19}{x+1} + \frac{128}{9}\frac{x^2+1}{x+1}H_{-1}\Big)H_{0,0,-1}$$

$$+ \Big(\frac{4}{27}\frac{357x^2+130x+93}{x+1} - \frac{128}{9}\frac{x^2+1}{x+1}H_{-1} + \frac{64}{9}(x+1)\big[2H_1-H_0\big]\Big)H_{0,0,1}$$

$$+ \frac{512}{27}\frac{4x^2+3x+4}{x+1}H_{0,1,-1} + \Big(-\frac{32}{9}(13x+1) + \frac{16}{3}(x+1)\big[H_0-2H_1\big]$$

$$+ \frac{256}{9}\frac{x^2+1}{x+1}H_{-1}\Big)H_{0,1,1} + \frac{128}{9}\frac{x^2+1}{x+1}\big[H_{0,0,-1,1} - 2H_{0,-1,-1,-1} - 2H_{0,-1,1,1}$$

$$- H_{0,0,-1,-1} - H_{0,0,0,-1} + H_{0,0,1,-1} - 2H_{0,1,-1,1} - 2H_{0,1,1,-1}\big]$$

$$+ \frac{8}{9}\frac{21x^2+10x+21}{x+1}H_{0,0,0,1} - \frac{32}{9}\frac{7x^2+6x+7}{x+1}H_{0,0,1,1} + \Big(\frac{64}{9}\frac{x^2+1}{x+1}H_{-1}^2$$

$$+ \frac{4}{81}\frac{1619x^2 + 1338x + 1511}{x+1} + \left(\frac{4}{27}\frac{147x^2 + 298x - 9}{x+1} + \frac{64}{9}\frac{x^2 + 1}{x+1}H_{-1}\right)H_0$$

$$+ \frac{64}{27}\frac{29x^2 + 18x + 29}{x+1}H_{-1} + \frac{4}{9}\frac{(x+5)(5x+1)}{x+1}H_0^2 - \frac{64}{9}(x+1)H_1^2$$

$$+ \left(\frac{16}{9}(x+9) - \frac{16}{3}(x+1)H_0\right)H_1 + \frac{16}{9}(x+1)H_{0,1}\right)\zeta_2 + \left(-\frac{80}{9}(x+1)H_1\right.$$

$$- \frac{8}{27}\frac{235x^2 + 404x + 409}{x+1} - \frac{256}{9}\frac{x^2+1}{x+1}H_{-1} + \frac{8}{9}\frac{15x^2 + 22x + 15}{x+1}H_0\right)\zeta_3$$

$$+ \frac{4}{9}\frac{131x^2 + 178x + 131}{x+1}\zeta_4 - \frac{32}{3}(x+1)B_4\bigg] + C_F T_F^2\bigg[-L_M^3\frac{64}{27}(x+1)$$

$$- L_Q^3\frac{32}{27}(x+1) + L_M^2\left[-\frac{32}{27}(11x-1) - \frac{32}{9}(x+1)H_0\right] + L_Q^2\left[\frac{32}{27}(14x+5)\right.$$

$$+ \frac{64}{9}(x+1)H_0 + \frac{32}{9}(x+1)H_1\right] - L_M\frac{992}{81}(x+1) + L_Q\left[-\frac{32}{81}(187x+16)\right.$$

$$- \frac{64}{27}(28x+13)H_0 - \frac{32}{3}(x+1)H_0^2 + \left(-\frac{64}{27}(14x+5) - \frac{64}{9}(x+1)H_0\right)H_1$$

$$- \frac{32}{9}(x+1)H_1^2 - \frac{64}{9}(x+1)H_{0,1} + \frac{128}{9}(x+1)\zeta_2\right] + \frac{16}{729}(431x+323)$$

$$+ \frac{64}{81}(6x-7)H_0 + \frac{16}{81}(11x-1)H_0^2 + \frac{16}{81}(x+1)H_0^3 - \frac{448}{27}(x+1)\zeta_3\bigg]$$

$$+ C_F N_F T_F^2\bigg[-\left[L_M^3 + 2L_Q^3\right]\frac{32}{27}(x+1) + L_Q^2\left[\frac{64}{27}(14x+5) + \frac{128}{9}(x+1)H_0\right.$$

$$+ \frac{64}{9}(x+1)H_1\right] + L_M\left[\frac{32}{81}(5x-73) + \frac{32}{27}(11x-1)H_0 + \frac{16}{9}(x+1)H_0^2\right]$$

$$+ L_Q\left[-\frac{64}{81}(187x+16) - \frac{128}{27}(28x+13)H_0 + \frac{64}{9}(x+1)\left[4\zeta_2 - 2H_{0,1} - H_1^2\right]\right.$$

$$- \frac{64}{3}(x+1)H_0^2 + \left(-\frac{128}{9}(x+1)H_0 - \frac{128}{27}(14x+5)\right)H_1\right] + \frac{32}{81}(x+1)H_0^3$$

$$- \frac{64}{729}(161x+215) + \frac{128}{81}(6x-7)H_0 + \frac{32}{81}(11x-1)H_0^2 + \frac{256}{27}(x+1)\zeta_3\bigg]$$

$$+ \hat{c}_{q,g_1}^{\mathrm{NS},(3)}(N_F)\bigg\}. \tag{E.12}$$

Here we denote the constant term of the massless non-singlet Wilson coefficient [153] by $\hat{c}_{q,g_1}^{\mathrm{NS},(3)}(N_F)$ and use the shorthand of Eq. (2.97).

E.3.3. The charged current Wilson coefficient $L_{q,3}^{\mathsf{NS}}$

For the x space expression of the asymptotic heavy flavour Wilson coefficient of the charged-current structure function $xF_3^{W^+}(x,Q^2) + xF_3^{W^-}(x,Q^2)$ we get

$$L_{q,3}^{\mathrm{NS},W^+-W^-}(x) =$$

$$a_s^2\left\{\left(\frac{1}{1-x}C_F T_F\left[L_M^2\frac{8}{3} + L_Q^2\frac{8}{3} + L_M\left[\frac{80}{9} + \frac{16}{3}H_0\right] + L_Q\left[-\frac{116}{9} - \frac{32}{3}H_0 - \frac{16}{3}H_1\right]\right.\right.$$

$$+ \frac{718}{27} - \frac{32}{3}\zeta_2 + \frac{268}{9}H_0 + 8H_0^2 + \left(\frac{116}{9} + \frac{16}{3}H_0\right)H_1 + \frac{8}{3}H_1^2 + \frac{16}{3}H_{0,1}\Bigg]\Bigg)_+$$

$$+ \delta(1-x)\left(C_F T_F\left[L_M^2 2 + L_Q^2 2 + L_M\frac{2}{3} - L_Q\frac{38}{3} + \frac{265}{9}\right]\right)$$

$$+ C_F T_F\left[-\left(L_M^2 + L_Q^2\right)\frac{4}{3}(x+1) + L_M\left[-\frac{8}{9}(11x-1) - \frac{8}{3}(x+1)H_0\right]\right.$$

$$+ L_Q\left[\frac{8}{9}(14x+5) + \frac{16}{3}(x+1)H_0 + \frac{8}{3}(x+1)H_1\right] - \frac{4}{27}(218x+47) + \frac{16}{3}(x+1)\zeta_2$$

$$- \frac{8}{9}(28x+13)H_0 - 4(x+1)H_0^2 + \left(-\frac{8}{9}(14x+5) - \frac{8}{3}(x+1)H_0\right)H_1$$

$$\left.- \frac{4}{3}(x+1)H_1^2 - \frac{8}{3}(x+1)H_{0,1}\right]\Bigg\}$$

$$+ a_s^3\Bigg\{\left(\frac{1}{(1-x)^2}C_A C_F T_F\left[\frac{32}{81}(94x-121)\zeta_2 - \frac{4}{81}(800x-773)H_0^2\right.\right.$$

$$\left.+ \frac{32}{9}(x+2)H_{0,1}\right] + \frac{1}{1-x}\left(C_A C_F T_F\left[-L_M^3\frac{176}{27} - L_Q^3\frac{352}{27} + L_M^2\left[\frac{184}{9} - \frac{32}{3}\zeta_2\right.\right.\right.$$

$$\left.+ \frac{16}{3}H_0^2\right] + L_Q^2\left[\frac{3104}{27} - \frac{32}{3}\zeta_2 + \frac{704}{9}H_0 + \frac{16}{3}H_0^2 + \frac{352}{9}H_1\right] + L_M\left[\frac{1240}{81} + \left(-\frac{320}{9}\right.\right.$$

$$\left.- \frac{64}{3}H_0\right)\zeta_2 + 96\zeta_3 + \frac{1792}{27}H_0 + \frac{248}{9}H_0^2 + \frac{32}{9}H_0^3 - 16H_0^2 H_1 + 32H_0 H_{0,1} - \frac{64}{3}H_{0,0,1}\right]$$

$$+ L_Q\left[-\frac{30124}{81} + \left(192 + \frac{128}{3}H_0 + 64H_1\right)\zeta_2 - \frac{256}{3}\zeta_3 - \frac{14144}{27}H_0 - \frac{1216}{9}H_0^2\right.$$

$$- \frac{80}{9}H_0^3 + \left(-\frac{6208}{27} - \frac{704}{9}H_0 - \frac{16}{3}H_0^2\right)H_1 + \left(-\frac{352}{9} + \frac{32}{3}H_0\right)H_1^2 - 64H_0 H_{0,-1}$$

$$\left.+ \left(-\frac{704}{9} + \frac{32}{3}H_0 - \frac{128}{3}H_1\right)H_{0,1} + 128H_{0,0,-1} - \frac{128}{3}H_{0,0,1} + 64H_{0,1,1}\right] + \frac{43228}{729}$$

$$- \frac{32}{3}B_4 + \left(-\frac{496}{27}H_0 - \frac{112}{9}H_0^2 + \left(8 - \frac{160}{9}H_0\right)H_1 - \frac{128}{9}H_1^2 + \frac{32}{9}H_{0,1}\right)\zeta_2$$

$$+ \left(-\frac{1196}{27} + \frac{160}{9}H_0 - \frac{32}{9}H_1\right)\zeta_3 + \frac{296}{3}\zeta_4 + \frac{3256}{81}H_0 + \frac{496}{81}H_0^3 + \frac{16}{27}H_0^4$$

$$+ \left(-\frac{32}{3}(x-2) - \frac{32}{9}H_0 - \frac{160}{9}H_0^2 - \frac{112}{27}H_0^3\right)H_1 + \frac{8}{9}H_0^2 H_1^2 - \frac{64}{27}H_0 H_1^3$$

$$+ \left(\frac{368}{9}H_0 + \frac{16}{3}H_0^2 + \left(-8 - \frac{128}{9}H_0\right)H_1 + \frac{128}{9}H_1^2\right)H_{0,1} - \frac{32}{9}H_{0,1}^2 + \left(-\frac{1072}{27}\right.$$

$$\left.+ \frac{32}{9}H_0 + \frac{320}{9}H_1\right)H_{0,0,1} + \left(24 + \frac{160}{9}H_0 - 32H_1\right)H_{0,1,1} - \frac{224}{9}\left(H_{0,0,1,1} - H_{0,1,1,1}\right)\Bigg]$$

$$+ C_F^2 T_F\left[L_Q^3\left[16 - \frac{32}{3}H_0 - \frac{64}{3}H_1\right] + L_M^2 L_Q\left[16 - \frac{32}{3}H_0 - \frac{64}{3}H_1\right] + L_Q^2\left[-\frac{334}{3}\right.\right.$$

$$- \frac{256}{3}\zeta_2 + \frac{32}{9}H_0 + \frac{80}{3}H_0^2 + \left(\frac{856}{9} + \frac{320}{3}H_0\right)H_1 + 48H_1^2\right] + L_M^2\left[-22 - \frac{64}{3}\zeta_2\right.$$

$$- 16H_0 + \frac{16}{3}H_0^2 + \left(8 + \frac{128}{3}H_0\right)H_1 + 16H_1^2\right] + L_M L_Q\left[\frac{88}{3} + \frac{64}{3}\zeta_2 - \frac{176}{9}H_0$$

$$- \frac{32}{3}H_0^2 + \left(-\frac{640}{9} - \frac{64}{3}H_0\right)H_1\right] + L_M\left[-\frac{206}{3} + \left(-\frac{784}{9} - \frac{128}{3}H_0 - \frac{64}{3}H_1\right)\zeta_2$$

$$- 64\zeta_3 - \frac{112}{3}H_0 + \frac{88}{9}H_0^2 + \frac{64}{9}H_0^3 + \left(\frac{152}{3} + \frac{1424}{9}H_0 + \frac{160}{3}H_0^2\right)H_1 + \left(\frac{160}{3}\right.$$

$$\left. + \frac{32}{3}H_0\right)H_1^2 - \frac{64}{3}H_0 H_{0,1}\right] + L_Q\left[\frac{2360}{9} + \left(\frac{2608}{9} + \frac{832}{3}H_0 + \frac{448}{3}H_1\right)\zeta_2 + 320\zeta_3\right.$$

$$+ \frac{4508}{27}H_0 - \frac{160}{3}H_0^2 - \frac{224}{9}H_0^3 + \left(-\frac{4556}{27} - \frac{3680}{9}H_0 - 128H_0^2\right)H_1 + \left(-\frac{512}{3}\right.$$

$$\left. - 128H_0\right)H_1^2 - \frac{320}{9}H_1^3 + 128H_0 H_{0,-1} + \left(48 - \frac{64}{3}H_0 + \frac{64}{3}H_1\right)H_{0,1} - 256H_{0,0,-1}$$

$$- 64H_{0,1,1}\right] - \frac{14197}{54} + \frac{64}{3}B_4 + \left(-\frac{2488}{27} - \frac{1192}{27}H_0 - \frac{80}{9}H_0^2 + \left(-\frac{160}{9} + \frac{32}{3}H_0\right)H_1\right.$$

$$\left. + \frac{128}{9}H_1^2 - \frac{32}{9}H_{0,1}\right)\zeta_2 + \left(\frac{3088}{27} - \frac{128}{9}H_0 + \frac{160}{9}H_1\right)\zeta_3 - \frac{664}{9}\zeta_4 - \frac{3262}{27}H_0$$

$$+ \frac{196}{27}H_0^2 + \frac{380}{81}H_0^3 + \frac{4}{3}H_0^4 + \left(\frac{302}{9} + \frac{13624}{81}H_0 + \frac{1628}{27}H_0^2 + \frac{304}{27}H_0^3\right)H_1$$

$$+ \left(\frac{448}{9} + \frac{80}{9}H_0 - \frac{8}{9}H_0^2\right)H_1^2 + \frac{128}{27}H_0 H_1^3 + \left(\frac{112}{9} - \frac{1304}{27}H_0 - \frac{32}{3}H_0^2 + \frac{160}{9}H_0 H_1\right.$$

$$\left. - \frac{128}{9}H_1^2\right)H_{0,1} - \frac{16}{9}H_{0,1}^2 + \left(\frac{1184}{27} + \frac{128}{9}H_0 - \frac{256}{9}H_1\right)H_{0,0,1} + \left(-16 - \frac{32}{3}H_0\right.$$

$$\left. + \frac{64}{3}H_1\right)H_{0,1,1} - \frac{128}{9}H_{0,0,0,1} + \frac{64}{3}H_{0,0,1,1}\right] + C_F T_F^2\left[L_M^3\frac{128}{27} + L_Q^3\frac{64}{27} + L_M^2\left[\frac{320}{27}\right.\right.$$

$$\left. + \frac{64}{9}H_0\right] + L_Q^2\left[-\frac{464}{27} - \frac{128}{9}H_0 - \frac{64}{9}H_1\right] + L_M\frac{1984}{81} + L_Q\left[\frac{3760}{81} - \frac{256}{9}\zeta_2\right.$$

$$\left. + \frac{2144}{27}H_0 + \frac{64}{3}H_0^2 + \left(\frac{928}{27} + \frac{128}{9}H_0\right)H_1 + \frac{64}{9}H_1^2 + \frac{128}{9}H_{0,1}\right] - \frac{12064}{729} + \frac{896}{27}\zeta_3$$

$$+ \frac{64}{81}H_0 - \frac{160}{81}H_0^2 - \frac{32}{81}H_0^3\right] + C_F N_F T_F^2\left[L_M^3\frac{64}{27} + L_Q^3\frac{128}{27} + L_Q^2\left[-\frac{928}{27} - \frac{256}{9}H_0\right.\right.$$

$$\left. - \frac{128}{9}H_1\right] + L_M\left[\frac{2176}{81} - \frac{320}{27}H_0 - \frac{32}{9}H_0^2\right] + L_Q\left[\frac{7520}{81} - \frac{512}{9}\zeta_2 + \frac{4288}{27}H_0\right.$$

$$\left. + \frac{128}{3}H_0^2 + \left(\frac{1856}{27} + \frac{256}{9}H_0\right)H_1 + \frac{128}{9}H_1^2 + \frac{256}{9}H_{0,1}\right] + \frac{24064}{729} - \frac{512}{27}\zeta_3 + \frac{128}{81}H_0$$

$$\left.\left. - \frac{320}{81}H_0^2 - \frac{64}{81}H_0^3\right]\right)\right)_+ + \delta(1-x)\left(C_A C_F T_F\left[-L_M^3\frac{44}{9} - L_Q^3\frac{88}{9} + L_M^2\left[\frac{34}{3} - \frac{16}{3}\zeta_3\right]\right.\right.$$

$$+ L_Q^2\left[\frac{938}{9} - \frac{16}{3}\zeta_3\right] + L_M\left[-\frac{1595}{27} + \frac{272}{9}\zeta_3 + \frac{68}{3}\zeta_4\right] + L_Q\left[-\frac{11032}{27} - \frac{32}{3}\zeta_2\right.$$

$$\left.\left. + \frac{1024}{9}\zeta_3 - \frac{196}{3}\zeta_4\right] + \frac{2647}{243} - 8B_4 - \frac{10045}{81}\zeta_3 - \frac{16}{9}\zeta_2\zeta_3 + \frac{2624}{27}\zeta_4 - \frac{176}{9}\zeta_5\right]$$

$$+ C_F^2 T_F\left[6L_Q\left(L_Q^2 + L_M^2\right) + L_M^2\left[-10 + \frac{32}{3}\zeta_3\right] + L_Q^2\left[-48 + \frac{32}{3}\zeta_3\right] + 2L_M L_Q\right.$$

$$+ L_M \left[-5 - \frac{112}{9}\zeta_3 - \frac{136}{3}\zeta_4 \right] + L_Q \left[\frac{368}{3} + \frac{64}{3}\zeta_2 - \frac{1616}{9}\zeta_3 + \frac{392}{3}\zeta_4 \right] - \frac{2039}{18}$$

$$+ 16B_4 + \frac{13682}{81}\zeta_3 + \frac{32}{9}\zeta_2\zeta_3 - \frac{3304}{27}\zeta_4 + \frac{352}{9}\zeta_5 + C_F T_F^2 \left[L_M^3 \frac{32}{9} + L_Q^3 \frac{16}{9} + L_M^2 \frac{8}{9} \right.$$

$$\left. - L_Q^2 \frac{152}{9} + L_M \frac{496}{27} + L_Q \frac{1624}{27} - \frac{3658}{243} + \frac{224}{9}\zeta_3 \right] + C_F N_F T_F^2 \left[L_M^3 \frac{16}{9} + L_Q^3 \frac{32}{9} \right.$$

$$\left. - L_Q^2 \frac{304}{9} + L_M \frac{700}{27} + L_Q \frac{3248}{27} + \frac{4732}{243} - \frac{128}{9}\zeta_3 \right] \right) + C_A C_F T_F \left[L_M^3 \frac{88}{27}(x+1) \right.$$

$$+ L_Q^3 \frac{176}{27}(x+1) + L_M^2 \left[-\frac{4}{9}(83x - 37) + \frac{32}{3}\frac{x}{x+1}\zeta_2 + \frac{32}{3}(x+1)H_0 \right.$$

$$- \frac{32}{3}\frac{x^2+1}{x+1}H_{-1}H_0 - \frac{16}{3}\frac{x}{x+1}H_0^2 + \frac{32}{3}\frac{x^2+1}{x+1}H_{0,-1} \right] + L_Q^2 \left[-\frac{4}{27}(865x + 109) \right.$$

$$+ \frac{32}{3}\frac{x}{x+1}\zeta_2 - \frac{256}{9}(x+1)H_0 - \frac{32}{3}\frac{x^2+1}{x+1}H_{-1}H_0 - \frac{16}{3}\frac{x}{x+1}H_0^2 - \frac{176}{9}(x+1)H_1$$

$$\left. + \frac{32}{3}\frac{x^2+1}{x+1}H_{0,-1} \right] + L_M \left[-\frac{4}{81}(4577x - 4267) + \left(\frac{16}{9}\frac{3x^2+14x-9}{x+1} \right. \right.$$

$$\left. - \frac{64}{3}\frac{x^2+1}{x+1}H_{-1} + \frac{16}{3}\frac{3x^2+4x+3}{x+1}H_0 \right)\zeta_2 - 32\frac{x^2+3x+1}{x+1}\zeta_3 - \frac{16}{27}(29x - 109)H_0$$

$$+ \frac{4}{9}\frac{19x^2+4x+25}{x+1}H_0^2 - \frac{32}{9}\frac{x}{x+1}H_0^3 + \left(\frac{32}{3}(x-1) + 8(x+1)H_0^2 \right)H_1$$

$$+ \frac{128}{9}\frac{4x^2+3x+4}{x+1}H_{0,-1} + \left(-\frac{16}{3}(x+1) - 16(x+1)H_0 \right)H_{0,1}$$

$$+ \left(-\frac{128}{9}\frac{4x^2+3x+4}{x+1}H_0 - \frac{16}{3}\frac{x^2+1}{x+1}H_0^2 + \frac{64}{3}\frac{x^2+1}{x+1}H_{0,1} \right)H_{-1} - \frac{64}{3}\frac{x^2+1}{x+1}H_{0,-1,1}$$

$$\left. + \frac{32}{3}\frac{x^2+1}{x+1}H_{0,0,-1} + \frac{64}{3}\frac{x}{x+1}H_{0,0,1} - \frac{64}{3}\frac{x^2+1}{x+1}H_{0,1,-1} \right] + L_Q \left[\frac{4}{81}(12329x - 577) \right.$$

$$+ \left(\frac{16}{9}\frac{12x^3 - 23x^2 - 72x - 17}{x+1} - \frac{32}{3}\frac{(x-1)^2}{x+1}H_{-1} - \frac{16}{3}\frac{3x^2+8x+3}{x+1}H_0 \right.$$

$$\left. - \frac{64}{3}(x+2)H_1 \right)\zeta_2 + \frac{64}{3}\frac{3x^2+3x+2}{x+1}\zeta_3 + \left(\frac{64}{27}\frac{181x^2+239x+49}{x+1} \right.$$

$$+ \frac{32}{9}\frac{6x^4 + 25x^3 + 18x^2 + 25x + 6}{(x+1)x}H_{-1} - \frac{32}{3}\frac{(x-1)^2}{x+1}H_{-1}^2 \right)H_0$$

$$+ \left(-\frac{8}{9}\frac{12x^3 - 21x^2 - 77x - 24}{x+1} + \frac{16}{3}\frac{5x^2 - 2x + 5}{x+1}H_{-1} \right)H_0^2 + \frac{80}{9}\frac{x}{x+1}H_0^3$$

$$+ \left(\frac{8}{27}(703x + 253) + \frac{352}{9}(x+1)H_0 - \frac{8}{3}(x-3)H_0^2 \right)H_1 + \left(\frac{176}{9}(x+1) \right.$$

$$\left. - \frac{16}{3}(x+1)H_0 \right)H_1^2 + \left(-\frac{32}{9}\frac{6x^4 + 25x^3 + 18x^2 + 25x + 6}{(x+1)x} + \frac{64}{3}\frac{(x-1)^2}{x+1}H_{-1} \right.$$

$$+ \frac{64}{3}\frac{3x+1}{x+1}H_0 \right)H_{0,-1} + \left(\frac{208}{9}(x+1) + \frac{16}{3}(x-3)H_0 + \frac{64}{3}(x+1)H_1 \right)H_{0,1}$$

$$- \frac{64}{3}\frac{(x-1)^2}{x+1}H_{0,-1,-1} - \frac{32}{3}\frac{5x^2+10x+9}{x+1}H_{0,0,-1} + \frac{32}{3}(x+3)H_{0,0,1}$$

$$- 32(x+1)H_{0,1,1}\Big] - \frac{2}{729}(108295x - 86681) + \frac{16}{3}(x+1)B_4$$

$$+ \left(\frac{16}{81}\frac{174x^2 + 209x - 189}{x+1} - \frac{32}{27}\frac{29x^2 + 18x + 29}{x+1}H_{-1} - \frac{32}{9}\frac{x^2+1}{x+1}H_{-1}^2\right.$$

$$+ \left(\frac{8}{27}\frac{63x^2 + 29x + 6}{x+1} - \frac{32}{9}\frac{x^2+1}{x+1}H_{-1}\right)H_0 + \frac{8}{9}\frac{3x^2 + 8x + 9}{x+1}H_0^2$$

$$+ \left(-\frac{8}{9}(3x+14) + \frac{80}{9}(x+1)H_0\right)H_1 + \frac{64}{9}(x+1)H_1^2 - \frac{16}{9}(7x+1)H_{0,1}\right)\zeta_2$$

$$+ \left(\frac{2}{27}\frac{497x^2 + 1102x + 1085}{x+1} + \frac{128}{9}\frac{x^2+1}{x+1}H_{-1} + \frac{32}{9}\frac{6x^2 + 4x - 3}{x+1}H_0\right.$$

$$+ \frac{16}{9}(x+1)H_1\right)\zeta_3 - \frac{8}{3}\frac{36x^2 + 51x + 22}{x+1}\zeta_4 + \left(-\frac{4}{81}(995x - 2807)\right.$$

$$- \frac{32}{81}\frac{199x^2 + 174x + 199}{x+1}H_{-1} + \frac{32}{9}(x+1)H_{-1}^2 - \frac{64}{27}\frac{x^2+1}{x+1}H_{-1}^3\right)H_0$$

$$+ \left(\frac{4}{81}\frac{253x^2 + 391x + 586}{x+1} - \frac{16}{27}\frac{19x^2 + 18x + 19}{x+1}H_{-1} + \frac{16}{9}\frac{x^2+1}{x+1}H_{-1}^2\right)H_0^2$$

$$+ \left(\frac{8}{81}\frac{22x^2 + 7x + 25}{x+1} - \frac{32}{27}\frac{x^2+1}{x+1}H_{-1}\right)H_0^3 - \frac{16}{27}\frac{x}{x+1}H_0^4 + \left(-\frac{8}{27}(65x+7)\right.$$

$$+ \frac{8}{9}(9x+4)H_0 + \frac{8}{9}(14x+3)H_0^2 + \frac{56}{27}(x+1)H_0^3\right)H_1 + \left(-\frac{4}{9}(43x - 46)\right.$$

$$- \frac{8}{9}(2x+5)H_0 - \frac{4}{9}(x+1)H_0^2\right)H_1^2 + \frac{32}{27}(x+1)H_0H_1^3 + \left(-\frac{64}{9}(x+1)H_{-1}\right.$$

$$+ \frac{32}{81}\frac{199x^2 + 174x + 199}{x+1} + \frac{64}{9}\frac{x^2+1}{x+1}H_{-1}^2\right)H_{0,-1} + \left(-\frac{8}{27}(143x+2)\right.$$

$$+ \frac{256}{27}\frac{4x^2 + 3x + 4}{x+1}H_{-1} - \frac{16}{9}(13x+6)H_0 - \frac{8}{3}(x+1)H_0^2 + \left(\frac{8}{9}(11x+20)\right.$$

$$+ \frac{64}{9}(x+1)H_0\right)H_1 - \frac{64}{9}(x+1)H_1^2\right)H_{0,1} + \frac{16}{9}(7x+1)H_{0,1}^2 + \left(\frac{64}{9}(x+1)\right.$$

$$- \frac{128}{9}\frac{x^2+1}{x+1}H_{-1}\right)H_{0,-1,-1} - \frac{256}{27}\frac{4x^2 + 3x + 4}{x+1}H_{0,-1,1} + \left(\frac{32}{27}\frac{19x^2 + 18x + 19}{x+1}\right.$$

$$- \frac{64}{9}\frac{x^2+1}{x+1}H_{-1}\right)H_{0,0,-1} + \left(\frac{8}{27}\frac{9x^2 + 101x + 12}{x+1} + \frac{64}{9}\frac{x^2+1}{x+1}H_{-1} - \frac{16}{9}(7x+1)H_0\right.$$

$$- \frac{160}{9}(x+1)H_1\right)H_{0,0,1} - \frac{256}{27}\frac{4x^2 + 3x + 4}{x+1}H_{0,1,-1} + \left(16(x+1)H_1 - \frac{16}{9}(x+7)\right.$$

$$- \frac{128}{9}\frac{x^2+1}{x+1}H_{-1} - \frac{16}{9}(11x+5)H_0\right)H_{0,1,1} + \frac{128}{9}\frac{x^2+1}{x+1}(H_{0,-1,-1,-1} + H_{0,-1,1,1})$$

$$+ \frac{1}{2}(H_{0,0,-1,-1} - H_{0,0,-1,1} + H_{0,0,0,-1} - H_{0,0,1,-1}) + H_{0,1,-1,1} + H_{0,1,1,-1})$$

$$+ \frac{64}{9}\frac{5x^2 + 6x - 1}{x+1}H_{0,0,0,1} - \frac{16}{9}\frac{x^2 - 2x - 11}{x+1}H_{0,0,1,1} - \frac{112}{9}(x+1)H_{0,1,1,1}\Bigg]$$

$$+ C_F^2T_F\Bigg[L_Q^3\Big[-\frac{8}{3}(x+5) + 8(x+1)H_0 + \frac{32}{3}(x+1)H_1\Big] + L_M^2L_Q\Big[-\frac{8}{3}(x+5)$$

$$+ 8(x+1)H_0 + \frac{32}{3}(x+1)H_1\Big] + L_M^2\Big[28(2x-1) + \frac{8}{3}\frac{9x^2 + 10x + 9}{x+1}\zeta_2$$

$$+ \left(-\frac{8}{3}(11x+5) + \frac{64}{3}\frac{x^2+1}{x+1}H_{-1} \right)H_0 - \frac{4}{3}\frac{9x^2+10x+9}{x+1}H_0^2 + \left(-\frac{16}{3}(2x+1) \right.$$

$$\left. -\frac{64}{3}(x+1)H_0 \right)H_1 - 8(x+1)H_1^2 - \frac{64}{3}\frac{x^2+1}{x+1}H_{0,-1} - \frac{8}{3}(x+1)H_{0,1} \right]$$

$$+ L_Q^2 \left[\frac{4}{9}(161x+130) + \frac{8}{3}\frac{23x^2+38x+23}{x+1}\zeta_2 + \left(\frac{64}{3}\frac{x^2+1}{x+1}H_{-1} - \frac{16}{3}(15x+4) \right)H_0 \right.$$

$$-\frac{4}{3}\frac{21x^2+34x+21}{x+1}H_0^2 + \left(-\frac{16}{9}(50x+17) - \frac{160}{3}(x+1)H_0 \right)H_1 - 24(x+1)H_1^2$$

$$-\frac{64}{3}\frac{x^2+1}{x+1}H_{0,-1} - 8(x+1)H_{0,1} \right] + L_M L_Q \left[\frac{4}{9}(19x-85) - \frac{32}{3}(x+1)\zeta_2 \right.$$

$$+ \frac{8}{3}(13x+1)H_0 + 8(x+1)H_0^2 + \left(\frac{128}{9}(4x+1) + \frac{32}{3}(x+1)H_0 \right)H_1 \right]$$

$$+ L_M \left[\frac{4}{3}(178x-125) + \left(\frac{8}{9}\frac{117x^2+118x+81}{x+1} + \frac{128}{3}\frac{x^2+1}{x+1}H_{-1} \right. \right.$$

$$\left. + \frac{16}{3}\frac{(x+3)(3x+1)}{x+1}H_0 + \frac{32}{3}(x+1)H_1 \right)\zeta_2 - \frac{4}{9}\frac{195x^2+238x+123}{x+1}H_0^2$$

$$+ \frac{16}{3}\frac{x^2+14x+1}{x+1}\zeta_3 - \frac{4}{9}(337x+235)H_0 - \frac{32}{9}\frac{3x^2+4x+3}{x+1}H_0^3 + \left(-\frac{4}{9}(287x-113) \right.$$

$$-\frac{224}{9}(5x+2)H_0 - \frac{80}{3}(x+1)H_0^2 \right)H_1 - \left(\frac{16}{3}(7x+3) + \frac{16}{3}(x+1)H_0 \right)H_1^2$$

$$-\frac{256}{9}\frac{4x^2+3x+4}{x+1}H_{0,-1} + \left(\frac{184}{9}(x+1) + \frac{32}{3}(x+1)H_0 \right)H_{0,1}$$

$$+ \left(\frac{256}{9}\frac{4x^2+3x+4}{x+1}H_0 + \frac{32}{3}\frac{x^2+1}{x+1}H_0^2 - \frac{128}{3}\frac{x^2+1}{x+1}H_{0,1} \right)H_{-1}$$

$$+ \frac{64}{3}\frac{x^2+1}{x+1}(2H_{0,-1,1} - H_{0,0,-1} + 2H_{0,1,-1}) + \frac{16}{3}\frac{3x^2-2x+3}{x+1}H_{0,0,1} \right]$$

$$+ L_Q \left[-\frac{8}{27}(557x+652) + \left(-\frac{16}{9}\frac{24x^3+245x^2+318x+137}{x+1} + \frac{64}{3}\frac{(x-1)^2}{x+1}H_{-1} \right. \right.$$

$$-\frac{16}{3}\frac{35x^2+66x+35}{x+1}H_0 - \frac{32}{3}(9x+5)H_1 \right)\zeta_2 - \frac{32}{3}\frac{21x^2+30x+17}{x+1}\zeta_3$$

$$+ \left(\frac{8}{9}\frac{115x^2+99x+32}{x+1} - \frac{64}{9}\frac{6x^4+25x^3+18x^2+25x+6}{(x+1)x}H_{-1} \right.$$

$$\left. + \frac{64}{3}\frac{(x-1)^2}{x+1}H_{-1}^2 \right)H_0 + \left(\frac{4}{9}\frac{48x^3+519x^2+706x+315}{x+1} - \frac{32}{3}\frac{5x^2-2x+5}{x+1}H_{-1} \right)H_0^2$$

$$+ \frac{32}{9}\frac{9x^2+13x+9}{x+1}H_0^3 + \left(\frac{8}{27}(908x-19) + \frac{16}{9}(169x+97)H_0 + \frac{32}{3}(7x+5)H_0^2 \right)H_1$$

$$+ \left(\frac{32}{3}(13x+6) + 64(x+1)H_0 \right)H_1^2 + \frac{160}{9}(x+1)H_1^3 + \left(-\frac{128}{3}\frac{(x-1)^2}{x+1}H_{-1} \right.$$

$$\left. + \frac{64}{9}\frac{6x^4+25x^3+18x^2+25x+6}{(x+1)x} - \frac{128}{3}\frac{3x+1}{x+1}H_0 \right)H_{0,-1} + \left(\frac{64}{9}(13x+1) \right.$$

$$\left. + \frac{16}{3}(x+9)H_0 - \frac{32}{3}(x+1)H_1 \right)H_{0,1} + \frac{128}{3}\frac{(x-1)^2}{x+1}H_{0,-1,-1} + \frac{16}{3}(5x-3)H_{0,0,1}$$

$$+ 48(x+1)H_{0,1,1} + \frac{64}{3}\frac{5x^2+10x+9}{x+1}H_{0,0,-1}\Bigg] + \frac{1}{27}\big(12332x - 4905\big) - \frac{32}{3}(x+1)B_4$$

$$+ \Bigg(\frac{4}{81}\frac{1619x^2+1338x+1511}{x+1} + \frac{64}{27}\frac{29x^2+18x+29}{x+1}H_{-1} + \frac{64}{9}\frac{x^2+1}{x+1}H_{-1}^2$$

$$+ \Bigg(\frac{4}{27}\frac{147x^2+298x-9}{x+1} + \frac{64}{9}\frac{x^2+1}{x+1}H_{-1}\Bigg)H_0 + \frac{4}{9}\frac{(x+5)(5x+1)}{x+1}H_0^2$$

$$+ \Bigg(\frac{16}{9}(x+9) - \frac{16}{3}(x+1)H_0\Bigg)H_1 - \frac{64}{9}(x+1)H_1^2 + \frac{16}{9}(x+1)H_{0,1}\Bigg)\zeta_2$$

$$+ \Bigg(-\frac{8}{27}\frac{235x^2+404x+409}{x+1} - \frac{256}{9}\frac{x^2+1}{x+1}H_{-1} + \frac{8}{9}\frac{15x^2+22x+15}{x+1}H_0$$

$$- \frac{80}{9}(x+1)H_1\Bigg)\zeta_3 + \frac{4}{9}\frac{131x^2+178x+131}{x+1}\zeta_4 + \Bigg(\frac{1}{81}\big(-10999x - 8399\big)$$

$$+ \frac{64}{81}\frac{199x^2+174x+199}{x+1}H_{-1} - \frac{64}{9}(x+1)H_{-1}^2 + \frac{128}{27}\frac{x^2+1}{x+1}H_{-1}^3\Bigg)H_0$$

$$+ \Bigg(-\frac{2}{81}\frac{4179x^2+5255x+2868}{x+1} + \frac{32}{27}\frac{19x^2+18x+19}{x+1}H_{-1} - \frac{32}{9}\frac{x^2+1}{x+1}H_{-1}^2\Bigg)H_0^2$$

$$+ \Bigg(-\frac{10}{81}\frac{177x^2+218x+105}{x+1} + \frac{64}{27}\frac{x^2+1}{x+1}H_{-1}\Bigg)H_0^3 - \frac{1}{27}\frac{51x^2+70x+51}{x+1}H_0^4$$

$$+ \Bigg(\frac{1}{27}\big(-3457x + 1951\big) - \frac{16}{81}\big(593x + 335\big)H_0 - \frac{8}{27}\big(146x + 71\big)H_0^2$$

$$- \frac{152}{27}(x+1)H_0^3\Bigg)H_1 + \Bigg(-\frac{8}{9}\big(3x + 55\big) - \frac{8}{9}\big(9x + 1\big)H_0 + \frac{4}{9}(x+1)H_0^2\Bigg)H_1^2$$

$$- \frac{64}{27}(x+1)H_0H_1^3 + \Bigg(-\frac{64}{81}\frac{199x^2+174x+199}{x+1} + \frac{128}{9}(x+1)H_{-1}$$

$$- \frac{128}{9}\frac{x^2+1}{x+1}H_{-1}^2\Bigg)H_{0,-1} + \Bigg(\frac{4}{27}\big(251x + 407\big) - \frac{512}{27}\frac{4x^2+3x+4}{x+1}H_{-1}$$

$$+ \frac{16}{27}\big(10x + 43\big)H_0 + \frac{16}{3}(x+1)H_0^2 + \Bigg(\frac{64}{9}(x-1) - \frac{80}{9}(x+1)H_0\Bigg)H_1$$

$$+ \frac{64}{9}(x+1)H_1^2\Bigg)H_{0,1} + \frac{8}{9}(x+1)H_{0,1}^2 + \Bigg(\frac{256}{9}\frac{x^2+1}{x+1}H_{-1} - \frac{128}{9}(x+1)\Bigg)H_{0,-1,-1}$$

$$+ \frac{512}{27}\frac{4x^2+3x+4}{x+1}H_{0,-1,1} + \Bigg(-\frac{64}{27}\frac{19x^2+18x+19}{x+1}$$

$$+ \frac{128}{9}\frac{x^2+1}{x+1}H_{-1}\Bigg)H_{0,0,-1} + \Bigg(\frac{4}{27}\frac{357x^2+130x+93}{x+1} - \frac{128}{9}\frac{x^2+1}{x+1}H_{-1}$$

$$- \frac{64}{9}(x+1)H_0 + \frac{128}{9}(x+1)H_1\Bigg)H_{0,0,1} + \frac{512}{27}\frac{4x^2+3x+4}{x+1}H_{0,1,-1}$$

$$+ \Bigg(-\frac{32}{9}\big(13x + 1\big) + \frac{256}{9}\frac{x^2+1}{x+1}H_{-1} + \frac{16}{3}(x+1)H_0 - \frac{32}{3}(x+1)H_1\Bigg)H_{0,1,1}$$

$$+ \frac{128}{9}\frac{x^2+1}{x+1}\big(-2H_{0,-1,-1,-1} - 2H_{0,-1,1,1} - H_{0,0,-1,-1} + H_{0,0,-1,1} - H_{0,0,0,-1}$$

$$+ H_{0,0,1,-1} - 2H_{0,1,-1,1} - 2H_{0,1,1,-1}\big) + \frac{8}{9}\frac{21x^2+10x+21}{x+1}H_{0,0,0,1}$$

$$- \frac{32}{9}\frac{7x^2+6x+7}{x+1}H_{0,0,1,1}\Bigg]$$

E. Results in x space

$$+ C_F T_F^2 \left[-(2L_M^3 + L_Q^3)\frac{32}{27}(x+1) + L_M^2 \left[-\frac{32}{27}(11x-1) - \frac{32}{9}(x+1)H_0 \right] \right.$$

$$+ L_Q^2 \left[\frac{32}{27}(14x+5) + \frac{64}{9}(x+1)H_0 + \frac{32}{9}(x+1)H_1 \right] - L_M \frac{992}{81}(x+1)$$

$$+ L_Q \left[-\frac{32}{81}(187x+16) + \frac{128}{9}(x+1)\zeta_2 - \frac{64}{27}(28x+13)H_0 - \frac{32}{3}(x+1)H_0^2 \right.$$

$$+ \left(-\frac{64}{27}(14x+5) - \frac{64}{9}(x+1)H_0 \right)H_1 - \frac{32}{9}(x+1)H_1^2 - \frac{64}{9}(x+1)H_{0,1} \right]$$

$$+ \frac{16}{729}(431x+323) - \frac{448}{27}(x+1)\zeta_3 + \frac{64}{81}(6x-7)H_0 + \frac{16}{81}(11x-1)H_0^2$$

$$+ \frac{16}{81}(x+1)H_0^3 \right] + C_F N_F T_F^2 \left[-(L_M^3 + 2L_Q^3)\frac{32}{27}(x+1) + L_Q^2 \left[\frac{64}{27}(14x+5) \right. \right.$$

$$+ \frac{128}{9}(x+1)H_0 + \frac{64}{9}(x+1)H_1 \right] + L_M \left[\frac{32}{81}(5x-73) + \frac{32}{27}(11x-1)H_0 \right.$$

$$+ \frac{16}{9}(x+1)H_0^2 \right] + L_Q \left[-\frac{64}{81}(187x+16) + \frac{256}{9}(x+1)\zeta_2 - \frac{128}{27}(28x+13)H_0 \right.$$

$$- \frac{64}{3}(x+1)H_0^2 + \left(-\frac{128}{27}(14x+5) - \frac{128}{9}(x+1)H_0 \right)H_1 - \frac{64}{9}(x+1)H_1^2$$

$$- \frac{128}{9}(x+1)H_{0,1} \right] - \frac{64}{729}(161x+215) + \frac{256}{27}(x+1)\zeta_3 + \frac{128}{81}(6x-7)H_0$$

$$+ \frac{32}{81}(11x-1)H_0^2 + \frac{32}{81}(x+1)H_0^3 \right]$$

$$+ \frac{d^{abc}d^{abc}}{N_c}\frac{1}{2}L_Q \left[-\frac{800}{3}(x-1) + \left(-\frac{4}{3}(41x+67) - 8\frac{(x+1)(4x^2-x+4)}{x}H_{-1} \right. \right.$$

$$+ \frac{4}{3}(32x^2+27x+3)H_0 - 4(3x+5)H_0^2 + \frac{8}{3}\frac{(x-1)(4x^2+7x+4)}{x}H_1$$

$$- 16(x-1)H_{0,-1} - 16(x+1)H_{0,1} \right)\zeta_2 + \left(\frac{32}{3}(5x^2+3) - 32H_0 \right)\zeta_3 + 10(5x+3)\zeta_4$$

$$+ \left(\frac{4}{3}(9x+100) - \frac{104}{3}(x+1)H_{-1} - \frac{8}{3}\frac{(x+1)(4x^2-7x+4)}{x}H_{-1}^2 \right)H_0$$

$$+ \left(\frac{2}{3}(29x+38) + \frac{4}{3}\frac{(x+1)(8x^2-5x+8)}{x}H_{-1} \right)H_0^2 - \frac{4}{9}(8x^2+3)H_0^3$$

$$+ \frac{2}{3}H_0^4 + \left(-\frac{364}{3}(x-1) + 6(x-1)H_0^2 \right)H_1 + \left(\frac{104}{3}(x+1) - \frac{32}{3}\frac{3x^2+2}{x}H_0 \right.$$

$$+ 8(x-1)H_0^2 + \frac{16}{3}\frac{(x+1)(4x^2-7x+4)}{x}H_{-1} \right)H_{0,-1} + 16(x-1)H_{0,-1}^2$$

$$+ \left(\frac{164}{3}(x+1) + \frac{32}{3}\frac{(x+1)(2x^2+x+2)}{x}H_{-1} - 12(x-1)H_0 \right.$$

$$- 4(x+1)H_0^2 \right)H_{0,1} + \left(-\frac{16}{3}\frac{(x+1)(4x^2-7x+4)}{x} - 32(x-1)H_0 \right)H_{0,-1,-1}$$

$$+ \left(-\frac{8}{3}\frac{8x^3-21x^2+3x-8}{x} - 16(x-1)H_0 \right)H_{0,0,-1}$$

284

$$- \frac{32}{3} \frac{(x+1)(2x^2+x+2)}{x} H_{0,-1,1} + \left(-\frac{8}{3}(8x^2+9x+3) + 16(x+1)H_0 \right) H_{0,0,1}$$

$$- \frac{32}{3} \frac{(x+1)(2x^2+x+2)}{x} H_{0,1,-1} \Bigg] + \hat{c}_{q,3}^{\mathrm{NS},W^+-W^-,(3)}(N_F) \Bigg\} . \tag{E.13}$$

Again, $\hat{c}_{q,3}^{\mathrm{NS},W^+-W^-,(3)}(N_F)$ refers to the constant term of the corresponding massless Wilson coefficient [153] after renormalisation. The second Wilson coefficient $H_{q,3}^{\mathrm{NS}}$ can be obtained from Eq. (E.13) together with the massless Wilson coefficient according to Eq. (4.189).

E.3.4. The pure-singlet Wilson coefficient $H_{q,2}^{\mathsf{PS}}$

In Section 5.2, we have calculated the pure-singlet heavy flavour Wilson coefficient at $Q^2 \gg m^2$. Its x space representation reads

$$H_{q,2}^{\mathrm{PS}}(x) = a_s^2 C_F T_F \Bigg[[L_Q^2 - L_M^2] \left[\frac{4}{3} \frac{4x^2+7x+4}{x}(1-x) + 8(1+x)H_0 \right] + L_M \left[8(1+x)H_0^2 \right.$$

$$- \frac{16}{9} \frac{28x^2+x+10}{x}(1-x) - \frac{8}{3}(8x^2+15x+3)H_0 \right] + L_Q \left[\left(\frac{16}{9} \frac{4x^2-26x+13}{x} \right. \right.$$

$$- \frac{8}{3} \frac{4x^2+7x+4}{x}H_1 \right)(1-x) + \left(-16H_0^2 - 16H_{0,1} \right)(1+x) + 32x^2 H_0$$

$$+ 16(1+x)\zeta_2 \Bigg] + \left(\frac{4}{3} \frac{4x^2+7x+4}{x}[4H_0 H_1 + H_1^2] - \frac{16}{9} \frac{52x^2-24x-5}{x} \right.$$

$$- \frac{16}{9} \frac{4x^2-26x+13}{x}H_1 \right)(1-x) - \frac{8}{9}(88x^2+99x-105)H_0 - 8(2x-5)xH_0^2$$

$$+ \frac{32}{3} \left[H_{0,-1} - H_{-1}H_0 \right] \frac{(1+x)^3}{x} + \left(\frac{16}{3}H_0^3 + 32H_0 H_{0,1} - 32H_{0,0,1} \right.$$

$$+ 16H_{0,1,1} \Bigg)(1+x) - \frac{16}{3} \frac{2x^3-3x^2+3x+4}{x}H_{0,1} + \left(\frac{32}{3} \frac{3x^3-3x^2-1}{x} \right.$$

$$- 32(1+x)H_0 \right)\zeta_2 + 16(1+x)\zeta_3 \Bigg] + a_s^3 \Bigg\{ C_A C_F T_F \Bigg[L_M^3 \left[\left(\frac{8}{9} \frac{44x^2-x+44}{x} \right. \right.$$

$$+ \frac{16}{9} \frac{4x^2+7x+4}{x}H_1 \right)(1-x) + \frac{32}{3}(1+x)H_{0,1} + \frac{16}{9} \frac{8x^2+11x+4}{x}H_0$$

$$+ \frac{16}{3}(2x-1)H_0^2 - \frac{32}{3}(1+x)\zeta_2 \Bigg] + L_Q^3 \left[\left(-\frac{8}{9} \frac{44x^2-x+44}{x} \right. \right.$$

$$- \frac{16}{9} \frac{4x^2+7x+4}{x}H_1 \right)(1-x) - \frac{32}{3}(1+x)H_{0,1} - \frac{16}{9} \frac{8x^2+11x+4}{x}H_0$$

$$- \frac{16}{3}(2x-1)H_0^2 + \frac{32}{3}(1+x)\zeta_2 \Bigg] + L_M^2 \left[\left(\frac{8}{27} \frac{1864x^2-485x+694}{x} + \frac{32}{3}H_0^3 \right. \right.$$

$$+ \left(\frac{8}{9} \frac{104x^2+119x+32}{x} - \frac{16}{3} \frac{4x^2+7x+4}{x}H_0 \right)H_1 + 64H_0 H_{0,-1}$$

$$- 128H_{0,0,-1} \Bigg)(1-x) + \left(\frac{32}{3} \frac{4x^2-7x+4}{x}[H_{0,-1} - H_{-1}H_0] - 32H_0 H_{0,1} \right.$$

$$+ 32H_{0,0,1} \Bigg)(1+x) + \frac{8}{9} \frac{272x^3+103x^2+139x+40}{x}H_0 + \frac{8}{3}(16x-17)H_0^2$$

$$+ \frac{32}{3}(10x+7)H_{0,1} + \left(32(1-x)H_0 - \frac{16}{3}\frac{4x^3+17x^2+11x+4}{x}\right)\zeta_2$$

$$- 64(2x-1)\zeta_3\Bigg] + L_Q^2\Bigg[\left(-\frac{8}{27}\frac{181x^2-413x+901}{x} + \frac{16}{9}\frac{62x^2-7x+44}{x}H_1\right.$$

$$+ \frac{16}{3}\frac{4x^2+7x+4}{x}\left[2H_0H_1+H_1^2\right] - 64H_0H_{0,-1} + 128H_{0,0,-1}\Bigg)(1-x)$$

$$+ \left(\frac{32}{3}\frac{4x^2-7x+4}{x}H_{-1}H_0 + \frac{224}{3}H_0^2 - \frac{32}{3}\frac{4x^2-7x+4}{x}H_{0,-1} + 64H_0H_{0,1}\right.$$

$$+ 64H_{0,1,1}\Bigg)(1+x) - \frac{32}{9}\frac{101x^3-53x^2+82x+13}{x}H_0 + \frac{16}{3}(4x-3)H_0^3$$

$$+ 16(2x-1)H_{0,1} - 96H_{0,0,1} + \left(\frac{16}{3}(8x^2-6x-3) - 32(2x+1)H_0\right)\zeta_2$$

$$+ 32(x-2)\zeta_3\Bigg] + L_M\Bigg[\left(\frac{8}{27}\frac{11542x^2+399x+3892}{x} + \frac{8}{9}\frac{210x^2-559x-186}{x}H_1\right.$$

$$+ \frac{4}{3}\frac{20x^2+21x+2}{x}H_1^2 - \frac{8}{9}\frac{4x^2+7x+4}{x}H_1^3 + \left(-\frac{16}{9}\frac{203x^2+47x+140}{x}H_1\right.$$

$$- 8\frac{4x^2+7x+4}{x}H_1^2\Bigg)H_0 + 64H_{0,-1}^2 + \left(4\frac{8x^2+17x+8}{x}H_1 - 32H_{0,-1}\right)H_0^2$$

$$+ \frac{32}{3}\frac{4x^2+7x+4}{x}H_1H_{0,1} - 128H_0H_{0,-1,-1} - 32\frac{x-2}{x}H_{0,0,-1}\Bigg)(1-x)$$

$$+ \left(\left(-\frac{32}{9}\frac{125x^2-20x+62}{x}H_{-1} + \frac{32}{3}\frac{4x^2-7x+4}{x}H_{-1}^2\right)H_0 + 32xH_{-1}H_0^2\right.$$

$$+ \left(\frac{32}{9}\frac{125x^2-20x+62}{x} - \frac{64}{3}\frac{4x^2-7x+4}{x}H_{-1}\right)H_{0,-1} - 96H_0H_{0,1,1}$$

$$+ \left(\frac{64}{3}\frac{2x^2+x+2}{x}H_{-1} + 56H_0^2\right)H_{0,1} + \frac{64}{3}\frac{4x^2-7x+4}{x}H_{0,-1,-1} + 32H_{0,1}^2$$

$$+ 32H_{0,0,1,1} - 32H_{0,1,1,1} - \frac{64}{3}\frac{2x^2+x+2}{x}\left[H_{0,-1,1}+H_{0,1,-1}\right]\Bigg)(1+x)$$

$$+ 32\frac{(1-x)(1+x)}{x}H_{-1}H_0^2 + \frac{16}{27}\frac{3729x^3+2093x^2+2330x+224}{x}H_0$$

$$- \frac{4}{9}(606x^2-346x+377)H_0^2 - \frac{8}{9}(35x-46)H_0^3 + \frac{4}{3}(4x-5)H_0^4$$

$$+ 16\frac{4x^3-13x^2+3x-4}{x}H_0H_{0,-1} + \left(\frac{8}{3}\frac{16x^3-41x^2-77x-40}{x}H_0\right.$$

$$- \frac{8}{9}\frac{274x^3-205x^2+659x-200}{x}\Bigg)H_{0,1} - \left(\frac{32}{3}\frac{4x^3-11x^2-17x-14}{x}\right.$$

$$+ 32(11x+5)H_0\Bigg)H_{0,0,1} - \left(192(x-2)x + 32(3x+1)H_0\right)H_{0,0,-1}$$

$$+ \frac{16}{3}\frac{8x^3+23x^2+5x-8}{x}H_{0,1,1} + 96(x+3)H_{0,0,0,-1} + 32(23x+5)H_{0,0,0,1}$$

$$+ \left(-\left(96H_{-1}+32H_{0,1}\right)(1+x) - \frac{8}{9}\frac{132x^3+313x^2-473x+168}{x}\right.$$

$$- \left(64H_{0,-1} + \frac{16}{3}\frac{4x^2+7x+4}{x}H_1 + 8H_0^2\right)(1-x) + \frac{8}{3}(8x^2-13x+59)H_0\Bigg)\zeta_2$$

$$+ \left(\frac{16}{3} \frac{52x^3 - 78x^2 - 33x - 48}{x} - 32(16x + 9)H_0 \right)\zeta_3 - 4(209x + 87)\zeta_4 \Bigg]$$

$$+ L_Q \Bigg[\left(-\frac{8}{27} \frac{3335x^2 + 2808x + 4604}{x} + \frac{8}{27} \frac{968x^2 + 1301x + 2210}{x}H_1 \right.$$

$$- \frac{4}{9} \frac{286x^2 + 25x + 106}{x}H_1^2 - \frac{40}{9} \frac{4x^2 + 7x + 4}{x}H_1^3 - \left(\frac{32}{9} \frac{76x^2 + 19x + 31}{x}H_1 \right.$$

$$\left. + \frac{40}{3} \frac{4x^2 + 7x + 4}{x}H_1^2 \right)H_0 + \left(-\frac{4}{3} \frac{56x^2 + 125x + 56}{x}H_1 + 112H_{0,-1} \right)H_0^2$$

$$- 32H_{0,-1}^2 + 64H_0 H_{0,-1,-1} + 128H_{0,-1,0,1} \Bigg)(1 - x) + \Bigg(96H_{0,-1,-1}$$

$$+ 128xH_{0,-1,1} + 128xH_{0,1,-1} + \left(\frac{32}{9} \frac{73x^2 + 38x + 118}{x}H_{-1} + 48H_{-1}^2 \right)H_0$$

$$- 160H_0 H_{0,1,1} - 160H_{0,1,1,1} + \left(-\frac{32}{9} \frac{73x^2 + 38x + 118}{x} - 96H_{-1} \right)H_{0,-1}$$

$$- 24\frac{4x^2 - 5x + 4}{x}H_{-1}H_0^2 - \left(128xH_{-1} + 136H_0^2 \right)H_{0,1} \Bigg)(1 + x)$$

$$+ 128\frac{(1 - x)(1 + x)}{x}\left[H_{0,-1,1} + H_{0,1,-1} - H_{-1}H_{0,1} \right] - \frac{4}{3}(12x - 11)H_0^4$$

$$- \frac{16}{27} \frac{466x^3 + 1961x^2 + 4007x + 284}{x}H_0 + \frac{4}{9}(1508x^2 - 1040x + 1297)H_0^2$$

$$- \frac{32}{3} \frac{2x^3 + 3x^2 + 24x - 22}{x}H_0 H_{0,-1} + \left(\frac{8}{9} \frac{542x^3 + 301x^2 + 853x + 332}{x} \right.$$

$$\left. - 8\frac{31x^2 - 19x - 8}{x}H_0 \right)H_{0,1} - \frac{8}{3}(41x + 34)H_0^3 + \left(\frac{16}{3} \frac{44x^3 + 3x^2 + 87x - 52}{x} \right.$$

$$\left. + 32(11x - 7)H_0 \right)H_{0,0,-1} + \frac{16}{3}(8x^2 - 19x + 14)H_{0,1,1} + \Bigg(32(7x + 13)H_0$$

$$- \frac{16}{3} \frac{8x^3 - 15x^2 + 33x - 4}{x} \Bigg)H_{0,0,1} - 384xH_{0,0,0,-1} - 128(2x + 3)H_{0,0,0,1}$$

$$- 32(x - 5)H_{0,0,1,1} + \left(\left(\frac{64}{3} \frac{5x^2 + 11x + 5}{x}H_1 - 96H_{0,-1} \right)(1 - x) \right.$$

$$- \frac{8}{9} \frac{846x^3 - 371x^2 + 901x - 264}{x} - \frac{8}{3} \frac{40x^3 - 93x^2 - 21x - 16}{x}H_0$$

$$+ 8(19x - 3)H_0^2 + \left(16\frac{8x^2 - 5x + 8}{x}H_{-1} + 192H_{0,1} \right)(1 + x) \Bigg)\zeta_2$$

$$+ \left(-\frac{16}{3} \frac{76x^3 + 35x^2 + 14x - 48}{x} + 32(14x + 15)H_0 \right)\zeta_3 + 4(41x + 35)\zeta_4 \Bigg]$$

$$+ \left(\frac{4}{729} \frac{1368812x^2 - 97732x + 353855}{x} - \frac{4}{243} \frac{724x^2 - 7160x + 17239}{x}H_1 \right.$$

$$- \frac{4}{27} \frac{152x^2 + 203x + 152}{x}H_0^3 H_1 + \frac{4}{81} \frac{770x^2 + 3230x - 859}{x}H_1^2$$

$$+ \frac{2}{9} \frac{112x^2 + 241x + 112}{x}H_0^2 H_1^2 - \frac{4}{81} \frac{14x^2 - 67x - 40}{x}H_1^3 - \frac{4}{27} \frac{4x^2 + 7x + 4}{x}H_1^4$$

$$+ \left(-\frac{232}{9}H_0^3 + \frac{32}{9} \frac{4x^2 - 11x + 4}{x}H_0 H_1 \right)H_{0,-1} - \left(\frac{8}{81} \frac{12284x^2 - 313x + 3392}{x}H_1 \right.$$

$$+ \frac{8}{27}\frac{367x^2 + 244x + 124}{x}H_1^2 + \frac{16}{27}\frac{4x^2 + 7x + 4}{x}H_1^3\Big)H_0 + \frac{56}{3}H_0 H_{0,-1}^2$$

$$+ \Big(-\frac{8}{9}\frac{112x^2 + 223x + 112}{x}H_0 H_1 + \frac{32}{9}\frac{4x^2 - 11x + 4}{x}H_{0,-1}\Big)H_{0,1} + \Big(\frac{248}{3}H_0^2$$

$$- \frac{64}{3}H_{0,-1}\Big)H_{0,-1,-1} - \Big(\frac{64}{9}\frac{4x^2 - 11x + 4}{x}H_1 + 240 H_{0,-1}\Big)H_{0,0,-1} + \Big(\frac{752}{3}H_{0,-1}$$

$$+ \frac{8}{9}\frac{176x^2 + 281x + 176}{x}H_1\Big)H_{0,0,1} + \frac{64}{3}H_0 H_{0,-1,-1,-1} - 320 H_0 H_{0,0,-1,-1}$$

$$- \frac{880}{3}H_0 H_{0,0,0,-1} - \frac{160}{3}H_{0,-1,-1,0,1} + \frac{128}{3}H_{0,-1,0,-1,-1} + \frac{256}{3}H_{0,0,-1,-1,-1}$$

$$+ 560 H_{0,0,-1,0,-1} + 1680 H_{0,0,0,-1,-1} + \frac{128}{9}\frac{4x^2 + 7x + 4}{x}H_1 H_{0,1,1}\Big)(1 - x)$$

$$+ \Big(\Big(-\frac{8}{27}\frac{3472x^2 - 1089x + 1048}{x}H_{-1} + \frac{32}{27}\frac{131x^2 - 35x + 50}{x}H_{-1}^2$$

$$- \frac{16}{27}\frac{4x^2 - 7x + 4}{x}H_{-1}^3\Big)H_0 + \frac{4}{3}\frac{16x^2 - 21x + 16}{x}H_{-1}H_0^3$$

$$- \frac{2}{3}\frac{56x^2 - 65x + 56}{x}H_{-1}^2 H_0^2 + \Big(\frac{8}{27}\frac{3472x^2 - 1089x + 1048}{x}$$

$$- \frac{64}{27}\frac{131x^2 - 35x + 50}{x}H_{-1} + \frac{8}{9}\frac{8x^2 + 67x + 8}{x}H_{-1}H_0$$

$$+ \frac{16}{9}\frac{4x^2 - 7x + 4}{x}H_{-1}^2\Big)H_{0,-1} + \Big(\frac{32}{3}\frac{8x^2 - 11x + 8}{x}H_{-1}H_0 - \frac{64}{3}H_0 H_{0,-1}$$

$$- \frac{248}{9}H_0^3 - \frac{8}{9}\frac{32x^2 + 61x + 32}{x}H_{-1}^2\Big)H_{0,1} + \Big(\frac{64}{27}\frac{131x^2 - 35x + 50}{x}$$

$$- \frac{32}{9}\frac{4x^2 - 7x + 4}{x}H_{-1}\Big)H_{0,-1,-1} + \frac{16}{9}\frac{32x^2 + 61x + 32}{x}H_{-1}H_{0,-1,1}$$

$$- \frac{248}{3}H_0 H_{0,1}^2 + \Big(\frac{8}{9}\frac{152x^2 - 329x + 152}{x}H_{-1} + \frac{128}{3}H_{0,1}\Big)H_{0,0,-1}$$

$$+ \frac{16}{9}\frac{32x^2 + 61x + 32}{x}H_{-1}H_{0,1,-1} + \Big(-\frac{8}{3}\frac{(7x - 8)(8x - 7)}{x}H_{-1}$$

$$+ \frac{656}{3}H_{0,1}\Big)H_{0,0,1} + \frac{32}{9}\frac{4x^2 - 7x + 4}{x}H_{0,-1,-1,-1} + \Big(\frac{64}{9}\frac{2x^2 + x + 2}{x}H_{-1}$$

$$+ 88 H_0^2\Big)H_{0,1,1} - \frac{16}{9}\frac{32x^2 + 61x + 32}{x}\big[H_{0,-1,-1,1} + H_{0,-1,1,-1}\big]$$

$$- \frac{64}{9}\frac{2x^2 + x + 2}{x}H_{0,-1,1,1} + \Big(\frac{8}{3}\frac{(7x - 8)(8x - 7)}{x} + \frac{128}{3}H_0\Big)H_{0,0,-1,1}$$

$$- \frac{8}{9}\frac{152x^2 - 329x + 152}{x}H_{0,0,-1,-1} + \Big(\frac{8}{3}\frac{(7x - 8)(8x - 7)}{x} + \frac{128}{3}H_0\Big)H_{0,0,1,-1}$$

$$- \frac{16}{9}\frac{32x^2 + 61x + 32}{x}H_{0,1,-1,-1} - \frac{64}{9}\frac{2x^2 + x + 2}{x}\big[H_{0,1,-1,1} + H_{0,1,1,-1}\big]$$

$$- \frac{64}{3}H_0 H_{0,1,1,1} + 32 H_{0,0,1,1,1} + \frac{256}{3}H_{0,1,0,1,1} - \frac{64}{3}H_{0,1,1,1,1}\Big)(1 + x)$$

$$+ \frac{16}{243}\frac{85213x^3 + 20744x^2 + 30011x + 3280}{x}H_0 + \frac{4}{81}\big(966x^2 + 790x + 721\big)H_0^3$$

$$+ \frac{4}{81} \frac{16316x^4 - 3871x^3 - 5796x^2 + 3628x - 11087}{1+x} \frac{H_0^2}{1-x} + \frac{2}{27}(83x - 121)H_0^4$$

$$- \frac{4}{9} \frac{692x^3 - 358x^2 + 115x - 458}{x} H_0^2 H_1 + \left(\frac{8}{27} \frac{874x^3 - 1866x^2 + 837x - 376}{x} H_0 \right.$$

$$\left. - \frac{4}{9} \frac{88x^3 - 9x^2 - 39x + 144}{x} H_0^2 \right) H_{0,-1} - \frac{8}{9} \frac{8x^3 + 81x^2 - 87x + 80}{x} H_{0,-1}^2$$

$$- \frac{4}{15}(3x - 4)H_0^5 - \frac{8}{81} \frac{12078x^4 + 4106x^3 - 4355x^2 + 797x - 2496}{(1+x)x} H_{0,1}$$

$$+ \left(\frac{8}{9} \frac{262x^3 - 306x^2 - 181x - 538}{x} H_0 - \frac{4}{9} \frac{144x^3 - 441x^2 - 357x - 296}{x} H_0^2 \right.$$

$$\left. - \frac{16}{27} \frac{167x^3 - 711x^2 + 657x - 140}{x} H_1 \right) H_{0,1} + \frac{4}{9} \frac{176x^3 - 237x^2 - 69x - 64}{x} H_{0,1}^2$$

$$+ \left(\frac{4}{27} \frac{430x^3 + 18x^2 - 63x + 376}{x} H_0^2 - \frac{16}{27} \frac{82x^3 - 78x^2 - 267x - 80}{x} H_{0,1} \right) H_{-1}$$

$$+ \frac{8}{9} \frac{8x^3 + 87x^2 - 249x + 152}{x} H_0 H_{0,-1,-1} + \left(\frac{16}{27} \frac{82x^3 - 78x^2 - 267x - 80}{x} \right.$$

$$\left. - \frac{64}{9} \frac{10x^3 + 3x^2 - 12x + 14}{x} H_0 \right) H_{0,-1,1} - \left(\frac{8}{27} \frac{2178x^3 - 3714x^2 + 1611x - 376}{x} \right.$$

$$+ \frac{8}{3} \frac{16x^3 - 15x^2 + 21x - 48}{x} H_0 + \frac{64}{3}(6x - 7)H_0^2 \bigg) H_{0,0,-1} + \left(\frac{16}{3}(57x + 31)H_0^2 \right.$$

$$+ \frac{8}{27} \frac{556x^3 + 187x^2 + 2011x + 1854}{x} + \frac{8}{9} \frac{136x^3 - 1365x^2 - 567x - 440}{x} H_0 \bigg) H_{0,0,1}$$

$$+ \left(\frac{16}{27} \frac{82x^3 - 78x^2 - 267x - 80}{x} - \frac{64}{9} \frac{10x^3 + 3x^2 - 12x + 14}{x} H_0 \right) H_{0,1,-1}$$

$$+ \left(-\frac{8}{27} \frac{188x^3 + 4040x^2 - 3271x + 392}{x} - \frac{128}{9} \frac{11x^3 + 18x^2 - 10}{x} H_0 \right) H_{0,1,1}$$

$$+ \frac{8}{3} \frac{88x^3 - 39x^2 + 39x - 48}{x} H_{0,0,0,-1} + \left(\frac{8}{9} \frac{88x^3 - 147x^2 - 39x + 56}{x} \right.$$

$$+ \frac{128}{3}(3x - 2)H_0 \bigg) H_{0,-1,0,1} - \left(\frac{16}{9} \frac{68x^3 - 1388x^2 - 395x - 292}{x} \right.$$

$$+ 16(73x + 39)H_0 \bigg) H_{0,0,0,1} + \left(-\frac{16}{9} \frac{20x^3 - 563x^2 - 164x + 104}{x} \right.$$

$$+ \frac{16}{3}(11x + 13)H_0 \bigg) H_{0,0,1,1} + \frac{16}{9} \frac{92x^3 + 83x^2 - 46x - 92}{x} H_{0,1,1,1}$$

$$+ \frac{32}{3}(21x - 29)H_{0,0,-1,0,1} + 16(39x - 55)H_{0,0,0,-1,1} - 256x H_{0,0,0,0,-1}$$

$$+ \frac{16}{3}(315x + 221)H_{0,0,0,0,1} + 16(39x - 55)H_{0,0,0,1,-1} - \frac{16}{3}(179x + 185)H_{0,0,0,1,1}$$

$$+ \frac{16}{3}(39x - 55)H_{0,0,1,0,-1} - \frac{32}{3}(41x + 40)H_{0,0,1,0,1} + \left(\left(\frac{8}{3} \frac{8x^2 + 11x + 8}{x} H_0 H_1 \right. \right.$$

$$+ \frac{8}{9} \frac{4x^2 + 7x + 4}{x} H_1^2 + \frac{160}{3} H_0 H_{0,-1} + 64 H_{0,-1,-1} - \frac{256}{3} H_{0,0,-1} \bigg)(1 - x)$$

$$+ \left(\frac{32}{9} \frac{7x^2 + 17x + 7}{x} H_{-1}^2 - \frac{16}{9} \frac{56x^2 - 17x + 56}{x} H_{-1}H_0 - \frac{8}{9}H_0^3 + \frac{80}{3}H_0 H_{0,1} \right.$$

$$+\frac{32}{3}H_{0,1,1}\bigg)(1+x)-\frac{16}{81}\frac{103x^4+1365x^3+1306x^2+1330x+1124}{(1+x)x}$$

$$+\frac{16}{27}\frac{344x^3+114x^2-237x+20}{x}H_{-1}-\frac{8}{27}\big(52x^2+1273x+580\big)H_0$$

$$+\frac{16}{27}\frac{62x^3-780x^2+807x-116}{x}H_1+\frac{16}{9}\frac{20x^3+81x^2+3x+56}{x}H_{0,-1}$$

$$+\frac{4}{9}\big(8x^2-37x-109\big)H_0^2-\frac{8}{3}\frac{32x^3-101x^2-41x+24}{x}H_{0,1}+\frac{64}{3}xH_{0,0,1}\bigg)\zeta_2$$

$$-\frac{512}{3}(1+x)\ln^3(2)\zeta_2+\bigg(-\bigg(\frac{8}{3}\frac{16x^2+55x+16}{x}H_1+\frac{320}{3}H_{0,-1}\bigg)(1-x)$$

$$-\bigg(160H_{-1}+112H_{0,1}\bigg)(1+x)-\frac{4}{27}\frac{4x^3+8314x^2+4402x+2103}{x}$$

$$-\frac{16}{9}\frac{52x^3+806x^2+71x+32}{x}H_0+\frac{16}{3}\big(6x-11\big)H_0^2\bigg)\zeta_3+\bigg(-896(1+x)H_0$$

$$+\frac{448}{3}\frac{4x^3-9x^2-6x-2}{x}\bigg)\ln(2)\zeta_3-896(1+x)\ln^2(2)\zeta_3+\frac{16}{3}\big(37x-45\big)\zeta_2\zeta_3$$

$$+\bigg(-\frac{2}{9}\frac{1632x^3+9285x^2+2223x+916}{x}-\frac{20}{3}\big(19x-51\big)H_0\bigg)\zeta_4-4\big(x-375\big)\zeta_5$$

$$-832(1+x)\ln(2)\zeta_4+\bigg(-64(1+x)H_0+\frac{16}{3}\frac{8x^3-30x^2-15x-2}{x}\bigg)B_4$$

$$-2048(1+x)\mathrm{Li}_5\left(\frac{1}{2}\right)-128(1+x)B_4\ln(2)+\frac{256}{15}(1+x)\ln^5(2)\bigg]$$

$$+C_F^2T_F\bigg[\big[L_M^3+2L_Q^3-3L_M^2L_Q\big]\bigg[-\bigg(\frac{92}{9}+\frac{16}{9}\frac{4x^2+7x+4}{x}H_1\bigg)(1-x)$$

$$-\bigg(\frac{8}{3}H_0^2+\frac{32}{3}H_{0,1}\bigg)(1+x)+\frac{16}{9}\big(4x+3\big)xH_0+\frac{32}{3}(1+x)\zeta_2\bigg]$$

$$+L_M^2\bigg[\bigg(80H_{0,0,1}-32H_{0,1,1}-8H_0^3-64H_0H_{0,1}\bigg)(1+x)-\bigg(\frac{4}{3}\frac{61x+12}{x}$$

$$+\frac{4}{3}\frac{88x^2+135x+40}{x}H_1+\frac{8}{3}\frac{4x^2+7x+4}{x}\big[4H_0H_1+H_1^2\big]\bigg)(1-x)$$

$$+\frac{4}{3}\big(88x^2+91x-37\big)H_0+\frac{8}{3}\big(8x-9\big)xH_0^2-\frac{16}{3}\frac{4x^3+30x^2+15x-8}{x}H_{0,1}$$

$$+\bigg(48(1+x)H_0-\frac{16}{3}\big(4x^2-24x-21\big)\bigg)\zeta_2-48(1+x)\zeta_3\bigg]$$

$$+L_Q^2\bigg[\bigg(8\frac{4x^2+7x+4}{x}\big[2H_0H_1+H_1^2\big]+\frac{8}{9}\frac{4x^2+337x-32}{x}H_1$$

$$-\frac{4}{9}\frac{120x^2-289x-36}{x}\bigg)(1-x)+\bigg(96H_{0,1,1}+96H_0H_{0,1}-32H_{0,0,1}$$

$$+16H_0^3\bigg)(1+x)-\frac{8}{9}\big(4x^2+315x-198\big)H_0-\frac{8}{3}\big(28x^2+3x+6\big)H_0^2$$

$$-\frac{16}{3}\frac{16x^3-15x^2-9x+12}{x}H_{0,1}+\bigg(-160(1+x)H_0+\frac{32}{3}\big(14x^2-3x-9\big)\bigg)\zeta_2$$

$$-64(1+x)\zeta_3\bigg]+L_ML_Q\bigg[\bigg(\frac{16}{9}\big(30x+23\big)+\frac{64}{9}\frac{28x^2+x+10}{x}H_1\bigg)(1-x)$$

$$-\left(\frac{16}{3}H_0^3 + 64H_{0,0,1}\right)(1+x) + \left(64(1+x)H_0 - \frac{32}{3}\left(8x^2+15x+3\right)\right)\zeta_2$$

$$+\frac{16}{3}\left(8x^2+9x+3\right)H_0^2 + \frac{32}{3}\left(8x^2+15x+3\right)H_{0,1} - \frac{8}{9}\left(224x^2-99x+81\right)H_0$$

$$+64(1+x)\zeta_3\Big] + L_M\Bigg[\left(\frac{8}{9}\frac{4x^2+7x+4}{x}H_1^3 - \frac{4}{27}\frac{1128x^2+1655x+180}{x}\right.$$

$$-\frac{16}{27}\frac{823x^2-1088x-59}{x}H_1 - \frac{4}{9}\frac{308x^2+71x+92}{x}H_1^2 + \left(\frac{16}{3}\frac{4x^2+7x+4}{x}H_1^2\right.$$

$$\left.-\frac{8}{9}\frac{364x^2-119x+184}{x}H_1\right)H_0 - \frac{32}{3}\frac{4x^2+7x+4}{x}H_1H_{0,1}\right)(1-x)$$

$$+\left(\frac{22}{3}H_0^4 - 32H_{0,1}^2 + 160H_0H_{0,0,1} + 64H_0H_{0,1,1} - 256H_{0,0,0,1} + 64H_{0,0,1,1}\right.$$

$$+32H_{0,1,1,1}\Bigg)(1+x) + \frac{16}{27}\left(1003x^2-1527x-291\right)H_0 - \frac{64}{9}\left(8x^2+3x+3\right)H_0^3$$

$$+\frac{2}{9}\left(568x^2-1071x+585\right)H_0^2 - \left(\frac{16}{9}\frac{68x^3-75x^2-159x-92}{x}\right.$$

$$\left.+\frac{64}{3}\left(10x^2+12x+3\right)H_0\right)H_{0,1} - \frac{16}{3}\frac{28x^3+57x^2+9x-8}{x}H_{0,1,1}$$

$$+\frac{32}{3}\left(16x^2+30x+27\right)H_{0,0,1} + \left(32\left(2x-1\right)\left(4x+5\right)H_0 - 112(1+x)H_0^2\right.$$

$$\left.-\frac{8}{3}\left(76x^2-111x+207\right)\right)\zeta_2 + \left(224(1+x)H_0 - 16\frac{12x^3+9x^2+7x-8}{x}\right)\zeta_3$$

$$+288(1+x)\zeta_4\Bigg] + L_Q\Bigg[\left(-\frac{56}{9}\frac{4x^2+7x+4}{x}H_1^3 + \frac{4}{135}\frac{19536x^2-1103x+4056}{x}\right.$$

$$+\frac{8}{27}\frac{986x^2-4747x-292}{x}H_1 + \frac{4}{3}\frac{8x^2-305x+20}{x}H_1^2 + 128H_{0,-1}^2$$

$$+\left(\frac{8}{3}\frac{32x^2-299x+32}{x}H_1 - \frac{80}{3}\frac{4x^2+7x+4}{x}H_1^2\right)H_0 + 64\left[H_{0,-1}-xH_1\right]H_0^2$$

$$-256H_0H_{0,-1,-1}\Bigg)(1-x) + \left(\left(-\frac{32}{45}\frac{36x^4-36x^3-1069x^2+4x-4}{x^2}H_{-1}\right.\right.$$

$$\left.+\frac{64}{3}\frac{x^2-10x+1}{x}H_{-1}^2\right)H_0 + \left(\frac{32}{45}\frac{36x^4-36x^3-1069x^2+4x-4}{x^2}\right.$$

$$\left.-\frac{128}{3}\frac{x^2-10x+1}{x}H_{-1}\right)H_{0,-1} + 128H_{-1}H_0^2 - 14H_0^4 - 64H_0^2H_{0,1}$$

$$+\frac{128}{3}\frac{x^2-10x+1}{x}H_{0,-1,-1} - 224H_0H_{0,0,1} - 320H_0H_{0,1,1} - 384H_{0,0,0,-1}$$

$$+480H_{0,0,0,1} + 192H_{0,0,1,1} - 224H_{0,1,1,1}\Bigg)(1+x) - 64\frac{(1-x)(1+x)}{x}H_0^2H_1$$

$$-\frac{8}{135}\frac{6298x^3-32859x^2+606x+48}{x}H_0 + \frac{16}{9}\left(52x^2-22x+15\right)H_0^3$$

$$+\frac{2}{45}\left(288x^3+3680x^2+1525x-7695\right)H_0^2 - \frac{64}{3}\left(2x^2+7x-3\right)H_0H_{0,-1}$$

$$+\left(\frac{8}{9}\frac{536x^3-327x^2-453x-96}{x} + \frac{32}{3}\frac{32x^3+6x^2-21x+12}{x}H_0\right)H_{0,1}$$

$$
+ \left(\frac{128}{3} \left(2x^2 + x - 9 \right) + 256 x H_0 \right) H_{0,0,-1} - \frac{32}{3} \frac{20x^3 + 63x^2 - 12x + 12}{x} H_{0,0,1}
$$

$$
+ \frac{16}{3} \frac{36x^3 - 45x^2 - 27x + 40}{x} H_{0,1,1} + \frac{128}{3} \Big[H_{-1} H_{0,1} - H_{0,-1,1}
$$

$$
- H_{0,1,-1} \Big] \frac{(1+x)^3}{x} + \left(\left(32 \frac{6x^2 + 5x + 6}{x} H_1 - 128 H_{0,-1} \right) (1-x) \right.
$$

$$
- \frac{16}{45} \left(72x^3 + 1100x^2 - 545x - 3615 \right) + \left(-\frac{64}{3} \frac{x^2 + 14x + 1}{x} H_{-1} + 288 H_0^2 \right.
$$

$$
+ 192 H_{0,1} \Big) (1+x) - \frac{32}{3} \left(56x^2 - 61x - 30 \right) H_0 \Big) \zeta_2 + \left(\frac{16}{3} \frac{219x^2 + 51x - 16}{x} \right.
$$

$$
- 64 \left(3x - 1 \right) H_0 \Big) \zeta_3 - 16 \left(33x + 23 \right) \zeta_4 \Big] + \left(\frac{4}{81} \frac{6864x^2 - 2983x + 7131}{x} \right.
$$

$$
+ \left(-\frac{4}{27} \frac{4x^2 + 47x + 40}{x} + \frac{64}{27} \frac{4x^2 + 7x + 4}{x} H_0 \right) H_1^3 + \left(\frac{152}{27} \frac{4x^2 + 7x + 4}{x} H_0^3 \right.
$$

$$
- \frac{4}{81} \frac{8800x^2 + 5436x - 3701}{x} - \frac{8}{81} \frac{208x^2 - 6287x + 334}{x} H_0
$$

$$
- \frac{4}{27} \frac{508x^2 + 1729x - 572}{x} H_0^2 \right) H_1 + \left(-\frac{4}{81} \frac{3578x^2 + 8933x - 427}{x} \right.
$$

$$
+ \frac{4}{27} \frac{460x^2 + 475x + 136}{x} H_0 + \frac{40}{9} \frac{4x^2 + 7x + 4}{x} H_0^2 \right) H_1^2 + \frac{4}{3} \frac{4x^2 + 7x + 4}{x} \left(\frac{1}{9} H_1^3 \right.
$$

$$
+ \frac{112}{3} H_0 H_{0,1} + 4 H_1 H_{0,1} - \frac{224}{3} H_{0,0,1} - \frac{104}{3} H_{0,1,1} \right) H_1 \right) (1-x) + \left(-\frac{6}{5} H_0^5 \right.
$$

$$
+ \frac{304}{9} H_0^3 H_{0,1} + \frac{448}{3} H_0 H_{0,1}^2 - \left(144 H_0^2 + \frac{1792}{3} H_{0,1} \right) H_{0,0,1} + \frac{1408}{3} H_0 H_{0,0,0,1}
$$

$$
+ \left(\frac{160}{3} H_0^2 + 64 H_{0,1} \right) H_{0,1,1} - \frac{2080}{3} H_0 H_{0,0,1,1} + \frac{256}{3} H_0 H_{0,1,1,1} - \frac{3376}{3} H_{0,0,0,0,1}
$$

$$
+ 3456 H_{0,0,0,1,1} + \frac{4096}{3} H_{0,0,1,0,1} - 544 H_{0,0,1,1,1} - \frac{1024}{3} H_{0,1,0,1,1}
$$

$$
+ \frac{64}{3} H_{0,1,1,1,1} \right) (1+x) + \frac{2}{81} \left(8488x^3 + 16583x^2 - 20811x - 2964 \right) \frac{H_0^2}{1-x}
$$

$$
+ \frac{8}{81} \left(8810x^2 + 2429x - 1451 \right) H_0 - \frac{2}{27} \left(1128x^2 + 137x + 565 \right) H_0^3
$$

$$
+ \frac{2}{27} \left(164x^2 + 57x + 75 \right) H_0^4 + \left(\frac{8}{81} \frac{1942x^3 + 12447x^2 - 8514x + 334}{x} \right.
$$

$$
- \frac{32}{27} \frac{564x^3 + 966x^2 - 912x + 143}{x} H_0 + \frac{8}{9} \frac{4x^3 - 315x^2 - 63x - 76}{x} H_0^2 \right) H_{0,1}
$$

$$
+ \frac{32}{9} \frac{4x^3 - 207x^2 + 207x - 22}{x} H_1 H_{0,1} + \frac{32}{9} \frac{114x^3 - 849x^2 - 129x - 38}{x} H_{0,0,0,1}
$$

$$
+ \frac{16}{9} \frac{16x^3 - 843x^2 - 297x + 264}{x} H_{0,0,1,1} - \frac{64}{9} \frac{54x^3 + 45x^2 - 30x - 52}{x} H_{0,1,1,1}
$$

$$
- \frac{32}{9} \frac{46x^3 - 33x^2 - 57x - 28}{x} H_{0,1}^2 + \left(\frac{4}{27} \frac{5152x^3 + 12297x^2 - 12279x + 1144}{x} \right.
$$

$$
- \frac{32}{9} \frac{10x^3 - 465x^2 - 51x - 38}{x} H_0 \right) H_{0,0,1} + \left(\frac{8}{27} \frac{272x^3 + 7152x^2 - 6711x + 392}{x} \right.
$$

$$+ \frac{64}{3} \frac{18x^3 + 16x^2 - 13x - 22}{x} H_0 \bigg) H_{0,1,1} + \bigg(\bigg(- \frac{160}{9} \frac{4x^2 + 7x + 4}{x} H_0 H_1$$

$$- \frac{112}{9} \frac{4x^2 + 7x + 4}{x} H_1^2 \bigg)(1-x) - \frac{8}{81} \big(2150x^2 + 5952x - 1893 \big) + \bigg(\frac{248}{9} H_0^3$$

$$- \frac{320}{3} H_0 H_{0,1} - \frac{224}{3} H_{0,0,1} - \frac{448}{3} H_{0,1,1} \bigg)(1+x) + \frac{4}{9} \big(952x^2 + 239x + 763 \big) H_0$$

$$- \frac{16}{9} \big(52x^2 + 45x - 42 \big) H_0^2 + \frac{8}{27} \frac{412x^3 + 2499x^2 - 2823x + 128}{x} H_1$$

$$+ \frac{64}{9} \frac{20x^3 - 60x^2 - 39x + 10}{x} H_{0,1} \bigg) \zeta_2 + \frac{1024}{3} (1+x) \ln^3(2) \zeta_2$$

$$+ \bigg(\frac{608}{9} \frac{4x^2 + 7x + 4}{x} (1-x) H_1 + \bigg(\frac{904}{3} H_0^2 + \frac{1216}{3} H_{0,1} \bigg)(1+x)$$

$$- \frac{4}{27} \frac{3904x^3 + 2289x^2 - 15861x + 1938}{x} - \frac{16}{9} \big(232x^2 - 921x - 309 \big) H_0 \bigg) \zeta_3$$

$$+ \bigg(1792(1+x) H_0 - \frac{896}{3} \frac{4x^3 - 9x^2 - 6x - 2}{x} \bigg) \ln(2) \zeta_3 + 1792(1+x) \ln^2(2) \zeta_3$$

$$+ 192(1+x) \zeta_2 \zeta_3 + \bigg(\frac{328}{3} (1+x) H_0 - \frac{4}{9} \frac{184x^3 - 4083x^2 + 9x + 540}{x} \bigg) \zeta_4$$

$$+ 1664(1+x) \ln(2) \zeta_4 + \bigg(128(1+x) H_0 - \frac{32}{3} \frac{8x^3 - 30x^2 - 15x - 2}{x} \bigg) B_4$$

$$- 3304(1+x) \zeta_5 + 4096(1+x) \text{Li}_5 \bigg(\frac{1}{2} \bigg) + 256(1+x) B_4 \ln(2) - \frac{512}{15} (1+x) \ln^5(2) \bigg]$$

$$+ C_F T_F^2 \bigg[\big[\tfrac{1}{3} L_Q^3 - \tfrac{4}{3} L_M^3 + L_M^2 L_Q \big] \bigg[\frac{32}{9} \frac{4x^2 + 7x + 4}{x} (1-x) + \frac{64}{3} (1+x) H_0 \bigg]$$

$$+ L_M^2 \bigg[- \frac{32}{27} \frac{142x^2 + 103x + 34}{x} (1-x) - \frac{64}{9} \big(4x^2 + 26x + 11 \big) H_0 \bigg]$$

$$+ L_Q^2 \bigg[- \frac{32}{9} \frac{10x^2 + 33x - 2}{x} (1-x) - \frac{64}{3} (1+x) H_0^2 + \frac{64}{9} \big(4x^2 - 11x - 8 \big) H_0 \bigg]$$

$$+ L_M L_Q \bigg[\bigg(\frac{64}{27} \frac{38x^2 + 47x + 20}{x} - \frac{64}{9} \frac{4x^2 + 7x + 4}{x} H_1 \bigg)(1-x) - \frac{128}{3} (1+x) H_{0,1}$$

$$+ \frac{128}{9} \big(2x^2 + 11x + 8 \big) H_0 + \frac{128}{3} (1+x) \zeta_2 \bigg] + L_M \bigg[\bigg(- \frac{64}{81} \frac{616x^2 + 667x + 94}{x}$$

$$- \frac{128}{27} \frac{4x^2 - 26x + 13}{x} H_1 + \frac{32}{9} \frac{4x^2 + 7x + 4}{x} \big[4H_0 H_1 + H_1^2 \big] \bigg)(1-x)$$

$$+ \bigg(- \frac{928}{9} H_0^2 - \frac{64}{9} H_0^3 + \frac{256}{3} H_0 H_{0,1} - \frac{256}{3} H_{0,0,1} + \frac{128}{3} H_{0,1,1} \bigg)(1+x)$$

$$- \frac{128}{27} \big(14x^2 + 127x + 64 \big) H_0 - \frac{128}{9} \frac{2x^3 - 3x^2 + 3x + 4}{x} H_{0,1} + \frac{128}{3} (1+x) \zeta_3$$

$$+ \frac{256}{3} \big[x^2 - (1+x) H_0 \big] \zeta_2 \bigg] + L_Q \bigg[\frac{64}{81} \frac{304x^2 + 811x + 124}{x} (1-x) + \frac{64}{3} (1+x) H_0^3$$

$$- \frac{64}{27} \big(60x^2 - 155x - 233 \big) H_0 - \frac{32}{9} \big(12x^2 - 59x - 29 \big) H_0^2 - \frac{256}{9} \frac{3x^2 + 1}{x} \zeta_2$$

$$+ \frac{256}{9} \big[-H_{-1} H_0 + H_{0,-1} \big] \frac{(1+x)^3}{x} \bigg] + \bigg(\frac{16}{9} \frac{4x^2 + 7x + 4}{x} \big[H_0 H_1^2 + 2H_0^2 H_1$$

$$- \frac{10}{9}H_1^3 - 8H_1H_{0,1}\Big] - \Bigg(\frac{32}{405}\frac{24x^4 - 204x^3 - 1476x^2 + 295x + 690}{x}$$

$$+ \frac{32}{135}\frac{8x^5 - 72x^4 - 32x^3 + 58x^2 - 1077x - 100}{x}H_0\Bigg)H_1$$

$$+ \frac{64}{3645}\frac{216x^4 - 1836x^3 - 20863x^2 - 6610x + 5030}{x}$$

$$+ \frac{16}{405}\frac{24x^5 - 216x^4 - 96x^3 + 1334x^2 - 3061x + 590}{x}H_1^2\Bigg)(1 - x) + \Bigg(\frac{40}{27}H_0^4$$

$$+ \frac{64}{3}H_0^2H_{0,1} - \frac{128}{3}H_{0,1}^2 - \frac{128}{3}H_0H_{0,0,1} + \frac{64}{3}H_0H_{0,1,1} - \frac{256}{9}H_{0,0,0,1} + \frac{320}{9}H_{0,0,1,1}$$

$$- \frac{640}{9}H_{0,1,1,1}\Bigg)(1 + x) - \frac{32}{1215}\big(72x^4 - 684x^3 + 264x^2 + 21103x - 3845\big)H_0$$

$$+ \frac{32}{405}\big(12x^5 - 120x^4 + 60x^3 + 135x^2 - 3470x - 320\big)H_0^2$$

$$- \frac{16}{81}\big(24x^2 - 13x - 49\big)H_0^3 + \Bigg(\frac{64}{9}\frac{2x^3 + 21x^2 + 18x - 4}{x}H_0$$

$$- \frac{64}{405}\frac{24x^6 - 240x^5 + 120x^4 + 1050x^3 - 4405x^2 + 2048x + 150}{x}\Bigg)H_{0,1}$$

$$+ \frac{64}{27}\frac{18x^3 - 76x^2 - 103x + 12}{x}H_{0,0,1} - \frac{128}{27}\frac{3x^3 + 17x^2 - x - 21}{x}H_{0,1,1}$$

$$+ \Bigg(\frac{32}{405}\big(24x^5 - 240x^4 + 120x^3 + 1830x^2 - 5405x + 1165\big) + \Bigg(\frac{128}{9}H_0^2$$

$$+ 64H_{0,1}\Bigg)(1 + x) + \frac{32}{3}\frac{4x^2 + 7x + 4}{x}(1 - x)H_1 - \frac{64}{27}\big(18x^2 + 41x + 14\big)H_0\Bigg)\zeta_2$$

$$+ \Bigg(\frac{64}{9}(1 + x)H_0 - \frac{32}{27}\frac{20x^3 - 223x^2 - 199x + 112}{x}\Bigg)\zeta_3 + \frac{112}{3}(1 + x)\zeta_4\Bigg]$$

$$+ C_F N_F T_F^2 \Bigg[\big[L_Q^3 - L_M^3\big]\Bigg[\frac{32}{27}\frac{4x^2 + 7x + 4}{x}(1 - x) + \frac{64}{9}(1 + x)H_0\Bigg]$$

$$+ L_M^2\Bigg[\Bigg(-\frac{32}{3}\big(2x - 5\big) - \frac{32}{9}\frac{4x^2 + 7x + 4}{x}H_1\Bigg)(1 - x) - \frac{32}{9}\big(4x^2 - 7x - 13\big)H_0$$

$$+ \Bigg(\frac{32}{3}H_0^2 - \frac{64}{3}H_{0,1}\Bigg)(1 + x) + \frac{64}{3}(1 + x)\zeta_2\Bigg] + L_Q^2\Bigg[-\frac{32}{9}\frac{10x^2 + 33x - 2}{x}(1 - x)$$

$$- \frac{64}{3}(1 + x)H_0^2 + \frac{64}{9}\big(4x^2 - 11x - 8\big)H_0\Bigg] + L_M\Bigg[\Bigg(-\frac{128}{81}\frac{25x^2 + 94x + 34}{x}$$

$$- \frac{32}{27}\frac{74x^2 - 43x + 20}{x}H_1 + \frac{16}{9}\frac{4x^2 + 7x + 4}{x}\big[4H_0H_1 - H_1^2\big]\Bigg)(1 - x)$$

$$+ \frac{64}{27}\big(x^2 + 2x - 58\big)H_0 + \frac{32}{9}\big(4x^2 - 7x - 13\big)H_0^2 + \Bigg(-\frac{64}{9}H_0^3 + \frac{128}{3}H_0H_{0,1}$$

$$- \frac{128}{3}H_{0,0,1} - \frac{64}{3}H_{0,1,1}\Bigg)(1 + x) - \frac{64}{9}\frac{2x^3 + x^2 - 2x + 4}{x}H_{0,1}$$

$$+ \Bigg(-\frac{128}{3}(1 + x)H_0 + \frac{64}{9}\big(6x^2 + 4x - 5\big)\Bigg)\zeta_2 + 64(1 + x)\zeta_3\Bigg]$$

$$+ L_Q\Bigg[\frac{64}{3}\big[H_0^3 - H_{0,1,1}\big](1 + x) + \Bigg(\frac{64}{81}\frac{194x^2 + 683x + 68}{x} - \frac{16}{9}\frac{4x^2 + 7x + 4}{x}H_1^2$$

$$
\begin{aligned}
&+ \frac{32}{27}\frac{38x^2 + 47x + 20}{x}H_1\Bigg)(1-x) - \frac{64}{27}\left(79x^2 - 88x - 190\right)H_0 \\
&- \frac{32}{9}\left(12x^2 - 59x - 29\right)H_0^2 + \frac{64}{9}\left(2x^2 + 11x + 8\right)H_{0,1} + \frac{64}{3}(1+x)\zeta_3 \\
&+ \frac{256}{9}\left[H_{0,-1} - H_{-1}H_0\right]\frac{(1+x)^3}{x} - \frac{64}{9}\frac{2x^3 + 23x^2 + 8x + 4}{x}\zeta_2\Bigg] \\
&+ \Bigg(\frac{64}{3}(2x-5)H_1 H_0 - \frac{64}{81}\frac{150x^2 + 103x + 60}{x}H_1 - \frac{16}{81}\frac{74x^2 - 43x + 20}{x}H_1^2 \\
&- \frac{64}{729}\frac{1697x^2 - 2023x + 752}{x} + \frac{16}{9}\frac{4x^2 + 7x + 4}{x}\Bigg(2H_0 H_1^2 - 2H_0^2 H_1 \\
&- \frac{1}{9}H_1^3\Bigg)\Bigg)(1-x) + \Bigg(\frac{40}{27}H_0^4 - \frac{64}{3}H_0^2 H_{0,1} + \frac{128}{3}H_0 H_{0,0,1} + \frac{128}{3}H_0 H_{0,1,1} \\
&- \frac{256}{9}H_{0,0,0,1} - \frac{640}{9}H_{0,0,1,1} - \frac{64}{9}H_{0,1,1,1}\Bigg)(1+x) + \frac{32}{81}\left(54x^2 + 29x + 137\right)H_0^2 \\
&- \frac{16}{81}\left(24x^2 - 13x - 49\right)H_0^3 + \frac{64}{27}\frac{59x^2 + 59x - 12}{x}H_{0,0,1} - \Bigg(\frac{128}{9}\frac{5x^2 + 5x - 2}{x}H_0 \\
&+ \frac{64}{81}\left(57x^2 + 253x - 35\right)\Bigg)H_{0,1} - \frac{32}{243}\left(300x^2 - 967x - 769\right)H_0 \\
&+ \frac{64}{27}\frac{6x^3 + 5x^2 - 4x - 12}{x}H_{0,1,1} + \Bigg(-\frac{64}{9}\frac{4x^2 + 7x + 4}{x}(1-x)H_1 + \frac{128}{3}\Bigg(\frac{1}{3}H_0^2 \\
&- H_{0,1}\Bigg)(1+x) + \frac{64}{81}\left(111x^2 + 64x + 100\right) - \frac{128}{27}\left(6x^2 + 4x - 5\right)H_0\Bigg)\zeta_2 \\
&+ \Bigg(-\frac{128}{9}(1+x)H_0 + \frac{64}{27}\frac{2x^3 - 58x^2 - 61x + 16}{x}\Bigg)\zeta_3 + 160(1+x)\zeta_4\Bigg] \\
&+ a_{Qq}^{\mathrm{PS,b},(3)} + \tilde{c}_{q,2}^{\mathrm{PS},(3)}(N_F + 1)\Bigg\}, \tag{E.14}
\end{aligned}
$$

where $a_{Qq}^{\mathrm{PS,b},(3)}$ is the part of the OME containing HPLs with argument $1 - 2x$, cf. Eq. (5.64), and $\tilde{c}_{q,2}^{\mathrm{PS},(3)}(N_F + 1)$ denotes the massless Wilson coefficient [138]. We make use of the shorthand notation defined in Eq. (2.96).

Bibliography

[1] H. Geiger, "On the Scattering of the α-Particles by Matter", Proc. R. Soc. Lond. **A81** (1908) 174.

[2] H. Geiger and E. Marsden, "On a Diffuse Reflection of the α-Particles", Proc. R. Soc. Lond. **A82** (1909) 495.

[3] H. Geiger, "The Scattering of the α-Particles by Matter", Proc. R. Soc. Lond. **A83** (1910) 492.

[4] H. Geiger and E. Marsden, "The laws of deflexion of a particles through large angles", Phil. Mag., 6th ser. **25** (1913) 604.

[5] E. Rutherford, "The scattering of α and β particles by matter and the structure of the atom", Phil. Mag., 6th ser. **21** (1911) 669.

[6] J. J. Thomson, "On the structure of the atom: an investigation of the stability and periods of oscillation of a number of corpuscles arranged at equal intervals around the circumference of a circle; with application of the results to the theory of atomic structure", Phil. Mag., 6th ser. **7** (1904) 237.

[7] E. Rutherford, "Collision of α particles with light atoms. IV. An anomalous effect in nitrogen", Phil. Mag., 6th ser. **37** (1919) 581.

[8] J. Chadwick, "Possible Existence of a Neutron", Nature **129** (1932) 312.

[9] R. Frisch and O. Stern, "Über die magnetische Ablenkung von Wasserstoffmolekülen und das magnetische Moment des Protons. I", Z. Phys. **85** (1933) 4.

[10] R. F. Bacher, "Note on the Magnetic Moment of the Nitrogen Nucleus", Phys. Rev. **43** (1933) 1001.

[11] L. W. Alvarez and F. Bloch, "A Quantitative Determination of the Neutron Moment in Absolute Nuclear Magnetons", Phys. Rev. **57** (1940) 111.

[12] R. Hofstadter, *Electron scattering and nuclear and nucleon structure, a collection of reprints with an introduction* (W. A. Benjamin, New York, 1963), 690 pp., and references therein.

[13] W. K. H. Panofsky, "Low q^2 electrodynamics: Elastic and inelastic electron (and muon) scattering", in Proc. 14th Int. Conf. on High-Energy Physics, Vienna, edited by J. Prentki and J. Steinberger (1968), 23, SLAC-PUB-0502.

[14] R. E. Taylor, "Inelastic electron - proton scattering in the deep continuum region", in 4th Int. Symposium on Electron and Photon Interactions at High Energies Liverpool, England, edited by D. W. Braben and R. E. Rand (1969), 251, SLAC-PUB-0677.

[15] M. Breidenbach, J. I. Friedman, H. W. Kendall, E. D. Bloom, D. Coward et al., "Observed behavior of highly inelastic electron-proton scattering", Phys. Rev. Lett. **23** (1969) 935.

[16] E. D. Bloom, D. Coward, H. DeStaebler, J. Drees, G. Miller et al., "High-energy inelastic $e\,p$ scattering at 6 degrees and 10 degrees", Phys. Rev. Lett. **23** (1969) 930.

[17] R. E. Taylor, "Deep inelastic scattering: The early years", Rev. Mod. Phys. **63** (1991) 573.

Bibliography

[18] H. W. Kendall, "Deep inelastic scattering: Experiments on the proton and the observation of scaling", Rev. Mod. Phys. **63** (1991) 597.

[19] J. I. Friedman, "Deep inelastic scattering: Comparisons with the quark model", Rev. Mod. Phys. **63** (1991) 615.

[20] J. D. Bjorken, "Asymptotic Sum Rules at Infinite Momentum", Phys. Rev. **179** (1969) 1547.

[21] R. P. Feynman, "Very high-energy collisions of hadrons", Phys. Rev. Lett. **23** (1969) 1415.

[22] R. P. Feynman, "The behavior of hadron collisions at extreme energies", in 3rd International Conference on High Energy Collisions Stony Brook, New York, edited by C. N. Yang (1969), 237.

[23] R. P. Feynman, *Photon-hadron interactions* (Benjamin, Reading, MA, 1972), 282 pp.

[24] C. G. Callan, Jr. and D. J. Gross, "High-energy electroproduction and the constitution of the electric current", Phys. Rev. Lett. **22** (1969) 156.

[25] J. J. Sakurai, "Vector-meson dominance - present status and future prospects", in 4th Int. Symposium on Electron and Photon Interactions at High Energies Liverpool, England, edited by D. W. Braben and R. E. Rand (1969), 91.

[26] J. J. Sakurai, "Vector meson dominance and high-energy electron proton inelastic scattering", Phys. Rev. Lett. **22** (1969) 981.

[27] M. Gell-Mann, "The Eightfold Way: A Theory of strong interaction symmetry", preprint CTSL-20 (California Institute of Technology, 1961), unpublished.

[28] Y. Ne'eman, "Derivation of strong interactions from a gauge invariance", Nucl. Phys. **26** (1961) 222.

[29] M. Gell-Mann and Y. Ne'eman, eds., *The Eightfold way: a review with a collection of reprints* (W.A. Benjamin, New York, 1964), 317 pp.

[30] S. Okubo, "Note on unitary symmetry in strong interactions", Prog. Theor. Phys. **27** (1962) 949.

[31] S. Okubo, "Note on Unitary Symmetry in Strong Interaction. II Excited States of Baryons", Prog. Theor. Phys. **28** (1962) 24.

[32] V. E. Barnes et al., "Observation of a Hyperon with Strangeness -3", Phys. Rev. Lett. **12** (1964) 204.

[33] M. Gell-Mann, "A Schematic Model of Baryons and Mesons", Phys. Lett. **8** (1964) 214.

[34] G. Zweig, "An $SU(3)$ model for strong interaction symmetry and its breaking", preprint CERN-TH-401 (CERN, 1964); preprint CERN-TH-412 (CERN, 1964).

[35] J. D. Bjorken and E. A. Paschos, "Inelastic Electron-Proton and γ-Proton Scattering and the Structure of the Nucleon", Phys. Rev. **185** (1969) 1975.

[36] See section "Free Quark Searches" in Ref. [37] and references therein.

[37] K. A. Olive et al., "Review of Particle Physics", Chin. Phys. **C38** (2014) 090001.

[38] W. Pauli, "The Connection Between Spin and Statistics", Phys. Rev. **58** (1940) 716.

[39] G. Lüders and B. Zumino, "Connection between Spin and Statistics", Phys. Rev. **110** (1958) 1450.

[40] N. Burgoyne, "On the connection of spin with statistics", Nuovo Cim. **8** (1958) 607.

[41] R. F. Streater and A. S. Wightman, *PCT, spin and statistics, and all that* (Addison-Wesley, Redwood City, 1989), 207 pp.

[42] I. Duck and E. C. G. Sudarshan, *Pauli and the spin-statistics theorem* (Singapore, 1997), 512 pp., and references therein.

[43] O. W. Greenberg, "Spin and Unitary Spin Independence in a Paraquark Model of Baryons and Mesons", Phys. Rev. Lett. **13** (1964) 598.

[44] M. Y. Han and Y. Nambu, "Three Triplet Model with Double SU(3) Symmetry", Phys. Rev. **139** (1965) B1006.

[45] Y. Nambu, "A Systematics of Hadrons in Subnuclear Physics", in *Preludes in Theoretical Physics*, edited by A. De-Shalit, H. Feshbach and L. Van Hove (North-Holland, Amsterdam, 1966), 133.

[46] N. N. Bogolyubov, B. V. Struminsky and A. N. Tavkhelidze, "On the composite models in theories of elementary particles", preprint JINR-D-1968 (JINR, Dubna, 1965), unpublished.

[47] Y. Miyamoto, "Three Kinds of Triplet Model", Prog. Theor. Phys. Suppl. **E65** (1965) 187.

[48] C. N. Yang and R. L. Mills, "Conservation of Isotopic Spin and Isotopic Gauge Invariance", Phys. Rev. **96** (1954) 191.

[49] L. D. Faddeev and V. N. Popov, "Feynman Diagrams for the Yang-Mills Field", Phys. Lett. **B25** (1967) 29.

[50] G. 't Hooft, "Renormalization of Massless Yang-Mills Fields", Nucl. Phys. **B33** (1971) 173.

[51] G. 't Hooft, "Renormalizable Lagrangians for Massive Yang-Mills Fields", Nucl. Phys. **B35** (1971) 167.

[52] G. 't Hooft and M. J. G. Veltman, "Combinatorics of gauge fields", Nucl. Phys. **B50** (1972) 318.

[53] G. 't Hooft and M. J. G. Veltman, "DIAGRAMMAR", NATO Sci. Ser. B **4** (1974) 177.

[54] B. W. Lee and J. Zinn-Justin, "Spontaneously Broken Gauge Symmetries. 1. Preliminaries", Phys. Rev. **D5** (1972) 3121.

[55] B. W. Lee and J. Zinn-Justin, "Spontaneously Broken Gauge Symmetries. 4. General Gauge Formulation", Phys. Rev. **D7** (1973) 1049.

[56] S. L. Glashow, "Partial Symmetries of Weak Interactions", Nucl. Phys. **22** (1961) 579.

[57] S. Weinberg, "A Model of Leptons", Phys. Rev. Lett. **19** (1967) 1264.

[58] A. Salam, "Weak and Electromagnetic Interactions", in 8th Nobel Symposium Lerum, Sweden, edited by N. Svartholm (1968), 367.

[59] A. Zee, "Study of the renormalization group for small coupling constants", Phys. Rev. **D7** (1973) 3630.

[60] S. R. Coleman and D. J. Gross, "Price of asymptotic freedom", Phys. Rev. Lett. **31** (1973) 851.

[61] D. J. Gross and F. Wilczek, "Ultraviolet Behavior of Nonabelian Gauge Theories", Phys. Rev. Lett. **30** (1973) 1343.

[62] H. D. Politzer, "Reliable Perturbative Results for Strong Interactions?", Phys. Rev. Lett. **30** (1973) 1346.

[63] G. 't Hooft, 1972, unpublished; G. 't Hooft and M. Veltman, in Proc. Colloquium on Renormalization of Yang-Mills Fields, Marseille, 1972, edited by C. Korthals-Altes et al. (1972); G. 't Hooft, "The birth of asymptotic freedom", Nucl. Phys. **B254** (1985) 11.

[64] H. Fritzsch and M. Gell-Mann, "Current algebra: Quarks and what else?", in Proc. 16th Int. Conf. High-Energy Physics, ICHEP, Batavia, Illinois, edited by J. D. Jackson and A. Roberts (1972), 135, arXiv:`hep-ph/0208010` [`hep-ph`].

[65] H. Fritzsch, M. Gell-Mann and H. Leutwyler, "Advantages of the Color Octet Gluon Picture", Phys. Lett. **B47** (1973) 365.

[66] S. Weinberg, "Nonabelian Gauge Theories of the Strong Interactions", Phys. Rev. Lett. **31** (1973) 494.

[67] D. J. Gross and F. Wilczek, "Asymptotically Free Gauge Theories. 1", Phys. Rev. **D8** (1973) 3633.

[68] K. G. Wilson, "Nonlagrangian models of current algebra", Phys. Rev. **179** (1969) 1499.

[69] R. A. Brandt, "Field equations in quantum electrodynamics", Fortsch. Phys. **18** (1970) 249.

[70] W. Zimmermann, "Lectures on Elementary Particle Physics and Quantum Field Theory", in Proc. 1970 Brandeis Summer Institue in Theor. Phys., edited by S. Deser, M. Grisaru and H. Pendelton (1971), 396.

[71] N. H. Christ, B. Hasslacher and A. H. Mueller, "Light cone behavior of perturbation theory", Phys. Rev. **D6** (1972) 3543.

[72] W. Zimmermann, "Composite operators in the perturbation theory of renormalizable interactions", Annals Phys. **77** (1973) 536.

[73] W. Zimmermann, "Normal products and the short distance expansion in the perturbation theory of renormalizable interactions", Annals Phys. **77** (1973) 570.

[74] K. G. Wilson and W. Zimmermann, "Operator product expansions and composite field operators in the general framework of quantum field theory", Commun. Math. Phys. **24** (1972) 87.

[75] T. Muta, *Foundations of Quantum Chromodynamics: An Introduction to Perturbative Methods in Gauge Theories*, World Scientific Lecture Notes in Physics 78 (World Scientific, Singapore, 2010).

[76] F. J. Ynduráin, *The Theory of Quark and Gluon Interactions*, Theoretical and Mathematical Physics (Springer, Berlin, 2006).

[77] R. A. Brandt and G. Preparata, "Operator product expansions near the light cone", Nucl. Phys. **B27** (1972) 541.

[78] Y. Frishman, "Operator products at almost light like distances", Annals Phys. **66** (1971) 373.

[79] D. J. Gross and S. B. Treiman, "Light cone structure of current commutators in the gluon quark model", Phys. Rev. **D4** (1971) 1059.

[80] D. J. Gross and F. Wilczek, "Asymptotically Free Gauge Theories. 2", Phys. Rev. **D9** (1974) 980.

[81] H. Georgi and H. D. Politzer, "Electroproduction scaling in an asymptotically free theory of strong interactions", Phys. Rev. **D9** (1974) 416.

[82] E. C. G. Stueckelberg and A. Petermann, "The normalization group in quantum theory", Helv. Phys. Acta **24** (1951) 317.

[83] A. Petermann and E. C. G. Stueckelberg, "La normalisation des constantes dans la théorie des quanta", Helv. Phys. Acta **26** (1953) 499.

[84] M. Gell-Mann and F. E. Low, "Quantum electrodynamics at small distances", Phys. Rev. **95** (1954) 1300.

[85] N. N. Bogolyubov and D. V. Shirkov, *Introduction to the theory of quantized fields*, Intersci. Monogr. Phys. Astron. 3 (Interscience Publishers, New York, 1959), 720 pp.

[86] C. G. Callan, Jr., "Broken scale invariance in scalar field theory", Phys. Rev. **D2** (1970) 1541.

[87] K. Symanzik, "Small distance behavior in field theory and power counting", Commun. Math. Phys. **18** (1970) 227.

[88] C. Chang et al., "Observed Deviations from Scale Invariance in High-Energy Muon Scattering", Phys. Rev. Lett. **35** (1975) 901.

[89] Y. Watanabe et al., "Test of Scale Invariance in Ratios of Muon Scattering Cross-Sections at 150-GeV and 56-GeV", Phys. Rev. Lett. **35** (1975) 898.

[90] G. Parisi, "Experimental limits on the values of anomalous dimensions", Phys. Lett. **B43** (1973) 207.

[91] G. Parisi, "Detailed Predictions for the p n Structure Functions in Theories with Computable Large Momenta Behavior", Phys. Lett. **B50** (1974) 367.

[92] D. J. Gross, "How to Test Scaling in Asymptotically Free Theories", Phys. Rev. Lett. **32** (1974) 1071.

[93] A. Zee, F. Wilczek and S. B. Treiman, "Scaling Deviations for Neutrino Reactions in Asymptotically Free Field Theories", Phys. Rev. **D10** (1974) 2881.

[94] G. Parisi, "An Introduction to Scaling Violations", in Weak Interactions and Neutrino Physics. Proceedings: 11th Rencontre de Moriond, Flaine 1976, Feb 28-Mar 12, 1976. (1976), 83.

[95] K. J. Kim and K. Schilcher, "Scaling Violation in the Infinite Momentum Frame", Phys. Rev. **D17** (1978) 2800.

[96] G. Altarelli and G. Parisi, "Asymptotic Freedom in Parton Language", Nucl. Phys. **B126** (1977) 298.

[97] Y. L. Dokshitzer, "Calculation of the Structure Functions for Deep Inelastic Scattering and e^+e^- Annihilation by Perturbation Theory in Quantum Chromodynamics.", Sov. Phys. JETP **46** (1977) 641, [Zh. Eksp. Teor. Fiz. **73** (1977) 1216].

[98] V. N. Gribov and L. N. Lipatov, "Deep inelastic $e\,p$ scattering in perturbation theory", Sov. J. Nucl. Phys. **15** (1972) 438, [Yad. Fiz. **15** (1972) 781].

[99] *HERA - A Proposal for a Large Electron Proton Colliding Beam Facility at DESY* (DESY, Hamburg, 1981), 292 pp., DESY-HERA-81-10.

[100] H. Abramowicz et al., "Combination of measurements of inclusive deep inelastic $e^{\pm}p$ scattering cross sections and QCD analysis of HERA data", Eur. Phys. J. **C75** (2015) 580, arXiv:1506.06042 [hep-ex].

[101] I. Abt et al., *The H1 detector at HERA* (1993), 194 pp., DESY-93-103.

[102] M. Derrick et al., "Initial study of deep inelastic scattering with ZEUS at HERA", Phys. Lett. **B303** (1993) 183.

[103] K. Ackerstaff et al., "The HERMES spectrometer", Nucl. Instrum. Meth. **A417** (1998) 230, arXiv:hep-ex/9806008 [hep-ex].

[104] E. G. Floratos, D. A. Ross and C. T. Sachrajda, "Higher Order Effects in Asymptotically Free Gauge Theories. 2. Flavor Singlet Wilson Operators and Coefficient Functions", Nucl. Phys. **B152** (1979) 493.

[105] W. A. Bardeen, A. J. Buras, D. W. Duke and T. Muta, "Deep Inelastic Scattering Beyond the Leading Order in Asymptotically Free Gauge Theories", Phys. Rev. **D18** (1978) 3998.

[106] W. Furmanski and R. Petronzio, "Lepton - Hadron Processes Beyond Leading Order in Quantum Chromodynamics", Z. Phys. **C11** (1982) 293, and references therein.

[107] E. G. Floratos, D. A. Ross and C. T. Sachrajda, "Higher Order Effects in Asymptotically Free Gauge Theories: The Anomalous Dimensions of Wilson Operators", Nucl. Phys. **B129** (1977) 66, [Erratum: Nucl. Phys. **B139** (1978) 545].

[108] A. González-Arroyo, C. López and F. J. Ynduráin, "Second Order Contributions to the Structure Functions in Deep Inelastic Scattering. 1. Theoretical Calculations", Nucl. Phys. **B153** (1979) 161.

[109] A. González-Arroyo, C. López and F. J. Ynduráin, "Second order contributions to the structure functions in deep inelastic scattering. II. Comparison with experiment for the nonsinglet contributions to e, μ-nucleon scattering", Nucl. Phys. **B159** (1979) 512.

[110] A. González-Arroyo and C. López, "Second Order Contributions to the Structure Functions in Deep Inelastic Scattering. 3. The Singlet Case", Nucl. Phys. **B166** (1980) 429.

[111] G. Curci, W. Furmanski and R. Petronzio, "Evolution of Parton Densities Beyond Leading Order: The Nonsinglet Case", Nucl. Phys. **B175** (1980) 27.

[112] W. Furmanski and R. Petronzio, "Singlet Parton Densities Beyond Leading Order", Phys. Lett. **B97** (1980) 437.

[113] E. G. Floratos, R. Lacaze and C. Kounnas, "Space and Timelike Cut Vertices in QCD Beyond the Leading Order. 1. Nonsinglet Sector", Phys. Lett. **B98** (1981) 89.

[114] E. G. Floratos, R. Lacaze and C. Kounnas, "Space and Timelike Cut Vertices in QCD Beyond the Leading Order. 2. The Singlet Sector", Phys. Lett. **B98** (1981) 285.

[115] E. G. Floratos, C. Kounnas and R. Lacaze, "Higher Order QCD Effects in Inclusive Annihilation and Deep Inelastic Scattering", Nucl. Phys. **B192** (1981) 417.

[116] R. Hamberg and W. L. van Neerven, "The Correct renormalization of the gluon operator in a covariant gauge", Nucl. Phys. **B379** (1992) 143.

[117] R. K. Ellis and W. Vogelsang, "The Evolution of parton distributions beyond leading order: The Singlet case", (1996), arXiv:`hep-ph/9602356` [`hep-ph`], unpublished.

[118] S. Moch and J. A. M. Vermaseren, "Deep inelastic structure functions at two loops", Nucl. Phys. **B573** (2000) 853, arXiv:`hep-ph/9912355` [`hep-ph`].

[119] W. L. van Neerven and E. B. Zijlstra, "Order α_s^2 contributions to the deep inelastic Wilson coefficient", Phys. Lett. **B272** (1991) 127.

[120] E. B. Zijlstra and W. L. van Neerven, "Contribution of the second order gluonic Wilson coefficient to the deep inelastic structure function", Phys. Lett. **B273** (1991) 476.

[121] E. B. Zijlstra and W. L. van Neerven, "Order α_s^2 QCD corrections to the deep inelastic proton structure functions F_2 and F_L", Nucl. Phys. **B383** (1992) 525.

[122] E. B. Zijlstra and W. L. van Neerven, "Order α_s^2 correction to the structure function $F_3(x, Q^2)$ in deep inelastic neutrino - hadron scattering", Phys. Lett. **B297** (1992) 377.

[123] D. W. Duke, J. D. Kimel and G. A. Sowell, "Fourth Order QCD Corrections to the Longitudinal Coefficient Function in Deep Inelastic Scattering", Phys. Rev. **D25** (1982) 71.

[124] A. Devoto, D. W. Duke, J. D. Kimel and G. A. Sowell, "Analytic Calculation of the Fourth Order Quantum Chromodynamic Contribution to the Nonsinglet Quark Longitudinal Structure Function", Phys. Rev. **D30** (1984) 541.

[125] D. I. Kazakov and A. V. Kotikov, "Total α_s Correction to Deep Inelastic Scattering Cross-section Ratio, $R = \sigma_L/\sigma_T$ in QCD", Nucl. Phys. **B307** (1988) 721, [Erratum: Nucl. Phys. **B345** (1990) 299].

[126] D. I. Kazakov, A. V. Kotikov, G. Parente, O. A. Sampayo and J. Sanchez Guillen, "Complete quartic α_s^2 correction to the deep inelastic longitudinal structure function F_L in QCD", Phys. Rev. Lett. **65** (1990) 1535, [Erratum: Phys. Rev. Lett. **65** (1990) 2921].

[127] D. I. Kazakov and A. V. Kotikov, "On the value of the α_s-correction to the Callan-Gross relation", Phys. Lett. **B291** (1992) 171.

[128] S. A. Larin and J. A. M. Vermaseren, "Two Loop QCD Corrections to the Coefficient Functions of the Deep Inelastic Structure Functions F_2 and F_L", Z. Phys. **C57** (1993) 93.

[129] S. A. Larin and J. A. M. Vermaseren, "The α_s^3 corrections to the Bjorken sum rule for polarized electroproduction and to the Gross-Llewellyn Smith sum rule", Phys. Lett. **B259** (1991) 345.

[130] S. A. Larin, F. V. Tkachov and J. A. M. Vermaseren, "The $O(\alpha_s^3)$ QCD correction to the lowest moment of the longitudinal structure function in deep inelastic electron-nucleon scattering", Phys. Lett. **B272** (1991) 121.

[131] S. A. Larin, T. van Ritbergen and J. A. M. Vermaseren, "The next-next-to-leading QCD approximation for nonsinglet moments of deep inelastic structure functions", Nucl. Phys. **B427** (1994) 41.

[132] S. A. Larin, P. Nogueira, T. van Ritbergen and J. A. M. Vermaseren, "The three loop QCD calculation of the moments of deep inelastic structure functions", Nucl. Phys. **B492** (1997) 338, arXiv:`hep-ph/9605317` [`hep-ph`].

[133] A. Retey and J. A. M. Vermaseren, "Some higher moments of deep inelastic structure functions at next-to-next-to-leading order of perturbative QCD", Nucl. Phys. **B604** (2001) 281, arXiv:`hep-ph/0007294` [`hep-ph`].

[134] J. Blümlein and J. A. M. Vermaseren, "The 16th moment of the non-singlet structure functions $F_2(x, Q^2)$ and $F_L(x, Q^2)$ to $O(\alpha_s^3)$", Phys. Lett. **B606** (2005) 130, arXiv:`hep-ph/0411111` [`hep-ph`].

[135] S. Moch, J. A. M. Vermaseren and A. Vogt, "The three loop splitting functions in QCD: The nonsinglet case", Nucl. Phys. **B688** (2004) 101, arXiv:`hep-ph/0403192` [`hep-ph`].

[136] A. Vogt, S. Moch and J. A. M. Vermaseren, "The three-loop splitting functions in QCD: The singlet case", Nucl. Phys. **B691** (2004) 129, arXiv:`hep-ph/0404111` [`hep-ph`].

[137] S. Moch, J. A. M. Vermaseren and A. Vogt, "The longitudinal structure function at the third order", Phys. Lett. **B606** (2005) 123, arXiv:`hep-ph/0411112` [`hep-ph`].

[138] J. A. M. Vermaseren, A. Vogt and S. Moch, "The third-order QCD corrections to deep-inelastic scattering by photon exchange", Nucl. Phys. **B724** (2005) 3, arXiv:`hep-ph/0504242` [`hep-ph`].

[139] P. A. Baikov and K. G. Chetyrkin, "New four loop results in QCD", Nucl. Phys. Proc. Suppl. **160** (2006) 76.

Bibliography

[140] P. A. Baikov, K. G. Chetyrkin and J. H. Kühn, "Massless Propagators, $R(s)$ and Multiloop QCD", Nucl. Part. Phys. Proc. **261-262** (2015) 3, arXiv:1501.06739 [hep-ph].

[141] V. N. Velizhanin, "Four loop anomalous dimension of the second moment of the non-singlet twist-2 operator in QCD", Nucl. Phys. **B860** (2012) 288, arXiv:1112.3954 [hep-ph].

[142] V. N. Velizhanin, "Four loop anomalous dimension of the third and fourth moments of the non-singlet twist-2 operator in QCD", (2014), arXiv:1411.1331 [hep-ph].

[143] J. A. M. Vermaseren, "Harmonic sums, Mellin transforms and integrals", Int. J. Mod. Phys. **A14** (1999) 2037, arXiv:hep-ph/9806280 [hep-ph].

[144] J. Blümlein and S. Kurth, "Harmonic sums and Mellin transforms up to two loop order", Phys. Rev. **D60** (1999) 014018, arXiv:hep-ph/9810241 [hep-ph].

[145] E. Remiddi and J. A. M. Vermaseren, "Harmonic polylogarithms", Int. J. Mod. Phys. **A15** (2000) 725, arXiv:hep-ph/9905237 [hep-ph].

[146] J. Blümlein, "Algebraic relations between harmonic sums and associated quantities", Comput. Phys. Commun. **159** (2004) 19, arXiv:hep-ph/0311046 [hep-ph].

[147] J. Blümlein, "Structural Relations of Harmonic Sums and Mellin Transforms up to Weight $w = 5$", Comput. Phys. Commun. **180** (2009) 2218, arXiv:0901.3106 [hep-ph].

[148] J. Blümlein, "Structural Relations of Harmonic Sums and Mellin Transforms at Weight $w = 6$", in Motives, Quantum Field Theory, and Pseudodifferential Operators, Vol. 12, edited by A. Carey, D. Ellwood, S. Paycha and S. Rosenberg, Clay Mathematics Proceedings (2010), 167, arXiv:0901.0837 [math-ph].

[149] J. Blümlein, M. Kauers, S. Klein and C. Schneider, "Determining the closed forms of the $O(a_s^3)$ anomalous dimensions and Wilson coefficients from Mellin moments by means of computer algebra", Comput. Phys. Commun. **180** (2009) 2143, arXiv:0902.4091 [hep-ph].

[150] G. T. Bodwin and J.-W. Qiu, "The Gluonic Contribution to g_1 and Its Relationship to the Spin Dependent Parton Distributions", Phys. Rev. **D41** (1990) 2755.

[151] W. Vogelsang, "The Gluonic contribution to $g_1^P(x, Q^2)$ in the parton model", Z. Phys. **C50** (1991) 275.

[152] E. B. Zijlstra and W. L. van Neerven, "Order α_s^2 corrections to the polarized structure function $g_1(x, Q^2)$", Nucl. Phys. **B417** (1994) 61, [Erratum: Nucl. Phys. **B426** (1994) 245, Nucl. Phys. **B773** (2007) 105].

[153] S. Moch, J. A. M. Vermaseren and A. Vogt, "Third-order QCD corrections to the charged-current structure function F_3", Nucl. Phys. **B813** (2009) 220, arXiv:0812.4168 [hep-ph].

[154] S. Wandzura and F. Wilczek, "Sum Rules for Spin Dependent Electroproduction: Test of Relativistic Constituent Quarks", Phys. Lett. **B72** (1977) 195.

[155] K. Sasaki, "Polarized Electroproduction in Asymptotically Free Gauge Theories", Prog. Theor. Phys. **54** (1975) 1816.

[156] M. A. Ahmed and G. G. Ross, "Spin-Dependent Deep Inelastic electron Scattering in an Asymptotically Free Gauge Theory", Phys. Lett. **B56** (1975) 385.

[157] R. Mertig and W. L. van Neerven, "The Calculation of the two loop spin splitting functions $P_{ij}^{(1)}(x)$", Z. Phys. **C70** (1996) 637, arXiv:hep-ph/9506451 [hep-ph].

[158] W. Vogelsang, "A Rederivation of the spin dependent next-to-leading order splitting functions", Phys. Rev. **D54** (1996) 2023, arXiv:hep-ph/9512218 [hep-ph].

[159] W. Vogelsang, "The Spin dependent two loop splitting functions", Nucl. Phys. **B475** (1996) 47, arXiv:hep-ph/9603366 [hep-ph].

[160] S. Moch, J. A. M. Vermaseren and A. Vogt, "The Three-Loop Splitting Functions in QCD: The Helicity-Dependent Case", Nucl. Phys. **B889** (2014) 351, arXiv:`1409.5131` [`hep-ph`].

[161] S. Moch, J. A. M. Vermaseren and A. Vogt, "On γ_5 in higher-order QCD calculations and the NNLO evolution of the polarized valence distribution", Phys. Lett. **B748** (2015) 432, arXiv:`1506.04517` [`hep-ph`].

[162] S. Moch and M. Rogal, "Charged current deep-inelastic scattering at three loops", Nucl. Phys. **B782** (2007) 51, arXiv:`0704.1740` [`hep-ph`].

[163] S. Moch, M. Rogal and A. Vogt, "Differences between charged-current coefficient functions", Nucl. Phys. **B790** (2008) 317, arXiv:`0708.3731` [`hep-ph`].

[164] J. E. Augustin et al., "Discovery of a Narrow Resonance in e^+e^- Annihilation", Phys. Rev. Lett. **33** (1974) 1406.

[165] G. S. Abrams et al., "The Discovery of a Second Narrow Resonance in e^+e^- Annihilation", Phys. Rev. Lett. **33** (1974) 1453.

[166] J. J. Aubert et al., "Experimental Observation of a Heavy Particle J", Phys. Rev. Lett. **33** (1974) 1404.

[167] J. D. Bjorken and S. L. Glashow, "Elementary Particles and SU(4)", Phys. Lett. **11** (1964) 255.

[168] Y. Hara, "Unitary triplets and the eightfold way", Phys. Rev. **134** (1964) B701.

[169] Z. Maki, "The Fourth baryon, Sakata model and modified $B - L$ symmetry. 1.", Prog. Theor. Phys. **31** (1964) 331.

[170] Z. Maki, "The Fourth baryon, Sakata model and modified $B - L$ symmetry. 2.", Prog. Theor. Phys. **31** (1964) 333.

[171] Z. Maki and Y. Ohnuki, "Quartet Scheme for Elementary Particles", Prog. Theor. Phys. **32** (1964) 144.

[172] D. Amati, H. Bacry, J. Nuyts and J. Prentki, "SU(4) and strong interactions", Phys. Lett. **11** (1964) 190.

[173] M. K. Gaillard, B. W. Lee and J. L. Rosner, "Search for Charm", Rev. Mod. Phys. **47** (1975) 277.

[174] C. Bouchiat, J. Iliopoulos and P. Meyer, "An Anomaly Free Version of Weinberg's Model", Phys. Lett. **B38** (1972) 519.

[175] D. J. Gross and R. Jackiw, "Effect of anomalies on quasirenormalizable theories", Phys. Rev. **D6** (1972) 477.

[176] S. L. Glashow, J. Iliopoulos and L. Maiani, "Weak Interactions with Lepton-Hadron Symmetry", Phys. Rev. **D2** (1970) 1285.

[177] S. W. Herb et al., "Observation of a Dimuon Resonance at 9.5 GeV in 400 GeV Proton-Nucleus Collisions", Phys. Rev. Lett. **39** (1977) 252.

[178] F. Abe et al., "Evidence for top quark production in $\bar{p}p$ collisions at $\sqrt{s} = 1.8$ TeV", Phys. Rev. Lett. **73** (1994) 225, arXiv:`hep-ex/9405005` [`hep-ex`].

[179] F. Abe et al., "Observation of top quark production in $\bar{p}p$ collisions", Phys. Rev. Lett. **74** (1995) 2626, arXiv:`hep-ex/9503002` [`hep-ex`].

[180] S. Abachi et al., "Observation of the top quark", Phys. Rev. Lett. **74** (1995) 2632, arXiv:`hep-ex/9503003` [`hep-ex`].

Bibliography

[181] E. Witten, "Heavy Quark Contributions to Deep Inelastic Scattering", Nucl. Phys. **B104** (1976) 445.

[182] J. Babcock, D. W. Sivers and S. Wolfram, "QCD Estimates for Heavy Particle Production", Phys. Rev. **D18** (1978) 162.

[183] M. A. Shifman, A. I. Vainshtein and V. I. Zakharov, "Remarks on Charm Electroproduction in QCD", Nucl. Phys. **B136** (1978) 157, [Yad. Fiz. **27** (1978) 455].

[184] J. P. Leveille and T. J. Weiler, "Characteristics of Heavy Quark Leptoproduction in QCD", Nucl. Phys. **B147** (1979) 147.

[185] M. Glück and E. Reya, "Deep Inelastic Quantum Chromodynamic Charm Leptoproduction", Phys. Lett. **B83** (1979) 98.

[186] E. Laenen, S. Riemersma, J. Smith and W. L. van Neerven, "Complete $O(\alpha_s)$ corrections to heavy flavor structure functions in electroproduction", Nucl. Phys. **B392** (1993) 162.

[187] E. Laenen, S. Riemersma, J. Smith and W. L. van Neerven, "$O(\alpha_s)$ corrections to heavy flavor inclusive distributions in electroproduction", Nucl. Phys. **B392** (1993) 229.

[188] S. Riemersma, J. Smith and W. L. van Neerven, "Rates for inclusive deep inelastic electroproduction of charm quarks at HERA", Phys. Lett. **B347** (1995) 143, arXiv:`hep-ph/9411431` [hep-ph].

[189] A. D. Watson, "Spin Spin Asymmetries in Inclusive Muon Proton Charm Production", Z. Phys. **C12** (1982) 123.

[190] J. Blümlein, V. Ravindran and W. L. van Neerven, "Twist-2 heavy flavor contributions to the structure function $g_2(x, Q^2)$", Phys. Rev. **D68** (2003) 114004, arXiv:`hep-ph/0304292` [hep-ph].

[191] M. Buza, Y. Matiounine, J. Smith and W. L. van Neerven, "$O(\alpha_s^2)$ corrections to polarized heavy flavor production at $Q^2 \gg m^2$", Nucl. Phys. **B485** (1997) 420, arXiv:`hep-ph/9608342` [hep-ph].

[192] I. Bierenbaum, J. Blümlein and S. Klein, "Two-loop massive operator matrix elements for polarized and unpolarized deep-inelastic scattering", PoS **ACAT** (2007) 070.

[193] S. W. G. Klein, *Mellin Moments of Heavy Flavor Contributions to $F_2(x, Q^2)$ at NNLO*, PhD thesis (DESY, Berlin, 2009), arXiv:`0910.3101` [hep-ph].

[194] T. Gottschalk, "Chromodynamic Corrections to Neutrino Production of Heavy Quarks", Phys. Rev. **D23** (1981) 56.

[195] M. Glück, S. Kretzer and E. Reya, "The Strange sea density and charm production in deep inelastic charged current processes", Phys. Lett. **B380** (1996) 171, arXiv:`hep-ph/9603304` [hep-ph], [Erratum: Phys. Lett. **B405** (1997) 391].

[196] J. Blümlein, A. Hasselhuhn, P. Kovačíková and S. Moch, "$O(\alpha_s)$ Heavy Flavor Corrections to Charged Current Deep-Inelastic Scattering in Mellin Space", Phys. Lett. **B700** (2011) 294, arXiv:`1104.3449` [hep-ph].

[197] M. Buza and W. L. van Neerven, "$O(\alpha_s^2)$ contributions to charm production in charged current deep inelastic lepton-hadron scattering", Nucl. Phys. **B500** (1997) 301, arXiv:`hep-ph/9702242` [hep-ph].

[198] J. Blümlein, A. Hasselhuhn and T. Pfoh, "The $O(\alpha_s^2)$ heavy quark corrections to charged current deep-inelastic scattering at large virtualities", Nucl. Phys. **B881** (2014) 1, arXiv:`1401.4352` [hep-ph].

[199] A. Hasselhuhn, *3-Loop Contributions to Heavy Flavor Wilson Coefficients of Neutral and Charged Current DIS*, PhD thesis (Techische Universität Dortmund, 2013).

[200] S. I. Alekhin and J. Blümlein, "Mellin representation for the heavy flavor contributions to deep inelastic structure functions", Phys. Lett. **B594** (2004) 299, arXiv:`hep-ph/0404034` [`hep-ph`].

[201] M. Buza, Y. Matiounine, J. Smith, R. Migneron and W. L. van Neerven, "Heavy quark coefficient functions at asymptotic values $Q^2 \gg m^2$", Nucl. Phys. **B472** (1996) 611, arXiv:`hep-ph/9601302` [`hep-ph`].

[202] M. Buza, Y. Matiounine, J. Smith and W. L. van Neerven, "Charm electroproduction viewed in the variable flavor number scheme versus fixed order perturbation theory", Eur. Phys. J. **C1** (1998) 301, arXiv:`hep-ph/9612398` [`hep-ph`].

[203] I. Bierenbaum, J. Blümlein and S. Klein, "Mellin Moments of the $O(\alpha_s^3)$ Heavy Flavor Contributions to unpolarized Deep-Inelastic Scattering at $Q^2 \gg m^2$ and Anomalous Dimensions", Nucl. Phys. **B820** (2009) 417, arXiv:`0904.3563` [`hep-ph`].

[204] I. Bierenbaum, J. Blümlein and S. Klein, "Calculation of massive 2-loop operator matrix elements with outer gluon lines", Phys. Lett. **B648** (2007) 195, arXiv:`hep-ph/0702265` [`hep-ph`].

[205] I. Bierenbaum, J. Blümlein and S. Klein, "Two-Loop Massive Operator Matrix Elements and Unpolarized Heavy Flavor Production at Asymptotic Values $Q^2 \gg m^2$", Nucl. Phys. **B780** (2007) 40, arXiv:`hep-ph/0703285` [`hep-ph`].

[206] I. Bierenbaum, J. Blümlein, S. Klein and C. Schneider, "Two-Loop Massive Operator Matrix Elements for Unpolarized Heavy Flavor Production to $O(\varepsilon)$", Nucl. Phys. **B803** (2008) 1, arXiv:`0803.0273` [`hep-ph`].

[207] I. Bierenbaum, J. Blümlein and S. Klein, "The Gluonic Operator Matrix Elements at $O(\alpha_s^2)$ for DIS Heavy Flavor Production", Phys. Lett. **B672** (2009) 401, arXiv:`0901.0669` [`hep-ph`].

[208] H. Mellin, "Om definita integraler, hvilka för obegränsadt växande värden af vissa heltaliga parametrar hafva till gränser hypergeometriska funktioner af särskilda ordningar", Acta Societatis Scientiarum Fennicae **XX** (1885) 1.

[209] E. W. Barnes, "A New Development of the Theory of the Hypergeometric Functions", Proc. London Math. Soc. **s2-6** (1908) 141.

[210] E. W. Barnes, "A Transformation of Generalised Hypergeometric Series", Quart. J. Math. **41** (1910) 136.

[211] C. F. Gauß, "Disquisitiones generales circa seriam infinitam $1 + \frac{\alpha\beta}{1\cdot\gamma}x + \frac{\alpha(\alpha+1)\beta(\beta+1)}{1\cdot2\cdot\gamma(\gamma+1)}x\ x +$ etc.", Commentationes societatis regiae scientarum Gottingensis recentiores (1812) 3.

[212] E. E. Kummer, "Über die hypergeometrische Reihe $1 + \frac{\alpha\cdot\beta}{1\cdot\gamma}x + \frac{\alpha(\alpha+1)\beta(\beta+1)}{1\cdot2\cdot\gamma(\gamma+1)}x^2 + \frac{\alpha(\alpha+1)(\alpha+2)\beta(\beta+1)(\beta+2)}{1\cdot2\cdot3\cdot\gamma(\gamma+1)(\gamma+2)}x^3 + \ldots$", J. reine angew. Math. **15** (1836) 39, 127.

[213] W. N. Bailey, *Generalized Hypergeometric Series*, Cambridge Tracts in Mathematics and Mathematical Physics 32 (Cambridge University Press, London, 1935), 108 pp.

[214] L. J. Slater, *Generalized hypergeometric functions* (Cambridge University Press, Cambridge, 1966), 273 pp.

[215] J. Blümlein, S. Klein and B. Tödtli, "$O(\alpha_s^2)$ and $O(\alpha_s^3)$ Heavy Flavor Contributions to Transversity at $Q^2 \gg m^2$", Phys. Rev. **D80** (2009) 094010, arXiv:`0909.1547` [`hep-ph`].

[216] J. A. M. Vermaseren, "New features of FORM", (2000), arXiv:`math-ph/0010025` [`math-ph`].

[217] M. Steinhauser, "MATAD: A Program package for the computation of MAssive TAD-poles", Comput. Phys. Commun. **134** (2001) 335, arXiv:`hep-ph/0009029` [`hep-ph`].

[218] S. Alekhin, J. Blümlein and S. Moch, "The ABM parton distributions tuned to LHC data", Phys. Rev. **D89** (2014) 054028, arXiv:`1310.3059` [`hep-ph`].

[219] P. Jimenez-Delgado and E. Reya, "Delineating parton distributions and the strong coupling", Phys. Rev. **D89** (2014) 074049, arXiv:`1403.1852` [`hep-ph`].

[220] S. Dulat, T. J. Hou, J. Gao, M. Guzzi, J. Huston, P. Nadolsky, J. Pumplin, C. Schmidt, D. Stump and C. P. Yuan, "The CT14 Global Analysis of Quantum Chromodynamics", (2015), arXiv:`1506.07443` [`hep-ph`].

[221] L. A. Harland-Lang, A. D. Martin, P. Motylinski and R. S. Thorne, "Parton distributions in the LHC era: MMHT 2014 PDFs", Eur. Phys. J. **C75** (2015) 204, arXiv:`1412.3989` [`hep-ph`].

[222] R. D. Ball et al., "Parton distributions for the LHC Run II", JHEP **04** (2015) 040, arXiv:`1410.8849` [`hep-ph`].

[223] S. Bethke et al., eds., *Workshop on Precision Measurements of α_s* (2011), arXiv:`1110.0016` [`hep-ph`].

[224] S. Moch et al., eds., *High precision fundamental constants at the TeV scale* (2014), arXiv:`1405.4781` [`hep-ph`].

[225] D. d'Enterria and P. Z. Skands, eds., *High-precision α_s measurements from LHC to FCC-ee* (2015), arXiv:`1512.05194` [`hep-ph`].

[226] S. Alekhin, J. Blümlein, K. Daum, K. Lipka and S. Moch, "Precise charm-quark mass from deep-inelastic scattering", Phys. Lett. **B720** (2013) 172, arXiv:`1212.2355` [`hep-ph`].

[227] J. L. Lagrange, "Nouvelle Recherches sur la nature et la Propagation du son", Miscellanea Taurinensia **II** (1760-61) 11, reprinted in J. A. Serret, ed., *Oeuvres de Lagrange*, Vol. 1 (Gauthier-Villars, Paris, 1867), pp. 151–316.

[228] C. F. Gauß, "Theoria attactionis corporum sphaeroidicorum ellipticorum homogeneorum methodo novo tractate", Commentationes scietas scientiarum Gottingensis recentiores **II** (1813), reprinted in *Werke*, Vol. 5 (Göttingen, 1867), pp. 3–22.

[229] G. Green, *An Essay on the Application of Mathematical Analysis to the Theories of Electricity and Magnetism* (Nottingham, 1828), reprinted in N. M. Ferrers, ed., *Mathematical papers of the late George Green* (Macmillan, London, 1871), pp. 1–115.

[230] M. Ostrogradski, "Note sur une intégrale qui se rencontre dans le calcul de l'attraction des sphéroïdes", Mem. Ac. Sci St. Peters., 6th ser. **1** (1831) 39.

[231] K. G. Chetyrkin, A. L. Kataev and F. V. Tkachov, "New Approach to Evaluation of Multiloop Feynman Integrals: The Gegenbauer Polynomial x Space Technique", Nucl. Phys. **B174** (1980) 345.

[232] K. G. Chetyrkin and F. V. Tkachov, "Integration by Parts: The Algorithm to Calculate beta Functions in 4 Loops", Nucl. Phys. **B192** (1981) 159.

[233] F. V. Tkachov, "A Theorem on Analytical Calculability of Four Loop Renormalization Group Functions", Phys. Lett. **B100** (1981) 65.

[234] P. Appell, *Sur les fonctions hypergéométriques de plusieurs variables, les polynômes d'Hermite et autres fonctions sphériques dans l'hyperespace* (Gauthier-Villars, Paris, 1925).

[235] P. Appell and J. Kampé de Fériet, *Fonctions hypergéométriques et hypersphériques: polynômes d'Hermite* (Gauthier-Villars, Paris, 1926).

[236] J. Kampé De Fériet, *La fonction hypergéométrique* (Gauthier-Villars, Paris, 1937).

[237] H. Exton, *Multiple Hypergeometric Functions and Applications* (Ellis Horwood, Chichester, 1976).

[238] H. Exton, *Handbook of hypergeometric integrals* (Ellis Horwood, Chichester, 1978).

[239] H. M. Srivastava and P. W. Karlsson, *Multiple Gaussian hypergeometric series* (Ellis Horwood, Chichester, 1985).

[240] M. Karr, "Summation in Finite Terms", J. ACM **28** (1981) 305.

[241] C. Schneider, *Symbolic Summation in Difference Fields*, PhD thesis (RISC, J. Kepler University Linz, 2001).

[242] C. Schneider, "A Collection of Denominator Bounds to Solve Parameterized Linear Difference Equations in $\Pi\Sigma$-Extensions", An. Univ. Timisoara Ser. Mat.-Inform. **42** (2004) 163.

[243] C. Schneider, "Solving Parameterized Linear Difference Equations in Terms of Indefinite Nested Sums and Products", J. Differ. Equations Appl. **11** (2005) 799.

[244] C. Schneider, "Degree Bounds to Find Polynomial Solutions of Parameterized Linear Difference Equations in $\Pi\Sigma$-Fields", Appl. Algebra Engrg. Comm. Comput. **16** (2005) 1.

[245] C. Schneider, "Simplifying Sums in $\Pi\Sigma^*$-Extensions", J. Algebra Appl. **6** (2007) 415.

[246] C. Schneider, "A Symbolic Summation Approach to Find Optimal Nested Sum Representations", in Motives, Quantum Field Theory, and Pseudodifferential Operators, Vol. 12, edited by A. Carey, D. Ellwood, S. Paycha and S. Rosenberg, Clay Mathematics Proceedings (2010), 285, arXiv:`0904.2323` [`cs.SC`].

[247] C. Schneider, "Parameterized Telescoping Proves Algebraic Independence of Sums", Ann. Comb. **14** (2010) 533, arXiv:`0808.2596` [`cs.SC`].

[248] C. Schneider, "Fast Algorithms for Refined Parameterized Telescoping in Difference Fields", in *Computer Algebra and Polynomials, Applications of Algebra and Number Theory*, edited by J. Gutierrez, J. Schicho and M. Weimann, Lecture Notes in Computer Science 8942 (Springer, 2015), pp. 157–191, arXiv:`1307.7887` [`cs.SC`].

[249] C. Schneider, "A refined difference field theory for symbolic summation", J. Symbolic Comput. **43** (2008) 611, arXiv:`0808.2543` [`cs.SC`].

[250] C. Schneider, "A difference ring theory for symbolic summation", J. Symbolic Comput. **72** (2016) 82, arXiv:`1408.2776` [`cs.SC`].

[251] C. Schneider, "Summation Theory II: Characterizations of $R\Pi\Sigma$-extensions and algorithmic aspects", (2016), arXiv:`1603.04285` [`cs.SC`].

[252] C. Schneider, "Symbolic Summation Assists Combinatorics", Sem. Lothar. Combin. **56** (2007) article 56b.

[253] C. Schneider, "Simplifying Multiple Sums in Difference Fields", in *Computer Algebra in Quantum Field Theory: Integration, Summation and Special Functions*, edited by C. Schneider and J. Blümlein (Springer, Vienna, 2013), 325, arXiv:`1304.4134` [`cs.SC`].

[254] J. Ablinger, J. Blümlein, S. Klein and C. Schneider, "Modern Summation Methods and the Computation of 2- and 3-loop Feynman Diagrams", Nucl. Phys. Proc. Suppl. **205-206** (2010) 110, arXiv:`1006.4797` [`math-ph`].

[255] J. Blümlein, A. Hasselhuhn and C. Schneider, "Evaluation of Multi-Sums for Large Scale Problems", PoS **RADCOR2011** (2011) 032, arXiv:`1202.4303` [`math-ph`].

Bibliography

[256] C. Schneider, "Symbolic Summation in Difference Fields and Its Application in Particle Physics", Computer Algebra Rundbrief **53** (2013) 8.

[257] C. Schneider, "Modern Summation Methods for Loop Integrals in Quantum Field Theory: The Packages Sigma, EvaluateMultiSums and SumProduction", J. Phys. Conf. Ser. **523** (2014) 012037, arXiv:`1310.0160` [`cs.SC`].

[258] J. Ablinger, *A Computer Algebra Toolbox for Harmonic Sums Related to Particle Physics*, Diploma thesis (J. Kepler University Linz, 2009), arXiv:`1011.1176` [`math-ph`].

[259] J. Ablinger, *Computer Algebra Algorithms for Special Functions in Particle Physics*, PhD thesis (J. Kepler University Linz, 2012), arXiv:`1305.0687` [`math-ph`].

[260] J. Ablinger, J. Blümlein and C. Schneider, "Harmonic Sums and Polylogarithms Generated by Cyclotomic Polynomials", J. Math. Phys. **52** (2011) 102301, arXiv:`1105.6063` [`math-ph`].

[261] J. Ablinger, J. Blümlein and C. Schneider, "Analytic and Algorithmic Aspects of Generalized Harmonic Sums and Polylogarithms", J. Math. Phys. **54** (2013) 082301, arXiv:`1302.0378` [`math-ph`].

[262] J. Ablinger, J. Blümlein, C. G. Raab and C. Schneider, "Iterated Binomial Sums and their Associated Iterated Integrals", J. Math. Phys. **55** (2014) 112301, arXiv:`1407.1822` [`hep-th`].

[263] J. Ablinger, "The package HarmonicSums: Computer Algebra and Analytic aspects of Nested Sums", PoS **LL2014** (2014) 019, arXiv:`1407.6180` [`cs.SC`].

[264] A. V. Kotikov, "Differential equations method: New technique for massive Feynman diagrams calculation", Phys. Lett. **B254** (1991) 158.

[265] M. Caffo, H. Czyż, S. Laporta and E. Remiddi, "Master equations for master amplitudes", Acta Phys. Polon. **B29** (1998) 2627, arXiv:`hep-th/9807119` [`hep-th`].

[266] M. Caffo, H. Czyż, S. Laporta and E. Remiddi, "The Master differential equations for the two loop sunrise selfmass amplitudes", Nuovo Cim. **A111** (1998) 365, arXiv:`hep-th/9805118` [`hep-th`].

[267] T. Gehrmann and E. Remiddi, "Differential equations for two loop four point functions", Nucl. Phys. **B580** (2000) 485, arXiv:`hep-ph/9912329` [`hep-ph`].

[268] J. Ablinger, A. Behring, J. Blümlein, A. De Freitas, A. von Manteuffel and C. Schneider, "Calculating Three Loop Ladder and V-Topologies for Massive Operator Matrix Elements by Computer Algebra", Comput. Phys. Commun. **202** (2016) 33, arXiv:`1509.08324` [`hep-ph`].

[269] J. A. M. Vermaseren, "Axodraw", Comput. Phys. Commun. **83** (1994) 45.

[270] A. Arbuzov, D. Y. Bardin, J. Blümlein, L. Kalinovskaya and T. Riemann, "Hector 1.00: A Program for the calculation of QED, QCD and electroweak corrections to ep and $l^{\pm}N$ deep inelastic neutral and charged current scattering", Comput. Phys. Commun. **94** (1996) 128, arXiv:`hep-ph/9511434` [`hep-ph`], and references therein.

[271] J. D. Bjorken, "Inelastic Scattering of Polarized Leptons from Polarized Nucleons", Phys. Rev. **D1** (1970) 1376.

[272] J. Blümlein, "The Theory of Deeply Inelastic Scattering", Prog. Part. Nucl. Phys. **69** (2013) 28, arXiv:`1208.6087` [`hep-ph`].

[273] O. Nachtmann, "Positivity constraints for anomalous dimensions", Nucl. Phys. **B63** (1973) 237.

[274] S. Wandzura, "Projection of Wilson Coefficients from Deep Inelastic Leptoproduction Data", Nucl. Phys. **B122** (1977) 412.

[275] H. Georgi and H. D. Politzer, "Freedom at Moderate Energies: Masses in Color Dynamics", Phys. Rev. **D14** (1976) 1829.

[276] J. Blümlein and A. Tkabladze, "Target mass corrections for polarized structure functions and new sum rules", Nucl. Phys. **B553** (1999) 427, arXiv:`hep-ph/9812478` [`hep-ph`].

[277] F. M. Steffens, M. D. Brown, W. Melnitchouk and S. Sanches, "Parton distributions in the presence of target mass corrections", Phys. Rev. **C86** (2012) 065208, arXiv:`1210.4398` [`hep-ph`].

[278] M. Anselmino, A. Efremov and E. Leader, "The Theory and phenomenology of polarized deep inelastic scattering", Phys. Rept. **261** (1995) 1, arXiv:`hep-ph/9501369` [`hep-ph`], [Erratum: Phys. Rept. **281** (1997) 399].

[279] B. Lampe and E. Reya, "Spin physics and polarized structure functions", Phys. Rept. **332** (2000) 1, arXiv:`hep-ph/9810270` [`hep-ph`].

[280] J. Blümlein and N. Kochelev, "On the twist-2 contributions to polarized structure functions and new sum rules", Phys. Lett. **B381** (1996) 296, arXiv:`hep-ph/9603397` [`hep-ph`].

[281] J. Blümlein and N. Kochelev, "On the twist-2 and twist-3 contributions to the spin dependent electroweak structure functions", Nucl. Phys. **B498** (1997) 285, arXiv:`hep-ph/9612318` [`hep-ph`].

[282] B. Geyer, D. Robaschik and E. Wieczorek, "Theory of Deep Inelastic Lepton-Hadron Scattering", Fortsch. Phys. **27** (1979) 75.

[283] E. Reya, "Perturbative Quantum Chromodynamics", Phys. Rept. **69** (1981) 195.

[284] A. J. Buras, "Asymptotic Freedom in Deep Inelastic Processes in the Leading Order and Beyond", Rev. Mod. Phys. **52** (1980) 199.

[285] J. C. Collins, *Renormalization*, Vol. 26, Cambridge Monographs on Mathematical Physics (Cambridge University Press, Cambridge, 1984), 380 pp.

[286] N. Cabibbo, "Unitary Symmetry and Leptonic Decays", Phys. Rev. Lett. **10** (1963) 531.

[287] M. Kobayashi and T. Maskawa, "CP Violation in the Renormalizable Theory of Weak Interaction", Prog. Theor. Phys. **49** (1973) 652.

[288] H. Mellin, "Über den Zusammenhang Zwischen den Linearen Differential- und Differenzengleichungen", Acta Math. **25** (1902) 139.

[289] F. Carlson, *Sur une classe de séries de Taylor*, PhD thesis (Uppsala University, 1914).

[290] E. C. Titchmarsh, *The Theory of Functions*, 2nd ed. (Oxford University Press, 1939).

[291] T. Kinoshita, "Mass singularities of Feynman amplitudes", J. Math. Phys. **3** (1962) 650.

[292] T. D. Lee and M. Nauenberg, "Degenerate Systems and Mass Singularities", Phys. Rev. **133** (1964) B1549.

[293] W. L. van Neerven and A. Vogt, "NNLO evolution of deep inelastic structure functions: The Singlet case", Nucl. Phys. **B588** (2000) 345, arXiv:`hep-ph/0006154` [`hep-ph`].

[294] G. A. Schuler, "Heavy Flavor Production at HERA", Nucl. Phys. **B299** (1988) 21.

[295] U. Baur and J. J. van der Bij, "Top Quark Production at HERA", Nucl. Phys. **B304** (1988) 451.

[296] J. J. van der Bij and G. J. van Oldenborgh, "QCD radiative corrections to charged current heavy quark production", Z. Phys. **C51** (1991) 477.

[297] M. Glück, R. M. Godbole and E. Reya, "Heavy Flavor Production at High-Energy *ep* Colliders", Z. Phys. **C38** (1988) 441, [Erratum: Z. Phys. **C39** (1988) 590].

[298] F. D. Aaron et al., "Search for Single Top Quark Production at HERA", Phys. Lett. **B678** (2009) 450, arXiv:`0904.3876` [`hep-ex`].

[299] H. Abramowicz et al., "Search for single-top production in *ep* collisions at HERA", Phys. Lett. **B708** (2012) 27, arXiv:`1111.3901` [`hep-ex`].

[300] O. Behnke, A. Geiser and M. Lisovyi, "Charm, Beauty and Top at HERA", Prog. Part. Nucl. Phys. **84** (2015) 1, arXiv:`1506.07519` [`hep-ex`].

[301] F. P. Wißbrock, $O(\alpha_s^3)$ *contributions to the heavy flavor Wilson coefficients of the structure function* $F_2(x, Q^2)$ *at* $Q^2 \gg m^2$, PhD thesis (Techische Universität Dortmund, 2015).

[302] J. Ablinger, J. Blümlein, A. De Freitas, A. Hasselhuhn, C. Schneider and F. Wißbrock, "Three Loop Massive Operator Matrix Elements and Asymptotic Wilson Coefficients for Two Different Masses", DESY-14-019, in preparation.

[303] M. A. G. Aivazis, J. C. Collins, F. I. Olness and W.-K. Tung, "Leptoproduction of heavy quarks. 2. A Unified QCD formulation of charged and neutral current processes from fixed target to collider energies", Phys. Rev. **D50** (1994) 3102, arXiv:`hep-ph/9312319` [`hep-ph`].

[304] W.-K. Tung, S. Kretzer and C. Schmidt, "Open heavy flavor production in QCD: Conceptual framework and implementation issues", J. Phys. **G28** (2002) 983, arXiv:`hep-ph/0110247` [`hep-ph`].

[305] R. S. Thorne and R. G. Roberts, "A Practical procedure for evolving heavy flavor structure functions", Phys. Lett. **B421** (1998) 303, arXiv:`hep-ph/9711223` [`hep-ph`].

[306] J. Blümlein and W. L. van Neerven, "Heavy flavor contributions to the deep inelastic scattering sum rules", Phys. Lett. **B450** (1999) 417, arXiv:`hep-ph/9811351` [`hep-ph`].

[307] S. Forte, E. Laenen, P. Nason and J. Rojo, "Heavy quarks in deep-inelastic scattering", Nucl. Phys. **B834** (2010) 116, arXiv:`1001.2312` [`hep-ph`].

[308] S. Alekhin, J. Blümlein, S. Klein and S. Moch, "The 3, 4, and 5-flavor NNLO Parton from Deep-Inelastic-Scattering Data and at Hadron Colliders", Phys. Rev. **D81** (2010) 014032, arXiv:`0908.2766` [`hep-ph`].

[309] G. 't Hooft and M. J. G. Veltman, "Regularization and Renormalization of Gauge Fields", Nucl. Phys. **B44** (1972) 189.

[310] J. F. Ashmore, "A Method of Gauge Invariant Regularization", Lett. Nuovo Cim. **4** (1972) 289.

[311] G. M. Cicuta and E. Montaldi, "Analytic renormalization via continuous space dimension", Lett. Nuovo Cim. **4** (1972) 329.

[312] C. G. Bollini and J. J. Giambiagi, "Dimensional Renormalization: The Number of Dimensions as a Regularizing Parameter", Nuovo Cim. **B12** (1972) 20.

[313] N. Nielsen, *Handbuch der Theorie der Gammafunktion* (Teubner, Leipzig, 1906), 326 pp.

[314] M. Abramowitz and I. A. Stegun, *Handbook of Mathematical Functions* (Dover Publications Inc., New York, 1972), 1046 pp.

[315] D. A. Akyeampong and R. Delbourgo, "Dimensional regularization, abnormal amplitudes and anomalies", Nuovo Cim. **A17** (1973) 578.

[316] D. A. Akyeampong and R. Delbourgo, "Dimensional regularization and PCAC", Nuovo Cim. **A18** (1973) 94.

[317] D. A. Akyeampong and R. Delbourgo, "Anomalies via dimensional regularization", Nuovo Cim. **A19** (1974) 219.

[318] P. Breitenlohner and D. Maison, "Dimensional Renormalization and the Action Principle", Commun. Math. Phys. **52** (1977) 11.

[319] S. A. Larin, "The Renormalization of the axial anomaly in dimensional regularization", Phys. Lett. **B303** (1993) 113, arXiv:`hep-ph/9302240` [`hep-ph`].

[320] J. C. Ward, "An Identity in Quantum Electrodynamics", Phys. Rev. **78** (1950) 182.

[321] Y. Takahashi, "On the generalized Ward identity", Nuovo Cim. **6** (1957) 371.

[322] G. 't Hooft, "Dimensional regularization and the renormalization group", Nucl. Phys. **B61** (1973) 455.

[323] J. C. Collins and R. J. Scalise, "The Renormalization of composite operators in Yang-Mills theories using general covariant gauge", Phys. Rev. **D50** (1994) 4117, arXiv:`hep-ph/9403231` [`hep-ph`].

[324] B. W. Harris and J. Smith, "Anomalous dimension of the gluon operator in pure Yang-Mills theory", Phys. Rev. **D51** (1995) 4550, arXiv:`hep-ph/9409405` [`hep-ph`].

[325] Y. Matiounine, J. Smith and W. L. van Neerven, "Two loop operator matrix elements calculated up to finite terms", Phys. Rev. **D57** (1998) 6701, arXiv:`hep-ph/9801224` [`hep-ph`].

[326] R. Tarrach, "The Pole Mass in Perturbative QCD", Nucl. Phys. **B183** (1981) 384.

[327] O. Nachtmann and W. Wetzel, "The Beta Function for Effective Quark Masses to Two Loops in QCD", Nucl. Phys. **B187** (1981) 333.

[328] D. J. Broadhurst, N. Gray and K. Schilcher, "Gauge invariant on-shell Z_2 in QED, QCD and the effective field theory of a static quark", Z. Phys. **C52** (1991) 111.

[329] J. Fleischer, F. Jegerlehner, O. V. Tarasov and O. L. Veretin, "Two loop QCD corrections of the massive fermion propagator", Nucl. Phys. **B539** (1999) 671, arXiv:`hep-ph/9803493` [`hep-ph`], [Erratum: Nucl. Phys. **B571** (2000) 511].

[330] I. B. Khriplovich, "Green's functions in theories with non-abelian gauge group.", Sov. J. Nucl. Phys. **10** (1969) 235, [Yad. Fiz. **10** (1969) 409].

[331] W. E. Caswell, "Asymptotic Behavior of Nonabelian Gauge Theories to Two Loop Order", Phys. Rev. Lett. **33** (1974) 244.

[332] D. R. T. Jones, "Two Loop Diagrams in Yang-Mills Theory", Nucl. Phys. **B75** (1974) 531.

[333] L. F. Abbott, "The Background Field Method Beyond One Loop", Nucl. Phys. **B185** (1981) 189.

[334] A. Rebhan, "Momentum Subtraction Scheme and the Background Field Method in QCD", Z. Phys. **C30** (1986) 309.

[335] F. Jegerlehner and O. V. Tarasov, "Exact mass dependent two loop $\bar{\alpha}_s(Q^2)$ in the background MOM renormalization scheme", Nucl. Phys. **B549** (1999) 481, arXiv:`hep-ph/9809485` [`hep-ph`].

[336] J. Ablinger, J. Blümlein, S. Klein, C. Schneider and F. Wißbrock, "The $O(\alpha_s^3)$ Massive Operator Matrix Elements of $O(n_f)$ for the Structure Function $F_2(x, Q^2)$ and Transversity", Nucl. Phys. **B844** (2011) 26, arXiv:`1008.3347` [`hep-ph`].

[337] J. Blümlein, A. Hasselhuhn, S. Klein and C. Schneider, "The $O(\alpha_s^3 n_f T_F^2 C_{A,F})$ Contributions to the Gluonic Massive Operator Matrix Elements", Nucl. Phys. **B866** (2013) 196, arXiv:`1205.4184` [`hep-ph`].

Bibliography

[338] A. Behring, J. Blümlein, A. De Freitas, T. Pfoh, C. Raab, M. Round, J. Ablinger, A. Hasselhuhn, C. Schneider, F. Wißbrock and A. von Manteuffel, "New Results on the 3-Loop Heavy Flavor Corrections in Deep-Inelastic Scattering", PoS **RADCOR2013** (2013) 058, arXiv:1312.0124 [`hep-ph`].

[339] J. Ablinger, J. Blümlein, A. De Freitas, A. Hasselhuhn, A. von Manteuffel, M. Round, C. Schneider and F. Wißbrock, "The Transition Matrix Element $A_{gq}(N)$ of the Variable Flavor Number Scheme at $O(\alpha_s^3)$", Nucl. Phys. **B882** (2014) 263, arXiv:1402.0359 [`hep-ph`].

[340] J. Ablinger, J. Blümlein, A. De Freitas, A. Hasselhuhn, A. von Manteuffel, M. Round and C. Schneider, "The $O(\alpha_s^3 T_F^2)$ Contributions to the Gluonic Operator Matrix Element", Nucl. Phys. **B885** (2014) 280, arXiv:1405.4259 [`hep-ph`].

[341] J. Ablinger, J. Blümlein, S. Klein, C. Schneider and F. Wißbrock, "3-Loop Heavy Flavor Corrections to DIS with two Massive Fermion Lines", in 19th International Workshop on Deep-Inelastic Scattering and Related Subjects (DIS 2011) Newport News, Virginia, April 11-15, 2011 (2011), arXiv:1106.5937 [`hep-ph`].

[342] J. Ablinger, J. Blümlein, A. Hasselhuhn, S. Klein, C. Schneider and F. Wißbrock, "New Heavy Flavor Contributions to the DIS Structure Function $F_2(x, Q^2)$ at $\mathcal{O}(\alpha_s^3)$", PoS **RADCOR2011** (2011) 031, arXiv:1202.2700 [`hep-ph`].

[343] J. Ablinger, J. Blümlein, A. Hasselhuhn, S. Klein, C. Schneider and F. Wißbrock, "Massive 3-loop Ladder Diagrams for Quarkonic Local Operator Matrix Elements", Nucl. Phys. **B864** (2012) 52, arXiv:1206.2252 [`hep-ph`].

[344] J. Ablinger, J. Blümlein, C. Raab, C. Schneider and F. Wißbrock, "Calculating Massive 3-loop Graphs for Operator Matrix Elements by the Method of Hyperlogarithms", Nucl. Phys. **B885** (2014) 409, arXiv:1403.1137 [`hep-ph`].

[345] F. Brown, "The Massless higher-loop two-point function", Commun. Math. Phys. **287** (2009) 925, arXiv:0804.1660 [`math.AG`].

[346] F. C. S. Brown, "On the periods of some Feynman integrals", (2009), arXiv:0910.0114 [`math.AG`].

[347] P. Nogueira, "Automatic Feynman graph generation", J. Comput. Phys. **105** (1993) 279.

[348] T. van Ritbergen, A. N. Schellekens and J. A. M. Vermaseren, "Group theory factors for Feynman diagrams", Int. J. Mod. Phys. **A14** (1999) 41, arXiv:`hep-ph/9802376` [`hep-ph`].

[349] C. Anastasiou and A. Lazopoulos, "Automatic integral reduction for higher order perturbative calculations", JHEP **07** (2004) 046, arXiv:`hep-ph/0404258` [`hep-ph`].

[350] A. V. Smirnov, "Algorithm FIRE – Feynman Integral REduction", JHEP **10** (2008) 107, arXiv:0807.3243 [`hep-ph`].

[351] R. N. Lee, "Presenting LiteRed: a tool for the Loop InTEgrals REDuction", (2012), arXiv:1212.2685 [`hep-ph`].

[352] A. V. Smirnov and V. A. Smirnov, "FIRE4, LiteRed and accompanying tools to solve integration by parts relations", Comput. Phys. Commun. **184** (2013) 2820, arXiv:1302.5885 [`hep-ph`].

[353] C. Studerus, "Reduze - Feynman Integral Reduction in C++", Comput. Phys. Commun. **181** (2010) 1293, arXiv:0912.2546 [`physics.comp-ph`].

[354] A. von Manteuffel and C. Studerus, "Reduze 2 - Distributed Feynman Integral Reduction", (2012), arXiv:1201.4330 [`hep-ph`].

314

[355] S. Laporta, "High precision calculation of multiloop Feynman integrals by difference equations", Int. J. Mod. Phys. **A15** (2000) 5087, arXiv:`hep-ph/0102033` [`hep-ph`].

[356] C. W. Bauer, A. Frink and R. Kreckel, "Introduction to the GiNaC framework for symbolic computation within the C++ programming language", J. Symb. Comput. **33** (2000) 1, arXiv:`cs/0004015` [`cs-sc`].

[357] R. H. Lewis, *Computer algebra system fermat*, `http://home.bway.net/lewis`.

[358] J. Ablinger, A. Behring, J. Blümlein, A. De Freitas, A. Hasselhuhn, A. von Manteuffel, M. Round, C. Schneider and F. Wißbrock, "The 3-Loop Non-Singlet Heavy Flavor Contributions and Anomalous Dimensions for the Structure Function $F_2(x, Q^2)$ and Transversity", Nucl. Phys. **B886** (2014) 733, arXiv:`1406.4654` [`hep-ph`].

[359] J. Ablinger and J. Blümlein, "Harmonic Sums, Polylogarithms, Special Numbers, and their Generalizations", in *Computer Algebra in Quantum Field Theory: Integration, Summation and Special Functions*, edited by C. Schneider and J. Blümlein (Springer, Vienna, 2013), 1, arXiv:`1304.7071` [`math-ph`].

[360] C. Duhr, "Mathematical aspects of scattering amplitudes", in Theoretical Advanced Study Institute in Elementary Particle Physics (TASI 2014) Boulder, Colorado, June 2-27, 2014 (2014), arXiv:`1411.7538` [`hep-ph`].

[361] J. Blümlein, D. J. Broadhurst and J. A. M. Vermaseren, "The Multiple Zeta Value Data Mine", Comput. Phys. Commun. **181** (2010) 582, arXiv:`0907.2557` [`math-ph`], and references therein.

[362] J. Blümlein, "Analytic continuation of Mellin transforms up to two loop order", Comput. Phys. Commun. **133** (2000) 76, arXiv:`hep-ph/0003100` [`hep-ph`].

[363] D. J. Broadhurst, "Three loop on-shell charge renormalization without integration: Λ_{MS}^{QED} to four loops", Z. Phys. **C54** (1992) 599.

[364] L. Avdeev, J. Fleischer, S. Mikhailov and O. Tarasov, "$O(\alpha\alpha_s^2)$ correction to the electroweak ρ parameter", Phys. Lett. **B336** (1994) [Erratum: Phys. Lett.B349,597(1995)], 560, arXiv:`hep-ph/9406363` [`hep-ph`], [Erratum: Phys. Lett. **B349** (1995) 597].

[365] S. Laporta and E. Remiddi, "The Analytical value of the electron $(g-2)$ at order α^3 in QED", Phys. Lett. **B379** (1996) 283, arXiv:`hep-ph/9602417` [`hep-ph`].

[366] D. J. Broadhurst, "Massive three-loop Feynman diagrams reducible to SC* primitives of algebras of the sixth root of unity", Eur. Phys. J. **C8** (1999) 311, arXiv:`hep-th/9803091` [`hep-th`].

[367] R. Boughezal, J. B. Tausk and J. J. van der Bij, "Three-loop electroweak correction to the Rho parameter in the large Higgs mass limit", Nucl. Phys. **B713** (2005) 278, arXiv:`hep-ph/0410216` [`hep-ph`].

[368] S. Moch, P. Uwer and S. Weinzierl, "Nested sums, expansion of transcendental functions and multiscale multiloop integrals", J. Math. Phys. **43** (2002) 3363, arXiv:`hep-ph/0110083` [`hep-ph`].

[369] J. Fleischer, A. V. Kotikov and O. L. Veretin, "Analytic two loop results for selfenergy type and vertex type diagrams with one nonzero mass", Nucl. Phys. **B547** (1999) 343, arXiv:`hep-ph/9808242` [`hep-ph`].

[370] A. I. Davydychev and M. Y. Kalmykov, "Massive Feynman diagrams and inverse binomial sums", Nucl. Phys. **B699** (2004) 3, arXiv:`hep-th/0303162` [`hep-th`].

[371] S. Weinzierl, "Expansion around half integer values, binomial sums and inverse binomial sums", J. Math. Phys. **45** (2004) 2656, arXiv:`hep-ph/0402131` [`hep-ph`].

Bibliography

[372] M. E. Hoffman, "Quasi-shuffle products", J. Algebraic Combin. **11** (2000) 49, arXiv:`math/9907173`.

[373] H. Poincaré, "Sur les groupes des équations linéaires", Acta Math. **4** (1884) 201.

[374] J. A. Lappo-Danilevsky, *Mémoires sur la théorie des systèmes des équations différentielles linéaires* (Chelsea Pub. Co., New York, 1953).

[375] K.-T. Chen, "Formal Differential Equations", Ann. Math. **73** (1961) 110.

[376] L. Lewin, *Polylogarithms and associated functions* (North Holland, New York, 1981).

[377] A. Devoto and D. W. Duke, "Table of Integrals and Formulae for Feynman Diagram Calculations", Riv. Nuovo Cim. **7N6** (1984) 1.

[378] N. Nielsen, "Der Eulersche Dilogarithmus und seine Verallgemeinerungen", Nova Acta Leopoldina **90** (1909) 123.

[379] K. S. Kölbig, J. A. Mignaco and E. Remiddi, "On Nielsen's generalized polylogarithms and their numerical calculation", BIT **10** (1970) 38.

[380] K. S. Kölbig, "Nielsen's generalized polylogarithms", SIAM J. Math. Anal. **17** (1986) 1232.

[381] S. Lang, *Algebra*, 3rd ed. (Springer, New York, 2002).

[382] B. Zürcher, *Rationale Normalformen von pseudo-linearen Abbildungen*, Diploma thesis (ETH Zürich, 1994).

[383] S. Gerhold, *Uncoupling Systems of Linear Ore Operator Equations*, Diploma thesis (RISC, J. Kepler University Linz, 2002).

[384] G. Almkvist and D. Zeilberger, "The method of differentiating under the integral sign", J. Symb. Comp. **10** (1990) 571.

[385] M. Apagodu and D. Zeilberger, "Multi-variable Zeilberger and Almkvist–Zeilberger algorithms and the sharpening of Wilf–Zeilberger theory", Adv. Appl. Math. **37** (2006) 139.

[386] S. W. G. Klein, *Heavy Flavor Coefficient Functions in Deep-Inelastic Scattering at $O(a_s^2)$ and Large Virtualities*, Diploma thesis (Universität Potsdam, 2006).

[387] R. Hamberg, *Second order gluonic contributions to physical quantities*, PhD thesis (Leiden University, 1991).

[388] I. S. Gradstein and I. M. Ryshik, *Tables of series, products and integrals* (Verlag Harri Deutsch, Thun, 1981).

[389] V. A. Smirnov, *Feynman integral calculus* (Springer, Berlin, 2006), 283 pp.

[390] V. A. Smirnov, "Analytical result for dimensionally regularized massless on shell double box", Phys. Lett. **B460** (1999) 397, arXiv:`hep-ph/9905323` [`hep-ph`].

[391] J. B. Tausk, "Nonplanar massless two loop Feynman diagrams with four on-shell legs", Phys. Lett. **B469** (1999) 225, arXiv:`hep-ph/9909506` [`hep-ph`].

[392] M. Czakon, "Automatized analytic continuation of Mellin-Barnes integrals", Comput. Phys. Commun. **175** (2006) 559, arXiv:`hep-ph/0511200` [`hep-ph`].

[393] A. V. Smirnov and V. A. Smirnov, "On the Resolution of Singularities of Multiple Mellin-Barnes Integrals", Eur. Phys. J. **C62** (2009) 445, arXiv:`0901.0386` [`hep-ph`].

[394] K. G. Chetyrkin and V. A. Smirnov, "Dimensional Regularization and Infrared Divergences", Theor. Math. Phys. **56** (1984) 770, [Teor. Mat. Fiz. **56** (1983) 206].

[395] C. Schneider, A. De Freitas and J. Blümlein, "Recent Symbolic Summation Methods to Solve Coupled Systems of Differential and Difference Equations", PoS **LL2014** (2014) 017, arXiv:1407.2537 [cs.SC].

[396] J. Ablinger, J. Blümlein, A. de Freitas and C. Schneider, "A toolbox to solve coupled systems of differential and difference equations", (2016), arXiv:1601.01856 [cs.SC].

[397] J. Ablinger, A. Behring, J. Blümlein, A. De Freitas, A. von Manteuffel and C. Schneider, "The 3-loop pure singlet heavy flavor contributions to the structure function $F_2(x, Q^2)$ and the anomalous dimension", Nucl. Phys. **B890** (2014) 48, arXiv:1409.1135 [hep-ph].

[398] J. Blümlein, S. Klein, C. Schneider and F. Stan, "A Symbolic Summation Approach to Feynman Integral Calculus", J. Symbolic Comput. **47** (2012) 1267, arXiv:1011.2656 [cs.SC].

[399] C. Itzykson and J. B. Zuber, *Quantum Field Theory*, International Series In Pure and Applied Physics (McGraw-Hill, New York, 1980).

[400] C. Bogner and S. Weinzierl, "Feynman graph polynomials", Int. J. Mod. Phys. **A25** (2010) 2585, arXiv:1002.3458 [hep-ph].

[401] D. J. Gross and C. H. Llewellyn Smith, "High-energy neutrino - nucleon scattering, current algebra and partons", Nucl. Phys. **B14** (1969) 337.

[402] A. Behring, J. Blümlein, A. De Freitas, A. von Manteuffel and C. Schneider, "The 3-Loop Non-Singlet Heavy Flavor Contributions to the Structure Function $g_1(x, Q^2)$ at Large Momentum Transfer", Nucl. Phys. **B897** (2015) 612, arXiv:1504.08217 [hep-ph].

[403] A. Behring, J. Blümlein, A. De Freitas, A. Hasselhuhn, A. von Manteuffel and C. Schneider, "$O(\alpha_s^3)$ heavy flavor contributions to the charged current structure function $xF_3(x, Q^2)$ at large momentum transfer", Phys. Rev. **D92** (2015) 114005, arXiv:1508.01449 [hep-ph].

[404] J. Ablinger, J. Blümlein, A. De Freitas, A. Hasselhuhn, A. von Manteuffel, M. Round, C. Schneider and F. Wißbrock, "3-Loop Heavy Flavor Corrections in Deep-Inelastic Scattering with Two Heavy Quark Lines", PoS **LL2014** (2014) 015, arXiv:1407.2821 [hep-ph].

[405] S. Kumano and M. Miyama, "Two loop anomalous dimensions for the structure function h_1", Phys. Rev. **D56** (1997) 2504, arXiv:hep-ph/9706420 [hep-ph].

[406] W. Vogelsang, "Next-to-leading order evolution of transversity distributions and Soffer's inequality", Phys. Rev. **D57** (1998) 1886, arXiv:hep-ph/9706511 [hep-ph].

[407] A. Hayashigaki, Y. Kanazawa and Y. Koike, "Next-to-leading order Q^2 evolution of the transversity distribution $h_1(x, Q^2)$", Phys. Rev. **D56** (1997) 7350, arXiv:hep-ph/9707208 [hep-ph].

[408] J. A. Gracey, "Three loop anomalous dimension of nonsinglet quark currents in the RI$'$ scheme", Nucl. Phys. **B662** (2003) 247, arXiv:hep-ph/0304113 [hep-ph].

[409] J. A. Gracey, "Three loop anomalous dimension of the second moment of the transversity operator in the $\overline{\text{MS}}$ and RI$'$ schemes", Nucl. Phys. **B667** (2003) 242, arXiv:hep-ph/0306163 [hep-ph].

[410] J. A. Gracey, "Three loop anomalous dimensions of higher moments of the non-singlet twist-2 Wilson and transversity operators in the $\overline{\text{MS}}$ and RI$'$ schemes", JHEP **10** (2006) 040, arXiv:hep-ph/0609231 [hep-ph].

[411] J. A. Gracey, "Three loop $\overline{\text{MS}}$ transversity operator anomalous dimensions for fixed moment $n \leq 8$", Phys. Lett. **B643** (2006) 374, arXiv:hep-ph/0611071 [hep-ph].

Bibliography

[412] A. A. Bagaev, A. V. Bednyakov, A. F. Pikelner and V. N. Velizhanin, "The 16th moment of the three loop anomalous dimension of the non-singlet transversity operator in QCD", Phys. Lett. **B714** (2012) 76, arXiv:1206.2890 [hep-ph].

[413] V. N. Velizhanin, "Three loop anomalous dimension of the non-singlet transversity operator in QCD", Nucl. Phys. **B864** (2012) 113, arXiv:1203.1022 [hep-ph].

[414] N. Gray, D. J. Broadhurst, W. Grafe and K. Schilcher, "Three Loop Relation of Quark (Modified) MS and Pole Masses", Z. Phys. **C48** (1990) 673.

[415] K. G. Chetyrkin and M. Steinhauser, "Short distance mass of a heavy quark at order α_s^3", Phys. Rev. Lett. **83** (1999) 4001, arXiv:hep-ph/9907509 [hep-ph].

[416] K. G. Chetyrkin and M. Steinhauser, "The Relation between the $\overline{\text{MS}}$ and the on-shell quark mass at order α_s^3", Nucl. Phys. **B573** (2000) 617, arXiv:hep-ph/9911434 [hep-ph].

[417] K. Melnikov and T. v. Ritbergen, "The Three loop relation between the $\overline{\text{MS}}$ and the pole quark masses", Phys. Lett. **B482** (2000) 99, arXiv:hep-ph/9912391 [hep-ph].

[418] K. Melnikov and T. van Ritbergen, "The Three loop on-shell renormalization of QCD and QED", Nucl. Phys. **B591** (2000) 515, arXiv:hep-ph/0005131 [hep-ph].

[419] R. Kirschner and L. N. Lipatov, "Double Logarithmic Asymptotics and Regge Singularities of Quark Amplitudes with Flavor Exchange", Nucl. Phys. **B213** (1983) 122.

[420] J. Blümlein and A. Vogt, "On the behavior of nonsinglet structure functions at small x", Phys. Lett. **B370** (1996) 149, arXiv:hep-ph/9510410 [hep-ph].

[421] J. Blümlein, A. De Freitas and G. Falcioni, DESY-15-171, in preparation.

[422] M. R. Whalley, D. Bourilkov and R. C. Group, "The Les Houches accord PDFs (LHAPDF) and LHAGLUE", in HERA and the LHC: A Workshop on the implications of HERA for LHC physics. Proceedings, Part B (2005), arXiv:hep-ph/0508110 [hep-ph], see also http://lhapdf.hepforge.org/.

[423] T. Gehrmann and E. Remiddi, "Numerical evaluation of harmonic polylogarithms", Comput. Phys. Commun. **141** (2001) 296, arXiv:hep-ph/0107173 [hep-ph].

[424] D. Boer et al., "Gluons and the quark sea at high energies: Distributions, polarization, tomography", (2011), arXiv:1108.1713 [nucl-th].

[425] A. Accardi et al., "Electron Ion Collider: The Next QCD Frontier - Understanding the glue that binds us all", edited by A. Deshpande, Z. E. Meziani and J. W. Qiu (2012), arXiv:1212.1701 [nucl-ex].

[426] S. Alekhin, J. Blümlein and S. Moch, "Parton Distribution Functions and Benchmark Cross Sections at NNLO", Phys. Rev. **D86** (2012) 054009, arXiv:1202.2281 [hep-ph].

[427] J. D. Jackson, G. G. Ross and R. G. Roberts, "Polarized Structure Functions in the Parton Model", Phys. Lett. **B226** (1989) 159.

[428] R. G. Roberts and G. G. Ross, "Quark model description of polarized deep inelastic scattering and the prediction of g_2", Phys. Lett. **B373** (1996) 235, arXiv:hep-ph/9601235 [hep-ph].

[429] A. Piccione and G. Ridolfi, "Target mass effects in polarized deep inelastic scattering", Nucl. Phys. **B513** (1998) 301, arXiv:hep-ph/9707478 [hep-ph].

[430] J. Blümlein and D. Robaschik, "On the structure of the virtual Compton amplitude in the generalized Bjorken region: Integral relations", Nucl. Phys. **B581** (2000) 449, arXiv:hep-ph/0002071 [hep-ph].

[431] J. Blümlein and D. Robaschik, "Polarized deep inelastic diffractive $e\,p$ scattering: Operator approach", Phys. Rev. **D65** (2002) 096002, arXiv:`hep-ph/0202077` [`hep-ph`].

[432] J. Blümlein, D. Robaschik and B. Geyer, "Target mass and finite t corrections to diffractive deeply inelastic scattering", Eur. Phys. J. **C61** (2009) 279, arXiv:`0812.1899` [`hep-ph`].

[433] J. Blümlein and A. Vogt, "On the resummation of $\alpha \ln^2 x$ terms for nonsinglet structure functions in QED and QCD", Acta Phys. Polon. **B27** (1996) 1309, arXiv:`hep-ph/9603450` [`hep-ph`].

[434] Y. Kiyo, J. Kodaira and H. Tochimura, "Does leading $\ln x$ resummation predict the rise of g_1 at small x?", Z. Phys. **C74** (1997) 631, arXiv:`hep-ph/9701365` [`hep-ph`].

[435] J. Blümlein and H. Böttcher, "QCD Analysis of Polarized Deep Inelastic Scattering Data", Nucl. Phys. **B841** (2010) 205, arXiv:`1005.3113` [`hep-ph`].

[436] J. Blümlein and A. Vogt, "The Evolution of unpolarized singlet structure functions at small x", Phys. Rev. **D58** (1998) 014020, arXiv:`hep-ph/9712546` [`hep-ph`].

[437] J. Blümlein, H. Bottcher and A. Guffanti, "Non-singlet QCD analysis of the structure function F_2 in 3-loops", Nucl. Phys. Proc. Suppl. **135** (2004) 152, arXiv:`hep-ph/0407089` [`hep-ph`].

[438] J. Blümlein, H. Böttcher and A. Guffanti, "Non-singlet QCD analysis of deep inelastic world data at $O(\alpha_s^3)$", Nucl. Phys. **B774** (2007) 182, arXiv:`hep-ph/0607200` [`hep-ph`].

[439] D. Mund, B. Märkisch, M. Deissenroth, J. Krempel, M. Schumann, H. Abele, A. Petoukhov and T. Soldner, "Determination of the Weak Axial Vector Coupling from a Measurement of the Beta-Asymmetry Parameter A in Neutron Beta Decay", Phys. Rev. Lett. **110** (2013) 172502, arXiv:`1204.0013` [`hep-ex`].

[440] J. Kodaira, S. Matsuda, T. Muta, K. Sasaki and T. Uematsu, "QCD Effects in Polarized Electroproduction", Phys. Rev. **D20** (1979) 627.

[441] S. G. Gorishnii and S. A. Larin, "QCD Corrections to the Parton Model Rules for Structure Functions of Deep Inelastic Scattering", Phys. Lett. **B172** (1986) 109.

[442] P. A. Baikov, K. G. Chetyrkin and J. H. Kühn, "Adler Function, Bjorken Sum Rule, and the Crewther Relation to Order α_s^4 in a General Gauge Theory", Phys. Rev. Lett. **104** (2010) 132004, arXiv:`1001.3606` [`hep-ph`].

[443] S. A. Larin, "The singlet contribution to the Bjorken sum rule for polarized deep inelastic scattering", Phys. Lett. **B723** (2013) 348, arXiv:`1303.4021` [`hep-ph`].

[444] I. Bierenbaum, J. Blümlein and S. Klein, "Two-loop massive operator matrix elements for polarized and unpolarized deep-inelastic scattering", in Proceedings, 15th International Workshop on Deep-inelastic scattering and related subjects (DIS 2007). Vol. 1 and 2 (2007), 821, arXiv:`0706.2738` [`hep-ph`].

[445] W. L. van Neerven, "Heavy flavor contributions to QCD sum rules and the running coupling constant", AIP Conf. Proc. **508** (2000) 162, arXiv:`hep-ph/9910356` [`hep-ph`].

[446] G. Altarelli, R. K. Ellis and G. Martinelli, "Leptoproduction and Drell-Yan Processes Beyond the Leading Approximation in Chromodynamics", Nucl. Phys. **B143** (1978) 521, [Erratum: Nucl. Phys. **B146** (1978) 521].

[447] B. Humpert and W. L. van Neerven, "Infrared and Mass Regularization in Af Field Theories 2. QCD", Nucl. Phys. **B184** (1981) 225.

[448] P. A. Baikov, K. G. Chetyrkin and J. H. Kühn, "Adler Function, DIS sum rules and Crewther Relations", Nucl. Phys. Proc. Suppl. **205-206** (2010) 237, arXiv:`1007.0478` [`hep-ph`].

Bibliography

[449] P. A. Baikov, K. G. Chetyrkin, J. H. Kühn and J. Rittinger, "Adler Function, Sum Rules and Crewther Relation of Order $O(\alpha_s^4)$: the Singlet Case", Phys. Lett. **B714** (2012) 62, arXiv:`1206.1288` [`hep-ph`].

[450] A. Behring, I. Bierenbaum, J. Blümlein, A. De Freitas, S. Klein and F. Wißbrock, "The logarithmic contributions to the $O(\alpha_s^3)$ asymptotic massive Wilson coefficients and operator matrix elements in deeply inelastic scattering", Eur. Phys. J. **C74** (2014) 3033, arXiv:`1403.6356` [`hep-ph`].

[451] C. Schneider, "A new Sigma approach to multi-summation", Adv. Appl. Math. **34** (2005) 740.

[452] J. Ablinger, J. Blümlein, M. Round and C. Schneider, "Advanced Computer Algebra Algorithms for the Expansion of Feynman Integrals", PoS **LL2012** (2012) 050, arXiv:`1210.1685` [`cs.SC`].

[453] M. Round et al., in preparation.

[454] J. Blümlein, "Mathematical structure of anomalous dimensions and QCD Wilson coefficients in higher order", Nucl. Phys. Proc. Suppl. **135** (2004) 225, arXiv:`hep-ph/0407044` [`hep-ph`].

[455] J. Blümlein, "QCD evolution of structure functions at small x", Lect. Notes Phys. **546** (2000) 42, arXiv:`hep-ph/9909449` [`hep-ph`].

[456] H. Kawamura, N. A. Lo Presti, S. Moch and A. Vogt, "On the next-to-next-to-leading order QCD corrections to heavy-quark production in deep-inelastic scattering", Nucl. Phys. **B864** (2012) 399, arXiv:`1205.5727` [`hep-ph`].

[457] D. Maitre, "HPL, a mathematica implementation of the harmonic polylogarithms", Comput. Phys. Commun. **174** (2006) 222, arXiv:`hep-ph/0507152` [`hep-ph`].

[458] D. Maitre, "Extension of HPL to complex arguments", Comput. Phys. Commun. **183** (2012) 846, arXiv:`hep-ph/0703052` [`hep-ph`].